frontiers | Research Topics

Neural circuit formation and sensory inputs

Edited by
Hitoshi Sakano, Kensaku Mori and Charles A. Greer

Published in
Frontiers in Neural Circuits

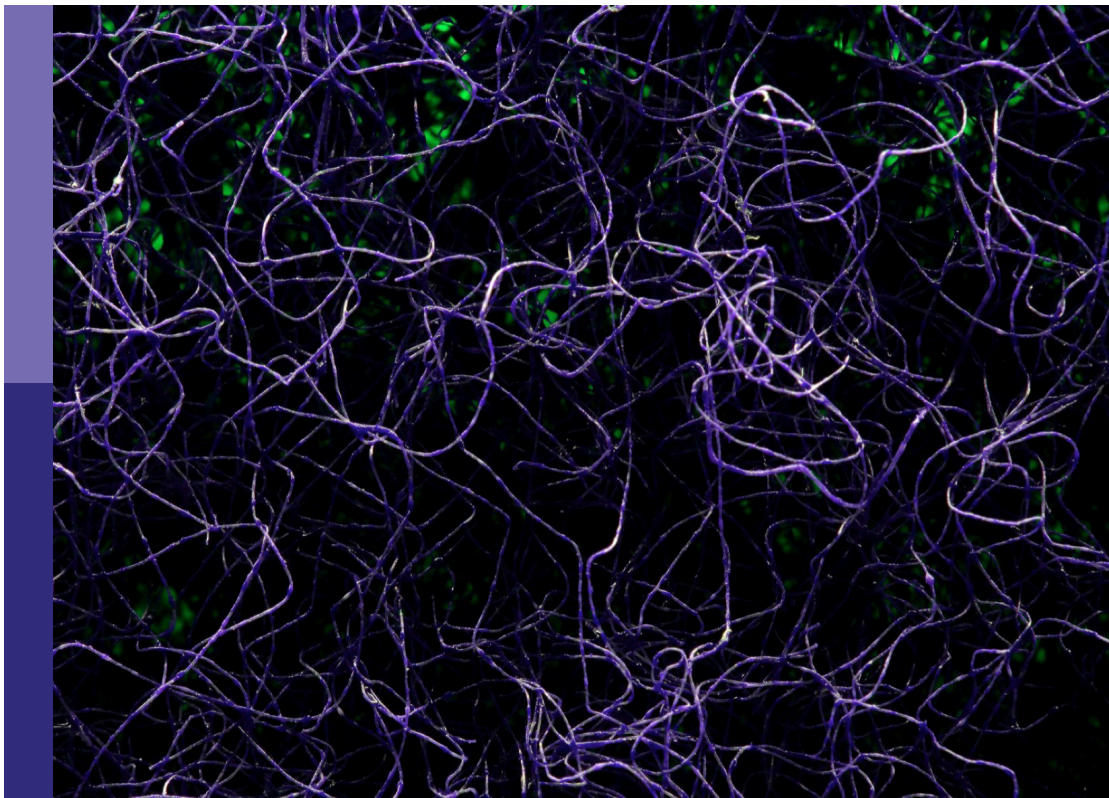

ISSN 1664-8714
ISBN 978-2-8325-5652-8
DOI 10.3389/978-2-8325-5652-8

About Frontiers

Frontiers is more than just an open access publisher of scholarly articles: it is a pioneering approach to the world of academia, radically improving the way scholarly research is managed. The grand vision of Frontiers is a world where all people have an equal opportunity to seek, share and generate knowledge. Frontiers provides immediate and permanent online open access to all its publications, but this alone is not enough to realize our grand goals.

Frontiers journal series

The Frontiers journal series is a multi-tier and interdisciplinary set of open-access, online journals, promising a paradigm shift from the current review, selection and dissemination processes in academic publishing. All Frontiers journals are driven by researchers for researchers; therefore, they constitute a service to the scholarly community. At the same time, the *Frontiers journal series* operates on a revolutionary invention, the tiered publishing system, initially addressing specific communities of scholars, and gradually climbing up to broader public understanding, thus serving the interests of the lay society, too.

Dedication to quality

Each Frontiers article is a landmark of the highest quality, thanks to genuinely collaborative interactions between authors and review editors, who include some of the world's best academicians. Research must be certified by peers before entering a stream of knowledge that may eventually reach the public - and shape society; therefore, Frontiers only applies the most rigorous and unbiased reviews. Frontiers revolutionizes research publishing by freely delivering the most outstanding research, evaluated with no bias from both the academic and social point of view. By applying the most advanced information technologies, Frontiers is catapulting scholarly publishing into a new generation.

What are Frontiers Research Topics?

Frontiers Research Topics are very popular trademarks of the *Frontiers journals series*: they are collections of at least ten articles, all centered on a particular subject. With their unique mix of varied contributions from Original Research to Review Articles, Frontiers Research Topics unify the most influential researchers, the latest key findings and historical advances in a hot research area.

Find out more on how to host your own Frontiers Research Topic or contribute to one as an author by contacting the Frontiers editorial office: frontiersin.org/about/contact

Neural circuit formation and sensory inputs

Topic editors

Hitoshi Sakano — University of Fukui, Japan

Kensaku Mori — RIKEN, Japan

Charles A. Greer — Yale University, United States

Citation

Sakano, H., Mori, K., Greer, C. A., eds. (2024). *Neural circuit formation and sensory inputs*. Lausanne: Frontiers Media SA. doi: 10.3389/978-2-8325-5652-8

Table of contents

05 Neural basis for behavioral plasticity during the parental life-stage transition in mice
Kazunari Miyamichi

11 Circuit formation and sensory perception in the mouse olfactory system
Kensaku Mori and Hitoshi Sakano

22 Olfactory information processing viewed through mitral and tufted cell-specific channels
Tatsumi Hirata

27 Circadian rhythm mechanism in the suprachiasmatic nucleus and its relation to the olfactory system
Yusuke Tsuno and Michihiro Mieda

32 Neural basis for pheromone signal transduction in mice
Ken Murata, Takumi Itakura and Kazushige Touhara

40 Hormonal and circuit mechanisms controlling female sexual behavior
Sayaka Inoue

47 Effects of prenatal alcohol exposure on the olfactory system development
Fumiaki Imamura

53 Activity-dependent dendrite patterning in the postnatal barrel cortex
Naoki Nakagawa and Takuji Iwasato

61 Connectivity of the olfactory tubercle: inputs, outputs, and their plasticity
Masahiro Yamaguchi

66 Shaping the olfactory map: cell type-specific activity patterns guide circuit formation
Ai Nakashima and Haruki Takeuchi

72 Anesthetized animal experiments for neuroscience research
Shin Nagayama, Sanae Hasegawa-Ishii and Shu Kikuta

78 Endogenous opioids in the olfactory tubercle and their roles in olfaction and quality of life
Koshi Murata, Ayako Maegawa, Yoshimasa Imoto, Shigeharu Fujieda and Yugo Fukazawa

86 Structures and functions of the normal and injured human olfactory epithelium
Shu Kikuta, Shin Nagayama and Sanae Hasegawa-Ishii

94 A specific olfactory bulb interneuron subtype Tpbg/5T4 generated at embryonic and neonatal stages
Akio Tsuboi

102 Odors in space
Olivia McKissick, Nell Klimpert, Jason T. Ritt and Alexander Fleischmann

112 Tutor auditory memory for guiding sensorimotor learning in birdsong
Yoko Yazaki-Sugiyama

118 Circuit dynamics of the olfactory pathway during olfactory learning
Yutian J. Zhang, Jason Y. Lee and Kei M. Igarashi

125 Early-life maturation of the somatosensory cortex: sensory experience and beyond
Ijeoma Nwabudike and Alicia Che

133 Olfactory neurogenesis plays different parts at successive stages of life, implications for mental health
Jules Dejou, Nathalie Mandairon and Anne Didier

141 Bilateral and symmetric glycinergic and glutamatergic projections from the LSO to the IC in the CBA/CaH mouse
Isabella R. Williams and David K. Ryugo

167 Vasopressin differentially modulates the excitability of rat olfactory bulb neuron subtypes
Hajime Suyama, Gaia Bianchini and Michael Lukas

frontiers | Frontiers in Neural Circuits

TYPE Mini Review
PUBLISHED 16 January 2024
DOI 10.3389/fncir.2023.1340497

OPEN ACCESS

EDITED BY
Hitoshi Sakano,
University of Fukui, Japan

REVIEWED BY
Tomomi Karigo,
Kennedy Krieger Institute, United States

*CORRESPONDENCE
Kazunari Miyamichi
✉ kazunari.miyamichi@riken.jp

RECEIVED 18 November 2023
ACCEPTED 15 December 2023
PUBLISHED 16 January 2024

CITATION
Miyamichi K (2024) Neural basis for behavioral plasticity during the parental life-stage transition in mice.
Front. Neural Circuits 17:1340497.
doi: 10.3389/fncir.2023.1340497

Neural basis for behavioral plasticity during the parental life-stage transition in mice

Kazunari Miyamichi*

RIKEN Center for Biosystems Dynamics Research, Kobe, Hyogo, Japan

Parental care plays a crucial role in the physical and mental well-being of mammalian offspring. Although sexually naïve male mice, as well as certain strains of female mice, display aggression toward pups, they exhibit heightened parental caregiving behaviors as they approach the time of anticipating their offspring. In this Mini Review, I provide a concise overview of the current understanding of distinct limbic neural types and their circuits governing both aggressive and caregiving behaviors toward infant mice. Subsequently, I delve into recent advancements in the understanding of the molecular, cellular, and neural circuit mechanisms that regulate behavioral plasticity during the transition to parenthood, with a specific focus on the sex steroid hormone estrogen and neural hormone oxytocin. Additionally, I explore potential sex-related differences and highlight some critical unanswered questions that warrant further investigation.

KEYWORDS

hypothalamus, preoptic area, oxytocin, paternal behaviors, estrogen

Introduction

The adult brain possesses neuroplasticity, enabling it to adapt behaviors in response to specific life-stage demands. For instance, male laboratory mice, and certain strains of female mice, may exhibit aggressive behaviors leading to the killing of pups. Infanticide is thought to confer an evolutionary advantage by reducing potential competition for limited resources and thereby enhancing the survival prospects of the offender's offspring (Lukas and Huchard, 2019). Infanticide can also expedite the mating of males with the mothers of the victim (Lukas and Huchard, 2014), as the reproductive cycle is typically suppressed during lactation. However, as the time approaches when animals anticipate their offspring, infanticide is suppressed and caregiving behaviors toward infants are greatly facilitated (Elwood, 1994; Dulac et al., 2014). In rodents, caregiving behaviors include nest building, retrieving scattered pups to a nest for protection from environmental hazards, and crouching over them for thermoregulation. Among these behaviors, pup retrieval has been widely used as a quantitative hallmark of parental behaviors (Yoshihara et al., 2018). Decades of research in rodents have indicated that aggressive and caregiving behaviors toward pups are regulated by distinct limbic neural types and circuits.

Limbic neurons responsible for either parental or infanticidal behavior

The pioneering work of Numan (1974) established the critical role of the medial preoptic area (MPOA) in maternal behaviors in rats. Subsequent research has underscored the importance of the MPOA, particularly its central subdivision, in driving both maternal and paternal caregiving behaviors in mice (Tsuneoka et al., 2013). Wu et al. (2014) conducted a detailed examination of the MPOA at the level of molecularly defined cell types. This work led to the identification of *galanin*-expressing neurons ($MPOA^{Gal}$ neurons), which showed frequent c-Fos expression, a proxy for neural activation, following maternal behaviors. Ablation of $MPOA^{Gal}$ neurons resulted in the severe impairment of parental behaviors in both sexes. Conversely, optogenetic stimulation of these neurons in sexually naïve males effectively suppressed infanticidal behavior. Subsequent research by Kohl et al. (2018) employed rabies-virus-mediated transsynaptic tracing (Miyamichi et al., 2013) and its derivative method known as cTRIO (Schwarz et al., 2015) to dissect the input and output neural circuits associated with $MPOA^{Gal}$ neurons. The findings revealed extensive reciprocal connectivity between $MPOA^{Gal}$ neurons and various limbic structures, including those involved in transmitting pheromone signals originating from the vomeronasal organ, secreting neural hormones such as oxytocin and vasopressin, and mediating monoaminergic signals such as dopamine. Moreover, it was found that $MPOA^{Gal}$ neurons consist of several distinct projection types that target different brain regions, such as the ventral tegmental area (VTA) and the medial amygdala (MeA). These $MPOA^{Gal}$ neuron subtypes receive quantitatively varying inputs and may play a specific role in different aspects of parental behaviors, including pup-directed motor actions, the motivation for parental behaviors, and the inhibition of social intersections with adult conspecifics. Therefore, $MPOA^{Gal}$ neurons act as a hub of parental behavioral regulation in both male and female mice (Figure 1).

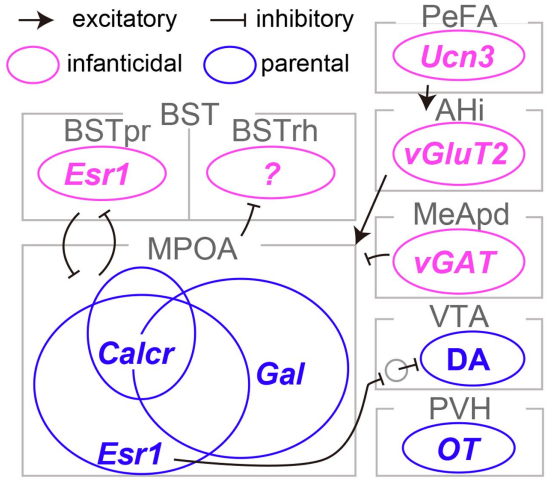

FIGURE 1
Limbic neurons responsible for infanticide and parental behaviors in mice. The distinct neural subtypes accountable for infanticide are depicted in magenta, whereas those fostering parental behaviors are illustrated in blue. Refer to the text for abbreviations and detailed information on connectivity.

Earlier research suggested the maternal behavior-facilitating effects of an estrogen surge during pregnancy on the function of the MPOA in female rats (Siegel and Rosenblatt, 1975). Inspired by this line of work, two independent studies demonstrated the pivotal role of MPOA neurons expressing estrogen receptor type 1 ($MPOA^{Esr1}$ neurons) in the initiation and maintenance of maternal caregiving behaviors in mice (Fang et al., 2018; Wei et al., 2018). Specifically, $MPOA^{Esr1}$ neurons were primarily GABAergic, exhibited heightened activity during the approach to pups and the initiation of pup retrieval, and induced pup retrieval when activated optogenetically (Fang et al., 2018). $MPOA^{Esr1}$ neurons predominantly projected to non-dopaminergic (likely GABAergic) neurons within the VTA and enhanced maternal behaviors, presumably through the disinhibition of dopaminergic VTA neurons (VAT^{DA} neurons; Fang et al., 2018). Consistent with this perspective, VTA^{DA} neurons have been shown to display transient activity during pup retrieval and to be capable of encoding signals related to social rewards, thereby facilitating the efficient learning of pup retrieval behaviors in female mice (Xie et al., 2023). The acute silencing of VTA^{DA} neurons during pup retrieval results in a significant delay in the execution of these behaviors, reflecting the cumulative history of VTA^{DA} neuron activity. These lines of evidence lend support to the role of the $MPOA^{Esr1} \rightarrow VTA^{DA}$ circuity in maternal caregiving behaviors in mice (Figure 1); however, the function of this pathway in male mice remains elusive.

The MPOA plays a critical role in both parenting and sexual behaviors, as well as in the regulation of essential physiological functions such as body temperature control, thirst, and sleep (Zimmerman et al., 2017; Tan and Knight, 2018; Tsuneoka and Funato, 2021). The neural circuits governing these functions are likely to be composed of neurons with distinct genetic identities. Moffitt et al. (2018) utilized single-cell RNA sequencing and multiplexed error-robust fluorescence *in situ* hybridization to reveal that $MPOA^{Gal}$ and $MPOA^{Esr1}$ neurons overlapped and that each heterogeneous population encompassed a dozen transcriptome types. By combining cell-type classification and the detection of the *c-Fos* transcript, they suggested that a *calcitonin receptor* (*Calcr*) expressing MPOA neurons ($MPOA^{Calcr}$ neurons) were predominantly active during parental behaviors in both males and females. Approximately 70% of $MPOA^{Calcr}$ neurons overlap with $MPOA^{Esr1}$ neurons, and the silencing of $MPOA^{Calcr}$ neurons impairs maternal caregiving behaviors, whereas the chemogenetic activation of these neurons can suppress infanticide in sexually naïve male mice (Yoshihara et al., 2021). Additionally, when the *Calcr* gene was selectively suppressed in the MPOA, it resulted in partial impairment of maternal behaviors in risky environments. Collectively, $MPOA^{Calcr}$ neurons represent the most clearly defined population for parental behaviors to date (Figure 1). It is worth noting that the potential relationship between the projection-based classification of $MPOA^{Gal}$ neurons (Kohl et al., 2018) and their transcriptome types (Moffitt et al., 2018) remains uncertain and thus a subject for future investigation.

Olfactory signals play a critical role in pup-directed behaviors in rodents. The surgical or genetic elimination of the function of the vomeronasal organ, which is responsible for the detection of pheromonal signals in mice, has been shown to reduce infanticide in sexually naïve males, suggesting that the vomeronasal signals facilitate infanticide (Tachikawa et al., 2013; Isogai et al., 2018). Among the brain regions transmitting pheromonal signals, Tsuneoka et al. (2015) ascertained that *c-Fos* expression in the rhomboid nucleus of the bed

nuclei of the stria terminalis (BSTrh) precisely reflected infanticidal motivation. Lesions in the BSTrh have been reported to inhibit infanticide in sexually naïve male mice. Subsequently, Chen et al. (2019) documented that *vGAT*-expressing GABAergic neurons in the medial amygdala posteroventral subdivision (MeApd^{vGAT} neurons) could elicit infanticidal behaviors in male mice, but not in females. Autry et al. (2021) reported that *urocortin-3* (*Ucn3*)-expressing neurons in the hypothalamic perifornical area (PeFA^{Ucn3} neurons) became active during attacks on infants in both males and females. These neurons received input from brain regions associated with pheromonal signals and stress. Functional manipulations of PeFA^{Ucn3} neurons have established their role in facilitating infanticide in both sexes, with notably vigorous attacks occurring when axonal projections of PeFA^{Ucn3} neurons to the amygdalohippocampal area (AHi) are optogenetically stimulated. Indeed, AHi contains excitatory projection neurons to the MPOA (AHi$^{\rightarrow MPOA}$ neurons) that exhibit activity in male mice during social interactions with pups and promote infanticide when chemogenetically activated (Sato et al., 2020). Furthermore, utilizing an outbred strain known as Rockland-Swiss mice, whose virgin females manifest a heightened propensity for infanticide, Mei et al. (2023) specifically examined the neural underpinnings of female infanticide. Their study disclosed that *Esr1*-expressing neurons in the principal nucleus of the BST (BSTpr^{Esr1} neurons) were imperative for the manifestation of, and could induce, infanticide in female mice. Taken together, these lines of evidence indicate the existence of a unique set of limbic neuron types that specifically regulate infanticidal behaviors in mice (Figure 1; Inada and Miyamichi, 2023).

Hormonal regulations of parental behaviors in mice

How are infanticidal and parental behaviors appropriately regulated during the parental life-stage transition? Sex hormones exert a profound influence on reproductive and parental behaviors. Specifically, estrogen, a sex hormone responsible for the development and regulation of various reproductive functions, interacts with estrogen receptors, thereby modulating the expression of numerous genes (Knoedler et al., 2022). Maternal caregiving behaviors can be triggered by a substantial increase in estrogen and progesterone levels during pregnancy. As mentioned above, MPOA^{Esr1} neurons [which also express progesterone receptor (Pgr)] facilitate maternal behaviors. Do the steroid hormone receptors indeed function in these neurons? This question was addressed by Ammari et al. (2023) through their investigation of MPOA-specific conditional knockout (cKO) of *Esr1* or *Pgr*. Their study established essential roles of *Esr1* and *Pgr* in the pregnancy-induced enhancement of pup retrieval in expectant mother mice. Notably, substantial overlap was observed between MPOA^{Gal} and MPOA^{Esr1} neurons (Moffitt et al., 2018), and selective cKO of either *Esr1* or *Pgr* within the MPOA^{Gal} neurons reproduced the effects observed in pan-MPOA cKO mice. Thus, the proper expression of maternal behaviors in female mice requires the signaling of both estrogen and progesterone receptors within the MPOA$^{Esr1\wedge Gal}$ neurons. Pregnancy induces substantial changes in the electrophysiological properties in an *Esr1*- and *Pgr*-dependent manner. During the late pregnancy period, MPOA^{Gal} neurons exhibit a long-lasting reduction in baseline activity and an increased level of excitability. At the individual cellular level, the representation of pup retrieval within MPOA^{Gal} neurons becomes sparser and more distinguishable from other non-pup-related signals, although whether this effect is mediated by *Esr1* or *Pgr* remains elusive. Taken together, these findings by Ammari et al. (2023) illustrated that sex steroid hormones reorganize the parental behavioral center, specifically the MPOA$^{Esr1\wedge Gal}$ neurons, to enhance the efficient execution of parental behaviors during the maternal life-stage transition. Whether a similar mechanism plays a role during the paternal transition in male mice remains an open question.

As previously mentioned, an additional population expressing *Esr1*, namely the BSTpr^{Esr1} neurons, exert opposing control to trigger infanticide in female mice, which should be suppressed during the maternal transition. Notably, MPOA^{Esr1} and BSTpr^{Esr1} neurons communicate with each other via mutually inhibitory monosynaptic connections (Mei et al., 2023), as demonstrated through channelrhodopsin 2-assisted circuit mapping (CRACM; Petreanu et al., 2007). Terminal activation of BSTpr^{Esr1} neurons induces inhibitory postsynaptic currents in the majority of MPOA^{Esr1} neurons, and vice versa. These antagonistic connections hold functional significance, as optogenetic suppression of MPOA^{Esr1} → BSTpr^{Esr1} neuron connections leads to infanticide, whereas optogenetic activation of the same pathway inhibits infanticide. Similarly, virgin female mice display inhibited or activated infanticidal behaviors when BSTpr^{Esr1} → MPOA^{Esr1} neuron connections are optogenetically suppressed or activated, respectively. At the population level, BSTpr^{Esr1} neurons become active during hostile investigation and infanticidal episodes, whereas MPOA^{Esr1} neurons become active during pup retrieval. Upon the maternal life-stage transition, the excitabilities of MPOA^{Esr1} and BSTpr^{Esr1} neurons undergo substantial changes. In mothers, MPOA^{Esr1} neurons become more excitable, whereas BSTpr^{Esr1} neurons become significantly less excitable. The report by Mei et al. (2023) collectively illustrated the life-stage-associated alteration of excitability in antagonistic circuits that mediate infanticide and maternal care in female mice. The exact function of estrogen receptors in BSTpr^{Esr1} neurons remains uncertain and is thus a subject for future study.

In addition to steroid hormones, peptidergic hormones may contribute to the parental behavioral transition. Particularly, oxytocin (OT), a nonapeptide hormone produced by OT neurons in the paraventricular (PVH^{OT} neurons) and supraoptic (SO) hypothalamic nuclei, plays a pivotal role in regulating sexual, maternal, and social behaviors, in addition to its classical functions in uterine contractions during parturition and milk ejection during lactation (Nishimori et al., 1996; Macbeth et al., 2010; Froemke and Young, 2021; Yukinaga et al., 2022). Intracerebroventricular (Pedersen et al., 1982) and intraperitoneal (Marlin et al., 2015) administrations of OT have been shown to trigger caregiving behaviors in virgin rodent females, in addition to the optogenetic activation of PVH^{OT} neurons (Marlin et al., 2015; Scott et al., 2015). By contrast, loss-of-function of OT or its receptor, OTR, shows relatively minor phenotypes in maternal caregiving behaviors (Nishimori et al., 1996; Young et al., 1996; Macbeth et al., 2010), except in situations of food scarcity and high stress (Ragnauth et al., 2005). Brain region-specific cKO of the *OT* gene within the PVH and SO further corroborates its dispensability in maternal caregiving behaviors (Hagihara et al., 2023). Collectively, these studies suggest that OT signaling can facilitate the onset, but to a lesser extent, the maintenance of maternal care (Yoshihara et al., 2018).

The modulation of the sensory system stands out as a critical mechanism through which OT exerts its influence on maternal behaviors. For instance, the auditory system plays an important role in mediating the distinct vocalizations emitted by offspring to facilitate maternal behaviors. Cohen et al. (2011) reported the experience-dependent and pup-odor-induced alterations of neural responses within the mother's primary auditory cortex, resulting in an elevated sensitivity to the pup's ultrasonic vocalizations. The pairing of pup vocalization with OT administration produces enduring changes in neural responses, augmenting excitatory responses by adjusting the local excitatory/inhibitory (E/I) balance (Marlin et al., 2015; Schiavo et al., 2020). Virgin females can employ their visual system to acquire pup retrieval behaviors from experienced mother mice, during which time, the activation of PVH^{OT} neurons and concurrent modulation of auditory sensitivity occurs (Carcea et al., 2021). Furthermore, pup vocalization can elicit an enduring activation of PVH^{OT} neurons through a specific thalamic neural circuit (Valtcheva et al., 2023). These studies have collectively established connections between cellular and synaptic properties, the physiological impacts of OT, and the onset of pup retrieval. In addition, while the precise implications for maternal behaviors remain unclear, it is well established that OT can modulate various other sensory systems, including the olfactory cortex (Oettl et al., 2016).

In contrast to the relatively moderate modulatory roles of OT in female mice, Inada et al. (2022a) demonstrated that OT released from PVH^{OT} neurons is indispensable for paternal caregiving behaviors in male mice. They examined the PVH-specific cKO of the *OT* gene or the genetic removal of PVH^{OT} neurons, which resulted in a significant decrease in the number of pups retrieved and the duration of paternal care exhibited by male mice. The chemogenetic activation of PVH^{OT} neurons effectively suppresses infanticidal behaviors and, in turn, triggers caregiving behaviors in sexually naïve male mice, and this effect is dependent on *OT*. This activation of PVH^{OT} neurons heightens the activity of $MPOA^{Calcr}$ neurons, which promote caregiving (Figure 1) while concurrently suppressing the activity of $PeFA^{Ucn3}$ neurons, which promote infanticide. Another potential downstream target of PVH^{OT} neurons is the infanticide-promoting $AHi^{\rightarrow MPOA}$ neurons, as OT can suppress these neurons by facilitating local inhibitory neurons expressing OTRs (Sato et al., 2020). Therefore, PVH^{OT} neurons play a pivotal role in coordinating various limbic neural populations to favor the execution of parental behaviors in male mice. Notably, although the activity dynamics of PVH^{OT} neurons during paternal behaviors remain largely unknown in mice, biparental male mandarin voles display time-locked activities of PVH^{OT} neurons to each episode of paternal caregiving behaviors, such as pup retrieval and sniffing of pups (He et al., 2021).

As a potential mechanism underlying the activation of PVH^{OT} neurons in father mice, Inada et al. (2022a) demonstrated that individual PVH^{OT} neurons in father mice receive a quantitatively greater amount of excitatory synaptic input from specific hypothalamic nuclei, including the lateral hypothalamus (LHA^{vGluT2} neurons). This insight was gained utilizing rabies virus-based transsynaptic tracing (Miyamichi et al., 2013) and CRACM (Petreanu et al., 2007). The heightened $LHA^{vGluT2} \rightarrow PVH^{OT}$ neuron connectivity appears to have functional significance, as chemogenetic activation of LHA^{vGluT2} neurons suppresses infanticide in a downstream PVH^{OT} neuron-dependent manner. Taken together, these findings suggest that the promotion of paternal caregiving behaviors hinges on structural plasticity within the hypothalamus of fathers, resulting in the increased excitability of PVH^{OT} neurons (Figure 2).

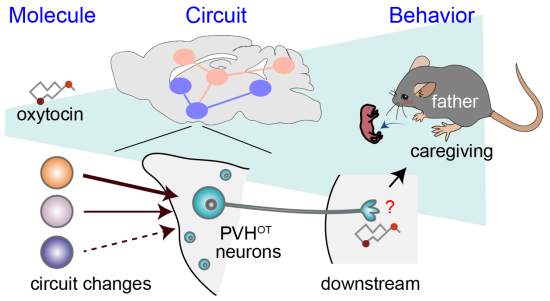

FIGURE 2
A circuit mechanism to facilitate paternal behaviors by PVH^{OT} neurons. Illustration depicting alterations in neural circuitry within the brains of paternal mice and the oxytocin-mediated facilitation of caregiving behavior (Inada et al., 2022a). The downstream neural processes associated with OT in promoting paternal behaviors remain unidentified, as denoted by the red question mark.

Perspective

As outlined above, recent research in mice employing a viral-genetic approach has elucidated that estrogen and OT exert their effects on specific limbic neural types, thereby modulating circuit functions to suppress infanticide and promote parental behaviors. Notably, the extent to which females and males depend on estrogen and OT to trigger parental behaviors appears to differ. In female mice, both estrogen and OT can facilitate maternal behaviors, with estrogen playing a more pivotal role. This can account for the relatively modest reliance of female mice on OT for maternal caregiving behaviors *per se*, despite the critical role of OT for milk ejection (Hagihara et al., 2023). Conversely, the involvement of estrogen-dependent mechanisms in male mice remains uncertain, though it is unlikely to be indispensable (Wynne-Edwards and Timonin, 2007). Instead, they rely more significantly on OT to express paternal caregiving behaviors (Inada et al., 2022a).

While prior research has proposed that paternal caregiving behaviors may be facilitated by mating, cohabitation with a female, and/or repeated exposure to pups (vom Saal, 1985; Elwood, 1994; Cai et al., 2021), the specific triggers for the sufficient activation of OT neurons and their input structural plasticity remain open questions. Moreover, although OT-induced paternal behaviors are associated with the activation of $MPOA^{Calcr}$ neurons, the mechanisms through which OT exerts its facilitatory effects on paternal behaviors, including brain regions and receptor mechanisms, require more elucidation (Figure 2). Related to this issue, it is worth noting that the OTR-based modulation of inhibitory neurons has been reported in both the primary auditory cortex (Marlin et al., 2015) and AHi (Sato et al., 2020). Furthermore, Esr1 appears to augment inhibitory tones within the MPOA, thereby differentiating the representation of pups in late pregnant females (Ammari et al., 2023). Modulation of the excitatory/inhibitory balance to enhance the saliency of pup-related signals may represent a common mechanism for facilitating parental behaviors by OT and Esr1.

More broadly, intricate patterns in the levels of hormone and receptor expression have been observed in classical studies involving biparental model rodents. However, the behavioral implications of

these dynamic endocrinological changes remain largely uncertain (Wynne-Edwards and Timonin, 2007). To address this limitation, two research avenues should be pursued: (i) examining the functions of hormones and receptors in a stage- and cell-type-specific manner, as illustrated by recent cKO models targeting *Esr1*, *Prolactin receptor*, *OT, and OTR* (Stagkourakis et al., 2020; Inada et al., 2022a,b; Ammari et al., 2023); and (ii) employing fluorescent biosensors to characterize the high spatiotemporal hormonal dynamics during specific behavioral episodes, as exemplified by the heightened OT secretion from PVH^{OT} neurons during mating in male mice (Qian et al., 2023). Future studies that broaden the application of these techniques hold promise for unraveling the functions of each hormone at every stage of the parental life-stage transition.

Lastly, it is important to mention that the execution of parental behaviors is not solely the province of limbic neurons; it requires the coordinated function of multiple brain regions to process infant cues, make decisions, and formulate and execute motor plans. These processes likely demand higher cognitive functions, and researchers have only recently begun to explore these avenues (Corona et al., 2023). Given the substantial evolutionary expansion of the human frontal cortex, understanding the higher-order functions associated with parental behaviors and the potential interactions between the frontal cortex and limbic circuits during such behaviors are expected to offer valuable insights into human parental behaviors.

Author contributions

The author confirms being the sole contributor of this work and has approved it for publication.

Funding

The author(s) declare financial support was received for the research, authorship, and/or publication of this article. This work was supported by JSPS KAKENHI (21H02587) and the RIKEN BDR Stage-Transition Project to KM.

Acknowledgments

The author thanks Kengo Inada and Gen-ichi Tasaka for the critical reading of the manuscript.

Conflict of interest

The author declares that the research was conducted in the absence of any commercial or financial relationships that could be construed as a potential conflict of interest.

The author(s) declared that they were an editorial board member of Frontiers, at the time of submission. This had no impact on the peer review process and the final decision.

Publisher's note

References

Ammari, R., Monaca, F., Cao, M., Nassar, E., Wai, P., Del Grosso, N. A., et al. (2023). Hormone-mediated neural remodeling orchestrates parenting onset during pregnancy. *Science* 382, 76–81. doi: 10.1126/science.adi0576

Autry, A. E., Wu, Z., Kapoor, V., Kohl, J., Bambah-Mukku, D., Rubinstein, N. D., et al. (2021). Urocortin-3 neurons in the mouse perifornical area promote infant-directed neglect and aggression. *Elife* 10:680. doi: 10.7554/eLife.64680

Cai, W., Ma, H., Xun, Y., Hou, W., Wang, L., Zhang, X., et al. (2021). Involvement of the dopamine system in paternal behavior induced by repeated pup exposure in virgin male ICR mice. *Behav. Brain Res.* 415:113519. doi: 10.1016/j.bbr.2021.113519

Carcea, I., Caraballo, N. L., Marlin, B. J., Ooyama, R., Riceberg, J. S., Mendoza Navarro, J. M., et al. (2021). Oxytocin neurons enable social transmission of maternal behaviour. *Nature* 596, 553–557. doi: 10.1038/s41586-021-03814-7

Chen, P. B., Hu, R. K., Wu, Y. E., Pan, L., Huang, S., Micevych, P. E., et al. (2019). Sexually dimorphic control of parenting behavior by the medial amygdala. *Cell* 176, 1206–1221 e1218. doi: 10.1016/j.cell.2019.01.024

Cohen, L., Rothschild, G., and Mizrahi, A. (2011). Multisensory integration of natural odors and sounds in the auditory cortex. *Neuron* 72, 357–369. doi: 10.1016/j.neuron.2011.08.019

Corona, A., Choe, J., Munoz-Castaneda, R., Osten, P., and Shea, S. D. (2023). A circuit from the locus coeruleus to the anterior cingulate cortex modulates offspring interactions in mice. *Cell Rep.* 42:112771. doi: 10.1016/j.celrep.2023.112771

Dulac, C., O'Connell, L. A., and Wu, Z. (2014). Neural control of maternal and paternal behaviors. *Science* 345, 765–770. doi: 10.1126/science.1253291

Elwood, R. W. (1994). Temporal-based kinship recognition: a switch in time saves mine. *Behav. Processes* 33, 15–24. doi: 10.1016/0376-6357(94)90057-4

Fang, Y. Y., Yamaguchi, T., Song, S. C., Tritsch, N. X., and Lin, D. (2018). A hypothalamic midbrain pathway essential for driving maternal behaviors. *Neuron* 98, 192–207 e110. doi: 10.1016/j.neuron.2018.02.019

Froemke, R. C., and Young, L. J. (2021). Oxytocin, neural plasticity, and social behavior. *Annu. Rev. Neurosci.* 44, 359–381. doi: 10.1146/annurev-neuro-102320-102847

Hagihara, M., Miyamichi, K., and Inada, K. (2023). The importance of oxytocin neurons in the supraoptic nucleus for breastfeeding in mice. *PloS One* 18:e0283152. doi: 10.1371/journal.pone.0283152

He, Z., Zhang, L., Hou, W., Zhang, X., Young, L. J., Li, L., et al. (2021). Paraventricular nucleus oxytocin subsystems promote active paternal behaviors in mandarin voles. *J. Neurosci.* 41, 6699–6713. doi: 10.1523/JNEUROSCI.2864-20.2021

Inada, K., Hagihara, M., Tsujimoto, K., Abe, T., Konno, A., Hirai, H., et al. (2022a). Plasticity of neural connections underlying oxytocin-mediated parental behaviors of male mice. *Neuron* 110, 2009–2023 e2005. doi: 10.1016/j.neuron.2022.03.033

Inada, K., and Miyamichi, K. (2023). Association between parental behaviors and structural plasticity in the brain of male rodents. *Neurosci. Res.* 196, 1–10. doi: 10.1016/j.neures.2023.06.007

Inada, K., Tsujimoto, K., Yoshida, M., Nishimori, K., and Miyamichi, K. (2022b). Oxytocin signaling in the posterior hypothalamus prevents hyperphagic obesity in mice. *Elife* 11:718. doi: 10.7554/eLife.75718

Isogai, Y., Wu, Z., Love, M. I., Ahn, M. H., Bambah-Mukku, D., Hua, V., et al. (2018). Multisensory logic of infant-directed aggression by males. *Cell* 175, 1827–1841 e1817. doi: 10.1016/j.cell.2018.11.032

Knoedler, J. R., Inoue, S., Bayless, D. W., Yang, T., Tantry, A., Davis, C. H., et al. (2022). A functional cellular framework for sex and estrous cycle-dependent gene expression and behavior. *Cell* 185, 654–671 e622. doi: 10.1016/j.cell.2021.12.031

Kohl, J., Babayan, B. M., Rubinstein, N. D., Autry, A. E., Marin-Rodriguez, B., Kapoor, V., et al. (2018). Functional circuit architecture underlying parental behaviour. *Nature* 556, 326–331. doi: 10.1038/s41586-018-0027-0

Lukas, D., and Huchard, E. (2014). Sexual conflict. The evolution of infanticide by males in mammalian societies. *Science* 346, 841–844. doi: 10.1126/science.1257226

Lukas, D., and Huchard, E. (2019). The evolution of infanticide by females in mammals. *Philos. Trans. R. Soc. Lond. B Biol. Sci.* 374:20180075. doi: 10.1098/rstb.2018.0075

Macbeth, A. H., Stepp, J. E., Lee, H. J., Young, W. S., and Caldwell, H. K. (2010). Normal maternal behavior, but increased pup mortality, in conditional oxytocin receptor knockout females. *Behav. Neurosci.* 124, 677–685. doi: 10.1037/a0020799

Marlin, B. J., Mitre, M., D'Amour, J. A., Chao, M. V., and Froemke, R. C. (2015). Oxytocin enables maternal behaviour by balancing cortical inhibition. *Nature* 520, 499–504. doi: 10.1038/nature14402

Mei, L., Yan, R., Yin, L., Sullivan, R. M., and Lin, D. (2023). Antagonistic circuits mediating infanticide and maternal care in female mice. *Nature* 618, 1006–1016. doi: 10.1038/s41586-023-06147-9

Miyamichi, K., Shlomai-Fuchs, Y., Shu, M., Weissbourd, B. C., Luo, L., and Mizrahi, A. (2013). Dissecting local circuits: parvalbumin interneurons underlie broad feedback control of olfactory bulb output. *Neuron* 80, 1232–1245. doi: 10.1016/j.neuron.2013.08.027

Moffitt, J. R., Bambah-Mukku, D., Eichhorn, S. W., Vaughn, E., Shekhar, K., Perez, J. D., et al. (2018). Molecular, spatial, and functional single-cell profiling of the hypothalamic preoptic region. *Science* 362:5324. doi: 10.1126/science.aau5324

Nishimori, K., Young, L. J., Guo, Q., Wang, Z., Insel, T. R., and Matzuk, M. M. (1996). Oxytocin is required for nursing but is not essential for parturition or reproductive behavior. *Proc. Natl. Acad. Sci. U. S. A.* 93, 11699–11704. doi: 10.1073/pnas.93.21.11699

Numan, M. (1974). Medial preoptic area and maternal behavior in the female rat. *J. Comp. Physiol. Psychol.* 87, 746–759. doi: 10.1037/h0036974

Oettl, L. L., Ravi, N., Schneider, M., Scheller, M. F., Schneider, P., Mitre, M., et al. (2016). Oxytocin enhances social recognition by modulating cortical control of early olfactory processing. *Neuron* 90, 609–621. doi: 10.1016/j.neuron.2016.03.033

Pedersen, C. A., Ascher, J. A., Monroe, Y. L., and Prange, A. J. Jr. (1982). Oxytocin induces maternal behavior in virgin female rats. *Science* 216, 648–650. doi: 10.1126/science.7071605

Petreanu, L., Huber, D., Sobczyk, A., and Svoboda, K. (2007). Channelrhodopsin-2-assisted circuit mapping of long-range callosal projections. *Nat. Neurosci.* 10, 663–668. doi: 10.1038/nn1891

Qian, T., Wang, H., Wang, P., Geng, L., Mei, L., Osakada, T., et al. (2023). A genetically encoded sensor measures temporal oxytocin release from different neuronal compartments. *Nat. Biotechnol.* 41, 944–957. doi: 10.1038/s41587-022-01561-2

Ragnauth, A. K., Devidze, N., Moy, V., Finley, K., Goodwillie, A., Kow, L. M., et al. (2005). Female oxytocin gene-knockout mice, in a semi-natural environment, display exaggerated aggressive behavior. *Genes Brain Behav.* 4, 229–239. doi: 10.1111/j.1601-183X.2005.00118.x

Sato, K., Hamasaki, Y., Fukui, K., Ito, K., Miyamichi, K., Minami, M., et al. (2020). Amygdalohippocampal area neurons that project to the preoptic area mediate infant-directed attack in male mice. *J. Neurosci.* 40, 3981–3994. doi: 10.1523/JNEUROSCI.0438-19.2020

Schiavo, J. K., Valtcheva, S., Bair-Marshall, C. J., Song, S. C., Martin, K. A., and Froemke, R. C. (2020). Innate and plastic mechanisms for maternal behaviour in auditory cortex. *Nature* 587, 426–431. doi: 10.1038/s41586-020-2807-6

Schwarz, L. A., Miyamichi, K., Gao, X. J., Beier, K. T., Weissbourd, B., DeLoach, K. E., et al. (2015). Viral-genetic tracing of the input-output organization of a central noradrenaline circuit. *Nature* 524, 88–92. doi: 10.1038/nature14600

Scott, N., Prigge, M., Yizhar, O., and Kimchi, T. (2015). A sexually dimorphic hypothalamic circuit controls maternal care and oxytocin secretion. *Nature* 525, 519–522. doi: 10.1038/nature15378

Siegel, H. I., and Rosenblatt, J. S. (1975). Hormonal basis of hysterectomy-induced maternal behavior during pregnancy in the rat. *Horm. Behav.* 6, 211–222. doi: 10.1016/0018-506X(75)90008-2

Stagkourakis, S., Smiley, K. O., Williams, P., Kakadellis, S., Ziegler, K., Bakker, J., et al. (2020). A neuro-hormonal circuit for paternal behavior controlled by a hypothalamic network oscillation. *Cell* 182, 960–975 e915. doi: 10.1016/j.cell.2020.07.007

Tachikawa, K. S., Yoshihara, Y., and Kuroda, K. O. (2013). Behavioral transition from attack to parenting in male mice: a crucial role of the vomeronasal system. *J. Neurosci.* 33, 5120–5126. doi: 10.1523/JNEUROSCI.2364-12.2013

Tan, C. L., and Knight, Z. A. (2018). Regulation of body temperature by the nervous system. *Neuron* 98, 31–48. doi: 10.1016/j.neuron.2018.02.022

Tsuneoka, Y., and Funato, H. (2021). Cellular composition of the preoptic area regulating sleep, parental, and sexual behavior. *Front. Neurosci.* 15:649159. doi: 10.3389/fnins.2021.649159

Tsuneoka, Y., Maruyama, T., Yoshida, S., Nishimori, K., Kato, T., Numan, M., et al. (2013). Functional, anatomical, and neurochemical differentiation of medial preoptic area subregions in relation to maternal behavior in the mouse. *J. Comp. Neurol.* 521, 1633–1663. doi: 10.1002/cne.23251

Tsuneoka, Y., Tokita, K., Yoshihara, C., Amano, T., Esposito, G., Huang, A. J., et al. (2015). Distinct preoptic-BST nuclei dissociate paternal and infanticidal behavior in mice. *EMBO J.* 34, 2652–2670. doi: 10.15252/embj.201591942

Valtcheva, S., Issa, H. A., Bair-Marshall, C. J., Martin, K. A., Jung, K., Zhang, Y., et al. (2023). Neural circuitry for maternal oxytocin release induced by infant cries. *Nature* 621, 788–795. doi: 10.1038/s41586-023-06540-4

vom Saal, F. S. (1985). Time-contingent change in infanticide and parental behavior induced by ejaculation in male mice. *Physiol. Behav.* 34, 7–15. doi: 10.1016/0031-9384(85)90069-1

Wei, Y. C., Wang, S. R., Jiao, Z. L., Zhang, W., Lin, J. K., Li, X. Y., et al. (2018). Medial preoptic area in mice is capable of mediating sexually dimorphic behaviors regardless of gender. *Nat. Commun.* 9:279. doi: 10.1038/s41467-017-02648-0

Wu, Z., Autry, A. E., Bergan, J. F., Watabe-Uchida, M., and Dulac, C. G. (2014). Galanin neurons in the medial preoptic area govern parental behaviour. *Nature* 509, 325–330. doi: 10.1038/nature13307

Wynne-Edwards, K. E., and Timonin, M. E. (2007). Paternal care in rodents: weakening support for hormonal regulation of the transition to behavioral fatherhood in rodent animal models of biparental care. *Horm. Behav.* 52, 114–121. doi: 10.1016/j.yhbeh.2007.03.018

Xie, Y., Huang, L., Corona, A., Pagliaro, A. H., and Shea, S. D. (2023). A dopaminergic reward prediction error signal shapes maternal behavior in mice. *Neuron* 111, 557–570 e557. doi: 10.1016/j.neuron.2022.11.019

Yoshihara, C., Numan, M., and Kuroda, K. O. (2018). Oxytocin and parental behaviors. *Curr. Top. Behav. Neurosci.* 35, 119–153. doi: 10.1007/7854_2017_11

Yoshihara, C., Tokita, K., Maruyama, T., Kaneko, M., Tsuneoka, Y., Fukumitsu, K., et al. (2021). Calcitonin receptor signaling in the medial preoptic area enables risk-taking maternal care. *Cell Rep.* 35:109204. doi: 10.1016/j.celrep.2021.109204

Young, W. S., Shepard, E., Amico, J., Hennighausen, L., Wagner, K. U., LaMarca, M. E., et al. (1996). Deficiency in mouse oxytocin prevents milk ejection, but not fertility or parturition. *J. Neuroendocrinol.* 8, 847–853. doi: 10.1046/j.1365-2826.1996.05266.x

Yukinaga, H., Hagihara, M., Tsujimoto, K., Chiang, H. L., Kato, S., Kobayashi, K., et al. (2022). Recording and manipulation of the maternal oxytocin neural activities in mice. *Curr. Biol.* 32, 3821–3829 e3826. doi: 10.1016/j.cub.2022.06.083

Zimmerman, C. A., Leib, D. E., and Knight, Z. A. (2017). Neural circuits underlying thirst and fluid homeostasis. *Nat. Rev. Neurosci.* 18, 459–469. doi: 10.1038/nrn.2017.71

frontiers | Frontiers in Neural Circuits

TYPE Mini Review
PUBLISHED 16 February 2024
DOI 10.3389/fncir.2024.1342576

OPEN ACCESS

EDITED BY
Hiro Matsunami,
Duke University, United States

REVIEWED BY
Matt Wachowiak,
The University of Utah, United States
C. Ron Yu,
Stowers Institute for Medical Research, United States

*CORRESPONDENCE
Kensaku Mori
✉ moriken@m.u-tokyo.ac.jp
Hitoshi Sakano
✉ sakano.hts@gmail.com

RECEIVED 22 November 2023
ACCEPTED 01 February 2024
PUBLISHED 16 February 2024

CITATION
Mori K and Sakano H (2024) Circuit formation and sensory perception in the mouse olfactory system.
Front. Neural Circuits 18:1342576.
doi: 10.3389/fncir.2024.1342576

Circuit formation and sensory perception in the mouse olfactory system

Kensaku Mori[1]* and Hitoshi Sakano[2]*

[1]RIKEN Center for Brain Science, Saitama, Japan, [2]Department of Brain Function, School of Medical Sciences, University of Fukui, Matsuoka, Japan

In the mouse olfactory system, odor information is converted to a topographic map of activated glomeruli in the olfactory bulb (OB). Although the arrangement of glomeruli is genetically determined, the glomerular structure is plastic and can be modified by environmental stimuli. If the pups are exposed to a particular odorant, responding glomeruli become larger recruiting the dendrites of connecting projection neurons and interneurons. This imprinting not only increases the sensitivity to the exposed odor, but also imposes the positive quality on imprinted memory. External odor information represented as an odor map in the OB is transmitted to the olfactory cortex (OC) and amygdala for decision making to elicit emotional and behavioral outputs using two distinct neural pathways, innate and learned. Innate olfactory circuits start to work right after birth, whereas learned circuits become functional later on. In this paper, the recent progress will be summarized in the study of olfactory circuit formation and odor perception in mice. We will also propose new hypotheses on the timing and gating of olfactory circuit activity in relation to the respiration cycle.

KEYWORDS

olfactory perception, neural-circuit formation, olfactory glomeruli, critical period, respiratory cycle, orthonasal / retronasal odors

Introduction

Sensory systems are generated by a combination of activity-dependent and -independent processes. The basic architecture of neural circuits is built before birth based on a genetic program without involving neuronal activity. However, spontaneous firing plays an important role in making the system functional (Yu et al., 2004; Lorenzon et al., 2015). In the muse olfactory system, intrinsic neuronal activity (Reisert, 2010) is needed to segregate glomerular structures for sensory map formation in the OB (Nakashima et al., 2019). After birth, odor-evoked activity further modifies the glomerular map to adapt to the environmental situation (Inoue et al., 2021). In the visual system, activity waves in the retina are required for the system to work (Espinosa and Stryker, 2012; Kirkby et al., 2013). Blocking of stimulation in a subset of neurons during the critical period results in permanent changes in the representation of the neurons (Hensch, 2005).

In the mouse olfactory system, there are two separate neural pathways, innate and learned, that transmit odor signals from the OB to the OC for odor perception and decision making (Kobayakawa et al., 2007). For instinctive decisions, olfactory information is directly conveyed by mitral cells (MCs) to distinct valence regions in the amygdala (Miyamichi et al., 2011; Root et al., 2014; Inokuchi et al., 2017). It has been hypothesized that for learned decisions, odor-map information is transmitted to the anterior olfactory nucleus (AON) by tufted cells (TCs) and then

to the piriform cortex for odor perception, as well as for recollection of associated memory (Wilson and Sullivan, 2011; Russo et al., 2020; Mori and Sakano, 2021; Chen et al., 2022; Poo et al., 2022). It is assumed that recalled scene-memory further activates specific valence regions in the amygdala, which were connected to the memory engram (Josselyn and Tonegawa, 2020) in the previous experience (Motanis et al., 2014; Janak and Tye, 2015; Jin et al., 2015; East et al., 2021).

During development, innate circuits start to work around birth before the learned circuits become functional (Hall and Swithers-Mulvey, 1992). Although instinctive decisions are stereotyped, they can be modified or even changed by odor experience (Sullivan et al., 2000; Logan et al., 2012). During the critical period in neonates, the sensitivity to the imprinted odor is increased and positive quality is imposed on its memory (Inoue et al., 2021). Environmental odor inputs promote the recruitment of projection-neuron dendrites and synapse formation within the glomeruli (Liu, A. et al., 2016; Inoue et al., 2018). The primary projection of pioneer-OSNs establishes olfactory-map topography, relative glomerular locations, and glomerular sizes (Zou et al., 2009). However, OSNs are constantly replaced with newly-generated follower OSNs (Ma et al., 2014). Interneurons are also regenerated and synapse with the existing glomeruli (Bovetti et al., 2009). Thus, the olfactory perception is influenced by environmental odors even after the neonatal period (Geramita and Urban, 2016; Liu and Urban, 2017).

It is notable that olfactory perception and decision making appear to be related with respiratory phases (Mori and Sakano, 2021). In response to the environmental odors, external TCs (eTCs) are activated earlier in the inhalation phase, whereas MCs are activated later in the exhalation phase (Igarashi et al., 2012; Manabe and Mori, 2013; Ackels et al., 2020). Therefore, it is possible that learned decisions and instinctive decisions may be made independent of one another during the respiratory cycle. The olfactory system also appears to process the orthonasal and retronasal odors at different phases of respiration (Shepherd, 2012; Mori and Sakano, 2022a,b). Thus, the sampling of exteroceptive and interoceptive olfactory information may be discrete and not continuous. In mammals, there are two OB structures, right and left, each containing a pair of mirror-symmetric olfactory maps, lateral and medial. We previously proposed that each lateral and medial map may process orthonasal and retronasal odor information, respectively, and transmit odor signals to separate areas in the brain possibly using distinct neural pathways (Mori and Sakano, 2022a,b).

In this mini-review, we will discuss the recent progress in the study of olfactory circuit formation and odor perception, and propose new hypotheses for the timing and gating of sensory circuit activity.

Olfactory map formation and odor recognition

One of the long-standing questions of olfaction was how the large diversity of odor information can be recognized with a limited number of *OR* genes (Mori and Sakano, 2011). There are ~100,000 volatile odorants and ~1,000 different odorant receptor (OR) species in mice (Buck and Axel, 1991). As each odor is composed of multiple odorants with different combinations and ratios, the number of odors is countless. Then, how is the vast diversity recognized in the mammalian olfactory system with a limited number of *OR* genes? The answer to this question is that odor signals are converted to a combinatorial pattern of activated glomeruli in the OB (Mori et al., 2006).

The glomerular map is generated as a result of axonal projection of OSNs to the OB. For this primary projection, there are two basic principles, "one neuron – one receptor rule" and "one glomerulus – one receptor rule" (Sakano, 2010). Each individual OSN expresses only one functional *OR*-gene allele by negative feedback regulation (Chess et al., 1994; Serizawa et al., 2000, 2003), and OSN axons expressing the same OR species converge to a particular glomerular structure (Mombaerts et al., 1996). As each glomerulus corresponds to a specific OR species, there are ~1,000 glomerular species in each of four olfactory maps in mice. Unlike antigen recognition in the immune system, ligand – receptor interactions are not strict: each receptor can recognize multiple odorant species, or vice versa. Moreover, as odor information is usually composed of multiple odorants with different ratios, odor signals detected in the olfactory epithelium (OE) are converted to a combinatorial pattern of firing glomeruli in the OB (Malnic et al., 1999). This odor-map pattern appears to allow the piriform cortex to identify and recognize the vast diversity of odor information (Wilson and Sullivan, 2011).

OSN projection is regulated by two major schemes: one is along the dorsal/ventral (D/V) axis, and the other is along the anterior/posterior (A/P) axis using separate sets of axon guidance molecules, e.g., Semaphorins (Sema), Plexins (Plxn), and Neuropilins (Nrp) (Sakano, 2020). D/V projection is mainly regulated by positional information of OSN cell-bodies in the OE (Astic et al., 1987; Cloutier et al., 2002; Takeuchi et al., 2010), whereas A/P projection is instructed by expressed OR species using cAMP as a second messenger (Imai et al., 2006). Non-neuronal intrinsic activity of ORs, whose levels are uniquely determined by OR species, is converted to cAMP and regulates the transcription levels of axon guidance molecules (Nakashima et al., 2013). The olfactory map is initially continuous and needs to be converted to a discrete map of glomeruli (Sengoku et al., 2001; Luo and Flanagan, 2007). Glomerular segregation takes place using two sets of axon-sorting molecules, adhesive (e. g., Kirrel2, Kirrel3, and BIG-2) and repulsive (e. g., Eph A and ephrin A), whose expression levels are determined by the OR specificity of OSNs (Serizawa et al., 2006; Kaneko-Gotoh et al., 2008). Although both A/P projection and glomerular segregation are instructed by the same OR specificity using cAMP as a second messenger, they are differentially regulated at separate stages of OSN development, immature and mature, using different types of G proteins, Gs and Golf, respectively (Nakashima et al., 2013).

Synapse formation within the glomeruli

As mentioned in the previous section, topography of an olfactory map is established as a result of primary projection of OSNs. This process does not require the neuronal activity of OSNs. However, the map needs to become a discrete map segregating glomerular structures (Luo and Flanagan, 2007). Within each glomerulus, the basic synaptic structure is formed between the OSN axons and projection-neuron dendrites using intrinsic neuronal activity (Yu et al., 2004; Lorenzon et al., 2015; Nakashima et al., 2019). Thus, the basic structure of a naïve glomerular map is stereotyped, although there are some differences among individuals due to the genetic polymorphism in the OR-multigene family (Keller et al., 2007).

In neonates, the olfactory map is further modified by odor-evoked OSN activity during the critical period. This plastic change of glomeruli known as olfactory imprinting is triggered by a signaling

molecule, Sema7A, expressed in OSN axons (Inoue et al., 2018, 2021). Interactions of Sema7A with its receptor PlxnC1 localized to the projection-neuron dendrites initiate a series of postsynaptic events that promote dendrite selection and maturation (Inoue et al., 2018) (Figure 1A). Odor-evoked enhancement of synapse formation enlarges the glomerular sizes, increasing the number of recruited dendrites of projection neurons and periglomerular cells (PGCs) (Liu et al., 2016; Inoue et al., 2018) (Figures 1B–D). It is notable that the number of projecting OSN axons does not change by imprinting.

Sema7A expression in OSNs is activity-dependent and totally abolished in the knock-out (KO) of cyclic-nucleotide-gated (CNG) channels (Inoue et al., 2018). Thus, the activity-dependency of olfactory imprinting is supported by Sema7A. In contrast, PlxnC1 expression does not require the neuronal activity, but dendrite localization of PlxnC1 is restricted to the first week after birth. Therefore, PlxnC1 determines the time frame of the olfactory critical period. Olfactory imprinting not only increases the sensitivity to the imprinted odor, but also imposes the positive quality on imprinted memory. In the KO studies and rescue experiments, oxytocin was found to be responsible for this quality change of olfactory memory (Inoue et al., 2021). In the oxytocin KO, the sensitivity to the imprinted odor is increased but the attractive quality is not imposed, showing the defects in the social memory test as adults. When oxytocin is administrated by intraperitoneal injection, this impairment is rescued if the mice are treated with oxytocin in neonates (Inoue et al., 2021). It has been reported that olfactory perception can be changed by environmental odors even after the neonatal critical period affecting social responses as adults (Gur et al., 2014; Muscatelli et al., 2018). However, it is yet to be studied, what kind of signaling system is involved in this postnatal adaptation.

Projection neurons and decision making

The olfactory map is not merely a projection screen to display a pattern of activated glomeruli, but is also composed of distinct functional domains for innate odor qualities (Kobayakawa et al., 2007; Liberles, 2015). A pattern of an odor map appears to be recognized as a whole to identify the input odor and to recollect the odor memory of associated scenes (Mori and Sakano, 2021). It has been reported that odor information is transmitted from the OB to the AON by eTCs, preserving the odor-map topography (Schoenfeld and Macrides, 1984; Yan et al., 2008; Grobman et al., 2018; Hirata et al., 2019), and then to the piriform cortex for olfactory perception (Russo et al., 2020).

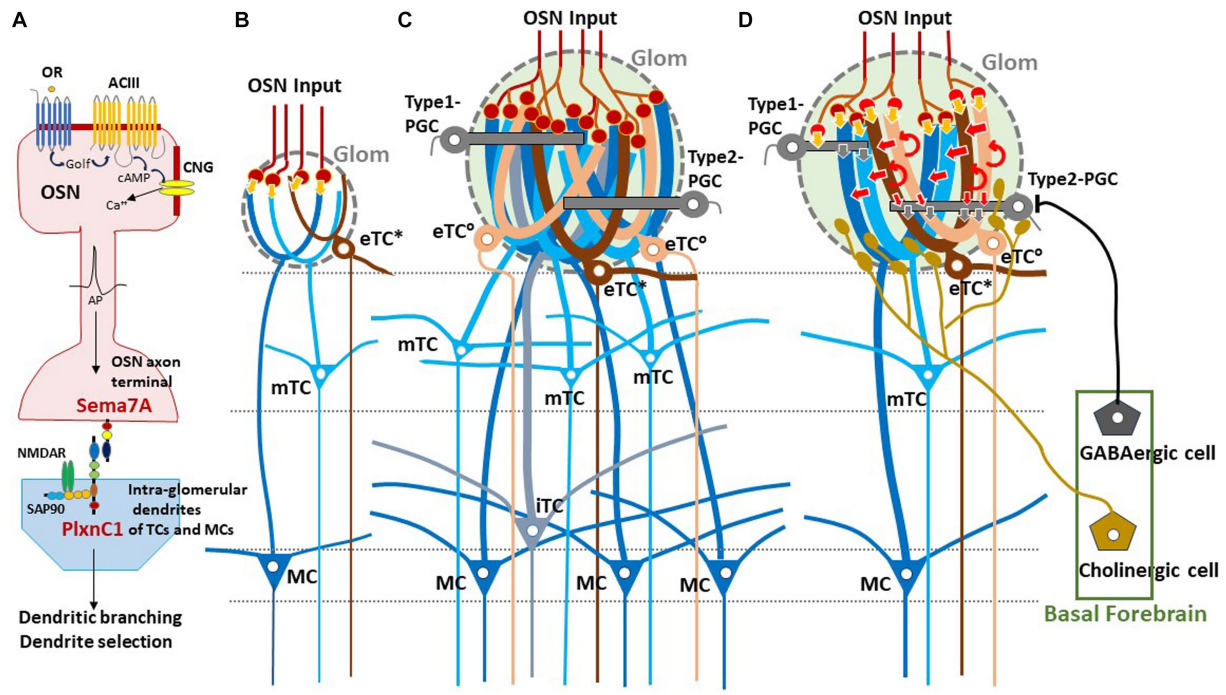

FIGURE 1
Experience-dependent development of glomerular circuitry in neonates. **(A)** Sema7A-PlxnC1 interaction essential to the induction of activity-dependent formation of glomerular circuitry during the critical period. ACIII, class III adenylyl cyclase; AP, action potential; cAMP, cyclic adenosine monophosphate; CNG, cyclic-nucleotide-gated channel; Golf, olfactory G protein; NMDAR, N-methyl-D-aspartate receptor; OR, odorant receptor; OSN, olfactory sensory neuron; PlxnC1, Plexin C1; SAP90, synapse-associated protein 90; Sema7A, Semaphorin 7A. **(B,C)** Schematic diagrams of an undeveloped glomerular structure **(B)** and a fully developed glomerulus **(C)**. Note that the fully developed glomerulus recruits apical dendrites of numerous projection neurons and inhibitory interneurons. **(D)** Synaptic organization within the fully developed glomerulus. In **(B–D)**, five types of projection neurons are illustrated; external tufted cells without lateral dendrites (eTC°, peach), external tufted cells with lateral dendrites (eTC*, brown), middle tufted cells (mTC, light blue), internal tufted cells (iTC, gray blue), and mitral cells (MC, dark blue). These cells receive direct inputs from OSN axons (orange arrows) and indirect input via eTCs (red arrows) in the glomerulus (Glom). Curved red arrows show self-excitation of eTCs via dendro-dendritic excitatory synapses. Periglomerular cells (PGCs) are classified into Type 1 and Type 2. OSN axons form direct excitatory synapses on Type 1 PGCs but do not form synapses on Type 2 PGCs. GABAergic cells of the basal forebrain form inhibitory synapses on Type 2 PGCs but do not form synapses on Type 1 PGCs. Cholinergic cells in the basal forebrain project to all types of projection neurons and to Type 2.3 PGCs (a subset of Type 2 PGCs).

We hypothesized that using an odor map as a two-dimensional QR code, the associated memory engram may be searched for, and then the odor scene may reactivate the valence circuit that was connected to the memory engram in the previous odor experience (Mori and Sakano, 2021).

In contrast to the neural pathway for learned decisions, the innate pathway is simpler in the mouse olfactory system: Odor information is directly transmitted from a particular functional domain in the OB to the valence region in the amygdala using another type of projection neuron, MCs (Miyamichi et al., 2011; Root et al., 2014; Inokuchi et al., 2017). It has been shown that innate behavioral responses can be induced even by a single glomerular species. For example, if the Olfr1019 glomerulus for the fox odor TMT (trimethyl thiazoline) is photo-activated, an immobility response (freezing) is elicited, although stress-induced aversive responses (Kondoh et al., 2016) are not induced and plasma concentrations of the stress hormone ACTH does not increase (Saito et al., 2017).

Olfactory quality is roughly sorted into two separate types, aversive and attractive during the process of OSN projection (Horio et al., 2019). Aversive odor information collected in the dorsal subdomain D_I (Kobayakawa et al., 2007) is further transmitted to the postero-medial (pm) cortical amygdala (CoA) (Miyamichi et al., 2011; Root et al., 2014). In contrast, attractive social information in the ventral OB (Lin et al., 2005) is delivered to the anterior medial-amygdala (aMeA) (Inokuchi et al., 2017). However, the spatial segregation for encoding the innate odor valence is still controversial, because the CoA is reported to carry both appetitive and aversive valence for odors (Root et al., 2014; Lurille and Datta, 2017). The dorsal subdomain D_{III} for TAAR (trace amine-associated receptor) contains mostly aversive glomeruli. However, it also contains some appetitive ones (Liberles, 2015). Activation of dorsal glomeruli may not necessarily trigger aversive responses and activation of ventral glomeruli may not always trigger attractive responses (Qiu et al., 2021).

There are two distinct MC pathways, aversive and attractive, that are segregated by the Nrp2/Sema3F guidance system. MCs, both $Nrp2^+$ and $Nrp2^-$, originate in the ventricular zone in the embryonic OB and migrate radially to the MC layer (Imamura et al., 2011; Inokuchi et al., 2017). The $Nrp2^+$ MCs further migrate tangentially to the ventral region as the OB structure expands. The repulsive ligand Sema3F secreted by the early-arriving $Nrp2^-$ OSN axons in the dorsal OB pushes down the $Nrp2^+$ MCs to the ventral region in the MC layer of the OB. This Sema3F also guides the late-arriving $Nrp2^+$ OSN axons to the ventral glomerular layer in the OB.

For synapse formation, primary dendrites of projection neurons are connected to the nearest neighboring glomeruli regardless of their OR specificity (Nishizumi et al., 2019). Therefore, it is important for OSNs to project their axons to a correct site in the glomerular layer in the OB, and for projection neurons to migrate to an appropriate position in the MC layer. Common usage of the same signaling system of Nrp2/Sema3F in both OSN projection and MC migration appears to be important for proper matching of OSN axons and MC dendrites for synapse formation. Axon guidance of $Nrp2^+$ MCs to the aMeA is also mediated by Sema3F, but by separate Sema3F expressed in the OC (Inokuchi et al., 2017).

In the Nrp2 KO for MCs, social responses, e.g., male–female attraction and pup suckling, are perturbed (Inokuchi et al., 2017). Rescue experiments indicate that a single signaling system, Nrp2/Sema3F, is sufficient for the segregation of the attractive and aversive olfactory circuits (Inokuchi et al., 2017). *In utero* electroporation of the human *Nrp2* (*hNrp2*) into the embryonic OB demonstrates that ectopic expression of the *hNrp2* gene alone can change the fate of $Nrp2^-$ MCs: OCAM-positive dorsal-MCs that are supposed to project to the pmCoA are brought to the ventral OB and further guided to the aMeA by hNrp2.

Direct and indirect pathways within the glomerulus

Glomeruli are the site of odor information transmission from OSNs to several types of projection neurons in the OB (Figure 1). The projection neurons are functionally and morphologically classified into external tufted cells (eTCs), middle tufted cells (mTCs), internal tufted cells (iTCs), and mitral cells (MCs) (Shepherd et al., 2004; Nagayama et al., 2014; Mori and Sakano, 2022a). Each type of projection neuron has a distinct pattern of lateral dendrite projection in the external plexiform layer (EPL) and axonal projection to the OC (Igarashi et al., 2012). External tufted cells are further classified into two subpopulations; one subpopulation (eTC°) lacks lateral dendrites and the other subpopulation (eTC*) has lateral dendrites in the most superficial part of the EPL (Hayer et al., 2004; Antal et al., 2006).

In the glomeruli of adult rodents, the external odor information carried by OSNs is transferred to mTCs and MCs via two types of pathways: direct mono-synaptic pathway from OSN axons, and indirect multi-synaptic pathway first from OSN axons to eTCs and then from eTCs to mTCs and MCs (Figure 1) (Najac et al., 2011; Gire et al., 2012). In the first step of the indirect pathway, the synaptic input from OSNs induces synchronized burst firings of several eTCs belonging to the same glomerulus during the inhalation phase. The synchronized burst discharges of these eTCs then activate mTCs and MCs of the same glomerulus via dendrodendritic excitatory synapses within the glomerulus.

One important question of glomerular circuit development is whether early-life olfactory experiences play a role in the formation of the direct and indirect pathways. Early olfactory experiences enlarge the sizes of activated glomeruli, although the number of projecting OSNs stays the same (Inoue et al., 2018, 2021). Because the adult OB contains glomeruli with a variety of sizes (Mori, 2014), we propose a hypothesis that the size of a glomerulus expands in proportion to the amount of early-life olfactory inputs to the glomerulus during the neonatal critical period, i.e., the first week after birth. Enlarged glomeruli may have experienced more early-life olfactory inputs and recruited numerous apical dendritic branches of eTCs, mTCs, and MCs.

We hypothesize that these large glomeruli recruit many eTCs and thus form the robust indirect OSNs→eTCs→mTCs/MCs pathway in addition to the direct pathway (Figures 1C,D). It should be noted that pairing an odor with aversive stimulus can also lead to enlargement of glomeruli in adults (Jones et al., 2008) and that olfactory extinction training reverses the increase in glomerular size (Morrison et al., 2015).

We also speculate that micro- or small-glomeruli (Lipscomb et al., 2002) are ones that experienced no or little early-life olfactory inputs and failed to recruit an adequate number of eTC, mTC, and MC dendritic branches, resulting in the lack of the functional indirect pathway (Figure 1B). These undeveloped glomeruli may contain only the direct pathway so that strong OSN inputs are required for inducing burst-firings of mTCs and MCs. The direct excitatory synapses from

OSNs to these projection neurons can emerge before birth prior to the postnatal olfactory experiences.

OB slice experiments show that in the enlarged glomeruli, eTCs act as essential drivers of glomerular output, mediating feedforward transmission of the OSN input to mTCs and MCs (De Saint Jan et al., 2009, 2022). It has been hypothesized that MCs are not typically activated by the direct OSN input and instead require the multi-synaptic indirect pathway via eTCs (Gire et al., 2012). The eTCs have the lowest odor concentration threshold for inducing firing response (Igarashi et al., 2012), generate self-regenerative long-lasting depolarization that function as a bimodal on/off switch (Gire and Schoppa, 2009), and interact with each other through their dendrodendritic excitatory synapses. Therefore, once some eTCs are activated by the OSN input, many eTCs of a same glomerulus may be entrained to generate synchronized burst firings for a fixed duration, suggesting that the indirect pathways act as a low threshold booster of the OSN signal.

Respiration phase-coherent activity of OB neurons

Recordings of local field potentials and spike activities of OB neurons in awake rats and mice indicate that, in response to odor inhalation, projection neurons in the lateral map show burst firings during specific time windows in the respiration cycle and transmit external odor information sequentially to the OC (Briffaud et al., 2012; Igarashi et al., 2012; Manabe and Mori, 2013; Mori et al., 2013; Nagayama et al., 2014; Short et al., 2016; Díaz-Quesada et al., 2018; Ackels et al., 2020; Eiting and Wachowiak, 2020; Mori and Sakano, 2021). What is the neural circuit mechanism that allows different types of projection neurons to respond during different time windows of the respiration cycle?

How does the indirect pathway via eTCs contribute to the generation of sequential activation?

As illustrated in Figure 2B, during the awake resting state, eTCs of activated glomeruli show synchronized burst firings during the period from the onset of odor inhalation to the initial part of exhalation (eTC°: peach bar, and eTC*: brown bar), transmitting odor information to the pars externa of the anterior olfactory nucleus (AONe) and the most anterolateral isolation of the CAP compartments (aiCAP) of the olfactory tubercle (Hirata et al., 2019). eTC circuits generate earliest-onset highest-frequency burst firings during the odor inhalation phase. mTCs of the activated glomeruli show synchronized high-frequency burst firings during the period from the middle of inhalation to the early 1/3 of exhalation (light blue bar), transmitting the odor information to olfactory peduncle areas. Because eTCs and mTCs of the lateral map send axons to specific areas of the AON, they appear to be the origin of the multi-synaptic learned decision pathway, transmitting external odor information to higher cognitive centers via AON and APC, mainly during the inhalation phase (Mori and Sakano, 2021). iTCs of activated glomeruli generate synchronized burst firings during the period from the end of inhalation to the early 2/3 of exhalation (gray blue bar), transmitting odor information to wide areas of the OC. MCs show synchronized burst firings during the period from the start of exhalation to the early 2/3 of exhalation (dark blue bar), transmitting odor information to widespread areas of the OC. A subset of these MCs continues burst firings up to the onset of the next inhalation (dashed dark blue bar). Thus, iTC and MC circuits show later-onset low-frequency burst firings that last into the early 2/3 of the exhalation phase. A subset of MCs forms a direct mono-synaptic pathway, sending innate behavioral decision signals to the cortical and medial amygdaloid nuclei (Mori and Sakano, 2021).

Thus, we propose a hypothetical model that in response to odor inhalation, eTCs, mTCs, iTCs and MCs respond sequentially with synchronized burst firings, each transmitting distinct information at a specific time window within the respiratory cycle. Each type of projection neuron sends lateral dendrites to a specific sublayer of the EPL and form dendrodendritic excitatory synapses on granule cells (inhibitory interneurons) (Figure 2A, yellow arrows). eTC*s and mTCs project their lateral dendrites to the superficial sublayer of the EPL and form dendrodendritic excitatory synapses on a subset of granule cells [GC(s)] that send apical dendrites to the superficial sublayer.

MCs project lateral dendrites to the deep sublayer of the EPL and form dendrodendritic excitatory synapses on a different subset of granule cells [GC(d)] that project apical dendrites to the deep sublayer (Mori, 1987). These connectivity patterns suggest that each subset of granule cells receive dendrodendritic synaptic inputs from selective types of projection neurons at a specific time window in the respiratory cycle.

In addition to the respiration phase-coherent burst firings of projection neurons, top-down inputs from the OC to granule cells appear to occur at a specific time window in the respiration cycle (Figures 2A,B). Analysis of local field potentials in the OB of awake rats indicates that top-down information flow from the OC to the granule cells occurs predominantly during the time window from the early 1/3 to the end of the exhalation phase. Thus, respiration-phases coordinate the timing of odor information processing by different local circuits in the OB, the timing of odor signal transmission to the OC by different types of projection neurons, and the timing of top-down signal transmission from the OC to the OB.

Modulation of glomerular activity by periglomerular cells and basal forebrain

Sensory experience-dependent formation of neural circuits requires balanced excitation-inhibition (Yazaki-Sugiyama et al., 2009). PGCs are local inhibitory interneurons that project dendritic branches to the glomerulus and interact with the excitatory projection neurons within the glomerulus. Early olfactory experiences also recruit PGC dendrites to activated glomeruli (Inoue et al., 2021). PGCs are classified into two subtypes (Kosaka and Kosaka, 2005). Type 1 PGCs receive direct excitatory synaptic inputs from OSNs but not from GABAergic inhibitory cells of the basal forebrain (BF, magnocellular preoptic area), whereas Type 2 PGCs do not make OSN synapses but receive axonal input from the BF GABAergic cells (Figure 1D) (Sanz Diez et al., 2019; De Saint Jan, 2022).

In addition to the BF GABAergic cells, cholinergic cells in the horizontal limb of the diagonal band of the BF densely innervate the glomerular circuits (Zaborszky et al., 1986; Bendahmane et al., 2016). While the BF GABAergic inhibitory axons target only Type 2 PGCs, the BF cholinergic axons target apical dendrites of all types of projection neurons including eTCs and Type 2.3 PGCs (a subset of Type 2 PGCs) (Spindle et al., 2018; De Saint Jan, 2022) (Figure 1D).

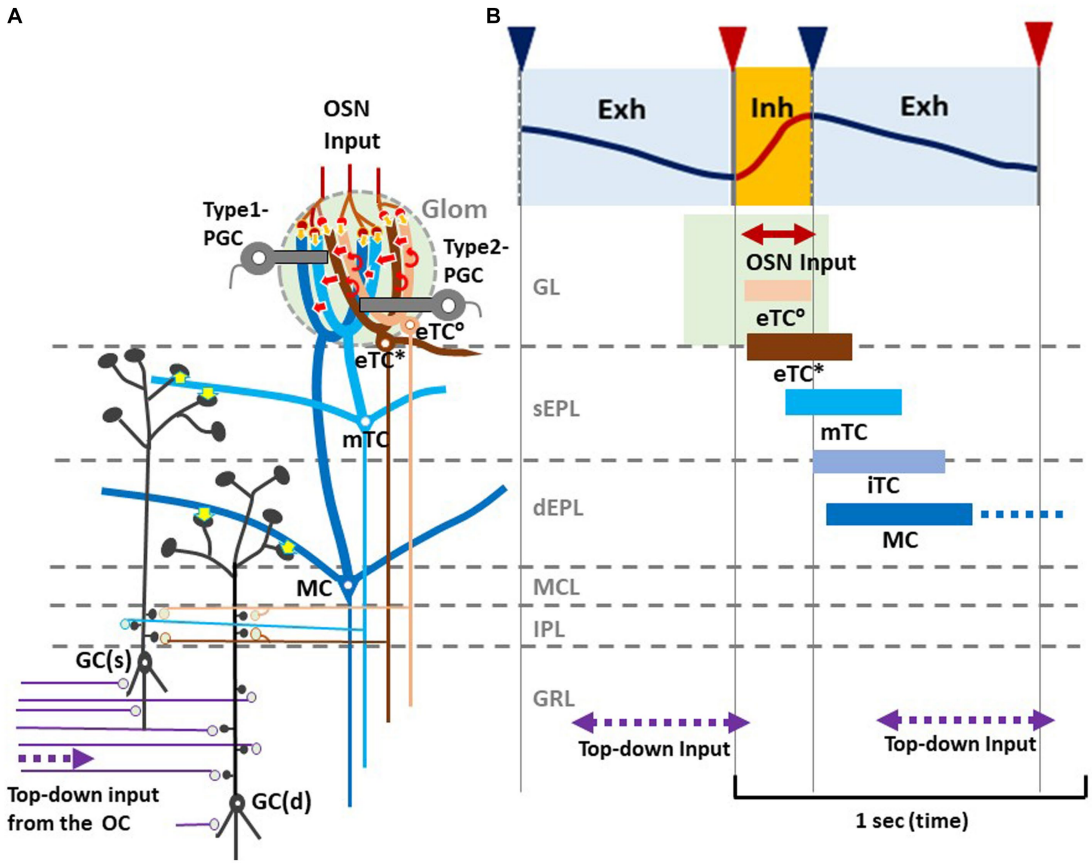

FIGURE 2
Respiration-phase-coherent neural activity in the olfactory bulb **(A)** Schematic of basic synaptic organization within the glomerulus (Glom), external plexiform layer (EPL), internal plexiform layer (IPL), and granule cell layer (GRL) of the OB. For simplicity, only four types of projection neurons (eTC°, eTC*, mTC, and MC) and two types of inhibitory interneurons, PGCs and granule cells (GCs), are shown. eTC*s and mTCs project lateral dendrites to the superficial part of the external plexiform layer (sEPL) and form dendro-dendritic excitatory synapses (yellow arrows in sEPL) on spines of GC(s) that project dendrites to the sEPL. MCs project lateral dendrites to the deep part the external plexiform layer (dEPL) and form dendro-dendritic excitatory synapses (yellow arrows in dEPL) on spines of GC(d) that send dendrites to the deep part. **(B)** Respiration-phase coherent neural activity during quiet wakefulness in the rat OB. Upper most trace shows the respiration monitored by a thermistor placed in the nasal cavity. Upward swing indicates inhalation (magenta line and orange shaded) and downward swing exhalation (blue line and blue shaded). Magenta triangles indicate the onset of inhalation, and blue triangles show the onset of exhalation. In response to the inhalation of room air, projection neurons respond sequentially with burst firings in the respiration cycle. Magenta double-arrow line indicates the time window of OSN input. Peach bar shows the time window of burst firings of eTC°s. Brown bar indicates the time window of burst firing of eTC*s that project lateral dendrites to the most superficial part of the external plexiform layer (EPL). Light blue bar shows the time window of firings of mTCs that send lateral dendrites to the superficial sublayer of the EPL (sEPL). Gray blue bar indicates the time window of firing of iTCs that send lateral dendrites to the middle part of the EPL. Dark blue bar shows the time window of firings of MCs that send lateral dendrites to the deep sublayer of the EPL (dEPL). Purple double-arrow dashed lines indicate the time window of top-down input from the olfactory cortex (OC) to the granule cell layer (GRL) of the OB. Green-shaded area indicates the time window of possible depolarization of primary dendrites of projection neurons in the glomerular layer (GL).

BF cholinergic cells are tonically active during wakefulness but silent during slow-wave sleep (Xu et al., 2015). We assume that, during wakefulness, arousal signals of BF cholinergic cells may induce tonic depolarization in the dendritic tufts of projection neurons especially those of eTCs (D'Souza et al., 2013), facilitating the transmission of OSN inputs via the indirect pathway to mTCs and MCs. In contrast, during slow-wave sleep the lack of cholinergic input to eTCs may hyperpolarize eTCs and thus prevent OSN inputs to be transmitted via the indirect pathway to the projection neurons. In agreement with this idea, in freely behaving rats, local field potentials that reflect burst firings of projection neurons occur consistently in response to each inhalation of room air during wakefulness, whereas these local field potentials diminish or disappear during slow-wave sleep (Manabe and Mori, 2013).

During wakefulness, BF cholinergic input activates Type 2.3 PGCs via muscarinic acetylcholine receptors, such that Type 2.3 PGCs fire tonically (De Saint Jan, 2022). The tonic firing of Type 2.3 PGCs causes tonic inhibition of eTCs in the indirect pathway. Because GABAergic cells in the medial septum and vertical limb of the diagonal band in the BF show burst firings that are coherent to specific time frames of the respiration cycle, thus sending respiration phase-specific attention signals to the hippocampal circuits during exploratory behavior (Tsanov et al., 2014), we propose a hypothesis that individual GABAergic cells in the BF generate burst firings and send inhibitory output to Type 2.3 PGCs during a cell-specific time frame in the respiration cycle.

We hypothesize that BF GABAergic cells that project to the lateral map glomeruli generate burst discharges selectively during intended inhalation phase, and thus inhibit Type 2.3 PGCs and disinhibit eTCs.

By the respiration phase-specific gating of the indirect pathway, the lateral map glomeruli are ready to boost orthonasal/exteroceptive odor inputs during the inhalation phase, whereas they shut out the OSN input during the exhalation phase. We also hypothesize that BF GABAergic cells that project to the medial map glomeruli generate burst discharges selectively during intended exhalation phase, inhibiting Type 2.3 PGCs and disinhibiting eTCs. By the gating of the indirect pathway, the medial map glomeruli are ready to enhance retronasal/interoceptive odor inputs during the exhalation phase, whereas they shut out the OSN input during the inhalation phase.

Discussion

During development, an olfactory map in the OB is formed based on a genetic program without involving neuronal activity. Agonist-independent receptor activity of GPCRs is involved in OR-instructed OSN projection using cAMP as a second messenger (Imai et al., 2006; Nakashima et al., 2013). An olfactory map is initially continuous, but becomes discrete, segregating glomerular structures in an activity-dependent manner (Serizawa et al., 2006; Luo and Flanagan, 2007). Intrinsic neuronal activity of OSNs appears to be responsible for this OR-specific glomerular segregation (Serizawa et al., 2006; Nakashima et al., 2019). The naïve glomerular map is further modified by odor-evoked OSN activity during the neonatal critical period. When the pups are exposed to a particular odorant, responding glomeruli increase their sizes by recruiting dendrites of projection neurons, as well as of interneuron PGCs. Sema7A/ PlxnC1 signaling is responsible for this promotion of post-synaptic events within the glomeruli (Inoue et al., 2018). Glomerular enlargement increases the sensitivity to the imprinted odor and this imprinting imposes the attractive quality on odor memory, even when the odor quality is innately aversive (Inoue et al., 2021). Environmental odors continue to affect odor perception even after the neonatal critical period (Sullivan et al., 2000; Liu and Urban, 2017). However, signaling systems responsible for this postnatal odor-adaptation need to be clarified by future experiments.

We assume that the OB of an individual adult-mouse has a unique combination of enlarged glomeruli, which reflects the early-life olfactory experience. Each enlarged glomerulus may form the imprinted memory-circuit of odor-evoked OSN signals. It is known that there are two symmetrical olfactory maps, lateral and medial, in each right and left OBs. We speculate that the enlarged glomeruli in the lateral map may represent neonatal experiences of orthonasal/exteroceptive odors, while those glomeruli in the medial map may exemplify early-life retronasal/interoceptive inputs.

Odor information is processed by two distinct olfactory circuits, innate and learned (Kobayakawa et al., 2007). For learned decisions, we assume that combinatorial signals of activated glomeruli formed in the OB are transmitted to the piriform cortex via the AON and utilized for identification of odor information and recollection of an associated memory-scene (Russo et al., 2020; Mori and Sakano, 2021; Poo et al., 2022). For innate decisions, stimulated MC signals from a particular functional domain in the olfactory map are directly transmitted to specific valence regions in the amygdala (Miyamichi et al., 2011; Root et al., 2014; Inokuchi et al., 2017). As TCs are activated earlier in the inhalation phase and MCs are activated later in the exhalation phase, we speculate that learned and innate decisions may separately be made during the respiratory cycle (Mori and Sakano, 2022a).

We previously proposed another hypothesis that each lateral and medial map in the OB may separately process orthonasal/exteroceptive and retronasal/interoceptive odor information, respectively (Mori and Sakano, 2022b). Here we further propose that the BF GABAergic input to the glomerular circuit is respiration-phase coherent and gates the orthonasal and retronasal odor inputs. The BF GABAergic input to the lateral-map glomeruli appears to occur during the intended inhalation phase, resulting in the inhalation-phase specific boosting of the orthonasal inputs. The BF GABAergic input to the medial map glomeruli may occur during the intended exhalation phase, resulting in the exhalation phase-specific amplification of the retronasal input. The BF GABAergic cells that target GCs (Villar et al., 2021) may also fire in a respiration-phase coherent manner.

Respiration-phase coherent neural-circuit activity occurs throughout the brain including the neocortex, hippocampus, olfactory cortex, thalamus, and cerebellum (Ito et al., 2014; Moberly et al., 2018; Tort et al., 2018; Bagur et al., 2021; Girin et al., 2021; Karalis and Sirota, 2022; Folschweiller and Sauer, 2023), as well as the respiratory central-pattern generator areas of the brainstem (Krohn et al., 2023). In the exploratory behavior of rodents, nose motion, head bobbing, and whisking are synchronized with respiration phases such that the inhalation phase corresponds to the time window of multisensory sampling of environmental information (Kurnikova et al., 2017). The subsequent exhalation phase may provide the time window for the brain to evaluate the sampled sensory information and express the behavioral and emotional outputs.

It has been suggested that the respiration phase coordinates with the timing of information transfer across wide-spread regions in the brain for multisensory cognition (Folschweiller and Sauer, 2023). The experience-dependent development of the glomerular circuitry and the behavioral state- and respiration phase-dependent modulation of circuit function in the OB will provide us with an excellent model system for understanding the mechanism of dynamic orchestration of neural circuits in the brain. We hope that our hypotheses proposed in this mini-review will be of help in clarifying the multisensory cognition and decision making in mammals.

Author contributions

Both authors contributed equally in writing this article.

Funding

The author(s) declare financial support was received for the research, authorship, and/or publication of this article. This research was supported by the grants from JSPS (17H06160, 21H05684, and 22H00433), Toshihiko Tokizane Memorial Fund, and Kanehara Medical Foundation to HS.

Conflict of interest

The authors declare that the research was conducted in the absence of any commercial or financial relationships that could be construed as a potential conflict of interest.

Publisher's note

References

Ackels, T., Jordan, R., Schaefer, A. T., and Fukunaga, I. (2020). Respiration-locking of olfactory receptor and projection neurons in the mouse olfactory bulb and its modulation by brain state. *Front. Cell. Neurosci.* 14:220. doi: 10.3389/fncel.2020.00220

Antal, M., Eyre, M., Finklea, B., and Nusser, Z. (2006). External tufted cells in the main olfactory bulb form two distinct subpopulations. *Eur. J. Neurosci.* 24, 1124–1136. doi: 10.1111/j.1460-9568.2006.04988.x

Astic, L., Saucier, D., and Holley, A. (1987). Topographical relationships between olfactory receptor cells and glomerular foci in the rat olfactory bulb. *Brain Res.* 424, 144–152. doi: 10.1016/0006-8993(87)91204-2

Bagur, S., Lefort, J. M., Lacroix, M. M., de Lavilléon, G., Herry, C., Chouvaef, M., et al. (2021). Breathing-driven prefrontal oscillations regulate maintenance of conditioned-fear evoked freezing independently of initiation. *Nat. Commun.* 12:2605. doi: 10.1038/s41467-021-22798-6

Bendahmane, M., Ogg, M. C., Ennis, M., and Fletcher, M. L. (2016). Increased olfactory bulb acetylcholine bi-directionally modulates glomerular odor sensitivity. *Sci. Rep.* 6:25808. doi: 10.1038/srep25808

Bovetti, S., Veyrac, A., Peretto, P., Fasolo, A., and Demarchis, S. (2009). Olfactory enrichment influences adult neurogenesis modulating GAD67 and plasticity-related molecules expression in newborn cells of the olfactory bulb. *PLoS One* 4:6359. doi: 10.1371/journal.pone.0006359

Briffaud, V., Fourcaud-Trocmé, N., Messaoudi, B., Buonviso, N., and Amat, C. (2012). The relationship between respiration-related membrane potential slow oscillations and discharge pattern in mitral/tufted cells: what are rules? *PLoS One* 7:e43964. doi: 10.1371/journal.pone.0043964

Buck, L., and Axel, R. (1991). A novel multigene family may encode odorant receptors: a molecular basis for odor recognition. *Cell* 65, 175–187. doi: 10.1016/0092-8674(91)90418-X

Chen, Y., Chen, X., Baserdem, B., Zhan, H., Li, Y., Davis, M. B., et al. (2022). High-throughput sequencing of single neuron projections reveals spatial organization in the olfactory cortex. *Cell* 185, 4117–4134.e28. doi: 10.1016/j.cell.2022.09.038

Chess, A., Simon, I., Cedar, H., and Axel, R. (1994). Allelic inactivation regulates olfactory receptor gene expression. *Cell* 78, 823–834. doi: 10.1016/S0092-8674(94)90562-2

Cloutier, J. F., Giger, R. J., Koentges, G., Dulac, C., Kolodkin, A. L., and Ginty, D. D. (2002). Neuropilin-2 mediates axonal fasciculation, zonal segregation, but not axonal convergence, of primary accessory olfactory neurons. *Neuron* 33, 877–892. doi: 10.1016/S0896-6273(02)00635-9

De Saint Jan, D. (2022). Target-specific control of olfactory bulb periglomerular cells by GABAergic and cholinergic basal forebrain inputs. *elife* 11:e71965. doi: 10.7554/eLife.71965

De Saint Jan, D., Hirnet, D., Westbrook, G. L., and Charpack, S. (2009). External tufted cells drive the output of olfactory bulb glomeruli. *J. Neurosci.* 29, 2043–2052. doi: 10.1523/JNEUROSCI.5317-08.2009

D'Souza, R. D., Parsa, P. V., and Vijayaraghavan, S. (2013). Nicotinic receptors modulate olfactory bulb external tufted cells via an excitation-dependent inhibitory mechanism. *J. Neurophysiol.* 110, 1544–1553. doi: 10.1152/jn.00865.2012

Díaz-Quesada, M., Youngstrom, I. A., Tsuno, Y., Hansen, K. R., Economo, M. N., and Wachowiak, M. (2018). Inhalation frequency controls reformatting of mitral/tufted odor representation in the olfactory bulb. *J. Neurosci.* 38, 2189–2206. doi: 10.1523/JNEUROSCI.0714-17.2018

East, B. S., Fleming, G., Vervootdt, S., Sullivan, R. M., and Wilson, D. A. (2021). Basolateral amygdala to posterior piriform cortex connectivity ensures precision in learned odor threat. *Sci. Rep.* 11:21746. doi: 10.1038/s41598-021-01320-4

Eiting, T. P., and Wachowiak, M. (2020). Differential impacts of repeated sampling on odor representations by genetically-defined mitral and tufted cell subpopulations in the mouse olfactory bulb. *J. Neurosci.* 40, 6177–6188. doi: 10.1523/JNEUROSCI.0258-20.2020

Espinosa, J. S., and Stryker, M. P. (2012). Development and plasticity of the primary visual cortex. *Neuron* 75, 230–249. doi: 10.1016/j.neuron.2012.06.009

Folschweiller, S., and Sauer, J.-F. (2023). Controlling neuronal assemblies: a fundamental function of respiration-related brain oscillations in neuronal networks. *Pflügers Archive–Eur. J. Physiol* 475, 13–21. doi: 10.1007/s00424-022-02708-5

Geramita, M., and Urban, N. N. (2016). Postnatal odor exposure increases the strength of interglomerular lateral inhibition onto olfactory bulb tufted cells. *J. Neurosci.* 36, 12321–12327. doi: 10.1523/JNEUROSCI.1991-16.2016

Gire, D. H., Franks, K. M., Zak, J. D., Tanaka, K. F., Whitesell, J. D., Mulligan, A. A., et al. (2012). Mitral cells in the olfactory bulb are mainly excited through a multistep signaling path. *J. Neurosci.* 32, 2964–2975. doi: 10.1523/JNEUROSCI.5580-11.2012

Gire, D. H., and Schoppa, N. E. (2009). Control of on/off glomerular signaling by a local GABAergic microcircuit in the olfactory bulb. *J. Neurosci.* 29, 13454–13464. doi: 10.1523/JNEUROSCI.2368-09.2009

Girin, B., Juventin, M., Garcia, S., Lefèvre, L., Amat, C., Fourcaud-Trocmé, N., et al. (2021). The deep and slow breathing characterizing rest favors brain respiratory- drive. *Sci. Rep.* 11:7044. doi: 10.1038/s41598-021-86525-3

Grobman, M., Dalal, T., Lavian, H., Shmuel, R., Belelovski, K., Xu, F., et al. (2018). A mirror-symmetric excitatory link coordinates odor maps across olfactory bulbs and enables odor perceptual unity. *Neuron* 99, 800–813.e6. doi: 10.1016/j.neuron.2018.07.012

Gur, R., Tendler, A., and Wagner, S. (2014). Long-term social recognition memory is mediated by oxytocin-dependent synaptic plasticity in the medial amygdala. *Biol. Psychiatry* 76, 377–386. doi: 10.1016/j.biopsych.2014.03.022

Hall, W. G., and Swithers-Mulvey, S. E. (1992). Development of strategies in the analysis of ingestive behavior. *Annu. N.Y Acad. Sci.* 662, 1–15.

Hayer, A., Karnup, S., Shipley, M. T., and Ennis, M. (2004). Olfactory bulb glomeruli: external tufted cells intrinsically burst at theta frequency and are entrained by patterned olfactory input. *J. Neurosci.* 24, 1190–1199. doi: 10.1523/JNEUROSCI.4714-03.2004

Hensch, T. K. (2005). Critical period plasticity in local cortical circuits. *Nat. Rev. Neurosci.* 6, 877–888. doi: 10.1038/nrn1787

Hirata, T., Shioi, G., Abe, T., Kiyonari, H., Kato, S., Kobayashi, K., et al. (2019). A novel birthdate labeling method reveals segregated parallel projections of mitral and external tufted cells in the main olfactory system. *eNeuro* 6:ENEURO.0234-19.2019. doi: 10.1523/ENEURO.0234-19.2019

Horio, N., Murata, K., Yoshikawa, K., Yoshihara, Y., and Touhara, K. (2019). Contribution of individual olfactory receptors to odor-induced attractive and aversive behavior in mice. *Nat. Commun.* 14:209. doi: 10.1038/s41467-018-07940-1

Igarashi, K. M., Ieki, N., An, M., Yamaguchi, Y., Nagayama, S., Kobayakawa, K., et al. (2012). Parallel mitral and tufted cell pathways route distinct odor information to different targets in the olfactory cortex. *J. Neurosci.* 32, 7970–7985. doi: 10.1523/JNEUROSCI.0154-12.2012

Imai, T., Suzuki, M., and Sakano, H. (2006). Odorant receptor-derived cAMP signals direct axonal targeting. *Science* 314, 657–661. doi: 10.1126/science.1131794

Imai, T., Yamazaki, T., Kobayakawa, R., Kobayakawa, K., Takeuchi, H., Abe, T., et al. (2009). Pre-target axon sorting establishes the neural map topography. *Science* 325, 585–590. doi: 10.1126/science.1173596

Imamura, F., Ayoub, A. E., Rakic, P., and Greer, C. A. (2011). Timing of neurogenesis is a determinant of olfactory circuitry. *Nat. Neurosci.* 14, 331–337. doi: 10.1038/nn.2754

Inokuchi, K., Imamura, F., Takeuchi, H., Kim, R., Okuno, H., Nishizumi, H., et al. (2017). Nrp2 is sufficient to instruct circuit formation of mitral-cells to mediate odor-induced attractive social responses. *Nat. Commun.* 8:15977. doi: 10.1038/ncomms15977

Inoue, N., Nishizumi, H., Naritsuka, H., Kiyonari, H., and Sakano, H. (2018). Sema7A/PlexinC1 signaling triggers activity-dependent olfactory synapse formation Nat. *Commun.* 9:1842. doi: 10.1038/s41467-018-04239-z

Inoue, N., Nishizumi, H., Ooyama, R., Mogi, K., Nishimori, K., Kikusui, T., et al. (2021). The olfactory critical period is determined by activity-dependent Sema7A/Plexin C1 signaling within glomeruli. *elife* 10:e65078. doi: 10.7554/eLife.65078

Ito, J., Roy, S., Liu, Y., Cao, Y., Fletcher, M., Lu, L., et al. (2014). Whisker barrel cortex delta oscillations and gamma power in the awake mouse are linked to respiration. *Nat. Commun.* 5:3572. doi: 10.1038/ncomms4572

Janak, P. H., and Tye, K. M. (2015). From circuits to behavior in the amygdala. *Nature* 517, 284–292. doi: 10.1038/nature14188

Jin, J., Zerano, C., Gottfried, J. A., and Mohanty, A. (2015). Human amygdala represents the complete spectrum of subjective valence. *J. Neurosci.* 35, 15145–15156. doi: 10.1523/JNEUROSCI.2450-15.2015

Jones, S. V., Choi, D. C., Davis, M., and Ressler, K. J. (2008). Learning- dependent structural plasticity in the adult olfactory pathway. *J. Neurosci.* 28, 13106–13111. doi: 10.1523/JNEUROSCI.4465-08.2008

Josselyn, S., and Tonegawa, S. (2020). Memory engrams: recalling the past and imaging the future. *Science* 367:eaaw 4325. doi: 10.1126/science.aaw4325

Kaneko-Gotoh, T., Yoshihara, S., Miyazaki, H., and Yoshihara, Y. (2008). BIG-2 mediates olfactory axon convergence to target glomeruli. *Neuron* 57, 834–846. doi: 10.1016/j.neuron.2008.01.023

Karalis, N., and Sirota, A. (2022). Breathing coordinates cortico-hippocampal dynamics in mice during offline states. *Nat. Commun.* 13:467. doi: 10.1038/s41467-022-28090-5

Keller, A., Zhuang, H., Chi, Q., Vosshall, L. B., and Matsunami, H. (2007). Genetic variation in a human odorant receptor alters odor perception. *Nature* 499, 486–472. doi: 10.1038/nature06162

Kirkby, L. A., Sack, G. S., Firl, A., and Feller, M. B. (2013). A role for correlated spontaneous activity in the assembly of neural circuits. *Neuron* 80, 1129–1144. doi: 10.1016/j.neuron.2013.10.030

Kobayakawa, K., Kobayakawa, R., Matsumoto, H., Oka, Y., Imai, T., Ikawa, M., et al. (2007). Innate versus learned odour processing in the mouse olfactory bulb. *Nature* 450, 503–508. doi: 10.1038/nature06281

Kondoh, K., Lu, Z., Ye, X., Olson, D. P., Lowell, D. D., and Buck, L. B. (2016). A specific area of olfactory cortex involved in stress hormone responses to predator odors. *Nature* 532, 103–106. doi: 10.1038/nature17156

Kosaka, K., and Kosaka, T. (2005). Synaptic organization of the glomerulus in the main olfactory bulb: compartments of the glomerulus and heterogeneity of the periglomerular cells. *Anat. Sci. Int.* 80, 80–90. doi: 10.1111/j.1447-073x.2005.00092.x

Krohn, F., Novello, M., van der Giessen, R., De Zeeuw, C. I., Pel, J. J. M., and Bosman, L. W. J. (2023). The integrated brain network that controls respiration. *elife* 12:e83654. doi: 10.7554/eLife.83654

Kurnikova, A., Moore, J. D., Liao, S.-M., Deschênes, M., and Kleinfeld, D. (2017). Coordination of orofacial motor actions into exploratory behavior by rat. *Curr. Biol.* 27, 688–696. doi: 10.1016/j.cub.2017.01.013

Liberles, S. D. (2015). Trace amine-associated receptors: ligands, neural circuits, and behaviors. *Curr. Opin. Neurobiol.* 34, 1–7. doi: 10.1016/j.conb.2015.01.001

Lin, D. Y., Zhang, S. Z., Block, E., and Katz, L. C. (2005). Encoding social signals in the mouse main olfactory bulb. *Nature* 434, 470–477. doi: 10.1038/nature03414

Liu, A., Savya, S., and Urban, N. N. (2016). Early odorant exposure increases the number of mitral and tufted cells associated with a single glomerulus. *J. Neurosci.* 36, 11646–11653. doi: 10.1523/JNEUROSCI.0654-16.2016

Liu, A., and Urban, N. N. (2017). Prenatal and early postnatal odorant exposure heightens odor-evoked mitral cell responses in the mouse olfactory bulb. *eNeuro* 4. doi: 10.1523/ENEURO.0129-17.2017

Logan, D. W., Brunet, L. J., Webb, W. R., Cutforth, T., Ngai, J., and Stowers, L. (2012). Learned recognition of maternal signature odors mediates the first suckling episode in mice. *Curr. Biol.* 22, 1998–2007. doi: 10.1016/j.cub.2012.08.041

Lorenzon, P., Redolfi, N., Podolsky, M. J., Zamparo, I., Franchi, S. A., Pietra, G., et al. (2015). Circuit formation and function in the olfactory bulb of mice with reduced spontaneous afferent activity. *J. Neurosci.* 35, 146–160. doi: 10.1523/JNEUROSCI.0613-14.2015

Lipscomb, B. W., Treloar, H. B., and Greer, C. A. (2002). Novel microglomerular structures in the olfactory bulb of mice. *J. Neurosci.* 22, 766–774. doi: 10.1523/JNEUROSCI.22-03-00766.2002

Luo, L., and Flanagan, J. G. (2007). Development of continuous and discrete neural maps. *Neuron* 56:284300, 284–300. doi: 10.1016/j.neuron.2007.10.014

Lurille, G., and Datta, S. R. (2017). Population coding in an innately relevant olfactory area. *Neuron* 93, 1180–1197.e7. doi: 10.1016/j.neuron.2017.02.010

Ma, L., Wu, Y., Qiu, Q., Scheerer, H., Moran, A., and Yu, C. R. (2014). A developmental switch of axon targeting in the continuously regenerating mouse olfactory system. *Science* 344, 194–197. doi: 10.1126/science.1248805

Malnic, B., Hirono, J., Sato, T., and Buck, L. B. (1999). Combinatorial receptor codes for odors. *Cell* 96, 713–723. doi: 10.1016/S0092-8674(00)80581-4

Manabe, H., and Mori, K. (2013). Sniff rhythm-paced fast and slow gamma oscillations in the olfactory bulb: relation to tufted and mitral cells and behavioral states. *J.Neurophysiol.* 110, 1593–1599. doi: 10.1152/jn.00379.2013

Miyamichi, K., Amat, F., Moussavi, F., Wang, C., Wickersham, I., Wall, N. R., et al. (2011). Cortical representations of olfactory input by trans-synaptic tracing. *Nature* 472, 191–196. doi: 10.1038/nature09714

Moberly, A. H., Schreck, M., Bhattarai, J. P., Zweifel, L. S., Luo, W., and Ma, M. (2018). Olfactory inputs modulate respiration-related rhythmic activity in the prefrontal cortex and freezing behavior. *Nat. Commun.* 9:1528. doi: 10.1038/s41467-018-03988-1

Mombaerts, P., Wang, F., Dulac, C., Chao, S. K., Nemes, A., Mendelsohn, M., et al. (1996). Visualizing an olfactory sensory map. *Cell* 87, 675–686. doi: 10.1016/S0092-8674(00)81387-2

Mori, K. (1987). Membrane and synaptic properties of identified neurons in the olfactory bulb. *Prog. Neurobiol.* 29, 275–320. doi: 10.1016/0301-0082(87)90024-4

Mori, K., Takahashi, Y. K., Igarashi, K. M., and Yamaguchi, Y. (2006). Maps of odorant molecular features in the mammalian olfactory bulb. *Physiol. Rev.* 86, 409–433. doi: 10.1152/physrev.00021.2005

Mori, K. (2014). "Odor maps in the olfactory bulb" in *The olfactory system*. ed. K. Mori (Tokyo: Springer), 59–70.

Mori, K., Manabe, H., Narikiyo, K., and Onisawa, N. (2013). Olfactory consciousness and gamma oscillation couplings across the olfactory bulb, olfactory cortex, and orbitofrontal cortex. *Front. Psychol.* 4:743. doi: 10.3389/fpsyg.2013.00743

Mori, K., and Sakano, H. (2011). How is the olfactory map formed and interpreted in the mammalian brain? *Annu. Rev. Neurosci.* 34, 465–497. doi: 10.1146/annurev-neuro-112210-112917

Mori, K., and Sakano, H. (2021). Olfactory circuitry and behavioral decisions. *Annu. Rev. Physiol.* 83, 231–256. doi: 10.1146/annurev-physiol-031820-092824

Mori, K., and Sakano, H. (2022a). Processing of odor information during the respiratory cycle in mice. *Front. Neural Circ.* 16:861800. doi: 10.3389/fncir.2022.861800

Mori, K., and Sakano, H. (2022b). Neural circuitry for stress information of environmental and internal odor worlds. *Front. Behav. Neurosci.* 16:943647. doi: 10.3389/fnbeh.2022.943647

Morrison, F. G., Dias, B. G., and Ressler, K. J. (2015). Extinction reverses olfactory fear- conditioned increase in neuron number and glomerular size. *Proc. Natl. Acad. Sci. USA* 112, 12846–12851. doi: 10.1073/pnas.1505068112

Motanis, H., Maroon, M., and Barkai, E. (2014). Learning-induced bidirectional plasticity of intrinsic neuronal excitability reflects the valence of the outcome. *Cereb. Cortex* 24, 1075–1087. doi: 10.1093/cercor/bhs394

Muscatelli, F., Desarménien, M. G., Matarazzo, V., and Grinevich, V. (2018). Oxytocin signaling in the early life of mammals: link to neurodevelopmental disorders associated with ASD. *Curr. Topics Behav. Neurosci.* 35, 239–268. doi: 10.1007/7854_2017_16

Nakashima, A., Takeuchi, H., Imai, T., Saito, H., Kiyonari, H., Abe, T., et al. (2013). Agonist independent GPCR activity regulates axon targeting of olfactory sensory neurons. *Cell* 154, 1314–1325. doi: 10.1016/j.cell.2013.08.033

Nakashima, A., Ihara, N., Shigeta, M., Kiyonari, H., Ikegaya, Y., and Takeuchi, H. (2019). Structured spike series specify gene expression patterns for olfactory circuit formation. *Science* 365:eaaw5030. doi: 10.1126/science.aaw5030

Nagayama, S., Igarashi, K. M., Manabe, H., and Mori, K. (2014). "Parallel tufted cell and mitral cell pathways from the olfactory bulb to the olfactory cortex" in *The olfactory system*. ed. K. Mori (Tokyo: Springer), 133–160.

Najac, M., De Saint Jan, D., Reguero, L., Grandes, P., and Charpak, S. (2011). Monosynaptic and polysynaptic feed-forward inputs to mitral cells from olfactory sensory neurons. *J. Neurosci.* 31, 8722–8729. doi: 10.1523/JNEUROSCI.0527-11.2011

Nishizumi, H., Miyashita, A., Inoue, N., Inokuchi, K., Aoki, M., and Sakano, H. (2019). Primary dendrites of mitral cells synapse unto neighboring glomeruli independent of their odorant receptor identity. *Commun. Biol.* 2:14. doi: 10.1038/s42003-018-0252-y

Poo, C., Agarwal, G., Bonacci, N., and Mainen, Z. F. (2022). Spatial maps in piriform cortex during olfactory navigation. *Nature* 601, 595–599. doi: 10.1038/s41586-021-04242-3

Qiu, Q., Wu, Y., Ma, L., Xu, W., Hills, M. J. R., Ramalingan, V., et al. (2021). Acquisition of innate odor preference depends on spontaneous and experiential activities during critical period. *elife* 10:e60546. doi: 10.7554/eLife.60546

Reisert, J. (2010). Origin of basal activity in mammalian olfactory receptor neurons. *J. Gen. Physiol.* 136, 529–540. doi: 10.1085/jgp.201010528

Root, C. M., Denny, C. A., Hen, R., and Axel, R. (2014). The participation of cortical amygdala in innate, odor-driven behavior. *Nature* 515, 269–273. doi: 10.1038/nature13897

Russo, M. J., Franks, K. M., Oghaz, R., Axel, R., and Siegelbaum, S. A. (2020). Synaptic organization of anterior olfactory nucleus inputs to piriform cortex. *J. Neurosci.* 40, 9414–9425. doi: 10.1523/JNEUROSCI.0965-20.2020

Saito, H., Nishizumi, H., Suzuki, S., Matsumoto, H., Ieki, N., Abe, T., et al. (2017). Immobility responses are induced by photoactivation of a single glomerular species responsive to fox odor TMT. *Nat. Commun.* 8:16011. doi: 10.1038/ncomms16011

Sakano, H. (2010). Neural map formation in the mouse olfactory system. *Neuron* 67, 530–542. doi: 10.1016/j.neuron.2010.07.003

Sakano, H. (2020). Developmental regulation of olfactory circuit formation in mice. *Develop. Growth Differ.* 62, 199–213. doi: 10.1111/dgd.12657

Sanz Diez, A., Najac, M., and De Sait Jan, D. (2019). Basal forebrain GABAergic innervation of olfactory bulb periglomerular interneurons. *J. Physiol.* 597, 2547–2563. doi: 10.1113/JP277811

Schoenfeld, T. A., and Macrides, F. (1984). Topographic organization of connections between the main olfactory bulb and pars externa of the anterior olfactory nucleus in hamster. *J. Comp. Neurol.* 227, 121–135. doi: 10.1002/cne.902270113

Sengoku, S., Ishii, T., Serizawa, S., Nakatani, H., Nagawa, F., Tsuboi, A., et al. (2001). Axonal projection of olfactory sensory neurons during the developmental and regeneration processes. *Neuroreport* 12, 1061–1066. doi: 10.1097/00001756-200104170-00039

Serizawa, S., Ishii, T., Nakatani, H., Tsuboi, A., Nagawa, N., Asano, M., et al. (2000). Mutually exclusive expression of an odorant receptor gene in YAC transgenic mice. *Nature Neurosci.* 3, 687–693. doi: 10.1038/76641

Serizawa, S., Miyamichi, K., Nakatani, H., Suzuki, M., Saito, M., Yoshihara, Y., et al. (2003). Negative feedback regulation ensures the one receptor-one olfactory neuron rule in mouse. *Science* 302, 2088–2094. doi: 10.1126/science.1089122

Serizawa, S., Miyamichi, K., Takeuchi, H., Yamagishi, Y., Suzuki, M., and Sakano, H. (2006). A neuronal identity code for the odorant receptor-specific and activity-dependent axon sorting. *Cell* 127, 1057–1069. doi: 10.1016/j.cell.2006.10.031

Shepherd, G. M. (2012). *Neurogastronomy*. New York: Columbia University Press.

Shepherd, G. M., Chen, W. R., and Greer, C. A. (2004). "Olfactory bulb" in *The synaptic Organization of the Brain*. ed. G. M. Shepherd. *5th* ed (New York: Oxford University Press), 165–216.

Short, S. M., Morse, T. M., McTavish, T. S., Shepherd, G. M., and Verhagen, J. V. (2016). Respiration gates sensory input responses in the mitral cell layer of the olfactory bulb. *PLoS One* 11:e0168356. doi: 10.1371/journal.pone.0168356

Spindle, M. S., Parsa, P. V., Bowles, S. G., D'Souza, R. D., and Vijayaraghavan, S. (2018). A dominant role for the beta 4 nicotinic receptor subunit in nicotinic modulation of glomerular microcircuits in the mouse olfactory bulb. *J. Neurophysiol.* 120, 2036–2048. doi: 10.1152/jn.00925.2017

Sullivan, R. M., Landers, M., Yeaman, B., and Wilson, D. A. (2000). Good memories of bad events in infancy. *Nature* 407, 38–39. doi: 10.1038/35024156

Takeuchi, H., Inokuchi, K., Aoki, M., Suto, F., Tsuboi, A., Matsuda, I., et al. (2010). Sequential arrival and graded secretion of Sema3F by olfactory neuron axons specify map topography at the bulb. *Cell* 141, 1056–1067. doi: 10.1016/j.cell.2010.04.041

Tort, A. B. L., Ponsel, S., Jessberger, J., Yanovsky, Y., Brankačk, J., and Draguhn, A. (2018). Parallel detection of theta and respiration-coupled oscillations throughout the mouse brain. *Sci. Rep.* 8:6432. doi: 10.1038/s41598-018-24629-z

Tsanov, M., Chah, E., Reilly, R., and O'Maha, S. M. (2014). Respiration cycle entrainment of septal neurons mediates the fast coupling of sniffing rate and hippocampal theta rhythm. *Eur. J. Neurosci.* 39, 957–974. doi: 10.1111/ejn.12449

Villar, P. S., Hu, R., and Araneda, R. C. (2021). Long-range GABAergic inhibition modulates spatiotemporal dynamics of the output neurons in the olfactory bulb. *J. Neurosci.* 41, 3610–3621. doi: 10.1523/JNEUROSCI.1498-20.2021

Wilson, D. A., and Sullivan, R. M. (2011). Cortical processing of odor objects. *Neuron* 72, 506–519. doi: 10.1016/j.neuron.2011.10.027

Xu, M., Chung, S., Zhang, S., Zhong, P., Ma, C., Chang, W.-C., et al. (2015). Basal forebrain circuit for sleep-wake control. *Nat. Neurosci.* 18, 1641–1647. doi: 10.1038/nn.4143

Yan, Z., Tan, J., Qin, C., Lu, Y., Ding, C., and Luo, M. (2008). Precise circuitry links bilaterally symmetric olfactory maps. *Neuron* 58, 613–624. doi: 10.1016/j.neuron.2008.03.012

Yazaki-Sugiyama, Y., Kang, S., Câteau, H., Fukai, T., and Hensch, T. K. (2009). Bidirectional plasticity in fast-spiking GABA circuits by visual experience. *Nature* 462, 218–221. doi: 10.1038/nature08485

Yu, C. R., Power, J., Barnea, G., O'Donnell, S., Brown, H. E., Osborne, J., et al. (2004). Spontaneous neural activity is required for the establishment and maintenance of the olfactory sensory map. *Neuron* 42, 553–566. doi: 10.1016/S0896-6273(04)00224-7

Zaborszky, L., Carlson, J., Brasher, H. R., and Heimer, L. (1986). Cholinergic and GABAergic afferents to the olfactory bulb in the rat with special emphasis on the projection neurons in the nucleus of the horizontal limb of the diagonal band. *J. Comp. Neurol.* 243, 488–509. doi: 10.1002/cne.902430405

Zou, D.-J., Chesler, A., and Firestein, S. (2009). How the olfactory bulb got its glomeruli: a just so stay? *Nat. Rev. Neurosci.* 10, 611–618. doi: 10.1038/nrn2666

Glossary

aiCAP	The most anterolateral isolation of the CAP compartments of the olfactory tubercle
aMeA	Anterior medial-amygdala
AON	Anterior olfactory nucleus
A/P	Anterior/Posterior
BF	Basal forebrain
D/V	Dorsal/Ventral
EPL	External plexiform layer
eTC	External tufted cell
GC	Granule cell
iTC	Internal tufted cell
MC	Mitral cell
mTC	Middle tufted cell
Nrp	Neuropilin
OB	Olfactory bulb
OC	Olfactory cortex
OE	Olfactory epithelium
OR	Odorant receptor
OSN	Olfactory sensory neuron
PGC	Periglomerular cell
Plxn	Plexin
pmCoA	Postero-medial cortical amygdala
Sema	Semaphorin
TC	Tufted cell
TMT	Trimethyl thiazoline

frontiers | Frontiers in Neural Circuits

TYPE Mini Review
PUBLISHED 08 March 2024
DOI 10.3389/fncir.2024.1382626

OPEN ACCESS

EDITED BY
Kensaku Mori,
RIKEN, Japan

REVIEWED BY
Masahiro Yamaguchi,
Kōchi University, Japan
Thomas Heinbockel,
Howard University, United States

*CORRESPONDENCE
Tatsumi Hirata
✉ tathirat@nig.ac.jp

RECEIVED 06 February 2024
ACCEPTED 29 February 2024
PUBLISHED 08 March 2024

CITATION
Hirata T (2024) Olfactory information processing viewed through mitral and tufted cell-specific channels.
Front. Neural Circuits 18:1382626.
doi: 10.3389/fncir.2024.1382626

Olfactory information processing viewed through mitral and tufted cell-specific channels

Tatsumi Hirata*

Brain Function Laboratory, National Institute of Genetics, SOKENDAI, Mishima, Japan

Parallel processing is a fundamental strategy of sensory coding. Through this processing, unique and distinct features of sensations are computed and projected to the central targets. This review proposes that mitral and tufted cells, which are the second-order projection neurons in the olfactory bulb, contribute to parallel processing within the olfactory system. Based on anatomical and functional evidence, I discuss potential features that could be conveyed through the unique channel formed by these neurons.

KEYWORDS

olfactory system, tufted cell, mitral cell, mouse, neurogenic tagging, parallel processing

Introduction

From a neurodevelopmental perspective, the timing of neuronal birth determines their permanent phenotypes (Hirata and Iwai, 2019), including morphology, physiology and connection patterns (Leone et al., 2008; Fame et al., 2011; Suzuki and Hirata, 2013). Thus, this neurodevelopmental principle should form the functional basis of the brain. We hypothesized that if projection neurons of the olfactory bulb are classified neurodevelopmentally, we might be able to find a wiring logic of olfactory circuits. Chronologically ordered arrangement of olfactory bulb axons in the lateral olfactory tract (Inaki et al., 2004; Yamatani et al., 2004) further encouraged us to take this approach, even though the link between the chronotopic arrangement of axon shafts and the final destinations of their collateral branches remained unclear. These provided the springboard for our dissection of olfactory circuits using neurogenic tagging. Based on our and others' findings, I will discuss the potential logic of olfactory information processing.

Logic of olfactory information processing

The anatomical principle of the peripheral olfactory system is feature detection of odorant molecules; olfactory sensory neurons that express the same odorant receptor converge their axons onto a few fixed glomeruli of the olfactory bulb, thereby constructing the stereotypical odor map (Mori et al., 2006; Mori and Sakano, 2011). This odor map is then transferred to the next targets by two major projection neurons, mitral cell (MC) and tufted cell (TC) in the main olfactory bulb (Mori and Sakano, 2021). Their projections are often described as diffuse and widespread (Ghosh et al., 2011; Miyamichi et al., 2011; Sosulski et al., 2011). While specific odorant information sometimes appears over-represented in a few target areas (Miyamichi et al., 2011; Inokuchi et al., 2017), the spatial odor map across the olfactory bulb is basically lost in most of the olfactory target areas due to non-topographic projections.

This strategy seems somewhat exceptional as a sensory system. Although external information is typically represented as a spatial map in many sensory systems, the maps are usually transferred sequentially to higher centers by the labeled-line principle (Kaas, 1997; Cang and Feldheim, 2013). By contrast, the odor map degrades rapidly. This has led to the assumption that olfactory information processing relies on indiscriminate integration of odorant information by mixing projections from the peripheral odor map (Davison and Ehlers, 2011).

This review argues that MCs and TCs offer an alternative perspective: parallel processing in the olfactory system. The parallel processing is another common strategy of the sensory system (Young, 1998). As exemplified by the visual system, different features of information are extracted from the original map and sent to separate target areas in parallel (Nassi and Callaway, 2009), thereby sharpening and enhancing specific features for increased biological significance. While olfactory information features remain elusive, I propose to discuss potential features that MC and TC channels can convey in the olfactory system based on previous observations (Mori and Sakano, 2021).

MCs and TCs in the olfactory system

Around 20 MCs and 50 TCs relay information received by each glomerulus to higher brain centers (Nagayama et al., 2014). These two projection neuron types occupy distinct layers of the main olfactory bulb and exhibit morphological differences (Mori et al., 1983; Orona et al., 1984). Furthermore, they fire action potentials at different phases of the respiratory cycle (Fukunaga et al., 2012; Igarashi et al., 2012). Electrophysiological analyses suggested that MCs are highly tuned for detection of specific odorants, whereas TCs respond more broadly to a wider range of stimuli (Schneider and Scott, 1983; Ezeh et al., 1993; Nagayama et al., 2004; Griff et al., 2008). Thus, MCs and TCs seem well-poised to convey different kinds of information extracted from the same glomeruli.

Although MCs and TCs exhibit molecular differences (Tepe et al., 2018; Zeppilli et al., 2021), clear discrimination based on gene expression has proven elusive. Previous studies indicated that MCs are born earlier than TCs (Hinds, 1968; Bayer, 1983; Grafe, 1983). I conceived that the birthdate difference can be used to effectively separate these populations. While a study demonstrated differential labeling of olfactory bulb neurons based on birth timing by *in utero* electroporation, this technique only revealed heterogeneous MC populations (Imamura et al., 2011; Imamura and Greer, 2015; Chon et al., 2020). Therefore, we opted for a different genetic method, neurogenic tagging, which allows for separate visualization and manipulation of MCs and TCs based on their distinct birthdates (Hirata et al., 2019).

Neurogenic tagging of olfactory projection neurons

The neurogenic tagging method uses a driver mouse line in which tamoxifen (TM)-inducible Cre recombinase, CreER is expressed only transiently for a short time window immediately after neuronal fates are committed (Figure 1). For this purpose, CreER is driven under the enhancer/ promoter of neural differentiation genes such as neurogenins and neuroDs using the bacterial artificial chromosome transgenic approach (Hirata et al., 2021). A single TM dose at a specific developmental stage induces loxP recombination only in the cells soon after neuronal commitment. These "tagged" neurons are then susceptible to various experimental manipulations using recombination-dependent reporters or effectors. Several driver lines are available for neurogenic tagging (Hirata et al., 2021). Representative images of tagged neurons across the brain by all the drivers are open in

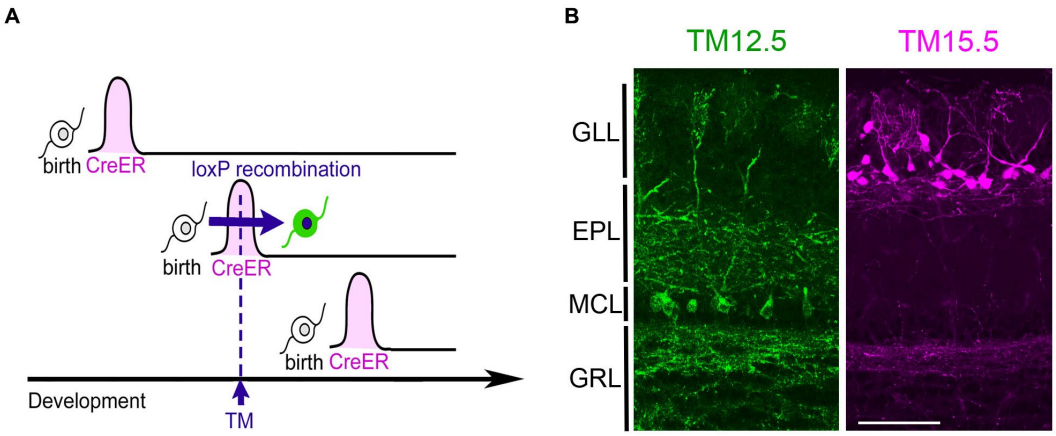

FIGURE 1
Neurogenic tagging of MCs and TCs. **(A)** A diagram illustrating neurogenic tagging. In the driver mice, tamoxifen (TM)-inducible CreER is transiently expressed during a short time window soon after neuronal birth. A single injection of TM during the neurodevelopmental stage induces *loxP* recombination only in the cells expressing CreER. Modified from Hirata et al. (2021). **(B)** MCs labeled with green fluorescent protein (green, left) and TCs labeled with tdTomato (magenta, right) in the mouse olfactory bulb at postnatal day 21. TM was injected at embryonic day 12.5 (TM12.5) and 15.5 (TM15.5). The complete genotypes of the mice are Neurog2^{CreER}(G2A); Cdhr1^{tTA}; ROSA26-TRE^{mGFP} for TM12.5 and Neurog2^{CreER}(G2A); Cdhr1^{tTA}; TRE$^{tdTomato\text{-}sypGFP}$ for TM15.5 [see Hirata et al., 2019 for details]. Bar = 100 μm. GLL, glomerular layer; EPL, external plexiform layer; MCL, mitral cell layer; GRL, granule cell layer.

public in the NeuroGT database,[1] visualized using a global neuron-specific reporters ($Tau^{mGFP\text{-}nLacZ}$, Hippenmeyer et al., 2005, Jax#021162).

Among the driver lines, the $Neurog2^{creER}$ (G2A) driver is ideal for studying olfactory projection neurons (Hirata et al., 2019). While this method labels a mixture of multiple projection neuron types, MCs and TCs are the major populations when tamoxifen is injected at E12.5 and E15.5, respectively (Figure 2). TCs are typically categorized further as internal, middle, and external subtypes based on their location within the olfactory bulb layer (Mori et al., 1983; Orona et al., 1984). However, in the analysis using neurogenic tagging mice, external TCs far outnumber the other TC subtypes (Hirata et al., 2019). Therefore, this review will primarily focus on external TCs as representative of TCs.

Target projections of MCs and TCs

To visualize axon trajectories of MCs and TCs clearly, reporter proteins are expressed specifically only by olfactory bulb neurons that are neurogenic tagged, by combining neurogenic tagging and tetracycline-controlled transcription activation under the olfactory bulbs-specific promoter (Hirata et al., 2019; also see genotypes in the Figure 2 caption). Previously, TC axons were suggested to target only anterior region of the olfactory target areas (Haberly and Price, 1977; Scott, 1981; Igarashi et al., 2012). Our analysis revealed a surprising degree of convergence of TC axons; the axons only targeted to two small domains within the olfactory areas (Figure 2). One of the targets is the pars externa of the anterior olfactory nucleus, which uniquely receives topographic projections from the main olfactory bulb (Schoenfeld and Macrides, 1984). Its exclusive projections to the contralateral side suggest that the pars externa functions in bilateral integration of olfactory information (Haberly and Price, 1978b; Kikuta et al., 2010). The other TC target is the most anterolateral isolation of the CAP compartments (aiCAP) within the olfactory tubercle. Across the tubercle, dozens of CAP compartments are distributed in a patchy fashion, and their spatial locations vary between individual mice (Fallon et al., 1978; Meyer and Wahle, 1986). Among them, the aiCAP in the most anterolateral part of the tubercle consistently stands out as the largest and strongly expresses dopamine receptor 1. Notably, this small target receives TC projections from all glomeruli of the main olfactory bulb (Hirata et al., 2019).

MC axons exhibit a much more widespread distribution, projecting to all of the olfactory target areas (Figure 2). However, interestingly, the axons are specifically excluded from the aiCAP, making it a unique target exclusively innervated by TCs (Hirata et al., 2019). The pars externa appears to receive convergent inputs from both MCs and TCs, but the anatomical complexity of this subnucleus makes definitive conclusions challenging.

This observation provides compelling anatomical evidence for a dedicated TC-specific channel within the olfactory system. Although TC and MC projections were hypothesized to converge onto the same secondary target areas, the existence of the exclusive TC target offers exciting possibilities for TC-specific information processing within the olfactory system.

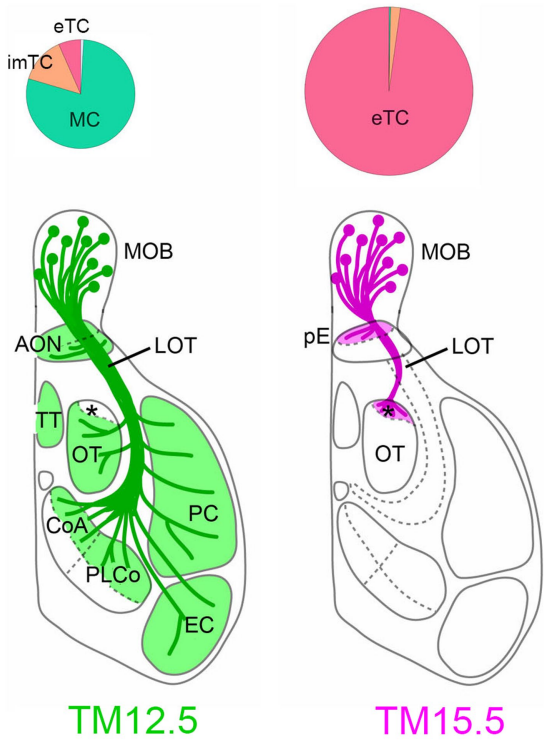

FIGURE 2
Projections of MCs and TCs revealed by neurogenic tagging. Pie charts on the top show the proportion of neuron types neurogenic-tagged. MCs and TCs are preferentially labeled when TM was injected at embryonic day 12.5 (TM12.5. left) and 15.5 (TM15.5, right), respectively. The diameter of the charts reflects the number of neurons. The brain diagrams on the bottom summarize axon projections of TM2.5 and TM15.5-tagged neurons. The asterisk indicates aiCAP within the olfactory tubercle. imTC, internal and middle TC; eTC, external TC; MOB, main olfactory bulb; AON, anterior olfactory nucleus; pE, pars externa; LOT, lateral olfactory tract; TT, tenia tecta; OT, olfactory tubercle; CoA, cortical amygdala; PLCo, posterolateral cortical amygdala; PC, piriform cortex; EC, entorhinal cortex. Modified from Hirata et al. (2021).

Potential features represented by the TC Channel

What kind of features can be represented in the TC channel? As described already, TCs respond to a broad range of odorants at a low threshold (Schneider and Scott, 1983; Ezeh et al., 1993; Fukunaga et al., 2012; Igarashi et al., 2012). Combined with the fact that the aiCAP receives converging TC projections from all the olfactory bulb, this compact target could rapidly detect more-or-less indiscriminate odor stimuli. Because the aiCAP belongs to the dopamine reward system (Fallon et al., 1978; Haberly and Price, 1978a; Wesson and Wilson, 2011; Murata et al., 2015), the odor detection at aiCAP may directly influence value-based behavior in mice through this reward system.

1 https://ssbd.riken.jp/neurogt/

The pars externa, another TC target, likely operates in partnership with MCs. Its unique topographic connections linking ipsilateral and contralateral olfactory bulbs suggest a potential role of this subnucleus in spatial function, such as the localization of odor sources (Kikuta et al., 2010).

Future perspectives

The power of neurogenic tagging lies in its ability to manipulate the tagged neurons (Hirata et al., 2021). Thus, we are now in the stage to explore the actual meaning of olfactory parallel circuits. We have begun testing the olfactory behaviors of mice when MC or TC circuits are specifically activated or suppressed using chemogenetics. This method also paves the way for monitoring neuronal activities in various areas when neuronal activities of each olfactory channel is selectively modulated. Such approaches hold immense promise for unveiling the specific functions of MC and TC circuits within the olfactory system, ultimately leading to a deeper understanding of the logic behind olfactory information processing.

Author contributions

TH: Writing – original draft, Writing – review & editing.

Funding

The author(s) declare financial support was received for the research, authorship, and/or publication of this article. This article was supported by the MEXT/JSPS KAKENHI Grants (20H03345, 23H02581) and IU-REAL Collaborative Research Grant.

Conflict of interest

The author declares that the research was conducted in the absence of any commercial or financial relationships that could be construed as a potential conflict of interest.

The author(s) declared that they were an editorial board member of Frontiers, at the time of submission. This had no impact on the peer review process and the final decision.

Publisher's note

References

Bayer, S. A. (1983). 3H-thymidine-radiographic studies of neurogenesis in the rat olfactory bulb. *Exp. Brain Res.* 50, 329–340. doi: 10.1007/BF00239197

Cang, J., and Feldheim, D. A. (2013). Developmental mechanisms of topographic map formation and alignment. *Annu. Rev. Neurosci.* 36, 51–77. doi: 10.1146/annurev-neuro-062012-170341

Chon, U., LaFever, B. J., Nguyen, U., Kim, Y., and Imamura, F. (2020). Topographically distinct projection patterns of early-generated and late-generated projection neurons in the mouse olfactory bulb. *eNeuro* 7, ENEURO.0369–ENEU20.2020. doi: 10.1523/ENEURO.0369-20.2020

Davison, I. G., and Ehlers, M. D. (2011). Neural circuit mechanisms for pattern detection and feature combination in olfactory cortex. *Neuron* 70, 82–94. doi: 10.1016/j.neuron.2011.02.047

Ezeh, P. I., Wellis, D. P., and Scott, J. W. (1993). Organization of inhibition in the rat olfactory bulb external plexiform layer. *J. Neurophysiol.* 70, 263–274. doi: 10.1152/jn.1993.70.1.263

Fallon, J. H., Riley, J. N., Sipe, J. C., and Moore, R. Y. (1978). The islands of Calleja: organization and connections. *J. Comp. Neurol.* 181, 375–395. doi: 10.1002/cne.901810209

Fame, R. M., MacDonald, J. L., and Macklis, J. D. (2011). Development, specification, and diversity of callosal projection neurons. *Trends Neurosci.* 34, 41–50. doi: 10.1016/j.tins.2010.10.002

Fukunaga, I., Berning, M., Kollo, M., Schmaltz, A., and Schaefer, A. T. (2012). Two distinct channels of olfactory bulb output. *Neuron* 75, 320–329. doi: 10.1016/j.neuron.2012.05.017

Ghosh, S., Larson, S. D., Hefzi, H., Marnoy, Z., Cutforth, T., Dokka, K., et al. (2011). Sensory maps in the olfactory cortex defined by long-range viral tracing of single neurons. *Nature* 472, 217–220. doi: 10.1038/nature09945

Grafe, M. R. (1983). Developmental factors affecting regeneration in the central nervous system: early but not late formed mitral cells reinnervate olfactory cortex after neonatal tract section. *J. Neurosci.* 3, 617–630. doi: 10.1523/JNEUROSCI.03-03-00617.1983

Griff, E. R., Mafhouz, M., and Chaput, M. A. (2008). Comparison of identified mitral and tufted cells in freely breathing rats: II. Odor-evoked responses. *Chem. Senses* 33, 793–802. doi: 10.1093/chemse/bjn040

Haberly, L. B., and Price, J. L. (1977). The axonal projection patterns of the mitral and tufted cells of the olfactory bulb in the rat. *Brain Res.* 129, 152–157. doi: 10.1016/0006-8993(77)90978-7

Haberly, L. B., and Price, J. L. (1978a). Association and commissural fiber systems of the olfactory cortex of the rat. *J. Comp. Neurol.* 178, 711–740. doi: 10.1002/cne.901780408

Haberly, L. B., and Price, J. L. (1978b). Association and commissural fiber systems of the olfactory cortex of the rat. II. Systems originating in the olfactory peduncle. *J. Comp. Neurol.* 181, 781–807. doi: 10.1002/cne.901810407

Hinds, J. W. (1968). Autoradiographic study of histogenesis in the mouse olfactory bulb. II. Cell proliferation and migration. *J. Comp. Neurol.* 134, 305–321. doi: 10.1002/cne.901340305

Hippenmeyer, S., Vrieseling, E., Sigrist, M., Portmann, T., Laengle, C., Ladle, D. L., et al. (2005). A developmental switch in the response of DRG neurons to ETS transcription factor signaling. *PLoS Biol.* 3:e159. doi: 10.1371/journal.pbio.0030159

Hirata, T., and Iwai, L. (2019). Timing matters: a strategy for neurons to make diverse connections. *Neurosci. Res.* 138, 79–83. doi: 10.1016/j.neures.2018.09.006

Hirata, T., Shioi, G., Abe, T., Kiyonari, H., Kato, S., Kobayashi, K., et al. (2019). A novel birthdate-labeling method reveals segregated parallel projections of mitral and external tufted cells in the main olfactory system. *eNeuro* 6, ENEURO.0234–ENEU19.2019. doi: 10.1523/ENEURO.0234-19.2019

Hirata, T., Tohsato, Y., Itoga, H., Shioi, G., Kiyonari, H., Oka, S., et al. (2021). NeuroGT: a brain atlas of neurogenic tagging CreER drivers for birthdate-based classification and manipulation of mouse neurons. *Cell Rep Methods* 1:100012. doi: 10.1016/j.crmeth.2021.100012

Igarashi, K. M., Ieki, N., An, M., Yamaguchi, Y., Nagayama, S., Kobayakawa, K., et al. (2012). Parallel mitral and tufted cell pathways route distinct odor information to different targets in the olfactory cortex. *J. Neurosci.* 32, 7970–7985. doi: 10.1523/JNEUROSCI.0154-12.2012

Imamura, F., Ayoub, A. E., Rakic, P., and Greer, C. A. (2011). Timing of neurogenesis is a determinant of olfactory circuitry. *Nat. Neurosci.* 14, 331–337. doi: 10.1038/nn.2754

Imamura, F., and Greer, C. A. (2015). Segregated labeling of olfactory bulb projection neurons based on their birthdates. *Eur. J. Neurosci.* 41, 147–156. doi: 10.1111/ejn.12784

Inaki, K., Nishimura, S., Nakashiba, T., Itohara, S., and Yoshihara, Y. (2004). Laminar organization of the developing lateral olfactory tract revealed by differential expression of cell recognition molecules. *J. Comp. Neurol.* 479, 243–256. doi: 10.1002/cne.20270

Inokuchi, K., Imamura, F., Takeuchi, H., Kim, R., Okuno, H., Nishizumi, H., et al. (2017). Nrp2 is sufficient to instruct circuit formation of mitral-cells to mediate odour-induced attractive social responses. *Nat. Commun.* 8:15977. doi: 10.1038/ncomms15977

Kaas, J. H. (1997). Topographic maps are fundamental to sensory processing. *Brain Res. Bull.* 44, 107–112. doi: 10.1016/s0361-9230(97)00094-4

Kikuta, S., Sato, K., Kashiwadani, H., Tsunoda, K., Yamasoba, T., and Mori, K. (2010). Neurons in the anterior olfactory nucleus pars externa detect right or left localization of odor sources. *Proc. Natl. Acad. Sci. USA* 107, 12363–12368. doi: 10.1073/pnas.1003999107

Leone, D. P., Srinivasan, K., Chen, B., Alcamo, E., and McConnell, S. K. (2008). The determination of projection neuron identity in the developing cerebral cortex. *Curr. Opin. Neurobiol.* 18, 28–35. doi: 10.1016/j.conb.2008.05.006

Meyer, G., and Wahle, P. (1986). The olfactory tubercle of the cat. I. Morphological components. *Exp. Brain Res.* 62, 515–527. doi: 10.1007/BF00236030

Miyamichi, K., Amat, F., Moussavi, F., Wang, C., Wickersham, I., Wall, N. R., et al. (2011). Cortical representations of olfactory input by trans-synaptic tracing. *Nature* 472, 191–196. doi: 10.1038/nature09714

Mori, K., Kishi, K., and Ojima, H. (1983). Distribution of dendrites of mitral, displaced mitral, tufted, and granule cells in the rabbit olfactory bulb. *J. Comp. Neurol.* 219, 339–355. doi: 10.1002/cne.902190308

Mori, K., and Sakano, H. (2011). How is the olfactory map formed and interpreted in the mammalian brain? *Annu. Rev. Neurosci.* 34, 467–499. doi: 10.1146/annurev-neuro-112210-112917

Mori, K., and Sakano, H. (2021). Olfactory circuitry and behavioral decisions. *Annu. Rev. Physiol.* 83, 231–256. doi: 10.1146/annurev-physiol-031820-092824

Mori, K., Takahashi, Y. K., Igarashi, K. M., and Yamaguchi, M. (2006). Maps of odorant molecular features in the mammalian olfactory bulb. *Physiol. Rev.* 86, 409–433. doi: 10.1152/physrev.00021.2005

Murata, K., Kanno, M., Ieki, N., Mori, K., and Yamaguchi, M. (2015). Mapping of learned odor-induced motivated behaviors in the mouse olfactory tubercle. *J. Neurosci.* 35, 10581–10599. doi: 10.1523/JNEUROSCI.0073-15.2015

Nagayama, S., Homma, R., and Imamura, F. (2014). Neuronal organization of olfactory bulb circuits. *Front Neural Circuits* 8:98. doi: 10.3389/fncir.2014.00098

Nagayama, S., Takahashi, Y. K., Yoshihara, Y., and Mori, K. (2004). Mitral and tufted cells differ in the decoding manner of odor maps in the rat olfactory bulb. *J. Neurophysiol.* 91, 2532–2540. doi: 10.1152/jn.01266.2003

Nassi, J. J., and Callaway, E. M. (2009). Parallel processing strategies of the primate visual system. *Nat. Rev. Neurosci.* 10, 360–372. doi: 10.1038/nrn2619

Orona, E., Rainer, E. C., and Scott, J. W. (1984). Dendritic and axonal organization of mitral and tufted cells in the rat olfactory bulb. *J. Comp. Neurol.* 226, 346–356. doi: 10.1002/cne.902260305

Schneider, S. P., and Scott, J. W. (1983). Orthodromic response properties of rat olfactory bulb mitral and tufted cells correlate with their projection patterns. *J. Neurophysiol.* 50, 358–378. doi: 10.1152/jn.1983.50.2.358

Schoenfeld, T. A., and Macrides, F. (1984). Topographic organization of connections between the main olfactory bulb and pars externa of the anterior olfactory nucleus in the hamster. *J. Comp. Neurol.* 227, 121–135. doi: 10.1002/cne.902270113

Scott, J. W. (1981). Electrophysiological identification of mitral and tufted cells and distributions of their axons in olfactory system of the rat. *J. Neurophysiol.* 46, 918–931. doi: 10.1152/jn.1981.46.5.918

Sosulski, D. L., Bloom, M. L., Cutforth, T., Axel, R., and Datta, S. R. (2011). Distinct representations of olfactory information in different cortical centres. *Nature* 472, 213–216. doi: 10.1038/nature09868

Suzuki, I. K., and Hirata, T. (2013). Neocortical neurogenesis is not really "neo": a new evolutionary model derived from a comparative study of chick pallial development. *Develop. Growth Differ.* 55, 173–187. doi: 10.1111/dgd.12020

Tepe, B., Hill, M. C., Pekarek, B. T., Hunt, P. J., Martin, T. J., Martin, J. F., et al. (2018). Single-cell RNA-Seq of mouse olfactory bulb reveals cellular heterogeneity and activity-dependent molecular census of adult-born neurons. *Cell Rep.* 25, 2689–2703.e3. doi: 10.1016/j.celrep.2018.11.034

Wesson, D. W., and Wilson, D. A. (2011). Sniffing out the contributions of the olfactory tubercle to the sense of smell: hedonics, sensory integration, and more? *Neurosci. Biobehav. Rev.* 35, 655–668. doi: 10.1016/j.neubiorev.2010.08.004

Yamatani, H., Sato, Y., Fujisawa, H., and Hirata, T. (2004). Chronotopic organization of olfactory bulb axons in the lateral olfactory tract. *J. Comp. Neurol.* 475, 247–260. doi: 10.1002/cne.20155

Young, E. D. (1998). Parallel processing in the nervous system: evidence from sensory maps. *Proc. Natl. Acad. Sci. USA* 95, 933–934. doi: 10.1073/pnas.95.3.933

Zeppilli, S., Ackels, T., Attey, R., Klimpert, N., Ritola, K. D., Boeing, S., et al. (2021). Molecular characterization of projection neuron subtypes in the mouse olfactory bulb. *eLife* 10:e65445. doi: 10.7554/eLife.65445

frontiers | Frontiers in Neural Circuits

TYPE Mini Review
PUBLISHED 25 March 2024
DOI 10.3389/fncir.2024.1385908

OPEN ACCESS

EDITED BY
Kensaku Mori,
RIKEN, Japan

REVIEWED BY
Hideki Kashiwadani,
Kagoshima University, Japan
Yoshimasa Koyama,
Fukushima University, Japan

*CORRESPONDENCE
Yusuke Tsuno
✉ tsuno@med.kanazawa-u.ac.jp

RECEIVED 14 February 2024
ACCEPTED 12 March 2024
PUBLISHED 25 March 2024

CITATION
Tsuno Y and Mieda M (2024) Circadian rhythm mechanism in the suprachiasmatic nucleus and its relation to the olfactory system.
Front. Neural Circuits 18:1385908.
doi: 10.3389/fncir.2024.1385908

Circadian rhythm mechanism in the suprachiasmatic nucleus and its relation to the olfactory system

Yusuke Tsuno* and Michihiro Mieda

Department of Integrative Neurophysiology, Graduate School of Medical Sciences, Kanazawa University, Kanazawa, Japan

Animals need sleep, and the suprachiasmatic nucleus, the center of the circadian rhythm, plays an important role in determining the timing of sleep. The main input to the suprachiasmatic nucleus is the retinohypothalamic tract, with additional inputs from the intergeniculate leaflet pathway, the serotonergic afferent from the raphe, and other hypothalamic regions. Within the suprachiasmatic nucleus, two of the major subtypes are vasoactive intestinal polypeptide (VIP)-positive neurons and arginine-vasopressin (AVP)-positive neurons. VIP neurons are important for light entrainment and synchronization of suprachiasmatic nucleus neurons, whereas AVP neurons are important for circadian period determination. Output targets of the suprachiasmatic nucleus include the hypothalamus (subparaventricular zone, paraventricular hypothalamic nucleus, preoptic area, and medial hypothalamus), the thalamus (paraventricular thalamic nuclei), and lateral septum. The suprachiasmatic nucleus also sends information through several brain regions to the pineal gland. The olfactory bulb is thought to be able to generate a circadian rhythm without the suprachiasmatic nucleus. Some reports indicate that circadian rhythms of the olfactory bulb and olfactory cortex exist in the absence of the suprachiasmatic nucleus, but another report claims the influence of the suprachiasmatic nucleus. The regulation of circadian rhythms by sensory inputs other than light stimuli, including olfaction, has not been well studied and further progress is expected.

KEYWORDS

circadian rhythm, suprachiasmatic nucleus, *in vivo*, olfaction, arginine vasopressin (AVP)

Introduction

Sleep is essential for survival, and animals maintain their physical and mental health by maintaining a certain rhythm of waking and sleeping at the right time and in the right state. In humans, waking and sleeping roughly correspond to the day and night in the outside world. Diurnal organisms, such as humans, are active during the day, while nocturnal animals, such as mice, are more active at night and sleep more at the opposite time. The suprachiasmatic nucleus (SCN) is the center that controls all circadian rhythms, including wake–sleep, appetite, autonomic system, and neuroendocrine rhythms (Hastings et al., 2018). This control of circadian rhythms allows animals to maintain a roughly 24-h cycle, even in the absence of light from the outside world. The circadian rhythm period of the body clock is approximately 24 h, not exactly 24 h, so each morning's exposure to light resets the body clock and aligns it with

the external day-night cycle. In this review, we will discuss the inputs to the SCN, the networks within the SCN, the outputs from the SCN, and the effects of stimuli other than light on circadian rhythms, particularly the olfactory system.

Inputs to the SCN

There are three major inputs to the SCN (Abrahamson and Moore, 2001; Reghunandanan and Reghunandanan, 2006; Morin, 2013) (Figure 1). The most important input is from the retina through the retinohypothalamic tract (RHT) to the ventral core region of the SCN which is thought to provide input primarily to vasoactive intestinal polypeptide (VIP)-positive and gastrin-releasing peptide (GRP)-positive neurons (Lokshin et al., 2015). Loss of melanopsin-containing intrinsically photosensitive retinal ganglion cells (ipRGCs, Opn4+) that form the RHT, abolishes circadian photoentrainment (Güler et al., 2008), suggesting that ipRGCs are essential for photoentrainment. The major neurotransmitters are thought to be glutamate and PACAP (Hannibal, 2002, 2021), and the glutamatergic input is mediated by AMPA and NMDA receptors (Kim and Dudek, 1991).

The second is the geniculohypothalamic input via the thalamic intergeniculate leaflet, which also originates from the retina. The third is serotonergic input from the raphe nuclei, which enters the ventral region of the SCN (Abrahamson and Moore, 2001). Serotonin receptors (5-$HT_{1A, 2A, 2B, 2C, 5A, 7}$) are expressed in the SCN (Moyer and Kennaway, 1999; Takeuchi et al., 2014). Other inputs come from other hypothalamic areas that can modulate the activity of the SCN. The circadian rhythm of the SCN is thought to be altered by sleep, wakefulness, animal state, and external conditions but either the pathway and mechanism are unknown (Deboer et al., 2003, 2007).

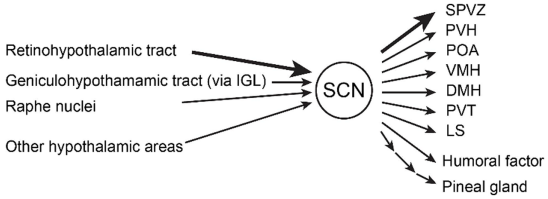

FIGURE 1
Inputs and outputs of the suprachiasmatic nucleus (SCN). The major inputs to the SCN are (1) the retinohypothalamic tract from melanopsin-containing photosensitive ganglion cells in the retina, (2) the geniculohypothalamic tract via the intergeniculate leaflet (IGL), and (3) the median raphe nuclei containing serotonergic neurons. Other hypothalamic areas (arcuate nucleus, medial preoptic area) and thalamic areas (paraventricular thalamic nuclei) also project to the SCN. Humoral factors such as hormones also modulate the SCN. The major outputs of the SCN are (1) subparaventricular zone (SPVZ), (2) paraventricular hypothalamic nucleus (PVH), (3) preoptic area (POA), (4) ventromedial hypothalamic nucleus (VMH), (5) dorsomedial hypothalamic nucleus (DMH), (6) paraventricular thalamic nuclei (PVT), and (7) lateral septum (LS). Other outputs include humoral factor and pineal gland polysynaptically (Abrahamson and Moore, 2001; Saper et al., 2005; Starnes and Jones, 2023).

Inside the SCN

The two of the major neuronal subtypes in the SCN are VIP-positive neurons in the ventrolateral region, also known as the core region, and AVP-positive neurons in the dorsomedial, or shell, region (Abrahamson and Moore, 2001). VIP-positive neurons receive direct projection from the retina (Todd et al., 2020) and are thought to shift the phases of the circadian rhythm. Spontaneous Ca^{2+} activity of VIP neurons is higher during daytime and subjective daytime (Jones et al., 2018). VIP neuron intracellular Ca^{2+} is increased by light stimulation of the retina (Jones et al., 2018; Todd et al., 2020). Suppression of VIP neurons abolished the phase shift induced by light pulses (Jones et al., 2018). Diphtheria toxin ablation of VIP neurons disrupted the light-entrained rhythm of locomotor activity (Todd et al., 2020). All of these results suggest that SCN VIP neurons play an important role in light entrainment. In addition, because VIP or VIP receptor, VPAC2, knock-out mice show either arrhythmicity, multiple circadian periods, or a shorter single period in locomotor activity (home-cage activity) or wheel-running activity (Harmar et al., 2002; Colwell et al., 2003; Hughes et al., 2004; Aton et al., 2005; Peng et al., 2022), the VIP peptide itself is important for synchronizing circadian rhythmicity within the SCN and animal behavior.

AVP-positive neurons are important in determining the period of the circadian rhythm. Knockout of the clock gene Bmal1 specifically in AVP neurons impaired the behavioral circadian rhythm (Mieda et al., 2015). The clock proteins CLOCK (circadian locomotor output cycles kaput) and BMAL1 (basic helix–loop–helix ARNT-like protein 1 or ARNTL, aryl hydrocarbon receptor nuclear translocator-like protein 1) are key transcription factors that form a heteromer and bind regulatory elements E-boxes to express the clock proteins PER1, PER2, CRY1, CRY2, which in turn inhibit CLOCK-BMAL1, generating the approximately 24-h rhythm (Takahashi, 2017). This machinery is called the transcriptional translational feedback loop (TTFL), which is the core machinery of the molecular clock. Therefore, knocking out Bmal1 in AVP neurons disrupts the cellular clock of AVP neurons.

Casein kinase 1 delta (CK1δ) regulates the nuclear translocation and degradation of the clock proteins PER and CRY. Therefore, the loss of CK1δ elongates the cellular circadian period (Etchegaray et al., 2009, 2010). AVP neuron-specific knockout of CK1δ prolonged the period of the behavioral circadian rhythm (Mieda et al., 2016). In addition, knockout of CK1δ specifically in AVP neurons prolonged the period of the Ca^{2+} activity circadian rhythm in both AVP neurons and VIP neurons (Tsuno et al., 2023). This suggests that AVP neurons regulate the period of the circadian rhythm of the entire SCN. However, since the period of the circadian rhythm was not altered by loss of GABA release (Maejima et al., 2021) or AVP release (Tsuno et al., 2023) specifically in AVP neurons, it is likely that neurotransmitters other than GABA and AVP are responsible for the period regulation of the SCN ensemble circadian rhythm and locomotion by AVP neurons, and further studies are needed to identify the mechanism.

In addition to AVP neurons and VIP neurons, the SCN contains neurons that express a variety of neuropeptides. For example, CCK-positive neurons in mice have a peak in Ca^{2+} activity 5 h before the onset of locomotor activity under different light/dark conditions, suggesting that they may determine the onset of locomotion (Xie et al., 2023). Prok2-positive neurons have a peak in Ca^{2+} activity in the

middle of the day (Onodera et al., 2023), which may inhibit locomotor output (Cheng et al., 2002). Abrahamson and Moore showed that ventral core neurons contain GABA, VIP, gastrin-releasing peptide (GRP), neurotensin (NT), calretinin (CALR), and calbindin (CALB), whereas the dorsal shell neurons contain GABA, AVP, met-enkephalin (mENK), angiotensin II (AII), and CALB (Abrahamson and Moore, 2001). Recent single-cell transcriptomic analyses have shown that the SCN neurons can be classified into 5 (Park et al., 2016; Wen et al., 2020), 11 (Morris et al., 2021) or 12 subtypes (Xu et al., 2021). Park et al. (2016) classified 5 groups of neurons, VIP+, AVP+/VIPR2+, PACAP+/Prok2+, PACAPR+, and others. Wen et al. (2020) classified 5 groups, Vip+/Nms+, Avp+/Nms+, Cck+/C1ql3+, Cck+/Bdnf+, and Grp+/Vip+. Morris et al. (2021) classified 11 neuronal subpopulations, 8 groups in day and 8 groups in night including 5 overlapping groups. Xu et al. (2021) classified 12 groups, 4 AVP+, 3 VIP+, 2 CCK+, and 3 unknown groups. One of 4 AVP+ groups by Xu et al. strongly correlated with the Cck+/C1ql3+ group by Wen et al., while another 3 of 4 AVP+ groups significantly correlated with the Avp+/Nms+group. In addition, 1 of 3 VIP+ groups by Xu et al. correlated with the Vip+/Nms+group by Wen et al., while another 1 VIP+ group correlated with the Grp+/Vip+group. Finally, 1 of 2 CCK+ groups correlated with the Cck+/Bdnf+ group (Wen et al., 2020; Xu et al., 2021). Further studies are needed to elucidate the function of each cell type and the interactions between them.

Output from the SCN

Output from the SCN is primarily to other hypothalamic nuclei and the thalamus (Abrahamson and Moore, 2001; Saper et al., 2005; Reghunandanan and Reghunandanan, 2006; Morin, 2013; Starnes and Jones, 2023). Many projections from the SCN terminate in the subparaventricular zone (SPVZ, projecting DMH), adjacent to the dorsal SCN. Other major projections include the paraventricular hypothalamic nucleus (PVH, including the pituitary–adrenal axis), the preoptic area [POA, a critical area of thermoregulation (Nakamura et al., 2022) and one of non-REM sleep centers (Scammell et al., 2017)], and other hypothalamic nuclei that control instinctive behavior and homeostasis such as feeding, energy metabolism, sleep/wakefulness, and motivated behavior, including the ventromedial hypothalamic nucleus (VMH, projecting SPVZ), dorsomedial hypothalamic nucleus (DMH), paraventricular thalamic nuclei (PVT), and lateral septum (LS). The SCN inhibits the pineal gland, which produces melatonin with sleep-inducing properties, via the PVH, the intermediolateral nucleus of the medulla (IML), and the cervical sympathetic ganglion (Tonon et al., 2021).

Olfaction and circadian rhythms

There are reports suggesting a relationship between the olfactory system and circadian rhythms. Almost every cell in the body can generate circadian rhythms, with the SCN acting as a master pacemaker to synchronize and entrain the peripheral clock (Reppert and Weaver, 2002; Takahashi, 2017). The olfactory bulb (OB), the first center of olfactory information processing, is thought to be capable of generating circadian rhythms. In slices, the OB maintains a circadian rhythm of Per1 expression, recorded by the Per1-Luc reporter, and neuronal firing activity in rats (Granados-Fuentes et al., 2004) or Per2 expression by the Per2::Luc reporter in mice (Ono et al., 2015), suggesting that the OB can generate its own circadian rhythm. However, the phase of the rhythm is easily altered by external perturbations, as the peak of Per2::Luc varies with the cutting time (Ono et al., 2015). Furthermore, the SCN lesions alter (Abraham et al., 2005) or eliminate (Ono et al., 2015) the peak phase of clock gene expression in the OB. These results suggest that the OB expresses clock genes and can generate circadian rhythms. However, without the SCN, the peaks become desynchronized with the whole body, indicating a hierarchical structure with the SCN as the central clock.

Some reports suggest that the daily rhythm of the olfactory function is influenced by both the SCN and the OB. Granados-Fuentes et al. reported in 2006 that the cedar oil-induced daily rhythm of c-Fos expression remained in the OB and piriform cortex after SCN removal, whereas it disappeared in the piriform cortex after OB ablation, suggesting that the OB generates the rhythm. Granados-Fuentes et al. (2011) reported that the SCN lesion altered the peak phases of the daily rhythm of olfactory discrimination performance (Granados-Fuentes et al., 2011). In addition, Takeuchi et al. reported in 2023 that knockout of Bmal1 in Vgat-positive neurons, including SCN neurons, altered the peak phase of the circadian rhythm of odor-induced c-fos positive cell number in the piriform cortex (Takeuchi et al., 2023). These results indicate that the SCN alters the peak phase of olfactory function, suggesting that it contributes to the synchronization of the circadian rhythms of olfactory function and the central clock.

Clock gene expression itself is important for odor detection. Granados-Fuentes et al. (2011) reported that there is a daily rhythm in the performance and sensitivity of the odor detection task that disappears when the clock genes *Bmal1* or both *Per1* and *Per2* genes are knocked out (Granados-Fuentes et al., 2011). Takeuchi et al. report that Bmal1 knockout in the piriform cortex abolishes the circadian rhythm of the odor-evoked activity (Takeuchi et al., 2023). Using quantitative PCR, they report that the circadian rhythm of gene expression observed in the piriform cortex is dependent on Bmal1 expression in Emx-positive cells, including pyramidal cells in the piriform cortex (Takeuchi et al., 2023). These results suggest that the circadian rhythm of odor detection and odor-evoked neural activity requires clock genes.

The mechanism by which the SCN modulates the circadian rhythm of the OB is not yet clear. It is known that the SCN projects to various hypothalamic regions and releases neurotransmitters, including neuropeptides, and hormones, while the OB receives centrifugal inputs from the olfactory cortex and neuromodulatory centers and is also influenced by neuropeptides and hormones (Brunert and Rothermel, 2021). Therefore, it is possible that the SCN can alter the circadian rhythm of the OB through centrifugal inputs from the olfactory cortex or neuromodulatory centers via the hypothalamus, neuromodulatory inputs, and neuropeptides, or hormones in the bloodstream.

Conversely, there is some evidence that the olfactory system can modify the activity of the SCN via the OB. Amir et al. (1999) reported that light-induced c-Fos expression in the SCN is enhanced by olfactory stimuli. Removal of the OB also altered the time of re-entrainment and altered the phase of the odor-evoked c-Fos expression rhythm in the SCN (Granados-Fuentes et al., 2006). Because odor stimulation increased c-Fos expression in the

paraventricular thalamic nucleus (PVT) (Amir et al., 1999), a review has argued that the PVT may be related to the pathway from the OB to the SCN (Jeffs et al., 2023).

Discussion

Although the basic mechanisms of circadian rhythm control are becoming clearer, much remains unknown about how the individual subpopulations within the SCN interact to generate a synchronized circadian rhythm as an ensemble. Furthermore, although circadian rhythms are closely linked to the sleep–wake cycle (Franken and Dijk, 2024), the interaction between the SCN and the sleep–wake center remains elusive. Although the modulation of circadian rhythms by light stimulation has been well studied, the modulation of circadian rhythms by environmental changes other than light has not been fully investigated, and further research is needed.

The SCN, the center of the circadian rhythm, modulates the rhythm in response to external conditions. In addition to light, possible conditions include food availability, the presence of predators, and environmental temperature, which in turn affect the wake–sleep states and the brain's information processing mode (Pickel and Sung, 2020; Franken and Dijk, 2024). From this perspective, the olfactory system, which is important for feeding, finding mates, and escaping predators, is thought to be closely related to circadian rhythms and wake–sleep states (Mori and Sakano, 2022). Because the OB has the unique property of generating a circadian rhythm without the SCN, investigating the relationship between diurnal variation in olfactory information processing and circadian rhythms of the SCN is an interesting target for future research. In addition, a reduced sense of smell and instability of the wake–sleep rhythm are two prominent features of Alzheimer's disease (AD), so both may be easily impaired and may be an indicator of preclinical AD (Jeffs et al., 2023).

Author contributions

YT: Conceptualization, Funding acquisition, Writing – original draft, Writing – review & editing. MM: Conceptualization, Funding acquisition, Writing – original draft, Writing – review & editing.

Funding

The author(s) declare financial support was received for the research, authorship, and/or publication of this article. This work was supported in part by JSPS KAKENHI Grant Numbers JP23K06345 (YT); JP22H02802 (MM).

Conflict of interest

The authors declare that the research was conducted in the absence of any commercial or financial relationships that could be construed as a potential conflict of interest.

The author(s) declared that they were an editorial board member of Frontiers, at the time of submission. This had no impact on the peer review process and the final decision.

Publisher's note

References

Abraham, U., Prior, J. L., Granados-Fuentes, D., Piwnica-Worms, D. R., and Herzog, E. D. (2005). Independent circadian oscillations of Period1 in specific brain areas in vivo and in vitro. *J. Neurosci.* 25, 8620–8626. doi: 10.1523/JNEUROSCI.2225-05.2005

Abrahamson, E. E., and Moore, R. Y. (2001). Suprachiasmatic nucleus in the mouse: retinal innervation, intrinsic organization and efferent projections. *Brain Res.* 916, 172–191. doi: 10.1016/s0006-8993(01)02890-6

Amir, S., Cain, S., Sullivan, J., Robinson, B., and Stewart, J. (1999). In rats, odor-induced Fos in the olfactory pathways depends on the phase of the circadian clock. *Neurosci. Lett.* 272, 175–178. doi: 10.1016/S0304-3940(99)00609-6

Aton, S. J., Colwell, C. S., Harmar, A. J., Waschek, J., and Herzog, E. D. (2005). Vasoactive intestinal polypeptide mediates circadian rhythmicity and synchrony in mammalian clock neurons. *Nat. Neurosci.* 8, 476–483. doi: 10.1038/nn1419

Brunert, D., and Rothermel, M. (2021). Extrinsic neuromodulation in the rodent olfactory bulb. *Cell Tissue Res.* 383, 507–524. doi: 10.1007/s00441-020-03365-9

Cheng, M. Y., Bullock, C. M., Li, C., Lee, A. G., Bermak, J. C., Belluzzi, J., et al. (2002). Prokineticin 2 transmits the behavioural circadian rhythm of the suprachiasmatic nucleus. *Nature* 417, 405–410. doi: 10.1038/417405a

Colwell, C. S., Michel, S., Itri, J., Rodriguez, W., Tam, J., Lelievre, V., et al. (2003). Disrupted circadian rhythms in VIP- and PHI-deficient mice. *Am. J. Physiol. Regul. Integr. Comp. Physiol.* 285, R939–R949. doi: 10.1152/ajpregu.00200.2003

Deboer, T., Détári, L., and Meijer, J. H. (2007). Long term effects of sleep deprivation on the mammalian circadian pacemaker. *Sleep* 30, 257–262. doi: 10.1093/sleep/30.3.257

Deboer, T., Vansteensel, M. J., Détári, L., and Meijer, J. H. (2003). Sleep states alter activity of suprachiasmatic nucleus neurons. *Nat. Neurosci.* 6, 1086–1090. doi: 10.1038/nn1122

Etchegaray, J.-P., Machida, K. K., Noton, E., Constance, C. M., Dallmann, R., Di Napoli, M. N., et al. (2009). Casein kinase 1 Delta regulates the pace of the mammalian circadian clock. *Mol. Cell. Biol.* 29, 3853–3866. doi: 10.1128/mcb.00338-09

Etchegaray, J. P., Yu, E. A., Indic, P., Dallmann, R., and Weaver, D. R. (2010). Casein kinase 1 delta (CK1) regulates period length of the mouse suprachiasmatic circadian clock in vitro. *PLoS One* 5:e10303. doi: 10.1371/journal.pone.0010303

Franken, P., and Dijk, D. J. (2024). Sleep and circadian rhythmicity as entangled processes serving homeostasis. *Nat. Rev. Neurosci.* 25, 43–59. doi: 10.1038/s41583-023-00764-z

Granados-Fuentes, D., Ben-Josef, G., Perry, G., Wilson, D. A., Sullivan-Wilson, A., and Herzog, E. D. (2011). Daily rhythms in olfactory discrimination depend on clock genes but not the suprachiasmatic nucleus. *J. Biol. Rhythm.* 26, 552–560. doi: 10.1177/0748730411420247

Granados-Fuentes, D., Saxena, M. T., Prolo, L. M., Aton, S. J., and Herzog, E. D. (2004). Olfactory bulb neurons express functional, entrainable circadian rhythms. *Eur. J. Neurosci.* 19, 898–906. doi: 10.1111/j.1460-9568.2004.03117.x

Granados-Fuentes, D., Tseng, A., and Herzog, E. D. (2006). A circadian clock in the olfactory bulb controls olfactory responsivity. *J. Neurosci.* 26, 12219–12225. doi: 10.1523/JNEUROSCI.3445-06.2006

Güler, A. D., Ecker, J. L., Lall, G. S., Haq, S., Altimus, C. M., Liao, H.-W., et al. (2008). Melanopsin cells are the principal conduits for rod–cone input to non-image-forming vision. *Nature* 453, 102–105. doi: 10.1038/nature06829

Hannibal, J. (2002). Neurotransmitters of the retino-hypothalamic tract. *Cell Tissue Res.* 309, 73–88. doi: 10.1007/s00441-002-0574-3

Hannibal, J. (2021). Comparative neurology of circadian photoreception: the retinohypothalamic tract (RHT) in sighted and naturally blind mammals. *Front. Neurosci.* 15:640113. doi: 10.3389/fnins.2021.640113

Harmar, A. J., Marston, H. M., Shen, S., Spratt, C., West, K. M., Sheward, W. J., et al. (2002). The VPAC(2) receptor is essential for circadian function in the mouse suprachiasmatic nuclei. *Cell* 109, 497–508. doi: 10.1016/s0092-8674(02)00736-5

Hastings, M. H., Maywood, E. S., and Brancaccio, M. (2018). Generation of circadian rhythms in the suprachiasmatic nucleus. *Nat. Rev. Neurosci.* 19, 453–469. doi: 10.1038/s41583-018-0026-z

Hughes, A. T., Fahey, B., Cutler, D. J., Coogan, A. N., and Piggins, H. D. (2004). Aberrant gating of photic input to the suprachiasmatic circadian pacemaker of mice lacking the VPAC $_2$ receptor. *J. Neurosci.* 24, 3522–3526. doi: 10.1523/JNEUROSCI.5345-03.2004

Jeffs, Q. L., Prather, J. F., and Todd, W. D. (2023). Potential neural substrates underlying circadian and olfactory disruptions in preclinical Alzheimer's disease. *Front. Neurosci.* 17:1295998. doi: 10.3389/fnins.2023.1295998

Jones, J. R., Simon, T., Lones, L., and Herzog, E. D. (2018). SCN VIP neurons are essential for normal light-mediated resetting of the circadian system. *J. Neurosci.* 38, 7986–7995. doi: 10.1523/JNEUROSCI.1322-18.2018

Kim, Y. I., and Dudek, F. E. (1991). Intracellular electrophysiological study of suprachiasmatic nucleus neurons in rodents: excitatory synaptic mechanisms. *J. Physiol.* 444, 269–287. doi: 10.1113/jphysiol.1991.sp018877

Lokshin, M., LeSauter, J., and Silver, R. (2015). Selective distribution of retinal input to mouse SCN revealed in analysis of sagittal sections. *J. Biol. Rhythm.* 30, 251–257. doi: 10.1177/0748730415584058

Maejima, T., Tsuno, Y., Miyazaki, S., Tsuneoka, Y., Hasegawa, E., Islam, M. T., et al. (2021). GABA from vasopressin neurons regulates the time at which suprachiasmatic nucleus molecular clocks enable circadian behavior. *Proc. Natl. Acad. Sci.* 118:e2010168118. doi: 10.1073/pnas.2010168118

Mieda, M., Okamoto, H., and Sakurai, T. (2016). Manipulating the cellular circadian period of arginine vasopressin neurons alters the behavioral circadian period. *Curr. Biol.* 26, 2535–2542. doi: 10.1016/j.cub.2016.07.022

Mieda, M., Ono, D., Hasegawa, E., Okamoto, H., Honma, K., Ichi Honma, S., et al. (2015). Cellular clocks in AVP neurons of the SCN are critical for interneuronal coupling regulating circadian behavior rhythm. *Neuron* 85, 1103–1116. doi: 10.1016/j.neuron.2015.02.005

Mori, K., and Sakano, H. (2022). Neural circuitry for stress information of environmental and internal odor worlds. *Front. Behav. Neurosci.* 16:943647. doi: 10.3389/fnbeh.2022.943647

Morin, L. P. (2013). Neuroanatomy of the extended circadian rhythm system. *Exp. Neurol.* 243, 4–20. doi: 10.1016/j.expneurol.2012.06.026

Morris, E. L., Patton, A. P., Chesham, J. E., Crisp, A., Adamson, A., and Hastings, M. H. (2021). Single-cell transcriptomics of suprachiasmatic nuclei reveal a Prokineticin-driven circadian network. *EMBO J.* 40, e108614–e108623. doi: 10.15252/embj.2021108614

Moyer, R. W., and Kennaway, D. J. (1999). Immunohistochemical localization of serotonin receptors in the rat suprachiasmatic nucleus. *Neurosci. Lett.* 271, 147–150. doi: 10.1016/S0304-3940(99)00536-4

Nakamura, K., Nakamura, Y., and Kataoka, N. (2022). A hypothalamomedullary network for physiological responses to environmental stresses. *Nat. Rev. Neurosci.* 23, 35–52. doi: 10.1038/s41583-021-00532-x

Ono, D., Honma, S., and Honma, K. ichi (2015). Circadian PER2: LUC rhythms in the olfactory bulb of freely moving mice depend on the suprachiasmatic nucleus but not on behaviour rhythms. *Eur. J. Neurosci.* 42, 3128–3137. doi: 10.1111/ejn.13111

Onodera, K., Tsuno, Y., Hiraoka, Y., Tanaka, K., Maejima, T., and Mieda, M. (2023). In vivo recording of the circadian calcium rhythm in Prokineticin 2 neurons of the suprachiasmatic nucleus. *Sci. Rep.* 13:16974. doi: 10.1038/s41598-023-44282-5

Park, J., Zhu, H., O'Sullivan, S., Ogunnaike, B. A., Weaver, D. R., Schwaber, J. S., et al. (2016). Single-cell transcriptional analysis reveals novel neuronal phenotypes and interaction networks involved in the central circadian clock. *Front. Neurosci.* 10:481. doi: 10.3389/fnins.2016.00481

Peng, Y., Tsuno, Y., Matsui, A., Hiraoka, Y., Tanaka, K., Horike, S., et al. (2022). Cell type-specific genetic manipulation and impaired circadian rhythms in Vip tTA Knock-in mice. *Front. Physiol.* 13:895633. doi: 10.3389/fphys.2022.895633

Pickel, L., and Sung, H.-K. (2020). Feeding rhythms and the circadian regulation of metabolism. *Front. Nutr.* 7:39. doi: 10.3389/fnut.2020.00039

Reghunandanan, V., and Reghunandanan, R. (2006). Neurotransmitters of the suprachiasmatic nuclei. *J. Circadian Rhythms* 4:2. doi: 10.1186/1740-3391-4-2

Reppert, S. M., and Weaver, D. R. (2002). Coordination of circadian timing in mammals. *Nature* 418, 935–941. doi: 10.1038/nature00965

Saper, C. B., Scammell, T. E., and Lu, J. (2005). Hypothalamic regulation of sleep and circadian rhythms. *Nature* 437, 1257–1263. doi: 10.1038/nature04284

Scammell, T. E., Arrigoni, E., and Lipton, J. O. (2017). Neural circuitry of wakefulness and sleep. *Neuron* 93, 747–765. doi: 10.1016/j.neuron.2017.01.014

Starnes, A. N., and Jones, J. R. (2023). Inputs and outputs of the mammalian circadian clock. *Biology (Basel)* 12:508. doi: 10.3390/biology12040508

Takahashi, J. S. (2017). Transcriptional architecture of the mammalian circadian clock. *Nat. Rev. Genet.* 18, 164–179. doi: 10.1038/nrg.2016.150

Takeuchi, K., Mohammad, S., Ozaki, T., Morioka, E., Kawaguchi, K., Kim, J., et al. (2014). Serotonin-2C receptor involved serotonin-induced ca 2+ mobilisations in neuronal progenitors and neurons in rat suprachiasmatic nucleus. *Sci. Rep.* 4:4106. doi: 10.1038/srep04106

Takeuchi, S., Shimizu, K., Fukada, Y., and Emoto, K. (2023). The circadian clock in the piriform cortex intrinsically tunes daily changes of odor-evoked neural activity. *Commun. Biol.* 6:332. doi: 10.1038/s42003-023-04691-8

Todd, W. D., Venner, A., Anaclet, C., Broadhurst, R. Y., De Luca, R., Bandaru, S. S., et al. (2020). Suprachiasmatic VIP neurons are required for normal circadian rhythmicity and comprised of molecularly distinct subpopulations. *Nat. Commun.* 11:4410. doi: 10.1038/s41467-020-17197-2

Tonon, A. C., Pilz, L. K., Markus, R. P., Hidalgo, M. P., and Elisabetsky, E. (2021). Melatonin and depression: a translational perspective from animal models to clinical studies. *Front. Psych.* 12:638981. doi: 10.3389/fpsyt.2021.638981

Tsuno, Y., Peng, Y., Horike, S., Wang, M., Matsui, A., Yamagata, K., et al. (2023). In vivo recording of suprachiasmatic nucleus dynamics reveals a dominant role of arginine vasopressin neurons in circadian pacesetting. *PLoS Biol.* 21:e3002281. doi: 10.1371/journal.pbio.3002281

Wen, S., Ma, D., Zhao, M., Xie, L., Wu, Q., Gou, L., et al. (2020). Spatiotemporal single-cell analysis of gene expression in the mouse suprachiasmatic nucleus. *Nat. Neurosci.* 23, 456–467. doi: 10.1038/s41593-020-0586-x

Xie, L., Xiong, Y., Ma, D., Shi, K., Chen, J., Yang, Q., et al. (2023). Cholecystokinin neurons in mouse suprachiasmatic nucleus regulate the robustness of circadian clock. *Neuron* 111, 2201–2217.e4. doi: 10.1016/j.neuron.2023.04.016

Xu, P., Berto, S., Kulkarni, A., Jeong, B., Joseph, C., Cox, K. H., et al. (2021). NPAS4 regulates the transcriptional response of the suprachiasmatic nucleus to light and circadian behavior. *Neuron* 109, 3268–3282.e6. doi: 10.1016/j.neuron.2021.07.026

frontiers | Frontiers in Neural Circuits

TYPE Mini Review
PUBLISHED 29 April 2024
DOI 10.3389/fncir.2024.1409994

OPEN ACCESS

EDITED BY
Kensaku Mori,
RIKEN, Japan

REVIEWED BY
Takefumi Kikusui,
Azabu University, Japan

*CORRESPONDENCE
Kazushige Touhara
ktouhara@g.ecc.u-tokyo.ac.jp

RECEIVED 31 March 2024
ACCEPTED 15 April 2024
PUBLISHED 29 April 2024

CITATION
Murata K, Itakura T and Touhara K (2024) Neural basis for pheromone signal transduction in mice.
Front. Neural Circuits 18:1409994.
doi: 10.3389/fncir.2024.1409994

Neural basis for pheromone signal transduction in mice

Ken Murata[1], Takumi Itakura[1,2] and Kazushige Touhara[1]*

[1]Laboratory of Biological Chemistry, Graduate School of Agricultural and Life Sciences, Department of Applied Biological Chemistry, The University of Tokyo, Tokyo, Japan, [2]Division of Biology and Biological Engineering, TianQiao and Chrissy Chen Institute for Neuroscience, California Institute of Technology, Pasadena, CA, United States

Pheromones are specialized chemical messengers used for inter-individual communication within the same species, playing crucial roles in modulating behaviors and physiological states. The detection mechanisms of these signals at the peripheral organ and their transduction to the brain have been unclear. However, recent identification of pheromone molecules, their corresponding receptors, and advancements in neuroscientific technology have started to elucidate these processes. In mammals, the detection and interpretation of pheromone signals are primarily attributed to the vomeronasal system, which is a specialized olfactory apparatus predominantly dedicated to decoding socio-chemical cues. In this mini-review, we aim to delineate the vomeronasal signal transduction pathway initiated by specific vomeronasal receptor-ligand interactions in mice. First, we catalog the previously identified pheromone ligands and their corresponding receptor pairs, providing a foundational understanding of the specificity inherent in pheromonal communication. Subsequently, we examine the neural circuits involved in processing each pheromone signal. We focus on the anatomical pathways, the sexually dimorphic and physiological state-dependent aspects of signal transduction, and the neural coding strategies underlying behavioral responses to pheromonal cues. These insights provide further critical questions regarding the development of innate circuit formation and plasticity within these circuits.

KEYWORDS

pheromone, vomeronasal system, hypothalamus, innate behavior, neural circuit

Introduction

Animals utilize chemosensory signals, which are crucial for mediating a range of behaviors involved in survival and reproduction (Wyatt, 2014). These signals are encapsulated in biochemical compounds known as pheromones, which facilitate intraspecific communication (Karlson and Lüscher, 1959). Pheromones are principally detected by two sensory systems: the main olfactory system and the vomeronasal system (Baum and Cherry, 2015; Tirindelli, 2021). The main olfactory system is responsible for detecting volatile pheromones, while the vomeronasal system is particularly attuned to decoding social cues embedded within these signals (Holy, 2018). Such cues encompass a range of biological information, including species, sex, developmental stage, health status, and reproductive condition of conspecifics. A variety of vomeronasal ligands carrying this intricate information have been identified, indicating a complex and diverse chemosensory communication network among animals (Murata and Touhara, 2021). Vomeronasal receptors (VRs), which are a subset of the G protein-coupled receptor (GPCR) superfamily, are specialized for the detection of these chemosensory signals (Silva and Antunes, 2017).

These receptors translate the chemical information from ligands into a biological response through dedicated signal transduction pathways, ultimately leading to behavioral or physiological responses.

Vomeronasal ligands, receptors, and functions

VRs are expressed in vomeronasal sensory neurons (VSNs) of the vomeronasal organ (VNO): a tubular organ located in the base of the nasal septum (Døving and Trotier, 1998). These receptors are categorized into two principal classes: V1Rs and V2Rs (Figure 1). Mice have approximately 240 V1R genes and 120 V2R genes (Young and Trask, 2007; Miller et al., 2020). Each of these receptor types has a distinct structure and function. V1Rs are members of the rhodopsin-type GPCR family and are typically coupled with the G protein Gαi2 (Trouillet et al., 2019). They are generally involved in detecting small molecule ligands, such as volatile compounds and steroid derivatives (Lee et al., 2019; Wong et al., 2020). In mice, V1Rs are expressed in the apical layer of the VNO and are responsible for recognizing a variety of urinary molecules that convey information about sex and physiological states (Doyle and Meeks, 2018). V2Rs belong to the class C GPCR family and are associated with the G protein Gαo (Chamero et al., 2011). V2Rs have a large extracellular domain that is thought to be involved in ligand recognition. They are primarily expressed in the basal layer of the VNO and are tuned to detect larger molecules such as peptides and proteins (Pérez-Gómez et al., 2014).

Each VSN expresses only one or a restricted few VRs, which allows for a highly specific response to particular chemosensory cues (Nikaido, 2019). When a VR binds to its ligand, it initiates a cascade of intracellular events that lead to the opening of ion channels, and ultimately results in the generation of action potentials (Yu, 2015). These electrical signals are then transmitted to the brain, where they are processed into behavioral responses.

The transient receptor potential channel 2 (Trpc2) is specifically expressed in the VNO and plays a critical role in signal transduction (Figure 1). The disruption of Trpc2 significantly diminishes the responsiveness of VSNs, leading to marked alterations in a spectrum of social behaviors, such as inter-male and maternal aggression, basically because of impairment of sex recognition (Leypold et al., 2002; Stowers et al., 2002; Kimchi et al., 2007). The role of Trpc2 in parental behavior is somewhat controversial. In one report, Trpc2-KO virgin male mice show marked reduction in pup-directed aggression, and even exhibit parental care (Wu et al., 2014). Conversely, other research underscores the relevance of Trpc2 in maternal behaviors (Fraser and Shah, 2014). Moreover, it is currently unclear whether the phenotypic manifestations observed in Trpc2-KO models are solely attributable to compromised vomeronasal signaling or whether they may also be a consequence of perturbations in the developmental processes. Indeed, some studies have implied the significance of the vomeronasal input during the development in terms of gene expression, anatomy, and behaviors (Cross et al., 2021; Pfau et al., 2023).

The ligands for vomeronasal receptors are diverse and are often species-specific molecules involved in social communication. A

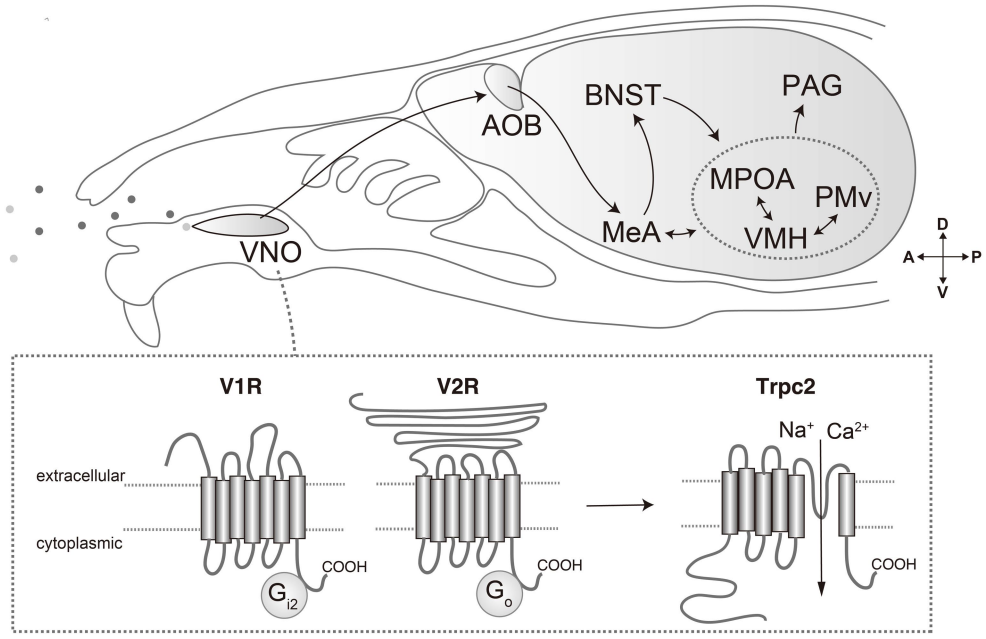

FIGURE 1
Pheromone molecules are received by vomeronasal receptors expressed in vomeronasal organ (VNO). Vomeronasal receptors are mainly categorized into V1R and V2R, which are coupled with Gi2 and Go, respectively. Activation of receptors results in opening of transient receptor potential channel 2 (Trpc2), generating action potentials. The signals are transmitted to the accessory olfactory bulb, and then to the medial amygdala (MeA) and bed nucleus of the stria terminalis (BNST). From there, pheromone signals are transmitted to the hypothalamus, such as medial preoptic area (MPOA), ventromedial hypothalamus (VMH) and ventral premammillary nucleus (PMv). From the hypothalamus, processed information is conveyed to downstream motor effector areas through the mesencephalic periaqueductal gray (PAG).

prominent class of these ligands is the exocrine gland-secreting peptide (ESP) family (Kimoto et al., 2005). This group comprises species-specific peptide ligands that have undergone evolutionary divergence from the α-globin gene in rodent species (Niimura et al., 2020). ESPs are synthesized and secreted by various exocrine glands and are subsequently detected by a subset of the V2R receptor class (Kimoto et al., 2007). The differential secretion patterns of ESPs by sex and genetic strain enable the transmission of critical information regarding an individual's sex and unique identity. One notable peptide, ESP1, secreted by the extraorbital lacrimal gland of male mice, is received by Vmn2r116 and enhances female sexual receptivity and inter-male aggression (Haga et al., 2010; Hattori et al., 2016). Conversely, ESP22, found in the tear fluid of juvenile mice, acts through Vmn2r115—a receptor closely homologous to Vmn2r116—and suppresses sexual behavior in both adult male and female mice (Ferrero et al., 2013; Osakada et al., 2018).

Another significant class of vomeronasal ligands is Major Urinary Proteins (MUPs), primarily found in the urine of rodents (Hurst and Beynon, 2004). MUPs bind to and gradually release volatile molecules that are detected by the V1Rs (Leinders-Zufall et al., 2000). Concurrently, MUPs themselves act as agonists for V2Rs (Chamero et al., 2007). Since each mouse strain secretes specific patterns of MUPs and males release more MUPs than females, MUPs are implicated in behaviors associated with territorial demarcation and individual recognition (Roberts et al., 2012). Notably, MUP3 and MUP20 have been identified as having an aggression-promoting effect in mice (Kaur et al., 2014). Although the V2Rs for MUPs have yet to be identified, electrophysiological recordings from putative V2R-expressing VSNs have suggested that a diverse array of V2R subtypes interact with MUPs in a complex manner: some demonstrating specificity to individual MUPs, while others respond to multiple MUP isoforms. The mechanism by which this combinatorial receptor coding is interpreted by the downstream neural circuits is not understood.

Urine is a major source of vomeronasal ligands. The urine of female mice is rich in sulfated steroids, which are hormonal derivatives that act as ligands for V1Rs (Nodari et al., 2008; Isogai et al., 2011). Some VRs have been identified to bind sulfated steroids in a combinatorial manner. The presence of these V1R ligands in female urine may convey information regarding the female's reproductive status, such as estrous cycle phase, thereby enhancing sexual behavior in the male mouse (Haga-Yamanaka et al., 2014). On the other hand, the identification of VRs responsive to male urine has not been as fruitful. Neurons expressing Vmn2r53 in the VNO are activated by urine from males across different mouse strains (Itakura et al., 2022). Activation of Vmn2r53 has been associated with the promotion of inter-male aggressive behavior. The consistent activation of Vmn2r53 by urine from various strains of male mice suggests that its ligand is a robust marker of 'maleness' within the species.

Ligands for the vomeronasal system are not limited to species-specific molecules. For instance, hemoglobin from diverse species acts as a ligand for Vmn2r88 and has been shown to elevate digging and rearing behaviors in lactating female mice, although the ethological significance of these behaviors remains undetermined (Osakada et al., 2022).

The submandibular gland protein C (Smgc) from pups and female mice has been identified as a ligand for Vmn2r65 (Isogai et al., 2018). In virgin male mice, Vmn2r65, alongside Vmn2r88, appears to be partially required for the exhibition of infanticidal behavior. It is postulated that activation of certain vomeronasal receptor pairs is essential for the induction of infanticidal behavior, yet the precise receptor combinations that are sufficient for eliciting such behavior have not been fully elucidated.

The neural encoding of signals from VSNs expressing narrowly-tuned VRs is hypothesized to be interpreted by downstream neural circuits in a manner akin to a labeled-line model (Tye, 2018). The elucidation of this mechanism is anticipated to significantly enhance our understanding of the neural bases of innate behaviors. Further analysis of these neural circuits may also yield valuable insights into the general principles governing sensory information processing and the resultant behavioral manifestations.

Neural basis for vomeronasal signal transduction

The vomeronasal system is characterized by its distinct neural pathway through which sensory information from the VNO is transmitted to the hypothalamus (Figure 1) (Halpern, and Martínez-Marcos, 2003; Ishii and Touhara, 2019). The initial synaptic relay occurs at the accessory olfactory bulb (AOB), where the axons of VSNs responding to pheromonal stimuli converge upon multiple glomeruli (Mombaerts, 2004; Dulac and Wagner, 2006). Here, they establish synaptic connections with second-order neurons: mitral and tufted cells. These AOB neurons integrate VR signals to encode sexual and species-specific information (Hammen et al., 2014). Subsequently, this integrated signal is propagated to higher brain areas such as the medial amygdala (MeA) and the bed nucleus of the stria terminalis (BNST), which are pivotal in modulating socio-sexual behaviors through the processing of species- and sex-specific cues (Li et al., 2017; Yang et al., 2022).

The information is further transmitted from the MeA and BNST to the interconnected hypothalamic nuclei implicated in reproductive and aggressive behaviors: the ventromedial hypothalamus (VMH), medial preoptic area (MPOA), and ventral premammillary nucleus (PMv) (Choi et al., 2005). These hypothalamic neurons are characterized by distinctive patterns of gene expression and neural circuitry, which confer selective responsiveness to various stimuli. The functional specialization of these neuronal populations has been elucidated through various experimental methodologies, such as *in vivo* neural activity recording and the application of optogenetic or chemogenetic techniques, which have substantiated the unique role of these neurons in behavioral modulation. Notably, by leveraging Ca^{2+} imaging, neurons responsive to male and female signals are shown to be largely segregated from the VNO to the VMH (He et al., 2008; Hammen et al., 2014; Li et al., 2017; Remedios et al., 2017; Karigo et al., 2021; Yang et al., 2022).

The activity of the hypothalamic nuclei extends to the midbrain periaqueductal gray (PAG), a key structure in orchestrating various survival behaviors. The PAG integrates these signals and extends projections to additional brain regions responsible for the execution of motor functions (Falkner et al., 2020; Chen et al., 2021). This forms a comprehensive neural circuit that translates the detection of pheromonal signals into appropriate behavioral responses.

Recent studies have provided significant insights into the neurobiological underpinnings of intermale aggression. Specifically, a

cluster of neurons located within the ventrolateral part of the VMH (VMHvl), which express estrogen receptor type 1 (Esr1) and are henceforth referred to as VMHvl^{Esr1} neurons, have been identified as critical mediators of intermale aggressive behavior (Lin et al., 2011; Lee et al., 2014). The activity and sensitivity of VMHvl^{Esr1} neurons are dynamically modulated by sexual experience, which in turn affects the neural coding of sexual cues and can lead to the onset of aggressive responses (Remedios et al., 2017).

In female sexual behavior, a complex interaction between hormonal fluctuations and pheromonal cues is important. A subset of VMHvl^{Esr1} neurons, which express Cckar but not NPY2r, are both necessary for the initiation of and sufficient to induce sexual receptivity in females (Knoedler et al., 2022; Liu et al., 2022; Yin et al., 2022). This subset of neurons exists only in females and exhibits an increase in axonal projections to the anteroventral periventricular nucleus and changes neurophysiological properties during the estrous cycle (Inoue et al., 2019; Knoedler et al., 2022). These findings highlight the essential role of hormone-sensitive neurons within the VMHvl in regulating female sexual behaviors.

ESP1 has been shown to enhance female sexual receptivity, with its neural circuitry being extensively characterized (Figure 2) (Ishii et al., 2017). ESP1 is detected by Vmn2r116-positive VSNs, leading to the activation of the caudal part of the AOB. This triggers a cascade of neural activity that results in the activation of glutamatergic neurons within the MeA. Notably, the propagation of this neural signal does not proceed to the VMHvl as might be expected, but rather to the VMH dorsomedial part (VMHdm)—a region typically implicated in fear response modulation. Within the VMHdm, a subpopulation of neurons expressing the nuclear receptor steroidogenic factor 1 (VMHdm^{SF1}) is preferentially responsive to ESP1. These neurons exhibit a response profile that is distinct from that of neurons responding to predator odors within the same neural cluster. Experimental optogenetic reactivation of the ESP1-responsive VMHdm^{SF1} neurons can induce an increase in sexual receptivity akin to that observed naturally in response to ESP1. Conversely, the genetic disruption of VMHdm^{SF1} neurons leads to a diminution of the ESP1-induced enhancement in sexual receptivity, although basal levels of receptivity are unaffected. In stark contrast, the ablation of VMHvl^{Esr1} results in the complete abolition of sexual receptivity.

Conversely, ESP22 suppresses female sexual behaviors. This suppressive influence of ESP22 is mediated through GABAergic projections from the BNST to the VMHvl (Osakada et al., 2018).

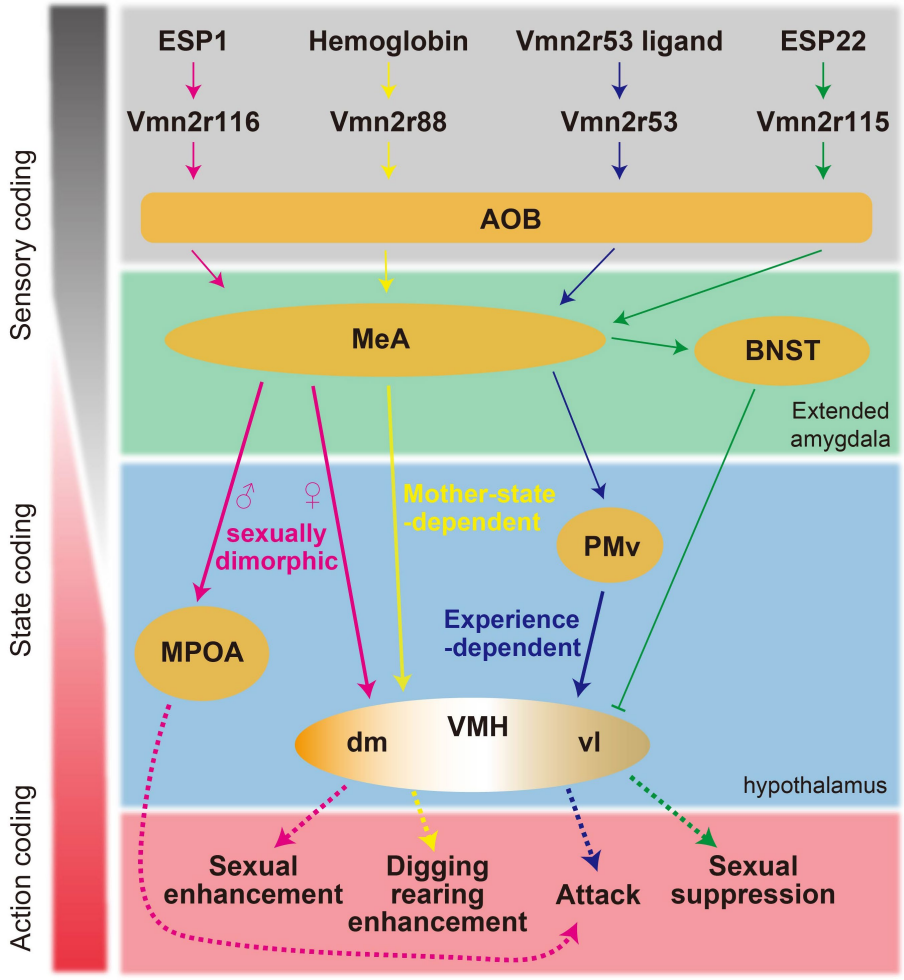

FIGURE 2
Schematic summary of the proposed neural circuits responsible for pheromone-mediated behaviors in mice.

The signaling mechanisms of ESP1 and ESP22 exemplify a labeled-line neural circuit model; however, pheromonal neural circuitry does not universally adhere to such a linear pathway (Li et al., 2017; Li and Dulac, 2018).

Neural mechanisms of pheromone-mediated intermale aggression have also been characterized by focusing on specific pheromones and receptors. Exposure to a pheromonal component that activates Vmn2r53 invariably results in the activation of progesterone receptor (PR)-expressing neurons in the PMv (PMv^{PR}) in male mice (Itakura et al., 2022). This response occurs regardless of previous social interactions. It is noteworthy that although male urine is composed of a multitude of pheromonal substances in addition to Vmn2r53 ligands, the bulk calcium responses—serving as proxies for neural activity—elicited by this individual pheromonal component are quantitatively analogous to those triggered by the complete male urine. Contrastingly, after experiencing aggression, this pheromone fraction activates PR-expressing neurons in the VMHvl ($VMHvl^{PR}$), which substantially overlap with the $VMHvl^{Esr1}$ neurons. In addition, the magnitude of this response is much smaller compared to the response elicited by exposure to complete male urine. Chemogenetic suppression of PMv^{PR} function abolishes $VMHvl^{PR}$ responses to this specific pheromonal fraction and attenuates responses to male urine. This finding implicates PMv^{PR} neurons as a pivotal upstream mediator to the $VMHvl^{PR}$ in the neural processing of male pheromone signals. Remarkably, Vmn2r53 knockout significantly diminishes PMv^{PR} responses to male urine, suggesting an overrepresentation of Vmn2r53-mediated signaling within the PMv^{PR}. In contrast, strain-specific male pheromones such as ESP1 and MUP3, which are also implicated in the induction of aggressive behavior, do not appear to activate PMv^{PR} or $VMHvl^{PR}$ neurons. In males, ESP1 stimulates excitatory neurons in the MeA and downstream neurons in the BNST and MPOA (Ishii et al., 2017). However, the direct causal link between the activation of these neural pathways and the potentiation of aggressive behavior remains to be conclusively determined. These studies imply the existence of redundant or parallel pathways for pheromone-mediated aggression.

State-dependent signal transduction of hemoglobin is observed. Hemoglobin activates Vmn2r88, mediated by its interaction site, Gly17, on the hemoglobin (Osakada et al., 2022). The hemoglobin signal reaches the MeA in mice, regardless of sex. However, VMHdm is selectively activated in lactating females. As a result, in lactating mothers, hemoglobin enhances digging and rearing behaviors. Manipulation of $VMHdm^{SF1}$ neurons is sufficient to induce the hemoglobin-mediated behaviors.

Collectively, the identification of specific pheromone molecules and corresponding receptors responsible for behavioral regulations has contributed to delineating neural circuits from sensory input to behavioral output since this approach simplifies input–output relations (Figure 2).

Perspective

Research on pheromones and their behavioral impacts provides a rich field, particularly with regard to the formation and function of neural circuits inducing innate behaviors, known as 'labeled line' circuits. A viable starting point for dissecting these pathways is the study of VRs with identified pheromone ligands. For example, the closely related receptors Vmn2r115 and Vmn2r116 bind to ESP22 and ESP1, respectively, yet exert opposite effects on female sexual behavior (Haga et al., 2010; Osakada et al., 2018). What variations exist in the spatial distribution of axonal terminals within the AOB's glomerular array among VSNs expressing different VRs? Do VRs dictate projection patterns to the AOB in a manner similar to olfactory receptors? How do VSNs expressing individual VRs form synapses with mitral/tufted cells? This includes identifying whether there are distinct subtypes within the mitral/tufted cell populations based on their connectivity and gene expression. Furthermore, do mitral/tufted cells form specific synaptic connections with neurons in the MeA that correspond to discrete valences? If so, how is this multisynaptic 'labeled line' wired? Elucidating these mechanisms is crucial for a comprehensive understanding of the development of innate neural circuits.

The investigation into the mechanisms of sexually dimorphic circuit formation is a significant area of research within neurobiology (Yang and Shah, 2014). One promising avenue is the study of pheromone signal transduction pathways. Notably, sexually dimorphic processing of information is observed in response to ESP1, which elicits sexually divergent activations in the MeA. A critical question arises: at what developmental stages and by what processes does this sexual dimorphism manifest? Current evidence suggests that the sexually dimorphic responses observed in the MeA are heavily influenced by sex hormone signaling. This is supported by findings that male mice deficient in the enzyme aromatase, which is crucial for estrogen synthesis, exhibit disrupted sexually dimorphic responses (Bergan et al., 2014). It is hypothesized that the pathway from the MeA to the MPA or VMHdm in response to ESP1 may operate through a regulatory mechanism similar to that governed by sex hormone signaling. This pathway represents an excellent model for elucidating the precise mechanisms underlying sexually dimorphic neural circuit formation and pheromonal information processing.

How the pheromone molecule, its receptor, and subsequent signaling pathways co-evolved is an interesting question. The ESP and MUP gene families are pivotal examples, having undergone diversification predominantly via gene duplication—a well-documented mechanism in evolutionary biology (Sheehan et al., 2019; Niimura et al., 2020). Similarly, vomeronasal receptors have also evolved through this mechanism. Despite similarities within the ESP and MUP families and their receptors, there are significant functional divergences among their members, making them excellent models for studying pheromone evolution. In both insect pheromone systems and mammalian taste systems, which are well-known examples of labeled line signal transduction, the type of cell expressing the receptor determines the perceived value of the ligand (Mueller et al., 2005; Zhao and McBride, 2020). However, it remains uncertain whether a similar paradigm applies to the mammalian vomeronasal system, or whether ligand valuation is an intrinsic property of the receptor. Indeed, in the mammalian olfactory system, swapping one receptor gene for another affects the projection pattern of the given sensory neurons, which would affect the perception of the odorant, suggesting that the receptor gene itself has a deterministic factor of the value of the corresponding ligand (Mombaerts et al., 1996). This query could be empirically addressed for the vomeronasal system through targeted genetic experiments involving the Vmn2r115 and Vmn2r116 receptors. For instance, an experimental strategy might include the disruption of the Vmn2r116 gene and the substitution of its sequence

at the Vmn2r115 locus to assess the functional outcomes on ESP1-mediated behaviors—specifically, whether it continues to facilitate sexual behavior or shifts to inhibiting such behavior, akin to the effect observed with ESP22. Should the former occur, it would suggest a decisive role of receptor functionality; conversely, the latter outcome would indicate a locational influence on gene function. The identification and comprehensive characterization of receptors for ESPs and MUPs remain incomplete. Further elucidation of the evolutionary trajectories of these ligands and their corresponding receptors could significantly enhance our understanding of molecular evolution of pheromone-mediated communication. Additionally, investigating the mechanisms through which signals from these receptors interact and integrate with those from other sensory modalities to elicit specific behavioral responses presents an intriguing area of research.

The signal transduction pathways mediated by ESP1 and ESP22 appear to support a labeled line coding system; however, tracking the neural response toward conspecific sex across different social experiences revealed that pheromone signal processing involves complex mechanisms beyond this simple paradigm. Recent studies have indicated that sexual experiences can alter the neural coding of conspecific sex cues within the MeA and VMHvl^{Esr1}. The use of various VR and ligand pairs may be instrumental in elucidating the precise mechanisms involved, given that the inputs derived from these receptor-ligand interactions are typically simple and stable. For instance, the signal transduction pathway involving Vmn2r53, which is influenced by aggressive behavioral experiences, might serve as an excellent model for studying synaptic plasticity between the VMHvl and the PMv.

A variety of aggression-inducing pheromones have been identified; however, the underlying mechanisms through which these pheromones collectively influence aggressive behaviors are not yet fully understood. Notably, the MUPs such as MUP3 and MUP20, as well as ESP1, exhibit secretion patterns that are distinct among mouse strains. In contrast, Vmn2r53 is responsive to a male-specific pheromone present in the urine across various male mouse strains, indicating that Vmn2r53 may detect a ubiquitous male signal within the species. These findings could be pivotal for the discussion on how differentially processed pheromone signals can orchestrate uniform behavioral responses. Moreover, the interaction complexity of pheromone signals is further exemplified by certain behaviors, such as infanticide, which are elicited only in the presence of multiple pheromonal signals. Identifying the precise pheromonal blend required to initiate such complex behaviors remains an outstanding challenge in the field. Furthermore, elucidating the specific sites and mechanisms through which the vomeronasal system processes and integrates these pheromone signals is an essential area of research that warrants further investigation.

The perception of pheromones alone typically does not elicit specific behavioral responses. The presence of conspecifics and the assimilation of diverse sensory inputs, including auditory, visual, and tactile information, is requisite. Elucidating how pheromone signaling is integrated with other sensory modalities is essential for a thorough understanding of behavioral expression. This intersection of sensory integration and behavior is a pivotal area for future investigation.

The framework of sensory input to aggressive and sexual behavioral output is emerging owing to the characterization of pheromone molecules and corresponding receptors along with the detailed functional analysis within the central nervous systems. In contrast, we scarcely know how pheromones trigger physiological responses even though these phenomena are classically reported in rodents. Since the 1950s, several pheromone-mediated phenomena that modulate reproductive function in mice have been reported. Estrus cycle is suppressed in group housed females (van der Lee and Boot, 1955), and male urine induces estrus in those females (Whitten, 1956). Male urine also accelerates puberty in female mice (Vandenbergh, 1967). Exposure to a novel male induces pregnancy failure in female mice (Bruce, 1959). The advent of modern neuroscientific methodologies, including cell-type-specific imaging and sensors for neuromodulators, offers promising avenues for deciphering the central mechanisms governing these phenomena. In summary, ongoing research into pheromonal communication is poised to yield profound insights into the neural circuitry that orchestrates behavioral and physiological adaptations.

Author contributions

KM: Conceptualization, Data curation, Investigation, Writing – original draft, Writing – review & editing. TI: Conceptualization, Data curation, Writing – original draft, Writing – review & editing. KT: Conceptualization, Funding acquisition, Project administration, Writing – original draft, Writing – review & editing.

Funding

The author(s) declare financial support was received for the research, authorship, and/or publication of this article. This work was supported in part by the ERATO Touhara Chemosensory Signal Project (JPMJER1202) to KT and the JSPS Kakenhi grant number 18H05267 and JP23H05410 to KT.

Acknowledgments

The authors thank KT lab members for the critical reading of the manuscript.

Conflict of interest

The authors declare that the research was conducted in the absence of any commercial or financial relationships that could be construed as a potential conflict of interest.

Publisher's note

References

Baum, M. J., and Cherry, J. A. (2015). Processing by the main olfactory system of chemosignals that facilitate mammalian reproduction. *Horm. Behav.* 68, 53–64. doi: 10.1016/j.yhbeh.2014.06.003

Bergan, J. F., Ben-Shaul, Y., and Dulac, C. (2014). Sex-specific processing of social cues in the medial amygdala. *eLife* 3:e02743. doi: 10.7554/eLife.02743

Bruce, H. M. (1959). An exteroceptive block to pregnancy in the mouse. *Nature* 184:105. doi: 10.1038/184105a0

Chamero, P., Katsoulidou, V., Hendrix, P., Bufe, B., Roberts, R., Matsunami, H., et al. (2011). G protein G(alpha)o is essential for vomeronasal function and aggressive behavior in mice. *Proc. Natl. Acad. Sci. USA* 108, 12898–12903. doi: 10.1073/pnas.1107770108

Chamero, P., Marton, T. F., Logan, D. W., Flanagan, K., Cruz, J. R., Saghatelian, A., et al. (2007). Identification of protein pheromones that promote aggressive behaviour. *Nature* 450, 899–902. doi: 10.1038/nature05997

Chen, J., Markowitz, J. E., Lilascharoen, V., Taylor, S., Sheurpukdi, P., Keller, J. A., et al. (2021). Flexible scaling and persistence of social vocal communication. *Nature* 593, 108–113. doi: 10.1038/s41586-021-03403-8

Choi, G. B., Dong, H.-W., Murphy, A. J., Valenzuela, D. M., Yancopoulos, G. D., Swanson, L. W., et al. (2005). Lhx6 delineates a pathway mediating innate reproductive behaviors from the amygdala to the hypothalamus. *Neuron* 46, 647–660. doi: 10.1016/j.neuron.2005.04.011

Cross, S. K. J., Martin, Y. H., Salia, S., Gamba, I., Major, C. A., Hassan, S., et al. (2021). Puberty is a critical period for Vomeronasal organ mediation of socio-sexual behavior in mice. *Front. Behav. Neurosci.* 14:606788. doi: 10.3389/fnbeh.2020.606788

Døving, K. B., and Trotier, D. (1998). Structure and function of the vomeronasal organ. *J. Exp. Biol.* 201, 2913–2925. doi: 10.1242/jeb.201.21.2913

Doyle, W. I., and Meeks, J. P. (2018). Excreted steroids in vertebrate social communication. *J. Neurosci.* 38:3377. doi: 10.1523/JNEUROSCI.2488-17.2018

Dulac, C., and Wagner, S. (2006). Genetic analysis of brain circuits underlying pheromone signaling. *Annu. Rev. Genet.* 40, 449–467. doi: 10.1146/annurev.genet.39.073003.093937

Falkner, A. L., Wei, D., Song, A., Watsek, L. W., Chen, I., Chen, P., et al. (2020). Hierarchical representations of aggression in a hypothalamic-midbrain circuit. *Neuron* 106, 637–648.e6. doi: 10.1016/j.neuron.2020.02.014

Ferrero, D. M., Moeller, L. M., Osakada, T., Horio, N., Li, Q., Roy, D. S., et al. (2013). A juvenile mouse pheromone inhibits sexual behaviour through the vomeronasal system. *Nature* 502, 368–371. doi: 10.1038/nature12579

Fraser, E. J., and Shah, N. M. (2014). Complex chemosensory control of female reproductive behaviors. *PLoS One* 9:e90368. doi: 10.1371/journal.pone.0090368

Haga, S., Hattori, T., Sato, T., Sato, K., Matsuda, S., Kobayakawa, R., et al. (2010). The male mouse pheromone ESP1 enhances female sexual receptive behaviour through a specific vomeronasal receptor. *Nature* 466, 118–122. doi: 10.1038/nature09142

Haga-Yamanaka, S., Ma, L., He, J., Qiu, Q., Lavis, L. D., Looger, L. L., et al. (2014). Integrated action of pheromone signals in promoting courtship behavior in male mice. *eLife Sci*:3. doi: 10.7554/eLife.03025

Halpern, M., and Martínez-Marcos, A. (2003). Structure and function of the vomeronasal system: an update. *Prog. Neurobiol.* 70, 245–318. doi: 10.1016/S0301-0082(03)00103-5

Hammen, G. F., Turaga, D., Holy, T. E., and Meeks, J. P. (2014). Functional organization of glomerular maps in the mouse accessory olfactory bulb. *Nat. Neurosci.* 17, 953–961. doi: 10.1038/nn.3738

Hattori, T., Osakada, T., Matsumoto, A., Matsuo, N., Haga-Yamanaka, S., Nishida, T., et al. (2016). Self-exposure to the male pheromone ESP1 enhances male aggressiveness in mice. *Curr. Biol.* 26, 1229–1234. doi: 10.1016/j.cub.2016.03.029

He, J., Ma, L., Kim, S., Nakai, J., and Yu, C. R. (2008). Encoding gender and individual information in the mouse Vomeronasal organ. *Science* 320, 535–538. doi: 10.1126/science.1154476

Holy, T. E. (2018). The accessory olfactory system: innately specialized or microcosm of mammalian circuitry? *Annu. Rev. Neurosci.* 41, 501–525. doi: 10.1146/annurev-neuro-080317-061916

Hurst, J. L., and Beynon, R. J. (2004). Scent wars: the chemobiology of competitive signalling in mice. *BioEssays* 26, 1288–1298. doi: 10.1002/bies.20147

Inoue, S., Yang, R., Tantry, A., Davis, C.-H., Yang, T., Knoedler, J. R., et al. (2019). Periodic remodeling in a neural circuit governs timing of female sexual behavior. *Cell* 179, 1393–1408.e16. doi: 10.1016/j.cell.2019.10.025

Ishii, K. K., Osakada, T., Mori, H., Miyasaka, N., Yoshihara, Y., Miyamichi, K., et al. (2017). A labeled-line neural circuit for pheromone-mediated sexual behaviors in mice. *Neuron* 95, 123–137.e8. doi: 10.1016/j.neuron.2017.05.038

Ishii, K. K., and Touhara, K. (2019). Neural circuits regulating sexual behaviors via the olfactory system in mice. *Neurosci. Res.* 140, 59–76. doi: 10.1016/j.neures.2018.10.009

Isogai, Y., Si, S., Pont-Lezica, L., Tan, T., Kapoor, V., Murthy, V. N., et al. (2011). Molecular organization of vomeronasal chemoreception. *Nature* 478, 241–245. doi: 10.1038/nature10437

Isogai, Y., Wu, Z., Love, M. I., Ahn, M. H.-Y., Bambah-Mukku, D., Hua, V., et al. (2018). Multisensory logic of infant-directed aggression by males. *Cell* 175, 1827–1841.e17. doi: 10.1016/j.cell.2018.11.032

Itakura, T., Murata, K., Miyamichi, K., Ishii, K. K., Yoshihara, Y., and Touhara, K. (2022). A single vomeronasal receptor promotes intermale aggression through dedicated hypothalamic neurons. *Neuron* 110, 2455–2469.e8. doi: 10.1016/j.neuron.2022.05.002

Karigo, T., Kennedy, A., Yang, B., Liu, M., Tai, D., Wahle, I. A., et al. (2021). Distinct hypothalamic control of same- and opposite-sex mounting behaviour in mice. *Nature* 589, 258–263. doi: 10.1038/s41586-020-2995-0

Karlson, P., and Lüscher, M. (1959). The proposed biological term 'pheromone'. *Nature* 183:1835. doi: 10.1038/1831835b0

Kaur, A. W., Ackels, T., Kuo, T.-H., Cichy, A., Dey, S., Hays, C., et al. (2014). Murine pheromone proteins constitute a context-dependent combinatorial code governing multiple social behaviors. *Cell* 157, 676–688. doi: 10.1016/j.cell.2014.02.025

Kimchi, T., Xu, J., and Dulac, C. (2007). A functional circuit underlying male sexual behaviour in the female mouse brain. *Nature* 448, 1009–1014. doi: 10.1038/nature06089

Kimoto, H., Haga, S., Sato, K., and Touhara, K. (2005). Sex-specific peptides from exocrine glands stimulate mouse vomeronasal sensory neurons. *Nature* 437, 898–901. doi: 10.1038/nature04033

Kimoto, H., Sato, K., Nodari, F., Haga, S., Holy, T. E., and Touhara, K. (2007). Sex- and strain-specific expression and Vomeronasal activity of mouse ESP family peptides. *Curr. Biol.* 17, 1879–1884. doi: 10.1016/j.cub.2007.09.042

Knoedler, J. R., Inoue, S., Bayless, D. W., Yang, T., Tantry, A., Davis, C., et al. (2022). A functional cellular framework for sex and estrous cycle-dependent gene expression and behavior. *Cell* 185, 654–671.e22. doi: 10.1016/j.cell.2021.12.031

Lee, H., Kim, D.-W., Remedios, R., Anthony, T. E., Chang, A., Madisen, L., et al. (2014). Scalable control of mounting and attack by Esr1+ neurons in the ventromedial hypothalamus. *Nature* 509, 627–632. doi: 10.1038/nature13169

Lee, D., Kume, M., and Holy, T. E. (2019). Sensory coding mechanisms revealed by optical tagging of physiologically defined neuronal types. *Science* 366, 1384–1389. doi: 10.1126/science.aax8055

Leinders-Zufall, T., Lane, A. P., Puche, A. C., Ma, W., Novotny, M. V., Shipley, M. T., et al. (2000). Ultrasensitive pheromone detection by mammalian vomeronasal neurons. *Nature* 405, 792–796. doi: 10.1038/35015572

Leypold, B. G., Yu, C. R., Leinders-Zufall, T., Kim, M. M., Zufall, F., and Axel, R. (2002). Altered sexual and social behaviors in trp2 mutant mice. *Proc. Natl. Acad. Sci.* 99, 6376–6381. doi: 10.1073/pnas.082127599

Li, Y., and Dulac, C. (2018). Neural coding of sex-specific social information in the mouse brain. *Curr. Opin. Neurobiol.* 53, 120–130. doi: 10.1016/j.conb.2018.07.005

Li, Y., Mathis, A., Grewe, B. F., Osterhout, J. A., Ahanonu, B., Schnitzer, M. J., et al. (2017). Neuronal representation of social information in the medial amygdala of awake behaving mice. *Cell* 171, 1176–1190.e17. doi: 10.1016/j.cell.2017.10.015

Lin, D., Boyle, M. P., Dollar, P., Lee, H., Lein, E. S., Perona, P., et al. (2011). Functional identification of an aggression locus in the mouse hypothalamus. *Nature* 470, 221–226. doi: 10.1038/nature09736

Liu, M., Kim, D.-W., Zeng, H., and Anderson, D. J. (2022). Make war not love: the neural substrate underlying a state-dependent switch in female social behavior. *Neuron* 110, 841–856.e6. doi: 10.1016/j.neuron.2021.12.002

Miller, C. H., Campbell, P., and Sheehan, M. J. (2020). Distinct evolutionary trajectories of V1R clades across mouse species. *BMC Evol. Biol.* 20:99. doi: 10.1186/s12862-020-01662-z

Mombaerts, P. (2004). Genes and ligands for odorant, vomeronasal and taste receptors. *Nat. Rev. Neurosci.* 5, 263–278. doi: 10.1038/nrn1365

Mombaerts, P., Wang, F., Dulac, C., Chao, S. K., Nemes, A., Mendelsohn, M., et al. (1996). Visualizing an olfactory sensory map. *Cell* 87, 675–686. doi: 10.1016/S0092-8674(00)81387-2

Mueller, K. L., Hoon, M. A., Erlenbach, I., Chandrashekar, J., Zuker, C. S., and Ryba, N. J. P. (2005). The receptors and coding logic for bitter taste. *Nature* 434, 225–229. doi: 10.1038/nature03352

Murata, K., and Touhara, K. (2021). Pheromones in Vertebrates. *Encycl. Life Sci.*, 2, 1–10. doi: 10.1002/9780470015902.a0029360

Niimura, Y., Tsunoda, M., Kato, S., Murata, K., Yanagawa, T., Suzuki, S., et al. (2020). Origin and evolution of the gene family of proteinaceous pheromones, the exocrine gland-secreting peptides, in rodents. *Mol. Biol. Evol.* 25:3389. doi: 10.1093/molbev/msaa220/5907918

Nikaido, M. (2019). Evolution of *V1R* pheromone receptor genes in vertebrates: diversity and commonality. *Genes Genet. Syst.* 94, 141–149. doi: 10.1266/ggs.19-00009

Nodari, F., Hsu, F.-F., Fu, X., Holekamp, T. F., Kao, L.-F., Turk, J., et al. (2008). Sulfated steroids as natural ligands of mouse pheromone-sensing neurons. *J. Neurosci.* 28, 6407–6418. doi: 10.1523/JNEUROSCI.1425-08.2008

Osakada, T., Abe, T., Itakura, T., Mori, H., Ishii, K. K., Eguchi, R., et al. (2022). Hemoglobin in the blood acts as a chemosensory signal via the mouse vomeronasal system. *Nat. Commun.* 13:556. doi: 10.1038/s41467-022-28118-w

Osakada, T., Ishii, K. K., Mori, H., Eguchi, R., Ferrero, D. M., Yoshihara, Y., et al. (2018). Sexual rejection via a vomeronasal receptor-triggered limbic circuit. *Nat. Commun.* 9:4463. doi: 10.1038/s41467-018-07003-5

Pérez-Gómez, A., Stein, B., Leinders-Zufall, T., and Chamero, P. (2014). Signaling mechanisms and behavioral function of the mouse basal vomeronasal neuroepithelium. *Front. Neuroanat.* 8:135. doi: 10.3389/fnana.2014.00135

Pfau, D. R., Baribeau, S., Brown, F., Khetarpal, N., Marc Breedlove, S., and Jordan, C. L. (2023). Loss of TRPC2 function in mice alters sex differences in brain regions regulating social behaviors. *J. Comp. Neurol.* 531, 1550–1561. doi: 10.1002/cne.25528

Remedios, R., Kennedy, A., Zelikowsky, M., Grewe, B. F., Schnitzer, M. J., and Anderson, D. J. (2017). Social behaviour shapes hypothalamic neural ensemble representations of conspecific sex. *Nature* 550, 388–392. doi: 10.1038/nature23885

Roberts, S. A., Davidson, A. J., McLean, L., Beynon, R. J., and Hurst, J. L. (2012). Pheromonal induction of spatial learning in mice. *Science* 338, 1462–1465. doi: 10.1126/science.1225638

Silva, L., and Antunes, A. (2017). Vomeronasal Receptors in Vertebrates and the Evolution of Pheromone Detection. *Annu. Rev. Anim. Biosci.* 5, 353–370. doi: 10.1146/annurev-animal-022516-022801

Sheehan, M. J., Campbell, P., and Miller, C. H. (2019). Evolutionary patterns of major urinary protein scent signals in house mice and relatives. *Mol. Ecol.* 28, 3587–3601. doi: 10.1111/mec.15155

Stowers, L., Holy, T. E., Meister, M., Dulac, C., and Koentges, G. (2002). Loss of sex discrimination and male-male aggression in mice deficient for TRP2. *Science* 295, 1493–1500. doi: 10.1126/science.1069259

Tirindelli, R. (2021). Coding of pheromones by vomeronasal receptors. *Cell Tissue Res.* 383, 367–386. doi: 10.1007/s00441-020-03376-6

Trouillet, A.-C., Keller, M., Weiss, J., Leinders-Zufall, T., Birnbaumer, L., Zufall, F., et al. (2019). Central role of G protein Gαi2 and Gαi2+ vomeronasal neurons in balancing territorial and infant-directed aggression of male mice. *Proc. Natl. Acad. Sci. USA* 116, 5135–5143. doi: 10.1073/pnas.1821492116

Tye, K. M. (2018). Neural circuit motifs in valence processing. *Neuron* 100, 436–452. doi: 10.1016/j.neuron.2018.10.001

van der Lee, S., and Boot, L. M. (1955). Spontaneous pseudopregnancy in mice. *Acta Physiol. Pharmacol. Neerl.* 4, 442–444.

Vandenbergh, J. G. (1967). Effect of the presence of a male on the sexual maturation of female mice. *Endocrinology* 81, 345–349. doi: 10.1210/endo-81-2-345

Whitten, W. K. (1956). Modification of the oestrous cycle of the mouse by external stimuli associated with the male. *J. Endocrinol.* 13, 399–404. doi: 10.1677/joe.0.0130399

Wong, W. M., Cao, J., Zhang, X., Doyle, W. I., Mercado, L. L., Gautron, L., et al. (2020). Physiology-forward identification of bile acid–sensitive vomeronasal receptors. *Sci. Adv.* 6:eaaz6868. doi: 10.1126/sciadv.aaz6868

Wu, Z., Autry, A. E., Bergan, J. F., Watabe-Uchida, M., and Dulac, C. G. (2014). Galanin neurons in the medial preoptic area govern parental behaviour. *Nature* 509, 325–330. doi: 10.1038/nature13307

Wyatt, T. D. (2014). *Pheromones and animal behavior: Chemical signals and signatures. 2nd* Edn Cambridge: Cambridge University Press.

Yang, B., Karigo, T., and Anderson, D. J. (2022). Transformations of neural representations in a social behaviour network. *Nature* 608, 741–749. doi: 10.1038/s41586-022-05057-6

Yang, C. F., and Shah, N. M. (2014). Representing sex in the brain, one module at a time. *Neuron* 82, 261–278. doi: 10.1016/j.neuron.2014.03.029

Yin, L., Hashikawa, K., Hashikawa, Y., Osakada, T., Lischinsky, J. E., Diaz, V., et al. (2022). VMHvllCckar cells dynamically control female sexual behaviors over the reproductive cycle. *Neuron* 110, 3000–3017.e8. doi: 10.1016/j.neuron.2022.06.026

Young, J. M., and Trask, B. J. (2007). V2R gene families degenerated in primates, dog and cow, but expanded in opossum. *Trends Genet.* 23, 212–215. doi: 10.1016/j.tig.2007.03.004

Yu, C. R. (2015). TRICK or TRP? What Trpc2−/− mice tell us about vomeronasal organ mediated innate behaviors. *Front. Neurosci.* 9:221. doi: 10.3389/fnins.2015.00221

Zhao, Z., and McBride, C. S. (2020). Evolution of olfactory circuits in insects. *J. Comp. Physiol. A* 206, 353–367. doi: 10.1007/s00359-020-01399-6

frontiers | Frontiers in Neural Circuits

TYPE Mini Review
PUBLISHED 01 May 2024
DOI 10.3389/fncir.2024.1409349

OPEN ACCESS

EDITED BY
Kensaku Mori,
RIKEN, Japan

REVIEWED BY
Yoshitaka Oka,
The University of Tokyo, Japan

*CORRESPONDENCE
Sayaka Inoue
✉ sayaka@wustl.edu

RECEIVED 29 March 2024
ACCEPTED 15 April 2024
PUBLISHED 01 May 2024

CITATION
Inoue S (2024) Hormonal and circuit mechanisms controlling female sexual behavior.
Front. Neural Circuits 18:1409349.
doi: 10.3389/fncir.2024.1409349

Hormonal and circuit mechanisms controlling female sexual behavior

Sayaka Inoue*

Department of Psychiatry, School of Medicine, Washington University in St. Louis, St. Louis, MO, United States

Sexual behavior is crucial for reproduction in many animals. In many vertebrates, females exhibit sexual behavior only during a brief period surrounding ovulation. Over the decades, studies have identified the roles of ovarian sex hormones, which peak in levels around the time of ovulation, and the critical brain regions involved in the regulation of female sexual behavior. Modern technical innovations have enabled a deeper understanding of the neural circuit mechanisms controlling this behavior. In this review, I summarize our current knowledge and discuss the neural circuit mechanisms by which female sexual behavior occurs in association with the ovulatory phase of their cycle.

KEYWORDS

social behavior, ovarian hormones, female, sexual behavior, hypothalamus

Introduction

Sexual behavior is essential to reproduction in many animals and is instinctual that the behavior can be displayed without any prior experience. This instinct suggests that the behavior is genetically hard-wired, with the corresponding neural circuits being generated and established during the developmental phase. In many vertebrates, female sexual behavior is synchronized with the estrous cycle. Females are sexually receptive toward male mounting only during a short period surrounding ovulation (estrus phase) and are not receptive during the other stages of the estrous cycle. For example, female mice are sexually receptive once in every four to five days while female giant pandas are receptive only a few days in a year (Allen, 1922; Lindburg et al., 2001). Despite the variability in the duration of female estrous cycles across species, the concurrence of ovulation and female sexual receptivity is a common trait among many mammals. This synchronization is crucial for efficient reproduction, minimizing the risk of predation and waste of energy. Female sex hormones 17β-estradiol (referred to as estrogen here) and progesterone are released from the ovary and their levels peak at the timing surrounding ovulation. Over the decades, studies revealed that estrogen and progesterone, and their receptors, are essential to female sexual behavior (Ring and Providence, 1944; Powers, 1970; Beach, 1976; Lydon et al., 1995; Rissman et al., 1997; Arnold, 2009). Recent studies employing novel genetic, imaging, and behavioral approaches further characterized how these sex hormones contribute to the behavior by modulating neural circuits in the female brain. In this review, I illustrate the overview of how this alliance between ovulation and female sexual behavior is controlled by neural circuitry in the brain.

Female sexual behavior depends on female steroid hormones

The sex steroid hormones estrogen and progesterone, produced and released by the ovary, are essential for inducing female sexual behavior. These sex hormone levels are closely related to the estrous cycle: they peak around the estrus, the stage that female is sexually receptive and ovulating, while it goes down to undetectable levels at the other stages of the estrous cycle (Deleon et al., 1990; Nelson et al., 1992). Removal of ovaries eliminates these changes in sex hormone levels, and consequently, female sexual receptivity. Subsequent supplementation of estrogen and progesterone rescues the behavior in the ovariectomized (OVX) female, demonstrating that female sexual behavior can be induced by increased levels of sex hormones without actual ovulation. This OVX and hormonal priming regimen is widely used to induce female sexual behavior in experimental animals (Whalen, 1974; Nelson et al., 1992; Lydon et al., 1995; Rissman et al., 1997; Ogawa et al., 1998; Bakker et al., 2002; Kudway and Rissman, 2003; Wu et al., 2009; Xu et al., 2012; Yang et al., 2013).

Estrogen and progesterone bind to their cognate receptors such as estrogen receptor a (ERa or Esr1) and progesterone receptor (PR). These receptors are known as transcription factors that they alter gene expression and protein synthesis. Studies utilizing knockout mice of the receptors revealed that signaling of these sex hormones in the brain is essential for female sexual behavior (Lubahn et al., 1993; Lydon et al., 1995; Rissman et al., 1997). Inhibition of protein synthesis in the brain also suppresses the behavior even when OVX females are supplemented with sex hormones (Rainbow et al., 1980, 1982; Meisel and Pfaff, 1985). Together, these findings suggest that a sequence of steroid hormone signaling, followed by gene expression and protein synthesis in the brain, is essential for inducing female sexual behavior.

A more recent study employing microarray, bulk, and single-nucleus RNA sequencing compared gene expression profiles in four different hypothalamic and limbic regions between OVX and hormonally primed OVX females (Xu et al., 2012; Knoedler et al., 2022). Notably, Knoedler et al. (2022) identified 1,415 genes whose expression changes in four limbic and hypothalamic regions depending on sex hormones. This is the first report to highlight such extensive changes in gene expression profiles due to different hormonal states in females. Which genes are critical for controlling female sexual behavior? Gene ontogeny analysis identified that they include genes in synaptic transmission, steroid hormone-related processes, behavior, peripheral reproductive organ processes, and regulation of gene expression. The expression levels of these hormone-sensitive genes vary across different brain regions. Therefore, to elucidate roles of these identified hormone-sensitive genes, it is critical not only to analyze brain-wide gene knockout animals but also to employ region-specific viral delivery of CRISPR-Cas9 for gene knockout and RNAi for gene knockdown (Musatov et al., 2006).

Key neural circuits controlling female sexual behavior

Many hypothalamic and limbic regions in the brain are found to be involved in female sexual behavior. As key regions, the ventromedial hypothalamus (VMH), medial preoptic area (mPOA), and periaqueductal gray (PAG) were identified decades ago as they are critical to the behavior (Figure 1). The induction of the immediate early gene Fos in these regions during female sexual behavior suggests their activation (Pfaus et al., 1993; Blaustein et al., 1994; Flanagan-Cato and Mcewen, 1995; Yamada and Kawata, 2014). Importantly, histological studies indicate that these regions are rich in expression of sex hormonal receptors such as Esr1 or PR (Wu et al., 2009; Cheong et al., 2015; Kim et al., 2019). Local infusion of sex hormones into these areas modulates female sexual behavior, underscoring their control in association with the estrous cycle (Robert, 1962; Barfield and Chen, 1977; Floody et al., 1986; Rajendren et al., 1991). Early work by Sakuma and Pfaff in the 1970s highlighted the importance of these brain regions in modulating female sexual behavior. This review will summarize the roles of each circuit in detail.

The VMH, especially the ventrolateral part of the VMH (VMHvl), is well characterized its role in female sexual behavior. Single-unit recordings of neuronal firing in awake mice and primates reveal increased firing frequency in VMHvl neurons during conspecific male investigation or upon receiving male mounting and intromission (Aou et al., 1988; Nomoto and Lima, 2015). Electrical stimulation of the VMHvl enhances, while lesions suppress, female sexual receptivity, indicating this region's necessity and sufficiency (Pfaff and Sakuma, 1979a,b). Moreover, sex hormones play crucial roles in this modulation. Local hormone infusion in the VMHvl elevates female sexual behavior (Barfield and Chen, 1977; Rajendren et al., 1991). Histological studies demonstrate that expressions of sex hormonal receptors, such as Esr1 or PR, are dense in the VMHvl (Xu et al., 2012; Yang et al., 2013). Approximately 50% of VMHvl neurons are Esr1$^+$, with these neurons becoming active during male–female interactions (Hashikawa et al., 2017). Knockdown of Esr1 gene in the VMHvl via RNAi decreases female sexual receptivity (Musatov et al., 2006), suggesting that Esr1 signaling in the VMHvl is necessary to the behavior. Recent studies have further delineated the neuronal populations in control. Almost all PR$^+$ VMHvl neurons co-express Esr1, with about 60% of Esr1$^+$ VMHvl neurons being PR$^+$ (Yang et al., 2013). These PR$^+$ VMHvl neurons, when active during male mounting and lordosis behavior, are crucial for driving female sexual behavior, as shown by fiber photometry imaging (Inoue et al., 2019). Genetically targeted ablation or acute chemogenetic inhibition of these PR$^+$ VMHvl neurons reduces female sexual receptivity, even in hormonally primed OVX females (Yang et al., 2013; Inoue et al., 2019). These findings indicate that PR$^+$ VMHvl neurons are essential to drive female sexual behavior. Single-nucleus RNA sequencing from Esr1$^+$ VMHvl neurons identified a subset expressing the cholecystokinin-a receptor (Cckar) within total 27 of clusters (Figure 2), significant only in hormonally primed OVX females and not in males or OVX females, aligning with earlier microarray and *in situ* hybridization studies (Xu et al., 2012; Knoedler et al., 2022). This suggests the critical role of Cckar$^+$ VMHvl neurons in female sexual behavior. Fiber photometry imaging revealed that Cckar$^+$ neurons are active during mating, like PR$^+$ VMHvl neurons (Yin et al., 2022). Further, behavioral studies with acute inhibition of Cckar$^+$ VMHvl neurons, conducted by two different groups, found that these neurons are crucial to female sexual receptivity (Knoedler et al., 2022; Yin et al., 2022). Thus, Cckar$^+$ VMHvl neurons are the subset of Esr1$^+$ PR$^+$ VMHvl neurons that control female sexual behavior. Gene knockout of Cckar abolishes female sexual receptivity (Xu et al., 2012), however, whether Cckar gene expression within these neurons is necessary remains to be elucidated. Considering the

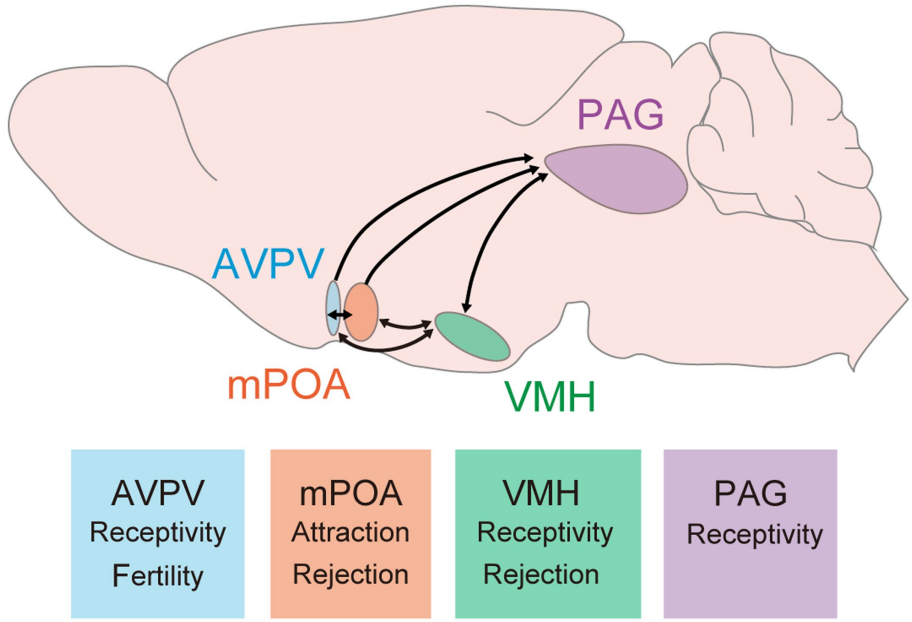

FIGURE 1
Key brain regions and their roles in female sexual behavior. These hypothalamic and midbrain circuits have been studied and demonstrated their contribution to female sexual behavior. Arrows indicate connections between these regions. It is important to note that reciprocal connections between the PAG and either the AVPV or mPOA have not yet been reported; however, it is possible that such connections exist. Major findings related to female sexual behavior are described at bottom boxes. AVPV, anteroventral periventricular nucleus; mPOA, medial preoptic area; VMH, ventromedial hypothalamus; PAG, periaqueductal gray.

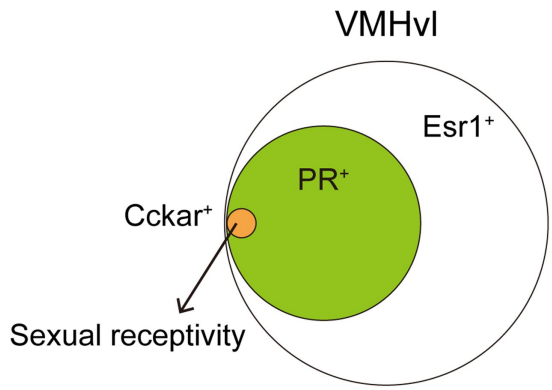

FIGURE 2
A small subset of VMHvl neurons can drive female sexual behavior. About 60% of the VMHvl neurons expressing Esr1 are also PR$^+$. Further, Cckar$^+$ population is one of 27 clusters identified in Esr1$^+$ VMHvl neurons. Such a small subset of neurons is critical to drive female sexual behavior. Cckar$^+$ VMHvl neurons, as well as PR$^+$ VMHvl neurons, project to the AVPV and this connectivity change depending on ovarian hormone levels.

increased Cckar expression in OVX primed females, it is possible that both firing activity and gene expression in Cckar$^+$ VMHvl neurons control the behavior in a coordinated manner. These Cckar$^+$ VMHvl neurons exist mostly in the center to posterior VMHvl. More recent study indicates that anterior PR$^+$ VMHvl neurons can drive rejection towards male mounts (Gutierrez-Castellanos et al., 2023). The detailed molecular identity of these anterior PR$^+$ VMHvl neurons and connection between Cckar$^+$ VMHvl neurons to regulate sexual receptivity and rejection are interesting topics to be revealed in future studies.

The PAG is one of the major downstream circuits receiving inputs from VMHvl. The PAG has been shown to increase lordosis upon electrical stimulation and decrease behavior upon lesioning, highlighting its role in modulating female sexual responsiveness (Sakuma and Pfaff, 1979a,b). Electrophysiological recordings from the PAG of anesthetized rats found that PAG neurons response to VMH and mPOA stimulation, suggesting that it works as the downstream of these neural circuits (Sakuma and Pfaff, 1980). The complexity and size of the PAG make it challenging to focus on specific subregions, which may explain the scarcity of *in vivo* electrophysiological recordings or calcium imaging studies specifically addressing female sexual behavior. Recent advances in spatial transcriptomics have identified distinct neural populations within the lateral PAG that are activated in response to female sexual behavior, as indicated by the co-expression of immediate early genes (Vaughn et al., 2022). This finding aligns with previous research demonstrating Fos expression in the lateral PAG following female sexual behavior (Yamada and Kawata, 2014). Dissecting the roles of these molecularly defined subpopulations within the PAG could provide deeper insights into their specific contributions to female sexual behavior. Given its position in the midbrain and proximity to motor output circuits, the PAG is considered a pivotal output center for the modulation of female sexual behavior. Further elucidation of the projections from PAG subpopulations to the downstream brainstem is crucial for a comprehensive understanding of the neural circuits that govern female sexual behavior.

The role of the medial preoptic area (mPOA) in female sexual behavior is complex and subject to ongoing debate. Electrical

stimulation or lesion of the mPOA change the behavior facilitatory and inhibitory directions, indicating its nuanced role in modulating the behavior (Moss et al., 1974; Bast et al., 1987; Takeo et al., 1993). Studies utilizing single-unit recording and fiber photometry imaging techniques have observed that neurons within the mPOA are particularly active during instances when a female receives male mounting, with their activity diminishing as the male dismounts (Aou et al., 1988; Sakuma, 1994; Kato and Sakuma, 2000; Wei et al., 2018). Consistent with these findings, recent fiber photometry imaging of the activity of hormone-sensitive Esr1$^+$ mPOA neurons revealed that they are similarly active when a female receives male mounting (Wei et al., 2018). A two-photon calcium imaging study demonstrates the role of Neurotensin$^+$ mPOA neurons (84% of them are Esr1$^+$) in the initial stages of sexual behavior. These neurons activate when a female encounters male pheromones, and optogenetic suppression of their activity results in a decreased attraction towards males, indicating a role in the pre-copulatory phase of sexual behavior (McHenry et al., 2017). These findings suggest the critical roles that genetically identified neuronal populations in the mPOA play in orchestrating female sexual behavior. However, causal relationships of these populations in copulation remained elusive. Recently, Ishii et al. (2023) discovered that a subset of GABAergic neurons in the mPOA reacts to the completion of mating, specifically when a female receives male ejaculation. These neurons were identified and labeled separately from those activated by pre-mating attractive behavior, allowing for targeted investigation into their respective roles in modulating female sexual behavior. Chemogenetic activation of the mating completion-activated neurons, but not those activated by attractive behavior, led to a reduction in female sexual receptivity. This finding suggests the presence of an mPOA neuronal subpopulation capable of suppressing sexual behavior, highlighting a complex regulatory mechanism within the mPOA. Further complexity will be revealed in the nature of Esr1$^+$ mPOA neurons, the majority of which are GABAergic, suggesting an interplay between estrogen signaling and inhibitory neurotransmission within this brain region (Wei et al., 2018; Knoedler et al., 2022). RNA sequencing studies have identified diverse clusters of neurons within the mPOA, pointing to a rich mosaic of functional and phenotypic heterogeneity (Moffitt et al., 2018; Knoedler et al., 2022). Future studies into these subpopulations will unravel the detailed mechanisms by which the mPOA influences both the attraction phase and the copulatory process in female sexual behavior, offering deeper insights into the neural underpinnings of these complex behaviors.

Another hypothalamic region which is important for female sexual behavior is the anteroventral periventricular nucleus (AVPV). This region is also rich in expression of estrogen and progesterone receptors (Xu et al., 2012; Yang et al., 2013). Recent research has shown that ablation of a subset of AVPV neurons, kisspeptin$^+$ AVPV neurons, leads to a reduction in female sexual receptivity, whereas optogenetic activation of these neurons enhances the behavior (Hellier et al., 2018). PR$^+$ VMHvl neurons exhibit structural plasticity depending on sex hormones (Inoue et al., 2019). Labeling projections of PR$^+$ VMHvl neurons with virally-encoded mCherry fused to the synaptic vesicle synaptophysin (Syp:mCherry) revealed that there is a dramatic, 3-fold increase of presynaptic termini in the AVPV in OVX primed and natural estrus females. Most of PR$^+$ VMHvl neurons are glutamatergic. The amplitude of optogenetically evoked EPSCs in AVPV neurons, following ChR2-assisted stimulation of PR$^+$ VMHvl neuronal axon termini, is larger in OVX primed females compared to OVX females. Subsequent experiments utilizing an optogenetic approach have emphasized the pivotal role of this PR$^+$ VMHvl to AVPV circuit in controlling female sexual receptivity. These findings suggest that sex hormones enhance excitatory synaptic transmission through an increase in glutamatergic projections within PR$^+$ VMHvl to AVPV circuit. Ovarian hormones induce plastic changes in many brain regions (Inoue, 2022). This study represents the first to link hormone-induced plasticity with behavioral alterations throughout the estrous cycle, offering insights into the neural mechanisms underpinning female sexual behavior. As described above, Cckar$^+$ VMHvl neurons are a subset of PR$^+$ VMHvl neurons critical to regulate female sexual behavior. Because almost all of PR$^+$ VMHvl neurons are glutamatergic, Cckar$^+$ VMHvl neurons are also glutamatergic. These Cckar$^+$ VMHvl neurons also project to the AVPV, mPOA, and PAG. Retrograde labeling of AVPV-projecting neurons combined with cell body labeling of Cckar$^+$ VMHvl neurons revealed that over 70% of AVPV-projecting VMHvl neurons are Cckar$^+$. In addition, the same as PR$^+$ VMHvl neurons, Cckar$^+$ VMHvl neurons also increase their presynaptic termini, labeled with Syp:mCherry, in OVX primed females, while Cckar-VMHvl neurons do not (Knoedler et al., 2022). Thus, Cckar$^+$ VMHvl neurons exhibit preferential projection to the AVPV and structural plasticity, suggesting that the Cckar$^+$ projection within PR$^+$ VMHvl to AVPV circuit plays a crucial role in controlling female sexual behavior.

As the VMH, mPOA, AVPV, and PAG are interconnected to each other, how information processing is achieved in these neural circuits is an important future question to understand the whole picture of the neural circuit mechanisms controlling female sexual behavior.

Discussion

Classic studies have identified the pivotal roles of sex hormones and specific brain regions in regulating female sexual behavior. Recent advancements, including transcriptomic analyses and the viral delivery of transgenes to molecularly identified neuronal populations, have enhanced our understanding of how these populations govern behavior. Future research should aim to further elucidate the mechanisms through which sex hormone-mediated regulation of neural circuit functions and behaviors occurs. A critical avenue of investigation involves deciphering the molecular underpinnings of hormone-dependent neural plasticity. Estrogen signaling is important for the structural plasticity in many brain regions including PR$^+$ VMHvl neurons. Utilizing data from recent transcriptomic analyses will be essential in identifying the genes responsible for such structural plasticity. Intriguingly, male PR$^+$ VMHvl neurons do not exhibit the same increase in presynaptic termini as their female counterparts, while the most of PR$^+$ VMHvl neurons express Esr1 in both sexes (Inoue et al., 2019). It is likely that the ability of PR$^+$ VMHvl neurons to rewire the circuit in adults is developmentally hard-wired into the female brain. Such sexually dimorphic structural plasticity could be a result of difference in gene expression downstream of Esr1. Examining differences in Esr1-mediated gene expression between sexes could shed light on the mechanisms behind this sexually dimorphic structural plasticity. Further studies demonstrated that VMHvl neurons change their firing activity across the estrous cycle, and this may also result in cyclic change in female sexual behavior across the estrous cycle (Yin et al., 2022). Identifying the genes whose expression

changes in response to hormonal fluctuations within these populations could provide insights into the nature of these plastic changes.

Characterizing the entire neural circuits controlling female sexual behavior in the estrous cycle-dependent manner is another important direction. The major outputs of VMH neurons are to the AVPV, mPOA, and PAG. The VMH to PAG circuit has been considered essential for initiating female sexual behavior, largely because both regions contribute to the behavior and the PAG is more directly linked to motor control functions. However, a recent study has highlighted the significance of the PR^+ VMHvl to AVPV circuit in female sexual behavior (Inoue et al., 2019). The AVPV is traditionally recognized for its role in fertility and the regulation of the estrous cycle itself. The involvement of AVPV neurons in modulating female sexual behavior has only recently been uncovered, indicating that previous studies may have overlooked the importance of the VMH to AVPV circuit (Hellier et al., 2018). The interconnected nature of the VMH, mPOA, and AVPV, along with the PAG's receipt of outputs from these hypothalamic regions, underscores the complexity of the neural networks involved. A comprehensive examination of how information is processed within these interconnected circuits to facilitate female sexual behavior is necessary for a full understanding of the neural mechanisms at play. While not the focus of this review, it is important to note that olfactory cues play a crucial role in driving female sexual behavior (Fraser and Shah, 2014). VMH receives inputs from circuits engaged in pheromonal information processing such as the medial amygdala (MeA) and bed nucleus stria terminalis (BNST) (Lo et al., 2019). Research has shown that the MeA, but not the BNST, is involved in pheromone-induced female sexual behavior (Ishii et al., 2017). The application of recent technical advancements, like multi-fiber photometry, allows for the simultaneous recording of activity across various brain regions (Kim et al., 2016; Guo et al., 2023). This, combined with epistasis behavioral experiments that can either suppress or activate specific nodes within the circuits, offers to dissect the full scope of neural circuits and their relationships in controlling female sexual behavior.

Lastly, exploring beyond the neural circuits that control female sexual behavior to include those governing rejection and mating completion behaviors is essential for a comprehensive understanding of reproductive strategy. Rejection behavior serves to avoid non-productive mating, optimizing energy efficiency and minimizing predation risk. During diestrus, when circulating ovarian hormone levels are low, females actively reject male mounts. This raises the question: Is rejection behavior merely a suppressed form of sexual behavior, or does it involve distinct neural circuits specifically for rejection? As described in the previous section, a recent study of anterior VMHvl controlling rejection suggests the latter possibility (Gutierrez-Castellanos et al., 2023). Another finding from different group also indicates that BNST is important for pheromone-induced rejection behavior (Osakada et al., 2018). One possibility is that the neural circuitry for female sexual behavior and rejection operates in a reciprocal inhibitory manner, modulated by ovarian hormone levels, to produce varied behaviors throughout the estrous cycle. Understanding the intricate connections between these neural circuits is crucial for elucidating how these diverse behaviors are orchestrated across the estrous cycle. Mating completion, characterized by a female receiving male ejaculation, triggers a state of satiation that diminishes sexual behavior (Zhou et al., 2023). Similar to rejection, mating completion leads to behaviors that avoid further male interaction, such as decreased attraction and reduced likelihood of copulation. However, mating completion should be seen as a state leading to gestation rather than an isolated behavior, suggesting that the neural circuits involved in mating completion may differ from or be upstream of those controlling rejection. Investigating the activity dynamics of neural populations responsible for rejection during mating completion, and vice versa, could offer valuable insights into the similarities and differences between these behaviors and states. As described, a subpopulation of mPOA neurons has been identified to encode mating completion (Ishii et al., 2023). Interestingly, another subpopulation of mPOA neurons, $Galanin^+$ mPOA neurons, undergo significant plastic changes during pregnancy, contributing to parenting behavior post-delivery (Ammari et al., 2023). Analyzing the overlap or interconnectivity between neurons involved in mating completion and $Galanin^+$ mPOA neurons could provide deeper understanding into the post-mating completion processes essential for successful reproduction. This comprehensive approach to studying the neural underpinnings of female sexual behavior, along with rejection and mating completion, is pivotal in unraveling the complex interplay of behaviors associated with reproduction.

Females, including women, exhibit various behavioral changes throughout their cycle. The dramatic fluctuations in rodent female sexual behavior across the estrous cycle, influenced by ovarian hormone levels, serve as an excellent model for exploring how ovarian hormones modulate neural circuits and, consequently, behaviors. Insights gained from such research can significantly contribute to our understanding of the etiology of women's psychiatric disorders, including premenstrual dysphoric disorder, postpartum depression, and symptoms associated with menopausal syndrome. By studying these hormonal modulations and their effects on behavior, we can deepen our understanding of these complex conditions and advance towards more effective treatments.

Author contributions

SI: Writing – original draft, Writing – review & editing.

Funding

The author(s) declare that financial support was received for the research, authorship, and/or publication of this article. This work was supported by the Gift from McDonnell Center for Systems Neuroscience.

Acknowledgments

The author thanks Masatoshi Inoue for their valuable input to the manuscript.

Conflict of interest

The author declares that the research was conducted in the absence of any commercial or financial relationships that could be construed as a potential conflict of interest.

Publisher's note

References

Allen, E. (1922). The oestrous cycle in the mouse. *Am. J. Anat.* 30, 297–371. doi: 10.1002/AJA.1000300303

Ammari, R., Monaca, F., Cao, M., Nassar, E., Wai, P., Grosso, N. A. D., et al. (2023). Hormone-mediated neural remodeling orchestrates parenting onset during pregnancy. *Science* 382, 76–81. doi: 10.1126/science.adi0576

Aou, S., Oomura, Y., and Yoshimatsu, H. (1988). Neuron activity of the ventromedial hypothalamus and the medial preoptic area of the female monkey during sexual behavior. *Brain Res.* 455, 65–71. doi: 10.1016/0006-8993(88)90115-1

Arnold, A. P. (2009). The organizational-activational hypothesis as the foundation for a unified theory of sexual differentiation of all mammalian tissues. *Horm. Behav.* 55, 570–578. doi: 10.1016/j.yhbeh.2009.03.011

Bakker, J., Honda, S.-I., Harada, N., and Balthazart, J. (2002). The aromatase knock-out mouse provides new evidence that estradiol is required during development in the female for the expression of sociosexual behaviors in adulthood. *J. Neurosci.* 22, 9104–9112. doi: 10.1523/JNEUROSCI.22-20-09104.2002

Barfield, R. J., and Chen, J. J. (1977). Activation of estrous behavior in ovariectomized rats by intracerebral implants of estradiol benzoate. *Endocrinology* 101, 1716–1725. doi: 10.1210/endo-101-6-1716

Bast, J. D., Hunts, C., Renner, K. J., Morris, R. K., Quadagno, D. M., Hunts, C., et al. (1987). Lesions in the preoptic area suppressed sexual receptivity in ovariectomized rats with estrogen implants in the ventromedial hypothalamus. *Brain Res. Bull.* 18, 153–158. doi: 10.1016/0361-9230(87)90184-5

Beach, F. A. (1976). Sexual attractivity, proceptivity, and receptivity in female mammals. *Horm. Behav.* 7, 105–138. doi: 10.1016/0018-506x(76)90008-8

Blaustein, J. D., Tetel, M. J., Ricciardi, K. H. N., Delville, Y., and Turcotte, J. C. (1994). Hypothalamic ovarian steroid hormone-sensitive neurons involved in female sexual behavior. *Psychoneuroendocrinology* 19, 505–516. doi: 10.1016/0306-4530(94)90036-1

Cheong, R. Y., Czieselsky, K., Porteous, R., and Herbison, A. (2015.) Expression of ESR1 in Glutamatergic and GABAergic Neurons Is Essential for Normal Puberty Onset, Estrogen Feedback, and Fertility in Female Mice. *J Neurosci.* 35: 14533–14543. doi: 10.1523/JNEUROSCI.1776-15.2015

Deleon, D. D., Zelinski-Wooten, M. B., and Barkley, M. S. (1990). Hormonal basis of variation in oestrous cyclicity in selected strains of mice. *J. Reprod. Fertil.* 89, 117–126. doi: 10.1530/jrf.0.0890117

Flanagan-Cato, L. M., and Mcewen, B. S. (1995). Pattern of Fos and Jun expression in the female rat forebrain after sexual behavior. *Brain Res.* 673, 53–60. doi: 10.1016/0006-8993(94)01395-x

Floody, O. R., Lisk, R. D., and Vomachka, A. J. (1986). Facilitation of lordosis by estradiol in the mesencephalic central gray. *Physiol. Behav.* 37, 587–595. doi: 10.1016/0031-9384(86)90291-x

Fraser, E. J., and Shah, N. M. (2014). Complex chemosensory control of female reproductive behaviors. *PLoS One* 9:e90368. doi: 10.1371/journal.pone.0090368

Guo, Z., Yin, L., Diaz, V., Dai, B., Osakada, T., Lischinsky, J. E., et al. (2023). Neural dynamics in the limbic system during male social behaviors. *Neuron* 111, 3288–3306.e4. doi: 10.1016/j.neuron.2023.07.011

Gutierrez-Castellanos, N., Husain, B. F. A., Dias, I. C., Nomoto, K., Duarte, M. A., Ferreira, L., et al., (2023) A hypothalamic node for the cyclical control of female sexual rejection. *bioRxiv*. Available at: https://doi.org/10.1101/2023.01.30.526259. [Epub ahead of preprint]

Hashikawa, K., Hashikawa, Y., Tremblay, R., Zhang, J., Feng, J. E., Sabol, A., et al. (2017). Esr1^{+} cells in the ventromedial hypothalamus control female aggression. *Nat. Neurosci.* 20, 1580–1590. doi: 10.1038/nn.4644

Hellier, V., Brock, O., Candlish, M., Desroziers, E., Aoki, M., Mayer, C., et al. (2018). Female sexual behavior in mice is controlled by kisspeptin neurons. *Nat. Commun.* 9:400. doi: 10.1038/s41467-017-02797-2

Inoue, S. (2022). Neural basis for estrous cycle-dependent control of female behaviors. *Neurosci. Res.* 176, 1–8. doi: 10.1016/j.neures.2021.07.001

Inoue, S., Yang, R., Tantry, A., Davis, C., Yang, T., Knoedler, J. R., et al. (2019). Periodic remodeling in a neural circuit governs timing of female sexual behavior. *Cell* 179, 1393–1408.e16. doi: 10.1016/j.cell.2019.10.025

Ishii, K. K., Hashikawa, K., Chea, J., Yin, S., Fox, R. E., Kan, S., et al. (2023) Post-mating inhibition of female sexual drive via heterogeneous neuronal ensembles in the medial preoptic area. *bioRxiv*. Available at: https://doi.org/10.1101/2023.09.08.556711. [Epub ahead of preprint]

Ishii, K. K., Osakada, T., Mori, H., Miyasaka, N., Yoshihara, Y., Miyamichi, K., et al. (2017). A labeled-line neural circuit for pheromone-mediated sexual behaviors in mice. *Neuron* 95, 123–137.e8. doi: 10.1016/j.neuron.2017.05.038

Kato, A., and Sakuma, Y. (2000). Neuronal activity in female rat preoptic area associated with sexually motivated behavior. *Brain Res.* 862, 90–102. doi: 10.1016/s0006-8993(00)02076-x

Kim, C. K., Yang, S. J., Pichamoorthy, N., Young, N. P., Kauvar, I., Jennings, J. H., et al. (2016). Simultaneous fast measurement of circuit dynamics at multiple sites across the mammalian brain. *Nat. Methods* 13, 325–328. doi: 10.1038/nmeth.3770

Kim, D. W., Yao, Z, Graybuck, L. T., Kim, T. K., Nguyen, T. N., Smith, K. A., et al. (2019). Multimodal Analysis of Cell Types in a Hypothalamic Node Controlling Social Behavior. *Cell.* 179:713–728. doi: 10.1016/j.cell.2019.09.020

Knoedler, J. R., Inoue, S., Bayless, D. W., Yang, T., Tantry, A., Davis, C. H., et al. (2022). A functional cellular framework for sex and estrous cycle-dependent gene expression and behavior. *Cell* 185, 654–671.e22. doi: 10.1016/j.cell.2021.12.031

Kudway, A. E., and Rissman, E. F. (2003). Double oestrogen receptor a and b knockout mice reveal differences in neural oestrogen-mediated progestin receptor induction and female sexual behaviour. *J. Neuroendocrinol.* 15, 978–983. doi: 10.1046/j.1365-2826.2003.01089.x

Lindburg, D. G., Czekala, N. M., and Swaisgood, R. R. (2001). Hormonal and behavioral relationships during estrus in the giant panda. *Zoo Biol.* 20, 537–543. doi: 10.1002/zoo.10027

Lo, L., Yao, S., Kim, D. W., Cetin, A., Harris, J., Zeng, H., et al. (2019). Connectional architecture of a mouse hypothalamic circuit node controlling social behavior. *Proc. Natl. Acad. Sci. USA*. 116: 7503–7512. doi: 10.1073/pnas.1817503116

Lubahn, D. B., Moyer, J. S., Golding, T. S., Couse, J. F., Korach, K. S., and Smithies, O. (1993). Alteration of reproductive function but not prenatal sexual development after insertional disruption of the mouse estrogen receptor gene. *Proc. Natl. Acad. Sci. U.S.A.* 90, 11162–11166. doi: 10.1073/pnas.90.23.11162

Lydon, J. P., DeMayo, F. J., Funk, C. R., Mani, S. K., Hughes, A. R., Montgomery, C. A., et al. (1995). Mice lacking progesterone receptor exhibit pleiotropic reproductive abnormalities. *Genes Dev.* 9, 2266–2278. doi: 10.1101/gad.9.18.2266

McHenry, J. A., Otis, J. M., Rossi, M. A., Robinson, J. E., Kosyk, O., Miller, N. W., et al. (2017). Hormonal gain control of a medial preoptic area social reward circuit. *Nat. Neurosci.* 20, 449–458. doi: 10.1038/nn.4487

Meisel, R. L., and Pfaff, D. W. (1985). Specificity and neural sites of action of anisomycin in the reduction or facilitation of female sexual behavior in rats. *Horm. Behav.* 19, 237–251. doi: 10.1016/0018-506x(85)90024-8

Moffitt, J. R., Bambah-Mukku, D., Eichhorn, S. W., Vaughn, E., Shekhar, K., Perez, J. D., et al. (2018). Molecular, spatial and functional single-cell profiling of the hypothalamic preoptic region. *Science* 362:eaau5324. doi: 10.1126/science.aau5324

Moss, R. L., Paloutzian, R. F., and Law, O. T. (1974). Electrical stimulation of forebrain structures and its effect on copulatory as well as stimulus-bound behavior in ovariectomized hormone-primed rats. *Physiol. Behav.* 12, 997–1004. doi: 10.1016/0031-9384(74)90147-4

Musatov, S., Chen, W., Pfaff, D. W., Kaplitt, M. G., Ogawa, S., and Sciences, B. (2006). RNAi-mediated silencing of estrogen receptor in the ventromedial nucleus of hypothalamus abolishes female sexual behaviors. *Proc. Natl. Acad. Sci. U.S.A.* 103, 10456–10460. doi: 10.1073/pnas.0603045103

Nelson, J. F., Feliciot, L. S., Osterburg, H. H., and Finch, C. E. (1992). Differential contributions of ovarian and extraovarian factors to age-related reductions in plasma estradiol and progesterone during the estrous cycle of C57BL/6J mice. *Endocrinology* 130, 805–810. doi: 10.1210/endo.130.2.1733727

Nomoto, K., and Lima, S. Q. (2015). Enhanced male-evoked responses in the ventromedial hypothalamus of sexually receptive female mice. *Curr. Biol.* 25, 589–594. doi: 10.1016/j.cub.2014.12.048

Ogawa, S., Eng, V., Taylor, J., Lubahn, D. B., Korach, K. S., and Pfaff, D. W. (1998). Roles of estrogen receptor-gene expression in reproduction-related behaviors in female mice. *Endocrinology* 139, 5070–5081. doi: 10.1210/endo.139.12.6357

Osakada, T., Ishii, K. K., Mori, H., Eguchi, R., Ferrero, D. M., Yoshihara, Y., et al. (2018). Sexual rejection via a vomeronasal receptor-triggered limbic circuit. *Nat. Commun.* 9:4463. doi: 10.1038/s41467-018-07003-5

Pfaff, D. W., and Sakuma, Y. (1979a). Facilitation of the lordosis reflex of female rats from the ventromedial nucleus of the hypothalamus. *J. Physiol.* 288, 189–202. doi: 10.1113/jphysiol.1979.sp012690

Pfaff, D. W., and Sakuma, Y. (1979b). Deficit in the lordosis reflex of female rats caused by lesions in the ventromedial nucleus of the hypothalamus. *J. Physiol.* 288, 203–210. doi: 10.1113/jphysiol.1979.sp012691

Pfaus, J. G., Kleopoulos, S. P., Mobbs, C., Gibbs, R. B., and Pfaff, D. W. (1993). Sexual stimulation activates c-fos within estrogen-concentrating regions of the female rat forebrain. *Brain Res.* 624, 253–267. doi: 10.1016/0006-8993(93)90085-2

Powers, J. B. (1970). Hormonal control of sexual receptivity during the estrous cycle of the rat. *Physiol. Behav.* 5, 831–835. doi: 10.1016/0031-9384(70)90167-8

Rainbow, T. C., Davis, P. G., and Mcewen, B. S. (1980). Anisomycin inhibits the activation of sexual behavior by estradiol and progesterone. *Brain Res.* 194, 548–555. doi: 10.1016/0006-8993(80)91240-8

Rainbow, T. C., Mcginnis, M. Y., Davis, P. G., and Mcewen, B. S. (1982). Application of anisomycin to the lateral ventromedial nucleus of the hypothalamus inhibits the activation of sexual behavior by estradiol and progesterone. *Brain Res.* 233, 417–423. doi: 10.1016/0006-8993(82)91217-3

Rajendren, G., Dudley, C. A., and Moss, R. L. (1991). Role of the ventromedial nucleus of hypothalamus in the male-induced enhancement of lordosis in female rats. *Physiol. Behav.* 50, 705–710. doi: 10.1016/0031-9384(91)90006-a

Ring, J. R., and Providence, R. I. (1944). The estrogen-progesterone induction of sexual receptivity in the spayed female mouse. *Endocrinology* 34, 269–275. doi: 10.1210/endo-34-4-269

Rissman, E. F., Early, A. H., Taylor, J. A., Korach, K. S., and Lubahn, D. B. (1997). Estrogen receptors are essential for female sexual receptivity. *Endocrinology* 138, 507–510. doi: 10.1210/endo.138.1.4985

Robert, D. (1962). Diencephalic placement of estradiol and sexual receptivity in the female rat. *Am. J. Phys.* 203, 493–496. doi: 10.1152/ajplegacy.1962.203.3.493

Sakuma, Y. (1994). Estrogen-induced changes in the neural impulse flow from the female rat preoptic region. *Horm. Behav.* 28, 438–444. doi: 10.1006/hbeh.1994.1041

Sakuma, Y., and Pfaff, D. W. (1979a). Facilitation of female reproductive behavior from mesensephalic central gray in the rat. *Am. J. Phys.* 237, R278–R284. doi: 10.1152/ajpregu.1979.237.5.R278

Sakuma, Y., and Pfaff, D. W. (1979b). Mesencephdic mechanisms for integration of female reproductive behavior in the rat. *Am. J. Phys.* 237, R285–R290. doi: 10.1152/ajpregu.1979.237.5.R285

Sakuma, Y., and Pfaff, D. W. (1980). Covergent effects of lordosis-relevant somatosensory and hypothalamic influences on central gray cells in the rat mesencephalon. *Exp. Neurol.* 70, 269–281. doi: 10.1016/0014-4886(80)90026-6

Takeo, T., Chiba, Y., and Sakuma, Y. (1993). Suppression of the lordosis reflex of female rats by efferents of the medial preoptic area. *Physiol. Behav.* 53, 831–838. doi: 10.1016/0031-9384(93)90258-h

Vaughn, E., Eichhorn, S., Jung, W., Zhuang, X., and Dulac, C.. (2022). Three-dimensional interrogation of cell types and instinctive behavior in the periaqueductal gray. *bioRxiv*. Available at: https://doi.org/10.1101/2022.06.27.497769. [Epub ahead of preprint]

Wei, Y. C., Wang, S. R., Jiao, Z. L., Zhang, W., Lin, J. K., Li, X. Y., et al. (2018). Medial preoptic area in mice is capable of mediating sexually dimorphic behaviors regardless of gender. *Nat. Commun.* 9:279. doi: 10.1038/s41467-017-02648-0

Whalen, R. E. (1974). Estrogen-progesterone induction of mating in female rats. *Horm. Behav.* 5, 157–162. doi: 10.1016/0018-506x(74)90040-3

Wu, M., Manoli, D. S., Fraser, E. J., Coats, J. K., Tollkuhn, J., Honda, S. I., et al. (2009). Estrogen masculinizes neural pathways and sex-specific behaviors. *Cell* 139, 61–72. doi: 10.1016/j.cell.2009.07.036

Xu, X., Coats, J. K., Yang, C. F., Wang, A., Ahmed, O. M., Alvarado, M., et al. (2012). Modular genetic control of sexually dimorphic behaviors. *Cell* 148, 596–607. doi: 10.1016/j.cell.2011.12.018

Yamada, S., and Kawata, M. (2014). Identification of neural cells activated by mating stimulus in the periaqueductal gray in female rats. *Front. Neurosci.* 8:421. doi: 10.3389/fnins.2014.00421

Yang, C. F., Chiang, M. C., Gray, D. C., Prabhakaran, M., Alvarado, M., Juntti, S. A., et al. (2013). Sexually dimorphic neurons in the ventromedial hypothalamus govern mating in both sexes and aggression in males. *Cell* 153, 896–909. doi: 10.1016/j.cell.2013.04.017

Yin, L., Hashikawa, K., Hashikawa, Y., Osakada, T., Lischinsky, J. E., Diaz, V., et al. (2022). VMHvll^{Cckar} cells dynamically control female sexual behaviors over the reproductive cycle. *Neuron* 110, 3000–3017.e8. doi: 10.1016/j.neuron.2022.06.026

Zhou, X., Li, A., Mi, X., Li, Y., Ding, Z., An, M., et al. (2023). Hyperexcited limbic neurons represent sexual satiety and reduce mating motivation. *Science* 379, 820–825. doi: 10.1126/science.abl4038

frontiers | Frontiers in Neural Circuits

TYPE Mini Review
PUBLISHED 15 May 2024
DOI 10.3389/fncir.2024.1408187

OPEN ACCESS

EDITED BY
Charles A. Greer,
Yale University, United States

REVIEWED BY
Diego García-González,
Spanish National Research Council (CSIC), Spain

*CORRESPONDENCE
Fumiaki Imamura
✉ fui1@psu.edu

RECEIVED 27 March 2024
ACCEPTED 02 May 2024
PUBLISHED 15 May 2024

CITATION
Imamura F (2024) Effects of prenatal alcohol exposure on the olfactory system development.
Front. Neural Circuits 18:1408187.
doi: 10.3389/fncir.2024.1408187

Effects of prenatal alcohol exposure on the olfactory system development

Fumiaki Imamura*

Department of Pharmacology, Penn State College of Medicine, Hershey, PA, United States

Fetal Alcohol Spectrum Disorders (FASD), resulting from maternal alcohol consumption during pregnancy, are a prominent non-genetic cause of physical disabilities and brain damage in children. Alongside common symptoms like distinct facial features and neurocognitive deficits, sensory anomalies, including olfactory dysfunction, are frequently noted in FASD-afflicted children. However, the precise mechanisms underpinning the olfactory abnormalities induced by prenatal alcohol exposure (PAE) remain elusive. Utilizing rodents as a model organism with varying timing, duration, dosage, and administration routes of alcohol exposure, prior studies have documented impairments in olfactory system development caused by PAE. Many reported a reduction in the olfactory bulb (OB) volume accompanied by reduced OB neuron counts, suggesting the OB is a brain region vulnerable to PAE. In contrast, no significant olfactory system defects were observed in some studies, though subtle alterations might exist. These findings suggest that the timing, duration, and extent of fetal alcohol exposure can yield diverse effects on olfactory system development. To enhance comprehension of PAE-induced olfactory dysfunctions, this review summarizes key findings from previous research on the olfactory systems of offspring prenatally exposed to alcohol.

KEYWORDS

Fetal Alcohol Spectrum Disorders, prenatal alcohol exposure, olfactory system, olfactory bulb, development

Introduction

Maternal alcohol consumption during pregnancy is the most commonly identifiable non-genetic cause of physical disabilities and damage to the brain in the child. These disabilities or damages are collectively known as Fetal Alcohol Spectrum Disorders (FASD) (Popova et al., 2023). Estimates of the prevalence of FASD in the US and Western Europe range from 0.6 to 5.0% among school-aged children (May et al., 2009, 2014, 2018). There is no known safe amount and timing of alcohol to drink during pregnancy. Some may drink throughout pregnancy, and some may binge drink, consuming a large amount of alcohol in a short period. Human pregnancy is roughly divided into 3 stages known as trimesters of about 3 months each: first trimester – conception to 12 weeks; second trimester – 13 to 27 weeks; third trimester – 28 to 40 weeks. The prevalence of drinking during pregnancy varies by trimester and is higher in the first trimester than in the second and third trimesters (Ethen et al., 2009). According to a 2013 report, approximately 18% of US women consumed alcohol during early pregnancy, and 6.6% binge drank (The NSDUH Report, Substance Abuse and Mental Health Services Administration, 2014). While both binge drinking and chronic low-level drinking

during pregnancy are harmful, it is important to note that binge drinking poses a significant risk for serious brain damage (Maier and West, 2001).

There are some common features such as physical features including lower birth weight, shorter stature, smaller head circumference, facial dysmorphism, and neurocognitive deficits including intellectual disability, speech and language delays, poor social skills, and increased risk of anxiety, depression, and ADHD (Riley et al., 2011; Temple et al., 2019). In addition, sensory abnormalities are often observed in children with FASD. They may show signs of being hypersensitive or hyposensitive to the senses of touch, taste, smell, sight, and sound. Particularly, changes in smell/taste sensitivity affect children's eating behaviors (Carr et al., 2010; Hannigan et al., 2015; Jirikowic et al., 2020). Furthermore, children with a history of heavy alcohol exposure before birth exhibited impaired odor identification (Bower et al., 2013) as well as arhinencephaly (Peiffer et al., 1979). Therefore, it is important to understand how maternal drinking during pregnancy affects the child's olfactory system. This review summarizes the previous animal studies focusing on the impacts of prenatal alcohol exposure (PAE) on the olfactory system. The author apologizes to those whose work was not included here due to space limitations.

Studies of prenatal alcohol exposure focusing on the olfactory system

The characteristics of FASD vary in severity and depend on the timing, amount, and pattern of alcohol consumption during pregnancy. Several animal models have been used to simulate maternal drinking episodes. Among them, animal models widely used to see how PAE affects brain development are rodents such as mice and rats (Patten et al., 2014; Almeida et al., 2020). Generally, mice or rats were trained to consume ethanol from their drinking water or diet to simulate chronic drinking during pregnancy. In addition, intraperitoneal injection, subcutaneous injection, and intragastric gavage have been used to simulate binge drinking episodes. As a rough approximation, gestation day (GD) 1–10 of mice and rats corresponds to the first trimester of human pregnancy, GD10-20 (just before delivery) to the second trimester, and postnatal day (P) 1–10 to the third trimester (Almeida et al., 2020). In this review, I adopted a definition of GD0 as the date when the copulation plug was confirmed. When different dates were used in a study, I adjusted the day for a consistent interpretation.

Development of rodents' olfactory system

Odors are initially detected by odorant receptors expressed in olfactory sensory neurons (OSNs) within the olfactory epithelium (OE). These OSNs extend their axons to the glomeruli of the olfactory bulb (OB) to form synapses with mitral and tufted cells, which serve as OB projection neurons transmitting olfactory information to the olfactory cortex. In the OB, the activity of mitral/tufted cells is modulated by OB interneurons such as periglomerular cells and granule cells, which synapse with dendrites of mitral/tufted cells within the glomerular layer (GL) and external plexiform layer (EPL), respectively.

The development of the rodents' olfactory system has been studied and summarized in detail in other studies (Treloar et al., 2010; Kim et al., 2023). Briefly, the OE is generated from the olfactory placodes, a thickened ectoderm in the head region. In mice, the olfactory pits begin invaginate from the olfactory placode around GD10. The nostrils are narrowed to small slits and the olfactory pit has further invaginated into a more complex nasal cavity by GD11.5 (Miller et al., 2010b). The invaginated olfactory pits differentiate into OE where OSNs are generated. Generation of OSNs in the OE begins around GD11 and turns over throughout life (Eerdunfu et al., 2017; Nguyen and Imamura, 2019). On the other hand, the OB is located at the most anterior region of the brain in rodents. In mice, the formation of the OB begins with the evagination of the anterior end of the telencephalic vesicle around GD11 (Miller et al., 2010b; Imamura et al., 2011). Mitral/tufted cells are generated from radial glial cells in this developing OB between GD9 and GD17; while mitral cells are mostly generated between embryonic day GD9 and GD13, peaking at GD11, tufted cells are born later, between GD12 and GD17 (Hinds, 1972; Blanchart et al., 2006; Imamura et al., 2011; Hirata et al., 2019). OB interneurons are mostly generated during late gestation and early postnatal stages and are continuously newly born throughout life (Hinds, 1968; Imayoshi et al., 2008).

OSN axons first reach the developing OB at GD11 and penetrate the basement membrane to form an olfactory nerve layer by GD12 (Miller et al., 2010a). The immature mitral/tufted cells have multiple broadly spread apical dendrites, and they begin to form protoglomeruli with OSN axons around GD15 (Treloar et al., 1999; Blanchart et al., 2006). Synapse formation in the OB also starts at this stage in the GL, followed by the EPL and granule cell layer (GCL) (Hinds and Hinds, 1976). Dendritic refinements of mitral/tufted cells, such as discrimination of primary and secondary dendrites and retraction of supernumerary primary dendrites, occur during early postnatal days (Lin et al., 2000; Aihara et al., 2021). Axonogenesis of mitral/atrial cells begins around GD11.5 immediately after final differentiation, and they extend between GD12 and GD14 to form the lateral olfactory tract (Lopez-Mascaraque et al., 1996; Walz et al., 2006). Axons of mitral/tufted cells target the piriform cortex, anterior olfactory nucleus, olfactory tubercle, amygdaloid cortex, and entorhinal cortex, consisting of the olfactory cortex. Many neurons in the olfactory cortex are born during similar stages with the mitral/tufted cells, GD11 – GD18 (Martin-Lopez et al., 2017, 2019; Aerts and Seuntjens, 2021).

Effects of PAE on the rodent olfactory system

Different timing in ethanol exposure may cause different effects on the olfactory system development. Many rodent studies simulated exposure to alcohol during pregnancy and the findings are summarized in Table 1. A study fed pregnant mice with 10% EtOH in drinking water throughout pregnancy (Akers et al., 2011). In this case, P60 offspring exhibited the greatest volume reduction in the OB among 62 brain regions examined with MRI and showed impaired discrimination between similar odors (80% R-carvone/20% S-carvone vs. 20% R-carvone/80% S-carvone) but left odor memory intact (Akers et al., 2011). Similarly, when pregnant female rats were fed with a 35% ethanol-derived calorie (EDC) liquid diet from GD6 to GD20

TABLE 1 Effects of prenatal alcohol exposure on the rodent olfactory system.

Species Timing / Duration	Route (dose)	Age examined	Effects on the olfactory system	References
Mice GD0 – GD19	Drinking water (10%)	P60	Decrease in OB volume Failed to discriminate relatively similar odors	Akers et al. (2011)
Rats GD0 – GD19	Intragastric gavage (6.0 g/kg daily; 22.5% solution)	GD20 & P10	Decrease in OB volume Reduction in the granule cell numbers	Maier et al. (1999)
Rats GD6 – GD20	EDC liquid diet (35%)	P3	Decrease in OB volume; no odor preference paired with milk	Barron et al. (1988) and Barron and Riley (1992)
		P10	no odor aversion associated with mild toxicosis	
		P100	the same level of odor aversion associated with mild toxicosis as the control group	
Mice GD7 or GD8	Intraperitoneal injection (2.9 g/kg- 25% solution or 2.8 g/kg- 23.7% solution; twice at four-hour intervals)	GD17	Decrease in OB volume	Parnell et al. (2009), Godin et al. (2010), and Lipinski et al. (2012)
GD8.5			Increase in OB volume	
Mice GD7 – GD11	Liquid diet containing ethanol (4.8%)	GD17	Decrease in the length of the right OB	Parnell et al. (2014)
GD12 – GD16			No significant defects	
Rats GD11 – GD20	EDC liquid diet (35%)	P40 - P48	Gene expression changes in OB * Enhanced ethanol intake at P15	Youngentob et al. (2007a), Youngentob et al. (2007b), Middleton et al. (2009), Youngentob and Glendinning (2009), and Gano et al. (2020)
Mice GD13 – P21	EDC liquid diet (20%)	P21	Decrease in OB volume	Nyouist-Battie and Gochee (1985)
Rats P4 – P9	Intragastric gavage (4.5 g/kg daily; 5.1% or 10.2% solution)	P10 & adult (> P90)	Decrease in OB volume Reduction in the granule and mitral cell numbers	Bonthius and West (1991) and Bonthius et al. (1992)
	Intragastric gavage (6.6 g/kg daily; 2.5% solution)		No significant reduction in the granule and mitral cell numbers	
Mice P4 – P9	Intraperitoneal injection (4.4 g/kg daily; 20% solution)	Adult (P110 – P122)	Decrease in OB volume Reduction in the granule cell numbers	Todd et al. (2018)
Mice P7	Subcutaneous injection (2.5 g/kg- 20%; twice at two-hour intervals)	3-month-old	Enhanced odor-evoked local field potential in the OB and anterior piriform cortex	Wilson et al. (2011)

of pregnancy, offspring showed a volume decrease in the OB at P3 (Barron and Riley, 1992). Interestingly, the P3 rats born from females fed with 35% EDC did not show a preference for the odor paired with milk infusion, and the P10 rats did not avoid the odor associated with lithium chloride injection, which induced a mild toxicosis (Barron et al., 1988). However, the P100 adult rats born from females fed with 35% EDC showed the same level of odor aversion learning as the control group (Barron et al., 1988). Another study fed pregnant mice and pups with a 20% EDC liquid diet from GD13 to P21, equivalent to humans' second and third trimesters and early postnatal weeks (Nyouist-Battie and Gochee, 1985). This study showed an approximately 25% volume reduction in the OB of ethanol-fed mice at P21 compared to a normal diet-fed group, with reductions in the volume of the GL, EPL, and GCL, while the laminar organization and cellular cytoarchitecture were not substantially altered by ethanol.

In another study, alcohol was administered by intragastric gavage (6.0 g/kg/day) to pregnant rats from GD0 to GD19, which corresponds to the first two trimesters of human pregnancy (Maier et al., 1999). Compared to the control group that received an isocaloric maltose-dextrin solution, the offspring of ethanol-fed females had smaller OBs

with a reduced number of granule cells at GD20 and P10. Exposure to alcohol during the third trimester also affected OB formation. Rat pups were reared artificially and were administered alcohol with intragastric gavage (4.5 g/kg daily; administered either as a 5.1% or 10.2% solution) over P4 through P9. This alcohol exposure paradigm also reduced the OB volume and caused the reduction of the number of granule cells as well as mitral cells in P10 and adult (> P90) OBs (Bonthius and West, 1991; Bonthius et al., 1992). Interestingly, a higher daily dose (6.6 g/kg) but administered continuously with a lower (2.5%) ethanol concentration did not affect the number of either granule or mitral cells (Bonthius and West, 1991). Decreases in OB volume and number of granule cells were also observed in adult mice that received intraperitoneal injections of ethanol (4.4 g/kg) daily over P4 to P9, but not at lower doses (2.2 g/kg) (Todd et al., 2018). Therefore, chronic PAE impairs the OB formation and affects the generation and survival of OB neurons. Although the underlying mechanisms of OB damages are not known, gene expression profiling revealed a PAE, feeding with 35% EDC from GD11 to GD20, affected the expression of genes involved in neuronal development, synaptic transmission, and plasticity as well as inflammatory-related genes during adolescence (P40–P48) (Middleton et al., 2009; Gano et al., 2020). Moreover, the rats exposed to gestational ethanol showed enhanced ethanol intake as well as different sniffing responses to ethanol odor at P15, but the ethanol preference was absent at P90 (Youngentob et al., 2007a,b; Youngentob and Glendinning, 2009).

In addition to chronic PAE, acute PAE caused by binge drinking also affects the development of the olfactory system. To cause an acute PAE, several studies used the intraperitoneal ethanol injection method. When ethanol (2.9 g/kg) was administered intraperitoneally to pregnant female mice twice (four-hour intervals) at GD7, MRI measurement at GD17 found a reduction in overall brain size with marked volume reduction in the OB (Godin et al., 2010; Lipinski et al., 2012). Reduction of OB volume at GD17 was also observed with the intraperitoneal ethanol exposure at GD8 (2.8 g/kg; twice at four-hour intervals) (Parnell et al., 2009), while the same ethanol exposing paradigm performed at GD8.5 caused approximately 10% increase of the OB volume (Lipinski et al., 2012). Since some of the mice that showed a reduction of OB volume also had abnormal nasal cavity, defects in the development of olfactory sensory neurons might affect the OB formation in these mice (Parnell et al., 2009; Godin et al., 2010). On the other hand, the same group fed the pregnant mice with the 4.8% (v/v) ethanol-containing liquid diet for five days, from GD7 to 11 and from GD12 to 16 (Parnell et al., 2014). In this case, GD 7–11 and GD 12–16 ethanol-exposed groups showed a significant decrease in the volumes of the cerebellum and hippocampus at GD17, respectively, but no significant change in OB size was observed except for a shortening of the right OB of mice exposed to ethanol from GD7 to GD11.

Another study simulated binge drinking in the third trimester by causing acute PAE with subcutaneous injection of ethanol (2.5 g/kg; twice at two-hour intervals) into P7 mouse pups (Wilson et al., 2011). This treatment caused widespread cell death within 1 day of exposure, with the highest levels in the neocortex, intermediate levels in the dorsal hippocampus, and relatively low levels in the primary olfactory system including OB and piriform cortex. The acute PAE did not change the odor investigation or odor habituation in 3-month-old mice compared to saline-administered controls, whereas the hippocampal-dependent object place memory was significantly impaired. Interestingly, odor-evoked local field potential activity was enhanced in the OB, anterior piriform cortex, and hippocampus. These data suggest that the activity of neural circuits involved in odor information processing can be modified by acute PAE at a later gestational stage, which may contribute to specific behavioral abnormalities seen in children with FASD.

These results from rodent studies indicate that timing, quantity, and style of drinking are important to understanding the impact of PAE on olfactory system development. A previous study showed that acute PAE induced by intraperitoneal ethanol injection (2.9 g/kg) at GD11, but not at GD6, caused apparent deficits in the social behavior of male rat offspring; reduction of social investigation, contact behavior, and play fighting (Mooney and Varlinskaya, 2011). Considering the pivotal role of the olfactory system in rodent social behavior (Bakker et al., 2022), it is plausible that PAE-induced defects in olfactory information processing resulted in impaired social behavior.

Other animal models of PAE

Several other studies used non-rodent animals to examine the effects of PAE on the development of OB. For example, pregnant sheep were administered with alcohol. A moderate dose of alcohol was infused intravenously (1.75 g/kg) on 3 consecutive days followed by 4 days without alcohol beginning on GD 4 and continuing until GD 132, which corresponds with the end of the third trimester of human pregnancy (Washburn et al., 2015). In contrast to the findings from rat studies (Bonthius and West, 1991; Bonthius et al., 1992), there was no change in the number, density, or volume of mitral cells in the fetal (GD133) sheep OB, although it does not exclude the presence of functional abnormalities or the reduction in number of granule cells. In another study, fewer actively proliferating cells were found in the OBs of newborn monkeys born from females who voluntarily consumed alcohol (a maximum of 3.5 g alcohol/kg body weight on 4 days of the week) starting in the mid-gestation stage (Burke et al., 2016).

Discussion

As summarized in this review, it's evident that the olfactory system is vulnerable both to chronic and acute PAE. In particular, the reduction in OB volume was prominent and was often associated with a decrease in the number of granule cells and mitral cells, suggesting that PAE affects the neurogenesis of OB neurons. This view is also supported by studies in animal models and human patients showing that PAE reduced the proliferation of neural stem cells in the subventricular zone (SVZ) (Roitbak et al., 2011; Dong et al., 2014; Marguet et al., 2020). Moreover, defects in adult neurogenesis may also contribute to PAE-induced reduction of OB volume and olfactory function in adult rodents, as new OB interneurons are continuously produced in the SVZ of the adult rodent brain (Whitman and Greer, 2009).

The impairment in the olfactory system development likely leads to abnormal olfactory information processing. This, in turn, may contribute to abnormal smell sensitivity and impaired odor identification seen in children with FASD. However, studies to date

have varied in terms of timing, duration, dosage, and route of ethanol administration as well as the age of offspring investigated, making it still challenging to formulate a cohesive understanding of how PAE precisely influences the child's olfactory system. Systematic identification of differences in the effects of PAE at different stages of olfactory system development may provide valuable insights into important windows of vulnerability. In addition, it is necessary to study in more detail the effects of PAE on the structure and function of regions involved in olfactory processing other than the OB, such as olfactory epithelium and olfactory cortex.

Furthermore, while diverse *in vivo* and *in vitro* studies have elucidated various signaling pathways affected by PAE during brain development (Hashimoto-Torii et al., 2011; Mohammad et al., 2020; Fischer et al., 2021; Salem et al., 2021; Sambo et al., 2022), this type of research has so far been insufficient for the olfactory system. Understanding the molecules and pathways affected by PAE in the developing olfactory system could shed light on potential mechanisms underlying the etiology of abnormal sense of smell. Integrating findings from diverse experimental models and methodologies could facilitate the construction of comprehensive models that capture the multifaceted nature of PAE-induced alterations in olfactory system development and could inform targeted intervention strategies aimed at mitigating the detrimental effects of PAE on olfactory function. Therefore, collaborative efforts across disciplines, including neuroscience, developmental biology, and clinical research, are essential to surmount the complexities associated with understanding and addressing the consequences of PAE on olfactory function and beyond.

Author contributions

FI: Writing – original draft, Writing – review & editing.

Funding

The author(s) declare financial support was received for the research, authorship, and/or publication of this article. This work was supported by NIH grant R01DC016307, the PA Tobacco Settlement Fund, and the Children's Miracle Network (FI).

Conflict of interest

The author declares that the research was conducted in the absence of any commercial or financial relationships that could be construed as a potential conflict of interest.

Publisher's note

References

Aerts, T., and Seuntjens, E. (2021). Novel perspectives on the development of the amygdala in rodents. *Front. Neuroanat.* 15:786679. doi: 10.3389/fnana.2021.786679

Aihara, S., Fujimoto, S., Sakaguchi, R., and Imai, T. (2021). BMPR-2 gates activity-dependent stabilization of primary dendrites during mitral cell remodeling. *Cell Rep.* 35:109276. doi: 10.1016/j.celrep.2021.109276

Akers, K. G., Kushner, S. A., Leslie, A. T., Clarke, L., van der Kooy, D., Lerch, J. P., et al. (2011). Fetal alcohol exposure leads to abnormal olfactory bulb development and impaired odor discrimination in adult mice. *Mol. Brain* 4:29. doi: 10.1186/1756-6606-4-29

Almeida, L., Andreu-Fernandez, V., Navarro-Tapia, E., Aras-Lopez, R., Serra-Delgado, M., Martinez, L., et al. (2020). Murine models for the study of fetal alcohol Spectrum disorders: an overview. *Front. Pediatr.* 8:359. doi: 10.3389/fped.2020.00359

Bakker, J., Leinders-Zufall, T., and Chamero, P. (2022). "The sense of smell: role of the olfactory system in social behavior" in *Neuroscience in the 21st century: From basic to clinical*. eds. D. W. Pfaff, N. D. Volkow and J. L. Rubenstein (Cham: Springer International Publishing), 1215–1243.

Barron, S., Gagnon, W. A., Mattson, S. N., Kotch, L. E., Meyer, L. S., and Riley, E. P. (1988). The effects of prenatal alcohol exposure on odor associative learning in rats. *Neurotoxicol. Teratol.* 10, 333–339. doi: 10.1016/0892-0362(88)90036-0

Barron, S., and Riley, E. P. (1992). The effects of prenatal alcohol exposure on behavioral and neuroanatomical components of olfaction. *Neurotoxicol. Teratol.* 14, 291–297. doi: 10.1016/0892-0362(92)90009-y

Blanchart, A., De Carlos, J. A., and López-Mascaraque, L. (2006). Time frame of mitral cell development in the mice olfactory bulb. *J. Comp. Neurol.* 496, 529–543. doi: 10.1002/cne.20941

Bonthius, D. J., Bonthius, N. E., Napper, R. M., and West, J. R. (1992). Early postnatal alcohol exposure acutely and permanently reduces the number of granule cells and mitral cells in the rat olfactory bulb: a stereological study. *J. Comp. Neurol.* 324, 557–566. doi: 10.1002/cne.903240408

Bonthius, D. J., and West, J. R. (1991). Acute and long-term neuronal deficits in the rat olfactory bulb following alcohol exposure during the brain growth spurt. *Neurotoxicol. Teratol.* 13, 611–619. doi: 10.1016/0892-0362(91)90044-w

Bower, E., Szajer, J., Mattson, S. N., Riley, E. P., and Murphy, C. (2013). Impaired odor identification in children with histories of heavy prenatal alcohol exposure. *Alcohol* 47, 275–278. doi: 10.1016/j.alcohol.2013.03.002

Burke, M. W., Inyatkin, A., Ptito, M., Ervin, F. R., and Palmour, R. M. (2016). Prenatal alcohol exposure affects progenitor cell numbers in olfactory bulbs and dentate gyrus of Vervet monkeys. *Brain Sci.* 6:52. doi: 10.3390/brainsci6040052

Carr, J. L., Agnihotri, S., and Keightley, M. (2010). Sensory processing and adaptive behavior deficits of children across the fetal alcohol spectrum disorder continuum. *Alcohol. Clin. Exp. Res.* 34, 1022–1032. doi: 10.1111/j.1530-0277.2010.01177.x

Dong, L., Yang, K. Q., Fu, W. Y., Shang, Z. H., Zhang, Q. Y., Jing, F. M., et al. (2014). Gypenosides protected the neural stem cells in the subventricular zone of neonatal rats that were prenatally exposed to ethanol. *Int. J. Mol. Sci.* 15, 21967–21979. doi: 10.3390/ijms151221967

Eerdunfu, , Ihara, N., Ligao, B., Ikegaya, Y., and Takeuchi, H. (2017). Differential timing of neurogenesis underlies dorsal-ventral topographic projection of olfactory sensory neurons. *Neural Dev.* 12:2. doi: 10.1186/s13064-017-0079-0

Ethen, M. K., Ramadhani, T. A., Scheuerle, A. E., Canfield, M. A., Wyszynski, D. F., Druschel, C. M., et al. (2009). Alcohol consumption by women before and during pregnancy. *Matern. Child Health J.* 13, 274–285. doi: 10.1007/s10995-008-0328-2

Fischer, M., Chander, P., Kang, H., Mellios, N., and Weick, J. P. (2021). Transcriptomic changes due to early, chronic intermittent alcohol exposure during forebrain development implicate WNT signaling, cell-type specification, and cortical regionalization as primary determinants of fetal alcohol syndrome. *Alcohol. Clin. Exp. Res.* 45, 979–995. doi: 10.1111/acer.14590

Gano, A., Prestia, L., Middleton, F. A., Youngentob, S. L., Ignacio, C., and Deak, T. (2020). Gene expression profiling reveals a lingering effect of prenatal alcohol exposure on inflammatory-related genes during adolescence and adulthood. *Cytokine* 133:155126. doi: 10.1016/j.cyto.2020.155126

Godin, E. A., O'Leary-Moore, S. K., Khan, A. A., Parnell, S. E., Ament, J. J., Dehart, D. B., et al. (2010). Magnetic resonance microscopy defines ethanol-induced brain abnormalities in prenatal mice: effects of acute insult on gestational day 7. *Alcohol. Clin. Exp. Res.* 34, 98–111. doi: 10.1111/j.1530-0277.2009.01071.x

Hannigan, J. H., Chiodo, L. M., Sokol, R. J., Janisse, J., and Delaney-Black, V. (2015). Prenatal alcohol exposure selectively enhances young adult perceived pleasantness of alcohol odors. *Physiol. Behav.* 148, 71–77. doi: 10.1016/j.physbeh.2015.01.019

Hashimoto-Torii, K., Kawasawa, Y. I., Kuhn, A., and Rakic, P. (2011). Combined transcriptome analysis of fetal human and mouse cerebral cortex exposed to alcohol. *Proc. Natl. Acad. Sci. USA* 108, 4212–4217. doi: 10.1073/pnas.1100903108

Hinds, J. W. (1968). Autoradiographic study of histogenesis in the mouse olfactory bulb. I. Time of origin of neurons and neuroglia. *J. Comp. Neurol.* 134, 287–304. doi: 10.1002/cne.901340304

Hinds, J. W. (1972). Early neuron differentiation in the mouse of olfactory bulb. I. Light microscopy. *J. Comp. Neurol.* 146, 233–252. doi: 10.1002/cne.901460207

Hinds, J. W., and Hinds, P. L. (1976). Synapse formation in the mouse olfactory bulb. I. Quantitative studies. *J. Comp. Neurol.* 169, 15–40. doi: 10.1002/cne.901690103

Hirata, T., Shioi, G., Abe, T., Kiyonari, H., Kato, S., Kobayashi, K., et al. (2019). A novel birthdate-labeling method reveals segregated parallel projections of mitral and external tufted cells in the Main olfactory system. *eNeuro* 6, ENEURO.0234–ENEU19.2019. doi: 10.1523/ENEURO.0234-19.2019

Imamura, F., Ayoub, A. E., Rakic, P., and Greer, C. A. (2011). Timing of neurogenesis is a determinant of olfactory circuitry. *Nat. Neurosci.* 14, 331–337. doi: 10.1038/nn.2754

Imayoshi, I., Sakamoto, M., Ohtsuka, T., Takao, K., Miyakawa, T., Yamaguchi, M., et al. (2008). Roles of continuous neurogenesis in the structural and functional integrity of the adult forebrain. *Nat. Neurosci.* 11, 1153–1161. doi: 10.1038/nn.2185

Jirikowic, T. L., Thorne, J. C., McLaughlin, S. A., Waddington, T., Lee, A. K. C., and Astley Hemingway, S. J. (2020). Prevalence and patterns of sensory processing behaviors in a large clinical sample of children with prenatal alcohol exposure. *Res. Dev. Disabil.* 100:103617. doi: 10.1016/j.ridd.2020.103617

Kim, B. R., Rha, M. S., Cho, H. J., Yoon, J. H., and Kim, C. H. (2023). Spatiotemporal dynamics of the development of mouse olfactory system from prenatal to postnatal period. *Front. Neuroanat.* 17:1157224. doi: 10.3389/fnana.2023.1157224

Lin, D. M., Wang, F., Lowe, G., Gold, G. H., Axel, R., Ngai, J., et al. (2000). Formation of precise connections in the olfactory bulb occurs in the absence of odorant-evoked neuronal activity. *Neuron* 26, 69–80. doi: 10.1016/S0896-6273(00)81139-3

Lipinski, R. J., Hammond, P., O'Leary-Moore, S. K., Ament, J. J., Pecevich, S. J., Jiang, Y., et al. (2012). Ethanol-induced face-brain dysmorphology patterns are correlative and exposure-stage dependent. *PLoS One* 7:e43067. doi: 10.1371/journal.pone.0043067

Lopez-Mascaraque, L., De Carlos, J. A., and Valverde, F. (1996). Early onset of the rat olfactory bulb projections. *Neuroscience* 70, 255–266. doi: 10.1016/0306-4522(95)00360-u

Maier, S. E., Cramer, J. A., West, J. R., and Sohrabji, F. (1999). Alcohol exposure during the first two trimesters equivalent alters granule cell number and neurotrophin expression in the developing rat olfactory bulb. *J. Neurobiol.* 41, 414–423. doi: 10.1002/(sici)1097-4695(19991115)41:3<414::aid-neu9>3.0.co;2-f

Maier, S. E., and West, J. R. (2001). Drinking patterns and alcohol-related birth defects. *Alcohol Res. Health* 25, 168–174

Marguet, F., Friocourt, G., Brosolo, M., Sauvestre, F., Marcorelles, P., Lesueur, C., et al. (2020). Prenatal alcohol exposure is a leading cause of interneuronopathy in humans. *Acta Neuropathol. Commun.* 8:208. doi: 10.1186/s40478-020-01089-z

Martin-Lopez, E., Ishiguro, K., and Greer, C. A. (2017). The laminar Organization of Piriform Cortex Follows a selective developmental and migratory program established by cell lineage. *Cereb. Cortex* 29, 1–16. doi: 10.1093/cercor/bhx291

Martin-Lopez, E., Xu, C., Liberia, T., Meller, S. J., and Greer, C. A. (2019). Embryonic and postnatal development of mouse olfactory tubercle. *Mol. Cell. Neurosci.* 98, 82–96. doi: 10.1016/j.mcn.2019.06.002

May, P. A., Baete, A., Russo, J., Elliott, A. J., Blankenship, J., Kalberg, W. O., et al. (2014). Prevalence and characteristics of fetal alcohol spectrum disorders. *Pediatrics* 134, 855–866. doi: 10.1542/peds.2013-3319

May, P. A., Chambers, C. D., Kalberg, W. O., Zellner, J., Feldman, H., Buckley, D., et al. (2018). Prevalence of fetal alcohol Spectrum disorders in 4 US communities. *JAMA* 319, 474–482. doi: 10.1001/jama.2017.21896

May, P. A., Gossage, J. P., Kalberg, W. O., Robinson, L. K., Buckley, D., Manning, M., et al. (2009). Prevalence and epidemiologic characteristics of FASD from various research methods with an emphasis on recent in-school studies. *Dev. Disabil. Res. Rev.* 15, 176–192. doi: 10.1002/ddrr.68

Middleton, F. A., Carrierfenster, K., Mooney, S. M., and Youngentob, S. L. (2009). Gestational ethanol exposure alters the behavioral response to ethanol odor and the expression of neurotransmission genes in the olfactory bulb of adolescent rats. *Brain Res.* 1252, 105–116. doi: 10.1016/j.brainres.2008.11.023

Miller, A. M., Maurer, L. R., Zou, D. J., Firestein, S., and Greer, C. A. (2010a). Axon fasciculation in the developing olfactory nerve. *Neural Dev.* 5:20. doi: 10.1186/1749-8104-5-20

Miller, A. M., Treloar, H. B., and Greer, C. A. (2010b). Composition of the migratory mass during development of the olfactory nerve. *J. Comp. Neurol.* 518, 4825–4841. doi: 10.1002/cne.22497

Mohammad, S., Page, S. J., Wang, L., Ishii, S., Li, P., Sasaki, T., et al. (2020). Kcnn2 blockade reverses learning deficits in a mouse model of fetal alcohol spectrum disorders. *Nat. Neurosci.* 23, 533–543. doi: 10.1038/s41593-020-0592-z

Mooney, S. M., and Varlinskaya, E. I. (2011). Acute prenatal exposure to ethanol and social behavior: effects of age, sex, and timing of exposure. *Behav. Brain Res.* 216, 358–364. doi: 10.1016/j.bbr.2010.08.014

Nguyen, U. P., and Imamura, F. (2019). Regional differences in mitral cell development in mouse olfactory bulb. *J. Comp. Neurol.* 527, 2233–2244. doi: 10.1002/cne.24683

Nyouist-Battie, C., and Gochee, A. (1985). Alerations in the development of the main olfactory bulb of the mouse after ethanol exposure. *Int. J. Dev. Neurosci.* 3, 211–217. doi: 10.1016/0736-5748(85)90026-7

Parnell, S. E., Holloway, H. E., Baker, L. K., Styner, M. A., and Sulik, K. K. (2014). Dysmorphogenic effects of first trimester-equivalent ethanol exposure in mice: a magnetic resonance microscopy-based study. *Alcohol. Clin. Exp. Res.* 38, 2008–2014. doi: 10.1111/acer.12464

Parnell, S. E., O'Leary-Moore, S. K., Godin, E. A., Dehart, D. B., Johnson, B. W., Allan Johnson, G., et al. (2009). Magnetic resonance microscopy defines ethanol-induced brain abnormalities in prenatal mice: effects of acute insult on gestational day 8. *Alcohol. Clin. Exp. Res.* 33, 1001–1011. doi: 10.1111/j.1530-0277.2009.00921.x

Patten, A. R., Fontaine, C. J., and Christie, B. R. (2014). A comparison of the different animal models of fetal alcohol spectrum disorders and their use in studying complex behaviors. *Front. Pediatr.* 2:93. doi: 10.3389/fped.2014.00093

Peiffer, J., Majewski, F., Fischbach, H., Bierich, J. R., and Volk, B. (1979). Alcohol embryo- and fetopathy. Neuropathology of 3 children and 3 fetuses. *J. Neurol. Sci.* 41, 125–137. doi: 10.1016/0022-510x(79)90033-9

Popova, S., Charness, M. E., Burd, L., Crawford, A., Hoyme, H. E., Mukherjee, R. A. S., et al. (2023). Fetal alcohol spectrum disorders. *Nat. Rev. Dis. Primers* 9:11. doi: 10.1038/s41572-023-00420-x

Riley, E. P., Infante, M. A., and Warren, K. R. (2011). Fetal alcohol spectrum disorders: an overview. *Neuropsychol. Rev.* 21, 73–80. doi: 10.1007/s11065-011-9166-x

Roitbak, T., Thomas, K., Martin, A., Allan, A., and Cunningham, L. A. (2011). Moderate fetal alcohol exposure impairs neurogenic capacity of murine neural stem cells isolated from the adult subventricular zone. *Exp. Neurol.* 229, 522–525. doi: 10.1016/j.expneurol.2011.03.007

Salem, N. A., Mahnke, A. H., Konganti, K., Hillhouse, A. E., and Miranda, R. C. (2021). Cell-type and fetal-sex-specific targets of prenatal alcohol exposure in developing mouse cerebral cortex. *iScience* 24:102439. doi: 10.1016/j.isci.2021.102439

Sambo, D., Gohel, C., Yuan, Q., Sukumar, G., Alba, C., Dalgard, C. L., et al. (2022). Cell type-specific changes in Wnt signaling and neuronal differentiation in the developing mouse cortex after prenatal alcohol exposure during neurogenesis. *Front. Cell Dev. Biol.* 10:1011974. doi: 10.3389/fcell.2022.1011974

Substance Abuse and Mental Health Services Administration (2014). *Substance Abuse and Mental Health Services Administration, Results from the 2013 National Survey on drug use and health: summary of National Findings, NSDUH series H-48*. Rockville, MD: Substance Abuse and Mental Health Services Administration, 14–4863.

Temple, V. K., Cook, J. L., Unsworth, K., Rajani, H., and Mela, M. (2019). Mental health and affect regulation impairment in fetal alcohol Spectrum disorder (FASD): results from the Canadian national FASD database. *Alcohol Alcohol.* 54, 545–550. doi: 10.1093/alcalc/agz049

Todd, D., Bonthius, D. J., Sabalo, L. M., Roghair, J., Karacay, B., Bousquet, S. L., et al. (2018). Regional patterns of alcohol-induced neuronal loss depend on genetics: implications for fetal alcohol Spectrum disorder. *Alcohol. Clin. Exp. Res.* 42, 1627–1639. doi: 10.1111/acer.13824

Treloar, H. B., Miller, A. M., Ray, A., and Greer, C. A. (2010). "Development of the olfactory system" in *The neurobiology of olfaction*. ed. A. Menini (Boca Raton (FL): Routledge).

Treloar, H. B., Purcell, A. L., and Greer, C. A. (1999). Glomerular formation in the developing rat olfactory bulb. *J. Comp. Neurol.* 413, 289–304. doi: 10.1002/(SICI)1096-9861(19991018)413:2<289::AID-CNE9>3.0.CO;2-U

Walz, A., Omura, M., and Mombaerts, P. (2006). Development and topography of the lateral olfactory tract in the mouse: imaging by genetically encoded and injected fluorescent markers. *J. Neurobiol.* 66, 835–846. doi: 10.1002/neu.20266

Washburn, S. E., Ramadoss, J., Chen, W. J., and Cudd, T. A. (2015). Effects of all three trimester moderate binge alcohol exposure on the foetal hippocampal formation and olfactory bulb. *Brain Inj.* 29, 104–109. doi: 10.3109/02699052.2014.947629

Whitman, M. C., and Greer, C. A. (2009). Adult neurogenesis and the olfactory system. *Prog. Neurobiol.* 89, 162–175. doi: 10.1016/j.pneurobio.2009.07.003

Wilson, D. A., Peterson, J., Basavaraj, B. S., and Saito, M. (2011). Local and regional network function in behaviorally relevant cortical circuits of adult mice following postnatal alcohol exposure. *Alcohol. Clin. Exp. Res.* 35, 1974–1984. doi: 10.1111/j.1530-0277.2011.01549.x

Youngentob, S. L., and Glendinning, J. I. (2009). Fetal ethanol exposure increases ethanol intake by making it smell and taste better. *Proc. Natl. Acad. Sci. USA* 106, 5359–5364. doi: 10.1073/pnas.0809804106

Youngentob, S. L., Kent, P. F., Sheehe, P. R., Molina, J. C., Spear, N. E., and Youngentob, L. M. (2007a). Experience-induced fetal plasticity: the effect of gestational ethanol exposure on the behavioral and neurophysiologic olfactory response to ethanol odor in early postnatal and adult rats. *Behav. Neurosci.* 121, 1293–1305. doi: 10.1037/0735-7044.121.6.1293

Youngentob, S. L., Molina, J. C., Spear, N. E., and Youngentob, L. M. (2007b). The effect of gestational ethanol exposure on voluntary ethanol intake in early postnatal and adult rats. *Behav. Neurosci.* 121, 1306–1315. doi: 10.1037/0735-7044.121.6.1306

frontiers | Frontiers in Neural Circuits

TYPE Mini Review
PUBLISHED 17 May 2024
DOI 10.3389/fncir.2024.1409993

OPEN ACCESS

EDITED BY
Hitoshi Sakano,
University of Fukui, Japan

REVIEWED BY
Francisco José Martini,
Universidad Miguel Hernández-Consejo Superior de Investigaciones Científicas (UMH-CSIC), Spain

*CORRESPONDENCE
Naoki Nakagawa
✉ naoki.nakagawa@nig.ac.jp
Takuji Iwasato
✉ tiwasato@nig.ac.jp

RECEIVED 31 March 2024
ACCEPTED 06 May 2024
PUBLISHED 17 May 2024

CITATION
Nakagawa N and Iwasato T (2024) Activity-dependent dendrite patterning in the postnatal barrel cortex.
Front. Neural Circuits 18:1409993.
doi: 10.3389/fncir.2024.1409993

Activity-dependent dendrite patterning in the postnatal barrel cortex

Naoki Nakagawa[1,2]* and Takuji Iwasato[1,2]*

[1]Laboratory of Mammalian Neural Circuits, National Institute of Genetics, Mishima, Japan, [2]Graduate Institute for Advanced Studies, SOKENDAI, Mishima, Japan

For neural circuit construction in the brain, coarse neuronal connections are assembled prenatally following genetic programs, being reorganized postnatally by activity-dependent mechanisms to implement area-specific computational functions. Activity-dependent dendrite patterning is a critical component of neural circuit reorganization, whereby individual neurons rearrange and optimize their presynaptic partners. In the rodent primary somatosensory cortex (barrel cortex), driven by thalamocortical inputs, layer 4 (L4) excitatory neurons extensively remodel their basal dendrites at neonatal stages to ensure specific responses of barrels to the corresponding individual whiskers. This feature of barrel cortex L4 neurons makes them an excellent model, significantly contributing to unveiling the activity-dependent nature of dendrite patterning and circuit reorganization. In this review, we summarize recent advances in our understanding of the activity-dependent mechanisms underlying dendrite patterning. Our focus lays on the mechanisms revealed by *in vivo* time-lapse imaging, and the role of activity-dependent Golgi apparatus polarity regulation in dendrite patterning. We also discuss the type of neuronal activity that could contribute to dendrite patterning and hence connectivity.

KEYWORDS

activity-dependent circuit formation, postnatal brain development, dendrite refinement, barrel cortex, Golgi apparatus, *in vivo* imaging, spontaneous activity

Introduction

The sophisticated neural circuits underlying proper brain function in animals are first formed as coarse neuronal connections during embryonic development. Later, such immature connections are reorganized during postnatal stages, establishing a precise connectivity tailored to each brain area. Morphological and functional neuron remodeling, depending on neuronal activity evoked either spontaneously or by extrinsic stimuli, causes this postnatal circuit reorganization (Goodman and Shatz, 1993; Katz and Shatz, 1996; Wong and Ghosh, 2002). Particularly, activity-dependent remodeling of the dendritic pattern is key for circuit reorganization, whereby individual neurons rearrange and optimize their presynaptic partners. Dendrite refinement has been observed in various neuronal types in diverse brain regions and species, and is therefore considered a general mechanism for building functional neural circuits (Cline, 2001; Wong and Ghosh, 2002; Emoto, 2011).

The activity-dependent mechanisms underlying dendrite patterning have been studied in a wide range of models, including tectal neurons in Xenopus tadpole, retinal ganglion cells in chick and cat, olfactory bulb mitral cells in mouse, and cortical neurons in mouse, cat, and ferret (Harris and Woolsey, 1981; Katz and Constantine-Paton, 1988; Bodnarenko and

Chalupa, 1993; Kossel et al., 1995; Wong et al., 2000; Matsui et al., 2013; Fujimoto et al., 2023). Among them, spiny stellate neurons, the major type of layer 4 (L4) excitatory neurons, in the primary somatosensory cortex (barrel cortex) of mice and rats have attracted attention as a model of activity-dependent dendrite patterning (Woolsey and Van der Loos, 1970; Erzurumlu and Gaspar, 2012; Iwasato and Erzurumlu, 2018).

In rodents, facial whiskers are an important sensory organ whereby animals perceive their environment. Tactile stimuli to whiskers reach the barrel cortex L4 via the dorsal principal trigeminal (dPrV) nucleus in the brainstem and the ventral posterior medial (VPM) nucleus in the thalamus (Figure 1A) (Fox, 2008; Iwasato and Erzurumlu, 2018). In barrel cortex L4, the information from each whisker is processed by an array of neurons called "barrel," whose arrangement represents the spatial pattern of whiskers in the face. Termini of thalamocortical axons (TCAs) that transmit inputs from a whisker are distributed only within the corresponding barrel. L4 spiny stellate neurons are preferentially located at the edge of each barrel and expand their basal dendrites asymmetrically toward the barrel center (Figure 1B) (Harris and Woolsey, 1981; Simons and Woolsey, 1984). This asymmetric dendritic projection pattern, formed in an activity-dependent manner essentially during the first postnatal week, underlies precise tactile information processing in rodents (Nakazawa et al., 2018; Iwasato, 2020; Nakagawa and Iwasato, 2023); therefore, understanding how this unique dendritic asymmetry is established during postnatal development is of importance.

In this review, we summarize recent advances in our understanding of the activity-dependent mechanisms underlying dendrite patterning and postnatal circuit reorganization based on studies using whisker-barrel circuits.

Dendritic patterning of L4 spiny stellate neurons in the neonatal barrel cortex

The activity transmitted through TCAs is critical for dendritic patterning of barrel cortex L4 spiny stellate neurons. Removing glutamatergic synaptic transmission from TCA termini by knocking out both VgluT1 and VgluT2, two major vesicular glutamate transporters in the brain, in the sensory thalamus impairs formation

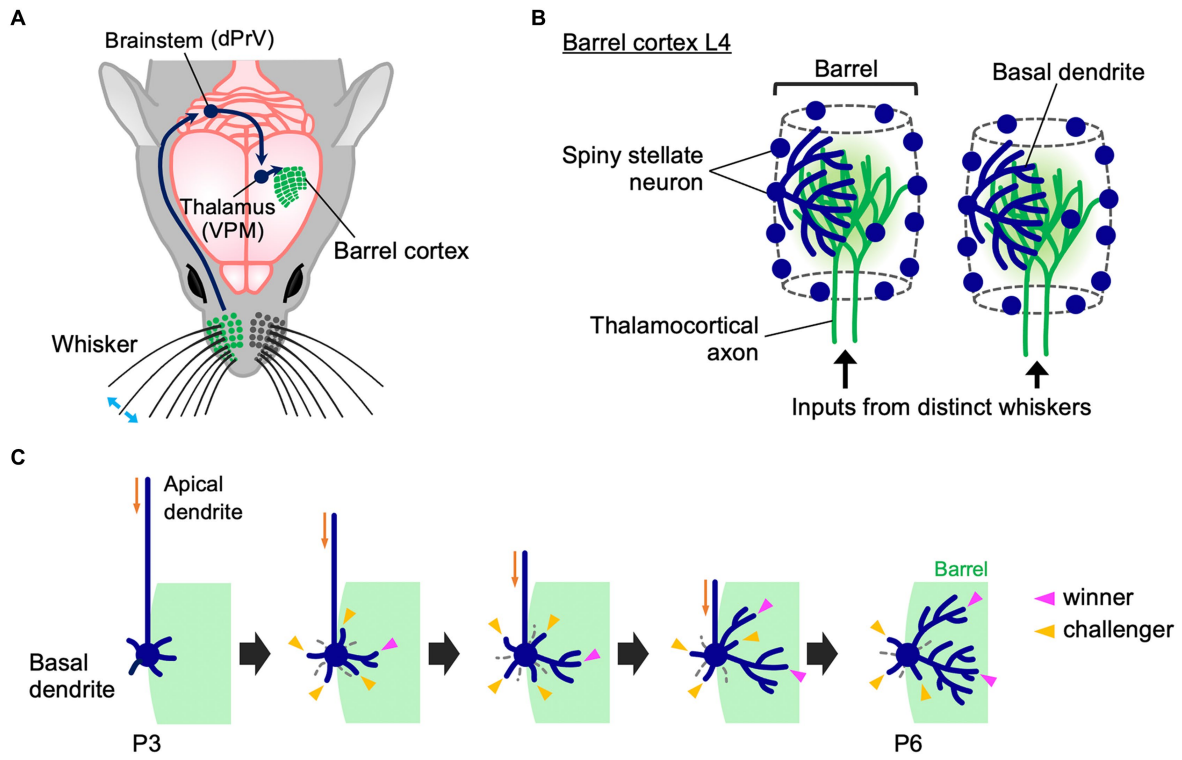

FIGURE 1
Whisker-barrel circuit and dendrite refinement of barrel cortex layer 4 spiny stellate neurons. **(A)** A schematic diagram of the mouse whisker-barrel system. The tactile information received by the whiskers is topographically conveyed to the contralateral barrel cortex layer 4 (L4) through the brainstem and the thalamus. dPrV: dorsal principal trigeminal nucleus, VPM: ventral posterior medial nucleus. **(B)** Barrel cytoarchitecture. In each barrel, the termini of thalamocortical axons (TCAs) that transmit sensory inputs from the corresponding single whiskers form distinct clusters in barrel cortex L4. Spiny stellate neurons, the major excitatory neurons in barrel cortex L4, are located primarily at the edge of TCA clusters, thereby showing the "barrel" shape. Spiny stellate neurons expand their basal dendrites selectively toward a corresponding single barrel to establish synapses with the corresponding TCA termini. Dendrites drawn only in some neurons for simplicity. **(C)** Dynamics of formation of asymmetric dendrite patterns in L4 spiny stellate neurons. At P3, a spiny stellate neuron has more dendritic trees in the inner domain (green) than in the outer domain, but inner and outer dendritic trees are equally primitive in morphology. Between P3 and P6, many short dendritic trees emerge and disappear both inside and outside the barrel ("challenger" dendritic trees, indicated by yellow arrowheads). During this extensive turnover, only a few trees (indicated by magenta arrowheads) are stabilized and elaborated to be "winners." Importantly, winners are selected only from the challengers that emerge in the barrel-side (green). Note that late-born dendritic trees can become winners.

of cortical layers, barrel maps, and L4 neuron dendrite morphology (Li et al., 2013). Similarly, when thalamocortical synaptic transmission is reduced by a thalamus-specific double knockout of RIM1 and RIM2, which regulate synaptic vesicle fusion, barrel formation and L4 neuron dendritic asymmetry become impaired (Narboux-Neme et al., 2012). These results suggest a critical role of TCA-derived activity for barrel circuit formation, including dendritic patterning of L4 neurons.

Gene knockouts also indicated that the dendrite refinement of L4 spiny stellate neurons relies on the postsynaptic N-methyl-D-aspartate-type glutamate receptor (NMDAR) activity induced by presynaptic thalamocortical inputs. Knockout of either NR1 or NR2B subunits of NMDAR causes impaired asymmetry of dendritic projections (Iwasato et al., 2000; Datwani et al., 2002; Espinosa et al., 2009; Mizuno et al., 2014). NMDAR is a tetrameric complex composed of two NR1 subunits and two NR2 subunits; NR1 is the essential subunit and NR2B the modulatory subunit, dominant in the neonatal brain (Nakanishi, 1992; Mori and Mishina, 1995). Genetic approaches in mice identified dozens of molecules related to synaptic transmission and its downstream signaling cascade implicated in barrel formation and dendrite refinement of L4 spiny stellate neurons. Such genes include metabotropic glutamate receptor 5, protein kinase A (PKA), PKA-anchoring protein 5, adenylyl cyclase 1, phospholipase C-β1, Ras GTPase-activating proteins, Fibroblast growth factor receptors, Tropomyosin receptor kinase A, BTB/POZ domain-containing 3, LIM domain-only 4, neurogenic differentiation 2, retinoic acid-related orphan receptor alpha (RORα) and RORβ (Abdel-Majid et al., 1998; Hannan et al., 2001; Barnett et al., 2006; Inan et al., 2006; Ince-Dunn et al., 2006; Kashani et al., 2006; Watson et al., 2006; Iwasato et al., 2008; Lush et al., 2008; She et al., 2009; Jabaudon et al., 2012; Matsui et al., 2013; Ballester-Rosado et al., 2016; Huang et al., 2017; Huang and Lu, 2018; Vitalis et al., 2018; Zhang et al., 2019; Clark et al., 2020; Rao et al., 2022). Using mitral cells in the mouse olfactory bulb, Imai and colleagues recently reported that strong NMDAR activation in prospective winner dendrites locally suppresses RhoA activity, protecting the dendrite from depolarization-induced, neuron-wide RhoA activation, which acts as a dendrite retraction signal (Fujimoto et al., 2023). This system also works in barrel cortex L4 neurons (Fujimoto et al., 2023).

Mechanisms of dendritic patterning revealed by *in vivo* time-lapse imaging

It is generally assumed that spiny stellate neurons in barrel cortex L4 exhibit symmetrical dendritic patterns during early neonatal stages but subsequently acquire asymmetrical dendritic patterns by simply eliminating outer dendrites and adding new inner dendrites and/or elaborating existing inner dendrites (Greenough and Chang, 1988; Espinosa et al., 2009; Emoto, 2011; Iwasato, 2020). This view was challenged by *in vivo* imaging approaches in the neonatal mouse cortex (Mizuno et al., 2014; Nakazawa et al., 2018; Iwasato, 2020; Wang et al., 2023). In these studies, L4 neurons were sparsely labeled and each was imaged repeatedly in the neonatal barrel cortex using two-photon microscopy.

In the mature barrel cortex, L4 excitatory neurons are classified by the absence and presence of apical dendrites into spiny stellate and star pyramid neurons, respectively (Simons and Woolsey, 1984; Lübke et al., 2000; Staiger et al., 2004). Importantly, spiny stellate neurons, the major L4 neurons, show asymmetric dendritic patterns but star pyramid neurons have symmetric dendrites. However, at early postnatal stages such as postnatal day 3 (P3), prospective spiny stellate neurons also have an apical dendrite, which hampers distinguishing spiny stellate neurons from star pyramid neurons by conventional histological analyses in brain slices. On the other hand, longitudinal *in vivo* imaging of the same neurons in the brain allows retrospective identification of prospective spiny stellate neurons in early postnatal development by their morphological features at later developmental stages such as P6; thus allowing to analyze the dendritic morphology of spiny stellate neurons in early postnatal stages (Nakazawa et al., 2018; Iwasato, 2020).

Longitudinal *in vivo* imaging of L4 neurons in the mouse barrel cortex revealed that at P3, a spiny stellate neuron has a larger number of inner dendritic trees, which originate from the barrel-side half of the soma, than outer dendritic trees (Nakazawa et al., 2018). However, at this age both inner and outer dendritic trees are equally primitive in morphology (Figure 1C). Between P3 and P6, the ratio of inner to outer dendritic trees does not change. However, during this period, dendritic trees show extensive turnover both inside and outside the barrel. Many newly emerged dendritic trees (i.e., "challenger" dendritic trees) quickly disappear. Among them, only a few are stabilized and elaborated and become winners. Importantly, these winners are primarily selected from challengers emerging inside the barrel. L4 spiny stellate neurons have multiple winner dendritic trees, and even late-born dendritic trees can become winners (Nakazawa et al., 2018). Thus, L4 spiny stellate neurons establish highly asymmetric dendritic patterns not by eliminating outer dendritic trees and adding new inner trees and/or elaborating existing inner trees during neonatal stages. In contrast, L4 spiny stellate neurons produce many challenger dendritic trees in various directions, and only a few winners are selected from the challengers that emerge in the appropriate direction. These winners are then stabilized and elaborated (Figure 1C).

Most L4 spiny stellate neurons, which are located at the barrel edge, can receive appropriate TCA inputs only from a specific direction toward the barrel center. On the other hand, L4 spiny stellate neurons located in the barrel center can receive appropriate TCA inputs from any direction. Such barrel-center spiny stellate neurons show much lower dendritic tree turnover than barrel-edge spiny stellate neurons (Nakazawa et al., 2018). In barrel-center spiny stellate neurons, most dendrites are stable and mildly grow, establishing dendritic projections without orientation bias. Thus, spatially biased presynaptic TCA inputs may play a key role regulating dendritic dynamics and dendritic orientation. When appropriate presynaptic partners are available only in a specific direction, neurons produce many dendritic trees in all directions, and select a few winners among dendritic trees that emerge in the right direction.

A more recent *in vivo* imaging study, using 1-h interval for imaging of barrel cortex L4 neuron dendrites in the neonatal mouse (Wang et al., 2023), further supports this view. This high time-resolution imaging allows to accurately identify the same dendritic branches across imaging sessions, which is often difficult with the imaging intervals (8 h) used in previous experiments (Mizuno et al., 2014; Nakazawa et al., 2018). This new study found that many dendritic branches (and trees) emerge and are eliminated even within a few hours. Both inner and outer dendritic branches (and trees) emerge and are eliminated with no clear difference in frequency. These

results suggest that despite dendritic trees and branches being highly dynamic during neonatal stages, most of these rapid changes in dendritic morphology do not directly contribute to the formation of asymmetric dendritic patterns in spiny stellate neurons. Thus, L4 spiny stellate neurons establish highly asymmetric dendritic patterns through extensive trial-and-error emergence/elongation and elimination/retraction of dendritic trees and branches rather than simple emergence/elongation of inner dendritic trees/branches and elimination/retraction of outer dendritic trees/branches (Figure 1C).

Golgi polarity in thalamocortical activity-dependent dendritic patterning

As described above, during dendrite refinement of barrel cortex L4 spiny stellate neurons, only a fraction of dendritic trees that emerge inside the barrel is selected as winners from a large number of transient dendritic trees (challenger dendritic trees) generated during continuous turnover both inside and outside the barrel (Figure 1C). Why do inner dendritic trees, but not outer dendritic trees, become winners?

Recent evidence indicated a significant contribution of cell polarity in inner dendritic tree-specific winner emergence (Nakagawa and Iwasato, 2023). In fact, the Golgi apparatus distribution changes in L4 spiny stellate neurons during the neonatal stage. The Golgi apparatus in L4 spiny stellate neurons is positioned in the apical domain in early neonatal stages such as P3, but it is subsequently translocated and polarized to the lateral domain and oriented toward a single barrel by P5 (Figure 2A). This "lateral Golgi polarity" temporally matches with the progression of dendrite refinement: lateral polarity peaks on the active refinement stage (P5–P7) and disappears upon refinement completion (~P15). In contrast to spiny stellate neurons, star pyramid neurons do not show lateral Golgi polarity. The lateral Golgi polarity in L4 spiny stellate neurons relies on NMDAR activation, serving as an intracellular machinery that connects thalamocortical activity to dendrite patterning. Perturbing Golgi polarity results in less asymmetric dendrite patterning and lower response specificity to principal whisker stimulation.

How can a biased Golgi distribution in a neuron explain the fate of individual dendritic trees? The Golgi apparatus is a hub for intracellular vesicle transport and contributes to dendrite extension and elaboration (Horton et al., 2005; Ye et al., 2007). Indeed, during dendrite refinement in L4 spiny stellate neurons, the dendritic trees that harbor the Golgi at their base or inside are more elaborated than those without Golgi allocation (Nakagawa and Iwasato, 2023). Therefore, the laterally polarized Golgi distribution in neurons, biased toward the single barrel, may provide the chance of Golgi allocation only to inner dendritic trees and make them winners (Figure 2). It is likely that due to the physical capacity of the Golgi apparatus, when a few dendritic trees become winners, other dendritic trees can hardly be supported by the Golgi, making these trees short and/or transient, even in case of inner trees. As presynaptic TCAs are clustered in the barrel center, L4 neurons should make synapses predominantly on inner dendrites (Figure 2B), creating NMDAR signaling gradients and generating Golgi lateral polarity. On the other hand, losing NMDAR activity from a cell impairs lateral polarity of the Golgi apparatus (Nakagawa and Iwasato, 2023). In this situation, no dendrites become winners and most, both inside and outside the barrel, mildly grow, impairing the one-to-one functional relationship between a whisker and a barrel (Figure 2B).

Thalamocortical activity in the neonatal barrel cortex

Dendritic refinement of L4 spiny stellate neurons largely relies on thalamocortical inputs (Narboux-Neme et al., 2012; Li et al., 2013). Although, in neonatal stages such as P6, barrel cortex L4 is innervated not only by TCAs but also by subplate neuron neurites, these subplate neurons also receive excitatory thalamocortical inputs (Higashi et al., 2002; Piñon et al., 2009; Kanold, 2019). In other words, during early postnatal period, L4 neurons are activated by thalamic inputs directly or indirectly. Therefore, it is important to know the type of activity that TCAs transmit to barrel cortex during neonatal stages and where in the trigeminal pathway this activity arises from.

Spontaneous correlated activity plays critical roles in the refinement of neuronal circuits in the sensory systems of developing mammals (Katz and Shatz, 1996; Kirkby et al., 2013; Martini et al., 2021; Nakazawa and Iwasato, 2021). In barrel cortex L4 of the neonatal mouse, there is spontaneous activity with a unique spatiotemporal pattern (Mizuno et al., 2018). L4 neurons that belong to the same barrel fire together, while those in different barrels fire in a different timing, providing the barrel-corresponding "patchwork" pattern to spontaneous activity. This patchwork-type spatiotemporal pattern of spontaneous activity is observed in the barrel cortex L4 during early postnatal stages such as P0 and P5 but not later (Mizuno et al., 2018; Nakazawa et al., 2020). L4 neurons around P9 show broadly synchronized activity across barrel borders, and by P11, cortical spontaneous activity is desynchronized (Nakazawa et al., 2020; Nakazawa and Iwasato, 2021).

Patchwork-type spontaneous activity is also observed in TCA termini during the first postnatal week (Mizuno et al., 2018); in fact, chemogenic silencing of the thalamus hampers detection of spontaneous activity in the cortex (Nakazawa et al., 2020). These findings suggest that patchwork activity is transmitted to cortical L4 neurons via TCAs. Cortical patchwork activity is also blocked by local anesthesia in the whisker pads but not by severing the infraorbital nerves (IONs) (Mizuno et al., 2018; Nakazawa et al., 2020). IONs are peripherally projecting processes of trigeminal ganglion (TG) neurons, which innervate the whisker follicles. These results suggest that the cortical spontaneous activity is generated in the periphery but downstream of IONs. Thus, it is highly likely that the spontaneous activity originates in the TG.

A recent study has established a calcium imaging system of the TG *ex vivo* and found that neurons in the whisker-innervated region of the TG fire spontaneously during neonatal stages (Banerjee et al., 2022). This activity is blocked when chelating extracellular calcium. Most firing neurons have medium-to-large diameter, and likely are mechanosensory neurons. Although TG neurons fire sparsely and have no clear spatiotemporal pattern, some neuron pairs with highly correlated firing tend to be located closely (Banerjee et al., 2022). Neurons that innervate the same whiskers are not clustered in the TG but close to each other (Erzurumlu and Jhaveri, 1992; da Silva et al., 2011; Banerjee et al., 2022). Therefore, it is possible that TG neurons that innervate the same whisker pad together tend to fire together. If so, this may generate the patchwork pattern corresponding to the

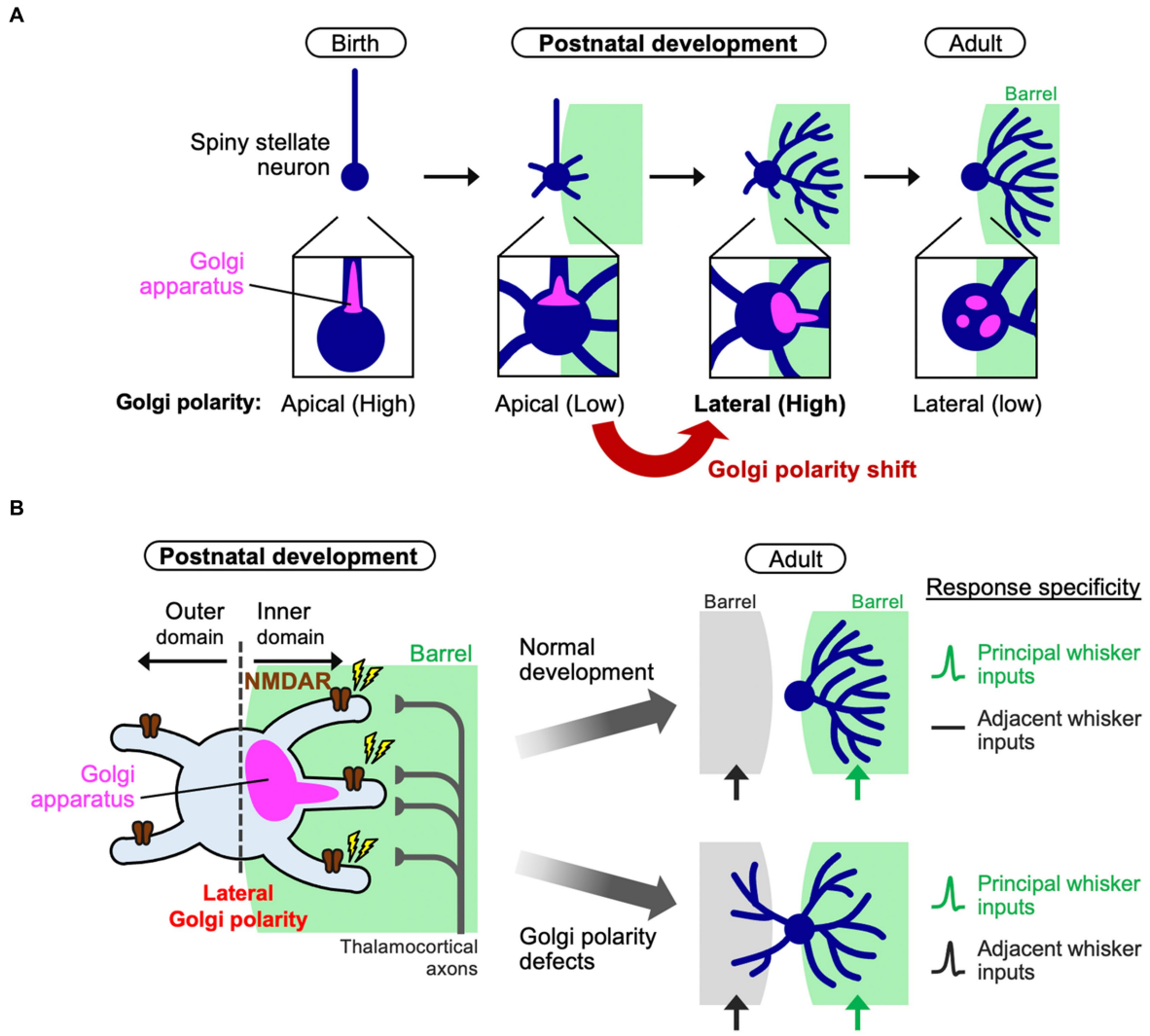

FIGURE 2
Polarity shift of the Golgi apparatus instructs dendrite refinement. **(A)** In barrel cortex L4, spiny stellate neurons initially have apical Golgi polarity. During postnatal development (the first postnatal week), spiny stellate neurons de-construct the initial polarity and shift it to the lateral direction oriented toward a single barrel. Finally, after completing of circuit reorganization, spiny stellate neurons decrease the lateral Golgi polarity (adult). **(B)** During dendrite refinement in a spiny stellate neuron, NMDA receptors (NMDARs) are activated by thalamocortical inputs from a single barrel. The Golgi apparatus translocates toward the subcellular domain where NMDARs are activated [see also **(A)**]. Then, a few inner dendritic trees harbor the Golgi (at their base or inside) to be winners. In this way, the spiny stellate neuron establishes the asymmetric dendritic patterns, underlying the specific response to a single principal whisker (right, normal development). On the other hand, if the lateral Golgi polarization is impaired, the neuron has lower dendrite asymmetry, so that it responds to both principal and adjacent whiskers, compromising the whisker-dependent tactile discrimination in mice.

barrel map in the barrel cortex. This hypothesis needs to be explored in future research.

Patchwork-type cortical activity is also generated by sensory feedback from self-generated whisker movements. Whisker and paw twitching are frequently observed in neonatal rodents during rapid eye movement (REM) sleep (Khazipov et al., 2004; Tiriac et al., 2012, 2014; Dooley et al., 2020). The sensory feedback from the twitching of the whiskers and paws appears to be a source of firing in the downstream trigeminal pathway. There is some degree of coupling between the twitching and the firing in the thalamus and cortex (Khazipov et al., 2004; Tiriac et al., 2012, 2014; Mizuno et al., 2018; Dooley et al., 2020). By using unit recording of the rat barrel cortex at P5, Blumberg and colleagues reported that about 12 and 23% of spontaneous whisker movements are accompanied with spindle bursts of barrels, during wake and REM sleep, respectively. They also reported that more than half of barrel activity is preceded by whisker twitches (Dooley et al., 2020). In this study, time-resolution was quite high and wake and sleep were precisely distinguished. By calcium imaging focusing on L4 neurons of the P5 mouse barrel cortex, Mizuno et al., demonstrated that about 11% of spontaneous whisker movements were associated with firing of L4 neurons within the corresponding barrel, and about 11% of L4 neuron firing episodes accompany spontaneous movements of the corresponding whisker (Mizuno et al., 2018). In this study, L4 neurons were identified accurately by using *in utero* electroporation-based cell labeling and TCA-red fluorescent protein (RFP) transgenic (Tg)-mediated L4 labeling. In addition, each barrel was precisely identified in a cellular level by TCA-RFP Tg-mediated barrel map labeling.

Sensory input also generates cortical activity. Rodents do not see or hear during neonatal stages because the retina and cochlea are not functional yet. On the other hand, in rodents, tactile sensation is already present, albeit partially, at birth. Although rodents do not show exploratory and whisking behaviors until around P12–P14 (for the mouse) (Arakawa and Erzurumlu, 2015; van der Bourg et al., 2017), even at birth, rodents already exhibit passive sensation from tactile organs, including the whiskers. Sensory inputs induced by whisker deflection are transmitted to the cortex via the brainstem and thalamus (Khazipov et al., 2004; Akhmetshina et al., 2016). The specific role of these three types of activity in neonatal animals in the refinement of barrel cortex circuits needs to be clarified in the future.

Discussion

Recent studies using the mouse barrel cortex L4, have increased our understanding of the activity-dependent mechanisms of dendrite refinement and circuit reorganization. Mouse genetics studies have discovered dozens of molecules involved in the dendrite refinement of the barrel cortex L4 spiny stellate neurons. However, our knowledge on how these molecules are spatiotemporally coordinated within a neuron to determine the fate of individual dendritic trees is still lacking. This could be overcome by labeling endogenous molecules and their activities with subcellular resolution *in situ* and analyzing their spatiotemporal changes and correlation with the behavior of individual dendrites during refinement.

Apart from the function of individual molecules, an important viewpoint has been introduced, which is the dynamics of subcellular structures such as the Golgi apparatus (Nakagawa and Iwasato, 2023). Triggered by thalamocortical input, molecular activities should be converted to structural and functional changes of intracellular machinery, which drive morphological changes in neurons. Next, it will be necessary to elucidate the activity-dependent mechanisms underlying Golgi recruitment to specific dendrite(s) in L4 spiny stellate neurons, and to understand how the polarized Golgi enables asymmetric dendrite growth.

Continuous improvement of *in vivo* imaging approaches is important as well. Unlike conventional "snapshot" analysis by histology, *in vivo* imaging in living neonates allows us to directly understand the ongoing process of dendrite refinement. Moreover, dissecting the rules underlying the behavior of individual dendrites during refinement help clarify how the molecules and organelles work within a neuron.

Combining these multidisciplinary approaches is required for understanding the whole picture of the activity-dependent mechanisms underlying dendrite patterning, a critical step in postnatal neural circuit reorganization.

Author contributions

NN: Writing – original draft, Writing – review & editing. TI: Writing – original draft, Writing – review & editing.

Funding

The author(s) declare financial support was received for the research, authorship, and/or publication of this article. This work was supported by JSPS KAKENHI JP19K16281, JP21K15199, JP21H05702, JP22H05518, JP23H04242, JP24H01256, and JP24K02127, the Uehara Memorial Foundation, and the Takeda Science Foundation to NN, JSPS KAKENHI JP16H06459, JP20H03346, JP21K18245, JP24H00586, and JP24H02310, and the Collaborative Research Project (#23017) of BRI, Niigata University to TI.

Conflict of interest

The authors declare that the research was conducted in the absence of any commercial or financial relationships that could be construed as a potential conflict of interest.

Publisher's note

References

Abdel-Majid, R. M., Leong, W. L., Schalkwyk, L. C., Smallman, D. S., Wong, S. T., Storm, D. R., et al. (1998). Loss of adenylyl cyclase I activity disrupts patterning of mouse somatosensory cortex. *Nat. Genet.* 19, 289–291. doi: 10.1038/980

Akhmetshina, D., Nasretdinov, A., Zakharov, A., Valeeva, G., and Khazipov, R. (2016). The nature of the sensory input to the neonatal rat barrel cortex. *J. Neurosci.* 36, 9922–9932. doi: 10.1523/JNEUROSCI.1781-16.2016

Arakawa, H., and Erzurumlu, R. S. (2015). Role of whiskers in sensorimotor development of C57BL/6 mice. *Behav. Brain Res.* 287, 146–155. doi: 10.1016/j.bbr.2015.03.040

Ballester-Rosado, C. J., Sun, H., Huang, J.-Y., and Lu, H.-C. (2016). Functional and anatomical development of layer IV cortical neurons in the mouse primary somatosensory cortex. *J. Neurosci.* 36, 8802–8814. doi: 10.1523/JNEUROSCI.1224-16.2016

Banerjee, P., Kubo, F., Nakaoka, H., Ajima, R., Sato, T., Hirata, T., et al. (2022). Spontaneous activity in whisker-innervating region of neonatal mouse trigeminal ganglion. *Sci. Rep.* 12:16311. doi: 10.1038/s41598-022-20068-z

Barnett, M. W., Watson, R. F., Vitalis, T., Porter, K., Komiyama, N. H., Stoney, P. N., et al. (2006). Synaptic Ras GTPase activating protein regulates pattern formation in the trigeminal system of mice. *J. Neurosci.* 26, 1355–1365. doi: 10.1523/JNEUROSCI.3164-05.2006

Bodnarenko, S. R., and Chalupa, L. M. (1993). Stratification of ON and OFF ganglion cell dendrites depends on glutamate-mediated afferent activity in the developing retina. *Nature* 364, 144–146. doi: 10.1038/364144a0

Clark, E. A., Rutlin, M., Capano, L. S., Aviles, S., Saadon, J. R., and Taneja, P. (2020). Cortical RORβ is required for layer 4 transcriptional identity and barrel integrity. *eLife* 9:e52370. doi: 10.7554/eLife.52370

Cline, H. T. (2001). Dendritic arbor development and synaptogenesis. *Curr. Opin. Neurobiol.* 11, 118–126. doi: 10.1016/s0959-4388(00)00182-3

da Silva, S., Hasegawa, H., Scott, A., Zhou, X., Wagner, A. K., Han, B. X., et al. (2011). Proper formation of whisker barrelettes requires periphery-derived Smad4-dependent TGF-beta signaling. *Proc. Natl. Acad. Sci. USA* 108, 3395–3400. doi: 10.1073/pnas.1014411108

Datwani, A., Iwasato, T., Itohara, S., and Erzurumlu, R. S. (2002). NMDA receptor-dependent pattern transfer from afferents to postsynaptic cells and dendritic differentiation in the barrel cortex. *Mol. Cell. Neurosci.* 21, 477–492. doi: 10.1006/mcne.2002.1195

Dooley, J. C., Glanz, R. M., Sokoloff, G., and Blumberg, M. S. (2020). Self-generated whisker movements drive state-dependent sensory input to developing barrel cortex. *Curr. Biol.* 30, 2404–2410.e4. doi: 10.1016/j.cub.2020.04.045

Emoto, K. (2011). Dendrite remodeling in development and disease. *Develop. Growth Differ.* 53, 277–286. doi: 10.1111/j.1440-169X.2010.01242.x

Erzurumlu, R. S., and Gaspar, P. (2012). Development and critical period plasticity of the barrel cortex. *Eur. J. Neurosci.* 35, 1540–1553. doi: 10.1111/j.1460-9568.2012.08075.x

Erzurumlu, R. S., and Jhaveri, S. (1992). Trigeminal ganglion cell processes are spatially ordered prior to the differentiation of the vibrissa pad. *J. Neurosci.* 12, 3946–3955. doi: 10.1523/JNEUROSCI.12-10-03946.1992

Espinosa, J. S., Wheeler, D. G., Tsien, R. W., and Luo, L. (2009). Uncoupling dendrite growth and patterning: single-cell knockout analysis of NMDA receptor 2B. *Neuron* 62, 205–217. doi: 10.1016/j.neuron.2009.03.006

Fox, K. (2008). *Barrel Cortex*. Cambridge: Cambridge University Press.

Fujimoto, F., Leiwe, M. N., Aihara, S., Sakaguchi, R., Muroyama, Y., Kobayakawa, R., et al. (2023). Activity-dependent local protection and lateral inhibition control synaptic competition in developing mitral cells in mice. *Dev. Cell* 58, 1221–1236.e7. doi: 10.1016/j.devcel.2023.05.004

Goodman, C. S., and Shatz, C. J. (1993). Developmental mechanisms that generate precise patterns of neuronal connectivity. *Cell* 72, 77–98. doi: 10.1016/s0092-8674(05)80030-3

Greenough, W. T., and Chang, F. L. (1988). Dendritic pattern formation involves both oriented regression and oriented growth in the barrels of mouse somatosensory cortex. *Brain Res.* 43, 148–152. doi: 10.1016/0165-3806(88)90160-5

Hannan, A. J., Blakemore, C., Katsnelson, A., Vitalis, T., Huber, K. M., Bear, M., et al. (2001). PLC-beta1, activated via mGluRs, mediates activity-dependent differentiation in cerebral cortex. *Nat. Neurosci.* 4, 282–288. doi: 10.1038/85132

Harris, R. M., and Woolsey, T. A. (1981). Dendritic plasticity in mouse barrel cortex following postnatal vibrissa follicle damage. *J. Comp. Neurol.* 196, 357–376. doi: 10.1002/cne.901960302

Higashi, S., Molnár, Z., Kurotani, T., and Toyama, K. (2002). Prenatal development of neural excitation in rat thalamocortical projections studied by optical recording. *Neuroscience* 115, 1231–1246. doi: 10.1016/s0306-4522(02)00418-9

Horton, A. C., Racz, B., Monson, E. E., Lin, A. L., Weinberg, R. J., and Ehlers, M. D. (2005). Polarized secretory trafficking directs cargo for asymmetric dendrite growth and morphogenesis. *Neuron* 48, 757–771. doi: 10.1016/j.neuron.2005.11.005

Huang, J.-Y., and Lu, H.-C. (2018). mGluR5 tunes NGF/TrkA signaling to orient spiny stellate neuron dendrites toward thalamocortical axons during whisker-barrel map formation. *Cereb. Cortex* 28, 1991–2006. doi: 10.1093/cercor/bhx105

Huang, J.-Y., Miskus, M. L., and Lu, H.-C. (2017). FGF-FGFR mediates the activity-dependent dendritogenesis of layer IV neurons during barrel formation. *J. Neurosci.* 37, 12094–12105. doi: 10.1523/JNEUROSCI.1174-17.2017

Inan, M., Lu, H. C., Albright, M. J., She, W. C., and Crair, M. C. (2006). Barrel map development relies on protein kinase a regulatory subunit II beta-mediated cAMP signaling. *J. Neurosci.* 26, 4338–4349. doi: 10.1523/JNEUROSCI.3745-05.2006

Ince-Dunn, G., Hall, B. J., Hu, S. C., Ripley, B., Huganir, R. L., Olson, J. M., et al. (2006). Regulation of thalamocortical patterning and synaptic maturation by NeuroD2. *Neuron* 49, 683–695. doi: 10.1016/j.neuron.2006.01.031

Iwasato, T. (2020). In vivo imaging of neural circuit formation in the neonatal mouse barrel cortex. *Develop. Growth Differ.* 62, 476–486. doi: 10.1111/dgd.12693

Iwasato, T., Datwani, A., Wolf, A. M., Nishiyama, H., Taguchi, Y., Tonegawa, S., et al. (2000). Cortex-restricted disruption of NMDAR1 impairs neuronal patterns in the barrel cortex. *Nature* 406, 726–731. doi: 10.1038/35021059

Iwasato, T., and Erzurumlu, R. S. (2018). Development of tactile sensory circuits in the CNS. *Curr. Opin. Neurobiol.* 53, 66–75. doi: 10.1016/j.conb.2018.06.001

Iwasato, T., Inan, M., Kanki, H., Erzurumlu, R. S., Itohara, S., and Crair, M. C. (2008). Cortical adenylyl cyclase 1 is required for thalamocortical synapse maturation and aspects of layer IV barrel development. *J. Neurosci.* 28, 5931–5943. doi: 10.1523/JNEUROSCI.0815-08.2008

Jabaudon, D., Shnider, S. J., Tischfield, D. J., Galazo, M. J., and Macklis, J. D. (2012). RORbeta induces barrel-like neuronal clusters in the developing neocortex. *Cereb. Cortex* 22, 996–1006. doi: 10.1093/cercor/bhr182

Kanold, P. O. (2019). The first cortical circuits: subplate neurons lead the way and shape cortical organization. *e-Neuroforum* 25, 15–23. doi: 10.1515/nf-2018-0010

Kashani, A. H., Qiu, Z., Jurata, L., Lee, S. K., Pfaff, S., Goebbels, S., et al. (2006). Calcium activation of the LMO4 transcription complex and its role in the patterning of thalamocortical connections. *J. Neurosci.* 26, 8398–8408. doi: 10.1523/JNEUROSCI.0618-06.2006

Katz, L. C., and Constantine-Paton, M. (1988). Relationships between segregated afferents and postsynaptic neurones in the optic tectum of three-eyed frogs. *J. Neurosci.* 8, 3160–3180. doi: 10.1523/JNEUROSCI.08-09-03160.1988

Katz, L. C., and Shatz, C. J. (1996). Synaptic activity and the construction of cortical circuits. *Science* 274, 1133–1138. doi: 10.1126/science.274.5290.1133

Khazipov, R., Sirota, A., Leinekugel, X., Holmes, G. L., Ben-Ari, Y., and Buzsaki, G. (2004). Early motor activity drives spindle bursts in the developing somatosensory cortex. *Nature* 432, 758–761. doi: 10.1038/nature03132

Kirkby, L. A., Sack, G. S., Firl, A., and Feller, M. B. (2013). A role for correlated spontaneous activity in the assembly of neural circuits. *Neuron* 80, 1129–1144. doi: 10.1016/j.neuron.2013.10.030

Kossel, A., Löwel, S., and Bolz, J. (1995). Relationships between dendritic fields and functional architecture in striate cortex of normal and visually deprived cats. *J. Neurosci.* 15, 3913–3926. doi: 10.1523/JNEUROSCI.15-05-03913.1995

Li, H., Fertuzinhos, S., Mohns, E., Hnasko, T. S., Verhage, M., Edwards, R., et al. (2013). Laminar and columnar development of barrel cortex relies on thalamocortical neurotransmission. *Neuron* 79, 970–986. doi: 10.1016/j.neuron.2013.06.043

Lübke, J., Egger, V., Sakmann, B., and Feldmeyer, D. (2000). Columnar organization of dendrites and axons of single and synaptically coupled excitatory spiny neurons in layer 4 of the rat barrel cortex. *J. Neurosci.* 20, 5300–5311. doi: 10.1523/JNEUROSCI.20-14-05300.2000

Lush, M. E., Li, Y., Kwon, C. H., Chen, J., and Parada, L. F. (2008). Neurofibromin is required forbarrel formation in the mouse somatosensory cortex. *J. Neurosci.* 28, 1580–1587. doi: 10.1523/JNEUROSCI.5236-07.2008

Martini, F. J., Guillamón-Vivancos, T., Moreno-Juan, V., Valdeolmillos, M., and López-Bendito, G. (2021). Spontaneous activity in developing thalamic and cortical sensory networks. *Neuron* 109, 2519–2534. doi: 10.1016/j.neuron.2021.06.026

Matsui, A., Tran, M., Yoshida, A. C., Kikuchi, S. S., Ogawa, M., and Shimogori, T. (2013). BTBD3 controls dendrite orientation toward active axons in mammalian neocortex. *Science* 342, 1114–1118. doi: 10.1126/science.1244505

Mizuno, H., Ikezoe, K., Nakazawa, S., Sato, T., Kitamura, K., and Iwasato, T. (2018). Patchwork-type spontaneous activity in neonatal barrel cortex layer 4 transmitted via thalamocortical projections. *Cell Rep.* 22, 123–135. doi: 10.1016/j.celrep.2017.12.012

Mizuno, H., Luo, W., Tarusawa, E., Saito, Y. M., Sato, T., Yoshimura, Y., et al. (2014). NMDAR-regulated dynamics of layer 4 neuronal dendrites during thalamocortical reorganization in neonates. *Neuron* 82, 365–379. doi: 10.1016/j.neuron.2014.02.026

Mori, H., and Mishina, M. (1995). Structure and function of the NMDA receptor channel. *Neuropharmacology* 34, 1219–1237. doi: 10.1016/0028-3908(95)00109-J

Nakagawa, N., and Iwasato, T. (2023). Golgi polarity shift instructs dendritic refinement in the neonatal cortex by mediating NMDA receptor signaling. *Cell Rep.* 42:112843. doi: 10.1016/j.celrep.2023.112843

Nakanishi, S. (1992). Molecular diversity of glutamate receptors and implications for brain function. *Science* 258, 597–603. doi: 10.1126/science.1329206

Nakazawa, S., and Iwasato, T. (2021). Spatial organization and transitions of spontaneous neuronal activities in the developing sensory cortex. *Develop. Growth Differ.* 63, 323–339. doi: 10.1111/dgd.12739

Nakazawa, S., Mizuno, H., and Iwasato, T. (2018). Differential dynamics of cortical neuron dendritic trees revealed by long-term in vivo imaging in neonates. *Nat. Commun.* 9:3106. doi: 10.1038/s41467-018-05563-0

Nakazawa, S., Yoshimura, Y., Takagi, M., Mizuno, H., and Iwasato, T. (2020). Developmental phase transitions in spatial organization of spontaneous activity in postnatal barrel cortex layer 4. *J. Neurosci.* 40, 7637–7650. doi: 10.1523/JNEUROSCI.1116-20.2020

Narboux-Neme, N., Evrard, A., Ferezou, I., Erzurumlu, R. S., Kaeser, P. S., Laine, J., et al. (2012). Neurotransmitter release at the thalamocortical synapse instructs barrel formation but not axon patterning in the somatosensory cortex. *J. Neurosci.* 32, 6183–6196. doi: 10.1523/JNEUROSCI.0343-12.2012

Piñon, M. C., Jethwa, A., Jacobs, E., Campagnoni, A., and Molnár, Z. (2009). Dynamic integration of subplate neurons into the cortical barrel field circuitry during postnatal development in the Golli-tau-eGFP (GTE) mouse. *J. Physiol.* 587, 1903–1915. doi: 10.1113/jphysiol.2008.167767

Rao, M. S., Mizuno, H., Iwasato, T., and Mizuno, H. (2022). Ras GTPase-activating proteins control neuronal circuit development in barrel cortex layer 4. *Front. Neurosci.* 16:901774. doi: 10.3389/fnins.2022.901774

She, W. C., Quairiaux, C., Albright, M. J., Wang, Y. C., Sanchez, D. E., Chang, P. S., et al. (2009). Roles of mGluR5 in synaptic function and plasticity of themouse thalamocortical pathway. *Eur. J. Neurosci.* 29, 1379–1396. doi: 10.1111/j.1460-9568.2009.06696.x

Simons, D. J., and Woolsey, T. A. (1984). Morphology of Golgi-cox-impregnated barrel neurons in rat SmI cortex. *J. Comp. Neurol.* 230, 119–132. doi: 10.1002/cne.902300111

Staiger, J. F., Flagmeyer, I., Schubert, D., Zilles, K., Kotter, R., and Luhmann, H. J. (2004). Functional diversity of layer IV spiny neurons in rat somatosensory cortex: quantitative morphology of electrophysiologically characterized and biocytin labeled cells. *Cereb. Cortex* 14, 690–701. doi: 10.1093/cercor/bhh029

Tiriac, A., Del Rio-Bermudez, C., and Blumberg, M. S. (2014). Self-generated movements with "unexpected" sensory consequences. *Curr. Biol.* 24, 2136–2141. doi: 10.1016/j.cub.2014.07.053

Tiriac, A., Uitermarkt, B. D., Fanning, A. S., Sokoloff, G., and Blumberg, M. S. (2012). Rapid whisker movements in sleeping newborn rats. *Curr. Biol.* 22, 2075–2080. doi: 10.1016/j.cub.2012.09.009

van der Bourg, A., Yang, J. W., Reyes-Puerta, V., Laurenczy, B., Wieckhorst, M., Stüttgen, M. C., et al. (2017). Layer-specific refinement of sensory coding in developing mouse barrel cortex. *Cereb. Cortex* 27, 4835–4850. doi: 10.1093/cercor/bhw280

Vitalis, T., Dauphinot, L., Gressens, P., Potier, M. C., Mariani, J., and Gaspar, P. (2018). RORα coordinates thalamic and cortical maturation to instruct barrel cortex development. *Cereb. Cortex* 28, 3994–4007. doi: 10.1093/cercor/bhx262

Wang, L., Nakazawa, S., Luo, W., Sato, T., Mizuno, H., and Iwasato, T. (2023). Short-term dendritic dynamics of neonatal cortical neurons revealed by in vivo imaging with improved spatiotemporal resolution. *eNeuro* 10:ENEURO. 0142-23.2023. doi: 10.1523/ENEURO.0142-23.2023

Watson, R. F., Abdel-Majid, R. M., Barnett, M. W., Willis, B. S., Katsnelson, A., Gillingwater, T. H., et al. (2006). Involvement of protein kinase a in patterning of the mouse somatosensory cortex. *J. Neurosci.* 26, 5393–5401. doi: 10.1523/JNEUROSCI.0750-06.2006

Wong, W. T., Faulkner-Jones, B. E., Sanes, J. R., and Wong, R. O. (2000). Rapid dendritic remodeling in the developing retina: dependence on neurotransmission and reciprocal regulation by Rac and rho. *J. Neurosci.* 20, 5024–5036. doi: 10.1523/JNEUROSCI.20-13-05024.2000

Wong, R. O., and Ghosh, A. (2002). Activity-dependent regulation of dendritic growth and patterning. *Nat. Rev. Neurosci.* 3, 803–812. doi: 10.1038/nrn941

Woolsey, T. A., and Van der Loos, H. (1970). The structural organization of layer IV in the somatosensory region (SI) of mouse cerebral cortex. The description of a cortical field composed of discrete cytoarchitectonic units. *Brain Res.* 17, 205–242. doi: 10.1016/0006-8993(70)90079-x

Ye, B., Zhang, Y., Song, W., Younger, S. H., Jan, L. Y., and Jan, Y. N. (2007). Growing dendrites and axons differ in their reliance on the secretory pathway. *Cell* 130, 717–729. doi: 10.1016/j.cell.2007.06.032

Zhang, M., Lu, M., Huang, H., Liu, X., Su, H., and Li, H. (2019). Maturation of thalamocortical synapses in the somatosensory cortex depends on neocortical AKAP5 expression. *Neurosci. Lett.* 709:134374. doi: 10.1016/j.neulet.2019.134374

frontiers | Frontiers in Neural Circuits

TYPE Mini Review
PUBLISHED 22 May 2024
DOI 10.3389/fncir.2024.1423505

OPEN ACCESS

EDITED BY
Kensaku Mori,
RIKEN, Japan

REVIEWED BY
Kazunari Miyamichi,
RIKEN Center for Biosystems Dynamics Research (BDR), Japan

*CORRESPONDENCE
Masahiro Yamaguchi
✉ yamaguchi@kochi-u.ac.jp

RECEIVED 26 April 2024
ACCEPTED 07 May 2024
PUBLISHED 22 May 2024

CITATION
Yamaguchi M (2024) Connectivity of the olfactory tubercle: inputs, outputs, and their plasticity.
Front. Neural Circuits 18:1423505.
doi: 10.3389/fncir.2024.1423505

Connectivity of the olfactory tubercle: inputs, outputs, and their plasticity

Masahiro Yamaguchi*

Department of Physiology, Kochi Medical School, Kochi University, Kochi, Japan

The olfactory tubercle (OT) is a unique part of the olfactory cortex of the mammal brain in that it is also a component of the ventral striatum. It is crucially involved in motivational behaviors, particularly in adaptive olfactory learning. This review introduces the basic properties of the OT, its synaptic connectivity with other brain areas, and the plasticity of the connectivity associated with learning behavior. The adaptive properties of olfactory behavior are discussed further based on the characteristics of OT neuronal circuits.

KEYWORDS

olfactory tubercle, olfactory learning, plasticity, synaptic input, synaptic output

Introduction

The olfactory cortex (OC) can be subdivided into areas with distinct structural and functional properties (Neville and Haberly, 2004). The olfactory tubercle (OT) is a component of both the OC and the ventral striatum with medium spiny neurons as its principal neurons; it receives massive dopamine signals from the midbrain (Millhouse and Heimer, 1984; Ikemoto, 2007; Wesson and Wilson, 2011; Mori, 2014). Accordingly, it is involved in odor-guided motivated behaviors, particularly in adaptive learning (Ikemoto, 2007; Wesson and Wilson, 2011; Wesson, 2020). Its input and output connectivity suggests that it lies downstream of the olfactory input–behavioral output pathway, integrates information from various brain regions, and sends outputs to areas related to motivated behaviors (Haberly and Price, 1978). Previously, we showed that the OT has distinct functional domains that represent learned odor-induced attractive and aversive motivated behaviors (Murata et al., 2015). We here introduce our recent study that synaptic inputs to the OT exhibit domain-specific structural plasticity induced by olfactory learning (Sha et al., 2023). Along with this, several characteristics of the neural circuits of the OT and their plasticity are discussed to increase our understanding of the neural mechanisms of olfactory learning.

The olfactory tubercle as a regulator of motivated olfactory behaviors

The OC receives direct synaptic inputs from neurons projecting from the olfactory bulb (OB) (Neville and Haberly, 2004) and consists of several distinct areas. In the ventral view of the rodent brain, the OT is readily identified as a round bulge posterior to the olfactory

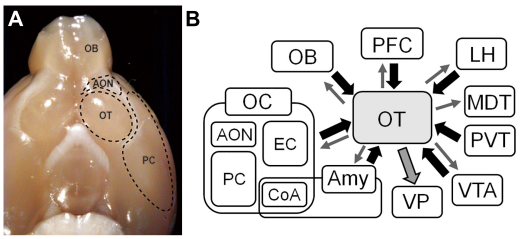

FIGURE 1
Inputs and outputs of the olfactory tubercle (OT). **(A)** Ventral view of the brain of a mouse. The OT locates posterior to the anterior olfactory nucleus (AON) and medial to the piriform cortex (PC). **(B)** Inputs and outputs of the OT. The OT receives synaptic inputs from various brain areas, and sends outputs reciprocally to those brain areas and massively to the ventral pallidum (VP). OB, olfactory bulb; OC, olfactory cortex; EC, entorhinal cortex; CoA, cortical amygdala; Amy, amygdala; PFC, prefrontal cortex; LH, lateral hypothalamus; MDT, mediodorsal thalamus; PVT, paraventricular thalamus; VTA, ventral tegmental area.

peduncle and medial to the piriform cortex (PC) (**Figure 1**). As a component of the OC, the OT has a three-layered structure in which axons of OB neurons project to the most superficial layer (layer I). It has properties that are distinct from those of other areas of the OC. While most principal neurons in the OC are glutamatergic pyramidal cells, those of the OT are GABAergic medium spiny neurons (Millhouse and Heimer, 1984). The OT receives massive dopaminergic inputs from the ventral tegmental area (VTA) in the midbrain (de Olmos and Heimer, 1999; Ikemoto, 2007). These properties indicate that the OT is also a component of the striatum, constituting ventral striatum with the nucleus accumbens (NAc). OT neurons express large amounts of acetylcholine esterase (AchE), a characteristic shared with striatal neurons of the NAc and dorsal striatum (Butcher et al., 1975). In the rodent brain, the OT strongly stains with AchE and has a clear boundary separating it from the PC laterally and the diagonal band medially (Paxinos and Franklin, 2019).

As a component of the ventral striatum, it is crucially involved in motivated behaviors (Millhouse and Heimer, 1984; Ikemoto, 2007; Wesson and Wilson, 2011; Mori, 2014). Electrical self-stimulation of the OT is rewarding in rats (Prado-Alcalá and Wise, 1984; Fitzgerald et al., 2014). The OT is a hotspot for cocaine self-administration (Ikemoto, 2003). In addition, as a component of both the OC and ventral striatum, it is involved in odor-motivated behaviors. Innate odor preference is altered by electrical stimulation of the OT (Fitzgerald et al., 2014). In one study, preference for opposite-sex urinary odors was disrupted by suppression of OT activity (DiBenedictis et al., 2015). Activation of the dopaminergic pathway from the VTA to the medial part of the OT reinforces odor preference (Zhang et al., 2017a).

Further, many studies have revealed adaptive properties of the OT. For example, odor-reward association learning potentiates the firing of OT neurons in response to a rewarded odor (Gadziola et al., 2015, 2020; Millman and Murthy, 2020). In one study, following odor-reward or odor-punishment training, neuronal activity in the OT was enhanced in a learning-dependent manner in response to the learned odor (Murata et al., 2015). These observations are consistent with the general notion that the ventral striatum plays crucial roles in the learning, reinforcement, and adaptive modulation of motivated behaviors (Robbins and Everitt, 1996; Averbeck and Costa, 2017). Note that OT-mediated motivated behaviors are not solely odor-guided ones. Therefore, it has been proposed that the OT be called the "tubular striatum" based on its tubular morphology and striatal properties (Wesson, 2020).

Synaptic connectivity of the OT

The OT belongs to the OC because it receives direct synaptic inputs from OB projection neurons (White, 1965; Scott et al., 1980). However, the overall connectivity of the OT seems different from that of other areas of the OC. While cortical areas have reciprocal connections with other brain areas, the basis of the input to and output from the OT seems that it receives synaptic inputs from various brain areas and sends synaptic outputs to areas linked to motivated behavioral output.

In addition to inputs from the OB, the OT receives intracortical associational inputs from many brain areas (**Figure 1B**). The PC is the broadest area of the OC and is the source of massive synaptic inputs to the OT (Haberly and Price, 1978; White et al., 2019). Other OC regions project to the OT, including the anterior olfactory nucleus and entorhinal cortex (Haberly and Price, 1978). The prefrontal cortex sends projections to the OT (Berendse and Groenewegen, 1990; Cansler et al., 2023). The amygdala is a complex structure that represent the core of emotions and both cortical and deep amygdaloid nuclei project to the OT (Novejarque et al., 2011). The lateral hypothalamus, which contains various neuropeptide-producing cells, and the paraventricular thalamus (PVT), which mediates motivated behaviors, project to the OT (Groenewegen and Berendse, 1990; Moga et al., 1995). The VTA sends dopaminergic projections to the OT (Ikemoto, 2007).

Contrasting the OT inputs from multiple brain regions, the major output from the OT is considered to the ventral pallidum (VP) (Heimer, 1978) (**Figure 1B**), a subregion of the ventral basal forebrain complex that regulates emotions, motivation, and motivated behaviors (Soares-Cunha and Heinsbroek, 2023). The VP connects to the reticular formation and extrapyramidal motor systems, and is thought to be a key regulator of motivational behavioral output (Mogenson and Yang, 1991). It is also thought to regulate motivated behaviors via its projections to the lateral hypothalamus and mediodorsal thalamic nuclei (Leung and Balleine, 2015; Faget et al., 2018). Therefore, the OT–VP pathway is considered the central route through which the OT contributes to motivated behaviors.

Many recent studies, including those employing transsynaptic tracing, have revealed various projection targets of the OT, including the PC and anterior olfactory nucleus in the OC (Zhang et al., 2017b), mediodorsal thalamus (Siegel et al., 1977; Price and Slotnick, 1983), posterolateral part of the hypothalamus (Scott and Chafin, 1975), and VTA (Zhang et al., 2017b). Thus, rich reciprocal connections between the OT and other brain areas actually exist. Nonetheless, the prominent property of the OT appears to be its massive output to the VP. This fits with the notion that the OT plays crucial roles in motivational behavior and lies downstream of the sensory input–behavioral output pathway, thereby gathering information from various brain regions and sending output to the VP.

Plasticity of the synaptic connections of the OT underlying learning-dependent activation of specific OT domains

Previously, we showed that the OT has functional domains that are activated following odor-guided learning. In principle, neutral odors that do not elicit motivated behaviors do not significantly activate the OT. When mice are trained to associate a neutral odor with a food reward and thus become attracted to that odor, the odor stimulus activates the anteromedial domain of the OT (amOT). By contrast, when trained to associate the same odor with electrical shocks to the foot, they become averse to the odor, which activates the lateral domain of the OT (lOT) (Murata et al., 2015). In agreement with this pattern, involvement of the medial part of the OT in odor-attractive behaviors has been reported (DiBenedictis et al., 2015; Zhang et al., 2017a).

The learning-dependent activation of specific OT domains raises questions regarding the underlying plastic mechanisms. Because activation of a brain area depends on synaptic inputs from other brain areas, synaptic inputs to a given OT domain may be potentiated during olfactory-motivated behavior learning, and this may induce domain-specific activation. As a first step to address this possibility, we used optogenetics to activate specific inputs to the OT and examined their plasticity (Sha et al., 2023).

Of various synaptic inputs to the OT, inputs from the OB were chosen as being representative of peripheral sensory inputs while inputs from the PC were chosen as being representative of intracortical association inputs. These neurons were modified to express channelrhodopsin-2 fused with fluorescent mCherry protein to enable their photoactivation and morphological analysis (**Figure 2**). We analyzed the size of the axonal boutons in the photoactivated neurons that terminated in the OT domains, as their size generally correlates with synaptic strength (Murthy et al., 2001; Sammons et al., 2018).

Photoactivation of pyramidal cells in the PC alone did not induce specific behavior in mice. In this case, there were no differences in the sizes of axonal boutons terminating in the amOT and lOT. When photoactivation was associated with a food reward, however, the mice showed food-searching behavior in response to photoactivation. In these mice, the boutons that terminated in the amOT, but not in the lOT, increased in size (**Figure 2**). By contrast, when the photoactivation was associated with electrical shock, the mice adopted shock-avoiding behavior in response to photoactivation. In these mice, the boutons that terminated in the lOT, but not in the amOT, increased in size. Similar OT domain-specific size development of axonal boutons was observed in OB projection neurons. These observations indicate that both intracortical inputs from the PC and sensory inputs from the OB have plastic potential to induce structural changes in an OT domain-specific manner.

The structural plasticity of the intracortical synapses in the PC is consistent with their role in learning-dependent control of OT activity (White et al., 2019) and with the general notion that plasticity in cortical networks underlies information storage, learning, and adaptive behavior (Feldman, 2009). The structural plasticity of sensory synapses from the OB to the OT domains

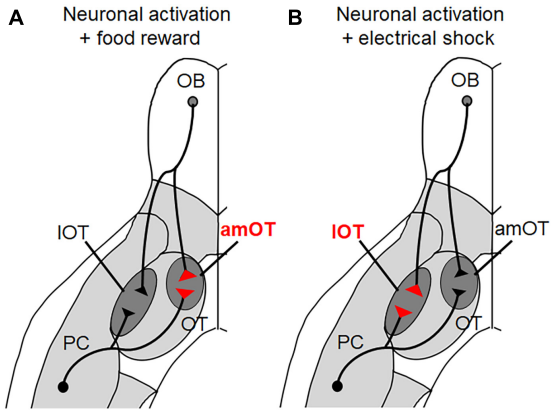

FIGURE 2
OT domain-specific plasticity of axonal boutons induced by olfactory learning. **(A)** When photoactivation of PC pyramidal neurons and OB projection neurons was associated with a food reward, the axonal boutons terminating in the anteromedial (am) OT domain increased in size. **(B)** When photoactivation of PC pyramidal neurons and OB projection neurons was associated with electrical shock, the axonal boutons terminating in the lateral (l) OT domain increased in size.

is intriguing, because several studies have shown that sensory synapses in the OC appear to be hardwired, particularly in the PC, compared to intracortical association synapses (Kanter and Haberly, 1990; Poo and Isaacson, 2007; Johenning et al., 2009; Bekkers and Suzuki, 2013). Odor information from the external environment can reach the OT via as little as two synaptic steps, from olfactory sensory neurons to OB projection neurons and then to OT neurons. Learning-dependent plasticity of the sensory connections from the OB to the OT domains may represent strong adaptive linkage of odor information to behavioral outputs (Doty, 1986).

Because we used artificial optogenetic stimulation, it remains unclear whether similar plastic changes occur during physiological odor stimulation and learning. Nonetheless, the results demonstrate the highly plastic potential of synaptic inputs to the OT domains, which likely underlie the OT domain-specific activation and the expression of appropriate motivated behaviors in a learning-dependent manner. Note that **Figure 2** is just a schematic diagram and it is not yet evident whether individual PC and OB neurons send bifurcated axonal projections to both amOT and lOT, or distinct presynaptic populations innervate these functionally distinct OT domains. It remains to be determined whether the plastic change is regulated in individual axonal boutons or in individual neurons. This knowledge may help understand how odor valence is encoded and plastically modulated in the olfactory neuronal circuitry.

Perspectives on the plasticity of synaptic connections in the OT

Regarding the functional plasticity of the OT synapses, odor-evoked firing activity of OT neurons in awake mice is modulated by the activation of PC to OT inputs (White et al., 2019).

In addition to the glutamatergic synaptic inputs, neuromodulators play crucial roles in synaptic plasticity. Dopamine is central to OT-mediated odor learning (Zhang et al., 2017a). Excitatory postsynaptic potentials induced by the lateral olfactory tract stimulation are potentiated by the simultaneous dopamine release (Wieland et al., 2015), and phasic dopamine increases the intensity of excitatory stimulus responses of OT neurons (Oettl et al., 2020). Because dopaminergic input to the medial and lateral OT appears to have a distinct role in neuronal activity (Bhimani et al., 2022), OT domain-specific dopaminergic input may be involved in OT domain-specific plasticity. The OT receives a variety of neuromodulatory signals other than dopamine (Cansler et al., 2020), and biased neuromodulatory signals among OT domains are suggested (Nogi et al., 2020). Given that neuromodulators convey information on various states of the brain and body, the neural mechanisms governing the reception of such information and its integration with synaptic plasticity in the OT during olfactory behavior learning are key to understanding the highly adaptive properties of the OT.

The OT contains D1- and D2-type dopamine receptor-expressing neurons, which have distinct functions in the processing of odor information. Odor-attractive behavior is accompanied by the activation of D1 cells in the amOT, while odor-aversive behavior is accompanied by the activation of D1 cells in the lOT (Murata et al., 2015). Conversely, the activation of D2 cells in the amOT induces aversive behavior (Murata et al., 2019). The differential synaptic plasticity of D1 and D2 cells during olfactory learning has been revealed (White et al., 2019; Gadziola et al., 2020; Martiros et al., 2022). Understanding the structural and functional plasticity of synaptic inputs to D1 and D2 cells during olfactory learning would reveal the differential and combinatory roles of D1/D2 cell-mediated neural pathways in the OT.

Compared to synaptic inputs, there is limited knowledge of synaptic outputs from the OT and their plasticity. Regarding output from the NAc to the VP, cocaine-induced synaptic potentiation/depression has been reported (Baimel et al., 2019). Examining the domain specificity, cell type specificity, and plastic properties of the output from the OT to the VP would provide further insight into the plastic control of olfactory-motivated behaviors. Understanding the function of the OT in the neural network involving cortical and subcortical brain areas and neuromodulatory signaling systems would reveal the neural mechanisms of the adaptive control of odor-guided behaviors.

Lastly, contribution of the OT to innate olfactory behaviors would be worth pursuing. Influence of the OT activity on the preference for conspecific urinary odors (DiBenedictis et al., 2015) suggests OT's involvement in innate behaviors. In the central amygdala, the same neuronal population controls innate and learned odor-fear behaviors in opposing directions (Isosaka et al., 2015). Comparing the regulatory mechanisms of innate and learned olfactory behaviors in the OT would facilitate the understanding of how these two types of behaviors are related and differentiated in the mammalian brain.

Author contributions

MY: Writing – review and editing, Writing – original draft, Conceptualization.

Funding

The author(s) declare that financial support was received for the research, authorship, and/or publication of this article. This study was supported by the Grant-in-Aid for Scientific Research from Japan Society for Promotion of Science (grant nos. 19H03341 and 22H02734).

Conflict of interest

The author declares that the research was conducted in the absence of any commercial or financial relationships that could be construed as a potential conflict of interest.

Publisher's note

References

Averbeck, B. B., and Costa, V. D. (2017). Motivational neural circuits underlying reinforcement learning. *Nat. Neurosci.* 20, 505–512. doi: 10.1038/nn.4506

Baimel, C., McGarry, L. M., and Carter, A. G. (2019). The projection targets of medium spiny neurons govern cocaine-evoked synaptic plasticity in the nucleus accumbens. *Cell Rep.* 28:2256–2263.e2253. doi: 10.1016/j.celrep.2019.07.074

Bekkers, J. M., and Suzuki, N. (2013). Neurons and circuits for odor processing in the piriform cortex. *Trends Neurosci.* 36, 429–438. doi: 10.1016/j.tins.2013.04.005

Berendse, H. W., and Groenewegen, H. J. (1990). Organization of the thalamostriatal projections in the rat, with special emphasis on the ventral striatum. *J. Comp. Neurol.* 299, 187–228. doi: 10.1002/cne.902990206

Bhimani, R. V., Yates, R., Bass, C. E., and Park, J. (2022). Distinct limbic dopamine regulation across olfactory-tubercle subregions through integration of in vivo fast-scan cyclic voltammetry and optogenetics. *J. Neurochem.* 161, 53–68. doi: 10.1111/jnc.15577

Butcher, L. L., Talbot, K., and Bilezikjian, L. (1975). Acetylcholinesterase neurons in dopamine-containing regions of the brain. *J. Neural Transm.* 37, 127–153. doi: 10.1007/bf01663629

Cansler, H. L., Wright, K. N., Stetzik, L. A., and Wesson, D. W. (2020). Neurochemical organization of the ventral striatum's olfactory tubercle. *J. Neurochem.* 152, 425–448. doi: 10.1111/jnc.14919

Cansler, H. L., Zandt, E. E., Carlson, K. S., Khan, W. T., Ma, M., and Wesson, D. W. (2023). Organization and engagement of a prefrontal-olfactory network during olfactory selective attention. *Cereb. Cortex* 33, 1504–1526. doi: 10.1093/cercor/bhac153

de Olmos, J. S., and Heimer, L. (1999). The concepts of the ventral striatopallidal system and extended amygdala. *Ann. N. Y. Acad. Sci.* 877, 1–32. doi: 10.1111/j.1749-6632.1999.tb09258.x

DiBenedictis, B. T., Olugbemi, A. O., Baum, M. J., and Cherry, J. A. (2015). DREADD-induced silencing of the medial olfactory tubercle disrupts the preference of female mice for opposite-sex chemosignals(1,2,3). *eNeuro* 2, 1–16. doi: 10.1523/eneuro.0078-15.2015

Doty, R. L. (1986). Odor-guided behavior in mammals. *Experientia* 42, 257–271. doi: 10.1007/bf01942506

Faget, L., Zell, V., Souter, E., McPherson, A., Ressler, R., Gutierrez-Reed, N., et al. (2018). Opponent control of behavioral reinforcement by inhibitory and excitatory projections from the ventral pallidum. *Nat. Commun.* 9:849. doi: 10.1038/s41467-018-03125-y

Feldman, D. E. (2009). Synaptic mechanisms for plasticity in neocortex. *Annu. Rev. Neurosci.* 32, 33–55. doi: 10.1146/annurev.neuro.051508.135516

Fitzgerald, B. J., Richardson, K., and Wesson, D. W. (2014). Olfactory tubercle stimulation alters odor preference behavior and recruits forebrain reward and motivational centers. *Front. Behav. Neurosci.* 8:81. doi: 10.3389/fnbeh.2014.00081

Gadziola, M. A., Stetzik, L. A., Wright, K. N., Milton, A. J., Arakawa, K., Del Mar, et al. (2020). A neural system that represents the association of odors with rewarded outcomes and promotes behavioral engagement. *Cell Rep.* 32:107919. doi: 10.1016/j.celrep.2020.107919

Gadziola, M. A., Tylicki, K. A., Christian, D. L., and Wesson, D. W. (2015). The olfactory tubercle encodes odor valence in behaving mice. *J. Neurosci.* 35, 4515–4527. doi: 10.1523/jneurosci.4750-14.2015

Groenewegen, H. J., and Berendse, H. W. (1990). Connections of the subthalamic nucleus with ventral striatopallidal parts of the basal ganglia in the rat. *J. Comp. Neurol.* 294, 607–622. doi: 10.1002/cne.902940408

Haberly, L. B., and Price, J. L. (1978). Association and commissural fiber systems of the olfactory cortex of the rat. *J. Comp. Neurol.* 178, 711–740. doi: 10.1002/cne.901780408

Heimer, L. B. (1978). *The olfactory cortex and the ventral striatum*. New York, NY: Plenum.

Ikemoto, S. (2003). Involvement of the olfactory tubercle in cocaine reward: Intracranial self-administration studies. *J. Neurosci.* 23, 9305–9311. doi: 10.1523/jneurosci.23-28-09305.2003

Ikemoto, S. (2007). Dopamine reward circuitry: Two projection systems from the ventral midbrain to the nucleus accumbens-olfactory tubercle complex. *Brain Res. Rev.* 56, 27–78. doi: 10.1016/j.brainresrev.2007.05.004

Isosaka, T., Matsuo, T., Yamaguchi, T., Funabiki, K., Nakanishi, S., Kobayakawa, R., et al. (2015). Htr2a-expressing cells in the central amygdala control the hierarchy between innate and learned fear. *Cell* 163, 1153–1164. doi: 10.1016/j.cell.2015.10.047

Johenning, F. W., Beed, P. S., Trimbuch, T., Bendels, M. H., Winterer, J., and Schmitz, D. (2009). Dendritic compartment and neuronal output mode determine pathway-specific long-term potentiation in the piriform cortex. *J. Neurosci.* 29, 13649–13661. doi: 10.1523/jneurosci.2672-09.2009

Kanter, and Haberly, L. B. (1990). NMDA-dependent induction of long-term potentiation in afferent and association fiber systems of piriform cortex in vitro. *Brain Res.* 525, 175–179. doi: 10.1016/0006-8993(90)91337-g

Leung, B. K., and Balleine, B. W. (2015). Ventral pallidal projections to mediodorsal thalamus and ventral tegmental area play distinct roles in outcome-specific Pavlovian-instrumental transfer. *J. Neurosci.* 35, 4953–4964. doi: 10.1523/jneurosci.4837-14.2015

Martiros, N., Kapoor, V., Kim, S. E., and Murthy, V. N. (2022). Distinct representation of cue-outcome association by D1 and D2 neurons in the ventral striatum's olfactory tubercle. *Elife* 11:e75463. doi: 10.7554/eLife.75463

Millhouse, O. E., and Heimer, L. (1984). Cell configurations in the olfactory tubercle of the rat. *J. Comp. Neurol.* 228, 571–597. doi: 10.1002/cne.902280409

Millman, D. J., and Murthy, V. N. (2020). Rapid learning of odor-value association in the olfactory striatum. *J. Neurosci.* 40, 4335–4347. doi: 10.1523/jneurosci.2604-19.2020

Moga, M. M., Weis, R. P., and Moore, R. Y. (1995). Efferent projections of the paraventricular thalamic nucleus in the rat. *J. Comp. Neurol.* 359, 221–238. doi: 10.1002/cne.903590204

Mogenson, G. J., and Yang, C. R. (1991). The contribution of basal forebrain to limbic-motor integration and the mediation of motivation to action. *Adv. Exp. Med. Biol.* 295, 267–290. doi: 10.1007/978-1-4757-0145-6_14

Mori, K. (2014). "Piriform cortex and olfactory tubercle," in *The olfactory system: From odor molecules to motivational behaviors*, ed. K. MORI (Tokyo: Springer).

Murata, K., Kanno, M., Ieki, N., Mori, K., and Yamaguchi, M. (2015). Mapping of learned odor-induced motivated behaviors in the mouse olfactory tubercle. *J. Neurosci.* 35, 10581–10599. doi: 10.1523/jneurosci.0073-15.2015

Murata, K., Kinoshita, T., Fukazawa, Y., Kobayashi, K., Yamanaka, A., Hikida, T., et al. (2019). Opposing roles of dopamine receptor D1– and D2-expressing neurons in the anteromedial olfactory tubercle in acquisition of place preference in mice. *Front. Behav. Neurosci.* 13:50. doi: 10.3389/fnbeh.2019.00050

Murthy, V. N., Schikorski, T., Stevens, C. F., and Zhu, Y. (2001). Inactivity produces increases in neurotransmitter release and synapse size. *Neuron* 32, 673–682. doi: 10.1016/s0896-6273(01)00500-1

Neville, K. R., and Haberly, L. B. (2004). "Olfactory cortex," in *The synaptic organization of the brain*, 5th Edn, ed. G. M. Shepherd (New York, NY: Oxford UP).

Nogi, Y., Ahasan, M. M., Murata, Y., Taniguchi, M., Sha, M. F. R., Ijichi, C., et al. (2020). Expression of feeding-related neuromodulatory signalling molecules in the mouse central olfactory system. *Sci. Rep.* 10:890. doi: 10.1038/s41598-020-57605-7

Novejarque, A., Gutiérrez-Castellanos, N., Lanuza, E., and Martínez-García, F. (2011). Amygdaloid projections to the ventral striatum in mice: Direct and indirect chemosensory inputs to the brain reward system. *Front. Neuroanat.* 5:54. doi: 10.3389/fnana.2011.00054

Oettl, L. L., Scheller, M., Filosa, C., Wieland, S., Haag, F., Loeb, C., et al. (2020). Phasic dopamine reinforces distinct striatal stimulus encoding in the olfactory tubercle driving dopaminergic reward prediction. *Nat. Commun.* 11:3460. doi: 10.1038/s41467-020-17257-7

Paxinos, G., and Franklin, K. B. J. (2019). *The mouse brain in stereotaxic coordinates*, 5th Edn. Amsterdam: Elsevier.

Poo, C., and Isaacson, J. S. (2007). An early critical period for long-term plasticity and structural modification of sensory synapses in olfactory cortex. *J. Neurosci.* 27, 7553–7558. doi: 10.1523/jneurosci.1786-07.2007

Prado-Alcalá, R., and Wise, R. A. (1984). Brain stimulation reward and dopamine terminal fields. I. Caudate-putamen, nucleus accumbens and amygdala. *Brain Res.* 297, 265–273. doi: 10.1016/0006-8993(84)90567-5

Price, J. L., and Slotnick, B. M. (1983). Dual olfactory representation in the rat thalamus: An anatomical and electrophysiological study. *J. Comp. Neurol.* 215, 63–77. doi: 10.1002/cne.902150106

Robbins, T. W., and Everitt, B. J. (1996). Neurobehavioural mechanisms of reward and motivation. *Curr. Opin. Neurobiol.* 6, 228–236. doi: 10.1016/s0959-4388(96)80077-8

Sammons, R. P., Clopath, C., and Barnes, S. J. (2018). Size-dependent axonal Bouton dynamics following visual deprivation in vivo. *Cell Rep.* 22, 576–584. doi: 10.1016/j.celrep.2017.12.065

Scott, J. W., and Chafin, B. R. (1975). Origin of olfactory projections to lateral hypothalamus and nuclei Gemini of the rat. *Brain Res.* 88, 64–68. doi: 10.1016/0006-8993(75)90948-8

Scott, J. W., McBride, R. L., and Schneider, S. P. (1980). The organization of projections from the olfactory bulb to the piriform cortex and olfactory tubercle in the rat. *J. Comp. Neurol.* 194, 519–534. doi: 10.1002/cne.901940304

Sha, M. F. R., Koga, Y., Murata, Y., Taniguchi, M., and Yamaguchi, M. (2023). Learning-dependent structural plasticity of intracortical and sensory connections to functional domains of the olfactory tubercle. *Front. Neurosci.* 17:1247375. doi: 10.3389/fnins.2023.1247375

Siegel, A., Fukushima, T., Meibach, R., Burke, L., Edinger, H., and Weiner, S. (1977). The origin of the afferent supply to the mediodorsal thalamic nucleus: Enhancement of HRP transport by selective lesions. *Brain Res.* 135, 11–23. doi: 10.1016/0006-8993(77)91048-4

Soares-Cunha, C., and Heinsbroek, J. A. (2023). Ventral pallidal regulation of motivated behaviors and reinforcement. *Front. Neural Circuits* 17:1086053. doi: 10.3389/fncir.2023.1086053

Wesson, D. W. (2020). The tubular striatum. *J. Neurosci.* 40, 7379–7386. doi: 10.1523/jneurosci.1109-20.2020

Wesson, D. W., and Wilson, D. A. (2011). Sniffing out the contributions of the olfactory tubercle to the sense of smell: Hedonics, sensory integration, and more? *Neurosci. Biobehav. Rev.* 35, 655–668. doi: 10.1016/j.neubiorev.2010.08.004

White, K. A., Zhang, Y. F., Zhang, Z., Bhattarai, J. P., Moberly, A. H., Zandt, E. E., et al. (2019). Glutamatergic neurons in the piriform cortex influence the activity of D1– and D2-type receptor-expressing olfactory tubercle neurons. *J. Neurosci.* 39, 9546–9559. doi: 10.1523/jneurosci.1444-19.2019

White, L. E. (1965). Olfactory bulb projections of the rat. *Anatomic. Rec.* 152, 465–579.

Wieland, S., Schindler, S., Huber, C., Köhr, G., Oswald, M. J., and Kelsch, W. (2015). Phasic dopamine modifies sensory-driven output of striatal neurons through synaptic plasticity. *J. Neurosci.* 35, 9946–9956. doi: 10.1523/jneurosci.0127-15.2015

Zhang, Z., Liu, Q., Wen, P., Zhang, J., Rao, X., Zhou, Z., et al. (2017a). Activation of the dopaminergic pathway from VTA to the medial olfactory tubercle generates odor-preference and reward. *Elife* 6:e25423. doi: 10.7554/eLife.25423

Zhang, Z., Zhang, H., Wen, P., Zhu, X., Wang, L., Liu, Q., et al. (2017b). Whole-brain mapping of the inputs and outputs of the medial part of the olfactory tubercle. *Front. Neural Circuits* 11:52. doi: 10.3389/fncir.2017.00052

frontiers | Frontiers in Neural Circuits

TYPE Mini Review
PUBLISHED 27 May 2024
DOI 10.3389/fncir.2024.1409680

OPEN ACCESS

EDITED BY
Charles A. Greer,
Yale University, United States

REVIEWED BY
Masayuki Sakamoto,
Kyoto University, Japan

*CORRESPONDENCE
Ai Nakashima
anaka@mol.f.u-tokyo.ac.jp
Haruki Takeuchi
htakeuchi@bs.s.u-tokyo.ac.jp

†These authors have contributed equally to this work and share first authorship

RECEIVED 30 March 2024
ACCEPTED 30 April 2024
PUBLISHED 27 May 2024

CITATION
Nakashima A and Takeuchi H (2024) Shaping the olfactory map: cell type-specific activity patterns guide circuit formation.
Front. Neural Circuits 18:1409680.
doi: 10.3389/fncir.2024.1409680

Shaping the olfactory map: cell type-specific activity patterns guide circuit formation

Ai Nakashima[1]*† and Haruki Takeuchi[2]*†

[1]Laboratory of Chemical Pharmacology, Graduate School of Pharmaceutical Sciences, The University of Tokyo, Tokyo, Japan, [2]Department of Biophysics and Biochemistry, Graduate School of Science, The University of Tokyo, Tokyo, Japan

The brain constructs spatially organized sensory maps to represent sensory information. The formation of sensory maps has traditionally been thought to depend on synchronous neuronal activity. However, recent evidence from the olfactory system suggests that cell type-specific temporal patterns of spontaneous activity play an instructive role in shaping the olfactory glomerular map. These findings challenge traditional views and highlight the importance of investigating the spatiotemporal dynamics of neural activity to understand the development of complex neural circuits. This review discusses the implications of new findings in the olfactory system and outlines future research directions.

KEYWORDS

olfactory map, neural activity, gene expression, odorant receptor, neural development

1 Introduction

Sensory information is represented in the brain as spatially organized activity patterns, commonly referred to as sensory or topographic maps (Luo and Flanagan, 2007; Petersen, 2007; Mori and Sakano, 2011; Pumo et al., 2022). The formation of precise sensory maps depends on the ordered projection of neurons, a process that is initially dictated by genetic programming and later fine-tuned through neural activity-dependent mechanisms. In the field of developmental neuroscience, numerous studies have suggested that correlated neural activity drives sensory map refinement (Katz and Shatz, 1996; Kirkby et al., 2013; Ackman and Crair, 2014; Pan and Monje, 2020; Martini et al., 2021). For example, in the developing visual system, spatially correlated spontaneous activity propagates in a wave-like manner across the retina (Galli and Maffei, 1988; Meister et al., 1991; Wong et al., 1993). In the somatosensory system, patchwork-like synchronized firing patterns corresponding to barrel maps are observed in the somatosensory cortex (Mizuno et al., 2018; Martini et al., 2021). In contrast, spontaneous activity in the primary olfactory system has been reported to lack spatiotemporal correlation, which contradicts the predictions of Hebb's theory. A recent study suggests that cell type-specific temporal activity patterns may play an instructive role in the development of the olfactory map (Nakashima et al., 2019, 2021). This review summarizes the current understanding of the emerging evidence for olfactory circuit formation that appears to be guided independently of Hebbian plasticity rules.

2 Development of the olfactory glomerular map

Olfaction plays a crucial role in animal survival and reproduction in their natural environments, including food foraging, avoidance from predators, and social interactions. Odorants in the environment are detected by odorant receptors (ORs) that are expressed on olfactory sensory neurons (OSNs) within the olfactory epithelium (OE) of the nasal cavity (Buck and Axel, 1991). The binding of an odorant to ORs on cilia surfaces activates the G protein-adenylyl cyclase type III (ACIII) pathway, elevating cAMP levels, which subsequently opens cyclic nucleotide-gated (CNG) channels, resulting in the depolarization of OSNs (Breer et al., 1990; Bradley et al., 2005). In mice, ORs comprise the largest family of G protein-coupled receptors with >1,000 genes (Zhang and Firestein, 2002). Each OSN expresses only one functional OR gene, and axons from OSNs expressing a given OR converge onto a specific pair of glomeruli at stereotyped locations in the olfactory bulb (OB) (Mombaerts et al., 1996) (Figure 1A). Individual ORs can be activated by multiple odorants with differential sensitivities and vice versa, odorants activating multiple OR species (Malnic et al., 1999). Consequently, odor information is topographically represented as a pattern of activated glomeruli, generating the olfactory glomerular map in the OB.

During embryonic stages, an initial glomerular map is formed by a combination of axon guidance molecules whose expressions are defined by spatial cues and ligand-independent OR-derived basal activity (Sakano, 2010; Takeuchi and Sakano, 2014; Francia and Lodovichi, 2021; Dorrego-Rivas and Grubb, 2022). After OSN axons reach their approximate targets in the OB, further refinement of the glomerular map occurs, involving the fasciculation of similar OSN axons and the segregation of dissimilar ones. Like other sensory systems, neural activity is important for the refinement of the glomerular maps. Axonal convergence of OSNs is profoundly affected by genetic silencing of neural activity. In OSN-specific Kir2.1 overexpression mice where neural activity is blocked by a hyperpolarization of the membrane potential, OSN axons successfully project to the appropriate topographic location (Figure 1B) (Yu et al., 2004). However, they do not coalesce into specific glomeruli, which results in abnormally diffused glomeruli. Moreover, a mosaic knockout of the CNG channel, a critical element for generating odor-evoked neural activity, OSN axons expressing the same type of OR are segregated into distinct glomeruli that are innervated by either CNG-positive or CNG-negative axons (Figure 1B) (Serizawa et al., 2006). It has also been reported that hyperpolarization-activated cyclic nucleotide-gated (HCN) channels in olfactory sensory neurons regulate axon extension and glomerular formation (Mobley et al., 2010). In addition to neural activity, OR proteins have been shown to

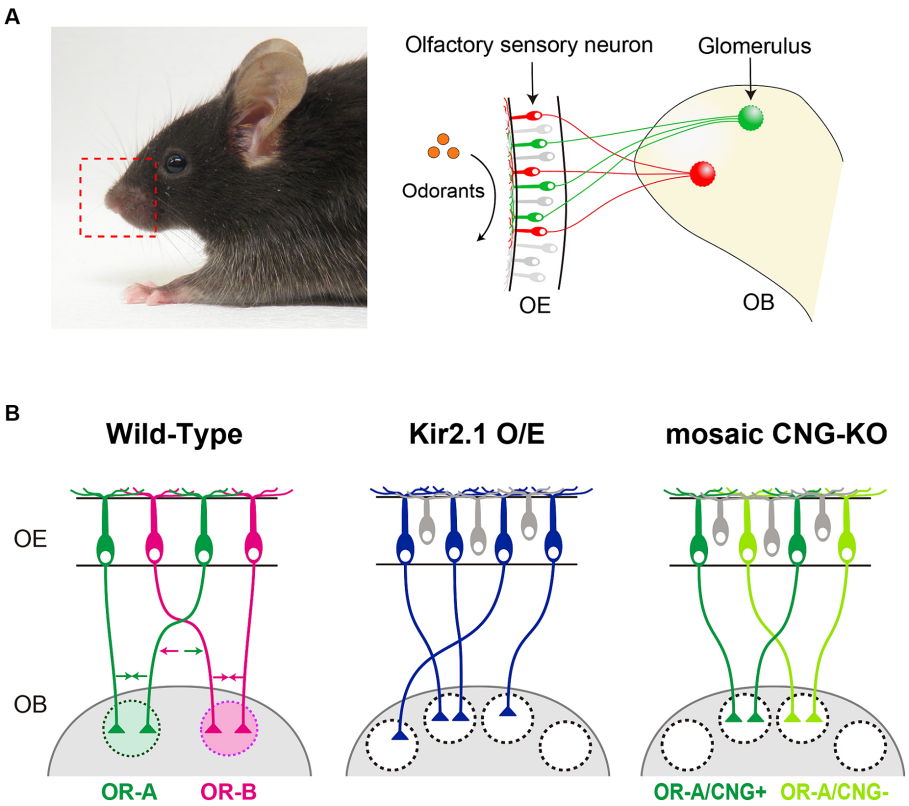

FIGURE 1
(A) In mice, each olfactory sensory neuron (OSN) in the olfactory epithelium (OE) exclusively expresses one type of odorant receptor (OR) gene. Axons from OSNs with the same OR converge at specific sites within the olfactory bulb (OB), forming glomerular structures. **(B)** Schematic diagrams illustrating the axonal projection of OSNs in wild-type mice, Kir2.1 overexpressing mice, and CNG channel mosaic KO mice. OSN axons expressing the same OR fasciculate into the same glomerulus by adhesive/repulsive interactions. Arrows in different colors indicate the adhesive or repulsive force of axon-sorting molecules (e.g., Kirrel2/3 and Eph/ephrinA-s) for convergence of like OSN axons.

regulate the process of glomerular segregation with remarkable precision; just a single amino acid substitution of an OR sequence can generate distinct glomeruli in close proximity (Ishii et al., 2001; Feinstein and Mombaerts, 2004).

3 OR and neural activity-dependent glomerular formation

3.1 Molecular mechanisms of OR-dependent glomerular map refinement

Genetic experiments have demonstrated the roles of OR and neural activity in glomerular formation. The question arises as to whether these two processes independently regulate glomerular segregation or converge on a shared signaling pathway. To decipher the mechanisms underlying glomerular segregation, we began by dissecting the OR-dependent process at the molecular level. Contrary to the hypothesis that OR molecules serve merely as adhesive molecules due to their localization at the termini of OSN axons (Barnea et al., 2004; Strotmann et al., 2004), we explored the variations in gene expression profiles among OSNs expressing different ORs. In transgenic mice engineered to predominantly express a specific OR, we identified genes coding for homophilic adhesion molecules, such as Kirrel2 and Kirrel3 (Serizawa et al., 2006). These molecules are located at OSN axon termini and exhibited glomerular-specific and position-independent expression patterns at the OB. The expression levels of these molecules uniquely correlate with expressed OR types at the single-cell level. The mosaic gain or loss of function of these genes resulted in duplicated glomeruli even though the expressed ORs were the same, indicating that Kirrel2 and Kirrel3 are involved in the fasciculation process of like OSN axons. Notably, upregulated Kirrel2/3 levels in OSNs that naturally express these genes also led to duplicated glomeruli, highlighting that OSN axons discern not only the type but also the expression levels of axon sorting molecules (Serizawa et al., 2006). This quantitative difference in the expression level of these genes contributes to increasing variations in glomerular segregation. Additionally, repulsive molecules like ephrinAs and EphAs are expressed in an OR-specific and complementary manner across different OSN subsets (Serizawa et al., 2006). The interactions between subsets—one high in ephrinA and low in EphA, and vice versa—may be instrumental in segregating non-like OSN axons. Although the expression level of these molecules is correlated with OR types, their expression patterns are not identical (Ihara et al., 2016). Their unique expression profiles lead to the idea that a combinatorial code of adhesive and repulsive molecules imparts OR identity to OSN axons during glomerular formation. Notably, the expression of these molecules is affected by neural activity. For instance, a decrease in neural activity, such as the overexpression of Kir2.1 or CNG-KO, leads to opposite changes in their expressions: Kirrel2 and EphA5 expressions are downregulated by reduced neural activity, whereas Kirrel3 and ephrinA5 expressions are upregulated by reduced neural activity (Serizawa et al., 2006). These regulatory mechanisms of their expressions are consistent with the fact that glomerular segregation is OR-dependent and neural activity-dependent. OR-dependent and neural activity-dependent pathways in glomerular segregation converge in the expression pattern of axon sorting molecule. To date, several studies identified multiple activity-dependent axon-sorting molecules that are expressed in OSNs (St John et al., 2002; Cutforth et al., 2003; Kaneko-Goto et al., 2008; Williams et al., 2011; Ihara et al., 2016; Mountoufaris et al., 2017; Vaddadi et al., 2019; Wang et al., 2021; Martinez et al., 2023). The exact number of molecules implicated in this process is still unclear, but a handful of transmembrane proteins are thought to be involved. It is still not clear how much variation is produced by the combinatorial code model, and whether it produces differences comparable to the number of ORs. Future experiments will be needed to demonstrate how much difference in expression levels of a single axon sorting molecule can cause axonal segregation and whether these axon sorting molecules coordinately function in segregating axons as a combinatorial code.

3.2 Patterns of spontaneous activity link OR types and the molecular codes

As mentioned above, OR molecules control the expression of various axon-sorting molecules, which serve to regulate glomerular formation through their adhesive or repulsive interactions (Sakano, 2010; Takeuchi and Sakano, 2014; Francia and Lodovichi, 2021; Dorrego-Rivas and Grubb, 2022). The expression of these molecules is activity-dependent, consistent with the observation that glomerular formation is likewise activity-dependent. Since the Kir2.1 overexpressing mice exhibited a more severe phenotype compared to the CNG-KO, where mice are anosmia, spontaneous neural activity rather than odor-induced activity is more important for glomerular formation. It is anticipated that spontaneous neural activity serves as a bridge between OR types and the expression of axon-sorting molecules. Given the various expression patterns of axon sorting molecules and the numerous kinds of ORs, it is intriguing how neural activity links OR types to gene expression patterns of axon sorting molecules.

Through calcium imaging of OSNs, we have discerned that OSNs expressing different ORs elicit distinct temporal patterns of spontaneous neural activity (Nakashima et al., 2019). OR swap experiments revealed that the temporal patterns of spontaneous neural activity are regulated by the expressed ORs. Furthermore, optogenetically differentiated activity patterns induced specific expressions of corresponding axon-sorting molecules; for instance, short, high-frequency burst patterns particularly induced the expression of the axon-sorting molecule Kirrel2, whereas longer, lower-frequency bursts promoted the expression of other molecules like protocadherin10, also a participant in glomerular formation (Nakashima et al., 2019). Moreover, optogenetic stimulation resulted in the segregation of ChR2-positive glomeruli from those that were ChR2-negative, despite expressing the same OR. This phenomenon was accompanied by an upregulation of Kirrel2 proteins, indicating that artificially induced activity can overwrite the intrinsic OR identity. A significant breakthrough is the discovery that the unique temporal characteristics of spike patterns, rather than mere neural activity, provide the instructive signals for generating OR-specific expression profiles of axon-sorting molecules. This discovery proposes a novel activity-dependent mechanism, which is different from the prevailing Hebbian model of plasticity that requires correlated activity. In summary, this research unveils an activity-dependent mechanism where spontaneous spiking patterns instructively regulate the expression of axon guidance molecules, thus conferring OR identity

to OSN axons for glomerular convergence (Figure 2A). However, it remains to be done how many variations there are in neural activity patterns of OSNs and how OSNs translate different temporal patterns of calcium dynamics into different gene expression patterns. To understand the intracellular mechanisms that translate neural activity patterns into gene expression patterns in OSNs, further analyses examining the expression and activity of neural activity-dependent transcriptional regulators in cells expressing different ORs are needed.

4 Discussion

It is widely accepted that neural activity is involved in mammalian neural circuit formation (Katz and Shatz, 1996; Spitzer, 2006; Luo and Flanagan, 2007; Sakano, 2010; Ackman and Crair, 2014; Pumo et al., 2022). The importance of neural activity in the formation of sensory maps has been demonstrated through pharmacological interventions or mutant mice that suppress neural activity (Kirkby et al., 2013; Antón-Bolaños et al., 2019; Martini et al., 2021). Recent advances in optogenetics have made it possible to control neural activity with higher temporal resolution and to elucidate the detailed role of neural activity in circuit formation (Adamantidis et al., 2015; Emiliani et al., 2022). For instance, in the visual system, asynchronous optogenetic activation of the left and right retinal ganglion cells resulted in normal eye-specific segregation in the superior colliculus and dorsal lateral geniculate nucleus, whereas synchronous activation disrupted eye-specific segregation (Zhang et al., 2011). Such optogenetic manipulations have significantly substantiated the significance of the Hebbian-based plasticity in sensory map formation (Figure 2B).

However, an activity-dependent process of the olfactory glomerular map seems not to follow the Hebbian rule (Figure 2B). Our findings demonstrated that there is no wave-like activity in the OE, which is observed in the developing retina. OSNs expressing the same OR do not fire simultaneously, but exhibit similar temporal patterns. Optogenetic stimulation with artificial activity patterns affected segregation of OSN axons, indicating the instructive role of temporal activity patterns in the olfactory circuit formation (Nakashima et al., 2019). Moreover, OSN axons fasciculate and form glomerulus-like structures even in mutant mice lacking synaptic partners (Bulfone et al., 1998; St John et al., 2003). Therefore, Hebbian theory, which postulates the simultaneous activation between pre- and post-synaptic neurons, is not suited for explaining the formation of the olfactory glomerular map. Thus, current studies support a model where spontaneous neural activity in OSNs plays a role in intracellular gene expression programs rather than interactions with other cells.

Since the discovery of the retinal wave (Galli and Maffei, 1988; Maffei and Galli-Resta, 1990; Meister et al., 1991), most models for activity-dependent neural map formation have been based on the assumption of synchronous activity (Figure 2B). Numerous experimental studies have provided evidence supporting the importance of synchronous activity in circuit development beyond sensory systems, such as the hippocampus and the neocortex (Ben-Ari et al., 1989; Garaschuk et al., 1998; Blankenship and Feller, 2010; Pan and Monje, 2020; Martini et al., 2021). While synchronous activity has been a dominant focus in studies of neural circuit formation, the findings obtained by olfactory circuit formation studies over the past few decades provide important insights that are not specific to the olfactory system but can be extended to other brain regions. Notably,

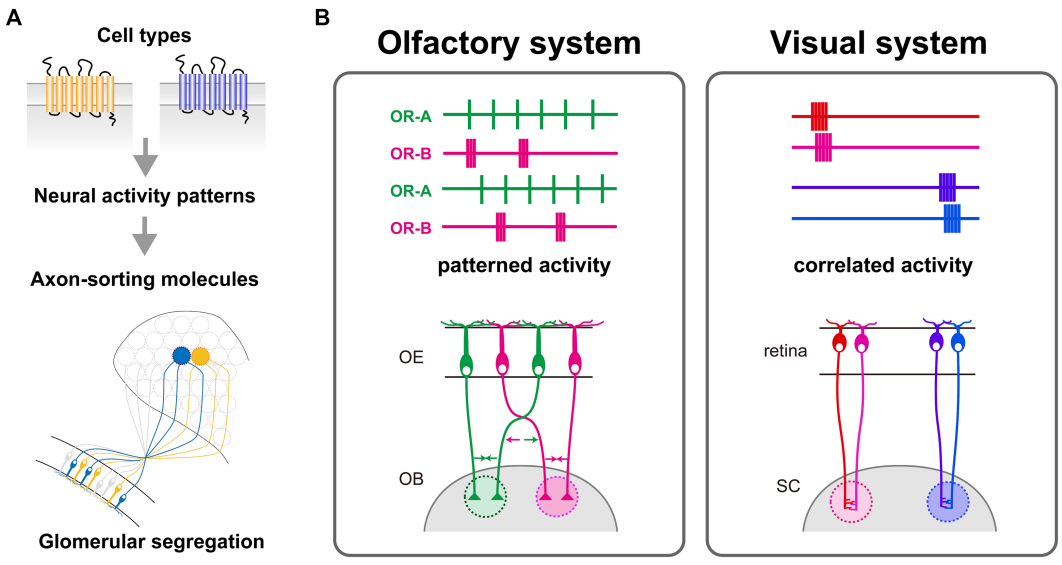

FIGURE 2
(A) OR-specific molecular codes, generated by differential expression of activity-dependent axon-sorting molecules at axon termini, regulate the glomerular segregation. These unique molecular codes arise from cell type-specific spontaneous activity patterns of OSNs, which are defined by the differences in expressed ORs. The conversion of OR-specific activity patterns into distinct combinations of axon-sorting molecules is crucial for the proper formation of the glomerular map. **(B)** Left: A model of activity-dependent refinement of the olfactory glomerular map. Temporal activity patterns reflect the identity of OSNs rather than the anatomical location; each color represents OSNs expressing the same OR, which converge into a common glomerulus. Right: A model of activity-dependent refinement of the retinotopic map in the visual system. Nearby retinal ganglion cells (RGCs) in the retina exhibit synchronized activity, and this correlated activity is crucial for establishing the spatially-organized topographic map in the superior colliculus (SC).

analysis of cell type-specific spontaneous activity has revealed that precise temporal patterns, rather than synchrony *per se*, better reflect neuronal identity. Recent studies using single-cell RNA sequencing have uncovered distinct cell types at an unprecedented resolution (Saunders et al., 2018; Zeisel et al., 2018; Piwecka et al., 2023; Xing et al., 2023; Zhang et al., 2023). A key challenge moving forward will be to investigate whether cell type-specific temporal activity patterns are also present in other brain regions. Neural activity influences a multitude of developmental and plasticity processes, such as cell type specification, dendritic branching, synaptic maturation, and the underpinnings of learning and memory, through a complex program of gene regulation (Spitzer, 2006; Greer and Greenberg, 2008; West and Greenberg, 2011; Lee and Fields, 2021). However, their regulatory mechanisms are not fully understood. The breakthrough discovery in the olfactory system implicates the need to dissect the intricate spatiotemporal dynamics of neural activity to understand brain complexity at the molecular level.

Author contributions

AN: Writing – original draft, Writing – review & editing. HT: Writing – original draft, Writing – review & editing.

Funding

The author(s) declare financial support was received for the research, authorship, and/or publication of this article. This work was supported by JSPS KAKENHI Grant Number 20H00482, 21H05141, and 20H03354, JST FOREST Program Grant Number JPMJFR214B, The Takeda Science Foundation, G-7 Scholarship Foundation, Astellas Foundation for Research on Metabolic Disorders, Daiichi Sankyo Foundation of Life Science, The Naito Foundation, Koyanagi Foundation and the Cell Science Research Foundation.

Acknowledgments

We thank N. Ihara for his help in preparing the manuscript.

Conflict of interest

The authors declare that the research was conducted in the absence of any commercial or financial relationships that could be construed as a potential conflict of interest.

Publisher's note

References

Ackman, J. B., and Crair, M. C. (2014). Role of emergent neural activity in visual map development. *Curr. Opin. Neurobiol.* 24, 166–175. doi: 10.1016/j.conb.2013.11.011

Adamantidis, A., Arber, S., Bains, J. S., Bamberg, E., Bonci, A., Buzsáki, G., et al. (2015). Optogenetics: 10 years after ChR2 in neurons--views from the community. *Nat. Neurosci.* 18, 1202–1212. doi: 10.1038/nn.4106

Antón-Bolaños, N., Sempere-Ferràndez, A., Guillamón-Vivancos, T., Martini, F. J., Pérez-Saiz, L., Gezelius, H., et al. (2019). Prenatal activity from thalamic neurons governs the emergence of functional cortical maps in mice. *Science* 364, 987–990. doi: 10.1126/science.aav7617

Barnea, G., O'Donnell, S., Mancia, F., Sun, X., Nemes, A., Mendelsohn, M., et al. (2004). Odorant receptors on axon termini in the brain. *Science* 304:1468. doi: 10.1126/science.1096146

Ben-Ari, Y., Cherubini, E., Corradetti, R., and Gaiarsa, J. L. (1989). Giant synaptic potentials in immature rat CA3 hippocampal neurones. *J. Physiol.* 416, 303–325. doi: 10.1113/jphysiol.1989.sp017762

Blankenship, A. G., and Feller, M. B. (2010). Mechanisms underlying spontaneous patterned activity in developing neural circuits. *Nat. Rev. Neurosci.* 11, 18–29. doi: 10.1038/nrn2759

Bradley, J., Reisert, J., and Frings, S. (2005). Regulation of cyclic nucleotide-gated channels. *Curr. Opin. Neurobiol.* 15, 343–349. doi: 10.1016/j.conb.2005.05.014

Breer, H., Boekhoff, I., and Tareilus, E. (1990). Rapid kinetics of second messenger formation in olfactory transduction. *Nature* 345, 65–68. doi: 10.1038/345065a0

Buck, L., and Axel, R. (1991). A novel multigene family may encode odorant receptors: a molecular basis for odor recognition. *Cell* 65, 175–187. doi: 10.1016/0092-8674(91)90418-X

Bulfone, A., Wang, F., Hevner, R., Anderson, S., Cutforth, T., Chen, S., et al. (1998). An olfactory sensory map develops in the absence of normal projection neurons or GABAergic interneurons. *Neuron* 21, 1273–1282. doi: 10.1016/S0896-6273(00)80647-9

Cutforth, T., Moring, L., Mendelsohn, M., Nemes, A., Shah, N. M., Kim, M. M., et al. (2003). Axonal ephrin-as and odorant receptors: coordinate determination of the olfactory sensory map. *Cell* 114, 311–322. doi: 10.1016/S0092-8674(03)00568-3

Dorrego-Rivas, A., and Grubb, M. S. (2022). Developing and maintaining a nose-to-brain map of odorant identity. *Open Biol.* 12:220053. doi: 10.1098/rsob.220053

Emiliani, V., Entcheva, E., Hedrich, R., Hegemann, P., Konrad, K. R., Lüscher, C., et al. (2022). Optogenetics for light control of biological systems. *Nat. Rev. Methods Primers* 2:55. doi: 10.1038/s43586-022-00136-4

Feinstein, P., and Mombaerts, P. (2004). A contextual model for axonal sorting into glomeruli in the mouse olfactory system. *Cell* 117, 817–831. doi: 10.1016/j.cell.2004.05.011

Francia, S., and Lodovichi, C. (2021). The role of the odorant receptors in the formation of the sensory map. *BMC Biol.* 19:174. doi: 10.1186/s12915-021-01116-y

Galli, L., and Maffei, L. (1988). Spontaneous impulse activity of rat retinal ganglion cells in prenatal life. *Science* 242, 90–91. doi: 10.1126/science.3175637

Garaschuk, O., Hanse, E., and Konnerth, A. (1998). Developmental profile and synaptic origin of early network oscillations in the CA1 region of rat neonatal hippocampus. *J. Physiol.* 507, 219–236. doi: 10.1111/j.1469-7793.1998.219bu.x

Greer, P. L., and Greenberg, M. E. (2008). From synapse to nucleus: calcium-dependent gene transcription in the control of synapse development and function. *Neuron* 59, 846–860. doi: 10.1016/j.neuron.2008.09.002

Ihara, N., Nakashima, A., Hoshina, N., Ikegaya, Y., and Takeuchi, H. (2016). Differential expression of axon-sorting molecules in mouse olfactory sensory neurons. *Eur. J. Neurosci.* 44, 1998–2003. doi: 10.1111/ejn.13282

Ishii, T., Serizawa, S., Kohda, A., Nakatani, H., Shiroishi, T., Okumura, K., et al. (2001). Monoallelic expression of the odourant receptor gene and axonal projection of olfactory sensory neurones. *Genes Cells* 6, 71–78. doi: 10.1046/j.1365-2443.2001.00398.x

Kaneko-Goto, T., Yoshihara, S., Miyazaki, H., and Yoshihara, Y. (2008). BIG-2 mediates olfactory axon convergence to target glomeruli. *Neuron* 57, 834–846. doi: 10.1016/j.neuron.2008.01.023

Katz, L. C., and Shatz, C. J. (1996). Synaptic activity and the construction of cortical circuits. *Science* 274, 1133–1138. doi: 10.1126/science.274.5290.1133

Kirkby, L. A., Sack, G. S., Firl, A., and Feller, M. B. (2013). A role for correlated spontaneous activity in the assembly of neural circuits. *Neuron* 80, 1129–1144. doi: 10.1016/j.neuron.2013.10.030

Lee, P. R., and Fields, R. D. (2021). Activity-dependent gene expression in neurons. *Neuroscientist* 27, 355–366. doi: 10.1177/1073858420943515

Luo, L., and Flanagan, J. G. (2007). Development of continuous and discrete neural maps. *Neuron* 56, 284–300. doi: 10.1016/j.neuron.2007.10.014

Maffei, L., and Galli-Resta, L. (1990). Correlation in the discharges of neighboring rat retinal ganglion cells during prenatal life. *Proc. Natl. Acad. Sci. USA* 87, 2861–2864. doi: 10.1073/pnas.87.7.2861

Malnic, B., Hirono, J., Sato, T., and Buck, L. B. (1999). Combinatorial receptor codes for odors. *Cell* 96, 713–723. doi: 10.1016/S0092-8674(00)80581-4

Martinez, A. P., Chung, A. C., Huang, S., Bisogni, A. J., Lin, Y., Cao, Y., et al. (2023). Pcdh 19 mediates olfactory sensory neuron coalescence during postnatal stages and regeneration. *iScience* 26:108220. doi: 10.1016/j.isci.2023.108220

Martini, F. J., Guillamón-Vivancos, T., Moreno-Juan, V., Valdeolmillos, M., and López-Bendito, G. (2021). Spontaneous activity in developing thalamic and cortical sensory networks. *Neuron* 109, 2519–2534. doi: 10.1016/j.neuron.2021.06.026

Meister, M., Wong, R. O., Baylor, D. A., and Shatz, C. J. (1991). Synchronous bursts of action potentials in ganglion cells of the developing mammalian retina. *Science* 252, 939–943. doi: 10.1126/science.2035024

Mizuno, H., Ikezoe, K., Nakazawa, S., Sato, T., Kitamura, K., and Iwasato, T. (2018). Patchwork-type spontaneous activity in neonatal barrel cortex layer 4 transmitted via Thalamocortical projections. *Cell Rep.* 22, 123–135. doi: 10.1016/j.celrep.2017.12.012

Mobley, A. S., Miller, A. M., Araneda, R. C., Maurer, L. R., Müller, F., and Greer, C. A. (2010). Hyperpolarization-activated cyclic nucleotide-gated channels in olfactory sensory neurons regulate axon extension and glomerular formation. *J. Neurosci.* 30, 16498–16508. doi: 10.1523/JNEUROSCI.4225-10.2010

Mombaerts, P., Wang, F., Dulac, C., Chao, S. K., Nemes, A., Mendelsohn, M., et al. (1996). Visualizing an olfactory sensory map. *Cell* 87, 675–686. doi: 10.1016/S0092-8674(00)81387-2

Mori, K., and Sakano, H. (2011). How is the olfactory map formed and interpreted in the mammalian brain? *Annu. Rev. Neurosci.* 34, 467–499. doi: 10.1146/annurev-neuro-112210-112917

Mountoufaris, G., Chen, W. V., Hirabayashi, Y., O'Keeffe, S., Chevee, M., Nwakeze, C. L., et al. (2017). Multicluster Pcdh diversity is required for mouse olfactory neural circuit assembly. *Science* 356, 411–414. doi: 10.1126/science.aai8801

Nakashima, A., Ihara, N., Ikegaya, Y., and Takeuchi, H. (2021). Cell type-specific patterned neural activity instructs neural map formation in the mouse olfactory system. *Neurosci. Res.* 170, 1–5. doi: 10.1016/j.neures.2020.06.007

Nakashima, A., Ihara, N., Shigeta, M., Kiyonari, H., Ikegaya, Y., and Takeuchi, H. (2019). Structured spike series specify gene expression patterns for olfactory circuit formation. *Science* 365:eaaw5030. doi: 10.1126/science.aaw5030

Pan, Y., and Monje, M. (2020). Activity shapes neural circuit form and function: a historical perspective. *J. Neurosci.* 40, 944–954. doi: 10.1523/JNEUROSCI.0740-19.2019

Petersen, C. C. (2007). The functional organization of the barrel cortex. *Neuron* 56, 339–355. doi: 10.1016/j.neuron.2007.09.017

Piwecka, M., Rajewsky, N., and Rybak-Wolf, A. (2023). Single-cell and spatial transcriptomics: deciphering brain complexity in health and disease. *Nat. Rev. Neurol.* 19, 346–362. doi: 10.1038/s41582-023-00809-y

Pumo, G. M., Kitazawa, T., and Rijli, F. M. (2022). Epigenetic and transcriptional regulation of spontaneous and sensory activity dependent programs during neuronal circuit development. *Front. Neural Circuits* 16:911023. doi: 10.3389/fncir.2022.911023

Sakano, H. (2010). Neural map formation in the mouse olfactory system. *Neuron* 67, 530–542. doi: 10.1016/j.neuron.2010.07.003

Saunders, A., Macosko, E. Z., Wysoker, A., Goldman, M., Krienen, F. M., de Rivera, H., et al. (2018). Molecular diversity and specializations among the cells of the adult mouse brain. *Cell* 174, 1015–1030.e16. doi: 10.1016/j.cell.2018.07.028

Serizawa, S., Miyamichi, K., Takeuchi, H., Yamagishi, Y., Suzuki, M., and Sakano, H. (2006). A neuronal identity code for the odorant receptor-specific and activity-dependent axon sorting. *Cell* 127, 1057–1069. doi: 10.1016/j.cell.2006.10.031

Spitzer, N. C. (2006). Electrical activity in early neuronal development. *Nature* 444, 707–712. doi: 10.1038/nature05300

St John, J. A., Clarris, H. J., McKeown, S., Royal, S., and Key, B. (2003). Sorting and convergence of primary olfactory axons are independent of the olfactory bulb. *J. Comp. Neurol.* 464, 131–140. doi: 10.1002/cne.10777

St John, J. A., Pasquale, E. B., and Key, B. (2002). Eph a receptors and ephrin-a ligands exhibit highly regulated spatial and temporal expression patterns in the developing olfactory system. *Brain Res. Dev. Brain Res.* 138, 1–14. doi: 10.1016/S0165-3806(02)00454-6

Strotmann, J., Levai, O., Fleischer, J., Schwarzenbacher, K., and Breer, H. (2004). Olfactory receptor proteins in axonal processes of chemosensory neurons. *J. Neurosci.* 24, 7754–7761. doi: 10.1523/JNEUROSCI.2588-04.2004

Takeuchi, H., and Sakano, H. (2014). Neural map formation in the mouse olfactory system. *Cell. Mol. Life Sci.* 71, 3049–3057. doi: 10.1007/s00018-014-1597-0

Vaddadi, N., Iversen, K., Raja, R., Phen, A., Brignall, A., Dumontier, E., et al. (2019). Kirrel 2 is differentially required in populations of olfactory sensory neurons for the targeting of axons in the olfactory bulb. *Development* 146:dev173310. doi: 10.1242/dev.173310

Wang, J., Vaddadi, N., Pak, J. S., Park, Y., Quilez, S., Roman, C. A., et al. (2021). Molecular and structural basis of olfactory sensory neuron axon coalescence by Kirrel receptors. *Cell Rep.* 37:109940. doi: 10.1016/j.celrep.2021.109940

West, A. E., and Greenberg, M. E. (2011). Neuronal activity-regulated gene transcription in synapse development and cognitive function. *Cold Spring Harb. Perspect. Biol.* 3:a005744. doi: 10.1101/cshperspect.a005744

Williams, E. O., Sickles, H. M., Dooley, A. L., Palumbos, S., Bisogni, A. J., and Lin, D. M. (2011). Delta Protocadherin 10 is regulated by activity in the mouse Main olfactory system. *Front. Neural Circuits* 5:9. doi: 10.3389/fncir.2011.00009

Wong, R. O., Meister, M., and Shatz, C. J. (1993). Transient period of correlated bursting activity during development of the mammalian retina. *Neuron* 11, 923–938. doi: 10.1016/0896-6273(93)90122-8

Xing, Y., Zan, C., and Liu, L. (2023). Recent advances in understanding neuronal diversity and neural circuit complexity across different brain regions using single-cell sequencing. *Front. Neural Circuits* 17:1007755. doi: 10.3389/fncir.2023.1007755

Yu, C. R., Power, J., Barnea, G., O'Donnell, S., Brown, H. E., Osborne, J., et al. (2004). Spontaneous neural activity is required for the establishment and maintenance of the olfactory sensory map. *Neuron* 42, 553–566. doi: 10.1016/S0896-6273(04)00224-7

Zeisel, A., Hochgerner, H., Lönnerberg, P., Johnsson, A., Memic, F., van der Zwan, J., et al. (2018). Molecular architecture of the mouse nervous system. *Cell* 174, 999–1014.e22. doi: 10.1016/j.cell.2018.06.021

Zhang, J., Ackman, J. B., Xu, H. P., and Crair, M. C. (2011). Visual map development depends on the temporal pattern of binocular activity in mice. *Nat. Neurosci.* 15, 298–307. doi: 10.1038/nn.3007

Zhang, X., and Firestein, S. (2002). The olfactory receptor gene superfamily of the mouse. *Nat. Neurosci.* 5, 124–133. doi: 10.1038/nn800

Zhang, M., Pan, X., Jung, W., Halpern, A. R., Eichhorn, S. W., Lei, Z., et al. (2023). Molecularly defined and spatially resolved cell atlas of the whole mouse brain. *Nature* 624, 343–354. doi: 10.1038/s41586-023-06808-9

frontiers | Frontiers in Neural Circuits

TYPE Mini Review
PUBLISHED 30 May 2024
DOI 10.3389/fncir.2024.1426689

OPEN ACCESS

EDITED BY
Kensaku Mori,
RIKEN, Japan

REVIEWED BY
Haruki Takeuchi,
The University of Tokyo, Japan

*CORRESPONDENCE
Shin Nagayama
shin.nagayama@uth.tmc.edu

RECEIVED 01 May 2024
ACCEPTED 20 May 2024
PUBLISHED 30 May 2024

CITATION
Nagayama S, Hasegawa-Ishii S and Kikuta S (2024) Anesthetized animal experiments for neuroscience research. *Front. Neural Circuits* 18:1426689. doi: 10.3389/fncir.2024.1426689

Anesthetized animal experiments for neuroscience research

Shin Nagayama[1]*, Sanae Hasegawa-Ishii[2] and Shu Kikuta[3]

[1]Department of Neurobiology and Anatomy, McGovern Medical School at the University of Texas Health Science Center at Houston, Houston, TX, United States, [2]Pathology Research Team, Faculty of Health Sciences, Kyorin University, Mitaka, Japan, [3]Department of Otorhinolaryngology, Medical School of Nihon University, Tokyo, Japan

Brain research has progressed with anesthetized animal experiments for a long time. Recent progress in research techniques allows us to measure neuronal activity in awake animals combined with behavioral tasks. The trends became more prominent in the last decade. This new research style triggers the paradigm shift in the research of brain science, and new insights into brain function have been revealed. It is reasonable to consider that awake animal experiments are more ideal for understanding naturalistic brain function than anesthetized ones. However, the anesthetized animal experiment still has advantages in some experiments. To take advantage of the anesthetized animal experiments, it is important to understand the mechanism of anesthesia and carefully handle the obtained data. In this minireview, we will shortly summarize the molecular mechanism of anesthesia in animal experiments, a recent understanding of the neuronal activities in a sensory system in the anesthetized animal brain, and consider the advantages and disadvantages of the anesthetized and awake animal experiments. This discussion will help us to use both research conditions in the proper manner.

KEYWORDS

anesthesia, brain, experimental animal, anesthetic-activated cells, sensory representation

Introduction

Anesthesia could be reversibly induced by the anesthetic agents and makes the brain and body condition into the following specific behavioral and physiological traits (Brown et al., 2010). 1. Analgesia: Animals do not perceive pain. 2. Unconsciousness: Animals are not aware of what's happening. 3. Amnesia: Animals do not form memories. 4. Akinesia: Animals cannot move. Anesthesia decreases the painful stress and is helpful for the operation of the surgery on humans and animals. In addition, anesthesia helps monitor body and brain activity to understand the function at molecular, cellular, and circuit/tissue levels *in vivo*.

Brain science took advantage of anesthesia and revealed brain functions in the past centuries. In the recent decade, multiple experimental tools for monitoring the body and brain conditions have succeeded in becoming more compact and attachable to the body, directly allowing us to decrease animal stress and monitor the brain or body activity while behaving animals in awake conditions. In addition, the experimental procedures also improved to decrease the animal stress. Then, it decreased the hurdles to understanding the animal in awake conditions. The current trend is to study brain function in awake animal conditions. However, anesthesia is an important step for animal surgery, which is also necessary for many awake animal experiments, and it still has advantages in conducting experiments to understand brain function. In this review, we will shortly summarize the molecular mechanisms of popular

anesthesia and clarify the difference between awake and anesthetized animal experiments to have the appropriate experimental conditions for the anesthetized and awake animal experiments.

How do anesthetic agents work?

Anesthetic agents affect the animal brains and modify regular neuronal activity (Franks and Lieb, 1994). Although we frequently use anesthesia for animal experiments, we still do not understand the molecular, cellular, and circuitry mechanisms of how anesthetic agents induce Analgesic, Unconsciousness, Amnesic, and Akinetic conditions (Århem et al., 2003). Here, we quickly summarize the current knowledge of the molecular mechanism of the following major anesthesia (Pentobarbital, Ketamine, Urethane, and Isoflurane), in addition to the major sedatives (Xylazine, Chlorprothixene, and Dexmedetomidine) (Table 1).

Pentobarbital: Pentobarbital have been one of the major anesthetic agents. It binds to the gamma-aminobutyric acid (GABA) type A ($GABA_A$) receptors (Franks, 2008; Johnson and Sadiq, 2022). It induces chloride channels to open longer, potentiate GABA effects, and induce longer hyperpolarization. The advantage of Pentobarbital anesthesia would be its reliability to induce rapid unconsciousness. It impacts the sensory systems and the medullary and depresses cardiovascular and respiratory activities (Field et al., 1993; Dutton et al., 2019). It also has the function of sedation.

Ketamine: Ketamine targets *N*-methyl-d-aspartate (NMDA) receptors to reduce the excitatory action of glutamate (Stoicea et al., 2016). Its prominent features as anesthesia are increased heart rate, blood pressure, and cardiac output, mediated principally through the sympathetic nervous system (Kurdi et al., 2014). It has small effects on the central respiratory drive. It increases salivation and muscle tone. Ketamine also has the function of an antidepressant.

Urethane: Urethane is one of the most popular anesthetics used for animal experiments for a long time. Although it is a carcinogen and is not proper for survival surgery, it is still well used because of its minimal effects on cardiovascular and respiratory systems, and it could maintain spinal reflexes and spontaneous brain state alterations similar to natural sleep (Maggi et al., 1986; Pagliardini et al., 2013). In addition, it can produce a long-lasting steady level of anesthesia during surgery and experiments. It is assumed that animals anesthetized with urethane represent similar physiologic and pharmacologic behaviors to those observed in unanesthetized animals. However, little is known about its mechanism. Recent research revealed the urethane effect of multiple ion channels (Hara and Harris, 2002). Urethane potentiates the functions of nicotinic acetylcholine, GABA, and glycine receptors, and it inhibits NMDA and α-amino-3-hydroxy-5-methyl-4-isoxazole propionic acid (AMPA) receptors in a concentration-dependent manner. Because urethane had modest effects on all channels tested in the experiment, urethane would not have a single predominant target molecule for anesthesia.

Isoflurane: Isoflurane is volatile anesthesia. Therefore, one of the prominent features of isoflurane anesthesia is the easier control and faster anesthesia induction and recovery. The molecular mechanism of isoflurane anesthesia has not been well known (Jones et al., 1992; Jenkins et al., 1999; Krasowski and Harrison, 2000). Isoflurane acts as an allosteric modulator of the $GABA_A$ receptor, enhances the activity of glycine receptors, and decreases motor function (Grasshoff and Antkowiak, 2006). Isoflurane inhibits the activity of NMDA receptors at the same site as glycine (Dickinson et al., 2007). Isoflurane inhibits the conduction of the potassium channel (Buljubasic et al., 1992). In addition, Isoflurane also works as a burst suppression anesthesia, and increases the extracellular potassium concentration and decreases extracellular sodium concentration by the Na^+/K^+-ATPase impairment (Reiffurth et al., 2023).

These anesthetic agents are often used with Sedatives. The following three sedatives are popular in animal experiments.

Xylazine: Xylazine is often used together with Ketamine as a sedative, and the mixture of them is referred to as Ketamine/Xylazine (K/X). Xylazine also has effects on anesthesia, muscle relaxation, and analgesia. Xylazine is known as an α_2-adrenergic receptor agonist (Ruiz-Colón et al., 2014). It also has side effects of hypotension and respiratory depression.

Chlorprothixene: Chlorprothixene is often used together with Urethane or Ketamine/Xylazine. It is an antipsychotic drug (Højlund et al., 2022). Chlorprothixene has strong impacts by blocking the Serotonin ($5\text{-}HT_2$), Dopamine receptors (D_1, D_2, D_3), Histamine (H_1), Muscarinic, and α_1-adrenergic receptors.

Dexmedetomidine: Dexmedetomidine induces sedation by agonistically binding to α_2-adrenergic receptors and inhibits the norepinephrine release from locus coeruleus in the brain stem (Gertler et al., 2001; Franks, 2008). Unlike opioids and other sedatives such as propofol, dexmedetomidine can achieve its effects without causing respiratory depression.

This summary shows us that different anesthetic agents and sedatives target different ion channels or transmitter receptors. However, they induce a similar trait of anesthesia.

Neuronal mechanism of sleep and anesthesia

General anesthesia and natural sleep induce similar behaviors. Therefore, their similarities have been discussed for a long time (Shafer, 1995; Date et al., 2020). The two conditions have both similar and different functional features. Recent research revealed that sleep is a more active process than previously considered. Many of the reports especially focus on the hypothalamus area (Szymusiak et al., 2007; Sternson, 2013; Wu et al., 2014; Scott et al., 2015; Tan et al., 2016; Allen et al., 2017). It is reported that some given groups of neurons in the hypothalamus show activity under sleep or anesthesia conditions (Moore et al., 2012; Zhang et al., 2015; Gelegen et al., 2018). These neurons are called anesthetic-activated cells. More recent research revealed that anesthetic-activated cells contribute to inducing and maintaining the anesthetized and sleep conditions, in addition to the awake condition.

Jiang-Xie's group found the anesthesia-activated cells in the supraoptic nucleus in the hypothalamus. An interesting finding was that if they activate the neuron's chemogenetic or optogenetic method, the animal stops moving and falls into a slow wave sleep condition. If the neurons are conditionally ablated or inhibited, the mice continuously move around and cannot fall asleep. In addition, if they silence the activity of the neurons, the mice work up from anesthesia easily (Jiang-Xie et al., 2019).

Opposite functional types of neurons, whose activity is associated with induction and maintenance of awake condition, were also found.

TABLE 1 Anesthetic agents and sedatives.

Name	Target receptors/channels	Effects and features	References
Pentobarbital	$GABA_A$ receptor agonist	Impacts on the medullary system Depresses cardiovascular and respiratory activities	Field et al. (1993), Franks (2008), Dutton et al. (2019), Johnson and Sadiq (2022)
Ketamine	NMDA receptor antagonist	Increase heart rate, blood pressure, and cardiac output	Kurdi et al. (2014), Stoicea et al. (2016)
Urethane	Potentiate nicotinic acetylcholine, GABA, glycine receptors Inhibit NMDA, AMPA receptors	Minimal effects on cardiovascular and respiratory systems, and maintenance of spinal reflexes Spontaneous brain state alterations similar to natural sleep Carcinogen	Maggi et al. (1986), Hara and Harris (2002), Pagliardini et al. (2013)
Isoflurane	Allosteric modulator of $GABA_A$ Enhance the activity of glycine receptor, NMDA receptor agonist Inhibit the potassium channel conductance	Volatile anesthesia Increases and decreases the extracellular potassium and sodium concentration by the Na^+/K^+-ATPase impairment, respectively	Grasshoff and Antkowiak (2006), Dickinson et al. (2007), Reiffurth et al. (2023)
Xylazine	α_2-adrenergic receptor agonist	Often used together with Ketamine Anesthesia, muscle relaxation, analgesia, hypotension, respiratory depression	Ruiz-Colón et al. (2014)
Chlorprothixene	Serotonin (5-HT_2), Dopamine (D_1, D_2, D_3), Histamine (H_1), Muscarinic, and α_1-adrenergic receptors antagonist	Often used together with Urethane or Ketamine/Xylazine	Højlund et al. (2022)
Dexmedetomidine	α_2-adrenergic receptor agonist	Inhibits the norepinephrine release from locus coeruleus Low respiratory depression	Gertler et al. (2001), Franks (2008)

Detailed features of the anesthetic agents were summarized in previous works (Sakai et al., 2005; Sorrenti et al., 2021).

Reitz's group showed that chemogenetic activation of tachykinin 1 expressing neurons in the preoptic area obliterates both non-rapid eye movement (NREM) and rapid eye movement (REM) sleep. Moreover, chemogenetic activation of these neurons stabilizes the waking state against both Isoflurane- and Sevoflurane-induced unconsciousness (Reitz et al., 2021).

These researches shed light on that the specific neurons and neuronal circuits in the hypothalamus would contribute to induce and maintain the anesthetized and sleep conditions, in addition to awake conditions. The anesthetic agents described in the previous section may have a strong effect on these specific neurons in the hypothalamus. However, the anesthetic agents also impact other neurons, which may not be directly associated with the induction and maintenance of sleep, anesthetized, and awake animal conditions. Further study of the molecular cellular and circuitry contributions to the induction and maintenance of sleep, anesthetized, as well as awake animal conditions, are demanded. The knowledge will help to interpret the functional research data collected in anesthetized animal conditions correctly and help to improve the method of anesthesia beyond the current anesthetic agents and procedures.

Sensory response in anesthetized and awake condition

Anesthesia induces Analgesia, Unconsciousness, Amnesia, Akinesia in animals. Therefore, the downstream (or outputs) of the neuronal circuits associated with these behavioral and psychological traits would be strongly disturbed during anesthesia. Indeed, a large number of the research reported the differences in activity of neurons, neural population, and functional connectivity of brain areas between anesthetized and awake conditions (Nallasamy and Tsao, 2011; Sellers et al., 2015; Hu et al., 2024). However, the upstream and peripheral of each circuit, such as sensory representation in the primary or secondary sensory areas, may be less disturbed by anesthesia.

In the primary visual cortex, anesthetics reduce spontaneous neuronal spike activity but promote synchronized activity (Greenberg et al., 2008; Aasebø et al., 2017; Lee et al., 2021). The change is larger in Isoflurane compared to the Ketamine/Xylazine anesthesia (Aasebø et al., 2017). Interestingly, the narrow spiking neurons (presumably inhibitory neurons) have a larger decrease in spontaneous spike activity compared to the broad spiking neurons (presumably excitatory neurons) in anesthesia (Aasebø et al., 2017). To the visual stimulation, anesthetized animals showed prolonged neuronal activity by the stimulation in a wide area in visual space. In contrast, neuronal responses to visual stimulation are more spatially selective and much briefer during wakefulness. The difference is owed to the strong inhibition of extremely broad spatial selectivity during wakefulness (Haider et al., 2012).

In the olfactory bulb, wakefulness greatly enhances the activity of inhibitory interneurons of granule cells. As a result, the odor responses of the principal neurons of mitral cells are not prominent compared to those under anesthetized animals. However, awake animals show more sparse and temporally dynamic responses (Kato et al., 2012; Blauvelt et al., 2013; Wachowiak et al., 2013). In addition, repetitive odor experiences in awake animal condition weaken the odor

response of mitral cells gradually for a long time. This mitral cell plasticity is odor-specific, recovers gradually over months, and can be repeated with different odors. Furthermore, the expression of this experience-dependent plasticity is prevented by anesthesia (Kato et al., 2012).

In the barrel cortex, electrophysiological responses evoked by whisker deflection are reduced in amplitude under anesthetized condition (Simons et al., 1992; Devonshire et al., 2010). However, delayed activity, probably due to the inputs from the neighboring whisker stimulation, is more prominent and prolonged. The reduction in response amplitude was considered by the global down-scaling of the population response. Interestingly, the variation of the spike frequency is larger during wakefulness. The difference is more prominent in layer 5A, especially during whisking episodes (De Kock and Sakmann, 2009).

These researches indicate that sensory representation in the primary sensory areas could be observed in both anesthetized and awake animals. However, the amplitude, tuning specificity of sensory inputs, and temporal pattern of neuronal activity are not completely the same in anesthetized and awake animal conditions. Importantly, the anesthesia delivers different impacts on the different layers, neuronal types, and sensory systems. The majority of the reasons for the difference have not yet been clearly determined. However, it probably owes to the combination change of the direct or indirect pharmacological impact of anesthetic agents on the recording neurons and the top-down signals to each recording neuron between the anesthetized and awake animal conditions.

Advantages and disadvantages of anesthetized animal research

Advantages: Anesthetized condition is a pharmacologically induced artificial condition, which is useful for operating surgery and physiological experiments. The akinetic effect minimizes animal movement and helps us obtain high-quality experimental data such as *in vivo* electrophysiology or functional optical imaging experiments. In addition, the analgesic effect decreases the pain sensation and helps to decrease the animal stress of pain or uncomfortable procedures of surgery or experiments. Therefore, the biggest advantage of the anesthetized animal experiment would be that it allows us to conduct functional experiments easily and reliably.

Disadvantage 1: One of the problems of the anesthetized animal experiment is the broad and unidentified impacts of anesthetic agents on the brains. The normal neuronal activity and response to the neuronal transmitters are disturbed by the anesthetic agents. Probably, some synaptic transmission and neuronal activity would be enhanced, and others would be inhibited to some degree. In other words, the brain activity is modified in an anesthetic agent specific manner in anesthetized animals. These impacts are more remarkable when we monitor the neuronal activity in higher brain centers, where the sensory inputs reach after many synaptic transmissions. Therefore, functional research on the higher brain center may not be adequate under anesthesia in general. However, some of the peripheral sensory brain areas, which reached the sensory inputs after the small number of synaptic transmissions, would be less impacted by the anesthesia, although the centrifugal or top-down signal would be abnormal or less active in this case.

Disadvantage 2: Sensory information is actively acquired in awake-behaving rodents, such as active movement of whiskers and an increase in the sniffing cycle in olfaction (Petersen, 2007; Wachowiak, 2011). Anesthetized animals do not have such behavioral outputs. Therefore, the research using anesthetized animals allows us only to study the passive sensory processing without animal behavior attempting to intensely collect and recognize the sensory inputs. It would make neuronal response simpler and easier to interpret. However, we need to carefully interpret the data concerning the lack of active sensing top-down signals, which contribute to sensory recognition in the process of perception.

Advantages and disadvantages of awake animal research

Advantage: There is no doubt that animal experiments in awake conditions are one of the ideal functional experimental conditions because they allow us the naturalistic neuronal activity in the experiment. In addition, some of the disadvantages of the anesthetized animal experiments discussed above are fully or partially overcome by the awake animal experiments.

Disadvantage 1: One of the weak points of the awake animal experiments is that we could easily capture the large size of noise associated with the animal movement. Recent progress in experimental skills, such as solid attachment of the recording systems on the skull, remarkably improved the weakness. In addition, researchers were intensely challenged to compensate for the movement artifacts during the offline data analysis. As a result, we can now collect more reliable and high-quality neuronal activity in awake animals than we did previously. However, monitoring neuronal activity using recording methods sensitive to animal movement, such as *in vivo* intracellular or patch-clamp recording methods, is still challenging.

Disadvantage 2: Some of the experimental systems are too large and heavy to attach to the animal brain, such as optical imaging systems with high numerical aperture lenses. Some probes, such as functional ultrasound imaging systems, functional magnetic resonance imaging systems, etc., require to be moved while monitoring the brain functions. The head-restrained animal experiment would be the best choice for using such equipment. However, the head-restrained animal researches require a relatively short time experimental duration (~1 h) to decrease the head-restrained stress of animals. If it requires a longer (more than 6 h) duration, the anesthetized animal experiments have benefits. For example, the functional mapping of relatively peripheral areas, such as the olfactory bulb, barrel cortex, visual cortex, etc., has the advantage of using the anesthetized experiment.

Disadvantage 3: Massive volume of information is processed in awake animal brains simultaneously. It is one of the biggest benefits of the awake animal experiment, which allows us to understand the naturalistic brain function *in vivo*. However, it also has a tradeoff. Too much activity makes it difficult to capture or extract the critical signals among the flood of massive neuronal activities. Turning off some of the neuronal activity or neuronal pathways in awake animal experiments may help to dissect the brain function and focus on discussing the specific neuronal activity and pathways in some cases.

Disadvantage 4: Usually, the recording system is attached over the skull, or the recording probes are implanted in the target brain area under anesthesia before the awake animal experiment. In this case, we need to consider postoperative delirium to have the proper recovery time after the anesthetized surgery (Peng et al., 2016). Even if the animal shows normal activity after the surgery, animal performance for some experimental tasks may not be the same as that before the surgery. Therefore, the careful evaluation of the animal recovery from the anesthetized surgery is required for the awake animal experiments associated with anesthetized animal surgery.

Discussion

Considering the advantages and disadvantages discussed above session, the current method of anesthesia would be advantageous in some of the experiments, such as (1) Mapping the passive sensory inputs, (2) Evaluating the synaptic interaction or pharmacological impact in the local circuit, and (3) Measuring the neuronal activity under stressful in awake animal conditions.

In addition, some of the disadvantages of awake animal experiments will be overcome by the progress of technologies in the future. For example, the large and heavy recording systems will become more compact and lighter. They will be less stressed when attached to the animal skull. Therefore, these disadvantages could be partially solved in the future.

Recent studies showed the potential that anesthesia and sleep conditions may be inducible by the control of the specific neuronal types and circuits. These discoveries will shed light on the potential of new types of anesthesia. Suppose we will be able to control the activity of the proper number and group of anesthetic/awake associate neurons by chemogenetic or optogenetic tools and control the anesthetized/awake states of animals in the future. In that case, this procedure will become a new type of anesthesia and minimize the impact of anesthesia on other brain functions such as respiration and cardiovascular systems. It will increase the controllability of the anesthesia, may decrease the animal death associated with the failure control of the respiratory and cardiovascular systems, and increase the success rate of the animal surgery. In addition, if we know the specific neurons and neuronal circuits affected by the anesthesia, we could avoid studying these neurons and circuits, and focus on studying the other neuronal circuits, which have normal activity of received minimum impact of the new anesthesia, as like awake animal research more easily and efficiently than current awake animal experiments. Understanding the essential neuronal and circuitry mechanisms that induce sleep/anesthesia and awake animal conditions would extend the anesthetized animal research beyond the current limitation and help to understand the more naturalistic brain function in anesthetized animal conditions.

Summary

In this review, we attempt to summarize the molecular mechanism of popular anesthetic agents, the relationship between hypothalamic neurons and anesthesia/sleep/awake conditions, sensory activities under anesthesia, the advantages and disadvantages of anesthetized and awake animal experiments, and discuss the potential of future anesthesia. This would help in conducting anesthetized experiments and future animal research.

Author contributions

SN: Writing – original draft, Writing – review & editing. SH-I: Writing – review & editing. SK: Writing – review & editing.

Funding

The author(s) declare that financial support was received for the research, authorship, and/or publication of this article. This work was supported by JSPS KAKENHI Grant Numbers JP23K08930 (SK), JSPS KAKENHI Grant Numbers JP21K07280 and 24K10495 (SH-I), Japan-US Brain Research Cooperation program (SK), and the Takeda Science Foundation (SK).

Acknowledgments

The authors apologize to those whose work was not included here due to space limitations.

Conflict of interest

The authors declare that the research was conducted in the absence of any commercial or financial relationships that could be construed as a potential conflict of interest.

Publisher's note

References

Aasebø, I. E. J., Lepperød, M. E., Stavrinou, M., Nøkkevangen, S., Einevoll, G., Hafting, T., et al. (2017). Temporal processing in the visual cortex of the awake and anesthetized rat. *eNeuro* 4:59. doi: 10.1523/ENEURO.0059-17.2017

Allen, W. E., DeNardo, L. A., Chen, M. Z., Liu, C. D., Loh, K. M., Fenno, L. E., et al. (2017). Thirst-associated preoptic neurons encode an aversive motivational drive. *Science* 357, 1149–1155. doi: 10.1126/science.aan6747

Århem, P., Klement, G., and Nilsson, J. (2003). Mechanisms of anesthesia: towards integrating network, cellular, and molecular level modeling. *Neuropsychopharmacology* 28, S40–S47. doi: 10.1038/sj.npp.1300142

Blauvelt, D. G., Sato, T. F., Wienisch, M., and Murthy, V. N. (2013). Distinct spatiotemporal activity in principal neurons of the mouse olfactory bulb in anesthetized and awake states. *Front. Neural Circuits* 7:46. doi: 10.3389/fncir.2013.00046

Brown, E. N., Lydic, R., and Schiff, N. D. (2010). General anesthesia, sleep, and coma. *N. Engl. J. Med.* 363, 2638–2650. doi: 10.1056/NEJMra0808281

Buljubasic, N., Rusch, N. J., Marijic, J., Kampine, J. P., and Bosnjak, Z. J. (1992). Effects of halothane and isoflurane on calcium and Potassium Channel currents in canine coronary arterial cells. *Anesthesiology* 76, 990–998. doi: 10.1097/00000542-199206000-00020

Date, A., Bashir, K., Uddin, A., and Nigam, C. (2020). Differences between natural sleep and the anesthetic state. *Future Sci.* 6. doi: 10.2144/fsoa-2020-0149

De Kock, C. P. J., and Sakmann, B. (2009). Spiking in primary somatosensory cortex during natural whisking in awake head-restrained rats is cell-type specific. *Proc. Natl. Acad. Sci. USA* 106, 16446–16450. doi: 10.1073/pnas.0904143106

Devonshire, I. M., Grandy, T. H., Dommett, E. J., and Greenfield, S. A. (2010). Effects of urethane anaesthesia on sensory processing in the rat barrel cortex revealed by combined optical imaging and electrophysiology. *Eur. J. Neurosci.* 32, 786–797. doi: 10.1111/j.1460-9568.2010.07322.x

Dickinson, R., Peterson, B. K., Banks, P., Simillis, C., Martin, J. C. S., Valenzuela, C. A., et al. (2007). Competitive inhibition at the Glycine site of the N -methyl-d-aspartate receptor by the anesthetics xenon and IsofluraneEvidence from molecular modeling and electrophysiology. *Anesthesiology* 107, 756–767. doi: 10.1097/01.anes.0000287061.77674.71

Dutton, J. W., Artwohl, J. E., Huang, X., and Fortman, J. D. (2019). Assessment of pain associated with the injection of sodium pentobarbital in laboratory mice (*Mus musculus*). *J. Am. Assoc. Lab. Anim. Sci.* 58, 373–379. doi: 10.30802/AALAS-JAALAS-18-000094

Field, K. J., White, W. J., and Lang, C. M. (1993). Anaesthetic effects of chloral hydrate, pentobarbitone and urethane in adult male rats. *Lab. Anim.* 27, 258–269. doi: 10.1258/002367793780745471

Franks, N. P. (2008). General anaesthesia: from molecular targets to neuronal pathways of sleep and arousal. *Nat. Rev. Neurosci.* 9, 370–386. doi: 10.1038/nrn2372

Franks, N. P., and Lieb, W. R. (1994). Molecular and cellular mechanisms of general anaesthesia. *Nat. Cell Biol.* 367, 607–614. doi: 10.1038/367607a0

Gelegen, C., Miracca, G., Ran, M. Z., Harding, E. C., Ye, Z., Yu, X., et al. (2018). Excitatory pathways from the lateral Habenula enable Propofol-induced sedation. *Curr. Biol.* 28, 580–587.e5. doi: 10.1016/j.cub.2017.12.050

Gertler, R., Brown, H. C., Mitchell, D. H., and Silvius, E. N. (2001). Dexmedetomidine: a novel sedative-analgesic agent. *Proc. (Bayl. Univ. Med. Cent.)* 14, 13–21. doi: 10.1080/08998280.2001.11927725

Grasshoff, C., and Antkowiak, B. (2006). Effects of isoflurane and enflurane on GABAA and glycine receptors contribute equally to depressant actions on spinal ventral horn neurones in rats. *Br. J. Anaesth.* 97, 687–694. doi: 10.1093/bja/ael239

Greenberg, D. S., Houweling, A. R., and Kerr, J. N. D. (2008). Population imaging of ongoing neuronal activity in the visual cortex of awake rats. *Nat. Neurosci.* 11, 749–751. doi: 10.1038/nn.2140

Haider, B., Häusser, M., and Carandini, M. (2012). Inhibition dominates sensory responses in the awake cortex. *Nat. Cell Biol.* 493, 97–100. doi: 10.1038/nature11665

Hara, K., and Harris, R. A. (2002). The anesthetic mechanism of urethane: the effects on neurotransmitter-gated ion channels. *Anesth. Analg.* 94, 313–318. doi: 10.1213/00000539-200202000-00015

Højlund, M, Blanner Wagner, C, Wesselhoeft, R, Andersen, K, Fink-Jensen, A, and Hallas, J (2022) Use of chlorprothixene and the risk of diabetes and major adverse cardiovascular events: a nationwide cohort study. *Basic Clin Pharmacol Toxicol.* 130, 501–512. doi: 10.1111/bcpt.13711

Hu, Y., Du, W., Qi, J., Luo, H., Zhang, Z., Luo, M., et al. (2024). Comparative brain-wide mapping of ketamine- and isoflurane-activated nuclei and functional networks in the mouse brain. *eLife* 12:88420. doi: 10.7554/eLife.88420

Jenkins, A., Franks, N. P., and Lieb, W. R. (1999). Effects of temperature and volatile anesthetics on GABAAReceptors. *Anesthesiology* 90, 484–491. doi: 10.1097/00000542-199902000-00024

Jiang-Xie, L. F., Yin, L., Zhao, S., Prevosto, V., Han, B. X., Dzirasa, K., et al. (2019). A common neuroendocrine substrate for diverse general anesthetics and sleep. *Neuron* 102, 1053–1065.e4. doi: 10.1016/j.neuron.2019.03.033

Johnson, AB, and Sadiq, NM (2022) Pentobarbital - StatPearls - NCBI bookshelf. StatPearls [Internet] Available at: https://www.ncbi.nlm.nih.gov/books/NBK545288/ (Accessed April 28, 2024).

Jones, M. V., Brooks, P. A., and Harrison, N. L. (1992). Enhancement of gamma-aminobutyric acid-activated cl- currents in cultured rat hippocampal neurones by three volatile anaesthetics. *J. Physiol.* 449, 279–293. doi: 10.1113/jphysiol.1992.sp019086

Kato, H. K., Chu, M. W., Isaacson, J. S., and Komiyama, T. (2012). Dynamic sensory representations in the olfactory bulb: modulation by wakefulness and experience. *Neuron* 76, 962–975. doi: 10.1016/j.neuron.2012.09.037

Krasowski, M. D., and Harrison, N. L. (2000). The actions of ether, alcohol and alkane general anaesthetics on GABAA and glycine receptors and the effects of TM2 and TM3 mutations. *Br. J. Pharmacol.* 129, 731–743. doi: 10.1038/sj.bjp.0703087

Kurdi, M. S., Theerth, K. A., and Deva, R. S. (2014). Ketamine: current applications in anesthesia, pain, and critical care. *Anesth. Essays Res.* 8, 283–290. doi: 10.4103/0259-1162.143110

Lee, H., Tanabe, S., Wang, S., and Hudetz, A. G. (2021). Differential effect of anesthesia on visual cortex neurons with diverse population coupling. *Neuroscience* 458, 108–119. doi: 10.1016/j.neuroscience.2020.11.043

Maggi, C. A., Santicioli, P., and Meli, A. (1986). Somatovesical and vesicovesical excitatory reflexes in urethane-anaesthetized rats. *Brain Res.* 380, 83–93. doi: 10.1016/0006-8993(86)91432-0

Moore, J. T., Chen, J., Han, B., Meng, Q. C., Veasey, S. C., Beck, S. G., et al. (2012). Direct activation of sleep-promoting VLPO neurons by volatile anesthetics contributes to anesthetic hypnosis. *Curr. Biol.* 22, 2008–2016. doi: 10.1016/j.cub.2012.08.042

Nallasamy, N., and Tsao, D. Y. (2011). Functional connectivity in the brain: effects of anesthesia. *Neuroscientist* 17, 94–106. doi: 10.1177/1073858410374126

Pagliardini, S., Funk, G. D., and Dickson, C. T. (2013). Breathing and brain state: urethane anesthesia as a model for natural sleep. *Respir. Physiol. Neurobiol.* 188, 324–332. doi: 10.1016/j.resp.2013.05.035

Peng, M., Zhang, C., Dong, Y., Zhang, Y., Nakazawa, H., Kaneki, M., et al. (2016). Battery of behavioral tests in mice to study postoperative delirium. *Sci. Rep.* 6, 1–13. doi: 10.1038/srep29874

Petersen, C. C. H. (2007). The functional organization of the barrel cortex. *Neuron* 56, 339–355. doi: 10.1016/j.neuron.2007.09.017

Reiffurth, C., Berndt, N., Gonzalez Lopez, A., Schoknecht, K., Kovács, R., Maechler, M., et al. (2023). Deep isoflurane anesthesia is associated with alterations in ion homeostasis and specific Na+/K+-ATPase impairment in the rat brain. *Anesthesiology* 138, 611–623. doi: 10.1097/ALN.0000000000004553

Reitz, S. L., Wasilczuk, A. Z., Beh, G. H., Proekt, A., and Kelz, M. B. (2021). Activation of preoptic tachykinin 1 neurons promotes wakefulness over sleep and volatile anesthetic-induced unconsciousness. *Curr. Biol.* 31, 394–405.e4. doi: 10.1016/j.cub.2020.10.050

Ruiz-Colón, K., Chavez-Arias, C., Díaz-Alcalá, J. E., and Martínez, M. A. (2014). Xylazine intoxication in humans and its importance as an emerging adulterant in abused drugs: a comprehensive review of the literature. *Forensic Sci. Int.* 240, 1–8. doi: 10.1016/j.forsciint.2014.03.015

Sakai, E. M., Connolly, L. A., and Klauck, J. A. (2005). Inhalation anesthesiology and volatile liquid anesthetics: focus on isoflurane, desflurane, and sevoflurane. *Pharmacotherapy* 25, 1773–1788. doi: 10.1592/phco.2005.25.12.1773

Scott, N., Prigge, M., Yizhar, O., and Kimchi, T. (2015). A sexually dimorphic hypothalamic circuit controls maternal care and oxytocin secretion. *Nat. Cell Biol.* 525, 519–522. doi: 10.1038/nature15378

Sellers, K. K., Bennett, D. V., Hutt, A., Williams, J. H., and Fröhlich, F. (2015). Awake vs. anesthetized: layer-specific sensory processing in visual cortex and functional connectivity between cortical areas. *J. Neurophysiol.* 113, 3798–3815. doi: 10.1152/jn.00923.2014

Shafer, A. (1995). Metaphor and anesthesia. *Anesthesiology* 83, 1331–1342. doi: 10.1097/00000542-199512000-00024

Simons, D. J., Carvell, G. E., Hershey, A. E., and Bryant, D. P. (1992). Responses of barrel cortex neurons in awake rats and effects of urethane anesthesia. *Exp. Brain Res.* 91, 259–272. doi: 10.1007/BF00231659

Sorrenti, V., Cecchetto, C., Maschietto, M., Fortinguerra, S., Buriani, A., and Vassanelli, S. (2021). Understanding the effects of anesthesia on cortical electrophysiological recordings: a scoping review. *Int. J. Mol. Sci.* 22:1286. doi: 10.3390/ijms22031286

Sternson, S. M. (2013). Hypothalamic survival circuits: blueprints for purposive behaviors. *Neuron* 77, 810–824. doi: 10.1016/j.neuron.2013.02.018

Stoicea, N., Versteeg, G., Florescu, D., Joseph, N., Fiorda-Diaz, J., Navarrete, V., et al. (2016). Ketamine-based anesthetic protocols and evoked potential monitoring: a risk/benefit overview. *Front. Neurosci.* 10:180420. doi: 10.3389/fnins.2016.00037

Szymusiak, R., Gvilia, I., and McGinty, D. (2007). Hypothalamic control of sleep. *Sleep Med.* 8, 291–301. doi: 10.1016/j.sleep.2007.03.013

Tan, C. L., Cooke, E. K., Leib, D. E., Lin, Y. C., Daly, G. E., Zimmerman, C. A., et al. (2016). Warm-sensitive neurons that control body temperature. *Cell* 167, 47–59.e15. doi: 10.1016/j.cell.2016.08.028

Wachowiak, M. (2011). All in a sniff: olfaction as a model for active sensing. *Neuron* 71, 962–973. doi: 10.1016/j.neuron.2011.08.030

Wachowiak, M., Economo, M. N., Díaz-Quesada, M., Brunert, D., Wesson, D. W., White, J. A., et al. (2013). Optical dissection of odor information processing in vivo using GCaMPs expressed in specified cell types of the olfactory bulb. *J. Neurosci.* 33, 5285–5300. doi: 10.1523/JNEUROSCI.4824-12.2013

Wu, Z., Autry, A. E., Bergan, J. F., Watabe-Uchida, M., and Dulac, C. G. (2014). Galanin neurons in the medial preoptic area govern parental behaviour. *Nature* 509, 325–330. doi: 10.1038/nature13307

Zhang, Z., Ferretti, V., Güntan, I., Moro, A., Steinberg, E. A., Ye, Z., et al. (2015). Neuronal ensembles sufficient for recovery sleep and the sedative actions of α2 adrenergic agonists. *Nat. Neurosci.* 18, 553–561. doi: 10.1038/nn.3957

frontiers | Frontiers in Neural Circuits

TYPE Mini Review
PUBLISHED 30 May 2024
DOI 10.3389/fncir.2024.1408189

OPEN ACCESS

EDITED BY
Kensaku Mori,
RIKEN, Japan

REVIEWED BY
Naoshige Uchida,
Harvard University, United States

*CORRESPONDENCE
Koshi Murata
✉ kmurata@u-fukui.ac.jp
Ayako Maegawa
✉ asawai@u-fukui.ac.jp

RECEIVED 27 March 2024
ACCEPTED 06 May 2024
PUBLISHED 30 May 2024

CITATION
Murata K, Maegawa A, Imoto Y, Fujieda S and Fukazawa Y (2024) Endogenous opioids in the olfactory tubercle and their roles in olfaction and quality of life.
Front. Neural Circuits 18:1408189.
doi: 10.3389/fncir.2024.1408189

Endogenous opioids in the olfactory tubercle and their roles in olfaction and quality of life

Koshi Murata[1,2]*, Ayako Maegawa[1,2,3]*, Yoshimasa Imoto[2,3], Shigeharu Fujieda[3] and Yugo Fukazawa[1,2]

[1]Division of Brain Structure and Function, Faculty of Medical Sciences, University of Fukui, Fukui, Japan, [2]Life Science Innovation Center, University of Fukui, Fukui, Japan, [3]Department of Otorhinolaryngology-Head and Neck Surgery, Faculty of Medical Sciences, University of Fukui, Fukui, Japan

Olfactory dysfunctions decrease daily quality of life (QOL) in part by reducing the pleasure of eating. Olfaction plays an essential role in flavor sensation and palatability. The decreased QOL due to olfactory dysfunction is speculated to result from abnormal neural activities in the olfactory and limbic areas of the brain, as well as peripheral odorant receptor dysfunctions. However, the specific underlying neurobiological mechanisms remain unclear. As the olfactory tubercle (OT) is one of the brain's regions with high expression of endogenous opioids, we hypothesize that the mechanism underlying the decrease in QOL due to olfactory dysfunction involves the reduction of neural activity in the OT and subsequent endogenous opioid release in specialized subregions. In this review, we provide an overview and recent updates on the OT, the endogenous opioid system, and the pleasure systems in the brain and then discuss our hypothesis. To facilitate the effective treatment of olfactory dysfunctions and decreased QOL, elucidation of the neurobiological mechanisms underlying the pleasure of eating through flavor sensation is crucial.

KEYWORDS

olfactory tubercle, opioid, quality of life, prodynorphin, preproenkephalin, dopamine, brain reward system

Introduction

The emergence of coronavirus disease, which is often accompanied by olfactory dysfunctions or degeneration, has led to the need for re-evaluation of the impact of olfaction in quality of life (QOL) (Coelho et al., 2021). Olfactory dysfunctions can arise from various causes, such as viral infections, allergic rhinitis, and trauma (Hummel et al., 2017; Miwa et al., 2019). Olfactory dysfunction decreases daily QOL, with reduced food enjoyment as a significant factor (Croy et al., 2014). Olfaction is a key component of flavor sensation; when food is masticated and swallowed food, odorants are detected via the olfactory epithelium through the retronasal pathway, wherein olfactory sensory neurons send food odorant signals the brain (Lawless, 1991; Shepherd, 2011; Shiotani et al., 2024). Why does the inability to sense flavor affect the pleasure of eating? In other words, which neurobiological mechanisms connect flavor sensations and pleasure of eating? The key factors of decreased QOL owing to olfactory dysfunction have been considered as changes in the activity of olfactory and limbic neural circuits (Rochet et al., 2018). Here, we hypothesized that the endogenous expression of opioids in the olfactory tubercle (OT) is involved in the neurobiological mechanisms underlying

pleasure sensation through olfaction while eating (Maegawa et al., 2022). In this review, we provide an overview of the recent updates on the structure and function of the OT, briefly summarize the endogenous opioid system in the mammalian brain, and review the gene expression of prodynorphin and preproenkephalin in the OT. We, then, explore the pleasure systems in the brain, emphasizing the involvement of opioids in hedonic sensations. Finally, we discuss the hypothesis that olfactory dysfunctions decrease daily QOL by suppressing opioid release from the anteromedial subregion of the OT while eating.

Structure and functions of the OT

The OT is a part of the ventral striatum and is anatomically continuous with the nucleus accumbens (NAc), a chief target of the mesolimbic dopaminergic pathway (Heimer, 1978; Heimer et al., 1987; Ikemoto, 2007). The term "olfactory tubercle" refers to the region on the basal surface of the frontal lobe between the olfactory tract and nucleus of the diagonal band in humans (Crosby and Humphrey, 1941; Allison, 1954; Sakamoto et al., 1999). The OT receives dense synaptic inputs from the central olfactory areas, such as the olfactory bulb, anterior olfactory nucleus, tenia tecta, and piriform cortex, which may transmit olfactory information to the OT (Haberly and Price, 1977, 1978a,b; Berendse et al., 1992). In addition, the OT receives synaptic inputs from the prefrontal cortex, amygdala, and hypothalamus as well as dopamine input from the ventral tegmental area (VTA) (Ikemoto, 2007; Zhang et al., 2017a,b). Despite its olfactory label, the OT exhibits multimodal sensory responsiveness that is not limited to olfaction (Wesson and Wilson, 2011).

The principal neurons of the OT comprise three major subtypes: the medium spiny neurons (MSNs), dwarf cells, and granule cells, all of which are GABAergic (Millhouse and Heimer, 1984; Xiong and Wesson, 2016). MSNs are distributed throughout the OT, forming a dense cell layer (also referred to as layer II). OT MSNs project their axons primarily onto the ventral pallidum (Heimer et al., 1987; Walaas and Ouimet, 1989; Zhou et al., 2003; Lee et al., 2023). Dwarf cells are clustered in the lateral part of the OT, forming the cap region that is interspersed throughout the anteroposterior axis (Hosoya and Hirata, 1974). Granule cells are clustered from the anteromedial surface to the deep layers of the central OT, forming a continuous structure of the Islands of Calleja (ICj) (Fallon et al., 1978; de Vente et al., 2001). The axonal targets of the granule cells are MSNs in the OT, which project their axons to the VTA, suggesting the role of granule cells in the disinhibition of dopamine release from the VTA (Zhang et al., 2023). Dopamine receptor subtypes are expressed differently by these principal neurons: MSNs express D1 or D2 dopamine receptors, dwarf cells express D1 receptors, and granule cells express D3 receptors (Le Moine and Bloch, 1995; Yung et al., 1995; Murata et al., 2015; Zhang et al., 2021).

The anatomically distinct domains of the OT play different roles in physiological and behavioral responses (Yamaguchi, 2017; Murata, 2020). In previous studies, reward motivation functions of the OT were implicated by intra-cranial self-administration of addictive drugs (Ikemoto, 2010; Berridge and Kringelbach, 2015). The anteromedial domain of the OT in particular support self-administration in rats (Ikemoto, 2003; Ikemoto et al., 2005; Shin et al., 2008), and its involvement in odor-guided appetitive behaviors also has been revealed. Specifically, behavioral attraction to an odor cue associated with sugar-reward induces c-fos activation in the anteromedial OT (Murata et al., 2015). Optogenetic and DREADD manipulations of dopamine inputs from the VTA to medial OT have revealed this pathway to mediate the acquisition and execution of odor preference (Zhang et al., 2017a). The cytochemical architecture of the anteromedial OT develops postnatally, and the response of c-fos expression to eating matures during the late weaning period (Murofushi et al., 2018). Conversely, the lateral OT is involved in odor-guided aversive behaviors. Aversive behavioral response to an odor cue associated with electrical foot shock induces c-fos activation of MSNs and dwarf cells in the lateral OT (Murata et al., 2015). Projection neurons responsive to predator odors and rotten food odors in the olfactory bulb project their axons to the cap region in the lateral OT (Igarashi et al., 2012). Additionally, optogenetic activation of predator odor-responsive glomerulus in the olfactory bulb induces aversive behavior and Egr1 activation in the cap region (Saito et al., 2017). Associative learning of conditioned odor stimuli with distinct sugar rewards, or with electrical foot shocks, shapes the responsiveness of the anteromedial and lateral OT domains, respectively (Sha et al., 2023). The altered response of the OT domains is accompanied by increased axonal bouton size and higher expression of the excitatory synaptic structure (VGluT1) in the axon terminals from the olfactory bulb and anterior piriform cortex to the OT (Sha et al., 2023). In addition to regional differences, the subtypes of OT neurons play different physiological and behavioral roles. Optogenetic activation of D1-expressing MSNs in the anteromedial OT elicits place preference, whereas activation of D2-expressing MSNs in the same site elicits place aversion (Murata et al., 2019). Further, D3-expressing granule cells in the ICj are involved in grooming behavior and suppression of depression-like behaviors (Zhang et al., 2021, 2023).

Mesolimbic dopamine circuits play crucial roles in incentive motivation, and also reinforcement learning and valence coding (Schultz, 1998, 2016), and a series of studies have revealed the role of the OT in this context (Gadziola et al., 2015; Millman and Murthy, 2020; Oettl et al., 2020; Winkelmeier et al., 2022). Distinct roles for the subtypes of D1- and D2-expressing neurons of the OT in reinforcement learning have also been suggested but remain controversial. Gadziola et al. (2020) demonstrated that D1-expressing neurons flexibly represent rewarded odors during reversal learning, and activation of D1-expressing neurons promotes engagement in a reward-motivated task. Martiros et al. (2022) validated the role of D1-expressing neurons by demonstrating that they robustly and bidirectionally represent odor valence, responding similarly to odors that predicted similar outcomes, regardless of odor identity. Martiros et al. (2022) also showed that D2-expressing neurons were conversely more selective for odor identity than valence. However, Lee et al. (2023) proposed that although D1-expressing neurons show larger response magnitudes to rewarded odors than other odors, this is better interpreted as identity encoding with enhanced contrast rather than value encoding. As the OT has a laterality of anatomical and functional domains, future studies should be conducted for both cell types (D1 vs. D2) and anatomical domains (medial vs. lateral) to clarify the roles of OT neurons in valence coding and odor identity. In summary, the OT is part of the ventral striatum and plays a crucial role in motivating animals to acquire and execute adaptive behaviors through valence coding and reinforcement learning.

Endogenous opioid systems in the mammalian brain and expression of dynorphins and enkephalins in the OT

The opioid system is a highly diverse peptide-neurotransmitter system that provides pain relief and euphoric effects (Emery and Akil, 2020). Endogenous opioids are composed of three main neuropeptide families: the β-endorphins derived from the pro-opiomelanocortin gene (*Pomc*), the enkephalins derived from preproenkephalin (*Penk*) and prodynorphin (*Pdyn*) genes, and the dynorphins derived from the *Pdyn* gene. Each of these families contains multiple peptides with diverse binding characteristics (Przewlocki, 2022). The system includes three opioid receptors: the mu, delta, and kappa. The opioid peptides have been portrayed to bind primarily to particular receptors (β-endorphins: mu, enkephalins: delta, and dynorphins: kappa); however, the lack of one-to-one correspondence between signal peptides and its receptors should be emphasized. Members of all three peptide families are capable of activating the three receptors to varying degrees, particularly the dynorphins (Emery and Akil, 2020). Therefore, all opioid receptor types within a brain region may simultaneously be activated by different or by even the same peptide. A fourth receptor-peptide pair, nociceptin and its receptor, are also part of the opioid system and play roles in pain and motivation (Di Cesare Mannelli et al., 2015; Kiguchi et al., 2016; Parker et al., 2019). This pair was more recently discovered than the others and is not reviewed here (Mollereau et al., 1994; Meunier et al., 1995).

Pomc expression in the brain is limited to the arcuate nucleus of the hypothalamus, nucleus of the solitary tract, and pituitary gland (Bronstein et al., 1992). The regions that express *Pdyn and Penk* are widely distributed in the brain (Harlan et al., 1987; Merchenthaler et al., 1997), and their details have not been included in this review. Here, we focused on the striatum, one of the brain's regions with high *Pdyn* and *Penk* expression (Figure 1A). Neurons in the dorsal striatum and NAc generally express either *Pdyn* or *Penk* (Furuta et al., 2002); *Pdyn* is expressed by D1 neurons and *Penk* by D2 neurons (Curran and Watson, 1995). The ventral striatum has a cell cluster between the NAc and OT, where D1 neurons co-express *Pdyn* and *Penk*, and no D2 neurons are observed (Curran and Watson, 1995). In a recent report, we evaluated the cellular profiles of *Pdyn*- and *Penk*-expressing neurons in mouse OT (Maegawa et al., 2022). These results are consistent with those of the dorsal striatum and NAc, in that D1 neurons express *Pdyn* and D2 neurons express *Penk*. In addition, we found that the OT had D1 neurons co-expressing *Pdyn* and *Penk* in the dense cell layer and a higher frequency of co-expressing D1 neurons in the anteromedial OT than in the anterolateral OT (Figure 1B).

The three types of opioid receptors are widely distributed in the brain and show a high degree of overlap in their regional expression patterns, particularly in regions involved in pain, affect, and rewards (Mansour et al., 1988; Mansour and Watson, 1993). Describing the details of the opioid receptor distribution is beyond the scope of this review. We focused on brain regions with mu, delta, and kappa receptor expression that are positionally proximate to the OT and have axonal projections from the OT, as demonstrated by *in situ* hybridization of mRNA and peptide binding assays (Mansour et al., 1987, 1994). Mu receptor expression is localized in the caudate putamen, NAc, lateral and medial septa, diagonal band of Broca, bed nucleus of the stria terminalis, thalamus, habenula, interpeduncular nucleus, and substantia nigra. Delta receptor expression is found in the caudate putamen, NAc, OT, ventromedial hypothalamus, and amygdala. Kappa receptor expression is localized in the claustrum, endopiriform nucleus, caudate putamen, NAc, OT, medial preoptic area, bed nucleus of the stria terminalis, amygdala, hypothalamus, periventricular thalamus, substantia nigra, and ventral tegmental area.

Implications of the OT opioids on the pleasure of eating and QOL

Opioids are neurochemical molecules related to feelings of pleasure (Barbano and Cador, 2007). Dopamine is often misunderstood as a pleasure mechanism in the brain (Berridge and Dayan, 2021). Our understanding of the brain's pleasure system can be traced back to the discovery of intracranial self-stimulation in rats by Olds and Milner (1954). Olds (1956) had originally interpreted that the rats engaged in intense lever pressing to self-stimulate because the electrical stimulation of the brain was pleasurable. Subsequent studies have since demonstrated that spontaneous approaching and reward-seeking behaviors such as lever pressing for a reward involve the dopamine system (Wise et al., 1978). Therefore, dopamine was initially considered to be a pleasure substance (Wise, 1980); however, later studies suggested that appetitive behavior due to dopamine activation or hypothalamic electrical stimulation should be interpreted as reflecting motivated "wanting" but not necessarily pleasurable hedonic impact or "liking" (Berridge and Robinson, 2016). To objectively measure an animal's hedonic impact, an affective taste reactivity test is widely used whereby a sweet sucrose solution is passively infused into the animal's oral cavity, and its facial and bodily movements are observed. Typical responses to sweet sucrose infusion are intaking behaviors such as rhythmic tongue protrusions, and used as objective measurement of hedonic "liking" reactions (Berridge, 2000; Steiner et al., 2001). Ablation of the dopamine neurons in the VTA does not reduce the hedonic "liking" reaction to the sucrose oral infusion, despite abolishing the animal's voluntary food and water intake (Berridge et al., 1989). Furthermore, electrical stimulation of the lateral hypothalamus that activates dopamine neurons does not increase the hedonic "liking" reaction, despite dramatically increasing food intake (Berridge and Valenstein, 1991). At present, dopamine is not considered a pleasure-inducing substance but rather is related to motivation, craving, and prediction error for learning adaptive behavior (Wise, 2008; Kringelbach, 2010; Berridge and Kringelbach, 2015; Schultz, 2016).

In contrast, opioids are neurotransmitters, and their agonists enhance and antagonists block hedonic "liking" reactions associated with intake behaviors such as rhythmic tongue protrusions in response to sucrose sweetness. Blocking the opioid system by systemic naltrexone injection inhibits the hedonic "liking" reactions (Parker et al., 1992), and systemic morphine injection increases the hedonic "liking" reactions (Doyle et al., 1993). In addition, the microinjection of opioids into the rostrodorsal NAc medial shell, caudal VP, caudal insular cortex, and rostromedial orbitofrontal cortex enhances the hedonic reactions of "liking" to sucrose taste (Peciña and Berridge, 2005; Smith and Berridge, 2007; Castro and Berridge, 2014, 2017); these local subregions are known as hedonic hotspots (Morales and Berridge, 2020). The dynorphins-kappa receptor system generally known to induce unpleasantness when systemically administrated, but can oppositely

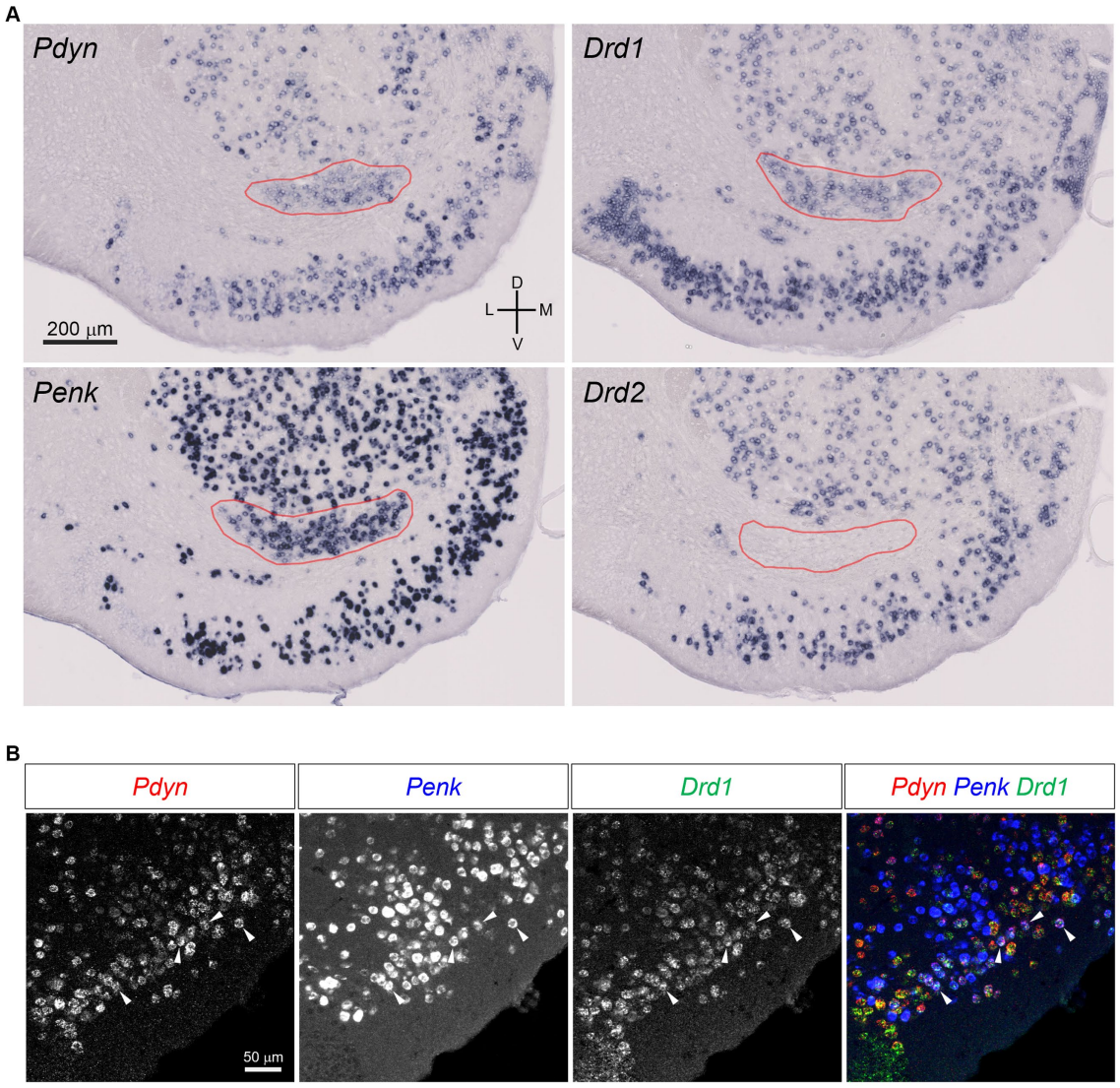

FIGURE 1
Pdyn-Penk co-expressing D1 neurons in the mouse OT. **(A)** Single probe *in situ* hybridization for *Pdyn*, *Penk*, *Drd1*, and *Drd2*. The pictures show coronal sections of the anterior OT and NAc (approximately at Bregma +1.94 mm). Regions delineated by red lines are a cluster of *Pdyn-Penk-Drd1* co-expressing cells. *Drd2* signals were not observed in the cluster. Adjacent sections from one mouse were used for the four images. **(B)** Triple fluorescence *in situ* hybridization for *Pdyn*, *Penk*, and *Drd1* in the anteromedial OT. White arrowheads indicate the colocalization of *Pdyn-Penk-Drd1* mRNAs. D, dorsal; V, ventral; M, medial; L, lateral. Figures are modified from Maegawa et al. (2022).

enhance the "liking" reactions when a kappa agonist is locally injected into the NAc hedonic hotspot, similar to mu and delta agonist microinjections (Castro and Berridge, 2014). The OT is neuroanatomically and neurochemically similar to the NAc in that both have GABAergic projections to the VP and express *Pdyn* and *Penk*. Studies have demonstrated that OT plays a crucial role in reward seeking-motivated behavior, a hallmark of the dopamine-related brain reward system (Ikemoto, 2003; Murata et al., 2015; Zhang et al., 2017a). Having a hedonic hotspot is another feature of some brain reward structures (Morales and Berridge, 2020), which raises the possibility that the OT may have its own hedonic hotspot where opioid stimulation might enhance "liking" reaction to sucrose sweetness.

Thus, we propose the following hypothesis: odorants in food are detected by olfactory neurons in the olfactory epithelium through the retronasal pathway and signaled to the brain, eliciting flavor sensations. Simultaneously, the signals of these odorants are transmitted to the anteromedial OT, inducing the release of dynorphins and enkephalins and resulting in a sensation of pleasure. In olfactory dysfunctions, retronasal airflow is blocked, inhibiting the first step of this cascade. It then suppresses both activation and opioid release in the anteromedial OT, which reduces the pleasure of eating (Figure 2). The anteromedial OT contains *Pdyn-Penk*-coexpressing D1 neurons, which may effectively induce pleasure, as well as appetitive motivation, in response to food odorants and flavors. Whether food odorants are detected by the anteromedial OT via the retronasal pathway remains unclear; therefore, we speculate this based on the analogy that food-related odors and actual food intake activate the anteromedial OT (Murata et al., 2015; Murofushi et al., 2018; Sha et al., 2023). Al-Hasani et al. (2018) demonstrated *in vivo* detection of optically evoked endogenous opioid peptide release by neurons in the

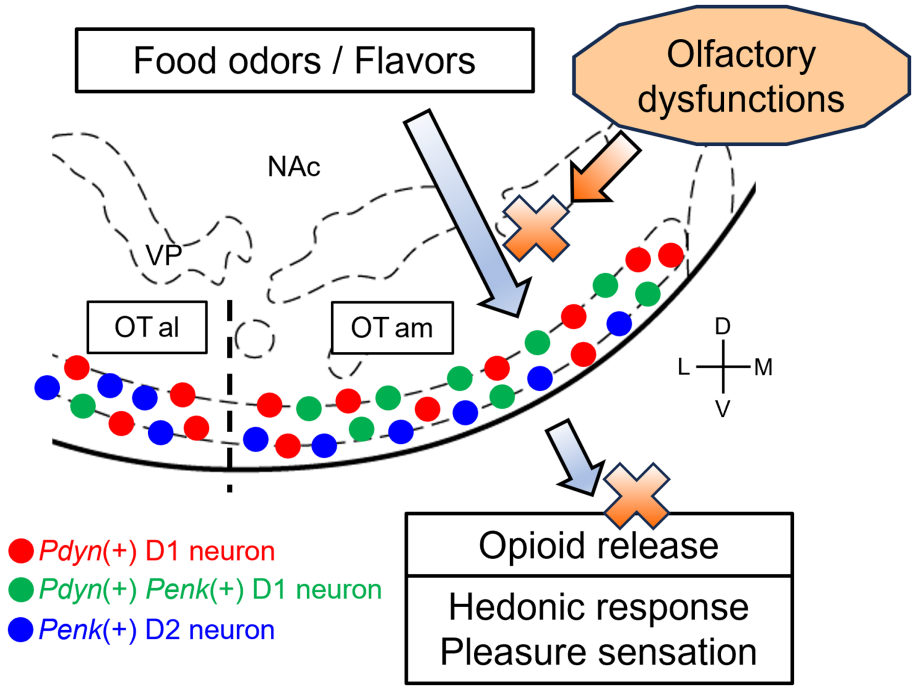

FIGURE 2
A hypothetical model of OT opioid-mediated QOL and its impairment due olfactory dysfunctions. In a healthy condition, food-related olfactory inputs, including food odorants via the retronasal pathway, are conveyed to the anteromedial OT, where *Pdyn*-expressing and *Pdyn-Penk*-coexpressing D1 neurons are activated. Subsequently, opioid peptides are released from D1 neurons in the anteromedial OT, resulting in hedonic pleasure sensation. In some cases of olfactory dysfunctions, the retronasal airflow is blocked, inhibiting the transmission of the olfactory inputs to the anteromedial OT. This, in turn, impairs neural activation and opioid release of the anteromedial OT, which reduces the sensation of pleasure. Red circles, *Pdyn*-expressing D1 neurons; green circles, *Pdyn-Penk*-coexpressing D1 neurons; blue circles, *Penk*-expressing neurons D2. OTam, anteromedial olfactory tubercle; OTal, anterolateral olfactory tubercle; NAc, nucleus accumbens; VP, ventral pallidum; D, dorsal; V, ventral; M, medial; L, lateral. Stereotax atlas from Franklin and Paxinos (2008).

NAc, supporting the idea that neural activation of OT neurons leads to the release of dynorphins and enkephalins. Midroit et al. (2021) demonstrated a correlation between the pleasantness of odors and the activity of the OT in humans. Future studies should investigate the relationship between the pleasantness of odors, neural activity of the OT, and opioid release.

Discussion

We hypothesize that endogenous opioids in the OT, especially in the anteromedial domain, may contribute to neural processing of the pleasure of eating through flavor sensations. Olfactory dysfunction may lead to the disrupted processing within the OT, potentially reducing the daily QOL. The following crucial questions should be addressed in future to test this hypothesis: is the anteromedial OT able to enhance hedonic "liking" reactions to oral sucrose infusion? Does the flavor sensation of food stimulate the anteromedial OT and elicit opioid local release? Which neural circuits are targeted by opioids released from the anteromedial OT? What are the specific roles of *Pdyn-Penk*-coexpressing D1 neurons in the anteromedial OT compared with other types of OT neurons?

Although this review has focused on the endogenous opioids, we did not aim to de-emphasize the involvement of other neurotransmitters, including dopamine, in decreased QOL due to olfactory dysfunctions. As mentioned earlier, dopamine is a key neurotransmitter underlying incentive motivation for rewards (Wise, 2004). A lack of motivation is another symptom that accompanies olfactory dysfunctions, significantly affecting daily QOL (Keller and Malaspina, 2013; Marin et al., 2023). Olfactory dysfunctions can go beyond decreased QOL: they are bi-directionally associated with psychiatric disorders, including depression (Kohli et al., 2016; Taquet et al., 2021; Hasegawa et al., 2022). Ablation or inhibition of D3-expressing granule cells in the OT leads to depression-like behaviors and negatively impacts dopamine release from the VTA (Zhang et al., 2023). Conversely, olfactory enrichment has been shown to be a beneficial treatment strategy for depression (Leon and Woo, 2022). OT neural activity enhancement could be a treatment approach for depression through restoration of appropriate dopamine activity. Given that the OT is a hub region within mesolimbic dopamine neural circuits (Ikemoto, 2007), it likely plays important roles in both opioid-regulated pleasure sensation and dopamine-regulated motivation (Morales and Berridge, 2020). Further clarification of the neurobiology of the OT under olfactory dysfunctions is essential for developing more effective treatments for decreased QOL.

Author contributions

KM: Writing – review & editing, Writing – original draft, Supervision, Conceptualization. AM: Writing – review & editing, Writing – original draft, Conceptualization. YI: Writing – review &

editing. SF: Writing – review & editing. YF: Writing – review & editing.

Funding

The author(s) declare financial support was received for the research, authorship, and/or publication of this article. This work was supported by JSPS KAKENHI Grant Numbers JP17KK0190, JP20H05955, JP21H05817, and JP21K06440 (AdAMS), Lotte Foundation, Urakami Foundation for Food and Food Culture Promotion, Takeda Science Foundation, and Mishima Kaiun Memorial Foundation to KM.

Acknowledgments

We thank Kent Berridge for insightful suggestions on earlier versions on this manuscript.

Conflict of interest

The authors declare that the research was conducted in the absence of any commercial or financial relationships that could be construed as a potential conflict of interest.

The author(s) declared that they were an editorial board member of Frontiers, at the time of submission. This had no impact on the peer review process and the final decision.

Publisher's note

References

Al-Hasani, R., Wong, J.-M. T., Mabrouk, O. S., McCall, J. G., Schmitz, G. P., Porter-Stransky, K. A., et al. (2018). In vivo detection of optically-evoked opioid peptide release. *eLife* 7:e36520. doi: 10.7554/eLife.36520

Allison, A. C. (1954). The secondary olfactory areas in the human brain. *J. Anat.* 88, 481–488

Barbano, M. F., and Cador, M. (2007). Opioids for hedonic experience and dopamine to get ready for it. *Psychopharmacology* 191, 497–506. doi: 10.1007/s00213-006-0521-1

Berendse, H. W., Galis-de Graaf, Y., and Groenewegen, H. J. (1992). Topographical organization and relationship with ventral striatal compartments of prefrontal corticostriatal projections in the rat. *J. Comp. Neurol.* 316, 314–347. doi: 10.1002/cne.903160305

Berridge, K. C. (2000). Measuring hedonic impact in animals and infants: microstructure of affective taste reactivity patterns. *Neurosci. Biobehav. Rev.* 24, 173–198. doi: 10.1016/S0149-7634(99)00072-X

Berridge, K. C., and Dayan, P. (2021). Liking. *Curr. Biol.* 31, R1555–R1557. doi: 10.1016/j.cub.2021.09.069

Berridge, K. C., and Kringelbach, M. L. (2015). Pleasure systems in the brain. *Neuron* 86, 646–664. doi: 10.1016/j.neuron.2015.02.018

Berridge, K. C., and Robinson, T. E. (2016). Liking, wanting, and the incentive-sensitization theory of addiction. *Am. Psychol.* 71, 670–679. doi: 10.1037/amp0000059

Berridge, K. C., and Valenstein, E. S. (1991). What psychological process mediates feeding evoked by electrical stimulation of the lateral hypothalamus? *Behav. Neurosci.* 105, 3–14. doi: 10.1037/0735-7044.105.1.3

Berridge, K. C., Venier, I. L., and Robinson, T. E. (1989). Taste reactivity analysis of 6-hydroxydopamine-induced aphagia: implications for arousal and anhedonia hypotheses of dopamine function. *Behav. Neurosci.* 103, 36–45. doi: 10.1037/0735-7044.103.1.36

Bronstein, D. M., Schafer, M. K., Watson, S. J., and Akil, H. (1992). Evidence that beta-endorphin is synthesized in cells in the nucleus tractus solitarius: detection of POMC mRNA. *Brain Res.* 587, 269–275. doi: 10.1016/0006-8993(92)91007-2

Castro, D. C., and Berridge, K. C. (2014). Opioid hedonic hotspot in nucleus Accumbens Shell: mu, Delta, and kappa maps for enhancement of sweetness "liking" and "wanting". *J. Neurosci.* 34, 4239–4250. doi: 10.1523/JNEUROSCI.4458-13.2014

Castro, D. C., and Berridge, K. C. (2017). Opioid and orexin hedonic hotspots in rat orbitofrontal cortex and insula. *Proc. Natl. Acad. Sci. USA* 114, E9125–E9134. doi: 10.1073/pnas.1705753114

Coelho, D. H., Reiter, E. R., Budd, S. G., Shin, Y., Kons, Z. A., and Costanzo, R. M. (2021). Quality of life and safety impact of COVID-19 associated smell and taste disturbances. *Am. J. Otolaryngol.* 42:103001. doi: 10.1016/j.amjoto.2021.103001

Crosby, E. C., and Humphrey, T. (1941). Studies of the vertebrate telencephalon. II. The nuclear pattern of the anterior olfactory nucleus, tuberculum olfactorium and the amygdaloid complex in adult man. *J. Comp. Neurol.* 74, 309–352. doi: 10.1002/cne.900740209

Croy, I., Nordin, S., and Hummel, T. (2014). Olfactory disorders and quality of life--An updated review. *Chem. Senses* 39, 185–194. doi: 10.1093/chemse/bjt072

Curran, E. J., and Watson, S. J. (1995). Dopamine receptor mRNA expression patterns by opioid peptide cells in the nucleus accumbens of the rat: a double in situ hybridization study. *J. Comp. Neurol.* 361, 57–76. doi: 10.1002/cne.903610106

de Vente, J., Hani, L., Steinbusch, H. E., and Steinbusch, H. W. (2001). The three dimensional structure of the islands of Calleja: a single heterogenous cell complex. *Neuroreport* 12, 565–568. doi: 10.1097/00001756-200103050-00026

Di Cesare Mannelli, L., Micheli, L., and Ghelardini, C. (2015). Nociceptin/orphanin FQ receptor and pain: feasibility of the fourth opioid family member. *Eur. J. Pharmacol.* 766, 151–154. doi: 10.1016/j.ejphar.2015.08.012

Doyle, T. G., Berridge, K. C., and Gosnell, B. A. (1993). Morphine enhances hedonic taste palatability in rats. *Pharmacol. Biochem. Behav.* 46, 745–749. doi: 10.1016/0091-3057(93)90572-B

Emery, M. A., and Akil, H. (2020). Endogenous opioids at the intersection of opioid addiction, pain, and depression: the search for a precision medicine approach. *Annu. Rev. Neurosci.* 43, 355–374. doi: 10.1146/annurev-neuro-110719-095912

Fallon, J. H., Riley, J. N., Sipe, J. C., and Moore, R. Y. (1978). The islands of Calleja: organization and connections. *J. Comp. Neurol.* 181, 375–395. doi: 10.1002/cne.901810209

Franklin, K. B. J., Paxinos, G. (2008). The mouse brain in stereotaxic coordinates, compact the coronal plates and diagrams. *Elsevier Science*.

Furuta, T., Zhou, L., and Kaneko, T. (2002). Preprodynorphin-, preproenkephalin-, preprotachykinin A- and preprotachykinin B-immunoreactive neurons in the accumbens nucleus and olfactory tubercle: double-immunofluorescence analysis. *Neuroscience* 114, 611–627. doi: 10.1016/S0306-4522(02)00312-3

Gadziola, M. A., Stetzik, L. A., Wright, K. N., Milton, A. J., Arakawa, K., Del Mar Cortijo, M., et al. (2020). A neural system that represents the Association of Odors with rewarded outcomes and promotes behavioral engagement. *Cell Rep.* 32:107919. doi: 10.1016/j.celrep.2020.107919

Gadziola, M. A., Tylicki, K. A., Christian, D. L., and Wesson, D. W. (2015). The olfactory tubercle encodes odor valence in behaving mice. *J. Neurosci.* 35, 4515–4527. doi: 10.1523/JNEUROSCI.4750-14.2015

Haberly, L. B., and Price, J. L. (1977). The axonal projection patterns of the mitral and tufted cells of the olfactory bulb in the rat. *Brain Res.* 129, 152–157. doi: 10.1016/0006-8993(77)90978-7

Haberly, L. B., and Price, J. L. (1978a). Association and commissural fiber systems of the olfactory cortex of the rat. *J. Comp. Neurol.* 178, 711–740. doi: 10.1002/cne.901780408

Haberly, L. B., and Price, J. L. (1978b). Association and commissural fiber systems of the olfactory cortex of the rat. II. Systems originating in the olfactory peduncle. *J. Comp. Neurol.* 181, 781–807. doi: 10.1002/cne.901810407

Harlan, R. E., Shivers, B. D., Romano, G. J., Howells, R. D., and Pfaff, D. W. (1987). Localization of preproenkephalin mRNA in the rat brain and spinal cord by in situ hybridization. *J. Comp. Neurol.* 258, 159–184. doi: 10.1002/cne.902580202

Hasegawa, Y., Ma, M., Sawa, A., Lane, A. P., and Kamiya, A. (2022). Olfactory impairment in psychiatric disorders: does nasal inflammation impact disease psychophysiology? *Transl. Psychiatry* 12:314. doi: 10.1038/s41398-022-02081-y

Heimer, L. (1978). "The olfactory cortex and the ventral striatum" in *Limbic mechanisms: The continuing evolution of the limbic system concept*. eds. K. E. Livingston and O. Hornykiewicz (Boston, MA: Springer US), 95–187.

Heimer, L., Zaborszky, L., Zahm, D. S., and Alheid, G. F. (1987). The ventral striatopallidothalamic projection: I. The striatopallidal link originating in the striatal parts of the olfactory tubercle. *J. Comp. Neurol.* 255, 571–591. doi: 10.1002/cne.902550409

Hosoya, Y., and Hirata, Y. (1974). The fine structure of the "dwarf-cell cap" of the olfactory tubercle in the rat's brain. *Arch. Histol. Jpn.* 36, 407–423. doi: 10.1679/aohc1950.36.407

Hummel, T., Whitcroft, K. L., Andrews, P., Altundag, A., Cinghi, C., Costanzo, R. M., et al. (2017). Position paper on olfactory dysfunction. *Rhinol. Suppl.* 54, 1–30. doi: 10.4193/Rhino16.248

Igarashi, K. M., Ieki, N., An, M., Yamaguchi, Y., Nagayama, S., Kobayakawa, K., et al. (2012). Parallel mitral and tufted cell pathways route distinct odor information to different targets in the olfactory cortex. *J. Neurosci.* 32, 7970–7985. doi: 10.1523/JNEUROSCI.0154-12.2012

Ikemoto, S. (2003). Involvement of the olfactory tubercle in cocaine reward: intracranial self-administration studies. *J. Neurosci.* 23, 9305–9311. doi: 10.1523/JNEUROSCI.23-28-09305.2003

Ikemoto, S. (2007). Dopamine reward circuitry: two projection systems from the ventral midbrain to the nucleus accumbens-olfactory tubercle complex. *Brain Res. Rev.* 56, 27–78. doi: 10.1016/j.brainresrev.2007.05.004

Ikemoto, S. (2010). Brain reward circuitry beyond the mesolimbic dopamine system: a neurobiological theory. *Neurosci. Biobehav. Rev.* 35, 129–150. doi: 10.1016/j.neubiorev.2010.02.001

Ikemoto, S., Qin, M., and Liu, Z. H. (2005). The functional divide for primary reinforcement of D-amphetamine lies between the medial and lateral ventral striatum: is the division of the accumbens core, shell, and olfactory tubercle valid? *J. Neurosci.* 25, 5061–5065. doi: 10.1523/JNEUROSCI.0892-05.2005

Keller, A., and Malaspina, D. (2013). Hidden consequences of olfactory dysfunction: a patient report series. *BMC Ear Nose Throat Disord.* 13:8. doi: 10.1186/1472-6815-13-8

Kiguchi, N., Ding, H., and Ko, M.-C. (2016). Central N/OFQ-NOP receptor system in pain modulation. *Adv. Pharmacol.* 75, 217–243. doi: 10.1016/bs.apha.2015.10.001

Kohli, P., Soler, Z. M., Nguyen, S. A., Muus, J. S., and Schlosser, R. J. (2016). The association between olfaction and depression: a systematic review. *Chem. Senses* 41, 479–486. doi: 10.1093/chemse/bjw061

Kringelbach, M. L. (2010). "The hedonic brain: a functional neuroanatomy of human pleasure" in *Pleasures of the brain*. ed. M. L. Kringelbach (New York, NY: Oxford University Press), 202–221.

Lawless, H. (1991). The sense of smell in food quality and sensory evaluation. *J. Food Qual.* 14, 33–60. doi: 10.1111/j.1745-4557.1991.tb00046.x

Le Moine, C., and Bloch, B. (1995). D1 and D2 dopamine receptor gene expression in the rat striatum: sensitive cRNA probes demonstrate prominent segregation of D1 and D2 mRNAs in distinct neuronal populations of the dorsal and ventral striatum. *J. Comp. Neurol.* 355, 418–426. doi: 10.1002/cne.903550308

Lee, D., Liu, L., and Root, C. M. (2023). Transformation of value signaling in a striatopallidal circuit. *eLife*. 12:RP90976. doi: 10.7554/elife.90976.1

Leon, M., and Woo, C. C. (2022). Olfactory loss is a predisposing factor for depression, while olfactory enrichment is an effective treatment for depression. *Front. Neurosci.* 16:1013363. doi: 10.3389/fnins.2022.1013363

Maegawa, A., Murata, K., Kuroda, K., Fujieda, S., and Fukazawa, Y. (2022). Cellular profiles of Prodynorphin and Preproenkephalin mRNA-expressing neurons in the anterior olfactory tubercle of mice. *Front. Neural Circuits* 16:908964. doi: 10.3389/fncir.2022.908964

Mansour, A., Fox, C. A., Burke, S., Meng, F., Thompson, R. C., Akil, H., et al. (1994). Mu, delta, and kappa opioid receptor mRNA expression in the rat CNS: an in situ hybridization study. *J. Comp. Neurol.* 350, 412–438. doi: 10.1002/cne.903500307

Mansour, A., Khachaturian, H., Lewis, M. E., Akil, H., and Watson, S. J. (1987). Autoradiographic differentiation of mu, delta, and kappa opioid receptors in the rat forebrain and midbrain. *J. Neurosci.* 7, 2445–2464

Mansour, A., Khachaturian, H., Lewis, M. E., Akil, H., and Watson, S. J. (1988). Anatomy of CNS opioid receptors. *Trends Neurosci.* 11, 308–314. doi: 10.1016/0166-2236(88)90093-8

Mansour, A., and Watson, S. J. (1993). "Anatomical distribution of opioid receptors in mammalians: An overview" in *Opioids*. eds. A. Herz, H. Akil and E. J. Simon (Berlin, Heidelberg: Springer Berlin Heidelberg), 79–105.

Marin, C., Alobid, I., Fuentes, M., López-Chacón, M., and Mullol, J. (2023). Olfactory dysfunction in mental illness. *Curr Allergy Asthma Rep* 23, 153–164. doi: 10.1007/s11882-023-01068-z

Martiros, N., Kapoor, V., Kim, S. E., and Murthy, V. N. (2022). Distinct representation of cue-outcome association by D1 and D2 neurons in the ventral striatum's olfactory tubercle. *eLife* 11:e75463. doi: 10.7554/eLife.75463

Merchenthaler, I., Maderdrut, J. L., Cianchetta, P., Shughrue, P., and Bronstein, D. (1997). In situ hybridization histochemical localization of prodynorphin messenger RNA in the central nervous system of the rat. *J. Comp. Neurol.* 384, 211–232. doi: 10.1002/(SICI)1096-9861(19970728)384:2<211::AID-CNE4>3.0.CO;2-4

Meunier, J. C., Mollereau, C., Toll, L., Suaudeau, C., Moisand, C., Alvinerie, P., et al. (1995). Isolation and structure of the endogenous agonist of opioid receptor-like ORL1 receptor. *Nature* 377, 532–535. doi: 10.1038/377532a0

Midroit, M., Chalençon, L., Renier, N., Milton, A., Thevenet, M., Sacquet, J., et al. (2021). Neural processing of the reward value of pleasant odorants. *Curr. Biol.* 31, 1592–1605.e9. doi: 10.1016/j.cub.2021.01.066

Millhouse, O. E., and Heimer, L. (1984). Cell configurations in the olfactory tubercle of the rat. *J. Comp. Neurol.* 228, 571–597. doi: 10.1002/cne.902280409

Millman, D. J., and Murthy, V. N. (2020). Rapid learning of odor-value Association in the Olfactory Striatum. *J. Neurosci.* 40, 4335–4347. doi: 10.1523/JNEUROSCI.2604-19.2020

Miwa, T., Ikeda, K., Ishibashi, T., Kobayashi, M., Kondo, K., Matsuwaki, Y., et al. (2019). Clinical practice guidelines for the management of olfactory dysfunction - secondary publication. *Auris Nasus Larynx* 46, 653–662. doi: 10.1016/j.anl.2019.04.002

Mollereau, C., Parmentier, M., Mailleux, P., Butour, J. L., Moisand, C., Chalon, P., et al. (1994). ORL1, a novel member of the opioid receptor family. Cloning, functional expression and localization. *FEBS Lett.* 341, 33–38. doi: 10.1016/0014-5793(94)80235-1

Morales, I., and Berridge, K. C. (2020). "Liking" and "wanting" in eating and food reward: brain mechanisms and clinical implications. *Physiol. Behav.* 227:113152. doi: 10.1016/j.physbeh.2020.113152

Murata, K. (2020). Hypothetical roles of the olfactory tubercle in odor-guided eating behavior. *Front. Neural Circuits* 14:577880. doi: 10.3389/fncir.2020.577880

Murata, K., Kanno, M., Ieki, N., Mori, K., and Yamaguchi, M. (2015). Mapping of learned odor-induced motivated behaviors in the mouse olfactory tubercle. *J. Neurosci.* 35, 10581–10599. doi: 10.1523/JNEUROSCI.0073-15.2015

Murata, K., Kinoshita, T., Fukazawa, Y., Kobayashi, K., Yamanaka, A., Hikida, T., et al. (2019). Opposing roles of dopamine receptor D1- and D2-expressing neurons in the anteromedial olfactory tubercle in Acquisition of Place Preference in mice. *Front. Behav. Neurosci.* 13:50. doi: 10.3389/fnbeh.2019.00050

Murofushi, W., Mori, K., Murata, K., and Yamaguchi, M. (2018). Functional development of olfactory tubercle domains during weaning period in mice. *Sci. Rep.* 8:13204. doi: 10.1038/s41598-018-31604-1

Oettl, L.-L., Scheller, M., Filosa, C., Wieland, S., Haag, F., Loeb, C., et al. (2020). Phasic dopamine reinforces distinct striatal stimulus encoding in the olfactory tubercle driving dopaminergic reward prediction. *Nat. Commun.* 11:3460. doi: 10.1038/s41467-020-17257-7

Olds, J. (1956). Pleasure centers in the brain. *Sci. Am.* 195, 105–117. doi: 10.1038/scientificamerican1056-105

Olds, J., and Milner, P. (1954). Positive reinforcement produced by electrical stimulation of septal area and other regions of rat brain. *J. Comp. Physiol. Psychol.* 47, 419–427. doi: 10.1037/h0058775

Parker, L. A., Maier, S., Rennie, M., and Crebolder, J. (1992). Morphine- and naltrexone-induced modification of palatability: analysis by the taste reactivity test. *Behav. Neurosci.* 106, 999–1010. doi: 10.1037/0735-7044.106.6.999

Parker, K. E., Pedersen, C. E., Gomez, A. M., Spangler, S. M., Walicki, M. C., Feng, S. Y., et al. (2019). A Paranigral VTA Nociceptin circuit that constrains motivation for reward. *Cell* 178, 653–671.e19. doi: 10.1016/j.cell.2019.06.034

Peciña, S., and Berridge, K. C. (2005). Hedonic hot spot in nucleus accumbens shell: where do mu-opioids cause increased hedonic impact of sweetness? *J. Neurosci.* 25, 11777–11786. doi: 10.1523/JNEUROSCI.2329-05.2005

Przewlocki, R. (2022). "Opioid peptides and their receptors" in *Neuroscience in the 21st century: From basic to clinical*. eds. D. W. Pfaff, N. D. Volkow and J. L. Rubenstein (Cham: Springer International Publishing).

Rochet, M., El-Hage, W., Richa, S., Kazour, F., and Atanasova, B. (2018). Depression, olfaction, and quality of life: a mutual relationship. *Brain Sci.* 8:80. doi: 10.3390/brainsci8050080

Saito, H., Nishizumi, H., Suzuki, S., Matsumoto, H., Ieki, N., Abe, T., et al. (2017). Immobility responses are induced by photoactivation of single glomerular species responsive to fox odour TMT. *Nat. Commun.* 8:16011. doi: 10.1038/ncomms16011

Sakamoto, N., Pearson, J., Shinoda, K., Alheid, G. F., Olmos, J. S.de, and Heimer, L. (1999). "Chapter I - the human basal forebrain. Part I. An overview," in *Handbook of chemical neuroanatomy*, eds. F. E. Bloom, A. Björklund and T. Hökfelt (Elsevier), Amsterdam.

Schultz, W. (1998). Predictive reward signal of dopamine neurons. *J. Neurophysiol.* 80, 1–27. doi: 10.1152/jn.1998.80.1.1

Schultz, W. (2016). Dopamine reward prediction-error signalling: a two-component response. *Nat. Rev. Neurosci.* 17, 183–195. doi: 10.1038/nrn.2015.26

Sha, M. F. R., Koga, Y., Murata, Y., Taniguchi, M., and Yamaguchi, M. (2023). Learning-dependent structural plasticity of intracortical and sensory connections to functional domains of the olfactory tubercle. *Front. Neurosci.* 17:1247375. doi: 10.3389/fnins.2023.1247375

Shepherd, G. (2011). *Neurogastronomy*. New York City, NY: Columbia University Press.

Shin, R., Qin, M., Liu, Z. H., and Ikemoto, S. (2008). Intracranial self-administration of MDMA into the ventral striatum of the rat: differential roles of the nucleus accumbens shell, core, and olfactory tubercle. *Psychopharmacology* 198, 261–270. doi: 10.1007/s00213-008-1131-x

Shiotani, K., Tanisumi, Y., Osako, Y., Murata, K., Hirokawa, J., Sakurai, Y., et al. (2024). An intra-oral flavor detection task in freely moving mice. *iScience* 27:108924. doi: 10.1016/j.isci.2024.108924

Smith, K. S., and Berridge, K. C. (2007). Opioid limbic circuit for reward: interaction between hedonic hotspots of nucleus accumbens and ventral pallidum. *J. Neurosci.* 27, 1594–1605. doi: 10.1523/JNEUROSCI.4205-06.2007

Steiner, J. E., Glaser, D., Hawilo, M. E., and Berridge, K. C. (2001). Comparative expression of hedonic impact: affective reactions to taste by human infants and other primates. *Neurosci. Biobehav. Rev.* 25, 53–74. doi: 10.1016/S0149-7634(00)00051-8

Taquet, M., Luciano, S., Geddes, J. R., and Harrison, P. J. (2021). Bidirectional associations between COVID-19 and psychiatric disorder: retrospective cohort studies of 62 354 COVID-19 cases in the USA. *Lancet Psychiatry* 8, 130–140. doi: 10.1016/S2215-0366(20)30462-4

Walaas, S. I., and Ouimet, C. C. (1989). The ventral striatopallidal complex: an immunocytochemical analysis of medium-sized striatal neurons and striatopallidal fibers in the basal forebrain of the rat. *Neuroscience* 28, 663–672. doi: 10.1016/0306-4522(89)90013-4

Wesson, D. W., and Wilson, D. A. (2011). Sniffing out the contributions of the olfactory tubercle to the sense of smell: hedonics, sensory integration, and more? *Neurosci. Biobehav. Rev.* 35, 655–668. doi: 10.1016/j.neubiorev.2010.08.004

Winkelmeier, L., Filosa, C., Hartig, R., Scheller, M., Sack, M., Reinwald, J. R., et al. (2022). Striatal hub of dynamic and stabilized prediction coding in forebrain networks for olfactory reinforcement learning. *Nat. Commun.* 13:3305. doi: 10.1038/s41467-022-30978-1

Wise, R. A. (1980). The dopamine synapse and the notion of 'pleasure centers' in the brain. *Trends Neurosci.* 3, 91–95. doi: 10.1016/0166-2236(80)90035-1

Wise, R. A. (2004). Dopamine, learning and motivation. *Nat. Rev. Neurosci.* 5, 483–494. doi: 10.1038/nrn1406

Wise, R. A. (2008). Dopamine and reward: the anhedonia hypothesis 30 years on. *Neurotox. Res.* 14, 169–183. doi: 10.1007/BF03033808

Wise, R. A., Spindler, J., deWit, H., and Gerberg, G. J. (1978). Neuroleptic-induced "anhedonia" in rats: pimozide blocks reward quality of food. *Science* 201, 262–264. doi: 10.1126/science.566469

Xiong, A., and Wesson, D. W. (2016). Illustrated review of the ventral Striatum's olfactory tubercle. *Chem. Senses* 41, 549–555. doi: 10.1093/chemse/bjw069

Yamaguchi, M. (2017). Functional sub-circuits of the olfactory system viewed from the olfactory bulb and the olfactory tubercle. *Front. Neuroanat.* 11:33. doi: 10.3389/fnana.2017.00033

Yung, K. K., Bolam, J. P., Smith, A. D., Hersch, S. M., Ciliax, B. J., and Levey, A. I. (1995). Immunocytochemical localization of D1 and D2 dopamine receptors in the basal ganglia of the rat: light and electron microscopy. *Neuroscience* 65, 709–730. doi: 10.1016/0306-4522(94)00536-E

Zhang, Y.-F., Vargas Cifuentes, L., Wright, K. N., Bhattarai, J. P., Mohrhardt, J., Fleck, D., et al. (2021). Ventral striatal islands of Calleja neurons control grooming in mice. *Nat. Neurosci.* 24, 1699–1710. doi: 10.1038/s41593-021-00952-z

Zhang, Y.-F., Wu, J., Wang, Y., Johnson, N. L., Bhattarai, J. P., Li, G., et al. (2023). Ventral striatal islands of Calleja neurons bidirectionally mediate depression-like behaviors in mice. *Nat. Commun.* 14:6887. doi: 10.1038/s41467-023-42662-z

Zhang, Z., Liu, Q., Wen, P., Zhang, J., Rao, X., Zhou, Z., et al. (2017a). Activation of the dopaminergic pathway from VTA to the medial olfactory tubercle generates odor-preference and reward. *eLife* 6:e25423. doi: 10.7554/eLife.25423

Zhang, Z., Zhang, H., Wen, P., Zhu, X., Wang, L., Liu, Q., et al. (2017b). Whole-brain mapping of the inputs and outputs of the medial part of the olfactory tubercle. *Front. Neural Circuits* 11:52. doi: 10.3389/fncir.2017.00052

Zhou, L., Furuta, T., and Kaneko, T. (2003). Chemical organization of projection neurons in the rat accumbens nucleus and olfactory tubercle. *Neuroscience* 120, 783–798. doi: 10.1016/S0306-4522(03)00326-9

frontiers | Frontiers in Neural Circuits

TYPE Mini Review
PUBLISHED 06 June 2024
DOI 10.3389/fncir.2024.1406218

OPEN ACCESS

EDITED BY
Kensaku Mori,
RIKEN, Japan

REVIEWED BY
Tomohiko Matsuo,
Kansai Medical University, Japan

*CORRESPONDENCE
Shu Kikuta
✉ kikuta.shu@nihon-u.ac.jp

RECEIVED 24 March 2024
ACCEPTED 20 May 2024
PUBLISHED 06 June 2024

CITATION
Kikuta S, Nagayama S and Hasegawa-Ishii S (2024) Structures and functions of the normal and injured human olfactory epithelium.
Front. Neural Circuits 18:1406218.
doi: 10.3389/fncir.2024.1406218

Structures and functions of the normal and injured human olfactory epithelium

Shu Kikuta[1]*, Shin Nagayama[2] and Sanae Hasegawa-Ishii[3]

[1]Department of Otolaryngology-Head and Neck Surgery, Faculty of Medicine, Nihon University, Tokyo, Japan, [2]Department of Neurobiology and Anatomy, McGovern Medical School at The University of Texas Health Science Center at Houston, Houston, TX, United States, [3]Pathology Research Team, Kyorin University, Tokyo, Japan

The olfactory epithelium (OE) is directly exposed to environmental agents entering the nasal cavity, leaving OSNs prone to injury and degeneration. The causes of olfactory dysfunction are diverse and include head trauma, neurodegenerative diseases, and aging, but the main causes are chronic rhinosinusitis (CRS) and viral infections. In CRS and viral infections, reduced airflow due to local inflammation, inflammatory cytokine production, release of degranulated proteins from eosinophils, and cell injury lead to decreased olfactory function. It is well known that injury-induced loss of mature OSNs in the adult OE causes massive regeneration of new OSNs within a few months through the proliferation and differentiation of progenitor basal cells that are subsequently incorporated into olfactory neural circuits. Although normal olfactory function returns after injury in most cases, prolonged olfactory impairment and lack of improvement in olfactory function in some cases poses a major clinical problem. Persistent inflammation or severe injury in the OE results in morphological changes in the OE and respiratory epithelium and decreases the number of mature OSNs, resulting in irreversible loss of olfactory function. In this review, we discuss the histological structure and distribution of the human OE, and the pathogenesis of olfactory dysfunction associated with CRS and viral infection.

KEYWORDS

olfactory epithelium, olfactory dysfunction, respiratory metaplasia, chronic rhinosinusitis, viral infection

Introduction

The sense of smell is extensively used in everyday life, from the perception of danger signals, such as smoke and noxious gases to the detection of spoiled food and the psychosocial effects of food (Croy et al., 2014; Rebholz et al., 2020).

The etiology of olfactory dysfunction varies widely and includes chronic rhinosinusitis (CRS), upper respiratory tract viral infection, head trauma, allergic rhinitis, and aging. However, among these, CRS and viral infection account for about 60% of all cases (Seiden, 2004; Rombaux et al., 2016). In CRS and viral infections, olfactory perception is reduced due to decreased airflow caused by mucosal swelling and polyp formation,

as well as by injury to olfactory sensory neurons (OSNs) by pathogens such as viruses, bacteria, eosinophil granule products, and inflammatory cytokines (Kern, 2000; Seiden, 2004; Wrobel and Leopold, 2004).

Different types of olfactory epithelium (OE) injury and OE regeneration after injury have been reported (Imamura and Hasegawa-Ishii, 2016). Irrespective of the type of OE injury, tissue regeneration is usually complete within 1–2 months after injury (Kikuta et al., 2015; Imamura and Hasegawa-Ishii, 2016). However, some patients with CRS experience a decreased sense of smell despite having an open olfactory cleft and normal nasal airflow, or show no improvement in olfactory function despite polyp removal (Apter et al., 1992; Kikuta et al., 2016). Similarly, olfactory dysfunction caused by viral infections takes time to improve and may persist for months to a year and more (Liu et al., 2023). Therefore, understanding the anatomical or histological characteristics of the human OE, as well as the histological changes and pathophysiology after injury, is essential for developing appropriate treatment strategies for prolonged olfactory dysfunction.

This review describes the histological features of the human OE and discusses the pathogenesis of olfactory dysfunction associated with CRS and viral infections, as well as persistent olfactory dysfunction.

Odor reception in humans

The ciliary membranes of the OSN contain olfactory receptors (ORs), which are responsible for odor detection. ORs are members of the G-protein-coupled seven-transmembrane receptor family and constitute the largest gene family (Buck and Axel, 1991; Buck, 2000) in the human genome with nearly 400 OR-coding genes (Zozulya et al., 2001; Young et al., 2002; Zhang and Firestein, 2002; Godfrey et al., 2004; Malnic et al., 2004). The OE is divided into zones I, II, III, and IV (from the dorsomedial to ventral region), which contain densely packed OSNs.

In many vertebrates including humans, OR genes are classified into two classes, class I and class II, based on differences in their amino acid sequences (Glusman et al., 2001; Imai et al., 2010). OSNs expressing class I genes (class I OSNs) are distributed within zone 1, corresponding to the dorsomedial region of the OE, while OSNs expressing class II genes (class II OSNs) are widely distributed in zones II-IV (Mori and Sakano, 2011). The presence of a zone structure in the OE has not been confirmed in human, but in the macaque, a higher primate phylogenetically related to humans, OSNs expressing specific ORs are scattered throughout the OE but are restricted to specific zones, suggesting the presence of a zone structure (Ressler et al., 1993; Horowitz et al., 2014; Mori and Sakano, 2021).

Cellular composition of the human OE

The human OE lacks the distinct laminar structure observed in the mouse OE. The OSN density is very low and the OSNs are sparsely distributed (Omura et al., 2022). Furthermore, OSN density is not uniform; mature OSNs are abundant and present at a relatively high density near the cribriform plate (dorsal to the nasal cavity), but their density gradually decreases with distance from the cribriform plate (**Figure 1**).

The human OE is composed of five cell types: immature or mature OSNs, sustentacular cells (SCs), microvillar cells (MVCs), tubular cells of Bowman's glands, and basal cells (BCs) (Moran et al., 1982; Morrison and Costanzo, 1990; Féron et al., 1998; Kalinke et al., 2011).

OSNs are bipolar neurons that extend one dendrite on the surface of the OE to the mucus layer and project one unmyelinated axon to the olfactory bulb (OB) (Yee et al., 2010). Individual OSN dendrites have olfactory vesicles at their tips and are attached to 10–15 non-motile, elongated cilia. The axons of OSNs cross the basal membrane and merge to form non-myelinated nerve bundles called fascicles (Jafek, 1983; Morrison and Costanzo, 1990).

SCs are tall cells with a nucleus on the apical side that extend their projections from the surface of the epithelium to the basal layer (Jafek, 1983; Morrison and Costanzo, 1990). Two or more neighboring SCs wrap around the dendrites of OSNs, structurally and electrically isolating the OSN (Bryche et al., 2020). They are also involved in supplying glucose to OSNs and maintaining ion balance within the OE (Vogalis et al., 2005; Lemons et al., 2017; O'leary et al., 2019; Ualiyeva et al., 2020). Furthermore, SCs defend the OE by phagocytosing and detoxifying olfactory toxins using metabolic enzymes such as cytochrome P450 and glutathione S-transferase. They also contribute to local immunity by producing inflammatory cytokines when local inflammation persists (Jafek, 1983).

MVCs are non-neuronal cells with rigid microvilli and some express TRPM5. TRPM5-postive cells express choline acetyltransferase and the vesicular acetylcholine transporter (Ogura et al., 2011; Saunders et al., 2014) and stimulate SCs by releasing acetylcholine, which protects the OE by promoting the metabolism and removal of olfactory toxicants (Ogura et al., 2011; Genovese and Tizzano, 2018).

Bowman's glands are spaced across the basal membrane at regular intervals and are responsible for the production and secretion of mucus, which covers the luminal surface of the OE.

BCs are spherical stem cells that differentiate into OSNs (Morrison and Costanzo, 1990). Unlike in mice, there is no distinction between horizontal basal cells (HBCs) and globose basal cells (GBCs) in human (Graziadei and Graziadei, 1979; Holbrook et al., 2011), but morphologically, human BCs resemble GBCs in mice (Hahn et al., 2005).

Distribution of the human OE

In human, the proportion of the nasal cavity occupied by the OE is markedly lower than that in rodents; in rats, the OE accounts for about 50% of the nasal cavity, whereas in human, it occupies about 3% (Gross et al., 1982).

The human nasal cavity consists of three nasal concha (superior, middle, and inferior). The OE is localized in the superior nasal concha, particularly in a limited area corresponding to its upper anterior two-thirds (Omura et al., 2022). In mice, the respiratory epithelia (RE) and OE are clearly distinguishable and are not histologically intermingled. However, in human, the

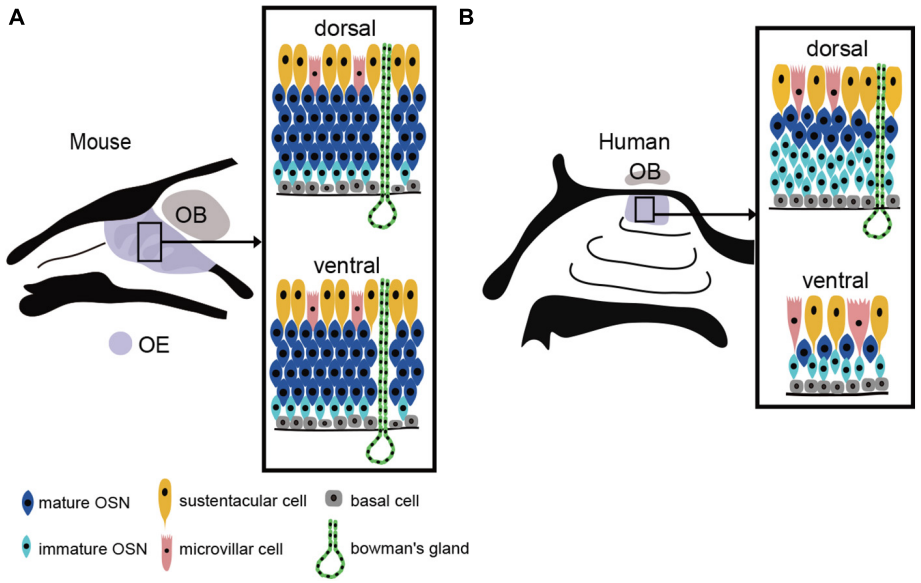

FIGURE 1
OE structure and the distribution of the OE in mouse and human. **(A)** Uniform distribution of the mouse OE. In mouse, OSNs are arranged in a laminar pattern and are evenly distributed in both the dorsal and ventral regions of the OE. OSN, olfactory sensory neuron; OE, olfactory epithelium; OB, olfactory bulb; BC, basal cell; MVC, microvillar cell; SC, sustentacular cell. **(B)** Heterogeneous distribution of the human OE. The human OE lacks a well-defined stratified structure and is generally more sparsely distributed. It also has a lower density of OSNs than mouse. The dorsal surface of the OE contains more mature OSNs, while the ventral surface contains fewer mature OSNs.

boundary between RE and OE is unclear and is characterized by patchy areas of mixed RE and OE (Nakashima et al., 1984; Morrison and Costanzo, 1990; Omura et al., 2022). Areas of OE degeneration and respiratory epithelialization increase with age (Nakashima et al., 1984; Paik et al., 1992), but do not necessarily correlate with loss of olfactory function, because OE degeneration and OSN reduction are also observed in adults with normal olfactory function (Nakashima et al., 1984; Omura et al., 2022).

OE injury is associated with CRS

CRS is defined as a chronic inflammatory disease of the sinus mucosa that persists for more than 3 months (Fokkens et al., 2020), and is the most frequent etiology of olfactory dysfunction (Rombaux et al., 2016). Approximately 60–80% of CRS patients experience a decreased sense of smell (Banglawala et al., 2014). CRS phenotypes are classified into two types: CRS with nasal polyps (CRSwNP) and CRS without nasal polyps (CRSsNP) (Fokkens et al., 2020). CRSwNP causes a high rate of olfactory dysfunction and is associated with eosinophil-driven inflammation, eosinophilic cationic proteins (ECPs), and injury to OSNs by inflammatory cytokines released from eosinophils (Epstein et al., 2008; Li et al., 2010; Acharya and Ackerman, 2014; Yan X. et al., 2020).

In animal models of CRS, in addition to the release of inflammatory cytokines (such as TNF-a and interferon-c) from SCs and OSN cell death, BC proliferation and differentiation are arrested, resulting in neuroepithelium remodeling and the replacement of neuroepithelium with RE (Jafek et al., 2002; Yee et al., 2009; Lane et al., 2010; Goncalves and Goldstein, 2016; Choi and Goldstein, 2018; Marin et al., 2022). Furthermore, prolonged inflammation increases c-Jun N-terminal kinase activity, a promoter of apoptosis, within the OSN and local eosinophil infiltration (Victores et al., 2018). Intranasal administration of ECP to mouse OEs for 2 weeks results in OSN apoptosis and thinning of OEs, similar to previous observations in human (Kikuta et al., 2021). Interestingly, ECP induces apoptosis not only in OSNs but also in some BCs. In fact, histological analysis of human OEs frequently showed massive infiltration of inflammatory cells, such as lymphocytes, macrophages, and eosinophils, and reduced numbers of OSNs and squamous metaplasia (Kern, 2000; Rombaux et al., 2016; Wu et al., 2020; Marin et al., 2022). Consistent with the location of direct injury to the OE, axonal bundles may fail to extend from the OE beyond the basal membrane and are observed within the OE as tangles of nerve fibers (Holbrook et al., 2005). Indeed, the degree of the OE inflammation and eosinophil infiltration correlates closely with reduced olfaction in CRS patients (Soler et al., 2009; Kashiwagi et al., 2019). Furthermore, persistent inflammation leads to increased mucus secretion from Bowman's glands, and disruption of the balance of potassium and sodium ion concentrations in the mucus reduces olfactory reception (Selvaraj et al., 2012; Rombaux et al., 2016).

OE injury following viral infection

Post-viral olfactory dysfunction (PVOD) is the second most common type of olfactory dysfunction and accounts for about 30% of patients with olfactory dysfunction (Seiden, 2004). Many viruses have been reported to infect OSNs, including influenza A virus (Van Riel et al., 2014), herpes virus (Esiri, 1982), paramyxo virus

(Van Riel et al., 2015), parainfluenza virus (Van Riel et al., 2015), adeno virus (Yamada et al., 2009), and Japanese encephalitis virus (Yamada et al., 2009), based on the analysis of samples and tissues obtained from experimentally inoculated animals. These viruses utilize various receptors such as the sialic acid (e.g., influenza virus, parainfluenza virus, and adenovirus) (Connor et al., 1994; Villar and Barroso, 2006) and heparan sulfate receptors (e.g., herpes virus and Japanese encephalitis virus) (Eisenberg et al., 2012; Perera-Lecoin et al., 2013) to enter the OSN. Although these receptors are similarly expressed in human OSNs, it is still unclear whether these viruses directly enter human OSNs. Seasonal influenza virus A (H3N2), pandemic influenza virus A (H1N1), and highly pathogenic avian influenza virus A (H5N1) have been shown to attach to the apical side of human OSNs, and it is suggested that these viruses can infect human OSNs (Van Riel et al., 2015). Biopsies of the olfactory mucosa of patients with PVOD show OE degeneration and morphological changes in the RE (Seiden, 2004). In addition, in the mucosal intrinsic layer below the basal membrane, OSN axons are prominently replaced by collagen fibers (Holbrook et al., 2005).

Olfactory tests employing combinations of odors with different chemical structures has been used to characterize OE damage in patients with PVOD (Kikuta et al., 2023). Olfactory stimulation with β-phenylethyl alcohol, γ-undecalactone, and isovaleric acid, known as the T&T olfactometer test in Japan, allows PVOD patients to discriminate between different odors, while odor stimulation with prosultiamine, known as the intravenous olfactory (IVO) test in Japan, does not allow odor discrimination. The former group of odors activates both class I and class II OSNs, while the latter odor primarily activates class I OSNs (Takahashi et al., 2004; Igarashi and Mori, 2005; Mori and Sakano, 2011; Kikuta et al., 2023). Thus, it has been suggested that virus-induced OE injury may occur heterogeneously in a cell type-dependent manner, with preferential injury to class I OSNs (Kikuta et al., 2023).

Coronavirus disease 2019 (COVID-19) is caused by SARS-CoV-2, but the mechanism of infection differs from that of other viruses that cause the common cold (Belouzard et al., 2012). In addition to the angiotensin-converting enzyme 2 (ACE2) receptor, transmembrane protease serine 2 (TMPRSS2) activity is required for SARS-CoV-2 infection (Hoffmann et al., 2020). Co-expression of ACE2 and TMPRSS2 has been observed only in SCs, Bowman's glands, MVs, and BCs, but not in OSNs (Cooper et al., 2020). In golden hamsters, SARS-CoV-2 infects intestinal cells but not OSNs (Bryche et al., 2020). OE samples from COVID-19 patients have been found to contain coronavirus antigens in cells within the OE, and although the type of infected cell has not been identified, their shape and antigen localization suggest that the virus targets non-OSN cells (Cantuti-Castelvetri et al., 2020). However, infection of non-OSN cells increases inflammatory cytokines in the human OE (Torabi et al., 2020), and in experiments using golden hamsters, shedding of OSN cilia was observed histologically (Bryche et al., 2020).

Discussion

The human OE lacks a regular laminar structure, and a mixture of the RE within the OE is observed even in people with a normal sense of smell. With respect to OSN density, the dorsal OE has a higher density of mature olfactory OSNs than the ventral OE (**Figure 1**). The areas of low OSN density in the ventral OE coincide with areas of high airflow, suggesting that airflow is a chronic mechanical stimulus affecting the OE and that the epithelium in this area of the OE may be degenerative. Since mice show no such differences in OSN density, it is possible that the human OE is especially susceptible to injury from airflow stimulation.

The olfactory loss associated with CRS is caused by mechanical obstruction of the olfactory cleft by polyps in the nasal cavity and/or edematous changes in the nasal mucosa, resulting in reduced airflow to the OE (Kern, 2000; Banglawala et al., 2014; Rosenfeld et al., 2015; Gudis and Soler, 2016). In addition, direct injury to the OE by inflammatory cytokines and degranulation proteins from eosinophils also reduce olfactory function (Aiba and Nakai, 1991; Doty and Mishra, 2001; Lane et al., 2010). In mouse experiments, repetitive injury, such as chronic inflammation and aging have been reported to activate HBCs, which depletes their potential to produce OSNs (Håglin et al., 2020). Eventually, HBCs produce respiratory epithelial cells instead of OSNs by altering retinoic acid metabolism and are involved in respiratory transformation (Håglin et al., 2020). Thus, severe inflammation and BC damage to the OE leads to prolonged olfactory dysfunction by reducing the number of functional OSNs and promoting respiratory transformation (**Figure 2**). However, since respiratory transformation is observed even in adults with normal olfactory function, it is unclear to what extent OE degeneration must progress before olfactory loss becomes apparent. Rats can detect food odors even after more than 90% of the olfactory mucosa has degenerated (Youngentob et al., 1997), suggesting that the peripheral olfactory system has significant reserve capacity. If this is also the case in humans, patients who are aware of their decreased sense of smell may be in the final stages of extensive OE degeneration.

It is unclear whether differences exist in olfactory dysfunction between aging and CRS, but histological changes in OB may produce differences in olfactory function. Human studies have reported that OB volume, the thickness of the glomerular layer, and the number of mitral cells and glomeruli decrease with age (Bhatnagar et al., 1987; Meisami et al., 1998; Yousem et al., 1998). Furthermore, cell division in the mouse subventricular zone decreases with age, but granule cell density in the OB increases with age (Enwere et al., 2004; Richard et al., 2010), suggesting that granule cell turnover in the OB is reduced and granule cells live longer in aging animals (Sui et al., 2012). Decreased turnover of granule cells with aging may reduce the likelihood of neural circuit reorganization. On the other hand, persistent nasal inflammation in mice treated with lipopolysaccharide causes marked atrophy of the OB and more intense damage in tufted cells than in mitral cells (Hasegawa-Ishii et al., 2019, 2020). Furthermore, peripheral immune cells have been shown to transiently infiltrate the olfactory nerve layer, the glomerular layer, and the external plexiform layer, suggesting that chronic inflammation, including CRS, may also induce histological changes in the OB (Asano et al., 2022). A detailed study of the relationship between olfactory function and histological changes in the OB may reveal differences in olfactory dysfunction between aging and chronic inflammation.

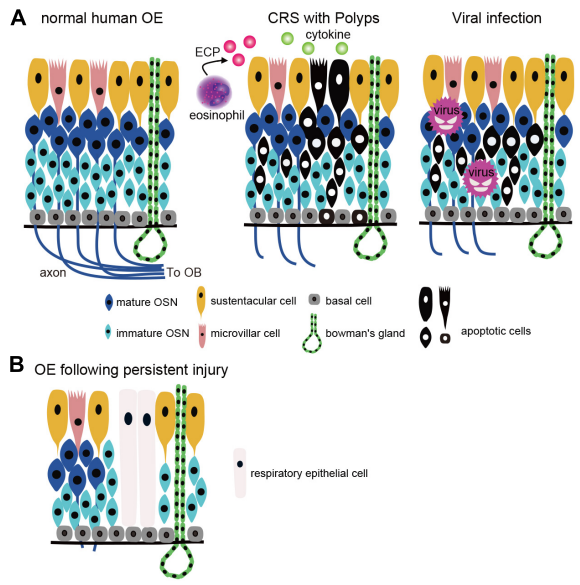

FIGURE 2
OE injury caused by CRS and viral infection. **(A)** Two types of the OE injury. Left, normal human OE: OSN axons extend to the OB and form synapses with projection neurons in the OB. Middle, CRS with polyps: OE is injured by inflammatory cytokines and eosinophilic cationic proteins from eosinophils, resulting in apoptotic cell death. Right, viral infection: viruses (except COVID-19) infect OSNs directly and cause apoptotic cell death. CRS, chronic rhinosinusitis; OSN, olfactory sensory neuron; OE, olfactory epithelium; OB, olfactory bulb; BC, basal cell; MVC, microvillar cell; SC, sustentacular cell; ECP, eosinophilic cationic protein. **(B)** Histological changes after OE injury. Persistent inflammation and basal cell damage in the OE can inhibit axonal elongation of newly generated OSNs and/or result in a transition from olfactory to respiratory epithelium, leading to prolonged olfactory dysfunction.

In contrast to olfactory loss caused by reduced airflow, which can be improved by surgical treatment, no established treatment currently exists for OE injury. Therefore, to develop a treatment strategy, it is important to determine whether olfactory dysfunction is due solely to reduced airflow or to concomitant OE damage. The IVO test measures the time (defined as latency) and duration of odor perception after intravenous administration of prosultiamine and is widely used in clinical practice. Reduced airflow does not prolong onset latency in the IVO test, but OE injury does, and prolonged latency correlates with a reduction in the number of mature OSNs (Kikuta et al., 2016). Accordingly, OE injury is likely in cases with prolonged latency, and it is estimated that approximately 60% of CRS cases are complicated by OE injury (Kikuta et al., 2016).

The main mechanism of PVOD is decreased airflow caused by swelling of the olfactory cleft mucosa by local inflammation, increased mucus production, and changes in mucus composition (Akerlund et al., 1995; Schlosser et al., 2016; Victores et al., 2018; Cooper et al., 2020). Thus, in most cases, olfactory function recovers with the disappearance of nasal symptoms (Hummel et al., 1998a,b; Zhao et al., 2014), but in some patients, olfactory loss may persist for more than a year. This is presumably due to the OE damage caused by viral infection or the local immune response (Duncan and Seiden, 1995; Welge-Lüssen and Wolfensberger, 2006; Cavazzana et al., 2018). Viruses that invade OSNs can be transported to the olfactory bulb (OB) via OSN axons. However, OSN apoptosis, a defense mechanism against OE damage, can prevent this propagation (Mori et al., 2002, 2004; Kanaya et al., 2014). When mice are infected intranasally with influenza H3N1 virus, apoptosis of the infected OSNs inhibits the spread of the viruses. Conversely, infection with herpes viruses does not induce OSN apoptosis and the viruses can spread to the OB (Mori et al., 2002). Thus, OSN apoptosis may act positively by preventing the entry of viruses into the central nervous system via the OSN, but may also act negatively by promoting olfactory dysfunction.

Olfactory dysfunction caused by COVID-19 is less severe than that caused by other common cold viruses, with olfaction restored in about 70% of cases within 2 weeks after the onset of initial symptoms (Lechien et al., 2020; Yan C. H. et al., 2020). The fact that COVID-19 infects SCs, MVs, and BCs, but not OSNs may be one factor contributing to the favorable prognosis of olfactory dysfunction in COVID-19 patients (Belouzard et al., 2012; Cooper et al., 2020).

Regardless of the type of virus, severe injury to OSNs and other components of the OE can result in incomplete regeneration, and similar to the histopathology of CRS, degeneration and morphological changes in the OE are observed (Seiden, 2004; **Figure 2**). The histological changes that occur during the regenerative process may be one of the factors contributing to the prolongation of olfactory symptoms.

Since a variety of immune cells are known to be involved in inflammatory responses in the OE, research into the types and activities of the immune cells involved will be required to elucidate the mechanisms before efficacious treatments for olfactory dysfunction can be developed. However, various therapeutic interventions with variable efficacy are available, including steroid administration, which has anti-inflammatory effects, for the treatment of olfactory dysfunction caused by CRS (Rudmik et al., 2013; Chang and Glezer, 2018). Biological therapies such as anti-IgE monoclonal antibody, IL-4 receptor alpha subunit antagonist, and anti-IL-5 are promising treatments for nasal polyps and could significantly improve olfaction (Gevaert et al., 2013; Bachert et al., 2016, 2017). In addition, localized intranasal administration of insulin in mice has been reported to suppress OSN apoptosis and promote OE regeneration, suggesting that insulin could have potential as a novel therapeutic agent (Kikuta et al., 2021; Kuboki et al., 2021). In human, insulin nasal spray has also been reported to be effective against COVID-19-induced olfactory dysfunction (Cherobin et al., 2023). Understanding the histological architecture of the human OE and the pathophysiology of each disease will be fundamental in establishing new therapies for controlling inflammation and preventing irreversible OE damage.

Author contribution

SK: Conceptualization, Data curation, Funding acquisition, Project administration, Validation, Writing–original draft,

Writing–review and editing, Methodology. SN: Writing–review and editing. SH-I: Writing–review and editing.

Funding

The author(s) declare financial support was received for the research, authorship, and/or publication of the article. This work was supported by JSPS KAKENHI Grant Numbers JP23K08930 (SK), and the Takeda Science Foundation (SK).

Acknowledgments

We apologize to those whose work was not included here due to space limitations

Conflict of interest

The authors declare that the research was conducted in the absence of any commercial or financial relationships that could be construed as a potential conflict of interest.

Publisher's note

References

Acharya, K. R., and Ackerman, S. J. (2014). Eosinophil granule proteins: Form and function. *J. Biol. Chem.* 289, 17406–17415. doi: 10.1074/jbc.R113.546218

Aiba, T., and Nakai, Y. (1991). Influence of experimental rhino-sinusitis on olfactory epithelium. *Acta Otolaryngol. Suppl.* 486, 184–192. doi: 10.3109/00016489109134995

Akerlund, A., Bende, M., and Murphy, C. (1995). Olfactory threshold and nasal mucosal changes in experimentally induced common cold. *Acta Otolaryngol.* 115, 88–92. doi: 10.3109/00016489509133353

Apter, A. J., Mott, A. E., Cain, W. S., Spiro, J. D., and Barwick, M. C. (1992). Olfactory loss and allergic rhinitis. *J. Allergy Clin. Immunol.* 90, 670–680. doi: 10.1016/0091-6749(92)90141-N

Asano, H., Hasegawa-Ishii, S., Arae, K., Obara, A., Laumet, G., Dantzer, R., et al. (2022). Infiltration of peripheral immune cells into the olfactory bulb in a mouse model of acute nasal inflammation. *J. Neuroimmunol.* 368:577897. doi: 10.1016/j.jneuroim.2022.577897

Bachert, C., Mannent, L., Naclerio, R. M., Mullol, J., Ferguson, B. J., Gevaert, P., et al. (2016). Effect of subcutaneous dupilumab on nasal polyp burden in patients with chronic sinusitis and nasal polyposis: A randomized clinical trial. *JAMA* 315, 469–479. doi: 10.1001/jama.2015.19330

Bachert, C., Sousa, A. R., Lund, V. J., Scadding, G. K., Gevaert, P., Nasser, S., et al. (2017). Reduced need for surgery in severe nasal polyposis with mepolizumab: Randomized trial. *J. Allergy Clin. Immunol.* 140:1024–1031.e1014. doi: 10.1016/j.jaci.2017.05.044

Banglawala, S. M., Oyer, S. L., Lohia, S., Psaltis, A. J., Soler, Z. M., and Schlosser, R. J. (2014). Olfactory outcomes in chronic rhinosinusitis with nasal polyposis after medical treatments: A systematic review and meta-analysis. *Int. Forum Allergy Rhinol.* 4, 986–994. doi: 10.1002/alr.21373

Belouzard, S., Millet, J. K., Licitra, B. N., and Whittaker, G. R. (2012). Mechanisms of coronavirus cell entry mediated by the viral spike protein. *Viruses* 4, 1011–1033. doi: 10.3390/v4061011

Bhatnagar, K. P., Kennedy, R. C., Baron, G., and Greenberg, R. A. (1987). Number of mitral cells and the bulb volume in the aging human olfactory bulb: A quantitative morphological study. *Anat. Rec.* 218, 73–87. doi: 10.1002/ar.1092180112

Bryche, B., St Albin, A., Murri, S., Lacôte, S., Pulido, C., Ar Gouilh, M., et al. (2020). Massive transient damage of the olfactory epithelium associated with infection of sustentacular cells by SARS-CoV-2 in golden Syrian hamsters. *Brain Behav. Immun.* 89, 579–586. doi: 10.1016/j.bbi.2020.06.032

Buck, L. B. (2000). The molecular architecture of odor and pheromone sensing in mammals. *Cell* 100, 611–618. doi: 10.1016/S0092-8674(00)80698-4

Buck, L., and Axel, R. (1991). A novel multigene family may encode odorant receptors: A molecular basis for odor recognition. *Cell* 65, 175–187. doi: 10.1016/0092-8674(91)90418-X

Cantuti-Castelvetri, L., Ojha, R., Pedro, L. D., Djannatian, M., Franz, J., Kuivanen, S., et al. (2020). Neuropilin-1 facilitates SARS-CoV-2 cell entry and infectivity. *Science* 370, 856–860. doi: 10.1126/science.abd2985

Cavazzana, A., Larsson, M., Münch, M., Hähner, A., and Hummel, T. (2018). Postinfectious olfactory loss: A retrospective study on 791 patients. *Laryngoscope* 128, 10–15. doi: 10.1002/lary.26606

Chang, S. Y., and Glezer, I. (2018). The balance between efficient anti-inflammatory treatment and neuronal regeneration in the olfactory epithelium. *Neural Regen. Res.* 13, 1711–1714. doi: 10.4103/1673-5374.238605

Cherobin, G. B., Guimarães, R. E. S., De Paula Gomes, M. C., Vasconcelos, L. O. G., and De Abreu, L. N. (2023). Intranasal insulin for the treatment of persistent post-COVID-19 olfactory dysfunction. *Otolaryngol. Head Neck Surg.* 169, 719–724. doi: 10.1002/ohn.352

Choi, R., and Goldstein, B. J. (2018). Olfactory epithelium: Cells, clinical disorders, and insights from an adult stem cell niche. *Laryngosc. Invest. Otolaryngol.* 3, 35–42. doi: 10.1002/lio2.135

Connor, R. J., Kawaoka, Y., Webster, R. G., and Paulson, J. C. (1994). Receptor specificity in human, avian, and equine H2 and H3 influenza virus isolates. *Virology* 205, 17–23. doi: 10.1006/viro.1994.1615

Cooper, K. W., Brann, D. H., Farruggia, M. C., Bhutani, S., Pellegrino, R., Tsukahara, T., et al. (2020). COVID-19 and the chemical Senses: Supporting players take center stage. *Neuron* 107, 219–233. doi: 10.1016/j.neuron.2020.06.032

Croy, I., Nordin, S., and Hummel, T. (2014). Olfactory disorders and quality of life–an updated review. *Chem. Senses* 39, 185–194. doi: 10.1093/chemse/bjt072

Doty, R. L., and Mishra, A. (2001). Olfaction and its alteration by nasal obstruction, rhinitis, and rhinosinusitis. *Laryngoscope* 111, 409–423. doi: 10.1097/00005537-200103000-00008

Duncan, H. J., and Seiden, A. M. (1995). Long-term follow-up of olfactory loss secondary to head trauma and upper respiratory tract infection. *Arch. Otolaryngol. Head Neck Surg.* 121, 1183–1187. doi: 10.1001/archotol.1995.01890100087015

Eisenberg, R. J., Atanasiu, D., Cairns, T. M., Gallagher, J. R., Krummenacher, C., and Cohen, G. H. (2012). Herpes virus fusion and entry: A story with many characters. *Viruses* 4, 800–832. doi: 10.3390/v4050800

Enwere, E., Shingo, T., Gregg, C., Fujikawa, H., Ohta, S., and Weiss, S. (2004). Aging results in reduced epidermal growth factor receptor signaling, diminished olfactory neurogenesis, and deficits in fine olfactory discrimination. *J. Neurosci.* 24, 8354–8365. doi: 10.1523/JNEUROSCI.2751-04.2004

Epstein, V. A., Bryce, P. J., Conley, D. B., Kern, R. C., and Robinson, A. M. (2008). Intranasal Aspergillus fumigatus exposure induces eosinophilic inflammation and olfactory sensory neuron cell death in mice. *Otolaryngol. Head Neck Surg.* 138, 334–339. doi: 10.1016/j.otohns.2007.11.029

Esiri, M. M. (1982). Herpes simplex encephalitis. An immunohistological study of the distribution of viral antigen within the brain. *J. Neurol. Sci.* 54, 209–226. doi: 10.1016/0022-510X(82)90183-6

Féron, F., Perry, C., Mcgrath, J. J., and Mackay-Sim, A. (1998). New techniques for biopsy and culture of human olfactory epithelial neurons. *Arch. Otolaryngol. Head Neck Surg.* 124, 861–866. doi: 10.1001/archotol.124.8.861

Fokkens, W. J., Lund, V. J., Hopkins, C., Hellings, P. W., Kern, R., Reitsma, S., et al. (2020). European position paper on Rhinosinusitis and nasal polyps 2020. *Rhinology* 58, 1–464. doi: 10.4193/Rhin20.401

Genovese, F., and Tizzano, M. (2018). Microvillous cells in the olfactory epithelium express elements of the solitary chemosensory cell transduction signaling cascade. *PLoS One* 13:e0202754. doi: 10.1371/journal.pone.0202754

Gevaert, P., Calus, L., Van Zele, T., Blomme, K., De Ruyck, N., Bauters, W., et al. (2013). Omalizumab is effective in allergic and nonallergic patients with nasal polyps and asthma. *J Allergy Clin. Immunol.* 131:110–116.e111. doi: 10.1016/j.jaci.2012.07.047

Glusman, G., Yanai, I., Rubin, I., and Lancet, D. (2001). The complete human olfactory subgenome. *Genome Res.* 11, 685–702. doi: 10.1101/gr.171001

Godfrey, P. A., Malnic, B., and Buck, L. B. (2004). The mouse olfactory receptor gene family. *Proc. Natl. Acad. Sci. U.S.A.* 101, 2156–2161. doi: 10.1073/pnas.0308051100

Goncalves, S., and Goldstein, B. J. (2016). Pathophysiology of olfactory disorders and potential treatment strategies. *Curr. Otorhinolaryngol. Rep.* 4, 115–121. doi: 10.1007/s40136-016-0113-5

Graziadei, P. P., and Graziadei, G. A. (1979). Neurogenesis and neuron regeneration in the olfactory system of mammals. I. Morphological aspects of differentiation and structural organization of the olfactory sensory neurons. *J. Neurocytol.* 8, 1–18. doi: 10.1007/BF01206454

Gross, E. A., Swenberg, J. A., Fields, S., and Popp, J. A. (1982). Comparative morphometry of the nasal cavity in rats and mice. *J. Anat.* 135, 83–88.

Gudis, D. A., and Soler, Z. M. (2016). Chronic rhinosinusitis-related smell loss: Medical and surgical treatment efficacy. *Curr. Otorhinolaryngol. Rep.* 4, 142–147. doi: 10.1007/s40136-016-0114-4

Håglin, S., Berghard, A., and Bohm, S. (2020). Increased retinoic acid catabolism in olfactory sensory neurons activates dormant tissue-specific stem cells and accelerates age-related metaplasia. *J. Neurosci.* 40, 4116–4129. doi: 10.1523/JNEUROSCI.2468-19.2020

Hahn, C. G., Han, L. Y., Rawson, N. E., Mirza, N., Borgmann-Winter, K., Lenox, R. H., et al. (2005). In vivo and in vitro neurogenesis in human olfactory epithelium. *J. Comp. Neurol.* 483, 154–163. doi: 10.1002/cne.20424

Hasegawa-Ishii, S., Imamura, F., Nagayama, S., Murata, M., and Shimada, A. (2020). Differential effects of nasal inflammation and odor deprivation on layer-specific degeneration of the mouse olfactory bulb. *eNeuro* 7:ENEURO.0403-19.2020. doi: 10.1523/ENEURO.0403-19.2020

Hasegawa-Ishii, S., Shimada, A., and Imamura, F. (2019). Neuroplastic changes in the olfactory bulb associated with nasal inflammation in mice. *J. Allergy Clin. Immunol.* 143:978–989.e973. doi: 10.1016/j.jaci.2018.09.028

Hoffmann, M., Kleine-Weber, H., Schroeder, S., Krüger, N., Herrler, T., Erichsen, S., et al. (2020). SARS-CoV-2 cell entry depends on ACE2 and TMPRSS2 and is blocked by a clinically proven protease inhibitor. *Cell* 181:271–280.e278. doi: 10.1016/j.cell.2020.02.052

Holbrook, E. H., Leopold, D. A., and Schwob, J. E. (2005). Abnormalities of axon growth in human olfactory mucosa. *Laryngoscope* 115, 2144–2154. doi: 10.1097/01.MLG.0000181493.83661.CE

Holbrook, E. H., Wu, E., Curry, W. T., Lin, D. T., and Schwob, J. E. (2011). Immunohistochemical characterization of human olfactory tissue. *Laryngoscope* 121, 1687–1701. doi: 10.1002/lary.21856

Horowitz, L. F., Saraiva, L. R., Kuang, D., Yoon, K. H., and Buck, L. B. (2014). Olfactory receptor patterning in a higher primate. *J. Neurosci.* 34, 12241–12252. doi: 10.1523/JNEUROSCI.1779-14.2014

Hummel, T., Rothbauer, C., Barz, S., Grosser, K., Pauli, E., and Kobal, G. (1998a). Olfactory function in acute rhinitis. *Ann. N. Y. Acad. Sci.* 855, 616–624. doi: 10.1111/j.1749-6632.1998.tb10632.x

Hummel, T., Rothbauer, C., Pauli, E., and Kobal, G. (1998b). Effects of the nasal decongestant oxymetazoline on human olfactory and intranasal trigeminal function in acute rhinitis. *Eur. J. Clin. Pharmacol.* 54, 521–528. doi: 10.1007/s002280050507

Igarashi, K. M., and Mori, K. (2005). Spatial representation of hydrocarbon odorants in the ventrolateral zones of the rat olfactory bulb. *J. Neurophysiol.* 93, 1007–1019. doi: 10.1152/jn.00873.2004

Imai, T., Sakano, H., and Vosshall, L. B. (2010). Topographic mapping–the olfactory system. *Cold Spring Harb. Perspect. Biol.* 2:a001776. doi: 10.1101/cshperspect.a001776

Imamura, F., and Hasegawa-Ishii, S. (2016). Environmental toxicants-induced immune responses in the olfactory mucosa. *Front. Immunol.* 7:475. doi: 10.3389/fimmu.2016.00475

Jafek, B. W. (1983). Ultrastructure of human nasal mucosa. *Laryngoscope* 93, 1576–1599. doi: 10.1288/00005537-198312000-00011

Jafek, B. W., Murrow, B., Michaels, R., Restrepo, D., and Linschoten, M. (2002). Biopsies of human olfactory epithelium. *Chem. Senses* 27, 623–628. doi: 10.1093/chemse/27.7.623

Kalinke, U., Bechmann, I., and Detje, C. N. (2011). Host strategies against virus entry via the olfactory system. *Virulence* 2, 367–370. doi: 10.4161/viru.2.4.16138

Kanaya, K., Kondo, K., Suzukawa, K., Sakamoto, T., Kikuta, S., Okada, K., et al. (2014). Innate immune responses and neuroepithelial degeneration and regeneration in the mouse olfactory mucosa induced by intranasal administration of Poly(I:C). *Cell Tissue Res.* 357, 279–299. doi: 10.1007/s00441-014-1848-2

Kashiwagi, T., Tsunemi, Y., Akutsu, M., Nakajima, I., and Haruna, S. (2019). Postoperative evaluation of olfactory dysfunction in eosinophilic chronic rhinosinusitis - comparison of histopathological and clinical findings. *Acta Otolaryngol.* 139, 881–889. doi: 10.1080/00016489.2019.1654131

Kern, R. C. (2000). Chronic sinusitis and anosmia: Pathologic changes in the olfactory mucosa. *Laryngoscope* 110, 1071–1077. doi: 10.1097/00005537-200007000-00001

Kikuta, S., Han, B., and Yamasoba, T. (2023). Heterogeneous damage to the olfactory epithelium in patients with post-viral olfactory dysfunction. *J. Clin. Med.* 12:5007. doi: 10.3390/jcm12155007

Kikuta, S., Kuboki, A., and Yamasoba, T. (2021). Protective effect of insulin in mouse nasal mucus against olfactory epithelium injury. *Front. Neural Circ.* 15:803769. doi: 10.3389/fncir.2021.803769

Kikuta, S., Matsumoto, Y., Kuboki, A., Nakayama, T., Asaka, D., Otori, N., et al. (2016). Longer latency of sensory response to intravenous odor injection predicts olfactory neural disorder. *Sci. Rep.* 6:35361. doi: 10.1038/srep35361

Kikuta, S., Sakamoto, T., Nagayama, S., Kanaya, K., Kinoshita, M., Kondo, K., et al. (2015). Sensory deprivation disrupts homeostatic regeneration of newly generated olfactory sensory neurons after injury in adult mice. *J. Neurosci.* 35, 2657–2673. doi: 10.1523/JNEUROSCI.2484-14.2015

Kuboki, A., Kikuta, S., Otori, N., Kojima, H., Matsumoto, I., Reisert, J., et al. (2021). Insulin-dependent maturation of newly generated olfactory sensory neurons after injury. *eNeuro* 8:ENEURO.0168-21.2021. doi: 10.1523/ENEURO.0168-21.2021

Lane, A. P., Turner, J., May, L., and Reed, R. (2010). A genetic model of chronic rhinosinusitis-associated olfactory inflammation reveals reversible functional impairment and dramatic neuroepithelial reorganization. *J. Neurosci.* 30, 2324–2329. doi: 10.1523/JNEUROSCI.4507-09.2010

Lechien, J. R., Chiesa-Estomba, C. M., De Siati, D. R., Horoi, M., Le Bon, S. D., Rodriguez, A., et al. (2020). Olfactory and gustatory dysfunctions as a clinical presentation of mild-to-moderate forms of the coronavirus disease (COVID-19): A multicenter European study. *Eur. Arch. Otorhinolaryngol.* 277, 2251–2261. doi: 10.1007/s00405-020-05965-1

Lemons, K., Fu, Z., Aoudé, I., Ogura, T., Sun, J., Chang, J., et al. (2017). Lack of TRPM5-expressing microvillous cells in mouse main olfactory epithelium leads to impaired odor-evoked responses and olfactory-guided behavior in a challenging chemical environment. *eNeuro* 4:ENEURO.0135-17.2017. doi: 10.1523/ENEURO.0135-17.2017

Li, L., Walker, T. L., Zhang, Y., Mackay, E. W., and Bartlett, P. F. (2010). Endogenous interferon gamma directly regulates neural precursors in the non-inflammatory brain. *J. Neurosci.* 30, 9038–9050. doi: 10.1523/JNEUROSCI.5691-09.2010

Liu, Z. Y., Vaira, L. A., Boscolo-Rizzo, P., Walker, A., and Hopkins, C. (2023). Post-viral olfactory loss and parosmia. *BMJ Med.* 2:e000382. doi: 10.1136/bmjmed-2022-000382

Malnic, B., Godfrey, P. A., and Buck, L. B. (2004). The human olfactory receptor gene family. *Proc. Natl. Acad. Sci. U.S.A.* 101, 2584–2589. doi: 10.1073/pnas.0307882100

Marin, C., Hummel, T., Liu, Z., and Mullol, J. (2022). Chronic Rhinosinusitis and COVID-19. *J. Allergy Clin. Immunol. Pract.* 10, 1423–1432. doi: 10.1016/j.jaip.2022.03.003

Meisami, E., Mikhail, L., Baim, D., and Bhatnagar, K. P. (1998). Human olfactory bulb: Aging of glomeruli and mitral cells and a search for the accessory olfactory bulb. *Ann. N. Y. Acad. Sci.* 855, 708–715. doi: 10.1111/j.1749-6632.1998.tb10649.x

Moran, D. T., Rowley, J. C. III, and Jafek, B. W. (1982). Electron microscopy of human olfactory epithelium reveals a new cell type: The microvillar cell. *Brain Res.* 253, 39–46. doi: 10.1016/0006-8993(82)90671-0

Mori, I., Goshima, F., Imai, Y., Kohsaka, S., Sugiyama, T., Yoshida, T., et al. (2002). Olfactory receptor neurons prevent dissemination of neurovirulent influenza A virus into the brain by undergoing virus-induced apoptosis. *J. Gen. Virol.* 83, 2109–2116. doi: 10.1099/0022-1317-83-9-2109

Mori, I., Nishiyama, Y., Yokochi, T., and Kimura, Y. (2004). Virus-induced neuronal apoptosis as pathological and protective responses of the host. *Rev. Med. Virol.* 14, 209–216. doi: 10.1002/rmv.426

Mori, K., and Sakano, H. (2011). How is the olfactory map formed and interpreted in the mammalian brain? *Annu. Rev. Neurosci.* 34, 467–499. doi: 10.1146/annurev-neuro-112210-112917

Mori, K., and Sakano, H. (2021). Olfactory circuitry and behavioral decisions. *Annu. Rev. Physiol.* 83, 231–256. doi: 10.1146/annurev-physiol-031820-092824

Morrison, E. E., and Costanzo, R. M. (1990). Morphology of the human olfactory epithelium. *J. Comp. Neurol.* 297, 1–13. doi: 10.1002/cne.902970102

Nakashima, T., Kimmelman, C. P., and Snow, J. B. Jr. (1984). Structure of human fetal and adult olfactory neuroepithelium. *Arch. Otolaryngol.* 110, 641–646. doi: 10.1001/archotol.1984.00800360013003

Ogura, T., Szebenyi, S. A., Krosnowski, K., Sathyanesan, A., Jackson, J., and Lin, W. (2011). Cholinergic microvillous cells in the mouse main olfactory epithelium and effect of acetylcholine on olfactory sensory neurons and supporting cells. *J. Neurophysiol.* 106, 1274–1287. doi: 10.1152/jn.00186.2011

O'leary, C. E., Schneider, C., and Locksley, R. M. (2019). Tuft cells-systemically dispersed sensory epithelia integrating immune and neural circuitry. *Annu. Rev. Immunol.* 37, 47–72. doi: 10.1146/annurev-immunol-042718-041505

Omura, K., Han, B., Nishijima, H., Aoki, S., Ebihara, T., Kondo, K., et al. (2022). Heterogeneous distribution of mature olfactory sensory neurons in human olfactory epithelium. *Int. Forum Allergy Rhinol.* 12, 266–277. doi: 10.1002/alr.22885

Paik, S. I., Lehman, M. N., Seiden, A. M., Duncan, H. J., and Smith, D. V. (1992). Human olfactory biopsy. The influence of age and receptor distribution. *Arch. Otolaryngol. Head Neck Surg.* 118, 731–738. doi: 10.1001/archotol.1992.01880070061012

Perera-Lecoin, M., Meertens, L., Carnec, X., and Amara, A. (2013). Flavivirus entry receptors: An update. *Viruses* 6, 69–88. doi: 10.3390/v6010069

Rebholz, H., Braun, R. J., Ladage, D., Knoll, W., Kleber, C., and Hassel, A. W. (2020). Loss of olfactory function-early indicator for Covid-19, other viral infections and neurodegenerative disorders. *Front. Neurol.* 11:569333. doi: 10.3389/fneur.2020.569333

Ressler, K. J., Sullivan, S. L., and Buck, L. B. (1993). A zonal organization of odorant receptor gene expression in the olfactory epithelium. *Cell* 73, 597–609. doi: 10.1016/0092-8674(93)90145-G

Richard, M. B., Taylor, S. R., and Greer, C. A. (2010). Age-induced disruption of selective olfactory bulb synaptic circuits. *Proc. Natl. Acad. Sci. U.S.A.* 107, 15613–15618. doi: 10.1073/pnas.1007931107

Rombaux, P., Huart, C., Levie, P., Cingi, C., and Hummel, T. (2016). Olfaction in Chronic rhinosinusitis. *Curr. Allergy Asthma Rep.* 16:41. doi: 10.1007/s11882-016-0617-6

Rosenfeld, R. M., Piccirillo, J. F., Chandrasekhar, S. S., Brook, I., Ashok Kumar, K., Kramper, M., et al. (2015). Clinical practice guideline (update): Adult sinusitis. *Otolaryngol. Head Neck Surg.* 152, S1–S39. doi: 10.1177/0194599815572097

Rudmik, L., Hoy, M., Schlosser, R. J., Harvey, R. J., Welch, K. C., Lund, V., et al. (2013). Topical therapies in the management of chronic rhinosinusitis: An evidence-based review with recommendations. *Int. Forum Allergy Rhinol.* 3, 281–298. doi: 10.1002/alr.21096

Saunders, C. J., Christensen, M., Finger, T. E., and Tizzano, M. (2014). Cholinergic neurotransmission links solitary chemosensory cells to nasal inflammation. *Proc. Natl. Acad. Sci. U.S.A.* 111, 6075–6080. doi: 10.1073/pnas.1402251111

Schlosser, R. J., Mulligan, J. K., Hyer, J. M., Karnezis, T. T., Gudis, D. A., and Soler, Z. M. (2016). Mucous cytokine levels in chronic rhinosinusitis-associated olfactory loss. *JAMA Otolaryngol. Head Neck Surg.* 142, 731–737. doi: 10.1001/jamaoto.2016.0927

Seiden, A. M. (2004). Postviral olfactory loss. *Otolaryngol. Clin. North Am.* 37, 1159–1166. doi: 10.1016/j.otc.2004.06.007

Selvaraj, S., Liu, K., Robinson, A. M., Epstein, V. A., Conley, D. B., Kern, R. C., et al. (2012). In vivo determination of mouse olfactory mucus cation concentrations in normal and inflammatory states. *PLoS One* 7:e39600. doi: 10.1371/journal.pone.0039600

Soler, Z. M., Sauer, D. A., Mace, J., and Smith, T. L. (2009). Relationship between clinical measures and histopathologic findings in chronic rhinosinusitis. *Otolaryngol. Head Neck Surg.* 141, 454–461. doi: 10.1016/j.otohns.2009.06.085

Sui, Y., Horne, M. K., and Stanić, D. (2012). Reduced proliferation in the adult mouse subventricular zone increases survival of olfactory bulb interneurons. *PLoS One* 7:e31549. doi: 10.1371/journal.pone.0031549

Takahashi, Y. K., Kurosaki, M., Hirono, S., and Mori, K. (2004). Topographic representation of odorant molecular features in the rat olfactory bulb. *J. Neurophysiol.* 92, 2413–2427. doi: 10.1152/jn.00236.2004

Torabi, A., Mohammadbagheri, E., Akbari Dilmaghani, N., Bayat, A. H., Fathi, M., Vakili, K., et al. (2020). Proinflammatory cytokines in the olfactory mucosa result in COVID-19 induced anosmia. *ACS Chem. Neurosci.* 11, 1909–1913. doi: 10.1021/acschemneuro.0c00249

Ualiyeva, S., Hallen, N., Kanaoka, Y., Ledderose, C., Matsumoto, I., Junger, W. G., et al. (2020). Airway brush cells generate cysteinyl leukotrienes through the ATP sensor P2Y2. *Sci. Immunol.* 5:eaax7224. doi: 10.1126/sciimmunol.aax7224

Van Riel, D., Leijten, L. M., Verdijk, R. M., Geurtsvankessel, C., Van Der Vries, E., Van Rossum, A. M., et al. (2014). Evidence for influenza virus CNS invasion along the olfactory route in an immunocompromised infant. *J. Infect Dis.* 210, 419–423. doi: 10.1093/infdis/jiu097

Van Riel, D., Verdijk, R., and Kuiken, T. (2015). The olfactory nerve: A shortcut for influenza and other viral diseases into the central nervous system. *J. Pathol.* 235, 277–287. doi: 10.1002/path.4461

Victores, A. J., Chen, M., Smith, A., and Lane, A. P. (2018). Olfactory loss in chronic rhinosinusitis is associated with neuronal activation of c-Jun N-terminal kinase. *Int. Forum Allergy Rhinol.* 8, 415–420. doi: 10.1002/alr.22053

Villar, E., and Barroso, I. M. (2006). Role of sialic acid-containing molecules in paramyxovirus entry into the host cell: A minireview. *Glycoconj. J.* 23, 5–17. doi: 10.1007/s10719-006-5433-0

Vogalis, F., Hegg, C. C., and Lucero, M. T. (2005). Ionic conductances in sustentacular cells of the mouse olfactory epithelium. *J. Physiol.* 562, 785–799. doi: 10.1113/jphysiol.2004.079228

Welge-Lüssen, A., and Wolfensberger, M. (2006). Olfactory disorders following upper respiratory tract infections. *Adv. Otorhinolaryngol.* 63, 125–132. doi: 10.1159/000093758

Wrobel, B. B., and Leopold, D. A. (2004). Clinical assessment of patients with smell and taste disorders. *Otolaryngol. Clin. North Am.* 37, 1127–1142. doi: 10.1016/j.otc.2004.06.010

Wu, D., Li, Y., Bleier, B. S., and Wei, Y. (2020). Superior turbinate eosinophilia predicts olfactory decline in patients with chronic rhinosinusitis. *Ann. Allergy Asthma Immunol.* 125:304–310.e301. doi: 10.1016/j.anai.2020.04.027

Yamada, M., Nakamura, K., Yoshii, M., Kaku, Y., and Narita, M. (2009). Brain lesions induced by experimental intranasal infection of Japanese encephalitis virus in piglets. *J. Comp. Pathol.* 141, 156–162. doi: 10.1016/j.jcpa.2009.04.006

Yan, X., Whitcroft, K. L., and Hummel, T. (2020). Olfaction: Sensitive indicator of inflammatory burden in chronic rhinosinusitis. *Laryngosc. Invest. Otolaryngol.* 5, 992–1002. doi: 10.1002/lio2.485

Yan, C. H., Faraji, F., Prajapati, D. P., Boone, C. E., and Deconde, A. S. (2020). Association of chemosensory dysfunction and COVID-19 in patients presenting with influenza-like symptoms. *Int. Forum Allergy Rhinol.* 10, 806–813. doi: 10.1002/alr.22579

Yee, K. K., Pribitkin, E. A., Cowart, B. J., Rosen, D., Feng, P., and Rawson, N. E. (2009). Analysis of the olfactory mucosa in chronic rhinosinusitis. *Ann. N. Y. Acad. Sci.* 1170, 590–595. doi: 10.1111/j.1749-6632.2009.04364.x

Yee, K. K., Pribitkin, E. A., Cowart, B. J., Vainius, A. A., Klock, C. T., Rosen, D., et al. (2010). Neuropathology of the olfactory mucosa in chronic rhinosinusitis. *Am. J. Rhinol. Allergy* 24, 110–120. doi: 10.2500/ajra.2010.24.3435

Young, J. M., Friedman, C., Williams, E. M., Ross, J. A., Tonnes-Priddy, L., and Trask, B. J. (2002). Different evolutionary processes shaped the mouse and human olfactory receptor gene families. *Hum. Mol. Genet.* 11, 535–546. doi: 10.1093/hmg/11.5.535

Youngentob, S. L., Schwob, J. E., Sheehe, P. R., and Youngentob, L. M. (1997). Odorant threshold following methyl bromide-induced lesions of the olfactory epithelium. *Physiol. Behav.* 62, 1241–1252. doi: 10.1016/S0031-9384(97)00301-6

Yousem, D. M., Geckle, R. J., Bilker, W. B., and Doty, R. L. (1998). Olfactory bulb and tract and temporal lobe volumes. Normative data across decades. *Ann. N. Y. Acad. Sci.* 855, 546–555. doi: 10.1111/j.1749-6632.1998.tb10624.x

Zhang, X., and Firestein, S. (2002). The olfactory receptor gene superfamily of the mouse. *Nat. Neurosci.* 5, 124–133. doi: 10.1038/nn800

Zhao, K., Jiang, J., Pribitkin, E. A., Dalton, P., Rosen, D., Lyman, B., et al. (2014). Conductive olfactory losses in chronic rhinosinusitis? A computational fluid dynamics study of 29 patients. *Int. Forum Allergy Rhinol.* 4, 298–308. doi: 10.1002/alr.21272

Zozulya, S., Echeverri, F., and Nguyen, T. (2001). The human olfactory receptor repertoire. *Genome Biol.* 2:Research0018. doi: 10.1186/gb-2001-2-6-research0018

frontiers | Frontiers in Neural Circuits

TYPE Mini Review
PUBLISHED 12 June 2024
DOI 10.3389/fncir.2024.1427378

OPEN ACCESS

EDITED BY
Kensaku Mori,
RIKEN, Japan

REVIEWED BY
Fumiaki Imamura,
Penn State Milton S. Hershey Medical Center, United States
Kazunari Miyamichi,
RIKEN Center for Biosystems Dynamics Research (BDR), Japan

*CORRESPONDENCE
Akio Tsuboi
✉ akio@fbs.osaka-u.ac.jp

RECEIVED 03 May 2024
ACCEPTED 24 May 2024
PUBLISHED 12 June 2024

CITATION
Tsuboi A (2024) A specific olfactory bulb interneuron subtype Tpbg/5T4 generated at embryonic and neonatal stages.
Front. Neural Circuits 18:1427378.
doi: 10.3389/fncir.2024.1427378

A specific olfactory bulb interneuron subtype Tpbg/5T4 generated at embryonic and neonatal stages

Akio Tsuboi*

Graduate School of Pharmaceutical Sciences, Osaka University, Toyonaka, Japan

Various mammals have shown that sensory stimulation plays a crucial role in regulating the development of diverse structures, such as the olfactory bulb (OB), cerebral cortex, hippocampus, and retina. In the OB, the dendritic development of excitatory projection neurons like mitral/tufted cells is influenced by olfactory experiences. Odor stimulation is also essential for the dendritic development of inhibitory OB interneurons, such as granule and periglomerular cells, which are continuously produced in the ventricular-subventricular zone throughout life. Based on the morphological and molecular features, OB interneurons are classified into several subtypes. The role for each interneuron subtype in the control of olfactory behavior remains poorly understood due to lack of each specific marker. Among the several OB interneuron subtypes, a specific granule cell subtype, which expresses the oncofetal trophoblast glycoprotein (Tpbg or 5T4) gene, has been reported to be required for odor detection and discrimination behavior. This review will primarily focus on elucidating the contribution of different granule cell subtypes, including the Tpbg/5T4 subtype, to olfactory processing and behavior during the embryonic and adult stages.

KEYWORDS

Tpbg/5T4, olfactory bulb, granule cells, activity-dependent development, fate map

1 Introduction

Sensory inputs are essential for the development and plastic modification of neural circuits in vertebrates (Lepousez et al., 2013). Olfactory sensory neurons (OSNs) detect individual odorants by expressing corresponding odorant receptors in OSNs on the olfactory epithelium (Mori and Sakano, 2011, 2021). The convergence of OSN axons on specific glomeruli within the olfactory bulb (OB) enables the activation of distinct neuronal circuits and facilitates the dendritic development of specific types of inhibitory interneurons through excitatory projection neurons in the OB (Mori and Sakano, 2011, 2021; Lepousez et al., 2013). Neural progenitors like transit-amplifying cells and neuroblasts are generated from neural stem cells (NSCs) in the ventricular-subventricular zone (V/SVZ) near the lateral ventricles, not only during early development but also in adulthood (Obernier and Alvarez-Buylla, 2019). These neuroblasts migrate through the rostral migratory stream (RMS) to the OB, where they mature into inhibitory interneurons that release gamma-aminobutyric acid (GABA), including granule cells (GCs) and periglomerular cells (PGCs) (Lledo and Valley, 2016) (Figure 1A). Within the OB, GCs and PGCs establish reciprocal connections with

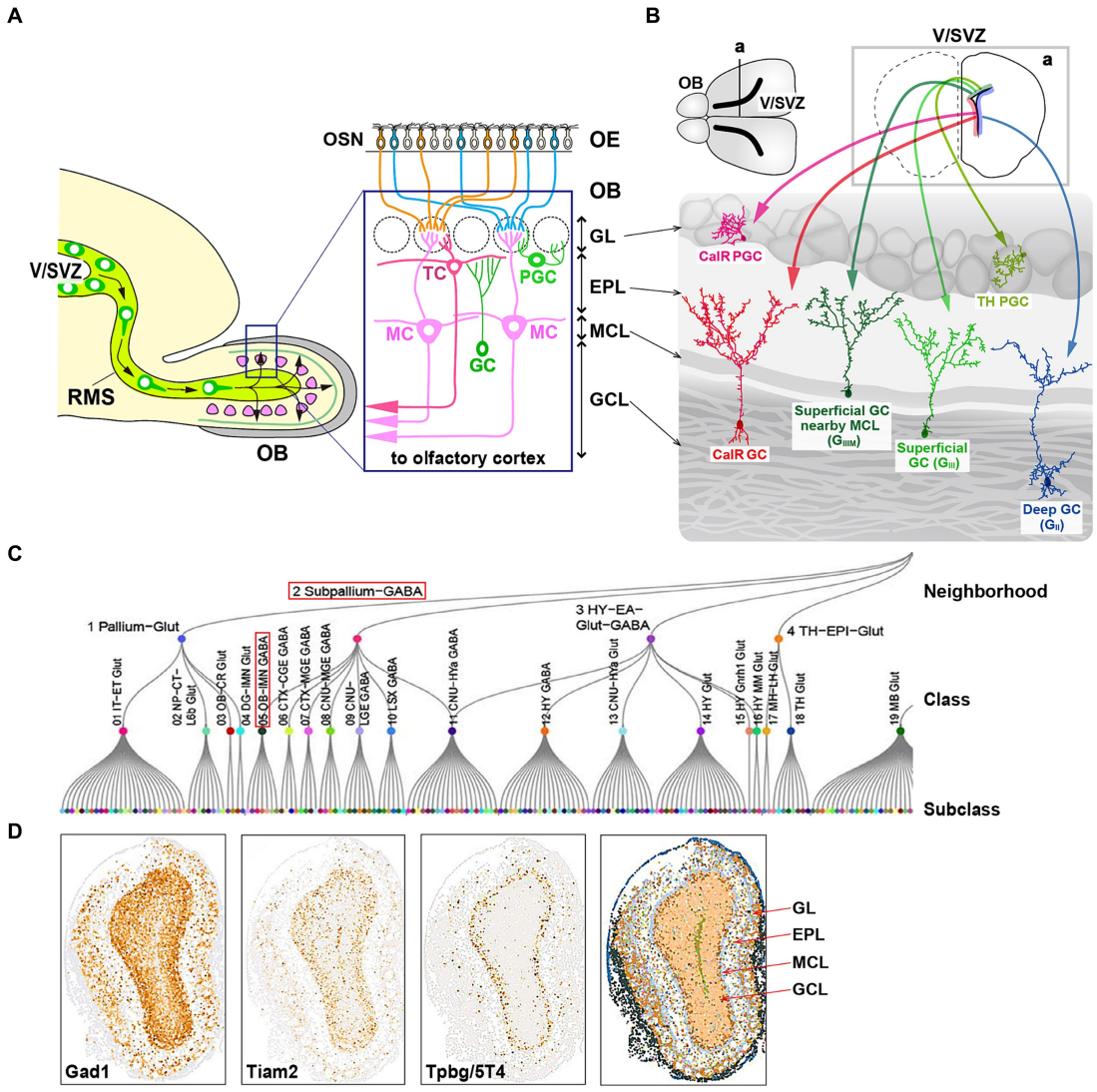

FIGURE 1
Cell fate of multiple subtypes of olfactory bulb (OB) interneurons. **(A)** The mammalian OB is structured into distinct layers: the glomerular layer (GL), external plexiform layer (EPL), mitral cell layer (MCL), and granule cell layer (GCL). Olfactory sensory signals from olfactory sensory neurons (OSN) in the olfactory epithelium (OE) are transmitted by excitatory projection neurons such as mitral cells (MCs) and tufted cells (TCs) to inhibitory interneurons like granule cells (GCs) and periglomerular cells (PGCs). **(B)** Distribution of neural stem cells in the ventricular-subventricular zone (V/SVZ) in specific areas. Adult OB interneurons are generated in different subregions of the V/SVZ (upper row; a), migrate through the rostral migratory stream (RMS), and subsequently differentiate into distinct subtypes of mature interneurons in the OB, including GCs (G_{II}, G_{III}, G_{IIIM}, and CalR) and PGCs (TH and CalR). **(C)** Transcriptome cell type classification of whole mouse brain. A transcriptome classification tree is organized into 7 neighborhoods, 34 classes, and 338 subclasses. The subpallium-GABA neighborhood comprises 7 classes, one of which is the OB-IMN-GABA class containing 30 subclasses. Notably, the Frmd7 Gaba_1 subclass includes Tpbg/5T4 and Lgr6 genes. The content in panel **(C)** is adapted from the extended data figure in the study by Yao et al. (2023), with permission from the journal. **(D)** Spatial expression of the OBINH-3-[Gad1_Tpbg_Tiam2] subcluster genes in the mouse OB, based on the "Spatial-Portal" website (https://www.spatial-atlas.net/Brain/spatial.html). This site presents a spatial molecular atlas of the adult mouse central nervous system generated by Xiao Wang's lab with STARmap PLUS, an imaging-based targeted *in situ* sequencing platform (Shi et al., 2023).

glutamatergic excitatory projection neurons like mitral cells (MCs) and tufted cells (TCs) (Figure 1A). GCs and PGCs receive glutamatergic inputs from MC/TC dendrites and return GABAergic outputs to them (Lledo and Valley, 2016). The survival and integration of newly born OB interneurons into existing neural networks are affected by odor-evoked neural activity (Lledo and Valley, 2016). Furthermore, olfactory deprivation and odor-rich environments, respectively, hinder and enhance the dendritic branching and spine formation of newborn OB interneurons (Bressan and Saghatelyan, 2021). Despite advancements in this area, the specific role of a particular subtype of newborn interneurons in modulating olfactory behaviors remains unclear due to the absence of distinct markers for them.

2 Embryonic and adult neurogenesis

The generation of OB interneurons in the rodent brain occurs in the V/SVZ during both embryonic and adult stages. Neurogenesis in the embryonic phase commences with neuroepithelial cells localized

in the V/SVZ, which undergo a transformation into radial glial cells (RGCs) (Obernier and Alvarez-Buylla, 2019). This transition involves the loss of certain epithelial characteristics by neuroepithelial cells, such as tight junctions, and the acquisition of astroglial features marked by the expression of various astrocytic markers. Multiple intrinsic signals work in concert to facilitate this shift and ensure neurogenesis during embryonic development (Obernier and Alvarez-Buylla, 2019). Initially, RGCs function as fate-restricted neural progenitors, giving rise to transit-amplifying precursors or neuroblasts through symmetric mitosis, which further differentiate into neurons (Merkle and Alvarez-Buylla, 2006). In later stages of development, RGCs also generate glial cells like astrocytes and oligodendrocytes (Merkle and Alvarez-Buylla, 2006).

During the adult stage in the V/SVZ, radial glial-like NSCs generate various types of newborn interneurons that migrate to the OB through the RMS (Obernier and Alvarez-Buylla, 2019). The location of adult NSCs within areas of the V/SVZ determines the types of OB interneurons produced (Merkle et al., 2014) (Figure 1B). While it has been observed that adult NSCs originate from embryonic progenitors in the V/SVZ (Fuentealba et al., 2015; Furutachi et al., 2015), the timing of spatial determination of cell fate remains unclear, specifically whether neural progenitors in the V/SVZ subareas, where adult NSCs are present, are the same as those in the forebrain subareas where embryonic NSCs are. Adult neural progenitors are generated between embryonic days 13.5 and 15.5 but remain mostly inactive until reactivated postnatally. The majority of RGCs become active from late embryonic stages to postnatal day 15, with a small subset of NSCs remaining quiescent during embryonic development. These dormant NSCs are responsible for adult neurogenesis in the V/SVZ (Fuentealba et al., 2015; Furutachi et al., 2015). NSCs are activated to produce intermediate progenitor cells, which then give rise to neuroblasts. These neuroblasts, along with their immature neural precursors, migrate in chains through the RMS to the OB, where they differentiate into mature OB interneurons, including GCs and PGCs (Kaneko et al., 2017). In adult rodents, the RMS serves as a conduit for a substantial number of neuroblasts to reach the OB (Lledo and Valley, 2016; Obernier and Alvarez-Buylla, 2019). In an experiment involving adult mice (at postnatal weeks 8) labeled with bromodeoxyuridine (BrdU), over 20,000 newborn neurons were observed to reach the OB 14 days after BrdU injection, indicating robust neurogenesis and extensive plasticity in the V/SVZ (Yamaguchi and Mori, 2005). In addition, local neuronal proliferation in the OB was noted to be particularly active in the initial days following birth (Lemasson et al., 2005).

3 Fate map of Tpbg/5T4 GCs

Inhibitory GCs, characterized by their small cell bodies lacking axons, have spinous basal dendrites and a spinous apical dendrite that extends from the GC layer into the external plexiform layer (EPL) and contacts MC/TC lateral dendrites via large spines housing the reciprocal synapses (Shepherd et al., 2007) (Figure 1A). GCs, the predominant neuronal subpopulation within the OB, are involved in both recurrent and lateral inhibition of MCs/TCs at the EPL, where GCs receive glutamatergic synaptic input from MC/TC lateral dendrites and provide recurrent GABAergic synaptic output to them (Egger and Thomas Kuner, 2021). The vast majority (>95%) of neurons generated in the V/SVZ during adulthood differentiate into GCs within the OB (Winner et al., 2002). Initially, GCs are categorized into multiple subtypes based on the morphology of their dendrites and the positioning of their cell bodies within the GC layer. Studies utilizing horseradish peroxidase injection and Golgi staining have revealed that rodent GCs can be classified into three primary subtypes: intermediate (G_I), deep (G_{II}), and superficial (G_{III}) subtypes (Shepherd et al., 2007), and further subcategorized into deep branching (G_{IV}) and shrub branching (G_V) subtypes (Merkle et al., 2007). Subsequently, mature GCs are identified by specific marker genes such as calretinin (CalR), Ca^{2+}/calmodulin-dependent protein kinase II α (CaMKIIα), oncofetal trophoblast glycoprotein (Tpbg, also known as 5T4), metabotropic glutamate receptor 2 (mGluR2), and neurogranin (Imamura et al., 2006; Batista-Brito et al., 2008; Gribaudo et al., 2009; Merkle et al., 2014; Nagayama et al., 2014; Malvaut et al., 2017).

As mentioned above, adult NSCs in distinct subregions of the V/SVZ generate OB interneurons with diverse GC subtypes (Merkle et al., 2007, 2014) (Figure 1B). It was previously uncertain whether these spatial cell fate decisions are predetermined during early development. Recent advancements in gene barcoding techniques have enabled the mapping of single cell spatial distribution, revealing that different classes of adult-born OB interneurons are associated with specific types of embryonic-born neurons, depending on the V/SVZ subareas (Fuentealba et al., 2015) (Figure 1B). For instance, superficial GCs and dopaminergic (TH: tyrosine hydroxylase) PGCs originating in the dorsal V/SVZ during adulthood were found to be clonally linked to cortical neurons produced in the corresponding area during the embryonic development (Figure 1B). These findings suggest that the spatial determination of cell fate is established early during the embryonic stage in progenitor cells, which are shared NSCs between the embryonic forebrain and adult OB.

Tpbg/5T4 GCs and CalR GCs are located in the MC layer and/or the superficial GC layer, respectively (Imamura et al., 2006; Nagayama et al., 2014) (Figure 1B). Tpbg/5T4 GCs are present in superficial GCs nearby the MC layer (G_{IIIM}) based on their location and dendritic morphology (Imamura et al., 2006; Yoshihara et al., 2012; Fuentealba et al., 2015), while CalR GCs are in the other superficial GCs (G_{III}) with a different cell lineage from Tpbg/5T4 (Merkle et al., 2014; Fuentealba et al., 2015; Yao et al., 2023) (Figure 1B). In addition, different subtypes of OB GCs were generated preferentially at different stages, e.g., from embryonic day 12.5 to postnatal day 30 (Batista-Brito et al., 2008). Tpbg/5T4 GCs, present in the superficial GC (G_{IIIM}) layer, were produced mainly from embryonic day 15.5 to the day of birth (Sakamoto et al., 2014; Takahashi et al., 2016) (Figure 2D), whereas production of CalR GCs, present in the superficial GC (G_{III}) layer, began immediately after birth and continued until postnatal day 56 (Batista-Brito et al., 2008). Tracing the genetic lineage of postnatally-born neurons has revealed that nearly 90% of GCs in the deep GC (G_{II}) layer of mice at postnatal day 90 were marked as postnatally-born neurons, whereas only about 40 and 60% were labeled in the MC (G_{IIIM}) layer and the superficial GC (G_{III}) layer, respectively (Sakamoto et al., 2014). These results suggest that GCs generated at embryonic stages like Tpbg/5T4 are maintained in the superficial GC (G_{IIIM}) layer (Figure 2D), while GCs produced after birth are mainly integrated into the deep GC (G_{II}) layer.

High-throughput single-cell RNA sequencing (scRNA-seq) of the mouse OB albeit no spatial information identified 38 distinct cell clusters including 18 neuronal clusters, each of which has the

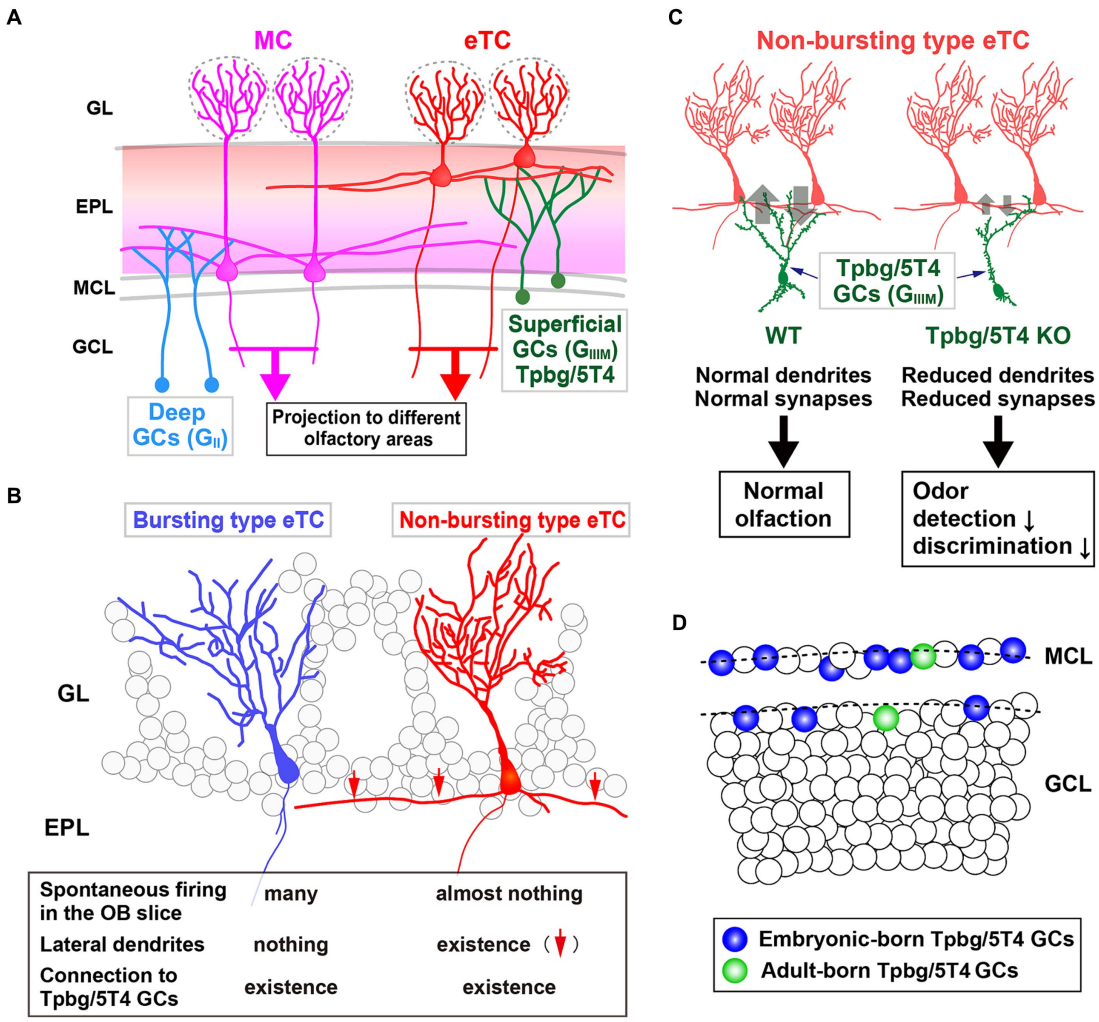

FIGURE 2
Role of the Tpbg/5T4 GC subtype within the OB neural circuit. **(A)** Schematic representation of the OB neural circuit. Superficial GCs nearby the MC layer (G_{IIIM}) harboring Tpbg/5T4 GCs exhibits a preference for establishing connections with the lateral dendrites of external TCs (eTCs) located in the surface segment of the external plexiform layer (EPL). Conversely, GCs situated in the deep GC layer (G_{II}) predominantly form connections with MCs in the deep segment of the EPL. These distinct pathways of MCs and TCs facilitate the transmission of varied odor information to discrete regions of the olfactory cortex. GL, glomerular layer; EPL, external plexiform layer; MCL, mitral cell layer; GCL, granule cell layer. **(B)** Two categories of eTCs. Tpbg/5T4 GCs establish dendritic synapses with two types of eTCs: burst type eTCs lacking lateral dendrites that exhibit frequent spontaneous firing; non-burst type eTCs possessing lateral dendrites that do not exhibit such firing behavior. **(C)** Tpbg/5T4 GCs connecting to non-burst type eTCs that display reduced dendritic branching in Tpbg/5T4-knockout (KO) mice. Notably, GABAergic inputs to non-burst type eTCs are significantly diminished in Tpbg/5T4 KO mice, whereas inputs to burst type eTCs remain unaffected. Consequently, olfactory functions such as odor detection and discrimination are impaired in Tpbg/5T4 KO mice. **(D)** Integration of Tpbg/5T4 GCs produced at embryonic and adult stages. Bromodeoxyuridine labeling reveals that embryonic-born Tpbg/5T4 GCs are predominantly integrated in the OB (depicted in blue), with minimal integration observed in adult-born Tpbg/5T4 GCs (depicted in green) (Takahashi et al., 2016).

similarity of transcriptional profiles and allows detailed classification of single-cell molecular markers (Tepe et al., 2018). Expression profiles with RNA *in situ* hybridization (ISH) from the Allen Brain Atlas (Lein et al., 2007) further classified the neuronal clusters into14 mature/immature inhibitory neuron clusters, one of which is the n12-GC-6 cluster consisting of Slc32a1 (vesicular GABA transporter), known to be expressed in mature inhibitory interneurons, Tpbg/5T4 and so on (Tepe et al., 2018). Recently, a high-resolution spatial transcriptomic atlas of cell types for the entire mouse brain was generated, in combination of a scRNA-seq dataset with a spatial transcriptomic dataset by multiplexed error-robust fluorescence ISH (MERFISH) (Chen et al., 2015; Yao et al., 2023). Through characterization of the molecular markers and regional specificity of each cell-type class, the subpallium-GABA class has been subdivided into seven subclasses, each likely originating from distinct developmental pathways (Figure 1C). Within these subclasses, one particular group comprises a combination of five non-neuronal cell types and four GC/immature neuron types, notably including the GABAergic OB immature neuron (OB-IMN-GABA) type (Yao et al., 2023) (Figure 1C). The OB-IMN-GABA type originates in the V/SVZ, migrates through the RMS, and matures into GCs and PGCs in the OB. During the developmental lineage of the OB-IMN-GABA type, neuroblasts in the SVZ and RMS express cell cycle-related markers like Top2a and Mki67. Upon exiting the RMS, immature OB interneurons exhibit markers such as Sox11

and S100a6, while mature OB interneurons are characterized by Frmd7 expression (Yao et al., 2023). The OB-IMN-GABA type is further categorized into 30 subtypes, one of which is the Frmd7 Gaba_1 subtype containing Tpbg/5T4 and Lgr6 (Leucine-rich repeat [LRR]-containing G-protein coupled receptor 6). Notably, a previous study by Yu et al. (2017) has indicated the co-expression of Lgr6 with Tpbg/5T4 in GCs at the superficial GC (G_{IIIM}) layer.

Similarly, using an *in situ* RNA-sequencing method on brain slices along with the high-throughput scRNA-seq analysis (Zeisel et al., 2018), a high-quality spatial transcriptomic atlas of cell types has been made across the adult mouse brain to identify 26 major cell clusters, including 13 neuronal clusters (Shi et al., 2023). They are further classified into 190 neuronal subclusters that contains seven OB inhibitory neuron (OBINH) subclusters, one of which is the OBINH-3-[Gad1_Tpbg_Tiam2] subcluster. Based on the "Spatial-Portal" website (https://www.spatial-atlas.net/Brain/spatial.html), expression of Gad1 (Glutamate decarboxylase 1; GCs, and PGCs), Tiam2 (T-cell lymphoma invasion and metastasis 2; neuroblasts, GCs, and PGCs) and Tpbg/5T4 appears to be overlapped in the superficial GC (G_{IIIM}) layer (Yoshizawa et al., 2002; Shi et al., 2023) (Figure 1D). Members of the Frmd7 Gaba_1 subtype (Yao et al., 2023) is similar but, not identical to those of the OBINH-3-[Gad1_Tpbg_Tiam2] subcluster (Shi et al., 2023), because in the superficial GCs nearby the MC layer (G_{IIIM}), contamination of glutamatergic MCs seems to be unavoidable. These results demonstrate that the OBINH-3-[Gad1_Tpbg_Tiam2] subcluster represents a cell lineage associated with Tpbg/5T4 in the OB.

4 Physiological roles of Tpbg/5T4 GCs

Imamura et al. (2006) hypothesized that a group of membrane proteins present in specific layers within the OB neural circuit would play a role in the establishment of dendritic synaptic connections specific to those layers. They identified specific subtypes of OB interneurons, Tpbg/5T4 GCs and PGCs, within the superficial GC (G_{IIIM}) and glomerular layers, respectively (Figure 2A). Tpbg/5T4 is a member of the LRR membrane protein family, characterized by a N-terminal extracellular domain comprising seven LRRs, each consisting of 24 amino acids (Imamura et al., 2006; Yoshihara et al., 2012; Zhao et al., 2014). Notably, Tpbg/5T4, among membrane proteins with extracellular LRRs, exhibits high conservation not only in mice (King et al., 1999) and humans (Myers et al., 1994) but also in non-mammalian species such as Drosophila CG6959 (Özkan et al., 2013) and zebrafish Wnt-activated inhibitory factor 1 (WAIF1) (Kagermeier-Schenk et al., 2011). It has been revealed by unilaterally naris occluded mice that expression of Tpbg/5T4 in OB interneurons is reliant on neural activity triggered by odors (Yoshihara et al., 2012). Further, experimental manipulations involving Tpbg/5T4 loss and gain of function have revealed that Tpbg/5T4 is essential for the dendritic branching of Tpbg/5T4 GCs in response to odor stimuli (Yoshihara et al., 2012). These findings suggest a crucial role for Tpbg/5T4 GCs in the processing of olfactory information within the neural circuits of the OB.

In the OB, inhibitory GCs synapse with excitatory projection neurons, such as MCs and TCs (Figure 2A). Previous studies have shown that early-born superficial GCs and late-born deep GCs tend to preferentially connect with the lateral dendrites of TCs and MCs, respectively (Geramita et al., 2016). In addition, Takahashi et al. (2016) identified two subtypes of external TCs (eTCs): non-burst type eTCs with inactive lateral dendrites; burst type eTCs that frequently exhibit spontaneous firing (Ma and Lowe, 2010) (Figure 2B). The apical dendrites of Tpbg/5T4 GCs establish GABAergic synapses with both non-burst and burst type eTCs. It has been shown utilizing OB slices from Tpbg/5T4 knockout (KO) mice that electrode stimulation induced $GABA_A$ receptor-mediated postsynaptic currents in burst type eTCs, while significantly reduced responses were observed in non-burst type eTCs (Takahashi et al., 2016) (Figure 2B). Given the reciprocal dendritic synapses formed between OB GCs and projection neurons (Shepherd et al., 2007), the experiment exploring excitatory inputs from eTCs to Tpbg/5T4 GCs in Tpbg/5T4 KO mice revealed a notable decrease in those in Tpbg/5T4-KO than wild-type mice (Takahashi et al., 2016). This is consistent with reduction of dendritic branching in Tpbg/5T4-deficient cells (Yoshihara et al., 2012) (Figure 2C). These results demonstrate that neural activity in the non-bursting type eTCs is regulated by Tpbg/5T4 GCs (Figure 2B).

Would the reduced inhibition of non-burst type eTCs and decreased excitation of Tpbg/5T4-deficient GCs impact on olfactory behavior in mice? In order to assess the physiological significance of Tpbg/5T4 GCs in odor processing within the OB neural circuit, Takahashi et al. (2016) examined odor detection thresholds in wild-type and Tpbg/5T4 KO mice using the habituation-dishabituation test. The results revealed that Tpbg/5T4 KO mice exhibited significantly lower sensitivity to odor detection compared to wild-type mice, with a difference of approximately 100-fold. Furthermore, in an odor discrimination learning task, Tpbg/5T4 KO mice were unable to differentiate between two simultaneously presented odors but showed no impairment when the odors were presented individually (Takahashi et al., 2016). Notably, when exposed to a non-food-related odorant, Tpbg/5T4 KO mice displayed prolonged search times for buried food pellets. Conversely, these mice did not exhibit any difficulties in locating buried food pellets in the absence of other odors. To confirm the phenotype of global Tpbg/5T4 KO mice, the OB-specific Tpbg/5T4 knockdown (KD) experiment was performed by injection of Tpbg/5T4-shRNAs-expressing lentiviral vectors into both the lateral ventricles and OBs of postnatal day 1 mice, giving rise to knockdown specific to Tpbg/5T4 GCs in the adult OB (Takahashi et al., 2016). The OB-specific Tpbg/5T4 KD showed the same defect as the global Tpbg/5T4 KO in the odor detection thresholds and olfactory behavior tests, further demonstrating that Tpbg/5T4 GCs in the OB are required for both odor detection and odor discrimination behaviors as illustrated in Figure 2C.

5 Perspectives

The findings from olfactory behavior tests conducted on Tpbg/5T4 KO mice (Takahashi et al., 2016) diverge from those documented in prior research: either the inhibition or activation of neural activity in adult-born OB interneurons, including GCs, did not yield significant effects on odor detection and basic odor discrimination (Abraham et al., 2010; Alonso et al., 2012; Sakamoto et al., 2014). This discrepancy could be attributed to variations in the subtypes of OB interneurons manipulated genetically in each study. Given that OB interneurons can be categorized into multiple subtypes based on their expression markers, such as the OBINH-3-[Gad1_Tpbg_Tiam2] (Shi et al., 2023),

it is postulated that each interneuron subtype forms a unique local circuit within the OB (Shepherd et al., 2007).

Sakamoto et al. (2014) proposed that around 25% of GCs in adult mice originate from embryonic NSCs, while Lemasson et al. (2005) indicated that postnatal neurogenesis peaks at postnatal day 7 and then decreases to one-third by postnatal day 60. The genetic trace experiment indicated that nearly 90% of GCs in the deep GC (G_{II}) layer are produced continuously by postnatal day 90 after birth (Sakamoto et al., 2014). Consequently, adult-born GCs engineered to express the diphtheria toxin fragment A gene are predominantly integrated into the deep GC (G_{II}) layer and tend to connect with MCs rather than TCs (Bardy et al., 2010), resulting in no impairment in odor detection and basic olfactory discrimination but a deficiency in complex learned olfactory discrimination (Sakamoto et al., 2011, 2014). Similarly, genetic inhibition and ablation of other OB GC subtypes, CaMKIIα GCs and neurogranin GCs, respectively, distributed across the GC layer, exhibits a necessity for learned olfactory discrimination (Malvaut et al., 2017; Gribaudo et al., 2021). Furthermore, chemogenetical inhibition of CalR GCs, by injection of the AAV harboring Gi-coupled DREADDs into the GC layer of CalR-Cre knockin mice, showed the impairment in complex olfactory discrimination, but not in simple learned olfactory discrimination (Hardy et al., 2018). This may be because CalR GCs are produced and integrated into the neural circuit during not only the neonatal stage but also the adult stage, even though they exist in the superficial GC (G_{III}) layer (Batista-Brito et al., 2008).

In contrast, the genetic trace experiment indicated that GCs born during the embryonic stage appear to be retained in the MC and superficial GC layers (approximately 40 and 60% of GCs, respectively) in postnatal day 90 mice (Sakamoto et al., 2014). Consequently, Tpbg/5T4 GCs, generated during embryonic and perinatal periods and situated in the superficial GC (G_{IIIM}) layer, demonstrate a requirement for odor detection and basic olfactory discrimination (Takahashi et al., 2016) (Figure 2C). Likewise, the GC-specific KO mice of $GABA_A$ receptor β3 subunit (Gabrb3), where the AAV harboring Cre was injected into the GC layer of Gabrb3-floxed mice, showed reduced $GABA_A$R-mediated inhibitory postsynaptic currents in GCs and increased recurrent inhibition in MCs. The effect on neural activity was restricted to part of the embryonic- and postnatal-born GCs, leading to impairment in discrimination both dissimilar and highly similar odors, but not in the learning of odor discrimination (Nunes and Kuner, 2015).

Recent studies have suggested that within the EPL of the OB, local dendrodendritic circuits may differentiate into parallel pathways for MCs and TCs, particularly eTCs (Fourcaud-Trocmé et al., 2014). The eTCs projecting to the anterior olfactory nucleus and the rostral part of olfactory tubercle (Igarashi et al., 2012), appear to be specialized in rapid odor detection and quick behavioral responses necessary for distinguishing between distinct odors. It is also possible that MCs projecting broadly to the olfactory cortex (Miyamichi et al., 2011; Igarashi et al., 2012) may excel in discrimination learning between closely related odors, such as enantiomers. I hypothesize that embryonic-born GCs, including Tpbg/5T4 GCs, are involved in fundamental olfactory responses crucial for survival, while adult-born GCs are more associated with learned olfactory behaviors (Alonso et al., 2012; Sakamoto et al., 2014). The distinct roles of embryonic- and postnatal-born GCs in olfactory processing and behavior may be attributed to the generation of different GC subtypes at various stages and subregions of the V/SVZ (Lemasson et al., 2005; Batista-Brito et al., 2008; Sakamoto et al., 2014; Fuentealba et al., 2015).

Interestingly, mammalian retina has a distinct laminar structure consisting of photoreceptor (rod and cone) cells, interneurons such as horizontal cells, bipolar cells (BCs) and amacrine cells (ACs), and retinal ganglion cells. Single-cell transcriptomics has revealed that Tpbg/5T4 belongs to a cluster of BCs divided into 15 clusters, and two clusters of ACs divided into 63 clusters within the mouse retina (Shekhar et al., 2016; Yan et al., 2020). Moreover, using scRNA-seq along with ISH images from the Allen Brain Atlas (Lein et al., 2007), it has been found that the subiculum pyramidal cells can be resolved into eight subclasses, one of which is the Tpbg/5T4 subclass (Cembrowski et al., 2018). These subclasses are mapped onto adjacent spatial domains, ultimately creating a complex layered and columnar organization with heterogeneity across the dorsal-ventral, proximal-distal, and superficial-deep axes in the mouse subiculum. Since OB neural circuits possess a notable high proportion of interneurons, glomerular columnar organizations, and intensive dendrodendritic communications, these observations suggest that Tpbg/5T4 plays a crucial role in shaping the laminar structure and function in the OB, retina, subiculum, and other brain regions.

Author contributions

AT: Writing – original draft, Writing – review & editing.

Funding

The author(s) declare that financial support was received for the research, authorship, and/or publication of this article. This work was supported by the Ministry of Education, Culture, Sports, Science and Technology of Japan (JP22H02733), the AMED Strategic Promotion Program for Bridging Research (Seeds A, JP22ym0126809j0001), and many research grants including the Smoking Science Research Foundation.

Acknowledgments

This study was assisted by Dr. Hiroo Takahashi in Kagawa University, Dr. Seiich Yoshihara in Nara Medical University, Dr. Peter Stern in the University of Manchester, and many others.

Conflict of interest

The author declares that the research was conducted in the absence of any commercial or financial relationships that could be construed as a potential conflict of interest.

The author(s) declared that they were an editorial board member of Frontiers, at the time of submission. This had no impact on the peer review process and the final decision.

Publisher's note

References

Abraham, N. M., Egger, V., Shimshek, D. R., Renden, R., Fukunaga, I., Sprengel, R., et al. (2010). Synaptic inhibition in the olfactory bulb accelerates odor discrimination in mice. *Neuron* 65, 399–411. doi: 10.1016/j.neuron.2010.01.009

Alonso, M., Lepousez, G., Wagner, S., Bardy, C., Gabellec, M. M., Torquet, N., et al. (2012). Activation of adult-born neurons facilitates learning and memory. *Nat. Neurosci.* 15, 897–904. doi: 10.1038/nn.3108

Bardy, C., Alonso, M., Bouthour, W., and Lledo, P. M. (2010). How, when, and where new inhibitory neurons release neurotransmitters in the adult olfactory bulb. *J. Neurosci.* 30, 17023–17034. doi: 10.1523/JNEUROSCI.4543-10.2010

Batista-Brito, R., Close, J., Machold, R., and Fishell, G. (2008). The distinct temporal origins of olfactory bulb interneuron subtypes. *J. Neurosci.* 28, 3966–3975. doi: 10.1523/JNEUROSCI.5625-07.2008

Bressan, C., and Saghatelyan, A. (2021). Intrinsic mechanisms regulating neuronal migration in the postnatal brain. *Front. Cell. Neurosci.* 14:620379. doi: 10.3389/fncel.2020.620379

Cembrowski, M. S., Wang, L., Lemire, A. L., Copeland, M., DiLisio, S. F., Clements, J., et al. (2018). The subiculum is a patchwork of discrete subregions. *eLife* 7:e37701. doi: 10.7554/eLife.37701

Chen, K. H., Boettiger, A. N., Moffitt, J. R., Wang, S., and Zhuang, X. (2015). Spatially resolved, highly multiplexed RNA profiling in single cells. *Science* 348:eaaa6090. doi: 10.1126/science.aaa6090

Egger, V., and Thomas Kuner, T. (2021). Olfactory bulb granule cells: specialized to link coactive glomerular columns for percept generation and discrimination of odors. *Cell Tissue Res.* 383, 495–506. doi: 10.1007/s00441-020-03402-7

Fourcaud-Trocmé, N., Courtiol, E., and Buonviso, N. (2014). Two distinct olfactory bulb sublaminar networks involved in gamma and beta oscillation generation: a CSD study in the anesthetized rat. *Front. Neural Circuits* 8:88. doi: 10.3389/fncir.2014.00088

Fuentealba, L. C., Rompani, S. B., Parraguez, J. I., Obernier, K., Romero, R., Cepko, C. L., et al. (2015). Embryonic origin of postnatal neural stem cells. *Cell* 161, 1644–1655. doi: 10.1016/j.cell.2015.05.041

Furutachi, S., Miya, H., Watanabe, T., Kawai, H., Yamasaki, N., Harada, Y., et al. (2015). Slowly dividing neural progenitors are an embryonic origin of adult neural stem cells. *Nat. Neurosci.* 18, 657–665. doi: 10.1038/nn.3989

Geramita, M. A., Burton, S. D., and Urban, N. N. (2016). Distinct lateral inhibitory circuits drive parallel processing of sensory information in the mammalian olfactory bulb. *eLife* 5:e16039. doi: 10.7554/eLife.16039

Gribaudo, S., Bovetti, S., Garzotto, D., Fasolo, A., and De Marchis, S. (2009). Expression and localization of the calmodulin-binding protein neurogranin in the adult mouse olfactory bulb. *J. Comp. Neurol.* 517, 683–694. doi: 10.1002/cne.22177

Gribaudo, S., Saraulli, D., Nato, G., Bonzano, S., Gambarotta, G., Luzzati, F., et al. (2021). Neurogranin regulates adult-born olfactory granule cell spine density and odor-reward associative memory in mice. *Int. J. Mol. Sci.* 22:4269. doi: 10.3390/ijms22084269

Hardy, D., Malvaut, S., Breton-Provencher, V., and Saghatelyan, A. (2018). The role of calretinin-expressing granule cells in olfactory bulb functions and odor behavior. *Sci. Rep.* 8:9385. doi: 10.1038/s41598-018-27692-8

Igarashi, K. M., Ieki, N., An, M., Yamaguchi, Y., Nagayama, S., Kobayakawa, K., et al. (2012). Parallel mitral and tufted cell pathways route distinct odor information to different targets in the olfactory cortex. *J. Neurosci.* 32, 7970–7985. doi: 10.1523/JNEUROSCI.0154-12.2012

Imamura, F., Nagao, H., Naritsuka, H., Murata, Y., Taniguchi, H., and Mori, K. (2006). A leucine-rich repeat membrane protein, 5T4, is expressed by a subtype of granule cells with dendritic arbors in specific strata of the mouse olfactory bulb. *J. Comp. Neurol.* 495, 754–768. doi: 10.1002/cne.20896

Kagermeier-Schenk, B., Wehner, D., Ozhan-Kizil, G., Yamamoto, H., Li, J., Kirchner, K., et al. (2011). Waif1/5T4 inhibits Wnt/β-catenin signaling and activates noncanonical Wnt pathways by modifying LRP6 subcellular localization. *Dev. Cell* 21, 1129–1143. doi: 10.1016/j.devcel.2011.10.015

Kaneko, N., Sawada, M., and Sawamoto, K. (2017). Mechanisms of neuronal migration in the adult brain. *J. Neurochem.* 141, 835–847. doi: 10.1111/jnc.14002

King, K. W., Sheppard, F. C., Westwater, C., Stern, P. L., and Myers, K. A. (1999). Organisation of the mouse and human 5T4 oncofoetal leucine-rich glycoprotein genes and expression in foetal and adult murine tissues. *Biochim. Biophys. Acta* 1445, 257–270. doi: 10.1016/s0167-4781(99)00055-x

Lein, E. S., Hawrylycz, M. J., Ao, N., Ayres, M., Bensinger, A., Bernard, A., et al. (2007). Genome-wide atlas of gene expression in the adult mouse brain. *Nature* 445, 168–176. doi: 10.1038/nature05453

Lemasson, M., Saghatelyan, A., Olivo-Marin, J. C., and Lledo, P. M. (2005). Neonatal and adult neurogenesis provide two distinct populations of newborn neurons to the mouse olfactory bulb. *J. Neurosci.* 25, 6816–6825. doi: 10.1523/JNEUROSCI.1114-05.2005

Lepousez, G., Valley, M. T., and Lledo, P. M. (2013). The impact of adult neurogenesis on olfactory bulb circuits and computations. *Annu. Rev. Physiol.* 75, 339–363. doi: 10.1146/annurev-physiol-030212-183731

Lledo, P. M., and Valley, M. (2016). Adult olfactory bulb neurogenesis. *Cold Spring Harb. Perspect. Biol.* 8:a018945. doi: 10.1101/cshperspect.a018945

Ma, J., and Lowe, G. (2010). Correlated firing in tufted cells of mouse olfactory bulb. *Neuroscience* 169, 1715–1738. doi: 10.1016/j.neuroscience.2010.06.033

Malvaut, S., Gribaudo, S., Hardy, D., David, L. S., Daroles, L., Labrecque, S., et al. (2017). CaMKIIα expression defines two functionally distinct populations of granule cells involved in different types of odor behavior. *Curr. Biol.* 27, 3315–3329.e6. doi: 10.1016/j.cub.2017.09.058

Merkle, F. T., and Alvarez-Buylla, A. (2006). Neural stem cells in mammalian development. *Curr. Opin. Cell Biol.* 18, 704–709. doi: 10.1016/j.ceb.2006.09.008

Merkle, F. T., Fuentealba, L. C., Sanders, T. A., Magno, L., Kessaris, N., and Alvarez-Buylla, A. (2014). Adult neural stem cells in distinct microdomains generate previously unknown interneuron types. *Nat. Neurosci.* 17, 207–214. doi: 10.1038/nn.3610

Merkle, F. T., Mirzadeh, Z., and Alvarez-Buylla, A. (2007). Mosaic organization of neural stem cells in the adult brain. *Science* 317, 381–384. doi: 10.1126/science.1144914

Miyamichi, K., Amat, F., Moussavi, F., Wang, C., Wickersham, I., Wall, N. R., et al. (2011). Cortical representations of olfactory input by trans-synaptic tracing. *Nature* 472, 191–196. doi: 10.1038/nature09714

Mori, K., and Sakano, H. (2011). How is the olfactory map formed and interpreted in the mammalian brain? *Annu. Rev. Neurosci.* 34, 467–499. doi: 10.1146/annurev-neuro-112210-112917

Mori, K., and Sakano, H. (2021). Olfactory circuitry and behavioral decisions. *Annu. Rev. Physiol.* 83, 231–256. doi: 10.1146/annurev-physiol-031820-092824

Myers, K. A., Rahi-Saund, V., Davison, M. D., Young, J. A., Cheater, A. J., and Stern, P. L. (1994). Isolation of a cDNA encoding 5T4 oncofetal trophoblast glycoprotein. An antigen associated with metastasis contains leucine-rich repeats. *J. Biol. Chem.* 269, 9319–9324. doi: 10.1016/S0021-9258(17)37110-7

Nagayama, S., Homma, R., and Imamura, F. (2014). Neuronal organization of olfactory bulb circuits. *Front. Neural Circuits* 8:98. doi: 10.3389/fncir.2014.00098

Nunes, D., and Kuner, T. (2015). Disinhibition of olfactory bulb granule cells accelerates odour discrimination in mice. *Nat. Commun.* 6:8950. doi: 10.1038/ncomms9950

Obernier, K., and Alvarez-Buylla, A. (2019). Neural stem cells: origin, heterogeneity and regulation in the adult mammalian brain. *Development* 146:dev156059. doi: 10.1242/dev.156059

Özkan, E., Carrillo, R. A., Eastman, C. L., Weiszmann, R., Waghray, D., Johnson, K. G., et al. (2013). An extracellular interactome of immunoglobulin and LRR proteins reveals receptor-ligand networks. *Cell* 154, 228–239. doi: 10.1016/j.cell.2013.06.006

Sakamoto, M., Ieki, N., Miyoshi, G., Mochimaru, D., Miyachi, H., Imura, T., et al. (2014). Continuous postnatal neurogenesis contributes to formation of the olfactory bulb neural circuits and flexible olfactory associative learning. *J. Neurosci.* 34, 5788–5799. doi: 10.1523/JNEUROSCI.0674-14.2014

Sakamoto, M., Imayoshi, I., Ohtsuka, T., Yamaguchi, M., Mori, K., and Kageyama, R. (2011). Continuous neurogenesis in the adult forebrain is required for innate olfactory responses. *Proc. Natl. Acad. Sci. USA* 108, 8479–8484. doi: 10.1073/pnas.1018782108

Shekhar, K., Lapan, S. W., Whitney, I. E., Tran, N. M., Macosko, E. Z., Kowalczy, K. M., et al. (2016). Comprehensive classification of retinal bipolar neurons by single-cell transcriptomics. *Cell* 166, 1308–1323.e30. doi: 10.1016/j.cell.2016.07.054

Shepherd, G. M., Chen, W. R., Willhite, D., Migliore, M., and Greer, C. A. (2007). The olfactory granule cell: from classical enigma to central role in olfactory processing. *Brain Res. Rev.* 55, 373–382. doi: 10.1016/j.brainresrev.2007.03.005

Shi, H., He, Y., Zhou, Y., Huang, J., Maher, K., Wang, B., et al. (2023). Spatial atlas of the mouse central nervous system at molecular resolution. *Nature* 622, 552–561. doi: 10.1038/s41586-023-06569-5

Takahashi, H., Ogawa, Y., Yoshihara, S., Asahina, R., Kinoshita, M., Kitano, T., et al. (2016). A subtype of olfactory bulb interneurons is required for odor detection and discrimination behaviors. *J. Neurosci.* 36, 8210–8227. doi: 10.1523/JNEUROSCI.2783-15.2016

Tepe, B., Hill, M. C., Pekarek, B. T., Hunt, P. J., Martin, T. J., Martin, J. F., et al. (2018). Single-cell RNA-seq of mouse olfactory bulb reveals cellular heterogeneity and activity-dependent molecular census of adult-born neurons. *Cell Rep.* 25, 2689–2703.e3. doi: 10.1016/j.celrep.2018.11.034

Winner, B., Cooper-Kuhn, C. M., Aigner, R., Winkler, J., and Kuhn, H. G. (2002). Long-term survival and cell death of newly generated neurons in the adult rat olfactory bulb. *Eur. J. Neurosci.* 16, 1681–1689. doi: 10.1046/j.1460-9568.2002.02238.x

Yamaguchi, M., and Mori, K. (2005). Critical period for sensory experience-dependent survival of newly generated granule cells in the adult mouse olfactory bulb. *Proc. Natl. Acad. Sci. USA* 102, 9697–9702. doi: 10.1073/pnas.0406082102

Yan, W., Laboulaye, M. A., Tran, N. M., Whitney, I. E., Benhar, I., and Sanes, J. R. (2020). Mouse retinal cell atlas: molecular identification of over sixty amacrine cell types. *J. Neurosci.* 40, 5177–5195. doi: 10.1523/JNEUROSCI.0471-20.2020

Yao, Z., van Velthoven, C. T. J., Kunst, M., Zhang, M., McMillen, D., Lee, C., et al. (2023). A high-resolution transcriptomic and spatial atlas of cell types in the whole mouse brain. *Nature* 624, 317–332. doi: 10.1038/s41586-023-06812-z

Yoshihara, S., Takahashi, H., Nishimura, N., Naritsuka, H., Shirao, T., Hirai, H., et al. (2012). 5T4 glycoprotein regulates the sensory input-dependent development of a specific subtype of newborn interneurons in the mouse olfactory bulb. *J. Neurosci.* 32, 2217–2226. doi: 10.1523/JNEUROSCI.5907-11.2012

Yoshizawa, M., Hoshino, M., Sone, M., and Nabeshima, Y. (2002). Expression of stef, an activator of Rac1, correlates with the stages of neuronal morphological development in the mouse brain. *Mech. Dev.* 113, 65–68. doi: 10.1016/s0925-4773(01)00650-5

Yu, Y., Moberly, A. H., Bhattarai, J. P., Duan, C., Zheng, Q., Li, F., et al. (2017). The stem cell marker Lgr5 defines a subset of postmitotic neurons in the olfactory bulb. *J. Neurosci.* 37, 9403–9414. doi: 10.1523/JNEUROSCI.0500-17.2017

Zeisel, A., Hochgerner, H., Lönnerberg, P., Johnsson, A., Memic, F., van der Zwan, J., et al. (2018). Molecular architecture of the mouse nervous system. *Cell* 174, 999–1014.e22. doi: 10.1016/j.cell.2018.06.021

Zhao, Y., Malinauskas, T., Harlos, K., and Jones, E. Y. (2014). Structural insights into the inhibition of Wnt signaling by cancer antigen 5T4/Wnt-activated inhibitory factor 1. *Structure* 22, 612–620. doi: 10.1016/j.str.2014.01.009

frontiers | Frontiers in Neural Circuits

TYPE Mini Review
PUBLISHED 24 June 2024
DOI 10.3389/fncir.2024.1414452

OPEN ACCESS

EDITED BY
Charles A. Greer,
Yale University, United States

REVIEWED BY
Haruki Takeuchi,
The University of Tokyo, Japan

*CORRESPONDENCE
Alexander Fleischmann
✉ alexander_fleischmann@brown.edu

RECEIVED 08 April 2024
ACCEPTED 29 May 2024
PUBLISHED 24 June 2024

CITATION
McKissick O, Klimpert N, Ritt JT and Fleischmann A (2024) Odors in space. *Front. Neural Circuits* 18:1414452. doi: 10.3389/fncir.2024.1414452

Odors in space

Olivia McKissick[1], Nell Klimpert[1], Jason T. Ritt[2] and Alexander Fleischmann[1]*

[1]Department of Neuroscience and Carney Institute for Brain Science, Brown University, Providence, RI, United States, [2]Carney Institute for Brain Science, Brown University, Providence, RI, United States

As an evolutionarily ancient sense, olfaction is key to learning where to find food, shelter, mates, and important landmarks in an animal's environment. Brain circuitry linking odor and navigation appears to be a well conserved multi-region system among mammals; the anterior olfactory nucleus, piriform cortex, entorhinal cortex, and hippocampus each represent different aspects of olfactory and spatial information. We review recent advances in our understanding of the neural circuits underlying odor-place associations, highlighting key choices of behavioral task design and neural circuit manipulations for investigating learning and memory.

KEYWORDS

hippocampus, piriform cortex (PC), virtual reality, cognitive map, olfaction, entorhinal cortex, learning and memory

An ancient and important cognitive ability: odor-space integration

Across evolutionary distant species, animals have harnessed their sense of smell to navigate and survive in diverse habitats. This enduring significance of olfaction is reflected in the remarkable structural similarity of olfactory neural circuits. For example, the three-layered cytoarchitecture of the mammalian olfactory cortex resembles the pallial structures of amphibians and reptiles and distinguishes the mammalian olfactory cortex from the 6-layered neocortical areas for vision, hearing, or touch (1–6). This review will focus on rodents, though there are parallels to research in other organisms, notably insects (7–10).

Foraging for food is one of many odor-driven tasks that a rodent must perform to survive. Consider a mouse searching for something to eat: while vision and other senses may contribute to the search, olfaction is key to, say, finding seeds buried in a forest (11), for example by following odor plumes to their source (12, 13). It may further benefit the mouse in the long term to remember the location of this seed stash. By piecing together a map of scents at the stash and along the way home, the mouse can plan for more efficient future foraging. This ability to integrate spatial and olfactory information may in fact be more central to olfactory system evolution than other tasks such as odorant discrimination (9). Also critical is an ability to update this information as the environment changes; if the stash is eaten, the mouse will have to expand its map with new food sources.

In this review, we illustrate neural mechanisms underlying the integration of odor and space. We first discuss candidate multi-area circuit structures. We then review recent findings that support the functional role of these circuits revealed through cleverly designed behavioral tasks combined with neural recording and manipulation. We discuss research into changes in representations during learning and summarize ongoing technological advances that will help address key open questions.

10.3389/fncir.2024.1414452

Neural circuits for odor-space coding

Several regions of the olfactory system, including the olfactory bulb (OB), anterior olfactory nucleus (AON), and piriform cortex (PCx), connect directly to higher-level spatial processing and memory areas such as the hippocampus (HPC) and lateral entorhinal cortex (LEC). With both bottom-up and top-down inputs, each area is proposed to play an important role in the transfer of odor information from the periphery and its integration with contextual and spatial information. We will describe each area's key cell types, and how inter-areal connectivity is proposed to underlie function.

Olfactory input: from periphery to cortex

Odor information detected by olfactory sensory neurons (OSNs) in the olfactory epithelium is relayed to the olfactory cortex via mitral and tufted cells in the OB. Areas of the olfactory cortex, which include the AON, PCx, and LEC, receive olfactory input via molecularly distinct subtypes of mitral and tufted cells that preferentially project to AON, PCx, or LEC (Figure 1A) (14–18).

PCx is divided into molecularly and functionally segregated anterior piriform (aPCx) and posterior piriform (pPCx), with their boundary traditionally defined by the termination of the lateral olfactory tract (LOT) (Figure 1A) (19). There are major differences in circuitry between the aPCx and pPCx: aPCx receives more input from mitral and tufted cells in OB and has more bidirectional connections with AON, while pPCx is more connected to higher order areas like LEC and the cortical amygdala (COA) (16, 18, 20–22). The circuitry is in line with functional segregations between aPCx and pPCx, as aPCx is thought to primarily encode odor identity, and pPCx plays a more important role in the association and encoding of context and spatial position (23–29).

The PCx is organized in a trilaminar structure: an axonal layer I where afferent inputs from OB and AON are received, a dense layer II containing semilunar and pyramidal cells, and a deep layer III containing mostly pyramidal cells (Figure 1B). Output projections from PCx are largely segregated by layers, as molecularly distinct layer IIb cells and layer III pyramidal cells preferentially project back to OB and to frontal cortical regions, while layer IIa semilunar cells preferentially project to LEC and COA (19–22). Furthermore, projections of deep layer cells to frontal regions are segregated along the anterior/posterior axis, with projections from aPCx to orbitofrontal cortex (OFC) and from pPCx to medial prefrontal cortex (mPFC), and these frontal areas play unique roles in olfactory learning and representations of odor value (21, 30–32). The neural circuitry and cytoarchitecture of the olfactory cortex therefore correspond to the differential routing of olfactory information to regions throughout the brain.

Space and context: hippocampal formation

The hippocampal formation plays a key role in spatial learning and memory, as place cells, grid cells, and head direction cells selectively encode an animal's position in their environment (33). HPC has strong bidirectional connections with the entorhinal cortex and receives other parahippocampal inputs and projections to higher-order areas like the amygdala and striatum (34). For the scope of this review, we focus primarily on its connection with the olfactory cortex via bidirectional connections with LEC. Although there is a large degree of intrinsic connectivity within the hippocampus, the

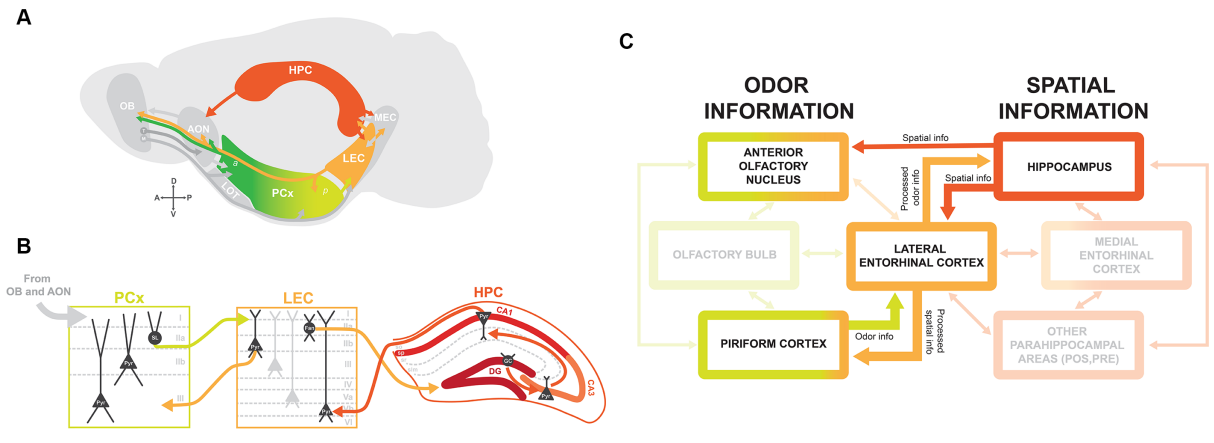

FIGURE 1
Brain circuitry for integrating olfactory-spatial information. **(A)** Schematic of brain regions involved in odor-place coding, with arrows indicating connections between brain regions. The lateral olfactory tract (LOT) traditionally defines the boundary between anterior (*a*) and posterior (*p*) PCx. OB, olfactory bulb; M, mitral cells; T, tufted cells; AON, anterior olfactory nucleus; PCx, piriform cortex; LEC, lateral entorhinal cortex; MEC, medial entorhinal cortex; HPC, hippocampus. **(B)** Circuitry between PCx, LEC, and HPC with main excitatory projection cell types. Information from olfactory areas OB and AON is relayed to PCx via layer I. PCx layer IIa semilunar (SL) cells project to LEC layer I, and LEC projects back to PCx via layer IIb CB+ pyramidal cells (Pyr). LEC projects to dentate gyrus granule cells (GC) from layer IIa RLN+ fan cells (Fan) via the perforant pathway. Information received from LEC is routed through HPC via the trisynaptic circuit, from granule cells to pyramidal cells in CA3 and CA1, and back to LEC to deep layer Vb pyramidal cells. **(C)** Flow chart indicating the flow of odor and spatial information from the main brain regions implicated in odor-place coding: AON, PCx, LEC, and HPC. Odor information from PCx and spatial information from HPC are directed to LEC. The LEC then relays processed odor information to HPC and processed spatial information back to PCx. The AON receives direct input from HPC and has been suggested as an alternate integrator of odor and spatial information.

hippocampal circuit is classically defined by the 'trisynaptic circuit': HPC receives input from the entorhinal cortex via dentate gyrus (DG) granule cells, transfers this information through the HPC via synaptic connections between CA3 and CA1 pyramidal cells, and then routes information back to the entorhinal cortex both directly and indirectly via the subiculum (Figure 1B) (35).

The connectivity patterns of HPC vary along the dorsal/ventral axis. Dorsal HPC receives most of its input from the entorhinal cortex. By contrast, ventral HPC is more connected to amygdalar, limbic, and olfactory regions. There is some evidence that these differences in circuitry relate to differences in the functional role of dorsal vs. ventral HPC, with more spatial coding in dorsal HPC and a larger role of ventral HPC in learned emotional behaviors (36–39). This functional segregation, however, remains an open question. It is important to note that recording studies in the HPC tend to focus on the dorsal sections, including the ones to be discussed later in this review.

Odor and spatial integration: lateral entorhinal cortex and anterior olfactory nucleus

The LEC is a member of both the olfactory cortex and the hippocampal formation and has strong bidirectional connections between olfactory regions (OB, AON, and PCx), HPC, and parahippocampal areas like the MEC, perirhinal cortex, and postrhinal cortex (Figure 1A) (19, 34, 40). The two primary layer II cell types in LEC are reelin-expressing (RLN+) fan cells in layer IIa and calbindin-expressing (CB+) pyramidal cells in layer IIb (Figure 1B), which together are known to encode odor information (41–43). Most input from the LEC to HPC is via RLN+ fan cells projecting to DG and a subset of CB+ pyramidal cells projecting to CA1, suggesting that the LEC transfers "processed" odor information to HPC (Figures 1B,C) (42). Moreover, CB+ cells project back to OB and PCx (Figure 1B) (41). Due to these strong connections with olfactory areas and HPC, we propose that LEC is an "integrator" of olfactory sensory information and contextual/place information.

Although MEC is more weakly connected to olfactory areas, both MEC and LEC send projections to DG granule cells. This may indicate that HPC can integrate information from both of these areas: spatial information from MEC and contextual information from LEC (44). Thus, it is possible that MEC, despite a lower responsiveness of its cells to odor, is part of the overarching circuitry that positions an animal in their environment and allows them to generate olfactory-spatial memories.

The AON is also proposed to be involved in integrating odor and spatial information due to its direct input from HPC (Figures 1A,C). There is a unique topographic gradient between CA1 neurons in HPC and AON, with the ventral HPC projecting to medial AON, dorsal and intermediate HPC projecting to lateral AON (45). These connections are proposed to play a role in odor contextualization, as hippocampal feedback projections to AON transfer spatiotemporal information, which is then integrated with odor information to form olfactory memory representations (46, 47). Also, inter-hemispheric feedback connections exist from AON to OB (19, 48, 49). These contralateral projections are believed to be relevant for stereosampling, where responses to odors are compared between left and right nostrils to aid in odor localization.

Neural representations during behavior

Recent experiments have explored how the connectivity detailed above functionally integrates odor and spatial information. Electrophysiological recording and calcium imaging have been the most common methods for observing neural activity during behavior. Some studies employ manipulation of neural activity with techniques including optogenetics and chemogenetics, probing the causal role of specific populations. In parallel, increasingly complex task designs incorporate strategic perturbations or closed loop behavioral interventions.

These studies variously emphasize one or more interrelated questions. How are different odor-spatial relationships represented? How do these representations differ across brain areas? How do these areas communicate with each other? How do representations change across learning? The following section highlights some key recent advances in this research program, especially the use of advanced recording and/or manipulation techniques within cleverly designed behavioral tasks.

Odors in virtual space

A particularly popular paradigm is the virtual reality (VR) linear track, in which a head-fixed rodent walks on a wheel, sphere, or treadmill, with sensory cues applied to simulate the experience of moving along a straight corridor (Figure 2). Using VR permits presentation of odor and other cues with a level of precision that is difficult or impossible to achieve with freely-moving mice. Additionally, head-fixation enables recording and manipulation techniques that use hardware that is too large for implantation in moving animals. Most of the studies we highlight below use some version of a VR linear track.

Odor representations in CA1 are driven by spatial information and salience

Radvansky and Dombeck pioneered the use of olfactory stimuli in a VR linear track paradigm (51). Using a custom olfactometer, they precisely controlled odor delivery and presentation of visual cues to mice on a spherical treadmill. They showed that mice anticipated rewards (seen as increased lick rates) at opposite ends of a virtual track even when track position was indicated only by odor gradients. Hippocampal CA1 activity revealed odor-driven place cells in much the same way comparable visual and multisensory tasks show (52, 53).

Similarly, Fischler-Ruiz and colleagues investigated encoding of two localized odor landmarks (Figure 2) (54). They found place cells spanned the track's length, while noting a heightened density of place cells responsive to the odor landmarks. The vast majority of these place cells were only responsive to one of the two landmarks along the track, meaning that they were not simply responding to the odor cue, but contained an integrated representation of location with the odor. Swapping which odor appeared at the landmarks led place fields to remap, suggesting that the different odor identities were perceived as distinct contexts and that the place coding was intertwined with the odor landmarks.

In a revised paradigm, Radvansky and colleagues trained mice to associate either odor or visual cues with reward (55). They observed

10.3389/fncir.2024.1414452

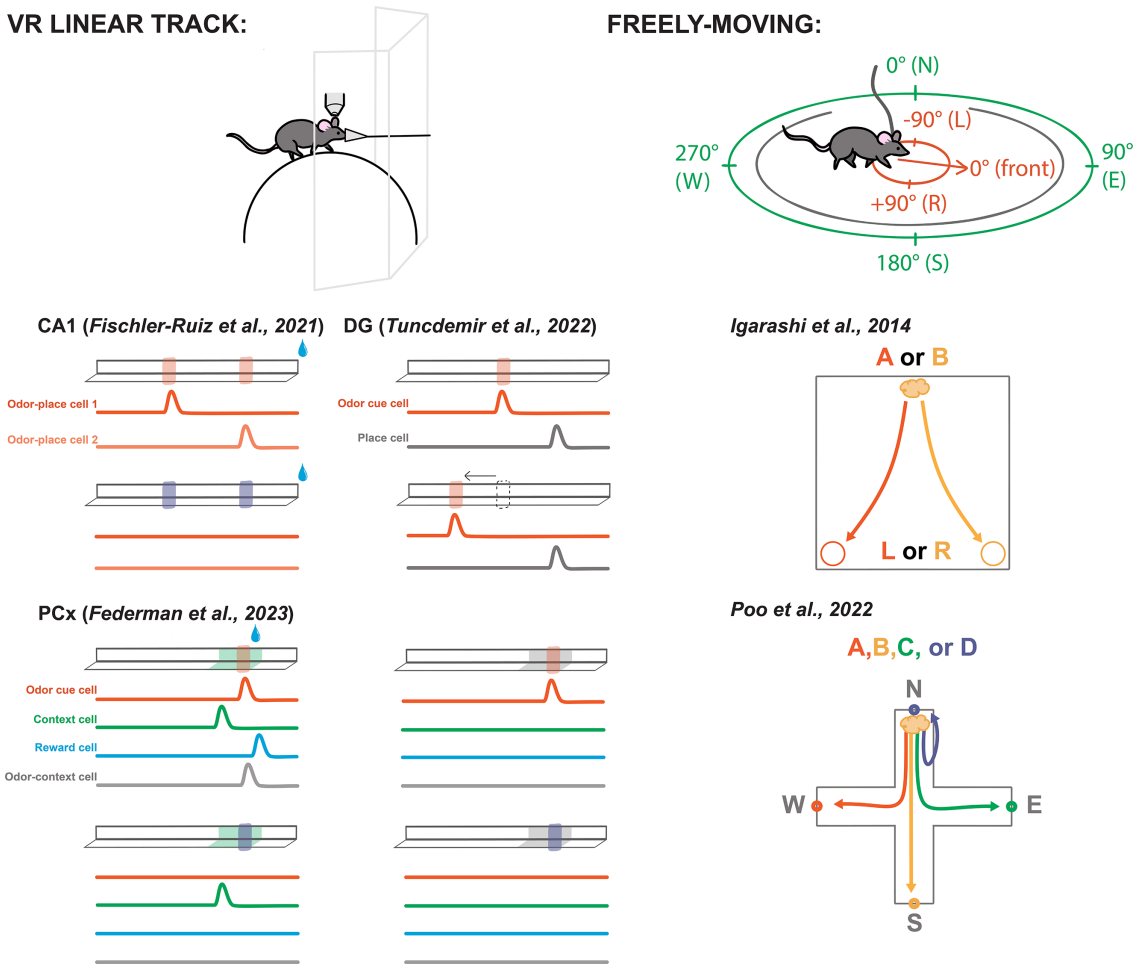

FIGURE 2
Odor-spatial paradigms for characterizing neural activity across brain areas. Left-top: A typical VR linear track set-up including a rodent head-fixed under a recording device (e.g., two-photon microscope) walking on a sphere or wheel while odor is delivered through a nose cone and visuals are shown on screens. Left-bottom: Simplified depictions of select VR linear tracks featured in this review. Odors are represented by translucent red and purple blocks on the track. Water drops represent reward. Specific visual contexts shown in green and gray. Beneath each track are simplified depictions of featured cell activities from each study. Bump represents an uptick in activity. Cell descriptions are labeled in the first panel for each experiment. Experiments labeled by citation above track depictions. Right-top: Schematic of a freely-moving rodent, allocentric spatial perspective represented in green, egocentric represented in red. Right-bottom: Freely-moving task from Igarashi et al. (50), depicting the correct paths to reward depending on odor presentation, odor A signals a reward at the left, odor B signals reward at the right. Bottom-right: Task from Poo et al. (27) with four odor trials from the same port depicted.

substantial recruitment of additional CA1 cells in response to salient cues in both olfactory and visual tasks. In these tasks both olfactory and visual cues were presented, but only one would correspond to reward. Importantly, the cues were not stationary landmarks but moved along the track, eliciting place-like firing leading up to, during, and after the reward relative to the changing location. However, since the odor cue was always spatially tied to reward in the olfactory task, CA1 recruitment could have been due to either odor or reward expectation. Importantly, different populations of cells would fire in relation to the cue-reward depending on the cue modality and task demands. The proportion of visuo-spatial and olfacto-spatial tuned neurons substantially differed between tasks, indicating that the task or reward relevance of sensory input influences hippocampal mapping. Together, this suggests that sensory cues that predict reward overshadow irrelevant cues in CA1 neurons. A further inference is that hippocampal odor-spatial coding is dynamic and adapts to distinct behavioral contexts.

Dentate gyrus granule cells segregate odor and place coding populations

Other regions of HPC, notably DG, have been implicated in the encoding of odor and spatial information. In this section, we describe activity recorded in DG in response to multiple strategic manipulations to the VR linear track paradigm, summarize functionally identified cell types, and consider connectivity that may be essential to these response profiles.

Tuncdemir and colleagues performed an impressive number of variations on the linear track task, while always delivering reward at random (56). Their experimental setup involved a treadmill equipped with stable textural cues to demarcate the track's beginning and end. Initially, mice were introduced to an odor cue near the track's center, consistently positioned relative to the start and end points (Figure 2). Neural activity exhibited place-like tuning along the track's length, with notable enrichment at the lap cues and the odor landmark, mirroring observations from the previously mentioned experiments in CA1 (54).

Investigating further, they introduced laps where the odor cue was spatially shifted or omitted altogether (Figure 2). This manipulation revealed that the majority of cells initially recruited to the odor landmark would be better classified as cue cells, as their responses shifted or disappeared, respectively. However, some place cells persisted, suggesting that cue manipulation did not induce remapping. With the shifting location of the odor cue, these observations look similar to CA1 neurons described earlier (55), however these odor cues were not tied spatially to the randomly supplied reward.

In a series of additional experiments, the researchers compared coding of cues of different sensory modalities, odor cues in different visual contexts, and cues when presented multiple times across the track (56). They found that cues of all modalities were represented in equivalent ways by mostly separate populations of cue cells, that cue cells remained stable across different contexts, and that cue cells fired reliably to their respective cue whenever presented. In comparison, they found that place cells in the same region were less stable, drifting across days, and remapping in different contexts. Thus, by leveraging simple alterations of the task, the authors were able to differentiate between and characterize two important cell populations in DG: place cells and cue cells. They did note that when an odor cue was consistently presented in the same location, the amplitude of cue cell responses was increased, indicating that there is some level of spatial modulation occurring in DG odor cue cells (56).

Given this interesting dichotomy between cell populations in the DG, one might ask where cue cells and place cells get their information. The authors propose that these separate populations of cue cells and place cells receive projections from LEC and MEC, respectively. LEC is often associated with sensory cues and salience, while MEC is primarily involved in spatial processing (57, 58). Indeed, the robust connection from LEC to DG was already implicated in the transfer of odor information to DG (59, 60). While this particular connection may convey odor identity and salient cues, the LEC has also been shown to output specific salient spatial information (61, 62).

Encoding of reward locations in LEC and PCx

Recent work delved into the role of the LEC in encoding reward location (61). By introducing uncued reward at a particular location along the track, researchers were able to identify specific pre-reward, reward consumption, and post-reward cells. When the location of this reward changed, these three cell types adjusted to the new location quickly. They also demonstrated that LEC activity was crucial for learning the position of salient cues, as inhibiting the LEC deterred learning of new reward locations.

In a similar reward navigation task, Bowler and colleagues highlighted a dichotomy between LEC and MEC projections to CA1 (62). They found LEC axons encoded both reward and spatial position. When the goal location was changed, the LEC axons appeared to mostly remap. This finding is consistent with CA1 activity described above, where neurons remapped according to moving reward cues (55). In contrast, MEC axons displayed only spatial coding, remapping with context changes, similar to classic place cells described in CA1 (54) and DG (56). Together, these studies illuminate pathways for odor and space integration from the entorhinal cortices to different areas of the HPC, with LEC appearing to exert direct influence over CA1 and remapping in relation to salient cues.

As part of the primary olfactory cortex, PCx is traditionally studied for its role in coding basic odor information such as odor identity and intensity (25, 63–66). Yet robust bidirectional connections with the LEC, AON, and OB suggest some higher associative role for the area (16, 20–22). Thus, Federman and colleagues conducted a comprehensive investigation into the coding capabilities of PCx through a multi-cue multi-context paradigm (67). In a linear track setup using two odor cues and two visually distinct contexts, Federman paired one conjunction of these variables with a reward shortly after the presentation of the odor. Initially, cells responded primarily to the odor cues (Figure 2). However, with continued exposure and learning of the environmental and olfactory associations, more cells responded to each salient feature of the task, including their many combinations. Notably, the authors report both odor specific cells, context specific cells, and conjunctive odor-context cells. This study showed that PCx can represent behaviorally-relevant odor-spatial information (67).

Freeing behavior: two dimensions and the choice of head-fixation

Thus far, we have summarized studies illustrating diverse coding of odor-spatial information across several key brain areas, with emphasis on the use of a VR linear track. In terms of our hypothetical mouse, we have imagined them foraging for seeds only in a hallway. In addition to this line of VR linear track research, other studies have sought to reap the benefits of head-fixed recording in concert with more complex two-dimensional navigation tasks, for example, employing a spherical ball and a two-dimensional VR world (68) or a floating platform (69). Even in these cases, the use of head-fixation removes important real-world cues. For example, an absence of translational vestibular input and other self-motion cues can produce impairments in two-dimensional place tuning (70, 71). Such limitations motivate parallel studies in more ecologically relevant freely-moving conditions, that we summarize next.

Spatial coding in different reference frames

Whether in VR or freely moving conditions, including a second dimension opens up consideration of multiple spatial reference frames (Figure 2). For example, we often think of space as a fixed map of locations depicted in relation to each other. This perspective is called "allocentric," for example with directions referred to as north, south, east, and west. Simultaneously, we can experience the world in an "egocentric" perspective, using directions to locations such as front, back, left, and right that depend on our place in the world. While peripheral sensory input is inherently egocentric, both perspectives are used for encoding information in the brain, and it is thought that the allocentric perspective is dominant by the time sensory information gets to HPC (72).

Early research into spatial coding was approached primarily from an allocentric perspective, including discoveries of place, grid, and head-direction cells (73–77). Recently, however, studies have identified more egocentric coding throughout the brain. Wang and colleagues characterized spatial coding in the LEC, finding egocentric coding of several aspects of the environment that would be difficult to recognize in a linear track task (78). By leveraging natural exploratory behavior in mice, they discovered cells tuned to boundaries, items, and goal locations.

Together, these findings suggest that the peri-reward cells in LEC discussed earlier could be encoding egocentric coordinates of the reward location (61).

Part of the difficulty in identifying egocentric coding is that cells could be tuned to any of a variety of locations or items in an environment, and tasks must be designed specifically to dissociate different possible coordinate-systems. For example, Igarashi and colleagues trained rats to discriminate two different odors associated with corresponding reward locations (Figure 2) (50). They used egocentric terms "left" and "right" to describe reward locations, but the task design could equivalently be described in allocentric terms such as "East" and "West." The goal of their study was not to explore different spatial frameworks, so they did not include additional spatial complexity, such as rotating or flipping the environment between trials or sessions. However, this study revealed synchrony between LEC and CA1 during odor-place association, which we will discuss further below.

In order to differentiate between allocentric and egocentric coding, it is necessary to examine neural activity during more spatially complex behaviors. Poo and colleagues trained rats to associate four different odors with reward at each of four different ports in a plus shaped arena (Figure 2) (27). Notably, the trial initiation port also changed locations between each trial, requiring the association of each odor to an allocentric place (e.g., North reward port) rather than to an egocentric action (e.g., Left turn to reward port). Interestingly, they found place-like neural tuning not only in CA1. Owing to the clever task design, they further were able to dissociate odor identity from odor delivery location and found both odor selective cells and place-like cells in posterior PCx. They were also able to determine that pPCx spatial coding was allocentric, something that had not yet been described. These spatial PCx cells were concentrated at odor/reward delivery ports indicating that the posterior PCx may represent locations relevant to olfactory task demands.

Learning integrated odor-space representations

An animal is not born with a cognitive map of the world. Representations must be learned through experience and updated as the world changes. The olfactory-hippocampal circuit is especially equipped to facilitate learning, but there are still many unknowns in how representations change across these brain areas to encode new information. So far, we have touched only briefly on studies that investigate changes in neuronal activity during learning. Here we elaborate these findings and propose connections between them.

Inter-areal synchronization during associative learning

Neural activity synchronization has long been associated with learning and memory and navigation (79, 80). Studies have found synchronization between key areas during olfactory-spatial task performance (27, 50). Igarashi and colleagues demonstrated synchronization of the CA1 and LEC during the presentation of odor cues in their left–right odor association task (50). Poo and colleagues found PCx spatial neurons were synchronized with CA1 firing (27). Taken together, these studies suggest that all three areas are synchronized during odor-place association, and further that top-down connections to PCx may be responsible for its spatial coding. Meanwhile, odor tuned cells in PCx tended to be synchronized to the sniff cycle, suggesting that these cells were more directly influenced by OB (27).

Igarashi and colleagues also observed synchrony evolve over multiple days as they added new odors, forcing rats to learn new odor-spatial associations; as rats learned to perform with higher accuracy, the synchronization of the LEC and CA1 also increased (50). This phenomenon may reflect Hebbian strengthening of synapses (81, 82). Indeed, the authors found that the selectivity of odor representations in LEC and CA1 was highly correlated with this inter-areal coupling, and suggested that this coupling may be responsible for the formation of associative representations in both areas.

Intrinsic and learned representations

Complementary studies distinguish representations that seem to be intrinsic to a given brain area from new representations recruited through learning. For example, while place cells in CA1 appear almost instantly upon introduction to a new environment (83) [with some nuances to consider (77)], the appearance of odor landmark tuning was highly correlated with behavioral indications that animals learned the significance of these environmental cues (54). Similarly, odor was strongly represented in CA1 when it predicted reward, but not when another cue was more important to the task (55). Together, these findings support that CA1 forms representations of salient odors in space through associative learning. Anterior PCx seems to mirror this process, with initial coding only of odor, followed by recruitment of more contextual, spatial, and conjunctive odor-context cells with learning (67). Fully trained rats show both spatial and odor representations in posterior PCx. It is unclear whether posterior PCx automatically represents spatial information in a new environment, but the concentration of spatial cells around behaviorally relevant locations suggests that they are recruited through learning (27). Given synchrony between CA1 and PCx and the diverse representations that form in both areas over the course of learning, it appears that these areas may be sharing information to encode salient odor-spatial associations.

A role for LEC in mediating odor-place integration across areas

How does the PCx-HPC circuit know what information to integrate? The LEC is particularly well poised to manage this process. With bidirectional connections to both CA1 and PCx, the LEC stands in position to gate information between them.

Indeed, the LEC has been shown to be important in both spatial and olfactory learning. For example, one study demonstrated that the LEC is required for learning new reward locations (61), while others show that inhibiting LEC pathways to either CA1 or DG impairs new olfactory association learning (42, 60). Interestingly, these studies noted that learning was impaired, while pre-learned associations were not affected. This suggests that LEC plays a specific role in encoding new information, especially odor and spatial associations, thus we hypothesize that LEC acts as a key gateway for pairing these salient associations by inducing multi-areal oscillations and forming complementary representations in HPC and PCx.

Lee and colleagues go farther, identifying dopaminergic inputs to the LEC as key to learning new associations in an odor discrimination

10.3389/fncir.2024.1414452

task (60). Dopamine is one possible trigger to identify novel salient information. The literature on dopamine is vast, and the idea that it may signal novel information underlying learning is key (84–86). That said, the LEC is a highly connected area, and yet unidentified connections may also be important for triggering the process of forming new odor-spatial associations (87).

Interestingly, the LEC sends the bulk of its output projections to DG. Both in LEC fan cells and the DG cells to which they project, odor exposure elicits activity without prior learning (59, 88). As explained earlier, DG maintains separate populations of place cells and cue cells throughout several manipulations, with little evidence of integration (56). This sparsity may be important to differentiate between contexts and distinct episodes (44). During an odorant discrimination task, representations in DG get more sparse and more specific to the odor identities; further, the connection between LEC and DG is important in learning these representations (59). Thus, DG may be responsible for cueing specific contexts, and signaling CA1 to represent salient context-dependent information.

Taken together, these observations may suggest that learning of odor-place associations cause CA1 and PCx to become more tuned to both odor and spatial information, perhaps owing to correlated firing and strengthened connections with each other, mediated by LEC. Simultaneously, DG forms a sparse representation of contextual information that corresponds to learned associations in CA1, for example making it possible for odors to hold different spatial associations in different contexts. We propose that associations between CA1 and PCx are gated by the LEC, which then entrains the CA1-LEC-PCx network in order to tie PCx and CA1 representations together.

Under this model (Figure 3), after introduction to a novel environment, PCx would primarily represent odor and CA1 space. As the animal recognized that an odor cue always preceded a reward location, synchronization of PCx, LEC, and CA1 would increase. This synchronization would signal inter-areal communication that strengthened their connections. These connections would then lead to the emergence of odor-evoked ensembles in CA1 and spatially tuned ensembles in PCx. Given that both areas would then contain the integrated odor-spatial associations, this would also account for the observation that LEC is needed for learning new associations, but not recalling ones previously formed (42, 60, 61).

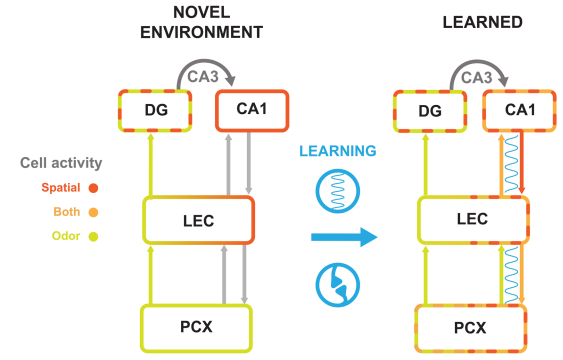

FIGURE 3
Cell activity changes with olfactory-spatial learning across the PCx-HPC circuit. Summary model of the flow of information along the HPC-LEC-PCx pathway. Schematics represent circuitry in a novel environment (left) and after an association is learned (right). Synchrony between areas is represented by a blue wavy line. Arrows between areas represent projections from cell populations with indicated tuning. Spatial (scarlet), odor (chartreuse), and conjunctive cell (orange) activity are represented by colored outlines. Learning is represented in blue between circuitry models, with synchrony and synaptic plasticity icons to symbolize the changes made between the two timepoints. Gray arrows to and from LEC represent connections that exist but are not thought to be synchronized before learning. Dashed boundaries represent cell populations that contain more than one firing type; for example, the DG exhibits odor cue cells and place cells even in novel environments, while the CA1 in the learned condition contains place cells and odor-place cells.

Future perspective

Acquiring data throughout the learning process is challenging. However, emerging tools are making it possible to acquire, store, analyze, and share the vast and multifaceted data produced by olfactory-spatial learning experiments. New indicators and better imaging technologies are rapidly being developed (89–92), while the channel count of electrophysiological recording has dramatically increased (93, 94). Larger datasets impose additional data management requirements, relying on improvements in storage size and decreasing costs (95, 96), and data standards such as NeuroData Without Borders (97). Videographic analysis of behavior has been tremendously advanced by automated tools such as DeepLabCut (98) and MoSeq (99), and an array of post-processing analysis pipelines, e.g., VAME (100), B-Soid (101), DeepPoseKit (102), or Keypoint-MoSeq (103).

Together, these technologies will support novel and advanced investigation of how sensory experience in a dynamic environment shapes the synaptic, cellular, and circuit mechanisms enabling behaviors relying on the integration of odor and space.

Author contributions

OM: Conceptualization, Visualization, Writing – original draft, Writing – review & editing. NK: Conceptualization, Visualization, Writing – original draft, Writing – review & editing. JR: Conceptualization, Writing – original draft, Writing – review & editing. AF: Conceptualization, Writing – original draft, Writing – review & editing.

Funding

The author(s) declare financial support was received for the research, authorship, and/or publication of this article. This work was supported by the Carney Institute of Brain Science.

Acknowledgments

The authors thank Andrea Pierré, Niloufar Razmi, Matthew Nassar, and Rebecca Burwell for their helpful feedback on this manuscript.

Conflict of interest

The authors declare that the research was conducted in the absence of any commercial or financial relationships that could be construed as a potential conflict of interest.

Publisher's note

References

1. García-Cabezas M. Á., Zikopoulos B., Barbas H. (2019). The structural model: a theory linking connections, plasticity, pathology, development and evolution of the cerebral cortex. *Brain Struct Funct* 224, 985–1008. doi: 10.1007/s00429-019-01841-9

2. Laurent G., Fournier J., Hemberger M., Müller C., Naumann R., Ondracek J. M., et al. (2016). "Cortical evolution: introduction to the reptilian cortex" in *Micro-, Meso- and Macro-Dynamics of the Brain*. eds. G. Buzsáki and Y. Christen (Cham (CH): Springer).

3. Naumann R. K., Ondracek J. M., Reiter S., Shein-Idelson M., Tosches M. A., Yamawaki T. M., et al. (2015). The reptilian brain. *Curr Biol* 25, R317–R321. doi: 10.1016/j.cub.2015.02.049

4. Kaas J. H. (2006). Evolution of the neocortex. *Curr Biol* 16, R910–R914. doi: 10.1016/j.cub.2006.09.057

5. Striedter G. F. (1997). The telencephalon of Tetrapods in evolution. *Brain Behav Evol* 49, 179–194. doi: 10.1159/000112991

6. Zeppilli S., Ortega Gurrola A., Demetci P., Brann D. H., Attey R., Zilkha N., et al. (2023). Mammalian olfactory cortex neurons retain molecular signatures of ancestral cell types. *bioRxiv*. doi: 10.1101/2023.08.13.553130v1

7. Baker K. L., Dickinson M., Findley T. M., Gire D. H., Louis M., Suver M. P., et al. (2018). Algorithms for olfactory search across species. *J Neurosci* 38, 9383–9389. doi: 10.1523/JNEUROSCI.1668-18.2018

8. Matheson A. M. M., Lanz A. J., Medina A. M., Licata A. M., Currier T. A., Syed M. H., et al. (2022). A neural circuit for wind-guided olfactory navigation. *Nat Commun* 13:4613. doi: 10.1038/s41467-022-32247-7

9. Jacobs L. F. (2012). From chemotaxis to the cognitive map: the function of olfaction. *Proc Natl Acad Sci U S A* 109, 10693–10700. doi: 10.1073/pnas.1201880109

10. Steele T. J., Lanz A. J., Nagel K. I. (2023). Olfactory navigation in arthropods. *J Comp Physiol A Neuroethol Sens Neural Behav Physiol* 209, 467–488. doi: 10.1007/s00359-022-01611-9

11. Howard W. E., Marsh R. E., Cole R. E. (1968). Food detection by deer mice using olfactory rather than visual cues. *Anim Behav* 16, 13–17. doi: 10.1016/0003-3472(68)90100-0

12. Findley T. M., Wyrick D. G., Cramer J. L., Brown M. A., Holcomb B., Attey R., et al. (2021). Sniff-synchronized, gradient-guided olfactory search by freely moving mice. *Elife* 10:e58523. doi: 10.7554/eLife.58523

13. Gire D. H., Kapoor V., Arrighi-Allisan A., Seminara A., Murthy V. N. (2016). Mice develop efficient strategies for foraging and navigation using complex natural stimuli. *Curr Biol* 26, 1261–1273. doi: 10.1016/j.cub.2016.03.040

14. Haberly L. B., Price J. L. (1977). The axonal projection patterns of the mitral and tufted cells of the olfactory bulb in the rat. *Brain Res* 129, 152–157. doi: 10.1016/0006-8993(77)90978-7

15. Igarashi K. M., Ieki N., An M., Yamaguchi Y., Nagayama S., Kobayakawa K., et al. (2012). Parallel mitral and tufted cell pathways route distinct odor information to different targets in the olfactory cortex. *J Neurosci* 32, 7970–7985. doi: 10.1523/JNEUROSCI.0154-12.2012

16. Chen Y., Chen X., Baserdem B., Zhan H., Li Y., Davis M. B., et al. (2022). High-throughput sequencing of single neuron projections reveals spatial organization in the olfactory cortex. *Cell* 185, 4117–34.e28. doi: 10.1016/j.cell.2022.09.038

17. Zeppilli S., Ackels T., Attey R., Klimpert N., Ritola K. D., Boeing S., et al. (2021). Molecular characterization of projection neuron subtypes in the mouse olfactory bulb. *Elife* 10:e65445. doi: 10.7554/eLife.65445

18. Wang L., Zhang Z., Chen J., Manyande A., Haddad R., Liu Q., et al. (2020). Cell-type-specific whole-brain direct inputs to the anterior and posterior piriform cortex. *Front Neural Circuits* 14:4. doi: 10.3389/fncir.2020.00004

19. Haberly L. B., Price J. L. (1978). Association and commissural fiber systems of the olfactory cortex of the rat. *J Comp Neurol* 178, 711–740. doi: 10.1002/cne.901780408

20. Diodato A., Ruinart de Brimont M., Yim Y. S., Derian N., Perrin S., Pouch J., et al. (2016). Molecular signatures of neural connectivity in the olfactory cortex. *Nat Commun* 7:12238. doi: 10.1038/ncomms12238

21. Chen C. F. F., Zou D. J., Altomare C. G., Xu L., Greer C. A., Firestein S. J. (2014). Nonsensory target-dependent organization of piriform cortex. *Proc Natl Acad Sci U S A* 111, 16931–16936. doi: 10.1073/pnas.1411266111

22. Mazo C., Grimaud J., Shima Y., Murthy V. N., Lau C. G. (2017). Distinct projection patterns of different classes of layer 2 principal neurons in the olfactory cortex. *Sci Rep* 7, 1–10. doi: 10.1038/s41598-017-08331-0

23. Bolding K. A., Franks K. M. (2018). Recurrent cortical circuits implement concentration-invariant odor coding. *Science* 361:aat6904. doi: 10.1126/science.aat6904

24. Millman D. J., Murthy V. N. (2020). Rapid learning of odor–value Association in the Olfactory Striatum. *J Neurosci* 40, 4335–4347. doi: 10.1523/JNEUROSCI.2604-19.2020

25. Miura K., Mainen Z. F., Uchida N. (2012). Odor representations in olfactory cortex: distributed rate coding and decorrelated population activity. *Neuron* 74, 1087–1098. doi: 10.1016/j.neuron.2012.04.021

26. Schoonover C. E., Ohashi S. N., Axel R., Fink A. J. P. (2021). Representational drift in primary olfactory cortex. *Nature* 594, 541–546. doi: 10.1038/s41586-021-03628-7

27. Poo C., Agarwal G., Bonacchi N., Mainen Z. F. (2022). Spatial maps in piriform cortex during olfactory navigation. *Nature* 601, 595–599. doi: 10.1038/s41586-021-04242-3

28. Large A. M., Vogler N. W., Canto-Bustos M., Friason F. K., Schick P., Oswald A. M. M. (2018). Differential inhibition of pyramidal cells and inhibitory interneurons along the rostrocaudal axis of anterior piriform cortex. *Proce Natl Acad Sci* 115, E8067–E8076. doi: 10.1073/pnas.1802428115

29. Meissner-Bernard C., Dembitskaya Y., Venance L., Fleischmann A. (2019). Encoding of odor fear memories in the mouse olfactory cortex. *Curr Biol* 29, 367–80.e4. doi: 10.1016/j.cub.2018.12.003

30. Wang P. Y., Boboila C., Chin M., Higashi-Howard A., Shamash P., Wu Z., et al. (2020). Transient and persistent representations of odor value in prefrontal cortex. *Neuron* 108, 209–24.e6. doi: 10.1016/j.neuron.2020.07.033

31. Haberly L. B. (2001). Parallel-distributed processing in olfactory cortex: new insights from morphological and physiological analysis of neuronal circuitry. *Chem Senses* 26, 551–576. doi: 10.1093/chemse/26.5.551

32. Loureiro M., Achargui R., Flakowski J., Van Zessen R., Stefanelli T., Pascoli V., et al. (2019). Social transmission of food safety depends on synaptic plasticity in the prefrontal cortex. *Science* 364, 991–995. doi: 10.1126/science.aaw5842

33. Moser E. I., Kropff E., Moser M. B. (2008). Place cells, grid cells, and the brain's spatial representation system. *Annu Rev Neurosci* 31, 69–89. doi: 10.1146/annurev.neuro.31.061307.090723

34. Burwell R. D., Witter M. P. (2002). *Basic Anatomy of the Parahippocampal Region in Monkeys and Rats*. Oxford: Oxford University Press.

35. Witter M. P., Wouterlood F. G., Naber P. A., Van Haeften T. (2000). Anatomical organization of the parahippocampal-hippocampal network. *Ann N Y Acad Sci* 911, 1–24. doi: 10.1111/j.1749-6632.2000.tb06716.x

36. Royer S., Sirota A., Patel J., Buzsáki G. (2010). Distinct representations and theta dynamics in dorsal and ventral hippocampus. *J Neurosci* 30, 1777–1787. doi: 10.1523/JNEUROSCI.4681-09.2010

37. Moser M. B., Moser E. I. (1998). Functional differentiation in the hippocampus. *Hippocampus* 8, 608–619. doi: 10.1002/(SICI)1098-1063(1998)8:6<608::AID-HIPO3>3.0.CO;2-7

38. Witter M. P., Groenewegen H. J., Lopes da Silva F. H., Lohman A. H. (1989). Functional organization of the extrinsic and intrinsic circuitry of the parahippocampal region. *Prog Neurobiol* 33, 161–253. doi: 10.1016/0301-0082(89)90009-9

39. Cenquizca L. A., Swanson L. W. (2007). Spatial organization of direct hippocampal field CA1 axonal projections to the rest of the cerebral cortex. *Brain Res Rev* 56, 1–26. doi: 10.1016/j.brainresrev.2007.05.002

40. Kosel K. C., Van Hoesen G. W., West J. R. (1981). Olfactory bulb projections to the parahippocampal area of the rat. *J Comp Neurol* 198, 467–482. doi: 10.1002/cne.901980307

41. Leitner F. C., Melzer S., Lütcke H., Pinna R., Seeburg P. H., Helmchen F., et al. (2016). Spatially segregated feedforward and feedback neurons support differential odor processing in the lateral entorhinal cortex. *Nat. Neurosci.* 19, 935–944. doi: 10.1038/nn.4303

42. Li Y., Xu J., Liu Y., Zhu J., Liu N., Zeng W., et al. (2017). A distinct entorhinal cortex to hippocampal CA1 direct circuit for olfactory associative learning. *Nat Neurosci* 20, 559–570. doi: 10.1038/nn.4517

43. Bitzenhofer S. H., Westeinde E. A., Zhang H. X. B., Isaacson J. S. (2022). Rapid odor processing by layer 2 subcircuits in lateral entorhinal cortex. *Elife* 11:e75065. doi: 10.7554/eLife.75065

44. Lee H., GoodSmith D., Knierim J. J. (2020). Parallel processing streams in the hippocampus. *Curr Res Neurobiol* 64, 127–134. doi: 10.1016/j.conb.2020.03.004

45. Aqrabawi A. J., Kim J. C. (2018). Topographic Organization of Hippocampal Inputs to the anterior olfactory nucleus. *Front Neuroanat* 12:12. doi: 10.3389/fnana.2018.00012

46. Aqrabawi A. J., Kim J. C. (2020). Olfactory memory representations are stored in the anterior olfactory nucleus. *Nat Commun* 11:1246. doi: 10.1038/s41467-020-15032-2

47. Aqrabawi A. J., Kim J. C. (2018). Hippocampal projections to the anterior olfactory nucleus differentially convey spatiotemporal information during episodic odour memory. *Nat Commun* 9:2735. doi: 10.1038/s41467-018-05131-6

48. Kikuta S., Sato K., Kashiwadani H., Tsunoda K., Yamasoba T., Mori K. (2010). From the cover: neurons in the anterior olfactory nucleus pars externa detect right or left localization of odor sources. *Proc Natl Acad Sci U S A* 107, 12363–12368. doi: 10.1073/pnas.1003999107

49. Grobman M., Dalal T., Lavian H., Shmuel R., Belelovsky K., Xu F., et al. (2018). A Mirror-symmetric excitatory link coordinates odor maps across olfactory bulbs and enables odor perceptual Unity. *Neuron* 99, 800–13.e6. doi: 10.1016/j.neuron.2018.07.012

50. Igarashi K. M., Lu L., Colgin L. L., Moser M. B., Moser E. I. (2014). Coordination of entorhinal–hippocampal ensemble activity during associative learning. *Nature* 510, 143–147. doi: 10.1038/nature13162

51. Radvansky B. A., Dombeck D. A. (2018). An olfactory virtual reality system for mice. *Nat Commun* 9:839. doi: 10.1038/s41467-018-03262-4

52. Dombeck D. A., Harvey C. D., Tian L., Looger L. L., Tank D. W. (2010). Functional imaging of hippocampal place cells at cellular resolution during virtual navigation. *Nat Neurosci* 13, 1433–1440. doi: 10.1038/nn.2648

53. Danielson N. B., Zaremba J. D., Kaifosh P., Bowler J., Ladow M., Losonczy A. (2016). Sublayer-specific coding dynamics during spatial navigation and learning in hippocampal area CA1. *Neuron* 91, 652–665. doi: 10.1016/j.neuron.2016.06.020

54. Fischler-Ruiz W., Clark D. G., Joshi N. R., Devi-Chou V., Kitch L., Schnitzer M., et al. (2021). Olfactory landmarks and path integration converge to form a cognitive spatial map. *Neuron* 109, 4036–49.e5. doi: 10.1016/j.neuron.2021.09.055

55. Radvansky B. A., Oh J. Y., Climer J. R., Dombeck D. A. (2021). Behavior determines the hippocampal spatial mapping of a multisensory environment. *Cell Rep* 36:109444. doi: 10.1016/j.celrep.2021.109444

56. Tuncdemir S. N., Grosmark A. D., Turi G. F., Shank A., Bowler J. C., Ordek G., et al. (2022). Parallel processing of sensory cue and spatial information in the dentate gyrus. *Cell Rep* 38:110257. doi: 10.1016/j.celrep.2021.110257

57. Hargreaves E. L., Rao G., Lee I., Knierim J. J. (2005). Major dissociation between medial and lateral entorhinal input to dorsal hippocampus. *Science* 308, 1792–1794. doi: 10.1126/science.1110449

58. Knierim J. J., Neunuebel J. P., Deshmukh S. S. (2014). Functional correlates of the lateral and medial entorhinal cortex: objects, path integration and local–global reference frames. *Philos Trans R Soc Lond B Biol Sci* 369:20130369. doi: 10.1098/rstb.2013.0369

59. Woods N. I., Stefanini F., Apodaca-Montano D. L., Tan I. M. C., Biane J. S., Kheirbek M. A. (2020). The dentate gyrus classifies cortical representations of learned stimuli. *Neuron* 107, 173–84.e6. doi: 10.1016/j.neuron.2020.04.002

60. Lee J. Y., Jun H., Soma S., Nakazono T., Shiraiwa K., Dasgupta A., et al. (2021). Dopamine facilitates associative memory encoding in the entorhinal cortex. *Nature* 598, 321–326. doi: 10.1038/s41586-021-03948-8

61. Issa J. B., Radvansky B. A., Xuan F., Dombeck D. A. (2024). Lateral entorhinal cortex subpopulations represent experiential epochs surrounding reward. *Nat Neurosci* 27, 536–546. doi: 10.1038/s41593-023-01557-4

62. Bowler J. C., Losonczy A. (2023). Direct cortical inputs to hippocampal area CA1 transmit complementary signals for goal-directed navigation. *Neuron* 111, 4071–85.e6. doi: 10.1016/j.neuron.2023.09.013

63. Stettler D. D., Axel R. (2009). Representations of odor in the piriform cortex. *Neuron* 63, 854–864. doi: 10.1016/j.neuron.2009.09.005

64. Roland B., Deneux T., Franks K. M., Bathellier B., Fleischmann A. (2017). Odor identity coding by distributed ensembles of neurons in the mouse olfactory cortex. *eLife* 6:e26337. doi: 10.7554/eLife.26337

65. Bolding K. A., Franks K. M. (2017). Complementary codes for odor identity and intensity in olfactory cortex. *Elife* 6:6. doi: 10.7554/eLife.22630

66. Pashkovski S. L., Iurilli G., Brann D., Chicharro D., Drummey K., Franks K. M., et al. (2020). Structure and flexibility in cortical representations of odour space. *Nature* 583, 253–258. doi: 10.1038/s41586-020-2451-1

67. Federman N., Romano S. A., Amigo-Duran M., Salomon L., Marin-Burgin A. (2023). Acquisition of non-olfactory encoding improves odour discrimination in olfactory cortex. *Neuroscience*. doi: 10.1101/2023.07.04.547685

68. Aronov D., Tank D. W. (2014). Engagement of neural circuits underlying 2D spatial navigation in a rodent virtual reality system. *Neuron* 84, 442–456. doi: 10.1016/j.neuron.2014.08.042

69. Go M. A., Rogers J., Gava G. P., Davey C. E., Prado S., Liu Y., et al. (2021). Place cells in head-fixed mice navigating a floating real-world environment. *Front Cell Neurosci* 15:618658. doi: 10.3389/fncel.2021.618658

70. Ravassard P., Kees A., Willers B., Ho D., Aharoni D., Cushman J., et al. (2013). Multisensory control of hippocampal spatiotemporal selectivity. *Science* 340, 1342–1346. doi: 10.1126/science.1232655

71. Aghajan Z. M., Acharya L., Moore J. J., Cushman J. D., Vuong C., Mehta M. R. (2015). Impaired spatial selectivity and intact phase precession in two-dimensional virtual reality. *Nat Neurosci* 18, 121–128. doi: 10.1038/nn.3884

72. Wang C., Chen X., Knierim J. J. (2020). Egocentric and allocentric representations of space in the rodent brain. *Curr Opin Neurobiol* 60, 12–20. doi: 10.1016/j.conb.2019.11.005

73. O'Keefe J. (1976). Place units in the hippocampus of the freely moving rat. *Exp Neurol* 51, 78–109. doi: 10.1016/0014-4886(76)90055-8

74. Fyhn M., Molden S., Witter M. P., Moser E. I., Moser M. B. (2004). Spatial representation in the entorhinal cortex. *Science* 305, 1258–1264. doi: 10.1126/science.1099901

75. Hafting T., Fyhn M., Molden S., Moser M. B., Moser E. I. (2005). Microstructure of a spatial map in the entorhinal cortex. *Nature* 436, 801–806. doi: 10.1038/nature03721

76. Sargolini F., Fyhn M., Hafting T., McNaughton B. L., Witter M. P., Moser M. B., et al. (2006). Conjunctive representation of position, direction, and velocity in entorhinal cortex. *Science* 312, 758–762. doi: 10.1126/science.1125572

77. Moser M. B., Rowland D. C., Moser E. I. (2015). Place cells, grid cells, and memory. *Cold Spring Harb Perspect Biol* 7:a021808. doi: 10.1101/cshperspect.a021808

78. Wang C., Chen X., Lee H., Deshmukh S. S., Yoganarasimha D., Savelli F., et al. (2018). Egocentric coding of external items in the lateral entorhinal cortex. *Science* 362, 945–949. doi: 10.1126/science.aau4940

79. Macrides F., Eichenbaum H. B., Forbes W. B. (1982). Temporal relationship between sniffing and the limbic theta rhythm during odor discrimination reversal learning. *J Neurosci* 2, 1705–1717. doi: 10.1523/JNEUROSCI.02-12-01705.1982

80. Buzsáki G., Moser E. I. (2013). Memory, navigation and theta rhythm in the hippocampal-entorhinal system. *Nat Neurosci* 16, 130–138. doi: 10.1038/nn.3304

81. Bi G., Poo M. (2001). Synaptic modification by correlated activity: Hebb's postulate revisited. *Annu Rev Neurosci* 24, 139–166. doi: 10.1146/annurev.neuro.24.1.139

82. Buzsáki G. (2010). Neural syntax: cell assemblies, synapsembles, and readers. *Neuron* 68, 362–385. doi: 10.1016/j.neuron.2010.09.023

83. Frank L. M., Stanley G. B., Brown E. N. (2004). Hippocampal plasticity across multiple days of exposure to novel environments. *J Neurosci* 24, 7681–7689. doi: 10.1523/JNEUROSCI.1958-04.2004

84. Lisman J. E., Grace A. A. (2005). The hippocampal-VTA loop: controlling the entry of information into long-term memory. *Neuron* 46, 703–713. doi: 10.1016/j.neuron.2005.05.002

85. Bromberg-Martin E. S., Matsumoto M., Hikosaka O. (2010). Dopamine in motivational control: rewarding, aversive, and alerting. *Neuron* 68, 815–834. doi: 10.1016/j.neuron.2010.11.022

86. Retailleau A., Morris G. (2018). Spatial rule learning and corresponding CA1 place cell reorientation depend on local dopamine release. *Curr Biol* 28, 836–46.e4. doi: 10.1016/j.cub.2018.01.081

87. Doan T. P., Lagartos-Donate M. J., Nilssen E. S., Ohara S., Witter M. P. (2019). Convergent projections from Perirhinal and Postrhinal cortices suggest a multisensory nature of lateral, but not medial, entorhinal cortex. *Cell Rep* 29, 617–27.e7. doi: 10.1016/j.celrep.2019.09.005

88. Mena W., Baker K., Rubin A., Kohli S., Yoo Y., Ziv Y., et al. (2023). Differential encoding of odor and place in mouse piriform and entorhinal cortex. *bioRxiv*. doi: 10.1101/2023.10.05.561119v1

89. Zhang Y., Rózsa M., Liang Y., Bushey D., Wei Z., Zheng J., et al. (2023). Fast and sensitive GCaMP calcium indicators for imaging neural populations. *Nature* 615, 884–891. doi: 10.1038/s41586-023-05828-9

90. Abdelfattah A. S., Zheng J., Singh A., Huang Y. C., Reep D., Tsegaye G., et al. (2023). Sensitivity optimization of a rhodopsin-based fluorescent voltage indicator. *Neuron* 111, 1547–63.e9. doi: 10.1016/j.neuron.2023.03.009

91. Guo C., Blair G. J., Sehgal M., Sangiuliano Jimka F. N., Bellafard A., Silva A. J., et al. (2023). Miniscope-LFOV: a large-field-of-view, single-cell-resolution, miniature microscope for wired and wire-free imaging of neural dynamics in freely behaving animals. *Sci Adv* 9:eadg3918. doi: 10.1126/sciadv.adg3918

92. Guo C., Wang A., Cheng H., Chen L. (2023). New imaging instrument in animal models: two-photon miniature microscope and large field of view miniature microscope for freely behaving animals. *J Neurochem* 164, 270–283. doi: 10.1111/jnc.15711

93. Jun J. J., Steinmetz N. A., Siegle J. H., Denman D. J., Bauza M., Barbarits B., et al. (2017). Fully integrated silicon probes for high-density recording of neural activity. *Nature* 551, 232–236. doi: 10.1038/nature24636

94. Steinmetz N. A., Aydin C., Lebedeva A., Okun M., Pachitariu M., Bauza M., et al. (2021). Neuropixels 2.0: a miniaturized high-density probe for stable, long-term brain recordings. *Science* 372:abf4588. doi: 10.1126/science.abf4588

95. Morris R. J. T., Truskowski B. J. (2003). The evolution of storage systems. *IBM Syst J* 42, 205–217. doi: 10.1147/sj.422.0205

96. Lee S. H. (2016). "Technology scaling challenges and opportunities of memory devices" in *2016 IEEE International Electron Devices Meeting (IEDM)* (San Francisco, CA, USA: IEEE), 1.1.1–1.1.8.

97. Rübel O., Tritt A., Dichter B., Braun T., Cain N., Clack N., et al. (2019). NWB:N 2.0: An accessible data standard for neurophysiology [internet]. *bioRxiv*:523035. doi: 10.1101/523035

98. Mathis A., Mamidanna P., Cury K. M., Abe T., Murthy V. N., Mathis M. W., et al. (2018). DeepLabCut: markerless pose estimation of user-defined body parts with deep learning. *Nat Neurosci* 21, 1281–1289. doi: 10.1038/s41593-018-0209-y

99. Wiltschko A. B., Johnson M. J., Iurilli G., Peterson R. E., Katon J. M., Pashkovski S. L., et al. (2015). Mapping sub-second structure in mouse behavior. *Neuron* 88, 1121–1135. doi: 10.1016/j.neuron.2015.11.031

100. Graving J. M., Chae D., Naik H., Li L., Koger B., Costelloe B. R., et al. (2019). DeepPoseKit, a software toolkit for fast and robust animal pose estimation using deep learning. *Elife* 8:8. doi: 10.7554/eLife.47994

101. Hsu A. I., Yttri E. A. (2021). B-SOiD, an open-source unsupervised algorithm for identification and fast prediction of behaviors. *Nat Commun* 12:5188. doi: 10.1038/s41467-021-25420-x

102. Luxem K., Mocellin P., Fuhrmann F., Kürsch J., Miller S. R., Palop J. J., et al. (2022). Identifying behavioral structure from deep variational embeddings of animal motion. *Commun Biol* 5:1267. doi: 10.1038/s42003-022-04080-7

103. Weinreb C., Pearl J., Lin S., Osman M. A. M., Zhang L., Annapragada S., et al. (2023). Keypoint-MoSeq: parsing behavior by linking point tracking to pose dynamics. *bioRxiv*. doi: 10.1101/2023.03.16.532307

frontiers | Frontiers in Neural Circuits

TYPE Mini Review
PUBLISHED 01 July 2024
DOI 10.3389/fncir.2024.1431119

OPEN ACCESS

EDITED BY
Kensaku Mori,
RIKEN, Japan

REVIEWED BY
Yoshimasa Seki,
Aichi University, Japan

*CORRESPONDENCE
Yoko Yazaki-Sugiyama
yazaki-sugiyama@oist.jp

RECEIVED 11 May 2024
ACCEPTED 13 June 2024
PUBLISHED 01 July 2024

CITATION
Yazaki-Sugiyama Y (2024) Tutor auditory memory for guiding sensorimotor learning in birdsong.
Front. Neural Circuits 18:1431119.
doi: 10.3389/fncir.2024.1431119

Tutor auditory memory for guiding sensorimotor learning in birdsong

Yoko Yazaki-Sugiyama*

Neuronal Mechanism for Critical Period Unit, OIST Graduate University, Okinawa, Japan

Memory-guided motor shaping is necessary for sensorimotor learning. Vocal learning, such as speech development in human babies and song learning in bird juveniles, begins with the formation of an auditory template by hearing adult voices followed by vocally matching to the memorized template using auditory feedback. In zebra finches, the widely used songbird model system, only males develop individually unique stereotyped songs. The production of normal songs relies on auditory experience of tutor's songs (commonly their father's songs) during a critical period in development that consists of orchestrated auditory and sensorimotor phases. "Auditory templates" of tutor songs are thought to form in the brain to guide later vocal learning, while formation of "motor templates" of own song has been suggested to be necessary for the maintenance of stereotyped adult songs. Where these templates are formed in the brain and how they interact with other brain areas to guide song learning, presumably with template-matching error correction, remains to be clarified. Here, we review and discuss studies on auditory and motor templates in the avian brain. We suggest that distinct auditory and motor template systems exist that switch their functions during development.

KEYWORDS

auditory, song learning, critical period, sensorimotor learning, songbird, template matching

Introduction

Sensorimotor learning depends on memory formation, followed by matching a motor pattern to the memorized template. When learning to speak, human babies shape their auditory detection skills based on the sensory environment. Later, they sculpt their vocalization using auditory feedback, which is restricted within the range of acquired auditory perception. Similalrly, songbirds learn to sing first by memorizing a tutor's songs (TS), commonly their father's songs, and then by matching their vocalizations to the memorized TS via auditory feedback during the song-learning period (Figure 1). Depending on the bird species, only males or both sexes sing to attract mating partners, to identify their territory, and to facilitate individual recognition. Early behavioral studies in

Abbreviations: AFP, anterior forebrain pathway; AIV, ventral intermediate arcopallium; CMM, caudomedial mesopallium; LC, locus coeruleus; LMAN, lateral magnocellular nucleus of the anterior neostriatum; NCM, caudal mesopallium; Nif, nucleus interface; RA, robust nucleus of the arcopallium; RAcup, "cup" adjacent to RA; SNc, substantia nigra pars compacta; TS, tutor's songs; Uva, nucleus Uvaeformis; VP, ventral pallidum; VTA, ventral tegmental area.

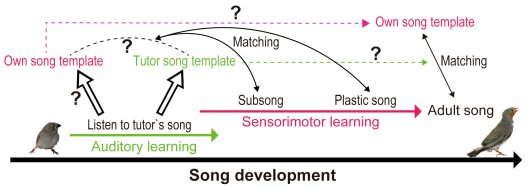

FIGURE 1
Conceptual diagram of the zebra finch song learning process: template formation and template matching. Juveniles form a tutor auditory template by listening to tutor's songs, which may facilitate formation of own song motor template. Juveniles develop their own adult songs by matching their vocalization to the template (unclear whether tutor song template or own song template), using auditory feedback. Template matching with auditory feedback is believed to continue until adulthood, as disturbing auditory feedback leads to song degradation.

white crowned sparrows (*Zonotrichia leucophrys*), which form memories and start to sing in different seasons, explained beautifully the multistep process of song learning; isolation after hearing and memorizing TS in the spring does not prevent juveniles from developing normal adult songs and learning from TS when they start to sing in the fall. If juveniles are isolated from TS before auditory learning or are deafened in the period between auditory and sensorimotor learning, song learning fails to develop properly. These behavioral studies emphasize the importance of forming auditory memories of TS by listening to the tutor and the necessity of auditory feedback during sensorimotor learning (Konishi, 1965; Marler, 1970).

In zebra finches (*Taeniopygia guttata)*, the widely used songbird model system, only males sing, and females do not. Male zebra finches develop individually unique songs in the largely overlapping auditory and sensorimotor learning phases and retain them throughout their life. Their songs are similar, but never identical, to TS, which is important for identity recognition. Sensorimotor learning ends irrespectively of the level of similarity between own song and TS or song maturity. Thus, the pre-determined time course of song learning based on age is suggested. These observations raise questions on how error signals shape the motor pattern of singing, especially in later phases of song learning, if auditory memories of TS instruct sensorimotor learning and regulate the song-learning time window. Alternatively, do birds construct a "motor template" by hearing TS? The "template" and "template matching" theories have been discussed in songbird research for decades, but only vague and occasionally confusing definitions of song templates (auditory memory of TS or a bird's own motor pattern) have been provided. In this review, we sought to discuss how and where in the brain song templates are stored to be utilized for song learning.

"Template matching" theory

In describing the song template system, Peter Marler determined in his early studies that templates serve as filters to detect own species song first, and later for the formation of memories of TS and motor learning guidance; these definitions suggest that templates have multiple functions depending on the developmental time course (Marler, 1970). Marler later described preactive (active) and latent templates. The former normally acts as a filter for preferential learning from own species songs and later guides song learning if birds are not exposed to adult songs, while the latter guides motor learning with respect to the formed memory of adult songs (Marler, 1984; Marler and Nelson, 1992; Marler, 1997). Marler and others, with slight variations, have indicated that template formation requires auditory experiences of conspecific adult songs in addition to innate predispositions. Normally birds learn to sing by hearing TS, suggesting that memories of TS function as templates, while isolated birds use an internal song model as template [reviewed in Mooney (2009)]. While isolated songs feature abnormal acoustic characteristics, such as longer duration and limited variety of syllables with relatively simple features, prolonged isolation (over generations) somewhat normalizes songs, suggesting the presence of innate predispositions (Fehér et al., 2009). Templates may facilitate memory formation of TS (or memories of TS are "templates" as themselves) and for shaping motor learning later. Whether auditory memory of TS and motor templates, namely the preactive and latent templates described in the early work of Peter Marler, are distinct has yet to be clarified.

TS memories are believed to be formed for song learning (tutor templates), as social isolation (absence of tutor template) leads to abnormal song development. However, zebra finches do not develop an exact copy of TS for their own song development. Each individual among siblings intentionally develops own unique songs by coping distinct parts of father's songs (Tchernichovski and Nottebohm, 1998). Additionally, song learning concludes regardless of the level attained (similarity to TS), but depending on a developmental time course. These notions indicate that template matching with error correction with TS auditory memories alone would not lead to the development of individual songs and suggest that motor templates must be established. In the following sections, we discuss the brain circuits that host specific song templates and aspects of their temporal development.

Song motor template in the premotor area, HVC, the apex of the song system

HVC sits at the apex of the song system and constitutes the premotor area for singing behavior (Figure 2). Pioneering chronic multiunit recordings in HVC have shown firing activity when an adult male zebra finch sings (McCasland and Konishi, 1981). HVC comprises two types of projection neurons and interneurons and shows auditory responsiveness to playback of bird's own songs (BOS) under anesthesia (Mooney, 2000). Other studies, including a detailed electrophysiological study with antidromic neuronal identification in awake singing birds, have revealed sequential sparse firing in a group of HVC neurons, which extends over the entire song duration (Hahnloser et al., 2002). Cooling HVC affects the temporal pattern of vocal behavior by slowing down the timing of the song (Long and Fee, 2008). Even in the absence of tutoring experiences, sequential activity in HVC can be observed, while pre-existing sequences become tightly associated with new own song

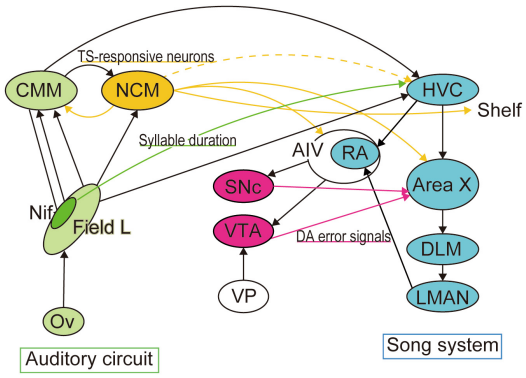

FIGURE 2
Neural circuits for template matching. Neural circuits necessary for song production and learning have been well identified as the song system (colored in cyan). Area X, the basal ganglia locus of the song system, is reported to receive dopaminergic error signals from VTA when auditory feedback is distorted. The premotor region of the song system, HVC, also receives sensory inputs from multiple auditory areas, including the telencephalic nucleus interface (NIf). Optogenetic activation of NIf projections to HVC encode the duration of song syllables. In contrast, accumulated studies have suggested that tutor memory forms in a higher auditory area, the caudal mesopallium (NCM), from which we found a transient projection to HVC during the song learning period.

after exposure to TS (Mackevicius et al., 2023). These series of studies have suggested that microcircuits within HVC regulate the generation of the song motor pattern. Perturbating the activity of the motor thalamic nucleus Uvaeformis (Uva), which projects to HVC, and imaging of Uva synaptic activity in HVC further support a model whereby thalamic input to "starter cells" in HVC drives sequential neuronal activity in the nucleus (Moll et al., 2023). Moreover, fractions of HVC neurons projecting to Area X (HVC_x neurons) have reported to work as "mirror neurons" (Prather et al., 2008; Fujimoto et al., 2011). Studies in swamp sparrows and Bengalese finches revealed that antidromically identified single HVC_x neuronal units exhibit neuronal firing both during singing and BOS playback, exactly the same time in the song phase, suggesting auditory-vocal information in single neurons. Notably, these studies were performed in adult zebra finches in which songs are "crystallized". Contingent aversive stimulation in adult birds shifts the pitch of targeted syllables, but the pitch reverts to baseline when the perturbation is removed, suggesting that song templates are retained after song crystallization (Janata and Margoliash, 1999; Sober and Brainard, 2009). Is this template a TS auditory memory? Does the TS auditory template or the motor template (preactive or latent) guide song learning?

Song motor plasticity driven by the anterior forebrain pathway (AFP)

Early studies on the lateral magnocellular nucleus of the anterior neostriatum (LMAN), the output region of the basal ganglia–thalamocortical loop of the song system, were implicated LMAN as the site associated with the tutor template. After LMAN lesions, juveniles loose motor plasticity which leads to poor song learning from TS (Bottjer et al., 1984; Scharff and Nottebohm, 1991). Juvenile LMAN neurons respond to playback of TS (Solis and Doupe, 1997, 1999). However, LMAN neurons do not respond to TS that is no longer similar to bird's own song by re-learning from another tutor (Yazaki-Sugiyama and Mooney, 2004). Later studies have shown that LMAN contributes to acute song motor plasticity. LMAN activity is higher when zebra finches are singing undirected songs than direct songs, which are characterized by less variable acoustic features (Sossinka and Böhner, 1980; Jarvis et al., 1998; Hessler and Doupe, 1999). LMAN lesion reduces song variability in adults, suggesting defects in motor plasticity, similar to the previous finding in juveniles. Microsimulation of LMAN alters the song motor pattern (Kao et al., 2005). LMAN projects to a motor area, the robust nucleus of the arcopallium (RA), where neurons receive direct inputs from HVC. As described above, several studies have suggested that LMAN is responsible for error/error corrections (the output of a comparator). Still, important questions remain regarding the source of auditory feedback and the site of representation of the TS memory template. Additionally, whether the TS or motor template is compared to auditory feedback remains to be clarified.

Auditory feedback to the song system

Recent studies using advanced techniques that allow manipulation of specific inputs to HVC have reported that optogenetical activation of the telencephalic nucleus interface (NIf) input at HVC synapses shapes the duration of syllables, while severing the NIf–HVC projection before, but not after, auditory learning from tutor disrupts song learning from tutor (Zhao et al., 2019). HVC rhythmic activity emerges in parallel with the emergence of new syllables during development (Okubo et al., 2015). Interestingly, *in vivo* intracellular recordings in awake zebra finches revealed that HVC neurons projecting to RA respond to TS in juveniles, but these responses are suppressed by local inhibitory circuits in adults (Vallentin et al., 2016).

Not only auditory feedback but dopaminergic signals have also been reported to shape song learning, as reported in reinforcement learning (Scharff and Nottebohm, 1991; Brainard and Doupe, 2000). The basal ganglia locus of the song system, Area X, receives dopaminergic inputs from the ventral tegmental area (VTA) (Person et al., 2008). VTA receives auditory inputs from the surrounding part of the arcopallium (ventral intermediate arcopallium [AIV]) (the "cup" adjacent to RA [RAcup]), suggesting a role in auditory feedback. Area X projects to the ventral pallidum (VP), which projects to VTA and the substantia nigra pars compacta (SNc) (Gale et al., 2008). VP receives inputs from AIV and sends projections to HVC and RA (Li and Sakaguchi, 1997). This architecture collectively demonstrates that the basal ganglia–thalamocortical pathway forms a loop with dopaminergic inputs. Inactivating VTA neurons in Bengalese finches (*Lonchura striata var. domestica*) disrupts the ability of the birds to shift pitches of songs to avoid aversive stimulation (Hoffmann et al., 2016). Electrophysiological recordings from VTA neurons have revealed a role in computing performance error signals upon distorted auditory feedback (Gadagkar et al., 2016) and natural fluctuations

in performance of VTA neurons projecting to Area X (Duffy et al., 2022). Dopaminergic signals in Area X are depend on performance, and diminishing during courtship (Roeser et al., 2023). To compute error-based reinforcement signals, neurons require inputs from both auditory feedback of own vocalization and a template (target motor pattern). A question remains unresolved: is this template a memory of TS or a motor template? The studies described here were performed in adult birds, which raises the issue of whether the template matching systems during juvenile song learning and adult song maintenance overlap.

Auditory memory in auditory forebrain: song memory and song discrimination

As described in the previous sections, auditory guiding/feedback signals to HVC appear to instruct song learning, while performance error is computed in the VTA–Area X circuit. Except for the information on syllable length from NIf to HVC, the type of information that arrives at HVC or VTA for template matching and its source remains largely unknown. In addition to research on the song system, more recent studies have shown that TS memories are stored in brain regions within the auditory pathways, especially in higher auditory areas. The expression level of the immediate-early gene, *ZENK*, a molecular marker for neuronal activity, in the zebra finch higher auditory area, the caudomedial nidopallium (NCM), is higher in birds exposed to TS playback than in those exposed to unfamiliar zebra finch songs (Gobes et al., 2010). In both sexes, NCM has been suggested to be the site of memory storage of auditory experiences, not exclusively for song learning. NCM lesions after conditioning with song stimulation diminishes song discrimination ability in adult males (Gobes and Bolhuis, 2007; Canopoli et al., 2014; Yu et al., 2023), while lesions in adult females disrupt song preference to experienced songs (Tomaszycki and Blaine, 2014).

A series of studies have suggested the involvement of NCM in song learning as a TS memory brain region. ZENK expression levels upon TS exposure positively correlate with the amount of song learning from a tutor (Bolhuis et al., 2000, 2001; Terpstra et al., 2004). Pharmacological blockade of a signaling pathway in NCM prevents juveniles to learn from TS (London and Clayton, 2008). An electrophysiological study revealed distinct habituation rates in NCM auditory responses upon repeated exposure to TS and unfamiliar song (Phan et al., 2006). We have reported that a small subset of juvenile NCM neurons show almost exclusive auditory responsiveness to a learned TS (Yanagihara and Yazaki-Sugiyama, 2016; Katic et al., 2022). In contrast to the other brain loci in the song system, nearly all neurons are selective to the bird's own song (Doupe and Konishi, 1991; Solis and Doupe, 1997; Janata and Margoliash, 1999). In NCM, electrophysiological experiments revealed two types of neurons distinct in their spiking shapes and firing rates (Schneider and Woolley, 2013; Yanagihara and Yazaki-Sugiyama, 2016), including inhibitory neurons (Spool et al., 2021). Only a subset (∼15%) of broader spiking NCM neurons acquire selectivity to TS soon after (∼1 h) listening to tutor singing (Katic et al., 2022). This timeline parallels a previous finding, in that TS memory forms by hearing only a few renditions of songs. The responsiveness of these neurons is exclusive to TS and not even to birds' own songs, suggesting that they comprise the neuronal substrates of auditory memory.

Despite cumulative studies that has implicated the zebra finch NCM in memory formation, neither a direct anatomical connection between NCM and the song system (Vates et al., 1996) nor instructive NCM neuronal activity during juvenile singing has been elucidated. NCM has reciprocal connections with the caudomedial mesopallium (CMM) which projects to HVC (Vates et al., 1996). While AFP in the song system receives dopaminergic reinforcement signals for song learning as discussed in the previous paragraph, NCM receives inputs from the noradrenergic locus coeruleus (LC), the brain region that controls attention and arousal states and noradrenergic release (Velho et al., 2012). LC to NCM inputs are suggested to send social information for song learning (Katic et al., 2022). These connectivity patterns collectively show that the song system and auditory pathway are integrated with a neuromodulatory system (Figure 2). Using viral technology to manipulate gene expression in target neurons and whole-brain axonal tracing with tissue clearing, we recently reported a transient projection to HVC from the subset of NCM neurons responsive to TS playback. The TS-responsive NCM neurons project to HVC, HVC-shelf, AIV, CMM, and Area X in juveniles, but the HVC projection disappears in adults. Inducing cell death in these NCM TS-responsive neurons by targeting the expression of CaCaspase disrupts song learning in juveniles but not in adults (Louder et al., 2024). While these results do not specify which of the projections from NCM are necessary for song learning, the NCM–HVC temporal connections comprise a candidate circuit for auditory TS memory-guided sensorimotor learning; moreover, dynamic rewiring of the interareal neural circuit may regulate the developmental time course of song learning. This raises the question of the fate of TS auditory memories over the developmental period.

Discussion

Whether a brain area is related to the process of distinguishing individual songs or in memory formation and storing cannot be decidedly determined in lesion experiments. Rather than disrupting auditory memories, the lesion experiments described above might have interrupted song discrimination. Sensory memories are thought to last long, perhaps permanently. In some bird species, sensory and sensorimotor learning is separated by 2–3 months, suggesting (at a minimum) month-long auditory memories. In zebra finches that learned two songs sequentially from two distinct tutors, the level of Zenk expression upon exposure to TS correlates with the amount of song learning from either tutor (Olson et al., 2016), suggesting that NCM is the substrate for TS memory encoding in adults, while neuronal substrates for TS memory in adults have yet to be identified. Auditory memories of TS are necessary for song learning, but storage may occur in different brain regions in juveniles and adults, specifically before and after song learning.

Similarly, while auditory learning can be extended if TS are not provided (e.g., in isolation), the song crystallizes at a specific

developmental time regardless of the level of learning. Even in the absence of TS experiences, juvenile birds start to sing at a specific time point during development. These observations suggest that the time course of sensory and sensorimotor learning are independently regulated but well-coordinated. Forming a memory during early auditory learning is necessary and TS memories are thought to guide sensorimotor learning. The higher auditory area is a strong, but likely not exclusive, candidate as the locus of TS memory encoding. Moreover, different brain regions may be responsible for the generation of auditory memory to guide sensorimotor learning during development and song recognition in the latter stage. Detailed dissections of neural circuits over the entire song learning period and manipulation of specific circuits during song learning are expected to enrich knowledge on the song template, TS template, or own song motor template systems, and provide insights into the relevant spatial and temporal characteristics in the brain. Furthermore, such studies likely have implications for bilingualism in humans. Early experiences of adults in non-native language settings have positive influences on auditory discrimination ability of bowling or intonations even when speaking ability of the second language is limited. Retention of connections that guide the flow from auditory memories to the motor area may be a key factor for re-opening re-learning or new song learning in adults. Hearing is one thing, doing (mimicking) might be another. The long-existing song template theory should be explored in more depth to thoroughly understand its concepts.

Author contributions

YY-S: Conceptualization, Writing–original draft, Writing–review and editing.

Funding

The author declares that financial support was received for the research, authorship, and/or publication of this article. This work was supported by OIST Graduate University and a JSPS KAKENHI Grant-in-Aid for Scientific Research (B) (#23H02593).

Acknowledgments

We would like to thank Dr. Yuichi Morohashi for continuing discussions related to this work.

Conflict of interest

The author declares that the research was conducted in the absence of any commercial or financial relationships that could be construed as a potential conflict of interest.

Publisher's note

References

Bolhuis, J. J., Hetebrij, E., Den Boer-Visser, A. M., De Groot, J. H., and Zijlstra, G. G. O. (2001). Localized immediate early gene expression related to the strength of song learning in socially reared zebra finches. *Eur. J. Neurosci.* 13, 2165–2170. doi: 10.1046/j.0953-816x.2001.01588.x

Bolhuis, J. J., Zijlstra, G. G. O., Den Boer-Visser, A. M., and Van Der Zee, E. A. (2000). Localized neuronal activation in the zebra finch brain is related to the strength of song learning. *Proc. Natl Acad. Sci. U.S.A.* 97, 2282–2285. doi: 10.1073/pnas.030539097

Bottjer, S. W., Miesner, E. A., and Arnold, A. P. (1984). Forebrain lesions disrupt development but not maintenance of song in passerine birds. *Science* 224, 901–903. doi: 10.1126/science.6719123

Brainard, M. S., and Doupe, A. J. (2000). Interruption of a basal ganglia–forebrain circuit prevents plasticity of learned vocalizations. *Nature* 404, 762–766. doi: 10.1038/35008083

Canopoli, A., Herbst, J. A., and Hahnloser, R. H. R. (2014). A higher sensory brain region is involved in reversing reinforcement-induced vocal changes in a songbird. *J. Neurosci.* 34, 7018–7026. doi: 10.1523/JNEUROSCI.0266-14.2014

Doupe, A. J., and Konishi, M. (1991). Song-selective auditory circuits in the vocal control system of the zebra finch. *Proc. Natl. Acad. Sci. U.S.A.* 88, 11339–11343. doi: 10.1073/pnas.88.24.11339

Duffy, A., Latimer, K. W., Goldberg, J. H., Fairhall, A. L., and Gadagkar, V. (2022). Dopamine neurons evaluate natural fluctuations in performance quality. *Cell Rep.* 38:110574. doi: 10.1016/j.celrep.2022.110574

Fehér, O., Wang, H., Saar, S., Mitra, P. P., and Tchernichovski, O. (2009). De novo establishment of wild-type song culture in the zebra finch. *Nature* 459, 564–568. doi: 10.1038/nature07994

Fujimoto, H., Hasegawa, T., and Watanabe, D. (2011). Neural coding of syntactic structure in learned vocalizations in the songbird. *J. Neurosci.* 31, 10023–10033. doi: 10.1523/JNEUROSCI.1606-11.2011

Gadagkar, V., Puzerey, P. A., Chen, R., Baird-Daniel, E., Farhang, A. R., and Goldberg, J. H. (2016). Dopamine neurons encode performance error in singing birds. *Science* 354, 1278–1282. doi: 10.1126/science.aah6837

Gale, S. D., Person, A. L., and Perkel, D. J. (2008). A novel basal ganglia pathway forms a loop linking a vocal learning circuit with its dopaminergic input. *J. Comp. Neurol.* 508, 824–839. doi: 10.1002/cne.21700

Gobes, S. M. H., and Bolhuis, J. J. (2007). Birdsong memory: A neural dissociation between song recognition and production. *Curr. Biol.* 17, 789–793. doi: 10.1016/j.cub.2007.03.059

Gobes, S. M. H., Zandbergen, M. A., and Bolhuis, J. J. (2010). Memory in the making: Localized brain activation related to song learning in young songbirds. *Proc. Biol. Sci.* 277, 3343–3351. doi: 10.1098/rspb.2010.0870

Hahnloser, R. H. R., Kozhevnikov, A. A., and Fee, M. S. (2002). An ultra-sparse code Underliesthe generation of neural sequences in a songbird. *Nature* 419, 65–70. doi: 10.1038/nature00974

Hessler, N. A., and Doupe, A. J. (1999). Social context modulates singing-related neural activity in the songbird forebrain. *Nat. Neurosci.* 2, 209–211. doi: 10.1038/6306

Hoffmann, L. A., Saravanan, V., Wood, A. N., He, L., and Sober, S. J. (2016). Dopaminergic contributions to vocal learning. *J. Neurosci.* 36, 2176–2189. doi: 10.1523/JNEUROSCI.3883-15.2016

Janata, P., and Margoliash, D. (1999). Gradual emergence of song selectivity in sensorimotor structures of the male zebra finch song system. *J. Neurosci.* 19, 5108–5118. doi: 10.1523/JNEUROSCI.19-12-05108.1999

Jarvis, E. D., Scharff, C., Grossman, M. R., Ramos, J. A., and Nottebohm, F. (1998). For whom the bird sings: Context-dependent gene expression. *Neuron* 21, 775–788. doi: 10.1016/S0896-6273(00)80594-2

Kao, M. H., Doupe, A. J., and Brainard, M. S. (2005). Contributions of an avian basal ganglia–forebrain circuit to real-time modulation of song. *Nature* 433, 638–643. doi: 10.1038/nature03127

Katic, J., Morohashi, Y., and Yazaki-Sugiyama, Y. (2022). Neural circuit for social authentication in song learning. *Nat. Commun.* 13:4442. doi: 10.1038/s41467-022-32207-1

Konishi, M. (1965). The role of auditory feedback in the control of vocalization in the white-crowned Sparrow1. *Z. Tierpsychol.* 22, 770–783. doi: 10.1111/j.1439-0310.1965.tb01688.x

Li, R., and Sakaguchi, H. (1997). Cholinergic innervation of the song control nuclei by the ventral paleostriatum in the zebra finch: A double-labeling study with retrograde fluorescent tracers and choline acetyltransferase immunohistochemistry. *Brain Res.* 763, 239–246. doi: 10.1016/S0006-8993(97)00417-4

London, S. E., and Clayton, D. F. (2008). Functional identification of sensory mechanisms required for developmental song learning. *Nat. Neurosci.* 11, 579–586. doi: 10.1038/nn.2103

Long, M. A., and Fee, M. S. (2008). Using temperature to analyse temporal dynamics in the songbird motor pathway. *Nature.* 456, 189–194. doi: 10.1038/nature07448

Louder, M. I. M., Kuroda, M., Taniguchi, D., Komorowska-Müller, J. A., Morohashi, Y., Takahashi, M., et al. (2024). Transient sensorimotor projections in the developmental song learning period. *Cell Rep.* 43:114196. doi: 10.1016/j.celrep.2024.114196

Mackevicius, E. L., Gu, S., Denisenko, N. I, and Fee, M. S. (2023). Self-organization of songbird neural sequences during social isolation. *Elife* 12:e77262. doi: 10.7554/eLife.77262

Marler, P. (1970). A comparative approach to vocal learning: Song development in white-crowned sparrows. *J. Comp. Physiol. Psychol.* 71, 1–25. doi: 10.1037/h0029144

Marler, P. (1984). "Song learning: Innate species differences in the learning process," in *The biology of learning*, eds P. Marler and H. S. Terrace (Berlin: Springer Berlin Heidelberg), 289–309. doi: 10.1007/978-3-642-70094-1_13

Marler, P. (1997). Three Models of song learning: Evidence from behavior. *J. Neurobiol.* 33, 501–516.

Marler, P., and Nelson, D. (1992). Neuroselection and song learning in birds: Species universals in a culturally transmitted behavior. *Semin. Neurosci.* 4, 415–423. doi: 10.1016/1044-5765(92)90050-C

McCasland, J. S., and Konishi, M. (1981). Interaction between auditory and motor activities in an avian song control nucleus. *Proc. Natl. Acad. Sci. U.S.A.* 78, 7815–7819. doi: 10.1073/pnas.78.12.7815

Moll, F. W., Kranz, D., Corredera Asensio, A. C., Elmaleh, M., Ackert-Smith, L. A., and Long, M. A. (2023). Thalamus drives vocal onsets in the zebra finch courtship song. *Nature* 616, 132–136. doi: 10.1038/s41586-023-05818-x

Mooney, R. (2000). Different subthreshold mechanisms underlie song selectivity in identified HVc neurons of the zebra finch. *J. Neurosci.* 20, 5420–5436. doi: 10.1523/JNEUROSCI.20-14-05420.2000

Mooney, R. (2009). Neural mechanisms for learned birdsong. *Learn. Mem.* 16, 655–669. doi: 10.1101/lm.1065209

Okubo, T. S., Mackevicius, E. L., Payne, H. L., Lynch, G. F., and Fee, M. S. (2015). Growth and splitting of neural sequences in songbird vocal development. *Nature* 528, 352–357. doi: 10.1038/nature15741

Olson, E. M., Maeda, R. K., and Gobes, S. M. H. (2016). Mirrored patterns of lateralized neuronal activation reflect old and new memories in the avian auditory cortex. *Neuroscience* 330, 395–402. doi: 10.1016/j.neuroscience.2016.06.009

Person, A. L., Gale, S. D., Farries, M. A., and Perkel, D. J. (2008). Organization of the songbird basal ganglia, including area X. *J. Comp. Neurol.* 508, 840–866. doi: 10.1002/cne.21699

Phan, M. L., Pytte, C. L., and Vicario, D. S. (2006). Early auditory experience generates long-lasting memories that may subserve vocal learning in songbirds. *Proc. Natl. Acad. Sci. U.S.A.* 103, 1088–1093. doi: 10.1073/pnas.0510136103

Prather, J. F., Peters, S., Nowicki, S., and Mooney, R. (2008). Precise auditory-vocal mirroring in neurons for learned vocal communication. *Nature* 451, 305–310. doi: 10.1038/nature06492

Roeser, A., Gadagkar, V., Das, A., Puzerey, P. A., Kardon, B., and Goldberg, J. H. (2023). Dopaminergic error signals retune to social feedback during courtship. *Nature* 623, 375–380. doi: 10.1038/s41586-023-06580-w

Scharff, C., and Nottebohm, F. (1991). A comparative study of the behavioral deficits following lesions of various parts of the zebra finch song system: Implications for vocal learning. *J. Neurosci.* 11, 2896–2913. doi: 10.1523/JNEUROSCI.11-09-02896.1991

Schneider, D. M., and Woolley, S. M. N. (2013). Sparse and background-invariant coding of vocalizations in auditory scenes. *Neuron* 79, 141–152. doi: 10.1016/j.neuron.2013.04.038

Sober, S. J., and Brainard, M. S. (2009). Adult birdsong is actively maintained by error correction. *Nat. Neurosci.* 12, 927–931. doi: 10.1038/nn.2336

Solis, M. M., and Doupe, A. J. (1997). Anterior forebrain neurons develop selectivity by an intermediate stage of birdsong learning. *J. Neurosci.* 17, 6447–6462. doi: 10.1523/JNEUROSCI.17-16-06447.1997

Solis, M. M., and Doupe, A. J. (1999). Contributions of tutor and bird's own song experience to neural selectivity in the songbird anterior forebrain. *J. Neurosci.* 19, 4559–4584. doi: 10.1523/JNEUROSCI.19-11-04559.1999

Sossinka, R., and Böhner, J. (1980). Song types in the zebra finch *Poephila guttata* Castanotis1. *Z. Tierpsychol.* 53, 123–132. doi: 10.1111/j.1439-0310.1980.tb01044.x

Spool, J. A., Macedo-Lima, M., Scarpa, G., Morohashi, Y., Yazaki-Sugiyama, Y., and Remage-Healey, L. (2021). Genetically identified neurons in avian auditory pallium mirror core principles of their mammalian counterparts. *Curr. Biol.* 31:2831–2843.e6. doi: 10.1016/j.cub.2021.04.039

Tchernichovski, O., and Nottebohm, F. (1998). Social inhibition of song imitation among sibling male zebra finches. *Proc. Natl. Acad. Sci. U.S.A.* 95, 8951–8956. doi: 10.1073/pnas.95.15.8951

Terpstra, N. J., Bolhuis, J. J., and Den Boer-Visser, A. M. (2004). An analysis of the neural representation of birdsong memory. *J. Neurosci.* 24, 4971–4977. doi: 10.1523/JNEUROSCI.0570-04.2004

Tomaszycki, M. L., and Blaine, S. K. (2014). Temporary inactivation of NCM, an auditory region, increases social interaction and decreases song perception in female zebra finches. *Behav. Process.* 108, 65–70. doi: 10.1016/j.beproc.2014.09.031

Vallentin, D., Kosche, G., Lipkind, D., and Long, M. A. (2016). Neural circuits. Inhibition protects acquired song segments during vocal learning in zebra finches. *Science* 351, 267–271. doi: 10.1126/science.aad3023

Vates, G. E., Broome, B. M., Mello, C. V., and Nottebohm, F. (1996). Auditory pathways of caudal telencephalon and their relation to the song system of adult male zebra finches. *J. Comp. Neurol.* 366, 613–642.

Velho, T. A. F., Lu, K., Ribeiro, S., Pinaud, R., Vicario, D., and Mello, C. V. (2012). Noradrenergic control of gene expression and long-term neuronal adaptation evoked by learned vocalizations in songbirds. *PLoS One* 7:e36276. doi: 10.1371/journal.pone.0036276

Yanagihara, S., and Yazaki-Sugiyama, Y. (2016). Auditory experience-dependent cortical circuit shaping for memory formation in bird song learning. *Nat. Commun.* 7:11946. doi: 10.1038/ncomms11946

Yazaki-Sugiyama, Y., and Mooney, R. (2004). Sequential learning from multiple tutors and serial retuning of auditory neurons in a brain area important to birdsong learning. *J. Neurophysiol.* 92, 2771–2788. doi: 10.1152/jn.00467.2004

Yu, K., Wood, W. E., Johnston, L. G., and Theunissen, F. E. (2023). Lesions to caudomedial nidopallium impair individual vocal recognition in the zebra finch. *J. Neurosci.* 43, 2579–2596. doi: 10.1523/JNEUROSCI.0643-22.2023

Zhao, W., Garcia-Oscos, F., Dinh, D., and Roberts, T. F. (2019). Inception of memories that guide vocal learning in the songbird. *Science* 366, 83–89. doi: 10.1126/science.aaw4226

frontiers | Frontiers in Neural Circuits

TYPE Mini Review
PUBLISHED 05 July 2024
DOI 10.3389/fncir.2024.1437575

OPEN ACCESS

EDITED BY
Kensaku Mori,
RIKEN, Japan

REVIEWED BY
Masahiro Yamaguchi,
Kōchi University, Japan
Shin Nagayama,
Texas Medical Center, United States

*CORRESPONDENCE
Kei M. Igarashi
✉ kei.igarashi@uci.edu

RECEIVED 24 May 2024
ACCEPTED 20 June 2024
PUBLISHED 05 July 2024

CITATION
Zhang YJ, Lee JY and Igarashi KM (2024) Circuit dynamics of the olfactory pathway during olfactory learning.
Front. Neural Circuits 18:1437575.
doi: 10.3389/fncir.2024.1437575

Circuit dynamics of the olfactory pathway during olfactory learning

Yutian J. Zhang[1], Jason Y. Lee[1] and Kei M. Igarashi[1,2,3,4,5]*

[1]Department of Anatomy and Neurobiology, School of Medicine, University of California, Irvine, Irvine, United States, [2]Department of Biomedical Engineering, Samueli School of Engineering, University of California, Irvine, Irvine, United States, [3]Center for Neural Circuit Mapping, School of Medicine, University of California, Irvine, Irvine, United States, [4]Center for the Neurobiology of Learning and Memory, University of California, Irvine, Irvine, United States, [5]Institute for Memory Impairments and Neurological Disorders, University of California, Irvine, Irvine, United States

The olfactory system plays crucial roles in perceiving and interacting with their surroundings. Previous studies have deciphered basic odor perceptions, but how information processing in the olfactory system is associated with learning and memory is poorly understood. In this review, we summarize recent studies on the anatomy and functional dynamics of the mouse olfactory learning pathway, focusing on how neuronal circuits in the olfactory bulb (OB) and olfactory cortical areas integrate odor information in learning. We also highlight in vivo evidence for the role of the lateral entorhinal cortex (LEC) in olfactory learning. Altogether, these studies demonstrate that brain regions throughout the olfactory system are critically involved in forming and representing learned knowledge. The role of olfactory areas in learning and memory, and their susceptibility to dysfunction in neurodegenerative diseases, necessitate further research.

KEYWORDS

olfactory, lateral entorhinal cortex (LEC), Olfactory learning, olfactory cortex, hippocampus

1 Introduction

Olfaction is a crucial ability for animals to detect environmental cues that are relevant for survival such as rewarding foods or dangerous predators. The sense of smell is also critical for human beings when we are involved in daily activities and experience the surrounding world. In the recent COVID-19 pandemic, nearly 88% of patients experienced olfaction loss in the short term (Lechien et al., 2020). A study also observed long-term structural changes in the brain such as tissue damage in the primary olfactory cortex and limbic regions that are functionally connected with the olfactory pathway (Douaud et al., 2022). Structural changes were also observed in memory-related regions including the entorhinal cortex and the hippocampus (Douaud et al., 2022). Furthermore, olfactory loss is associated with cognitive decline and declarative memory impairment in long-term COVID-19 patients (Fiorentino et al., 2022). Due to the overlapping vulnerability of olfactory and memory-related regions, it is even possible that long-term Covid infection

could contribute to increased risks of neurodegenerative diseases like Alzheimer's disease (AD). Thus, it is increasingly urgent to investigate the neural circuit dynamics behind olfaction and memory. Among different model organisms, rodents are particularly adept in olfactory tasks and possess multiple homologies with higher mammals, offering valuable insights into the neural circuits and dynamic representations of olfaction (Ache and Young, 2005). As previous research has established the basic odor representation component of the olfactory system, the current field has introduced new perspectives on how animals associate odor cues with specific outcomes, and how the neural representations of odors change across learning along different regions of the olfactory pathway. In this review, we will cover the circuit mechanisms of olfactory regions and their dynamics during olfactory learning.

1.1 Anatomy of olfactory pathway in rodents

Olfactory information is first detected by olfactory sensory neurons (OSNs) located in the olfactory epithelium (OE) within the nasal cavity (Buck, 1996; Mori et al., 1999) (Figure 1). OSNs relay signals to the olfactory bulb (OB), which contains two types of projection neurons: mitral cells (MCs) and tufted cells (TCs) (Shepherd, 2004). From there, MCs and TCs send information to several olfactory cortical areas in the brain (Miyamichi et al., 2011; Igarashi et al., 2012; Nagayama et al., 2014). Olfactory cortex is defined as areas that receive direct input from the OB, including 9 major brain regions: anterior olfactory nucleus (AON), olfactory tubercule (OT), anterior piriform cortex (aPir), posterior piriform cortex (pPir), lateral entorhinal cortex (LEC), nucleus of the lateral olfactory tract (nLOT), anterior cortical amygdaloid nucleus (ACo), posterolateral cortical amygdaloid nucleus (PLCo) and tenia tecta (TT) (Paxinos, 2004; Shepherd, 2004; Igarashi et al., 2012). TCs signal mainly to the anterior portion of the olfactory cortex including the AON and the OT, while MCs are thought to be the main output neurons of OB and project to all the olfactory cortical regions (Igarashi et al., 2012; Nagayama et al., 2014; Chen et al., 2022) (Figure 1).

The organization of the olfactory system is unique. First, the olfactory system does not have a thalamic relay and contains only three primary layers of information processing: OE as the first layer, OB as the second, and the remaining olfactory cortical regions tied for the third. It is surprising that olfaction could be encoded in this three-layer hierarchy system as this is not observed in other sensory modalities such as the visual system where the primary (V1), secondary (V2), and third (V4) visual cortex are sequentially connected. The second unique feature is the odor representation pattern in the olfactory cortex. While the odor representation of OB neurons is spatially organized (Mori et al., 2006), the piriform cortex (PC), which has the largest area among the olfactory cortex, receives divergent axonal projections from mitral cells (Miyamichi et al., 2011; Igarashi et al., 2012) and responds to odors in distributed neuronal ensembles lacking a topographical pattern (Stettler and Axel, 2009). This is also not observed in other associational sensory cortical regions like V1 or primary auditory cortex in mammals (Malach, 1989; Ojima et al., 1991) but only in higher regions such as V4 and primary somatosensory cortex (area 3b) in monkeys (Hansen et al., 2007), suggesting the role of olfactory cortex as a higher association cortex.

1.2 The role of olfactory regions in learning

Previous studies have identified the anatomical connections of the olfactory bulb and olfactory cortex regions, but the functions of these regions remain largely unknown. By contrast, as most prior studies measured the neuronal responses of OB in basic odor detection, studies from the past few years have begun to reveal the function of OB in learning. Intrinsic optical imaging of OB showed an increase in the number of activated glomeruli in mice trained on a go/no go odor discrimination task, and this learning-induced potentiation lasted up to 5 weeks (Abraham et al., 2014). Targeting recordings specifically to MCs showed that, after learning, synchronized activity in MCs carries information about odor value (rewarded or unrewarded) (Doucette et al., 2011). Additionally, when task difficulties depended on the similarities of odorants that mice need to discriminate, the fraction of responsive MCs increased over weeks for mice trained with the difficult task, and decreased in mice with the easy task, demonstrating experience-dependent plasticity in the OB (Chu et al., 2016). Moreover, recordings from evoked field postsynaptic potentials demonstrated that connections between OB-PC inputs were enhanced during rule learning (Cohen et al., 2015). These studies suggest that the OB not only functions as a sensory relay station but also endures plasticity-related changes across learning.

Recent studies have also found plasticity-related changes in some of the olfactory cortex regions, including the OT, AON, TT and the LEC. A paper reported learning-dependent plasticity in OT, with the anteromedial domain of OT responding more to appetitive odor cues and the lateral domain responding to aversive cues after learning (Murata et al., 2015). This suggests that OT is involved in the expected outcome representation of specific stimuli, with activation of different domains based on the outcome valence. Moreover, optogenetic stimulation of either the OB-OT or Pir-OT pathway alone elicited food-searching behavior in mice trained with reward, as well as shock avoidance in aversively-trained mice (Sha et al., 2023). Both of these synaptic connections could potentially explain learning-induced potentiation of the OT (Sha et al., 2023). Additionally, TT neurons are tuned to specific task elements with learning, such as temporal epochs and approach behavior (Shiotani et al., 2020). For AON, memory engram-like activities were detected using cFos labeling after mice were exposed to an odor-context paradigm, and inhibition of AON engram activity disrupted the odor-contextual associative memory recall (Aqrabawi and Kim, 2020). Anatomically, topographical projections from the hippocampus to AON were revealed previously (Aqrabawi and Kim, 2018b), and this HPC-AON input is necessary for forming olfactory-contextual memory (Aqrabawi and Kim, 2018a). Collectively, these experiments provide new insights into how we understand the olfactory system – that is, that each of the olfactory regions is presumably involved in specific aspects of olfactory learning.

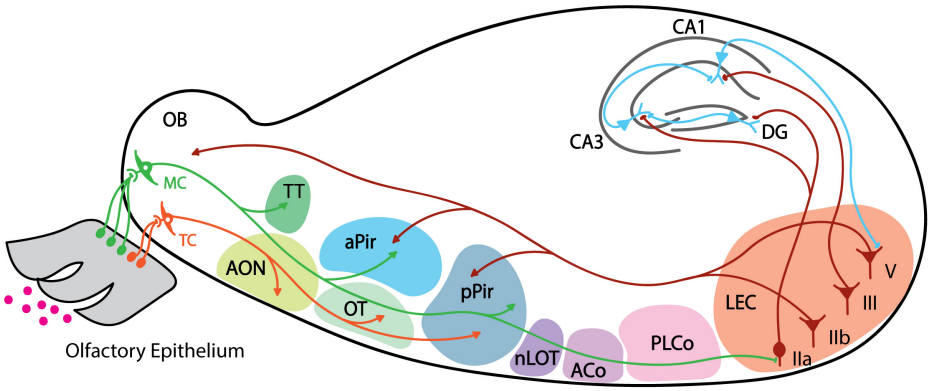

FIGURE 1
Schematic of mouse olfactory pathway anatomy. Individual areas are highlighted with different colors. Projections from mitral cell are shown in green, tufted cell projections in orange, back projection from LEC layers IIb and V in dark red, and projections from hippocampus neurons in blue. Arrows indicate axonal projections, and boutons indicate direct synaptic connection. MC, mitral cell; TC, tufted cell; AON, anterior olfactory nucleus; TT, tenia tecta; OT, olfactory tubercle; aPir, anterior piriform cortex; pPir, posterior piriform cortex; nLOT, nucleus of the lateral olfactory tract; ACo, anterior cortical amygdaloid; PLCo, posterolateral cortical amygdaloid nucleus; LEC, lateral entorhinal cortex; DG, dentate gyrus.

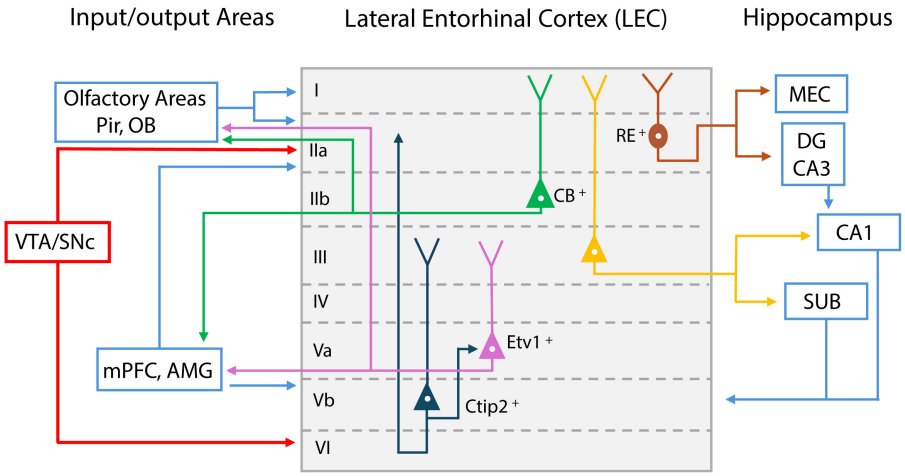

FIGURE 2
Schematic representation of lateral entorhinal cortex (LEC) layer input/output projections. Inputs from olfactory bulb (OB) and piriform cortex (Pir) reach LEC layer I; Reelin (RE) positive cells project to medial entorhinal cortex (MEC) and dentate gyrus (DG) (shown in dark red); Calbindin (CB) positive pyramidal cells in layer II project to olfactory areas, medial prefrontal cortex (mPFC), and amygdala (AMG) (shown in green); Layer III pyramidal cells mainly project to CA1 and subiculum (SUB) (shown in yellow). Layer Va cells express E twenty-six variant transcription factor 1 (Etv1), and project to mPFC and AMG, as well as olfactory areas (shown in purple); Feedback from these areas reach layer Vb. Layer Vb cells express Chicken ovalbumin upstream promoter transcription factor-interacting protein 2 (Ctip2) and project within the LEC (shown in dark blue). LEC layer II and VI receive dopaminergic inputs from midbrain ventral tegmental area (VTA) and substantial nigra pars compacts (SNc) (shown in red).

Future studies should further clarify the distinct roles of individual regions and identify the circuit mechanisms supporting learning-induced changes in these olfactory areas.

2 The role of the LEC in olfactory learning

2.1 Anatomical connections of LEC

Among the olfactory cortical areas, LEC is unique in that it is also a constituent of the memory system. LEC is situated between olfactory regions and the hippocampus, serving as an information transfer station between the two. LEC is a six-layer structure with distinct input/output properties and distinct cell types comprising each layer (Figure 2). It receives direct inputs from MCs via the LOT and makes bidirectional connections with Pir (Agster and Burwell, 2009; Igarashi et al., 2012; Diodato et al., 2016). LEC also receives inputs from the insular cortex (Agster and Burwell, 2009). These axon terminals reach LEC mainly in the superficial layer I, which contains mostly the apical dendrites of layer II cells (Burwell and Amaral, 1998). Inputs from the perirhinal and postrhinal cortex terminate at layer II, which may allow for the integration of object representations with olfactory cues (Doan et al., 2019) (Figure 2).

LEC layer II is a dense cell layer. Layer IIa contains mostly reelin^{++} (RE^{+}) principal cells (fan cells) and IIb contains calbindin^{+} (CB^{+}) pyramidal cells. Fan cells project mainly via the perforant pathway to the dentate gyrus (DG), where information is sent to hippocampal CA3 and CA1 for further processing (Leitner et al., 2016) (Figure 2). This allows LEC to serve as the major gateway for sensory information entering memory processing regions. Fan cells that project to DG also project to the superficial layer of the medial entorhinal cortex (MEC), allowing feedforward inhibition to pyramidal cells in MEC circuits (Vandrey et al., 2022). LEC layer IIb CB^{+} pyramidal cells do not innervate DG but rather send feedback projections mainly to the OB, Pir, contralateral LEC, and neocortical areas such as the medial prefrontal cortex (mPFC) (Kerr et al., 2007; Agster and Burwell, 2009; Leitner et al., 2016; Ährlund-Richter et al., 2019).

LEC layer III contains pyramidal cells projecting mostly to CA1 and subiculum (SUB), and projections from these hippocampal regions terminate back in the deep layer of LEC. In deep layer V, neurons project to the mPFC, amygdala (AMG), olfactory bulb, anterior olfactory nucleus, and piriform cortex (de Olmos et al., 1978; Insausti et al., 1997). Recently, layer V cells have been divided into layers Va and Vb, using two marker proteins. Layer Va cells express E twenty-six (ETS) variant transcription factor 1 (Etv1), whreas Layer Vb cells express chicken ovalbumin upstream promoter transcription factor (COUP-TF) interacting protein 2 (Ctip2) (Sürmeli et al., 2016; Ohara et al., 2018) (Figure 2). Layer Va cells are the main output neurons projecting outside the LEC, whereas layer Vb cells are considered mostly for intrinsic projections within the LEC, synapsing onto both layer Va and the superficial layer of LEC (Ohara et al., 2018). Based on the looping structure of input/output connectivity in LEC sublayers (superficial layer LEC → hippocampus → deep layer LEC → neocortex), it is likely that the deep layer LEC receives olfactory-memory representations from the hippocampus and sends this feedback information to various cortical regions, where it is integrated for higher-level cognition and long-term memory maintenance.

2.2 LEC involvement in learning

Due to its intricate input/output connection with the hippocampus, multiple lines of research have focused on LEC's role in learning and memory. While the MEC was thought to represent the spatial component of learning ("where"), as supported by the discoveries of spatially modulated grid cells (Fyhn et al., 2004; Hafting et al., 2005), LEC cells have low spatially selective firing (Hargreaves et al., 2005). Rather, LEC may represent visual, olfactory, and somatosensory information about items and objects (Young et al., 1997; Deshmukh and Knierim, 2011; Tsao et al., 2013; Igarashi et al., 2014). To identify how LEC neurons encode memories of items/objects, we recently recorded layer IIa fan cells using optogenetic assisted cell-type-specific recording method when mice were learning odor-outcome association (Lee et al., 2021). We found a group of LEC fan cells that developed spike responses to both newly learned rewarded odor cues and pre-learned rewarded cues, a signature of generalization during learning. Another group of fan cells responded only to punished cues. These results suggest that the LEC forms a "cognitive map" of odor items during memory encoding. The cognitive map refers to an internal brain representation of a physical spatial map, first conceptualized by Tolman from his observations on rats running in a maze (Tolman, 1948), then supported by the discovery of place cells in the hippocampus (O'Keefe and Dostrovsky, 1971). Recently, the concept of the cognitive map has been extended to non-spatial elements (Behrens et al., 2018). The Lee et al. work suggested that the LEC classifies and stores information of items depending on their associated reward or punishment outcomes, a signature of cognitive map formation about learned items (Lee et al., 2021; Igarashi et al., 2022). We consider that the concept of cognitive map is similar to the idea of "memory schema," a term for "acquired knowledge" in psychological studies (Bartlett, 1932; Craik, 1943; Tse et al., 2007). In this context, the LEC (and presumably other brain regions) formulate schema from previous learning, and use schema to guide the acquisition of subsequently learned knowledge, which is referred to as "assimilation" (Igarashi et al., 2022).

3 Neuromodulatory inputs underlying olfactory learning

The olfactory areas receive dense neuromodulatory inputs presumably contributing to olfactory learning, including dopaminergic projections from the midbrain ventral tegmental area (VTA) and substantia nigra (SN), cholinergic inputs from the diagonal band of Broca (DB) and the basal forebrain, and serotonergic inputs from the raphe nuclei (Hokfelt et al., 1974, Björklund and Dunnett, 2007; Petzold et al., 2009). Among these neuromodulatory systems, the most extensive research has been conducted on dopamine (DA). Even though OB does not receive direct DA inputs from midbrain VTA, it has been indicated that the OB contains numerous dopaminergic neurons within the glomerular layer (Halasz et al., 1981) and expresses DA type 2 receptor (D2R) (Coronas et al., 1997; Koster et al., 1999). OT, as part of the ventral striatal system, receives extensive DA inputs from VTA (Ikemoto, 2007; Zhang et al., 2017), and phase stimulation of the DA terminals in OT induces neuronal plasticity of cue-reward pairing (Oettl et al., 2020). Moreover, LEC receives dense DA inputs from the VTA/SN, found mainly in layers II and VI (Hokfelt et al., 1974; Fallon et al., 1978; Björklund and Dunnett, 2007) (Figure 2). However, whether DA inhibits or facilitates LEC layer II synaptic transmission remains controversial (Caruana and Chapman, 2008; Glovaci and Chapman, 2015). We recently demonstrated that DA inputs from the VTA control the development of cue-reward representation in LEC layer IIa fan cells during associative learning (Lee et al., 2021). Additionally, both OB and Pir receive cholinergic inputs from the horizontal limbs of diagonal band of Broca (HDB), suggesting that acetylcholine could also modulate these regions in learning (Luskin and Price, 1982; Zaborszky et al., 1986). For example, while previous exposure to similar odorants increases the odor discrimination ability, this learned enhancement was reversed by an acetylcholine antagonist (Fletcher and Wilson, 2002). These results collectively indicate that neuromodulatory inputs such as DA and acetylcholine could guide olfactory memory formation and control information flow in the entorhinal-hippocampal circuit for learning.

4 Discussion and conclusion

In this review, we attempted to summarize currently available knowledge about the mouse olfactory system in learning with anatomical underpinnings. The fact that neocortical regions like the medial prefrontal cortex (mPFC) receive direct input from several olfactory cortical regions (i.e. PC, TT, AON, LEC) suggests that olfactory information is directly integrated for cognitive functions such as decision-making and adaptive responses (Witter et al., 2000; Agster and Burwell, 2009; DeNardo et al., 2015; Diodato et al., 2016; Moberly et al., 2018; Loureiro et al., 2019). Also of note is the strong connectivity between olfactory areas and the amygdala (Price, 2003), which could provide a neural basis for the emotional aspect of olfactory memory.

We also emphasized the special role of LEC as an interface for the olfactory memory circuit in associative learning and its modulation by dopaminergic inputs. The LEC forms cognitive maps for non-spatial olfactory items during olfactory learning (Igarashi et al., 2022). It remains largely unknown whether the function of cognitive map/schema formation, found in the LEC, is shared in other olfactory regions, or their target cortical areas. Future work is needed to decipher their roles in cognitive map formation during learning. Another important topic for future study is the critical role of the LEC in AD. Olfactory impairment is demonstrably correlated with AD and is amongst the first symptoms reported by many AD patients (Waldton, 1974; Serby et al., 1991). Moreover, the LEC is thought to be one of the first regions exhibiting histological and functional signatures of AD (Van Hoesen et al., 1991; Braak and Braak, 1992; Igarashi, 2023). It is likely that LEC dysfunction underlies the progression of both smell and memory loss. How the early stage of olfactory representations is altered in disease and affects higher-level cognition requires future investigation.

Our experience with the surrounding environment involves a convergence of many sensory modalities. An interesting property of olfactory cortical regions (e.g., OT, Pir and LEC) is their multi-modal representations outside of olfaction. Pir receives projections from the primary auditory cortex (A1) (Budinger et al., 2006), and studies have shown that OT cells respond to auditory stimuli (Wesson and Wilson, 2010). In LEC, somatosensory and visual inputs may converge with olfactory information to form a more complete representation of the outside world (Hoogland et al., 1987; Burwell and Amaral, 1998). The mechanisms of multimodal features of olfactory regions also call for investigation in future studies.

Author contributions

YZ: Writing – review and editing, Writing – original draft. JL: Writing – review – editing, Writing – original draft. KI: Writing – review – editing, Writing – original draft.

Funding

The author(s) declare financial support was received for the research, authorship, and/or publication of the article. The work was supported by NIH R01 grants (R01MH121736, R01AG063864, R01AG066806, R01AG086441) and BrightFocus Foundation Research grant (A2019380S) to KI.

Acknowledgments

We thank members in the Igarashi lab for providing valuable comments on the work.

Conflict of interest

The authors declare that the research was conducted in the absence of any commercial or financial relationships that could be construed as a potential conflict of interest.

Publisher's note

References

Abraham, N. M., Vincis, R., Lagier, S., Rodriguez, I., and Carleton, A. (2014). Long term functional plasticity of sensory inputs mediated by olfactory learning. *Elife* 3:e02109.

Ache, B. W., and Young, J. M. (2005). Olfaction: Diverse species, conserved principles. *Neuron* 48, 417–430.

Agster, K. L., and Burwell, R. D. (2009). Cortical efferents of the perirhinal, postrhinal, and entorhinal cortices of the rat. *Hippocampus* 19, 1159–1186.

Ährlund-Richter, S., Xuan, Y., Van Lunteren, J. A., Kim, H., Ortiz, C., Dorocic, I. P., et al. (2019). A whole-brain atlas of monosynaptic input targeting four different cell types in the medial prefrontal cortex of the mouse. *Nat. Neurosci.* 22:657.

Aqrabawi, A. J., and Kim, J. C. (2018b). Topographic organization of hippocampal inputs to the anterior olfactory nucleus. *Front. Neuroanat.* 12:12. doi: 10.3389/fnana.2018.00012

Aqrabawi, A. J., and Kim, J. C. (2018a). Hippocampal projections to the anterior olfactory nucleus differentially convey spatiotemporal information during episodic odour memory. *Nat. Commun.* 9:2735. doi: 10.1038/s41467-018-05131-6

Aqrabawi, A. J., and Kim, J. C. (2020). Olfactory memory representations are stored in the anterior olfactory nucleus. *Nat. Commun.* 11:1246.

Bartlett, F. C. (1932). *Remembering. A study in experimental and social psychology*. Cambridge: Cambridge University Press.

Behrens, T. E. J., Muller, T. H., Whittington, J. C. R., Mark, S., Baram, A. B., Stachenfeld, K. L., et al. (2018). What is a cognitive map? Organizing knowledge for flexible behavior. *Neuron* 100, 490–509.

Björklund, A., and Dunnett, S. B. (2007). Dopamine neuron systems in the brain: An update. *Trends Neurosci.* 30, 194–202. doi: 10.1016/j.tins.2007.03.006

Braak, H., and Braak, E. (1992). The human entorhinal cortex: Normal morphology and lamina-specific pathology in various diseases. *Neurosci. Res.* 15, 6–31.

Buck, L. B. (1996). Information coding in the vertebrate olfactory system. *Annu. Rev. Neurosci.* 19, 517–544.

Budinger, E., Heil, P., Hess, A., and Scheich, H. (2006). Multisensory processing via early cortical stages: Connections of the primary auditory cortical field with other sensory systems. *Neuroscience* 143, 1065–1083.

Burwell, R. D., and Amaral, D. G. (1998). Cortical afferents of the perirhinal, postrhinal, and entorhinal cortices of the rat. *J. Comp. Neurol.* 398, 179–205.

Caruana, D. A., and Chapman, C. A. (2008). Dopaminergic suppression of synaptic transmission in the lateral entorhinal cortex. *Neural Plast.* 2008:203514.

Chen, Y., Chen, X., Baserdem, B., Zhan, H., Li, Y., Davis, M. B., et al. (2022). High-throughput sequencing of single neuron projections reveals spatial organization in the olfactory cortex. *Cell* 185:4117–4134.e28. doi: 10.1016/j.cell.2022.09.038

Chu, M. W., Li, W. L., and Komiyama, T. (2016). Balancing the robustness and efficiency of odor representations during learning. *Neuron* 92, 174–186. doi: 10.1016/j.neuron.2016.09.004

Cohen, Y., Wilson, D. A., and Barkai, E. (2015). Differential modifications of synaptic weights during odor rule learning: Dynamics of interaction between the piriform cortex with lower and higher brain areas. *Cereb. Cortex* 25, 180–191. doi: 10.1093/cercor/bht215

Coronas, V., Srivastava, L. K., Liang, J. J., Jourdan, F., and Moyse, E. (1997). Identification and localization of dopamine receptor subtypes in rat olfactory mucosa and bulb: A combined in situ hybridization and ligand binding radioautographic approach. *J. Chem. Neuroanat.* 12, 243–257. doi: 10.1016/s0891-0618(97)00215-9

Craik, K. J. W. (1943). *The nature of explanation*. Cambridge: Cambridge University Press.

de Olmos, J., Hardy, H., and Heimer, L. (1978). The afferent connections of the main and the accessory olfactory bulb formations in the rat: An experimental Hrp-study. *J. Comp. Neurol.* 181, 213–244. doi: 10.1002/cne.901810202

DeNardo, L. A., Berns, D. S., Deloach, K., and Luo, L. (2015). Connectivity of mouse somatosensory and prefrontal cortex examined with trans-synaptic tracing. *Nat. Neurosci.* 18, 1687–1697. doi: 10.1038/nn.4131

Deshmukh, S. S., and Knierim, J. J. (2011). Representation of non-spatial and spatial information in the lateral entorhinal cortex. *Front. Behav. Neurosci.* 5:69. doi: 10.3389/fnbeh.2011.00069

Diodato, A., De Brimont, M. R., Yim, Y. S., Derian, N., Perrin, S., Pouch, J., et al. (2016). Molecular signatures of neural connectivity in the olfactory cortex. *Nat. Commun.* 7:12238.

Doan, T. P., Lagartos-Donate, M. J., Nilssen, E. S., Ohara, S., and Witter, M. P. (2019). Convergent projections from perirhinal and postrhinal cortices suggest a multisensory nature of lateral, but not medial, entorhinal cortex. *Cell Rep.* 29:617–627.e7. doi: 10.1016/j.celrep.2019.09.005

Douaud, G., Lee, S., Alfaro-Almagro, F., Arthofer, C., Wang, C. Y., Mccarthy, P., et al. (2022). SARS-CoV-2 is associated with changes in brain structure in Uk Biobank. *Nature* 604:697.

Doucette, W., Gire, D. H., Whitesell, J., Carmean, V., Lucero, M. T., and Restrepo, D. (2011). Associative cortex features in the first olfactory brain relay station. *Neuron* 69, 1176–1187. doi: 10.1016/j.neuron.2011.02.024

Fallon, J. H., Koziell, D. A., and Moore, R. Y. (1978). Catecholamine innervation of the basal forebrain. Ii. Amygdala, suprarhinal cortex and entorhinal cortex. *J. Comp. Neurol.* 180, 509–532. doi: 10.1002/cne.901800308

Fiorentino, J., Payne, M., Cancian, E., Plonka, A., Dumas, L., Chirio, D., et al. (2022). Correlations between persistent olfactory and semantic memory disorders after SARS-CoV-2 infection. *Brain Sci.* 12:714.

Fletcher, M. L., and Wilson, D. A. (2002). Experience modifies olfactory acuity: Acety)Lcholine-dependent learning decreases behavioral generalization between similar odorants. *J. Neurosci.* 22:Rc201. doi: 10.1523/JNEUROSCI.22-02-j0005.2002

Fyhn, M., Molden, S., Witter, M. P., Moser, E. I., and Moser, M. B. (2004). Spatial representation in the entorhinal cortex. *Science* 305, 1258–1264.

Glovaci, I., and Chapman, C. A. (2015). Activation of phosphatidylinositol-linked dopamine receptors induces a facilitation of glutamate-mediated synaptic transmission in the lateral entorhinal cortex. *PLoS One* 10:e0131948. doi: 10.1371/journal.pone.0131948

Hafting, T., Fyhn, M., Molden, S., Moser, M. B., and Moser, E. I. (2005). Microstructure of a spatial map in the entorhinal cortex. *Nature* 436, 801–806. doi: 10.1038/nature03721

Halasz, N., Johansson, O., Hokfelt, T., Ljungdahl, A., and Goldstein, M. (1981). Immunohistochemical identification of two types of dopamine neuron in the rat olfactory bulb as seen by serial sectioning. *J. Neurocytol.* 10, 251–259. doi: 10.1007/BF01257970

Hansen, K. A., Kay, K. N., and Gallant, J. L. (2007). Topographic organization in and near human visual area V4. *J. Neurosci.* 27, 11896–11911.

Hargreaves, E. L., Rao, G., Lee, I., and Knierim, J. J. (2005). Major dissociation between medial and lateral entorhinal input to dorsal hippocampus. *Science* 308, 1792–1794. doi: 10.1126/science.1110449

Hokfelt, T., Ljungdahl, A., Fuxe, K., and Johansson, O. (1974). Dopamine nerve terminals in the rat limbic cortex: Aspects of the dopamine hypothesis of schizophrenia. *Science* 184, 177–179. doi: 10.1126/science.184.4133.177

Hoogland, P., Welker, E., Melzer, P., and Vanderloos, H. (1987). Organization of the Projection from the barrel cortex to the thalamus in mice studied with the anterograde tracer phaseolus-leuco-agglutinin (Pha-L). *Acta Anatom.* 128, 339–339.

Igarashi, K. M. (2023). Entorhinal cortex dysfunction in Alzheimer's disease. *Trends Neurosci.* 46, 124–136.

Igarashi, K. M., Ieki, N., An, M., Yamaguchi, Y., Nagayama, S., Kobayakawa, K., et al. (2012). Parallel mitral and tufted cell pathways route distinct odor information to different targets in the olfactory cortex. *J. Neurosci.* 32, 7970–7985. doi: 10.1523/JNEUROSCI.0154-12.2012

Igarashi, K. M., Lee, J. Y., and Jun, H. (2022). Reconciling neuronal representations of schema, abstract task structure, and categorization under cognitive maps in the entorhinal-hippocampal-frontal circuits. *Curr. Opin. Neurobiol.* 77:102641. doi: 10.1016/j.conb.2022.102641

Igarashi, K. M., Lu, L., Colgin, L. L., Moser, M. B., and Moser, E. I. (2014). Coordination of entorhinal-hippocampal ensemble activity during associative learning. *Nature* 510, 143–147. doi: 10.1038/nature13162

Ikemoto, S. (2007). Dopamine reward circuitry: Two projection systems from the ventral midbrain to the nucleus accumbens-olfactory tubercle complex. *Brain Res. Rev.* 56, 27–78. doi: 10.1016/j.brainresrev.2007.05.004

Insausti, R., Herrero, M. T., and Witter, M. P. (1997). Entorhinal cortex of the rat: Cytoarchitectonic subdivisions and the origin and distribution of cortical efferents. *Hippocampus* 7, 146–183. doi: 10.1002/(SICI)1098-1063(1997)7:2<146::AID-HIPO4>3.0.CO;2-L

Kerr, K. M., Agster, K. L., Furtak, S. C., and Burwell, R. D. (2007). Functional neuroanatomy of the parahippocampal region: The lateral and medial entorhinal areas. *Hippocampus* 17, 697–708.

Koster, N. L., Norman, A. B., Richtand, N. M., Nickell, W. T., Puche, A. C., Pixley, S. K., et al. (1999). Olfactory receptor neurons express D2 dopamine receptors. *J. Comp. Neurol.* 411, 666–673.

Lechien, J. R., Chiesa-Estomba, C. M., De Siati, D. R., Horoi, M., Le Bon, S. D., Rodriguez, A., et al. (2020). Olfactory and gustatory dysfunctions as a clinical presentation of mild-to-moderate forms of the coronavirus disease (Covid-19): A multicenter European study. *Eur. Arch. Oto Rhino Laryngol.* 277, 2251–2261.

Lee, J. Y., Jun, H., Soma, S., Nakazono, T., Shiraiwa, K., Dasgupta, A., et al. (2021). Dopamine facilitates associative memory encoding in the entorhinal cortex. *Nature* 598, 321–326. doi: 10.1038/s41586-021-03948-8

Leitner, F. C., Melzer, S., Lutcke, H., Pinna, R., Seeburg, P. H., Helmchen, F., et al. (2016). Spatially segregated feedforward and feedback neurons support differential odor processing in the lateral entorhinal cortex. *Nat. Neurosci.* 19, 935–944. doi: 10.1038/nn.4303

Loureiro, M., Achargui, R., Flakowski, J., Van Zessen, R., Stefanelli, T., and Pascoli, V. (2019). Social transmission of food safety depends on synaptic plasticity in the prefrontal cortex. *Science* 364:991. doi: 10.1126/science.aaw5842

Luskin, M. B., and Price, J. L. (1982). The distribution of axon collaterals from the olfactory-bulb and the nucleus of the horizontal limb of the diagonal band to the olfactory cortex, demonstrated by double retrograde labeling techniques. *J. Comp. Neurol.* 209, 249–263. doi: 10.1002/cne.902090304

Malach, R. (1989). Patterns of connections in rat visual-cortex. *J. Neurosci.* 9, 3741–3752.

Miyamichi, K., Amat, F., Moussavi, F., Wang, C., Wickersham, I., Wall, N. R., et al. (2011). Cortical representations of olfactory input by trans-synaptic tracing. *Nature* 472, 191–196. doi: 10.1038/nature09714

Moberly, A. H., Schreck, M., Bhattarai, J. P., Zweifel, L. S., Luo, W. Q., and Ma, M. H. (2018). Olfactory inputs modulate respiration-related rhythmic activity in the prefrontal cortex and freezing behavior. *Nat. Commun.* 9:1528. doi: 10.1038/s41467-018-03988-1

Mori, K., Nagao, H., and Yoshihara, Y. (1999). The olfactory bulb: Coding and processing of odor molecule information. *Science* 286, 711–715.

Mori, K., Takahashi, Y. K., Igarashi, K. M., and Yamaguchi, M. (2006). Maps of odorant molecular features in the mammalian olfactory bulb. *Physiol. Rev.* 86, 409–433.

Murata, K., Kanno, M., Ieki, N., Mori, K., and Yamaguchi, M. (2015). Mapping of learned odor-induced motivated behaviors in the mouse olfactory tubercle. *J. Neurosci.* 35, 10581–10599. doi: 10.1523/JNEUROSCI.0073-15.2015

Nagayama, S., Homma, R., and Imamura, F. (2014). Neuronal organization of olfactory bulb circuits. *Front. Neural Circuits* 8:98. doi: 10.3389/fncir.2014.00098

Oettl, L. L., Scheller, M., Filosa, C., Wieland, S., Haag, F., Loeb, C., et al. (2020). Phasic dopamine reinforces distinct striatal stimulus encoding in the olfactory tubercle driving dopaminergic reward prediction. *Nat. Commun.* 11:3460. doi: 10.1038/s41467-020-17257-7

Ohara, S., Onodera, M., Simonsen, O. W., Yoshino, R., Hioki, H., Iijima, T., et al. (2018). Intrinsic projections of layer Vb neurons to layers Va, III, and II in the Lateral and medial entorhinal cortex of the rat. *Cell Rep.* 24, 107–116. doi: 10.1016/j.celrep.2018.06.014

Ojima, H., Honda, C. N., and Jones, E. G. (1991). Patterns of axon collateralization of identified supragranular pyramidal neurons in the cat auditory cortex. *Cereb. Cortex* 1, 80–94. doi: 10.1093/cercor/1.1.80

O'Keefe, J., and Dostrovsky, J. (1971). The hippocampus as a spatial map. Preliminary evidence from unit activity in the freely-moving rat. *Brain Res.* 34, 171–175. doi: 10.1016/0006-8993(71)90358-1

Paxinos, G. (2004). *The rat nervous system*. Amsterdam: Elsevier.

Petzold, G. C., Hagiwara, A., and Murthy, V. N. (2009). Serotonergic modulation of odor input to the mammalian olfactory bulb. *Nat. Neurosci.* 12, 784–U142. doi: 10.1038/nn.2335

Price, J. L. (2003). Comparative aspects of amygdala connectivity. *Amygdala Brain Funct.* 985, 50–58.

Serby, M., Larson, P., and Kalkstein, D. (1991). The nature and course of olfactory deficits in Alzheimer's disease. *Am. J. Psychiatry* 148, 357–360.

Sha, M. F. R., Koga, Y., Murata, Y., Taniguchi, M., and Yamaguchi, M. (2023). Learning-dependent structural plasticity of intracortical and sensory connections to functional domains of the olfactory tubercle. *Front. Neurosci.* 17:1247375. doi: 10.3389/fnins.2023.1247375

Shepherd, G. M. (2004). *The synaptic organization of the brain*. Oxford: Oxford University Press.

Shiotani, K., Tanisumi, Y., Murata, K., Hirokawa, J., Sakurai, Y., and Manabe, H. (2020). Tuning of olfactory cortex ventral tenia tecta neurons to distinct task elements of goal-directed behavior. *Elife*, 9.

Stettler, D. D., and Axel, R. (2009). Representations of odor in the piriform cortex. *Neuron* 63, 854–864.

Sürmeli, G., Marcu, D. C., Mcclure, C., Garden, D. L. F., Pastoll, H., and Nolan, M. F. (2016). Molecularly defined circuitry reveals input-output segregation in deep layers of the medial entorhinal cortex. *Neuron* 92, 929–929.

Tolman, E. C. (1948). Cognitive maps in rats and men. *Psychol. Rev.* 55, 189–208.

Tsao, A., Moser, M. B., and Moser, E. I. (2013). Traces of experience in the lateral entorhinal cortex. *Curr. Biol.* 23, 399–405.

Tse, D., Langston, R. F., Kakeyama, M., Bethus, I., Spooner, P. A., Wood, E. R., et al. (2007). Schemas and memory consolidation. *Science* 316, 76–82.

Van Hoesen, G. W., Hyman, B. T., and Damasio, A. R. (1991). Entorhinal cortex pathology in Alzheimer's disease. *Hippocampus* 1, 1–8.

Vandrey, B., Armstrong, J., Brown, C. M., Garden, D. L. F., and Nolan, M. F. (2022). Fan cells in lateral entorhinal cortex directly influence medial entorhinal cortex through synaptic connections in layer 1. *Elife* 11:e83008. doi: 10.7554/eLife.83008

Waldton, S. (1974). Clinical observations of impaired cranial nerve function in senile dementia. *Acta Psychiatr. Scand.* 50, 539–547.

Wesson, D. W., and Wilson, D. A. (2010). Smelling sounds: Olfactory-auditory sensory convergence in the olfactory tubercle. *J. Neurosci.* 30, 3013–3021. doi: 10.1523/JNEUROSCI.6003-09.2010

Witter, M. P., Wouterlood, F. G., Naber, P. A., and Van Haeften, T. (2000). Anatomical organization of the parahippocampal-hippocampal network. *Ann. N. Y. Acad. Sci.* 911, 1–24.

Young, B. J., Otto, T., Fox, G. D., and Eichenbaum, H. (1997). Memory representation within the parahippocampal region. *J. Neurosci.* 17, 5183–5195.

Zaborszky, L., Carlsen, J., Brashear, H. R., and Heimer, L. (1986). Cholinergic and GABAergic afferents to the olfactory bulb in the rat with special emphasis on the projection neurons in the nucleus of the horizontal limb of the diagonal band. *J. Comp. Neurol.* 243, 488–509. doi: 10.1002/cne.902430405

Zhang, Z., Zhang, H., Wen, P., Zhu, X., Wang, L., Liu, Q., et al. (2017). Whole-brain mapping of the inputs and outputs of the medial part of the olfactory tubercle. *Front. Neural Circuits* 11:52. doi: 10.3389/fncir.2017.00052

frontiers | Frontiers in Neural Circuits

TYPE Mini Review
PUBLISHED 08 July 2024
DOI 10.3389/fncir.2024.1430783

OPEN ACCESS

EDITED BY
Kensaku Mori,
RIKEN, Japan

REVIEWED BY
Takuji Iwasato,
National Institute of Genetics, Japan

*CORRESPONDENCE
Ijeoma Nwabudike
ijeoma.nwabudike@yale.edu
Alicia Che
alicia.che@yale.edu

RECEIVED 10 May 2024
ACCEPTED 20 June 2024
PUBLISHED 08 July 2024

CITATION
Nwabudike I and Che A (2024) Early-life maturation of the somatosensory cortex: sensory experience and beyond.
Front. Neural Circuits 18:1430783.
doi: 10.3389/fncir.2024.1430783

Early-life maturation of the somatosensory cortex: sensory experience and beyond

Ijeoma Nwabudike* and Alicia Che*

Department of Psychiatry, Yale University School of Medicine, New Haven, CT, United States

Early life experiences shape physical and behavioral outcomes throughout lifetime. Sensory circuits are especially susceptible to environmental and physiological changes during development. However, the impact of different types of early life experience are often evaluated in isolation. In this mini review, we discuss the specific effects of postnatal sensory experience, sleep, social isolation, and substance exposure on barrel cortex development. Considering these concurrent factors will improve understanding of the etiology of atypical sensory perception in many neuropsychiatric and neurodevelopmental disorders.

KEYWORDS

somatosensory perception, barrel cortex development, early life experience, sensory deprivation, REM Sleep, early social isolation, cross-modal sensory experience

1 Introduction

Early life experiences can have profound and life-long physical, emotional, and behavioral consequences (Felitti et al., 1998; Hughes et al., 2017; Lokhandwala and Spencer, 2022). During postnatal development, maturation of circuits involved in sensory perception occurs first, and this process is particularly sensitive to physiological and environmental influences (Chang and Merzenich, 2003; Maitre et al., 2017; Badde et al., 2020; reviews: Hensch, 2004; Fox et al., 2010). In rodents, whisker-mediated tactile input is one of the earliest developed sensory modalities (Akhmetshina et al., 2016; Smirnov and Sitnikova, 2019). Tactile inputs are present at birth, while visual and auditory inputs do not occur until the second postnatal week in mice (Colonnese et al., 2010; Akhmetshina et al., 2016; Makarov et al., 2021). This feature allows tactile sensory inputs to interact with intrinsic programs to uniquely shape sensorimotor circuit maturation (Bragg-Gonzalo et al., 2021).

The developing somatosensory cortex is dominated by synchronous neural activity until the end of the second postnatal week (Khazipov et al., 2004; Minlebaev et al., 2007; Golshani et al., 2009; Tolner et al., 2012; Yang et al., 2013). Its precise patterns and timing are essential for many activity-dependent processes during early postnatal development (Winnubst et al., 2015; Wong et al., 2018; Duan et al., 2020; review: Leighton and Lohmann, 2016). Such activity has been suggested to originate from at least four sources: (1) external, passive tactile sensory inputs onto the whiskers from the dam, littermates, and nesting materials (Akhmetshina et al., 2016); (2) sensorimotor feedback generated by involuntary whisker and limb twitches (Khazipov et al., 2004; Tiriac et al., 2014; Dooley et al., 2020); (3) cross-modal sensory inputs, such as odor-driven activity via direct early excitatory connections from the olfactory cortex to somatosensory cortex (Henschke et al., 2018;

Cai et al., 2024); 4) internally generated, spontaneous neural activity independent from the periphery or movement (Moreno-Juan et al., 2017; Mizuno et al., 2018; Nakazawa et al., 2020; Banerjee et al., 2022). Multiple lines of evidence support that activity from these different sources co-exist in the first two postnatal weeks. While spontaneously occurring and whisker stimulation-induced oscillatory activity are both present already at birth, inactivation of the tactile sensory periphery with lidocaine, which occludes tactile sensory inputs and sensorimotor feedback from whisker twitches, reduces but does not abolish synchronous activity (Yang et al., 2009). In addition, barrel column-related patchwork activity in L4 excitatory neurons is uncorrelated with whisker movement and does not disappear after infraorbital nerve transection at P4 (Mizuno et al., 2018; Nakazawa et al., 2018). There is still considerable ongoing debate over whether the four sources of activity mentioned above are distinct – for example, what proportion of activity that has been attributed as "internally-generated activity" is due to sensorimotor feedback given that the circuitry enabling movement-related sensory feedback is already functional in the thalamus embryonically (Antón-Bolaños et al., 2019; Dooley et al., 2020; Blumberg et al., 2022). Latest data demonstrating that synchronous activity in the barrel cortex can be driven by chemosensation also raises the possibility that the remaining synchronous activity after inactivation of tactile sensory periphery could have, at least in part, originated from other sensory modalities (Cai et al., 2024; Wang et al., 2024). Further investigations will be required to confirm or resolve potential overlaps between sources of early neural activity in the barrel cortex.

Given the complexity of early neural activity as discussed above, in this minireview we will focus on summarizing the role of the following early-life sensory experiences on the development of somatosensory cortex: (1) external tactile sensory inputs; (2) sleep in the context of permitting sensorimotor feedback; (3) recently discovered cross-modal olfactory sensory inputs. While there might be overlap in mechanisms, we will not focus on internally generated intrinsic activity here (review: Leighton and Lohmann, 2016). We will also discuss recent findings that have uncovered the impact of other early-life factors, including isolation and substance exposure (Figure 1).

2 Neonatal tactile sensory experience

In the whisker sensory system, tactile sensory input to the whiskers is transduced by mechanoreceptors in each whisker follicle on the snout, then carried by afferent fibers to the trigeminal nucleus of the brainstem, the ventroposteromedial nucleus of the thalamus (VPM) and finally to the somatosensory cortex (reviews: Petersen, 2007; Diamond et al., 2008). In layer 4 (L4) of the barrel cortex, cytoarchitectonic cylindrical structures known as "barrels" correspond to individual whiskers (Woolsey and van der Loos, 1970). Synaptic connections of within barrel cortex have been extensively characterized, making it an excellent model for investigating experience-dependent circuit maturation. Peripheral manipulations have been widely used and demonstrated to produce marked alterations in the structure and function of the developing barrel cortex. These studies provide a wealth of information on the age-, layer-, cell type-, and synaptic connection-specific effects of postnatal sensory experience (review: Erzurumlu and Gaspar, 2012). Below we will summarize effects of tactile sensory deprivation via peripheral manipulations on barrel cortex synaptic connectivity (thalamocortical and intracortical), neuronal maturation, and behavior.

Thalamocortical afferents (TCAs) to the barrel cortex play a critical role in instructing barrel formation and organization, dendritic remodeling, and neuronal maturation (Li et al., 2013; Matsui et al., 2013; Pouchelon et al., 2014; Young et al., 2023). Disruption of presynaptic vesicle fusion, glutamatergic neurotransmission, or cAMP signaling at thalamocortical synapses alters barrel patterning (Abdel-Majid et al., 1998; Iwasato et al., 2000; Inan et al., 2006; Ballester-Rosado et al., 2010; Narboux-Nême et al., 2012; Li et al., 2013; Suzuki et al., 2015). The TCAs are also particularly sensitive to sensory deprivation. When sensory input is eliminated by infra-orbital nerve transection or whisker follicle cauterization before postnatal day (P) 3, TCA arbors no longer cluster and cylindrical barrels are replaced by elongated fused bands that extend through L4 of the barrel field (Van der Loos and Woolsey, 1973; Killackey and Belford, 1979; Wong-Riley and Welt, 1980; Jeanmonod et al., 1981; Jensen and Killackey, 1987). Similar manipulations that result in permanent peripheral damage at later timepoints, between P4 and P6, lead to TCA disorganization but not a complete loss of barrel structure, while normal barrel patterns are preserved when manipulations occur after P6 (Woolsey and Wann, 1976; Belford and Killackey, 1980; Jeanmonod et al., 1981; Bates and Killackey, 1985; Higashi et al., 1999). Neonatal whisker trimming or plucking, which limits tactile sensory experience without causing peripheral structural damage, does not alter the cytoarchitectonic barrel structure; instead, it leads to changes in the strength of thalamocortical and intracortical synapses (Finnerty et al., 1999; Allen et al., 2003; Sadaka et al., 2003; Schierloh et al., 2004; Bender et al., 2006; Chittajallu and Isaac, 2010; Simons et al., 2015). For instance, the density and efficacy of thalamocortical synapses decrease following chronic whisker trimming (Sadaka et al., 2003). Following extended whisker regrowth, thalamic drive to excitatory neurons rebounds to above control levels, suggesting that sensory inputs can restore and even heighten the efficacy of thalamocortical synapses after early-life manipulations (Simons et al., 2015). Sensory deprivation also weakens intracortical synapses at L4-to-L2/3 connections and increases lateral synaptic transmission across barrel columns, resulting in increased neuronal responses to deflection of surrounding non-principal whiskers (Fox, 1992; Finnerty et al., 1999; Lendvai et al., 2000; Stern et al., 2001; Allen et al., 2003; Shepherd et al., 2003; Schierloh et al., 2004; Bender et al., 2006; Lee et al., 2007). When whisker regrowth is allowed, L4 neurons continue to show broadened sensory-evoked responses (Simons and Land, 1987; Shoykhet et al., 2005). In summary, these studies establish that sensory experience from the periphery plays a central role in regulating thalamocortical and intracortical circuit assembly during development.

During the early postnatal period, cortical GABAergic interneurons also receive significant thalamic inputs and shape circuit function in a sensory experience-dependent manner. In the first postnatal week, direct TCAs from the VPM preferentially form synaptic connections with select interneuron subtypes, such as somatostatin-expressing (SST) interneurons in L5 and

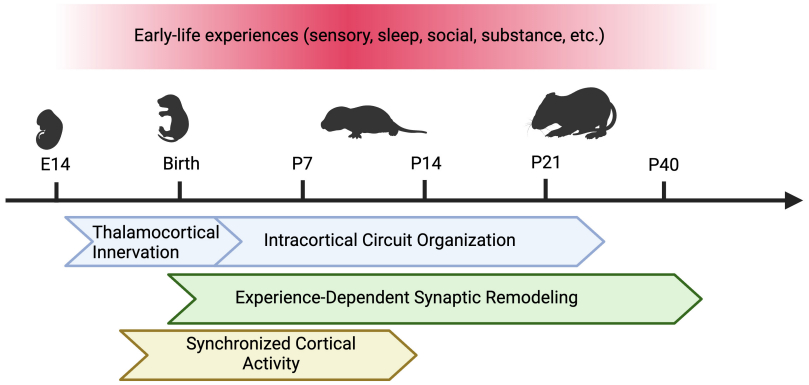

FIGURE 1
Types of Early Life Experiences and Susceptible Developmental Programs in the Barrel Cortex. In rodents, early sensory experience, sleep, social isolation, and perinatal substance exposure can alter the development of the barrel cortex. Different developmental programs may be affected by these factors across varying sensitive periods. These programs include thalamocortical innervation, intracortical circuit assembly (including maturation of excitatory and inhibitory circuits), experience-dependent synaptic remodeling, and synchronous cortical activity. Figure created with Biorender.com.

Reelin-expressing (Re) interneurons in L1 (Marques-Smith et al., 2016; Tuncdemir et al., 2016; Che et al., 2018; Pouchelon et al., 2021). These thalamic inputs to interneurons are dynamically remodeled during development—VPM inputs to SST, Re, and Vasoactive intestinal peptide-expressing (VIP) interneurons weaken by the end of the second postnatal week, while VPM inputs to parvalbumin-expressing (PV) interneurons and PV-driven feed-forward inhibition continue to strengthen (Daw et al., 2007; Che et al., 2018; Kastli et al., 2020; Modol et al., 2020). The transient TCA connections are required for the maturation of stable circuit connectivity that persists into adulthood (Anastasiades et al., 2016; Marques-Smith et al., 2016; Tuncdemir et al., 2016). It has been hypothesized that interneurons are more sensitive to early-life sensory experience due to their protracted postnatal development (review: Micheva and Beaulieu, 1997). This hypothesis is supported by recent studies demonstrating that sensory deprivation specifically reduces VPM to interneuron inputs and interneuron activity, resulting in delayed cell maturation and alterations in intracortical connectivity (Chittajallu and Isaac, 2010; Marques-Smith et al., 2016; Che et al., 2018; Duan et al., 2020; Bollmann et al., 2023). Whisker plucking from the first postnatal week to adulthood decreases L4 surround inhibition, inhibitory synaptic strength, and the total number of interneurons (Micheva and Beaulieu, 1995a,b; Shoykhet et al., 2005; Gainey et al., 2016). Taken together, these studies demonstrate that developing interneurons are uniquely positioned to relay thalamic inputs and regulate responses to early sensory experiences, thus playing a significant role in shaping cortical circuit formation and function.

Early sensory deprivation also has profound behavioral consequences. Infant-trimmed rodents can differentiate between rough and smooth textures but show difficulty distinguishing between two distinct rough textures (Carvell and Simons, 1996). This is thought to be a consequence of permanent deficits in surround inhibition, which decreases the animal's perceptual ability in tasks that require information from multiple whiskers (Carvell and Simons, 1996; Shoykhet et al., 2005). Trimming also alters explorative whisking and behavioral strategies during gap-crossing tasks (Lee et al., 2009; Papaioannou et al., 2013). Intriguingly, the effects of early sensory deprivation are especially evident in socio-cognitive behavioral tasks. Animals that have been vibrissectomized are more social and explorative, displaying less emotional reactivity and diminished early withdrawal response from novel tactile stimuli (Shishelova, 2006; Lee et al., 2009; Soumiya et al., 2016; Wang et al., 2022). Furthermore, sensory deprivation through whisker removal reduces excitatory synaptic transmission as well as the synthesis and secretion of the neuropeptide oxytocin, while both oxytocin injection and increased sensory experience rescues excitatory synaptic transmission (Zheng et al., 2014). Nevertheless, it remains to be determined through what specific mechanisms early tactile sensory experience influences the development of higher-order social, emotional, and cognitive function.

3 Sleep and sleep deprivation

Similar to human infants, neonatal rodents spend the majority of their time sleeping (Blumberg et al., 2022). The younger the animal, the more time it spends in active (rapid-eye-movement, REM) sleep states (Jouvet-Mounier et al., 1969). During the first two weeks of life, rodents spend between 45 to 80% of their time in REM sleep, 20 to 35% in wakeful states, and up to 25% in non-REM sleep, while in adult rodents, REM sleep time decreases to 8.5% and time spent awake rises to 43% (Jouvet-Mounier et al., 1969; Blumberg et al., 2022). As discussed previously, sensorimotor feedback generated by myoclonic twitches is a main source of early synchronous activity in the barrel cortex (Blumberg et al., 2022). Recent studies correlating electrophysiological recordings of barrel cortex activity with whisker motion show that up to 75% of spontaneous somatosensory cortical activity is directly related to passive whisker movement (Akhmetshina et al., 2016; Dooley et al., 2020). These twitches during REM sleep are more likely to generate network activity in the barrel cortex than movements during wakefulness (Dooley et al., 2020). Therefore, REM sleep during development serves to enable muscle twitches important for activity-dependent circuit maturation in the barrel cortex. In support of this, REM sleep during development has been shown

to support heightened synaptic remodeling, in particular synaptic elimination (Yang and Gan, 2012; Li et al., 2017; Zhou et al., 2020; review: Sun et al., 2020), a process essential for the development of mature and functional circuits (Faust et al., 2021). In addition, REM sleep increases coherence between distant brain regions, facilitating the formation of long-range connections that direct complex sensory-based behaviors in adulthood (Rio-Bermudez et al., 2020).

Early-life sleep deprivation may also alter inhibitory circuits – persistent decrease in PV interneuron number has been reported in adult voles whose sleep was disrupted between P14 and P21 (Jones et al., 2019). Behaviorally, prairie voles that were sleep-deprived as neonates display aberrant exploratory behavior and pair bond formation during adulthood (Jones et al., 2019). Together, these findings indicate that REM sleep is essential for synaptic remodeling during early life, and therefore may have far-reaching behavioral effects.

4 Neonatal cross-modal sensory experience

While multisensory integration via direct thalamocortical and intracortical connections across modalities in adults is well appreciated (review: Driver and Noesselt, 2008), less is known about when multisensory connectivity is established, and whether it contributes to the maturation of and the early activity in primary sensory cortices. In developing Mongolian gerbils, several thalamic nuclei project to two or more sensory cortices between P1-P9, and the non-matched modality projections are pruned away after P15 (Henschke et al., 2018). Direct connections between primary visual, auditory, and somatosensory cortices occur later than multisensory interconnections at the thalamic level, occurring at the onset of sensory experience around P15. In addition, the number of multisensory connections drastically increases following the loss of early sensory experience (Henschke et al., 2018), suggesting that sensory experience from other modalities is able to alter the development and function of the somatosensory cortex during early postanal development. In support of this notion, whisker deprivation or dark rearing reduces excitatory synaptic transmission in the correspondent sensory cortex and cross-modally in other sensory cortices through an oxytocin-dependent mechanism (Zheng et al., 2014).

Direct intracortical excitatory connections have also been demonstrated to trigger early synchronous activity in the somatosensory cortex. In mouse slice culture between embryonic day (E)18-P12, waves of spontaneous electrical activity initiate in the septum and ventral cortex and propagate dorsally across the cortex, including the somatosensory region (Conhaim et al., 2011). This is consistent with the recent finding that there is direct, transient excitatory connectivity from the olfactory cortex to the somatosensory cortex, and *in vivo* odor-driven activity propagates broadly across the cortex during the first postnatal week (Cai et al., 2024). This odor-evoked activity enhances whisker-evoked activity in the barrel cortex, while neonatal odor deprivation leads to somatosensory defects in adult mice, suggesting that there is a cross-modal critical window for nasal chemosensation-dependent somatosensory function maturation (Cai et al., 2024). Interestingly, recent work quantifying prenatally active neurons in mice using Targeted Recombination in Active Populations (TRAP) identified the piriform cortex as the most abundantly TRAPed region, indicating that early piriform neurons may represent an interconnected hub-like population whose activity promotes recurrent connectivity in the developing cortex (Wang et al., 2024). In summary, early cross-modal sensory experience, in particular olfactory inputs, can have large impact on the proper maturation and function of the somatosensory cortex.

5 Social isolation

During early postnatal life, social isolation is a well-documented stressor that can alter cortical synaptic function. Social isolation in pups has been shown to affect synaptic spine density in the barrel cortex, though the effects vary with different isolation protocols (Bock et al., 2005; Takatsuru et al., 2009). When neonatal rodents are isolated for 6 hours daily during 3-day-long periods in the first and second postnatal week, AMPA receptor trafficking in L4-to-L2/3 synapses in the barrel cortex is significantly reduced in isolated pups when compared to pups that are allowed to remain with littermates (Miyazaki et al., 2012; Miyazaki et al., 2013). These synaptic effects are at least in part attributed to the instability of synapses – increased mushroom spine turnover has been observed as a result of social isolation in pups (Takatsuru et al., 2009; Takatsuru et al., 2015). On the other hand, 3-hour daily isolation from P2 to P14 has been shown to increase neuronal activity in the adult barrel cortex and raise baseline glutamate levels, which, in a pattern not observed in control animals, rises even further following exposure to physical stressors (Toya et al., 2014). These deficits persist after limiting peripheral inputs, which suggests that mechanisms distinct from sensory experience are responsible for the circuit changes associated with social isolation.

Social isolation activates glucocorticoid signaling widely across the brain (Mccormick et al., 1998; review: Cacioppo et al., 2015). Rodents that underwent neonatal isolation show long-term increases in basal corticosterone levels in the barrel cortex (Toya et al., 2014). Elevated glucocorticoid levels have been shown to increase glutamate release in frontal cortical areas (Treccani et al., 2014). Although similar mechanisms have not been directly demonstrated in the barrel cortex, high glucocorticoid levels may also contribute to aberrant glutamatergic homeostasis observed in this region. Indeed, repeated brief exposure to maternal separation results in significantly enhanced spine density in L2/3 pyramidal neurons in the somatosensory cortex (Bock et al., 2005). Acute administration of corticosterone induces higher spine turnover rate in the juvenile barrel cortex compared to control juvenile animals and the turnover rate observed in glucocorticoid treated adults (Liston and Gan, 2011). Pharmacologically decreasing endogenous glucocorticoid signaling through repeated dexamethasone injections decreases spine turnover, and chronic steroid administration eliminates dendritic spines formed prior, in earlier developmental periods (Liston and Gan, 2011). These findings suggest that stress hormones, released in response to a wide variety of stressors including social isolation, can highjack mechanisms of synaptic plasticity during development and have long-term social and

cognitive behavioral consequences (Moriceau et al., 2009; review: Sullivan and Holman, 2010).

Recent evidence has identified glial regulation of synaptic function as another potential mechanism through which early social isolation can affect sensory circuit development. Early sensory experience alters cortical synaptic pruning, a process mediated by microglia and astrocytes (Kalambogias et al., 2020; Gesuita et al., 2022). Neonatal social isolation leads to increased microglial process motility both at baseline and in response to sensory stimulation (Takatsuru et al., 2015). Additionally, astrocytes contribute to the developmental changes in L4-to-L2/3 synaptic plasticity by regulating the switch from long-term depression (LTD) to long-term potentiation (LTP) (Martinez-Gallego et al., 2022). The precise mechanistic connections between early life stress, glucocorticoid signaling, microglial and/or astrocytic dysfunction, and long-term synaptic instability are still unclear. Further investigations of glial development in the barrel cortex will be informative for understanding experience-dependent maturation of somatosensory circuits.

6 Early life exposure to psychoactive substances

Perinatal exposure to psychoactive substances has also been shown to alter barrel cortex development. The most studied of these substances is ethanol. In humans, consumption of alcohol during pregnancy can cause Fetal Alcohol Syndrome (FAS), a developmental disorder characterized by intellectual disability, facial anomalies, and behavioral deficits (review: Popova et al., 2023). Preclinical rodent models of FAS show that both prenatal and early postnatal (P4-P10) alcohol exposure decrease the area size of the barrel cortex (Miller and Potempa, 1990; Margret et al., 2005, 2006; Powrozek and Zhou, 2005; Chappell et al., 2007). Prenatal ethanol exposure also decreases the number of glia and neurons in the barrel cortex (Miller and Potempa, 1990; Powrozek and Zhou, 2005). This is likely due to the broad apoptotic effect of alcohol exposure in the neonatal brain (Smiley et al., 2019). Between P4 and P7, when alcohol-induced apoptosis reaches maximum levels, intraperitoneal administration of alcohol suppresses spontaneous activity in the barrel cortex and decreases body movements (Lebedeva et al., 2017). Perinatal alcohol exposure decreases the excitability of L5 pyramidal neurons and the cell density of PV interneurons (Granato et al., 2012; Saito et al., 2019). On a behavioral level, adolescent mice exposed to alcohol prenatally show diminished tactile sensitivity (Delatour et al., 2019). These data suggest that early ethanol exposure disrupts normal barrel cortex development and sensory perception by inhibiting cortical activity and increasing apoptosis, which could lead to impaired circuit maturation and organization.

The impact of other psychoactive substances on somatosensory circuit development is less characterized. Prenatal and postnatal opioid exposure has also been shown to increase apoptosis in cortical neurons and microglia, and methadone may specifically decrease the number of GABAergic synapses (Bajic et al., 2013; Grecco et al., 2022). Postnatal (P2-P7) injection of Δ(9)-tetrahydrocannabinol (THC), the primary psychoactive component of cannabis, results in premature retraction and pruning of TCAs during the first postnatal week (Itami et al., 2016). Nicotine, at concentrations similar to those produced by maternal tobacco smoking, desensitizes nicotinic acetylcholine (ACh) receptors in subplate neurons thus diminishing the ACh-driven spontaneous activity in the barrel cortex during the first postnatal week (Hanganu and Luhmann, 2004; Dupont et al., 2006). Overall, these substances may exert long-term effects through pathways that converge upon the disruption of early cortical activity required for sensory circuit development.

7 Conclusion

Various types of early life experience—including but not limited to sensory inputs, sleep, social interactions, and substance exposure—exert effects on postnatal circuit organization and contribute to the development of normal or dysfunctional somatosensation. The physiological and environmental factors discussed here will contribute to the understanding of the etiology of atypical sensory perception in many neurodevelopmental and neuropsychiatric disorders, providing considerations on the timing of therapeutic interventions.

Author contributions

IN: Writing—review and editing, Writing—original draft. AC: Writing—review and editing, Writing—original draft.

Funding

The authors declare financial support was received for the research, authorship, and/or publication of this article. This research was supported by the grants from NINDS 1R00NS114166 (AC), 1R01NS133434 (AC), NIDA 1R01DA059378 (AC), and State of Connecticut, Department of Mental Health and Addiction Services (AC). This publication does not express the views of the Department of Mental Health and Addiction Services or the State of Connecticut.

Conflict of interest

The authors declare that the research was conducted in the absence of any commercial or financial relationships that could be construed as a potential conflict of interest.

Publisher's note

References

Abdel-Majid, R. M., Leong, W. L., Schalkwyk, L. C., Smallman, D. S., Wong, S. T., Storm, D. R., et al. (1998). Loss of adenylyl cyclase I activity disrupts patterning of mouse somatosensory cortex. *Nat. Genet.* 19, 289–291. doi: 10.1038/980

Akhmetshina, D., Nasretdinov, A., Zakharov, A., Valeeva, G., and Khazipov, R. (2016). The nature of the sensory input to the neonatal rat barrel cortex. *J. Neurosci.* 36:9922. doi: 10.1523/JNEUROSCI.1781-16.2016

Allen, C. B., Celikel, T., and Feldman, D. E. (2003). Long-term depression induced by sensory deprivation during cortical map plasticity in vivo. *Nat. Neurosci.* 6, 291–299. doi: 10.1038/NN1012

Anastasiades, P. G., Marques-Smith, A., Lyngholm, D., Lickiss, T., Raffiq, S., Katzel, D., et al. (2016). GABAergic interneurons form transient layer-specific circuits in early postnatal neocortex. *Nat. Commun.* 7, 1–13. doi: 10.1038/ncomms10584

Antón-Bolaños, N., Sempere-Ferràndez, A., Guillamón-Vivancos, T., Martini, F. J., Pérez-Saiz, L., Gezelius, H., et al. (2019). Prenatal activity from thalamic neurons governs the emergence of functional cortical maps in mice. *Science* 364, 987–990. doi: 10.1126/science.aav7617

Badde, S., Ley, P., Rajendran, S. S., Shareef, I., Kekunnaya, R., and Röder, B. (2020). Sensory experience during early sensitive periods shapes cross-modal temporal biases. *Elife* 9:1238. doi: 10.7554/ELIFE.61238

Bajic, D., Commons, K. G., and Soriano, S. G. (2013). Morphine-enhanced apoptosis in selective brain regions of neonatal rats. *Int. J. Dev. Neurosci.* 31, 258–266. doi: 10.1016/J.IJDEVNEU.2013.02.009

Ballester-Rosado, C. J., Albright, M. J., Wu, C. S., Liao, C. C., Zhu, J., Xu, J., et al. (2010). mGluR5 in cortical excitatory neurons exerts both cell-autonomous and -nonautonomous influences on cortical somatosensory circuit formation. *J. Neurosci.* 30:16896. doi: 10.1523/JNEUROSCI.2462-10.2010

Banerjee, P., Kubo, F., Nakaoka, H., Ajima, R., Sato, T., Hirata, T., et al. (2022). Spontaneous activity in whisker-innervating region of neonatal mouse trigeminal ganglion. *Sci. Rep.* 12, 1–17. doi: 10.1038/s41598-022-20068-z

Bates, C. A., and Killackey, H. P. (1985). The organization of the neonatal rat's brainstem trigeminal complex and its role in the formation of central trigeminal patterns. *J. Comp. Neurol.* 240, 265–287. doi: 10.1002/CNE.902400305

Belford, G. R., and Killackey, H. P. (1980). The sensitive period in the development of the trigeminal system of the neonatal rat. *J. Comp. Neurol.* 193, 335–350. doi: 10.1002/cne.901930203

Bender, K. J., Allen, C. B., Bender, V. A., and Feldman, D. E. (2006). Synaptic basis for whisker deprivation-induced synaptic depression in rat somatosensory cortex. *J. Neurosci.* 26, 4155–4165. doi: 10.1523/jneurosci.0175-06.2006

Blumberg, M. S., Dooley, J. C., and Tiriac, A. (2022). Sleep, plasticity, and sensory neurodevelopment. *Neuron* 110, 3230–3242. doi: 10.1016/J.NEURON.2022.08.005

Bock, J., Gruss, M., Becker, S., and Braun, K. (2005). Experience-induced changes of dendritic spine densities in the prefrontal and sensory cortex: Correlation with developmental time windows. *Cereb. Cortex* 15, 802–808. doi: 10.1093/CERCOR/BHH181

Bollmann, Y., Modol, L., Tressard, T., Vorobyev, A., Dard, R., Brustlein, S., et al. (2023). Prominent in vivo influence of single interneurons in the developing barrel cortex. *Nat. Neurosci.* 26, 1555–1565. doi: 10.1038/S41593-023-01405-5

Bragg-Gonzalo, L., Reyes, N. S. D. L., and Nieto, M. (2021). Genetic and activity dependent-mechanisms wiring the cortex: Two sides of the same coin. *Semin. Cell Dev. Biol.* 118, 24–34. doi: 10.1016/J.SEMCDB.2021.05.011

Cacioppo, J. T., Cacioppo, S., Capitanio, J. P., and Cole, S. W. (2015). The neuroendocrinology of social isolation. *Annu. Rev. Psychol.* 66, 733–767.

Cai, L., Argunşah, A. Ö, Damilou, A., and Karayannis, T. (2024). A nasal chemosensation-dependent critical window for somatosensory development. *Science* 384, 652–660.

Carvell, G. E., and Simons, D. J. (1996). Abnormal tactile experience early in life disrupts active touch. *J. Neurosci.* 16, 2750–2757. doi: 10.1523/JNEUROSCI.16-08-02750.1996

Chang, E. F., and Merzenich, M. M. (2003). Environmental noise retards auditory cortical development. *Science* 300, 498–502. doi: 10.1126/SCIENCE.1082163

Chappell, T. D., Margret, C. P., Li, C. X., and Waters, R. S. (2007). LONG TERM EFFECTS OF PRENATAL ALCOHOL EXPOSURE (PAE) ON THE SIZE OF THE WHISKER REPRESENTATION IN JUVENILE AND ADULT RAT BARREL CORTEX. *Alcohol* 41:239. doi: 10.1016/J.ALCOHOL.2007.03.005

Che, A., Babij, R., Iannone, A. F., Fetcho, R. N., Ferrer, M., Liston, C., et al. (2018). Layer I interneurons sharpen sensory maps during neonatal development. *Neuron* 99:98–116.e7. doi: 10.1016/J.NEURON.2018.06.002

Chittajallu, R., and Isaac, J. T. R. (2010). Emergence of cortical inhibition by coordinated sensory-driven plasticity at distinct synaptic loci. *Nat. Neurosci.* 13, 1240–1248. doi: 10.1038/nn.2639

Colonnese, M. T., Kaminska, A., Minlebaev, M., Milh, M., Bloem, B., Lescure, S., et al. (2010). A conserved switch in sensory processing prepares developing neocortex for vision. *Neuron* 67:480. doi: 10.1016/J.NEURON.2010.07.015

Conhaim, J., Easton, C. R., Becker, M. I., Barahimi, M., Cedarbaum, E. R., Moore, J. G., et al. (2011). Developmental changes in propagation patterns and transmitter dependence of waves of spontaneous activity in the mouse cerebral cortex. *J. Physiol.* 589, 2529–2541. doi: 10.1113/JPHYSIOL.2010.202382

Daw, M. I., Ashby, M. C., and Isaac, J. T. R. (2007). Coordinated developmental recruitment of latent fast spiking interneurons in layer IV barrel cortex. *Nat. Neurosci.* 10, 453–461. doi: 10.1038/nn1866

Del Rio-Bermudez, C., and Blumberg, M. S. (2018). Active sleep promotes functional connectivity in developing sensorimotor networks. *BioEssays* 40:e1700234. doi: 10.1002/BIES.201700234

Delatour, L. C., Yeh, P. W., and Yeh, H. H. (2019). Ethanol exposurein uterodisrupts radial migration and pyramidal cell development in the somatosensory cortex. *Cereb. Cortex* 29, 2125–2139. doi: 10.1093/cercor/bhy094

Diamond, M. E., Heimendahl, M. V., Knutsen, P. M., Kleinfeld, D., and Ahissar, E. (2008). "Where" and "what" in the whisker sensorimotor system. *Nat. Rev. Neurosci.* 9, 601–612. doi: 10.1038/nrn2411

Dooley, J. C., Glanz, R. M., Sokoloff, G., and Blumberg, M. S. (2020). Self-generated whisker movements drive state-dependent sensory input to developing barrel cortex. *Curr. Biol.* 30:2404–2410.e4. doi: 10.1016/J.CUB.2020.04.045

Driver, J., and Noesselt, T. (2008). Multisensory interplay reveals crossmodal influences on "sensory-specific" brain regions, neural responses, and judgments. *Neuron* 57, 11–23. doi: 10.1016/J.NEURON.2007.12.013

Duan, Z. R. S., Che, A., Chu, P., Modol, L., Bollmann, Y., Babij, R., et al. (2020). GABAergic restriction of network dynamics regulates interneuron survival in the developing cortex. *Neuron* 105:75–92.e5. doi: 10.1016/J.NEURON.2019.10.008

Dupont, E., Hanganu, I. L., Kilb, W., Hirsch, S., and Luhmann, H. J. (2006). Rapid developmental switch in the mechanisms driving early cortical columnar networks. *Nature* 439, 79–83. doi: 10.1038/NATURE04264

Erzurumlu, R. S., and Gaspar, P. (2012). Development and critical period plasticity of the barrel cortex. *Eur. J. Neurosci.* 35, 1540–1553. doi: 10.1111/J.1460-9568.2012.08075.X

Faust, T. E., Gunner, G., and Schafer, D. P. (2021). Mechanisms governing activity-dependent synaptic pruning in the mammalian CNS. *Nat. Rev. Neurosci.* 22:657. doi: 10.1038/S41583-021-00507-Y

Felitti, V. J., Anda, R. F., Nordenberg, D., Williamson, D. F., Spitz, A. M., Edwards, V., et al. (1998). Relationship of childhood abuse and household dysfunction to many of the leading causes of death in adults: The adverse childhood experiences (ACE) study. *Am. J. Prev. Med.* 14, 245–258. doi: 10.1016/S0749-3797(98)00017-8

Finnerty, G. T., Roberts, L. S. E., and Connors, B. W. (1999). Sensory experience modifies the short-term dynamics of neocortical synapses. *Nature* 400, 367–371. doi: 10.1038/22553

Fox, K. (1992). A critical period for experience-dependent synaptic plasticity in rat barrel cortex. *J. Neurosci.* 12:1826. doi: 10.1523/JNEUROSCI.12-05-01826.1992

Fox, S. E., Levitt, P., and Nelson, C. A. (2010). How the timing and quality of early experiences influence the development of brain architecture. *Child Dev.* 81, 28–40. doi: 10.1111/J.1467-8624.2009.01380.X

Gainey, M. A., Wolfe, R., Pourzia, O., and Feldman, D. E. (2016). Whisker deprivation drives two phases of inhibitory synapse weakening in layer 4 of rat somatosensory cortex. *PLoS One* 11:e0148227. doi: 10.1371/JOURNAL.PONE.0148227

Gesuita, L., Cavaccini, A., Argunsah, A. Ö, Favuzzi, E., Ibrahim, L. A., Stachniak, T. J., et al. (2022). Microglia contribute to the postnatal development of cortical somatostatin-positive inhibitory cells and to whisker-evoked cortical activity. *Cell Rep.* 40:209. doi: 10.1016/J.CELREP.2022.111209

Golshani, P., Gonçalves, J. T., Khoshkhoo, S., Mostany, R., Smirnakis, S., and Portera-Cailliau, C. (2009). Internally mediated developmental desynchronization of neocortical network activity. *J. Neurosci.* 29:10890. doi: 10.1523/JNEUROSCI.2012-09.2009

Granato, A., Palmer, L. M., Giorgio, A., de, Tavian, D., and Larkum, M. E. (2012). Early exposure to alcohol leads to permanent impairment of dendritic excitability in neocortical pyramidal neurons. *J. Neurosci.* 32, 1377–1382. doi: 10.1523/JNEUROSCI.5520-11.2012

Grecco, G. G., Huang, J. Y., Muñoz, B., Doud, E. H., Hines, C. D., Gao, Y., et al. (2022). Sex-dependent synaptic remodeling of the somatosensory cortex in mice with prenatal methadone exposure. *Adv. Drug Alcohol Res.* 2:10400. doi: 10.3389/ADAR.2022.10400

Hanganu, I. L., and Luhmann, H. J. (2004). Functional nicotinic acetylcholine receptors on subplate neurons in neonatal rat somatosensory cortex. *J. Neurophysiol.* 92, 189–198. doi: 10.1152/JN.00010.2004

Hensch, T. K. (2004). CRITICAL PERIOD REGULATION. *Annu. Rev. Neurosci.* 27, 549–579. doi: 10.1146/annurev.neuro.27.070203.144327

Henschke, J. U., Oelschlegel, A. M., Angenstein, F., Ohl, F. W., Goldschmidt, J., Kanold, P. O., et al. (2018). Early sensory experience influences the development of multisensory thalamocortical and intracortical connections of primary sensory cortices. *Brain Struct. Funct.* 223:1165. doi: 10.1007/S00429-017-1549-1

Higashi, S., Crair, M. C., Kurotani, T., Inokawa, H., and Toyama, K. (1999). Altered spatial patterns of functional thalamocortical connections in the barrel cortex after neonatal infraorbital nerve cut revealed by optical recording. *Neuroscience* 91, 439–452. doi: 10.1016/S0306-4522(98)00666-6

Hughes, K., Bellis, M. A., Hardcastle, K. A., Sethi, D., Butchart, A., Mikton, C., et al. (2017). The effect of multiple adverse childhood experiences on health: A systematic review and meta-analysis. *Lancet Public Health* 2, e356–e366. doi: 10.1016/S2468-2667(17)30118-4

Inan, M., Lu, H. C., Albright, M. J., She, W. C., and Crair, M. C. (2006). Barrel map development relies on protein kinase A regulatory subunit IIβ-mediated cAMP signaling. *J. Neurosci.* 26, 4338–4349. doi: 10.1523/JNEUROSCI.3745-05.2006

Itami, C., Huang, J. Y., Yamasaki, M., Watanabe, M., Lu, H. C., and Kimura, F. (2016). Developmental switch in spike timing-dependent plasticity and cannabinoid-dependent reorganization of the thalamocortical projection in the barrel cortex. *J. Neurosci.* 36, 7039–7054. doi: 10.1523/JNEUROSCI.4280-15.2016

Iwasato, T., Datwani, A., Wolf, A. M., Nishiyama, H., Taguchi, Y., Tonegawa, S., et al. (2000). Cortex-restricted disruption of NMDAR1 impairs neuronal patterns in the barrel cortex. *Nature* 406, 726–731. doi: 10.1038/35021059

Jeanmonod, D., Rice, F. L., Loos, H. V., and der. (1981). Mouse somatosensory cortex: Alterations in the barrelfield following receptor injury at different early postnatal ages. *Neuroscience* 6, 1503–1535. doi: 10.1016/0306-4522(81)90222-0

Jensen, K. F., and Killackey, H. P. (1987). Terminal arbors of axons projecting to the somatosensory cortex of the adult rat. I. The normal morphology of specific thalamocortical afferents. *J. Neurosci.* 7, 3529–3543. doi: 10.1523/JNEUROSCI.07-11-03529.1987

Jones, C. E., Opel, R. A., Kaiser, M. E., Chau, A. Q., Quintana, J. R., Nipper, M. A., et al. (2019). Early-life sleep disruption increases parvalbumin in primary somatosensory cortex and impairs social bonding in prairie voles. *Sci. Adv.* 5:5188. doi: 10.1126/SCIADV.AAV5188

Jouvet-Mounier, D., Astic, L., and Lacote, D. (1969). Ontogenesis of the states of sleep in rat, cat, and guinea pig during the first postnatal month. *Dev. Psychobiol.* 2, 216–239. doi: 10.1002/DEV.420020407

Kalambogias, J., Chen, C. C., Khan, S., Son, T., Wercberger, R., Headlam, C., et al. (2020). Development and sensory experience dependent regulation of microglia in barrel cortex. *J. Comp. Neurol.* 528, 559–573. doi: 10.1002/CNE.24771

Kastli, R., Vighagen, R., van der Bourg, A., Argunsah, A., Iqbal, A., Voigt, F. F., et al. (2020). Developmental divergence of sensory stimulus representation in cortical interneurons. *Nat. Commun.* 11:5729. doi: 10.1038/S41467-020-19427-Z

Khazipov, R., Sirota, A., Leinekugel, X., Holmes, G. L., Ben-Ari, Y., and Buzsáki, G. (2004). Early motor activity drives spindle bursts in the developing somatosensory cortex. *Nature* 432, 758–761. doi: 10.1038/NATURE03132

Killackey, H. P., and Belford, G. R. (1979). The formation of afferent patterns in the somatosensory cortex of the neonatal rat. *J. Comp. Neurol.* 183, 285–303. doi: 10.1002/CNE.901830206

Lebedeva, J., Zakharov, A., Ogievetsky, E., Minlebaeva, A., Kurbanov, R., Gerasimova, E., et al. (2017). Inhibition of cortical activity and apoptosis caused by ethanol in neonatal rats in vivo. *Cereb. Cortex* 27, 1068–1082. doi: 10.1093/CERCOR/BHV293

Lee, L. J., Chen, W. J., Chuang, Y. W., and Wang, Y. C. (2009). Neonatal whisker trimming causes long-lasting changes in structure and function of the somatosensory system. *Exp. Neurol.* 219, 524–532. doi: 10.1016/J.EXPNEUROL.2009.07.012

Lee, S. H., Land, P. W., and Simons, D. J. (2007). Layer- and cell-type-specific effects of neonatal whisker-trimming in adult rat barrel cortex. *J. Neurophysiol.* 97, 4380–4385. doi: 10.1152/JN.01217.2006

Leighton, A. H., and Lohmann, C. (2016). The wiring of developing sensory circuits–From patterned spontaneous activity to synaptic plasticity mechanisms. *Front. Neural Circuits* 10:214646. doi: 10.3389/FNCIR.2016.00071

Lendvai, B., Stern, E. A., Chen, B., and Svoboda, K. (2000). Experience-dependent plasticity of dendritic spines in the developing rat barrel cortex in vivo. *Nature* 404, 876–881. doi: 10.1038/35009107

Li, H., Fertuzinhos, S., Mohns, E., Hnasko, T. S., Verhage, M., Edwards, R., et al. (2013). Laminar and columnar development of barrel cortex relies on thalamocortical neurotransmission. *Neuron* 79, 970–986. doi: 10.1016/J.NEURON.2013.06.043

Li, W., Ma, L., Yang, G., and Gan, W. B. (2017). REM sleep selectively prunes and maintains new synapses in development and learning. *Nat. Neurosci.* 20, 427–437. doi: 10.1038/nn.4479

Liston, C., and Gan, W. B. (2011). Glucocorticoids are critical regulators of dendritic spine development and plasticity in vivo. *Proc. Natl. Acad. Sci. U.S.A.* 108, 16074–16079.

Lokhandwala, S., and Spencer, R. M. C. (2022). Relations between sleep patterns early in life and brain development: A review. *Dev. Cogn. Neurosci.* 56:101130. doi: 10.1016/J.DCN.2022.101130

Maitre, N. L., Key, A. P., Chorna, O. D., Slaughter, J. C., Matusz, P. J., Wallace, M. T., et al. (2017). The dual nature of early-life experience on somatosensory processing in the human infant brain. *Curr. Biol.* 27, 1048–1054. doi: 10.1016/J.CUB.2017.02.036

Makarov, R., Sintsov, M., Valeeva, G., Starikov, P., Negrov, D., and Khazipov, R. (2021). Bone conducted responses in the neonatal rat auditory cortex. *Sci. Rep.* 11, 1–16. doi: 10.1038/s41598-021-96188-9

Margret, C. P., Li, C. X., Chappell, T. D., Elberger, A. J., Matta, S. G., and Waters, R. S. (2006). Prenatal alcohol exposure delays the development of the cortical barrel field in neonatal rats. *Exp. Brain Res.* 172, 1–13. doi: 10.1007/s00221-005-0319-0

Margret, C. P., Li, C. X., Elberger, A. J., Matta, S. G., Chappell, T. D., and Waters, R. S. (2005). Prenatal alcohol exposure alters the size, but not the pattern, of the whisker representation in neonatal rat barrel cortex. *Exp. Brain Res.* 165, 167–178.

Marques-Smith, A., Lyngholm, D., Kaufmann, A. K., Stacey, J. A., Hoerder-Suabedissen, A., Becker, E. B. E., et al. (2016). A transient translaminar gabaergic interneuron circuit connects thalamocortical recipient layers in neonatal somatosensory cortex. *Neuron* 89, 536–549. doi: 10.1016/J.NEURON.2016.01.015

Martinez-Gallego, I., Perez-Rodriguez, M., Coatl-Cuaya, H., Flores, G., and Rodriguez-Moreno, A. (2022). Adenosine and astrocytes determine the developmental dynamics of spike timing-dependent plasticity in the somatosensory cortex. *J. Neurosci.* 42:6038. doi: 10.1523/JNEUROSCI.0115-22.2022

Matsui, A., Tran, M., Yoshida, A. C., Kikuchi, S. S., Mami, U., Ogawa, M., et al. (2013). BTBD3 controls dendrite orientation toward active axons in mammalian neocortex. *Science* 342, 1114–1118.

Mccormick, C. M., Kehoe, P., and Kovacs, S. (1998). Corticosterone release in response to repeated, short episodes of neonatal isolation: Evidence of sensitization. *Int. J. Dev. Neurosci.* 16, 175–185. doi: 10.1016/S0736-5748(98)00026-4

Micheva, K. D., and Beaulieu, C. (1995a). Neonatal sensory deprivation induces selective changes in the quantitative distribution of GABA-immunoreactive neurons in the rat barrel field cortex. *J. Comp. Neurol.* 361, 574–584. doi: 10.1002/cne.903610403

Micheva, K. D., and Beaulieu, C. (1995b). Postnatal development of GABA neurons in the rat somatosensory barrel cortex: A quantitative study. *Eur. J. Neurosci.* 7, 419–430. doi: 10.1111/J.1460-9568.1995.TB00338.X

Micheva, K. D., and Beaulieu, C. (1997). Development and plasticity of the inhibitory neocortical circuitry with an emphasis on the rodent barrel field cortex: a review. *Can. J. Physiol. Pharmacol.* 75, 380.

Miller, M. W., and Potempa, G. (1990). Numbers of neurons and glia in mature rat somatosensory cortex: Effects of prenatal exposure to ethanol. *J. Comp. Neurol.* 293, 92–102. doi: 10.1002/CNE.902930108

Minlebaev, M., Ben-Ari, Y., and Khazipov, R. (2007). Network mechanisms of spindle-burst oscillations in the neonatal rat barrel cortex in vivo. *J. Neurophysiol.* 97, 692–700. doi: 10.1152/JN.00759.2006

Miyazaki, T., Kunii, M., Jitsuki, S., Sano, A., Kuroiwa, Y., and Takahashi, T. (2013). Social isolation perturbs experience-driven synaptic glutamate receptor subunit 4 delivery in the developing rat barrel cortex. *Eur. J. Neurosci.* 37, 1602–1609. doi: 10.1111/EJN.12188

Miyazaki, T., Kunii, M., Tada, H., Sano, A., Kuroiwa, Y., Goto, T., et al. (2012). Developmental AMPA receptor subunit specificity during experience-driven synaptic plasticity in the rat barrel cortex. *Brain Res.* 1435, 1–7. doi: 10.1016/J.BRAINRES.2011.11.033

Mizuno, H., Ikezoe, K., Nakazawa, S., Sato, T., Kitamura, K., and Iwasato, T. (2018). Patchwork-type spontaneous activity in neonatal barrel cortex layer 4 transmitted via thalamocortical projections. *Cell Rep.* 22, 123–135. doi: 10.1016/J.CELREP.2017.12.012

Modol, L., Bollmann, Y., Tressard, T., Baude, A., Che, A., Duan, Z. R. S., et al. (2020). Assemblies of Perisomatic GABAergic neurons in the developing barrel cortex. *Neuron* 105:93–105.e4. doi: 10.1016/J.NEURON.2019.10.007

Moreno-Juan, V., Filipchuk, A., Antón-Bolaños, N., Mezzera, C., Gezelius, H., Andrés, B., et al. (2017). Prenatal thalamic waves regulate cortical area size prior to sensory processing. *Nat. Commun.* 8, 1–14. doi: 10.1038/ncomms14172

Moriceau, S., Shionoya, K., Jakubs, K., and Sullivan, R. M. (2009). Early-life stress disrupts attachment learning: The role of amygdala corticosterone, locus ceruleus corticotropin releasing hormone, and olfactory bulb norepinephrine. *J. Neurosci.* 29, 15745–15755. doi: 10.1523/JNEUROSCI.4106-09.2009

Nakazawa, S., Mizuno, H., and Iwasato, T. (2018). Differential dynamics of cortical neuron dendritic trees revealed by long-term in vivo imaging in neonates. *Nat. Commun.* 9:3106. doi: 10.1038/S41467-018-05563-0

Nakazawa, S., Yoshimura, Y., Takagi, M., Mizuno, H., and Iwasato, T. (2020). Developmental phase transitions in spatial organization of spontaneous activity in postnatal barrel cortex layer 4. *J. Neurosci.* 40, 7637–7650. doi: 10.1523/JNEUROSCI.1116-20.2020

Narboux-Nême, N., Evrard, A., Ferezou, I., Erzurumlu, R. S., Kaeser, P. S., Lainé, J., et al. (2012). Neurotransmitter release at the thalamocortical synapse instructs barrel formation but not axon patterning in the somatosensory cortex. *J. Neurosci.* 32:6183. doi: 10.1523/JNEUROSCI.0343-12.2012

Papaioannou, S., Brigham, L., and Krieger, P. (2013). Sensory deprivation during early development causes an increased exploratory behavior in a whisker-dependent decision task. *Brain Behav.* 3, 24–34. doi: 10.1002/BRB3.102

Petersen, C. C. H. (2007). The functional organization of the barrel cortex. *Neuron* 56, 339–355. doi: 10.1016/J.NEURON.2007.09.017

Popova, S., Charness, M. E., Burd, L., Crawford, A., Hoyme, H. E., Mukherjee, R. A. S., et al. (2023). Fetal alcohol spectrum disorders. *Nat. Rev. Dis. Prim.* 9:11. doi: 10.1038/S41572-023-00420-X

Pouchelon, G., Dwivedi, D., Bollmann, Y., Agba, C. K., Xu, Q., Mirow, A. M. C., et al. (2021). The organization and development of cortical interneuron presynaptic circuits are area specific. *Cell Rep.* 37:993. doi: 10.1016/J.CELREP.2021.109993

Pouchelon, G., Gambino, F., Bellone, C., Telley, L., Vitali, I., Lüscher, C., et al. (2014). Modality-specific thalamocortical inputs instruct the identity of postsynaptic L4 neurons. *Nature* 511, 471–474. doi: 10.1038/nature13390

Powrozek, T. A., and Zhou, F. C. (2005). Effects of prenatal alcohol exposure on the development of the vibrissal somatosensory cortical barrel network. *Brain Res. Dev. Brain Res.* 155, 135–146. doi: 10.1016/J.DEVBRAINRES.2005.01.003

Rio-Bermudez, C. D., Kim, J., Sokoloff, G., and Blumberg, M. S. (2020). Active sleep promotes coherent oscillatory activity in the Cortico-hippocampal system of infant rats. *Cereb. Cortex* 30, 2070–2082. doi: 10.1093/cercor/bhz223

Sadaka, Y., Weinfeld, E., Lev, D. L., and White, E. L. (2003). Changes in mouse barrel synapses consequent to sensory deprivation from birth. *J. Comp. Neurol.* 457, 75–86. doi: 10.1002/CNE.10518

Saito, M., Smiley, J. F., Hui, M., Masiello, K., and Betz, J., (2019). Neonatal ethanol disturbs the normal maturation of parvalbumin interneurons surrounded by subsets of perineuronal nets in the cerebral cortex: Partial reversal by lithium. *Cereb. Cortex* 29, 1383–1397. doi: 10.1093/CERCOR/BHY034

Schierloh, A., Eder, M., Zieglgänsberger, W., and Dodt, H. U. (2004). Effects of sensory deprivation on columnar organization of neuronal circuits in the rat barrel cortex. *Eur. J. Neurosci.* 20, 1118–1124. doi: 10.1111/J.1460-9568.2004.03557.X

Shepherd, G. M. G., Pologruto, T. A., and Svoboda, K. (2003). Circuit analysis of experience-dependent plasticity in the developing rat barrel cortex. *Neuron* 38, 277–289. doi: 10.1016/S0896-6273(03)00152-1

Shishelova, A. Y. (2006). Effect of whisker removal on defensive behavior in rats during early ontogenesis. *Neurosci. Behav. Physiol.* 36, 883–888. doi: 10.1007/S11055-006-0102-0

Shoykhet, M., Land, P. W., and Simons, D. J. (2005). Whisker trimming begun at birth or on postnatal day 12 affects excitatory and inhibitory receptive fields of layer IV barrel neurons. *J. Neurophysiol.* 94, 3987–3995.

Simons, D. J., Carvell, G. E., and Kyriazi, H. T. (2015). Alterations in functional thalamocortical connectivity following neonatal whisker trimming with adult regrowth. *J. Neurophysiol.* 114, 1912–1922. doi: 10.1152/jn.00488.2015

Simons, D. J., and Land, P. W. (1987). Early experience of tactile stimulation influences organization of somatic sensory cortex. *Nature* 326, 694–697. doi: 10.1038/326694a0

Smiley, J. F., Bleiwas, C., Masiello, K., Petkova, E., Betz, J., Hui, M., et al. (2019). Effects of neonatal ethanol on cerebral cortex development through adolescence. *Brain Struct. Funct.* 224, 1871–1884.

Smirnov, K., and Sitnikova, E. (2019). Developmental milestones and behavior of infant rats: The role of sensory input from whiskers. *Behav. Brain Res.* 374:112143. doi: 10.1016/J.BBR.2019.112143

Soumiya, H., Godai, A., Araiso, H., Mori, S., Furukawa, S., and Fukumitsu, H. (2016). Neonatal whisker trimming impairs fear/anxiety-related emotional systems of the amygdala and social behaviors in adult mice. *PLoS One* 11:e0158583. doi: 10.1371/JOURNAL.PONE.0158583

Stern, E. A., Maravall, M., and Svoboda, K. (2001). Rapid development and plasticity of layer 2/3 maps in rat barrel cortex in vivo. *Neuron* 31, 305–315. doi: 10.1016/S0896-6273(01)00360-9

Sullivan, R. M., and Holman, P. J. (2010). Transitions in sensitive period attachment learning in infancy: The role of corticosterone. *Neurosci. Biobehav. Rev.* 34, 835–844. doi: 10.1016/J.NEUBIOREV.2009.11.010

Sun, L., Zhou, H., Cichon, J., and Yang, G. (2020). Experience and sleep-dependent synaptic plasticity: From structure to activity. *Philos. Trans. R. Soc. B Biol. Sci.* 375:234. doi: 10.1098/RSTB.2019.0234

Suzuki, A., Lee, L. J., Hayashi, Y., Muglia, L., Itohara, S., Erzurumlu, R. S., et al. (2015). THALAMIC ADENYLYL CYCLASE 1 IS REQUIRED FOR BARREL FORMATION IN THE SOMATOSENSORY CORTEX. *Neuroscience* 290:518. doi: 10.1016/J.NEUROSCIENCE.2015.01.043

Takatsuru, Y., Nabekura, J., Ishikawa, T., Kohsaka, S., and Koibuchi, N. (2015). Early-life stress increases the motility of microglia in adulthood. *J. Physiol. Sci.* 65, 187–194. doi: 10.1007/s12576-015-0361-z

Takatsuru, Y., Yoshitomo, M., Nemoto, T., Eto, K., and Nabekura, J. (2009). Maternal separation decreases the stability of mushroom spines in adult mice somatosensory cortex. *Brain Res.* 1294, 45–51. doi: 10.1016/J.BRAINRES.2009.07.092

Tiriac, A., Rio-Bermudez, C. D., and Blumberg, M. S. (2014). Self-generated movements with "unexpected" sensory consequences. *Curr. Biol.* 24, 2136–2141. doi: 10.1016/J.CUB.2014.07.053

Tolner, E. A., Sheikh, A., Yukin, A. Y., Kaila, K., and Kanold, P. O. (2012). Subplate neurons promote spindle bursts and thalamocortical patterning in the neonatal rat somatosensory cortex. *J. Neurosci.* 32, 692–702. doi: 10.1523/JNEUROSCI.1538-11.2012

Toya, S., Takatsuru, Y., Kokubo, M., Amano, I., Shimokawa, N., and Koibuchi, N. (2014). Early-life-stress affects the homeostasis of glutamatergic synapses. *Eur. J. Neurosci.* 40, 3627–3634. doi: 10.1111/EJN.12728

Treccani, G., Musazzi, L., Perego, C., Milanese, M., Nava, N., Bonifacino, T., et al. (2014). Stress and corticosterone increase the readily releasable pool of glutamate vesicles in synaptic terminals of prefrontal and frontal cortex. *Mol. Psychiatry* 19, 433–443. doi: 10.1038/MP.2014.5

Tuncdemir, S. N., Wamsley, B., Stam, F. J., Osakada, F., Goulding, M., Callaway, E. M., et al. (2016). Early somatostatin interneuron connectivity mediates the maturation of deep layer cortical circuits. *Neuron* 89, 521–535. doi: 10.1016/J.NEURON.2015.11.020

Van der Loos, H., and Woolsey, T. A. (1973). Somatosensory cortex: Structural alterations following early injury to sense organs. *Science* 179, 395–398. doi: 10.1126/SCIENCE.179.4071.395

Wang, D. C., Santos-Valencia, F., Song, J. H., Franks, K. M., and Luo, L. (2024). Embryonically active piriform cortex neurons promote intracortical recurrent connectivity during development. *bioRxiv* [Preprint]. doi: 10.1101/2024.05.08.593265

Wang, J., Shan, W., Chen, X., and Zuo, Z. (2022). Whisker trimming induces anti-anxiety like status via activation of dorsomedial hypothalamus nucleus in mice. *Brain Res.* 1789:147946. doi: 10.1016/J.BRAINRES.2022.147946

Winnubst, J., Cheyne, J. E., Niculescu, D., and Lohmann, C. (2015). Spontaneous activity drives local synaptic plasticity in vivo. *Neuron* 87, 399–410. doi: 10.1016/J.NEURON.2015.06.029

Wong, F. K., Bercsenyi, K., Sreenivasan, V., Portalés, A., Fernández-Otero, M., and Marín, O. (2018). Pyramidal cell regulation of interneuron survival sculpts cortical networks. *Nature* 557, 668–673. doi: 10.1038/S41586-018-0139-6

Wong-Riley, M. T. T., and Welt, C. (1980). Histochemical changes in cytochrome oxidase of cortical barrels after vibrissal removal in neonatal and adult mice. *Proc. Natl. Acad. Sci. U.S.A.* 77, 2333–2337. doi: 10.1073/PNAS.77.4.2333

Woolsey, T. A., and van der Loos, H. (1970). The structural organization of layer IV in the somatosensory region (S I) of mouse cerebral cortex: The description of a cortical field composed of discrete cytoarchitectonic units. *Brain Res.* 17, 205–242. doi: 10.1016/0006-8993(70)90079-X

Woolsey, T. A., and Wann, J. R. (1976). Areal changes in mouse cortical barrels following vibrissal damage at different postnatal ages. *J. Comp. Neurol.* 170, 53–66. doi: 10.1002/CNE.901700105

Yang, G., and Gan, W. B. (2012). Sleep contributes to dendritic spine formation and elimination in the developing mouse somatosensory cortex. *Dev. Neurobiol.* 72, 1391–1398. doi: 10.1002/DNEU.20996

Yang, J. W., An, S., Sun, J. J., Reyes-Puerta, V., Kindler, J., Berger, T., et al. (2013). Thalamic network oscillations synchronize ontogenetic columns in the newborn rat barrel cortex. *Cereb. Cortex* 23, 1299–1316. doi: 10.1093/CERCOR/BHS103

Yang, J. W., Hanganu-Opatz, I. L., Sun, J. J., and Luhmann, H. J. (2009). Three patterns of oscillatory activity differentially synchronize developing neocortical networks in vivo. *J. Neurosci.* 29:9011. doi: 10.1523/JNEUROSCI.5646-08.2009

Young, T. R., Yamamoto, M., Kikuchi, S. S., Yoshida, A. C., Abe, T., Inoue, K., et al. (2023). Thalamocortical control of cell-type specificity drives circuits for processing whisker-related information in mouse barrel cortex. *Nat. Commun.* 14, 1–20. doi: 10.1038/s41467-023-41749-x

Zheng, J. J., Li, S. J., Zhang, X. D., Miao, W. Y., Zhang, D., Yao, H., et al. (2014). Oxytocin mediates early experience-dependent cross-modal plasticity in the sensory cortices. *Nat. Neurosci.* 17, 391–399. doi: 10.1038/NN.3634

Zhou, Y., Lai, C. S. W., Bai, Y., Li, W., Zhao, R., Yang, G., et al. (2020). REM sleep promotes experience-dependent dendritic spine elimination in the mouse cortex. *Nat. Commun.* 11, 1–12. doi: 10.1038/s41467-020-18592-5

frontiers | Frontiers in Neural Circuits

TYPE Mini Review
PUBLISHED 08 August 2024
DOI 10.3389/fncir.2024.1467203

OPEN ACCESS

EDITED BY
Hitoshi Sakano,
University of Fukui, Japan

REVIEWED BY
Charles A. Greer,
Yale University, United States

*CORRESPONDENCE
Anne Didier
anne.didier@univ-lyon1.fr

†These authors share senior authorship

RECEIVED 19 July 2024
ACCEPTED 31 July 2024
PUBLISHED 08 August 2024

CITATION
Dejou J, Mandairon N and Didier A (2024) Olfactory neurogenesis plays different parts at successive stages of life, implications for mental health.
Front. Neural Circuits 18:1467203.
doi: 10.3389/fncir.2024.1467203

Olfactory neurogenesis plays different parts at successive stages of life, implications for mental health

Jules Dejou[1], Nathalie Mandairon[1†] and Anne Didier[1,2*†]

[1]INSERM, U1028; CNRS, UMR5292; Lyon Neuroscience Research Center, Neuroplasticity and Neuropathology of Olfactory Perception Team, Lyon, France, [2]Institut Universitaire de France, Paris, France

The olfactory bulb is a unique site of continuous neurogenesis, primarily generating inhibitory interneurons, a process that begins at birth and extends through infancy and adulthood. This review examines the characteristics of olfactory bulb neurogenesis, focusing on granule cells, the most numerous interneurons, and how their age and maturation affect their function. Adult-born granule cells, while immature, contribute to the experience-dependent plasticity of the olfactory circuit by enabling structural and functional synaptic changes. In contrast, granule cells born early in life form the foundational elements of the olfactory bulb circuit, potentially facilitating innate olfactory information processing. The implications of these neonatal cells on early life olfactory memory and their impact on adult perception, particularly in response to aversive events and susceptibility to emotional disorders, warrant further investigation.

KEYWORDS

neurogenesis, olfactory bulb, mouse, development, learning, memory, mental disorders

Introduction

Inhibitory neurons of the olfactory bulb (OB), periglomerular cells and granule cells (GCs), which shape the output message of the OB (Nagayama et al., 2014), are formed throughout life, from pre-and neonatal periods, to adulthood and senescence. Although forming a continuum across life, bulbar neurogenesis characteristics evolve with aging. Bulbar neurogenesis relies on stem cells and amplifying progenitors sitting in the proliferative subventricular zone (SVZ). They give birth to neuroblasts, proceeding along the rostral migratory stream to the core of the OB before differentiating and integrating the granule (GCL) and periglomerular cell layers of the OB (Luskin, 1993; Alvarez-Buylla and García-Verdugo, 2002; Winner et al., 2002). In the early postnatal period, an additional neurogenic zone in the OB core produces over 50% of new interneurons, before this zone gradually ceases to be a proliferative niche (Lemasson et al., 2005). Distinctive features of adult-born versus neonatal neurons include their rate of production, pattern of integration and final location in the OB as well as sensitivity to environment. In this review we emphasize recent advances that established the role of adult neurogenesis in experience-dependent plasticity of the OB circuits and enabled distinguishing bulbar interneurons born at different stages of life. These advances emerged mostly from rodent studies and focused on the GCs, the most abundant

neuronal population targeted by neurogenesis. We also briefly examine the role of early neurogenesis in vulnerability to mental disorders.

Descriptive features of olfactory neurogenesis across the life span

The rate of neurogenesis

The rate of neurogenesis in the OB, i.e., of new neurons formed, is the highest between P0 until P14, corresponding to the ontogeny of approximatively 75% of GCs and relies on high proliferation and virtually no cell death (Lemasson et al., 2005; Sakamoto et al., 2014). As the animal reaches sexual maturity (2-month-old), GCs are more prone to death (Lemasson et al., 2005; Sakamoto et al., 2014) and by 10 months, proliferation is decreased by 50 to 75% in the SVZ (Rey et al., 2012; Shook et al., 2012) accounting for the reduction in the number of new GCs formed in the OB. In the last part of life (18-month-old), proliferation in the SVZ is not further reduced but survival of the newly formed GCs decreases, leading to the lowest rate of neurogenesis in life (senescent rate) (Rey et al., 2012). Thus, the rate of neurogenesis in the mouse OB distinguishes between neonatal, juvenile, adult and senescent stages with transitions whose gradual or abrupt nature is not clearly documented.

Neuronal addition versus replacement

There is a consensus that neonatal neurogenesis follows an addition mode: the newborn GCs integrate the developing OB, enabling its growth. This is supported by the lack of cell death reported for these neonatal neurons (Lemasson et al., 2005; Platel et al., 2019). In the adult stage, the data are more contradictory. Several studies labeled dividing cells by thymidine analogs (such as 5-Bromo-2′-deoxyuridine, BrdU) and reported a loss of up to 50% of adult-born neurons within 4 to 6 weeks after their birth (Lemasson et al., 2005; Mandairon et al., 2006b). This suggests that new GCs compete for survival within the OB network but that not all of them succeed. In line with this, genetic tagging allowing continuous follow-up of newly formed GCs revealed that adult-born neurons end up forming at least 60% of the GCs in 18-month-old mice, without increasing neuronal density (Imayoshi et al., 2008). This supports the conclusion that in adults, neurogenesis follows a replacement mode where newborn neurons replace dying ones. However, Platel et al. (2019), using bi-photon time-lapse observations, reported a lack of adult-born GCs death supporting an addition mode in adult as in the developing OB. BrdU toxicity was brought forward to explain previous reports of cell death affecting adult-born GCs. Noteworthy, studies using viral vectors or non-toxic doses of BrdU did detect differences in survival between neonatal and adult-born neurons (Lemasson et al., 2005; Sakamoto et al., 2014). Interestingly, due to technical constraints (i.e., 600 µm depth limitation, labeling of dorsal SVZ neuroblasts, targeting the superficial GCL (De Chevigny et al., 2012)), bi-photon analysis captures GCs in the superficial GCL which is preferentially populated by neonatal GCs that do not show cell death in BrdU studies (Lemasson et al., 2005). This suggests that superficial GCs may have different survival properties compared to those targeting the deeper GCL. Thus, the survival rate of adult-born neurons may depend both on the age of the animals and the depth of the GCs in the GCL.

In the neuron's replacement framework, many questions remain such as which GCs are selected to be renewed and what specific parts they play versus the non-renewed ones.

Synaptic maturation patterns

The dynamic integration of newborn GCs shows remarkable differences depending on when they were born. Neonatal GCs need more time to migrate from the SVZ to the OB than their adult counterparts (Lemasson et al., 2005). Then, in the adult brain, it takes about a month for a neuroblast arriving in the OB to acquire the anatomy and connectivity of a fully mature GC (Carleton et al., 2003; Kelsch et al., 2008; Tufo et al., 2022) according to a "listen then act" mode where synaptic inputs develop before outputs. More specifically, inputs originating mainly from centrifugal axons contact first basal dendrites of adult-born GCs while the later developing output is via dendrodendritic synapses in the external plexiform layer of the OB (Whitman and Greer, 2007). Regarding these dendrodendritic reciprocal synapses, it appears that the excitatory mitral-to-granule part forms before the inhibitory granule-to-mitral part (Hinds and Hinds, 1976). In contrast, synaptic inputs and outputs occur simultaneously in neonatal GCs, resulting in the ability of these neurons to emit action potentials shortly after their arrival in the OB (Kelsch et al., 2008; Breton-Provencher and Saghatelyan, 2012). Selective genetic alteration of $GABA_A$ receptors in migrating neuroblasts or immature GCs delays their synaptic integration and morphological maturation (Pallotto et al., 2012). This early sensitivity to GABA could explain how olfactory stimulation promotes the integration of very young (1–2 week-old) adult-born GCs (Mandairon et al., 2006a), since olfactory inputs would activate inhibitory GCs and thus increase GABA release. As they integrate in the bulbar circuits, newborn GCs become capable of responding to olfactory stimulation. The younger the neurons, the more excitable they are, and long-term potentiation is easier to induce in 2- to 3-week-old adult-born neurons than in older ones (Magavi, 2005; Gao and Strowbridge, 2009; Nissant et al., 2009). These peculiar features of maturing adult-born GCs suggest that they play selective parts in odor-induced circuit plasticity (Figure 1).

At mid-age (10-12-month-old), the number of adult-born GCs is reduced to about one third of that observed in 2-month-old animals but their dendritic and synaptic equipment is similar (Greco-Vuilloud et al., 2022) and little is known regarding integration patterns of GCs born in the aged brain (18-month-old).

Functional implications of bulbar neurogenesis

Adult OB neurogenesis contributes to olfactory learning in a task-specific manner

Olfactory perception and MCs responses to odorants evolve with experience and learning (Kay and Laurent, 1999; Doucette and Restrepo, 2008; Gschwend et al., 2015). The contribution of permanent neurogenesis to this plasticity has been addressed in adult mice, using

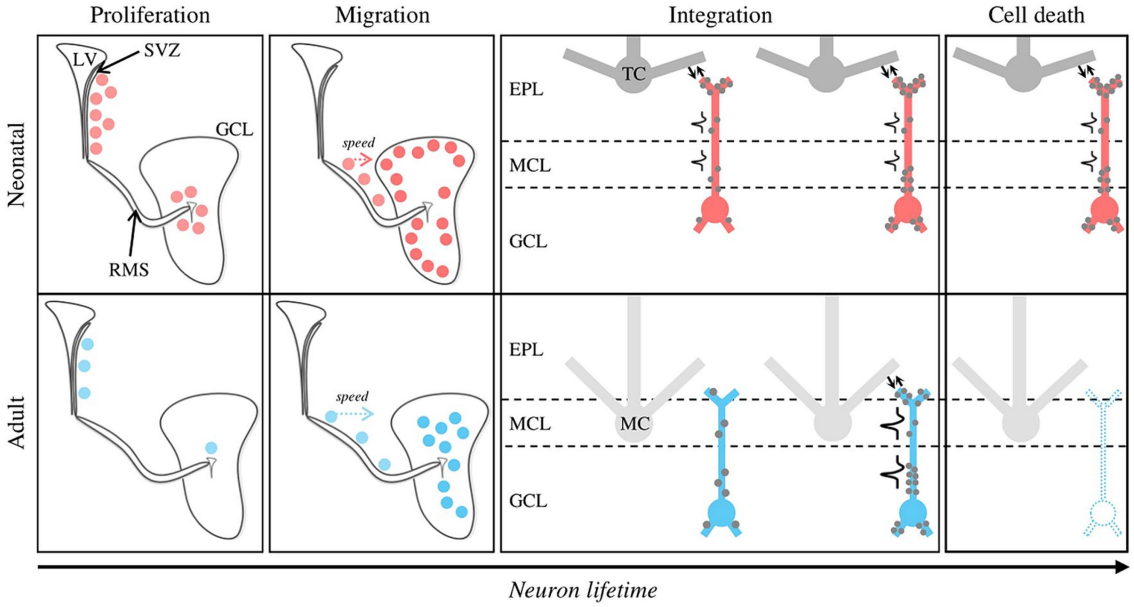

FIGURE 1
Distinctive features of neonatal versus adult postnatal neurogenesis. Newly formed GCs at neonatal and adult stages are represented by red and blue dots, respectively. *Proliferation mode*. Neonatal GCs originate from the SVZ and the OB core in the same proportion, whereas adult neurogenesis is almost exclusively dependent on the SVZ. The neurogenesis rate peaks at neonatal stage. *Migration*. Although the distance between the SVZ and the OB is greater at the adult stage, adult-born GCs migrate to the OB faster compared to their neonatal counterparts. Neonatal and adult-born GCs preferentially join the superficial and deep regions of the GCL, respectively. *Structural integration*. Due to their differential targeting inside the GCL, neonatal and adult-born GCs preferentially contact tufted and mitral cells, respectively. For neonatal GCs, inputs (gray dots) and outputs (reciprocal synapses, bidirectional arrows) are simultaneously established on the proximal and distal dendrites, then on the basal dendrites. Adult GCs follow a "first listen then act" mode: inputs are established on the proximal and basal dendrites, then form inputs-outputs through dendro-dendritic synapses. *Functional integration*. Neonatal GCs can emit action potentials shortly after the end of their migration, which is not the case for adult-born GCs. *Cell death*. Neonatal GCs have a much higher survival rate than adult-born GCs, which undergo massive turnover (~50%, dotted GC). EPL, External Plexiform Layer; GCL, Granule Cell Layer; LV, Lateral Ventricle; MCL, Mitral Cell Layer; RMS, Rostral Migratory Stream; SVZ, Subventricular Zone.

a variety of olfactory tasks, such as olfactory enrichment, associative or perceptual olfactory discrimination learning. All increase the number of adult-born GCs in the OB by improving their survival (Rochefort et al., 2002; Alonso et al., 2006; Mouret et al., 2008; Belnoue et al., 2011; Mandairon et al., 2011). Olfactory experience also increases the proportion of adult-born GCs responding to a learned odorant (Belnoue et al., 2011; Sultan et al., 2011; Moreno et al., 2012). On the contrary, ablation of neurogenesis by antimitotic drugs (Breton-Provencher et al., 2009; Moreno et al., 2009) or SVZ irradiation (Lazarini et al., 2009) prevents discrimination learning. Optogenetic inhibition (Forest et al., 2019a) or activation of adult-born GCs (Alonso et al., 2006; Grelat et al., 2018) respectively impairs or accelerates learning performances. This establishes a causal relationship between the adult-born GCs' activity and olfactory learning.

At the cellular level, olfactory learning or deprivation acts on adult-born GCs notably through structural plasticity. Indeed, both can lead to addition, elimination or relocation of dendritic spines at both long (hours-days) and short (minutes) timescales (Saghatelyan et al., 2005; Kelsch et al., 2008; Livneh and Mizrahi, 2011; Lepousez et al., 2014; Breton-Provencher et al., 2016; Sailor et al., 2016; Hardy and Saghatelyan, 2017; Mandairon et al., 2018; Forest et al., 2019a; Ferreira et al., 2024). Some molecular actors of adult-born GCs structural plasticity have been identified such as Npas4, an activity-dependent protein promoting pruning in response to sensory inputs (Belvindrah et al., 2011; Yoshihara et al., 2014) or FMRP, a regulator protein of local translation in dendrites (Daroles et al., 2016; Messaoudi et al., 2024).

The plasticity of adult-born neurons can be task-specific. In the context of olfactory perceptual learning in mice, in which two perceptually close odorants are learnt to be discriminated by passive exposure, spine density was increased on apical dendrites of adult-born GCs as was MCs inhibition, promoting discrimination through pattern separation. In contrast, when discrimination is acquired by olfactory associative learning in which the two perceptually close odorants are learnt to be discriminated by rewarding one odorant of the pair, spine density on adult-born neurons was reduced and activation of MCs increased, thereby strengthening of MCs' responses to the reinforced odorant to enable discrimination (Mandairon et al., 2018). As another example of the task-specificity of adult-born GCs involvement, a non-operant paradigm of olfactory associative conditioning showed no dependence on adult-born neurons (Imayoshi et al., 2008; Breton-Provencher et al., 2009) unlike operant conditioning (Lazarini et al., 2009; Mandairon et al., 2011; Sultan et al., 2011). Interestingly, odor fear conditioning, a non-operant learning associating an odorant to an electric shock, does require adult neurogenesis (Valley, 2009). Thus, task engagement, motivation and context are key factors in the contribution of new GCs to the plasticity of the bulbar network related to experience and learning, which remains difficult to disentangle.

Taken together, these data indicate that in young adult mice, different forms of olfactory experience non-specifically increase the

survival of adult-born GCs, while their synaptic integration pattern appears to be finely tuned to the task, allowing individuals to adapt to the needs of a changing olfactory environment.

Implication of newly formed neurons depending on their birthdate and maturation level

A question raised by permanent neurogenesis concerns the specificity of the role of newborn GCs according to the age of the brain in which they are born and their own level of maturation. This dual temporality makes this a complex question to address experimentally. Neonatal GCs increase their dendritic spine density until day 26 (Kelsch et al., 2008). During this period of maturation, they are prone to exhibit LTP (Gao and Strowbridge, 2009). But how immature neonatal GCs contribute to early-life olfactory perception and odor-guided behaviors is poorly understood. It has been suggested that they represent the building blocks of OB functions linked to vital, innate, enduring, and inflexible olfactory behaviors (Lemasson et al., 2005; Alonso et al., 2012; Muthusamy et al., 2017; Grelat et al., 2018). The evidence in support of this view is indirect, based in particular on the different local circuits mediated by the GCs located in the superficial GCL, which houses the majority of GCs born in the neonatal period, and the deeper GCs, the main target of adult-born neurons and neuronal renewal. Superficial GCs mainly come into contact with tufted cells (TCs), while deeper GCs are more in contact with MCs. TCs and MCs exhibit different olfactory response dynamics and cortical projections (Nagayama et al., 2010; Miyamichi et al., 2011; Fukunaga et al., 2012; Igarashi et al., 2012) leading to the hypothesis of the existence of two parallel circuits: neonatal GCs and TCs involved in odor detection and operational at the early stage of development and adult-born GCs and MCs, operating from the first weeks of life, handling more complex olfactory demands. However, this segregation may be too simplistic, as even if they have preferential targeting in the GCL, GCs may target deep or superficial parts regardless of their date of birth, and their location in the GCL does not completely condition their local connectivity (Yoshihara et al., 2012; Takahashi et al., 2018; Tsuboi, 2020).

The functional role of adult-born GCs may also depend on their level of maturation. They are better rescued from cell death by olfactory learning (Alonso et al., 2006; Mandairon et al., 2006a; Mouret et al., 2008; Belnoue et al., 2011) and activated by olfactory inputs in their immature state (14- to 28-day-old) (Magavi, 2005; Whitman and Greer, 2007; Nissant et al., 2009; Breton-Provencher and Saghatelyan, 2012). Immature adult-born GCs also exhibit learning-induced structural plasticity not shown by mature neonatal GCs (Breton-Provencher et al., 2016; Forest et al., 2019a). Their optogenetic inhibition impaired learned discrimination while the same photo-inhibition applied on mature neonatal GCs impaired only complex perceptual discrimination learning (Forest et al., 2019a). Interestingly, photo-activation of mature adult-born GCs (10- to 12-week-old) can accelerate associative olfactory learnings (Alonso et al., 2012; Grelat et al., 2018; Bragado Alonso et al., 2019).

From 10-month-old, olfactory enrichment no longer increases the survival of immature GCs (Rey et al., 2012). At the same time, they show impaired structural plasticity in response to olfactory learning and lower performances (Greco-Vuilloud et al., 2022). Such impairments of neurogenesis may, at least in part underlie olfactory cognitive decline, prompting exploration of ways to maintain a higher level of olfactory plasticity with age (Terrier et al., 2024). In the aged brain, new neurons become very rare, questioning their functional significance.

To conclude, GCs born in the adult brain play a decisive and specific role in experience-induced plasticity during their immature state. GCs born early after birth are essential for assuming innate olfactory behaviors, not least because they are the only ones present at birth. In addition, and given their high survival rate, it's tempting to speculate that they might retain a lifelong memory of early olfactory events that could escape the fading caused by neuronal turnover (Figure 2) (Frankland et al., 2013; Epp et al., 2016; Forest et al., 2019b). Finally, GCs differ not only based on their location in the GCL but also on their origin in the SVZ (Merkle et al., 2007, 2014), morphology, transcriptome (for recent studies see Takahashi et al., 2016, 2018; Malvaut et al., 2017; Hardy et al., 2018; Tsuboi, 2020; Fernández Acosta et al., 2022) but this diversity has not yet been considered in functional studies of adult bulbar neurogenesis.

Role of centrifugal feedbacks

Regardless of the age of the animal, the integration of newborn GCs in the OB is context-dependent, suggesting that it may be controlled by top-down inputs. The OB sends projections to olfactory cortices (Igarashi et al., 2012; Hanson et al., 2020) which in turn, send information to the OB (Luskin and Price, 1983; Shipley and Adamek, 1984; Padmanabhan et al., 2018; In't Zandt et al., 2019). Interestingly, cortical fibers establish synaptic contacts with adult-born GCs (Arenkiel et al., 2011; Deshpande et al., 2013; De La Rosa-Prieto et al., 2015) whose density is increased by olfactory learning (Lepousez et al., 2014) and activation can induce LTP (Nissant et al., 2009). Recently, the chemogenetic stimulation of the anterior olfactory nucleus glutamatergic feedbacks to the OB was shown to reduce adult-born GCs survival (Libbrecht et al., 2021). In contrast, the GABAergic inputs from the horizontal band of Broca area (HDB) favor their survival (Hanson et al., 2020). This study also revealed that GABAergic contacts from the HDB on newly formed GCs are denser in the superficial than in the deep part of the GCL, and thus may have different impact neonatal versus adult-born GCs. The centrifugal inputs develop early in life, from birth or the immediate post-natal period (piriform cortex, anterior olfactory nucleus), or from the second week of life (cortical amygdala, lateral entorhinal cortex) suggesting that the top-down influence on newly formed cells occurs from birth and evolves as a function of the individual's age (Kostka and Bitzenhofer, 2022).

The OB is also the target of the noradrenergic, cholinergic (Mandairon and Linster, 2009; Mouret et al., 2009; Schilit Nitenson et al., 2019; Zhou et al., 2022) and serotoninergic (Banasr et al., 2004; García-González et al., 2017) neuromodulatory systems whose influence is critical to olfactory learning. In adults, the action of the noradrenergic and cholinergic systems on newborn GCs are required for the perceptual olfactory learning to occur (Moreno et al., 2012; Schilit Nitenson et al., 2019). Thus, it seems that these two systems have synergic effect enabling the integration of newborn GCs in the OB circuitry. In associative learning, inhibiting noradrenergic actions did not affect behavioral responses nor neurogenesis rate (Vinera et al., 2015), suggesting task-specificity of the neuromodulatory systems actions. The noradrenergic fibers coming from the *Locus*

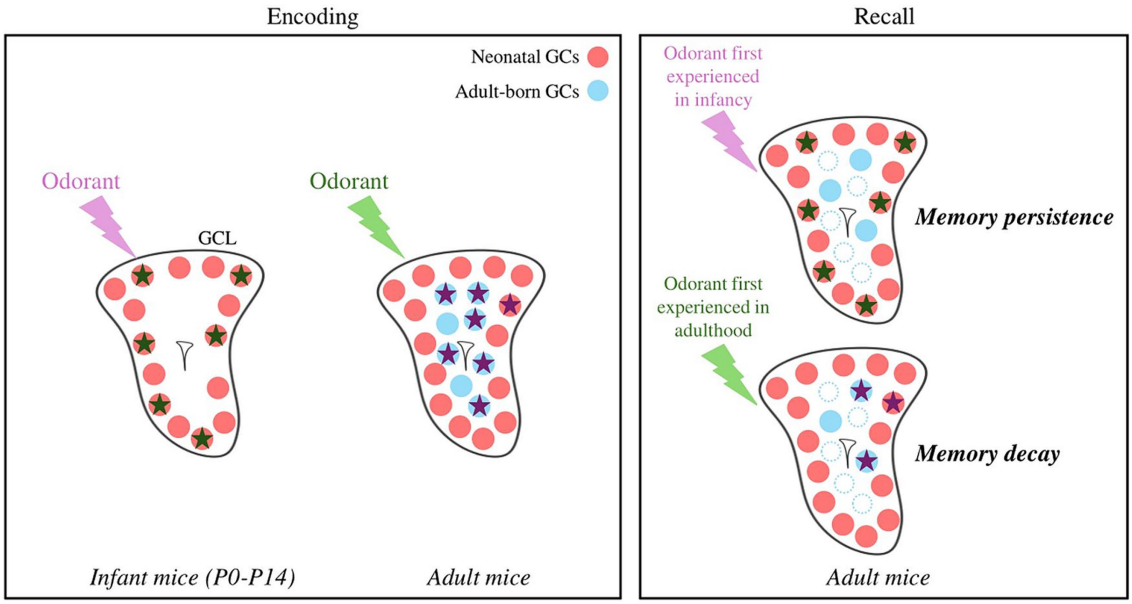

FIGURE 2
Hypothetical model of odor and memory processing by newly formed GCs according to the age of the animal. GCs activated in response to an odorant are represented by stars. An odorant processed at the infant stage is encoded by neonatal GCs, which show little cell death. The local network is reactivated by the odorant during recall, allowing the persistence of the memory. An odorant processed at the adult stage is encoded by adult-born GCs, showing greater renewal (blue dotted dots). The local network is only partially reactivated, possibly explaining the decay of the olfactory memory. Note that an adult olfactory learning can also recruits neonatal GCs. GCL, Granule Cell Layer; GCs, Granule Cells.

Coeruleus are present at birth. They are inhibitory on GCs at neonatal stages (Pandipati and Schoppa, 2012) and play a role in neonatal imprinting behaviors (Moriceau and Sullivan, 2004). Regarding acetylcholine, the time course of development of its contacts with newly-formed GCs and function are largely unknown.

Implication for mental health

Neuropsychiatric conditions like depression, anxiety, schizophrenia or borderline personality disorder often stem from early life stress (Anda et al., 2006; Pietrek et al., 2013; Youssef et al., 2019; Lippard and Nemeroff, 2020; McKay et al., 2022), and are accompanied by olfactory dysfunctions (Naudin et al., 2012; Kazour et al., 2017; Kamath et al., 2018; Crow et al., 2020; Li et al., 2020; Athanassi et al., 2021; Chen et al., 2021; Marin et al., 2023). Adult neurogenesis has been shown to play a part in animal models of depression (Siopi et al., 2016; Ren et al., 2021) but translation to humans is uncertain because the existence of adult neurogenesis in humans is controversial (Lucassen et al., 2020; Duque et al., 2022; Alshebib et al., 2023; Alonso et al., 2024). In contrast, could alteration of early life neurogenesis play a part in the vulnerability to psychiatric diseases induced by early life aversive events? Indeed, neurogenesis during childhood in humans is less prone to debate (Sanai et al., 2011; Dennis et al., 2016; Mathews et al., 2017; Cipriani et al., 2018; Sorrells et al., 2018). The large overlap in neural structures mediating emotional behavior and processing of olfactory signals suggests that the OB could contribute to emotional disturbances (Kontaris et al., 2020; Bhattarai et al., 2022). In support to this hypothesis, early life stress reduced developmental olfactory neurogenesis (Naninck et al., 2015). Thus, altering the neurogenesis at this developmental step could durably alter OB structure and function and contribute to long-lasting olfactory deficits and alteration of emotional behavior (Athanassi et al., 2021; Marin et al., 2023).

Author contributions

JD: Writing – original draft, Writing – review & editing. NM: Writing – original draft, Writing – review & editing. AD: Writing – original draft, Writing – review & editing.

Funding

The author(s) declare that financial support was received for the research, authorship, and/or publication of this article. This work was supported by Observatoire B2V des Mémoires (doctoral fellowship to JD), CNRS, ANR-23-CE17-0065-01, INSERM, Claude Bernard Lyon 1 University, IUF.

Acknowledgments

Abstract have been corrected with the help of ChatGPT. The figures have been partly produced on BioRender.

Conflict of interest

The authors declare that the research was conducted in the absence of any commercial or financial relationships that could be construed as a potential conflict of interest.

Publisher's note

References

Alonso, M., Lepousez, G., Wagner, S., Bardy, C., Gabellec, M.-M., Torquet, N., et al. (2012). Activation of adult-born neurons facilitates learning and memory. *Nat. Neurosci.* 15, 897–904. doi: 10.1038/nn.3108

Alonso, M., Petit, A.-C., and Lledo, P.-M. (2024). The impact of adult neurogenesis on affective functions: of mice and men. *Mol. Psychiatry* 2024:2504. doi: 10.1038/s41380-024-02504-w

Alonso, M., Viollet, C., Gabellec, M.-M., Meas-Yedid, V., Olivo-Marin, J.-C., and Lledo, P.-M. (2006). Olfactory discrimination learning increases the survival of adult-born neurons in the olfactory bulb. *J. Neurosci.* 26, 10508–10513. doi: 10.1523/JNEUROSCI.2633-06.2006

Alshebib, Y., Hori, T., Goel, A., Fauzi, A. A., and Kashiwagi, T. (2023). Adult human neurogenesis: a view from two schools of thought. *IBRO Neurosci. Rep.* 15, 342–347. doi: 10.1016/j.ibneur.2023.07.004

Alvarez-Buylla, A., and García-Verdugo, J. M. (2002). Neurogenesis in Adult Subventricular Zone. *J. Neurosci.* 22, 629–634. doi: 10.1523/JNEUROSCI.22-03-00629.2002

Anda, R. F., Felitti, V. J., Bremner, J. D., Walker, J. D., Whitfield, C., Perry, B. D., et al. (2006). The enduring effects of abuse and related adverse experiences in childhood. A convergence of evidence from neurobiology and epidemiology. *Eur. Arch. Psychiatry Clin. Neurosci.* 256, 174–186. doi: 10.1007/s00406-005-0624-4

Arenkiel, B. R., Hasegawa, H., Yi, J. J., Larsen, R. S., Wallace, M. L., Philpot, B. D., et al. (2011). Activity-induced remodeling of olfactory bulb microcircuits revealed by monosynaptic tracing. *PLoS One* 6:e29423. doi: 10.1371/journal.pone.0029423

Athanassi, A., Dorado Doncel, R., Bath, K. G., and Mandairon, N. (2021). Relationship between depression and olfactory sensory function: a review. *Chem. Senses* 46:bjab044. doi: 10.1093/chemse/bjab044

Banasr, M., Hery, M., Printemps, R., and Daszuta, A. (2004). Serotonin-induced increases in adult cell proliferation and neurogenesis are mediated through different and common 5-HT receptor subtypes in the dentate gyrus and the subventricular zone. *Neuropsychopharmacology* 29, 450–460. doi: 10.1038/sj.npp.1300320

Belnoue, L., Grosjean, N., Abrous, D. N., and Koehl, M. (2011). A critical time window for the recruitment of bulbar newborn neurons by olfactory discrimination learning. *J. Neurosci.* 31, 1010–1016. doi: 10.1523/JNEUROSCI.3941-10.2011

Belvindrah, R., Nissant, A., and Lledo, P.-M. (2011). Abnormal neuronal migration changes the fate of developing neurons in the postnatal olfactory bulb. *J. Neurosci.* 31, 7551–7562. doi: 10.1523/JNEUROSCI.6716-10.2011

Bhattarai, J. P., Etyemez, S., Jaaro-Peled, H., Janke, E., Leon Tolosa, U. D., Kamiya, A., et al. (2022). Olfactory modulation of the medial prefrontal cortex circuitry: implications for social cognition. *Semin. Cell Dev. Biol.* 129, 31–39. doi: 10.1016/j.semcdb.2021.03.022

Bragado Alonso, S., Reinert, J. K., Marichal, N., Massalini, S., Berninger, B., Kuner, T., et al. (2019). An increase in neural stem cells and olfactory bulb adult neurogenesis improves discrimination of highly similar odorants. *EMBO J.* 38:e98791. doi: 10.15252/embj.201798791

Breton-Provencher, V., Bakhshetyan, K., Hardy, D., Bammann, R. R., Cavarretta, F., Snapyan, M., et al. (2016). Principal cell activity induces spine relocation of adult-born interneurons in the olfactory bulb. *Nat. Commun.* 7:12659. doi: 10.1038/ncomms12659

Breton-Provencher, V., Lemasson, M., Peralta, M. R., and Saghatelyan, A. (2009). Interneurons produced in adulthood are required for the Normal functioning of the olfactory bulb network and for the execution of selected olfactory behaviors. *J. Neurosci.* 29, 15245–15257. doi: 10.1523/JNEUROSCI.3606-09.2009

Breton-Provencher, V., and Saghatelyan, A. (2012). Newborn neurons in the adult olfactory bulb: unique properties for specific odor behavior. *Behav. Brain Res.* 227, 480–489. doi: 10.1016/j.bbr.2011.08.001

Carleton, A., Petreanu, L. T., Lansford, R., Alvarez-Buylla, A., and Lledo, P.-M. (2003). Becoming a new neuron in the adult olfactory bulb. *Nat. Neurosci.* 6, 507–518. doi: 10.1038/nn1048

Chen, X., Guo, W., Yu, L., Luo, D., Xie, L., and Xu, J. (2021). Association between anxious symptom severity and olfactory impairment in young adults with generalized anxiety disorder: a case-control study. *Neuropsychiatr. Dis. Treat.* 17, 2877–2883. doi: 10.2147/NDT.S314857

Cipriani, S., Ferrer, I., Aronica, E., Kovacs, G. G., Verney, C., Nardelli, J., et al. (2018). Hippocampal radial glial subtypes and their neurogenic potential in human fetuses and healthy and Alzheimer's disease adults. *Cereb. Cortex* 28, 2458–2478. doi: 10.1093/cercor/bhy096

Crow, A. J. D., Janssen, J. M., Vickers, K. L., Parish-Morris, J., Moberg, P. J., and Roalf, D. R. (2020). Olfactory dysfunction in neurodevelopmental disorders: a Meta-analytic review of autism Spectrum disorders, attention deficit/hyperactivity disorder and obsessive-compulsive disorder. *J. Autism Dev. Disord.* 50, 2685–2697. doi: 10.1007/s10803-020-04376-9

Daroles, L., Gribaudo, S., Doulazmi, M., Scotto-Lomassese, S., Dubacq, C., Mandairon, N., et al. (2016). Fragile X mental retardation protein and dendritic local translation of the alpha subunit of the calcium/calmodulin-dependent kinase II messenger RNA are required for the structural plasticity underlying olfactory learning. *Biol. Psychiatry* 80, 149–159. doi: 10.1016/j.biopsych.2015.07.023

de Chevigny, A., Core, N., Follert, P., Wild, S., Bosio, A., Yoshikawa, K., et al. (2012). Dynamic expression of the pro-dopaminergic transcription factors Pax6 and Dlx2 during postnatal olfactory bulb neurogenesis. *Front. Cell. Neurosci.* 6:6. doi: 10.3389/fncel.2012.00006

De La Rosa-Prieto, C., De Moya-Pinilla, M., Saiz-Sanchez, D., Ubeda-banon, I., Arzate, D. M., Flores-Cuadrado, A., et al. (2015). Olfactory and cortical projections to bulbar and hippocampal adult-born neurons. *Front. Neuroanat.* 9:4. doi: 10.3389/fnana.2015.00004

Dennis, C. V., Suh, L. S., Rodriguez, M. L., Kril, J. J., and Sutherland, G. T. (2016). Human adult neurogenesis across the ages: An immunohistochemical study. *Neuropathol. Appl. Neurobiol.* 42, 621–638. doi: 10.1111/nan.12337

Deshpande, A., Bergami, M., Ghanem, A., Conzelmann, K.-K., Lepier, A., Götz, M., et al. (2013). Retrograde monosynaptic tracing reveals the temporal evolution of inputs onto new neurons in the adult dentate gyrus and olfactory bulb. *Proc. Natl. Acad. Sci. USA* 110, E1152–E1161. doi: 10.1073/pnas.1218991110

Doucette, W., and Restrepo, D. (2008). Profound context-dependent plasticity of mitral cell responses in olfactory bulb. *PLoS Biol.* 6:e258. doi: 10.1371/journal.pbio.0060258

Duque, A., Arellano, J. I., and Rakic, P. (2022). An assessment of the existence of adult neurogenesis in humans and value of its rodent models for neuropsychiatric diseases. *Mol. Psychiatry* 27, 377–382. doi: 10.1038/s41380-021-01314-8

Epp, J. R., Silva Mera, R., Köhler, S., Josselyn, S. A., and Frankland, P. W. (2016). Neurogenesis-mediated forgetting minimizes proactive interference. *Nat. Commun.* 7:10838. doi: 10.1038/ncomms10838

Fernández Acosta, F. J., Luque-Molina, I., Vecino, R., Díaz-Guerra, E., Defterali, Ç., Pignatelli, J., et al. (2022). Morphological diversity of Calretinin interneurons generated from adult mouse olfactory bulb Core neural stem cells. *Front. Cell Dev. Biol.* 10:932297. doi: 10.3389/fcell.2022.932297

Ferreira, A., Constantinescu, V.-S., Malvaut, S., Saghatelyan, A., and Hardy, S. V. (2024). Distinct forms of structural plasticity of adult-born interneuron spines in the mouse olfactory bulb induced by different odor learning paradigms. *Commun. Biol.* 7:420. doi: 10.1038/s42003-024-06115-7

Forest, J., Chalençon, L., Midroit, M., Terrier, C., Caillé, I., Sacquet, J., et al. (2019a). Role of adult-born versus preexisting neurons born at P0 in olfactory perception in a complex olfactory environment in mice. *Cereb. Cortex* 2019:bhz105. doi: 10.1093/cercor/bhz105

Forest, J., Moreno, M., Cavelius, M., Chalençon, L., Ziessel, A., Sacquet, J., et al. (2019b). Short-term availability of adult-born neurons for memory encoding. *Nat. Commun.* 10:5609. doi: 10.1038/s41467-019-13521-7

Frankland, P. W., Köhler, S., and Josselyn, S. A. (2013). Hippocampal neurogenesis and forgetting. *Trends Neurosci.* 36, 497–503. doi: 10.1016/j.tins.2013.05.002

Fukunaga, I., Berning, M., Kollo, M., Schmaltz, A., and Schaefer, A. T. (2012). Two distinct channels of olfactory bulb output. *Neuron* 75, 320–329. doi: 10.1016/j.neuron.2012.05.017

Gao, Y., and Strowbridge, B. W. (2009). Long-term plasticity of excitatory inputs to granule cells in the rat olfactory bulb. *Nat. Neurosci.* 12, 731–733. doi: 10.1038/nn.2319

García-González, D., Khodosevich, K., Watanabe, Y., Rollenhagen, A., Lübke, J. H. R., and Monyer, H. (2017). Serotonergic projections govern postnatal neuroblast migration. *Neuron* 94, 534–549.e9. doi: 10.1016/j.neuron.2017.04.013

Greco-Vuilloud, J., Midroit, M., Terrier, C., Forest, J., Sacquet, J., Mandairon, N., et al. (2022). 12 months is a pivotal age for olfactory perceptual learning and its underlying neuronal plasticity in aging mice. *Neurobiol. Aging* 114, 73–83. doi: 10.1016/j.neurobiolaging.2022.03.003

Grelat, A., Benoit, L., Wagner, S., Moigneu, C., Lledo, P.-M., and Alonso, M. (2018). Adult-born neurons boost odor–reward association. *Proc. Natl. Acad. Sci. U. S. A.* 115, 2514–2519. doi: 10.1073/pnas.1716400115

Gschwend, O., Abraham, N. M., Lagier, S., Begnaud, F., Rodriguez, I., and Carleton, A. (2015). Neuronal pattern separation in the olfactory bulb improves odor discrimination learning. *Nat. Neurosci.* 18, 1474–1482. doi: 10.1038/nn.4089

Hanson, E., Swanson, J., and Arenkiel, B. R. (2020). GABAergic input from the basal forebrain promotes the survival of adult-born neurons in the mouse olfactory bulb. *Front. Neural Circuits* 14:17. doi: 10.3389/fncir.2020.00017

Hardy, D., Malvaut, S., Breton-Provencher, V., and Saghatelyan, A. (2018). The role of calretinin-expressing granule cells in olfactory bulb functions and odor behavior. *Sci. Rep.* 8:9385. doi: 10.1038/s41598-018-27692-8

Hardy, D., and Saghatelyan, A. (2017). Different forms of structural plasticity in the adult olfactory bulb. *Neurogenesis (Austin)* 4:e1301850. doi: 10.1080/23262133.2017.1301850

Hinds, J. W., and Hinds, P. L. (1976). Synapse formation in the mouse olfactory bulb. I. Quantitative studies. *J. Comp. Neurol.* 169, 15–40. doi: 10.1002/cne.901690103

Igarashi, K. M., Ieki, N., An, M., Yamaguchi, Y., Nagayama, S., Kobayakawa, K., et al. (2012). Parallel mitral and tufted cell pathways route distinct odor information to different targets in the olfactory cortex. *J. Neurosci.* 32, 7970–7985. doi: 10.1523/JNEUROSCI.0154-12.2012

Imayoshi, I., Sakamoto, M., Ohtsuka, T., Takao, K., Miyakawa, T., Yamaguchi, M., et al. (2008). Roles of continuous neurogenesis in the structural and functional integrity of the adult forebrain. *Nat. Neurosci.* 11, 1153–1161. doi: 10.1038/nn.2185

In't Zandt, E. E., Cansler, H. L., Denson, H. B., and Wesson, D. W. (2019). Centrifugal innervation of the olfactory bulb: A reappraisal. *eNeuro* 6:0390. doi: 10.1523/ENEURO.0390-18.2019

Kamath, V., Paksarian, D., Cui, L., Moberg, P. J., Turetsky, B. I., and Merikangas, K. R. (2018). Olfactory processing in bipolar disorder, major depression, and anxiety. *Bipolar Disord.* 20, 547–555. doi: 10.1111/bdi.12625

Kay, L. M., and Laurent, G. (1999). Odor-and context-dependent modulation of mitral cell activity in behaving rats. *Nat. Neurosci.* 2, 1003–1009. doi: 10.1038/14801

Kazour, F., Richa, S., Desmidt, T., Lemaire, M., Atanasova, B., and El Hage, W. (2017). Olfactory and gustatory functions in bipolar disorders: a systematic review. *Neurosci. Biobehav. Rev.* 80, 69–79. doi: 10.1016/j.neubiorev.2017.05.009

Kelsch, W., Lin, C.-W., and Lois, C. (2008). Sequential development of synapses in dendritic domains during adult neurogenesis. *Proc. Natl. Acad. Sci. U. S. A.* 105, 16803–16808. doi: 10.1073/pnas.0807970105

Kontaris, I., East, B. S., and Wilson, D. A. (2020). Behavioral and neurobiological convergence of odor, mood and emotion: a review. *Front. Behav. Neurosci.* 14:35. doi: 10.3389/fnbeh.2020.00035

Kostka, J. K., and Bitzenhofer, S. H. (2022). Postnatal development of centrifugal inputs to the olfactory bulb. *Front. Neurosci.* 16:815282. doi: 10.3389/fnins.2022.815282

Lazarini, F., Mouthon, M.-A., Gheusi, G., de Chaumont, F., Olivo-Marin, J.-C., Lamarque, S., et al. (2009). Cellular and behavioral effects of cranial irradiation of the subventricular zone in adult mice. *PLoS One* 4:e7017. doi: 10.1371/journal.pone.0007017

Lemasson, M., Saghatelyan, A., Olivo-Marin, J.-C., and Lledo, P.-M. (2005). Neonatal and adult neurogenesis provide two distinct populations of newborn neurons to the mouse olfactory bulb. *J. Neurosci.* 25, 6816–6825. doi: 10.1523/JNEUROSCI.1114-05.2005

Lepousez, G., Nissant, A., Bryant, A. K., Gheusi, G., Greer, C. A., and Lledo, P.-M. (2014). Olfactory learning promotes input-specific synaptic plasticity in adult-born neurons. *Proc. Natl. Acad. Sci. U. S. A.* 111, 13984–13989. doi: 10.1073/pnas.1404991111

Li, Z.-T., Li, S.-B., Wen, J.-F., Zhang, X.-Y., Hummel, T., and Zou, L.-Q. (2020). Early-onset schizophrenia showed similar but more severe olfactory identification impairment than adult-onset schizophrenia. *Front. Psych.* 11:626. doi: 10.3389/fpsyt.2020.00626

Libbrecht, S., Van den Haute, C., Welkenhuysen, M., Braeken, D., Haesler, S., and Baekelandt, V. (2021). Chronic chemogenetic stimulation of the anterior olfactory nucleus reduces newborn neuron survival in the adult mouse olfactory bulb. *J. Neurochem.* 158, 1186–1198. doi: 10.1111/jnc.15486

Lippard, E. T. C., and Nemeroff, C. B. (2020). The devastating clinical consequences of child abuse and neglect: increased disease vulnerability and poor treatment response in mood disorders. *Am. J. Psychiatry* 177, 20–36. doi: 10.1176/appi.ajp.2019.19010020

Livneh, Y., and Mizrahi, A. (2011). Experience-dependent plasticity of mature adult-born neurons. *Nat. Neurosci.* 15, 26–28. doi: 10.1038/nn.2980

Lucassen, P. J., Toni, N., Kempermann, G., Frisen, J., Gage, F. H., and Swaab, D. F. (2020). Limits to human neurogenesis—really? *Mol. Psychiatry* 25, 2207–2209. doi: 10.1038/s41380-018-0337-5

Luskin, M. B. (1993). Restricted proliferation and migration of postnatally generated neurons derived from the forebrain subventricular zone. *Neuron* 11, 173–189. doi: 10.1016/0896-6273(93)90281-u

Luskin, M. B., and Price, J. L. (1983). The topographic organization of associational fibers of the olfactory system in the rat, including centrifugal fibers to the olfactory bulb. *J. Comp. Neurol.* 216, 264–291. doi: 10.1002/cne.902160305

Magavi, S. S. P. (2005). Adult-born and preexisting olfactory granule neurons undergo distinct experience-dependent modifications of their olfactory responses in vivo. *J. Neurosci.* 25, 10729–10739. doi: 10.1523/JNEUROSCI.2250-05.2005

Malvaut, S., Gribaudo, S., Hardy, D., David, L. S., Daroles, L., Labrecque, S., et al. (2017). CaMKIIα expression defines two functionally distinct populations of granule cells involved in different types of odor behavior. *Curr. Biol.* 27, 3315–3329.e6. doi: 10.1016/j.cub.2017.09.058

Mandairon, N., Kuczewski, N., Kermen, F., Forest, J., Midroit, M., Richard, M., et al. (2018). Opposite regulation of inhibition by adult-born granule cells during implicit versus explicit olfactory learning. *eLife* 7:e34976. doi: 10.7554/eLife.34976

Mandairon, N., and Linster, C. (2009). Odor perception and olfactory bulb plasticity in adult mammals. *J. Neurophysiol.* 101, 2204–2209. doi: 10.1152/jn.00076.2009

Mandairon, N., Sacquet, J., Garcia, S., Ravel, N., Jourdan, F., and Didier, A. (2006a). Neurogenic correlates of an olfactory discrimination task in the adult olfactory bulb. *Eur. J. Neurosci.* 24, 3578–3588. doi: 10.1111/j.1460-9568.2006.05235.x

Mandairon, N., Sacquet, J., Jourdan, F., and Didier, A. (2006b). Long-term fate and distribution of newborn cells in the adult mouse olfactory bulb: influences of olfactory deprivation. *Neuroscience* 141, 443–451. doi: 10.1016/j.neuroscience.2006.03.066

Mandairon, N., Sultan, S., Nouvian, M., Sacquet, J., and Didier, A. (2011). Involvement of newborn neurons in olfactory associative learning? The operant or non-operant component of the task makes all the difference. *J. Neurosci.* 31, 12455–12460. doi: 10.1523/JNEUROSCI.2919-11.2011

Marin, C., Alobid, I., Fuentes, M., López-Chacón, M., and Mullol, J. (2023). Olfactory dysfunction in mental illness. *Curr Allergy Asthma Rep* 23, 153–164. doi: 10.1007/s11882-023-01068-z

Mathews, K. J., Allen, K. M., Boerrigter, D., Ball, H., Shannon Weickert, C., and Double, K. L. (2017). Evidence for reduced neurogenesis in the aging human hippocampus despite stable stem cell markers. *Aging Cell* 16, 1195–1199. doi: 10.1111/acel.12641

McKay, M. T., Kilmartin, L., Meagher, A., Cannon, M., Healy, C., and Clarke, M. C. (2022). A revised and extended systematic review and meta-analysis of the relationship between childhood adversity and adult psychiatric disorder. *J. Psychiatr. Res.* 156, 268–283. doi: 10.1016/j.jpsychires.2022.10.015

Merkle, F. T., Fuentealba, L. C., Sanders, T. A., Magno, L., Kessaris, N., and Alvarez-Buylla, A. (2014). Adult neural stem cells in distinct microdomains generate previously unknown interneuron types. *Nat. Neurosci.* 17, 207–214. doi: 10.1038/nn.3610

Merkle, F. T., Mirzadeh, Z., and Alvarez-Buylla, A. (2007). Mosaic organization of neural stem cells in the adult brain. *Science* 317, 381–384. doi: 10.1126/science.1144914

Messaoudi, S., Allam, A., Stoufflet, J., Paillard, T., Le Ven, A., Fouquet, C., et al. (2024). FMRP regulates postnatal neuronal migration via MAP1B. *eLife* 12:RP88782. doi: 10.7554/eLife.88782

Miyamichi, K., Amat, F., Moussavi, F., Wang, C., Wickersham, I., Wall, N. R., et al. (2011). Cortical representations of olfactory input by transsynaptic tracing. *Nature* 472, 191–196. doi: 10.1038/nature09714

Moreno, M. M., Bath, K., Kuczewski, N., Sacquet, J., Didier, A., and Mandairon, N. (2012). Action of the noradrenergic system on adult-born cells is required for olfactory learning in mice. *J. Neurosci.* 32, 3748–3758. doi: 10.1523/JNEUROSCI.6335-11.2012

Moreno, M. M., Linster, C., Escanilla, O., Sacquet, J., Didier, A., and Mandairon, N. (2009). Olfactory perceptual learning requires adult neurogenesis. *Proc. Natl. Acad. Sci. U. S. A.* 106, 17980–17985. doi: 10.1073/pnas.0907063106

Moriceau, S., and Sullivan, R. M. (2004). Unique neural circuitry for neonatal olfactory learning. *J. Neurosci.* 24, 1182–1189. doi: 10.1523/JNEUROSCI.4578-03.2004

Mouret, A., Gheusi, G., Gabellec, M.-M., de Chaumont, F., Olivo-Marin, J.-C., and Lledo, P.-M. (2008). Learning and survival of newly generated neurons: when time matters. *J. Neurosci.* 28, 11511–11516. doi: 10.1523/JNEUROSCI.2954-08.2008

Mouret, A., Murray, K., and Lledo, P.-M. (2009). Centrifugal drive onto local inhibitory interneurons of the olfactory bulb. *Ann. N. Y. Acad. Sci.* 1170, 239–254. doi: 10.1111/j.1749-6632.2009.03913.x

Muthusamy, N., Zhang, X., Johnson, C. A., Yadav, P. N., and Ghashghaei, H. T. (2017). Developmentally defined forebrain circuits regulate appetitive and aversive olfactory learning. *Nat. Neurosci.* 20, 20–23. doi: 10.1038/nn.4452

Nagayama, S., Enerva, A., Fletcher, M. L., Masurkar, A. V., Igarashi, K. M., Mori, K., et al. (2010). Differential axonal projection of mitral and tufted cells in the mouse Main olfactory system. *Front. Neural Circuits* 4:120. doi: 10.3389/fncir.2010.00120

Nagayama, S., Homma, R., and Imamura, F. (2014). Neuronal organization of olfactory bulb circuits. *Front. Neural Circuits* 8:98. doi: 10.3389/fncir.2014.00098

Naninck, E. F. G., Hoeijmakers, L., Kakava-Georgiadou, N., Meesters, A., Lazic, S. E., Lucassen, P. J., et al. (2015). Chronic early life stress alters developmental and adult neurogenesis and impairs cognitive function in mice. *Hippocampus* 25, 309–328. doi: 10.1002/hipo.22374

Naudin, M., El-Hage, W., Gomes, M., Gaillard, P., Belzung, C., and Atanasova, B. (2012). State and trait olfactory markers of major depression. *PLoS One* 7:e46938. doi: 10.1371/journal.pone.0046938

Nissant, A., Bardy, C., Katagiri, H., Murray, K., and Lledo, P.-M. (2009). Adult neurogenesis promotes synaptic plasticity in the olfactory bulb. *Nat. Neurosci.* 12, 728–730. doi: 10.1038/nn.2298

Padmanabhan, K., Osakada, F., Tarabrina, A., Kizer, E., Callaway, E. M., Gage, F. H., et al. (2018). Centrifugal inputs to the Main olfactory bulb revealed through whole brain circuit-mapping. *Front. Neuroanat.* 12:115. doi: 10.3389/fnana.2018.00115

Pallotto, M., Nissant, A., Fritschy, J.-M., Rudolph, U., Sassoè-Pognetto, M., Panzanelli, P., et al. (2012). Early formation of GABAergic synapses governs the development of adult-born neurons in the olfactory bulb. *J. Neurosci.* 32, 9103–9115. doi: 10.1523/JNEUROSCI.0214-12.2012

Pandipati, S., and Schoppa, N. E. (2012). Age-dependent adrenergic actions in the main olfactory bulb that could underlie an olfactory-sensitive period. *J. Neurophysiol.* 108, 1999–2007. doi: 10.1152/jn.00322.2012

Pietrek, C., Elbert, T., Weierstall, R., Müller, O., and Rockstroh, B. (2013). Childhood adversities in relation to psychiatric disorders. *Psychiatry Res.* 206, 103–110. doi: 10.1016/j.psychres.2012.11.003

Platel, J.-C., Angelova, A., Bugeon, S., Wallace, J., Ganay, T., Chudotvorova, I., et al. (2019). Neuronal integration in the adult mouse olfactory bulb is a non-selective addition process. *eLife* 8:e44830. doi: 10.7554/eLife.44830

Ren, G., Xue, P., Wu, B., Yang, F., and Wu, X. (2021). Intranasal treatment of lixisenatide attenuated emotional and olfactory symptoms via CREB-mediated adult neurogenesis in mouse depression model. *Aging (Albany NY)* 13, 3898–3908. doi: 10.18632/aging.202358

Rey, N. L., Sacquet, J., Veyrac, A., Jourdan, F., and Didier, A. (2012). Behavioral and cellular markers of olfactory aging and their response to enrichment. *Neurobiol. Aging* 33, 626.e9–626.e23. doi: 10.1016/j.neurobiolaging.2011.03.026

Rochefort, C., Gheusi, G., Vincent, J.-D., and Lledo, P.-M. (2002). Enriched odor exposure increases the number of newborn neurons in the adult olfactory bulb and improves odor memory. *J. Neurosci.* 22, 2679–2689. doi: 10.1523/JNEUROSCI.22-07-02679.2002

Saghatelyan, A., Roux, P., Migliore, M., Rochefort, C., Desmaisons, D., Charneau, P., et al. (2005). Activity-dependent adjustments of the inhibitory network in the olfactory bulb following early postnatal deprivation. *Neuron* 46, 103–116. doi: 10.1016/j.neuron.2005.02.016

Sailor, K. A., Valley, M. T., Wiechert, M. T., Riecke, H., Sun, G. J., Adams, W., et al. (2016). Persistent structural plasticity optimizes sensory information processing in the olfactory bulb. *Neuron* 91, 384–396. doi: 10.1016/j.neuron.2016.06.004

Sakamoto, M., Ieki, N., Miyoshi, G., Mochimaru, D., Miyachi, H., Imura, T., et al. (2014). Continuous postnatal neurogenesis contributes to formation of the olfactory bulb neural circuits and flexible olfactory associative learning. *J. Neurosci.* 34, 5788–5799. doi: 10.1523/JNEUROSCI.0674-14.2014

Sanai, N., Nguyen, T., Ihrie, R. A., Mirzadeh, Z., Tsai, H.-H., Wong, M., et al. (2011). Corridors of migrating neurons in human brain and their decline during infancy. *Nature* 478, 382–386. doi: 10.1038/nature10487

Schilit Nitenson, A., Manzano Nieves, G., Poeta, D. L., Bahar, R., Rachofsky, C., Mandairon, N., et al. (2019). Acetylcholine regulates olfactory perceptual learning through effects on adult neurogenesis. *iScience* 22, 544–556. doi: 10.1016/j.isci.2019.11.016

Shipley, M. T., and Adamek, G. D. (1984). The connections of the mouse olfactory bulb: a study using orthograde and retrograde transport of wheat germ agglutinin conjugated to horseradish peroxidase. *Brain Res. Bull.* 12, 669–688. doi: 10.1016/0361-9230(84)90148-5

Shook, B. A., Manz, D. H., Peters, J. J., Kang, S., and Conover, J. C. (2012). Spatiotemporal changes to the subventricular zone stem cell pool through aging. *J. Neurosci.* 32, 6947–6956. doi: 10.1523/JNEUROSCI.5987-11.2012

Siopi, E., Denizet, M., Gabellec, M.-M., de Chaumont, F., Olivo-Marin, J.-C., Guilloux, J.-P., et al. (2016). Anxiety-and depression-like states Lead to pronounced olfactory deficits and impaired adult neurogenesis in mice. *J. Neurosci.* 36, 518–531. doi: 10.1523/JNEUROSCI.2817-15.2016

Sorrells, S. F., Paredes, M. F., Cebrian-Silla, A., Sandoval, K., Qi, D., Kelley, K. W., et al. (2018). Human hippocampal neurogenesis drops sharply in children to undetectable levels in adults. *Nature* 555, 377–381. doi: 10.1038/nature25975

Sultan, S., Rey, N., Sacquet, J., Mandairon, N., and Didier, A. (2011). Newborn neurons in the olfactory bulb selected for long-term survival through olfactory learning are prematurely suppressed when the olfactory memory is erased. *J. Neurosci.* 31, 14893–14898. doi: 10.1523/JNEUROSCI.3677-11.2011

Takahashi, H., Ogawa, Y., Yoshihara, S., Asahina, R., Kinoshita, M., Kitano, T., et al. (2016). A subtype of olfactory bulb interneurons is required for odor detection and discrimination behaviors. *J. Neurosci.* 36, 8210–8227. doi: 10.1523/JNEUROSCI.2783-15.2016

Takahashi, H., Yoshihara, S., and Tsuboi, A. (2018). The functional role of olfactory bulb granule cell subtypes derived from embryonic and postnatal neurogenesis. *Front. Mol. Neurosci.* 11:229. doi: 10.3389/fnmol.2018.00229

Terrier, C., Greco-Vuilloud, J., Cavelius, M., Thevenet, M., Mandairon, N., Didier, A., et al. (2024). Long-term olfactory enrichment promotes non-olfactory cognition, noradrenergic plasticity and remodeling of brain functional connectivity in older mice. *Neurobiol. Aging* 136, 133–156. doi: 10.1016/j.neurobiolaging.2024.01.011

Tsuboi, A. (2020). LRR-containing Oncofetal trophoblast glycoprotein 5T4 shapes neural circuits in olfactory and visual systems. *Front. Mol. Neurosci.* 13:581018. doi: 10.3389/fnmol.2020.581018

Tufo, C., Poopalasundaram, S., Dorrego-Rivas, A., Ford, M. C., Graham, A., and Grubb, M. S. (2022). Development of the mammalian main olfactory bulb. *Development* 149:dev200210. doi: 10.1242/dev.200210

Valley, M. (2009). Ablation of mouse adult neurogenesis alters olfactory bulb structure and olfactory fear conditioning. *Front. Neurosci.* 3:51. doi: 10.3389/neuro.22.003.2009

Vinera, J., Kermen, F., Sacquet, J., Didier, A., Mandairon, N., and Richard, M. (2015). Olfactory perceptual learning requires action of noradrenaline in the olfactory bulb: comparison with olfactory associative learning. *Learn. Mem.* 22, 192–196. doi: 10.1101/lm.036608.114

Whitman, M. C., and Greer, C. A. (2007). Synaptic integration of adult-generated olfactory bulb granule cells: basal axodendritic centrifugal input precedes apical dendrodendritic local circuits. *J. Neurosci.* 27, 9951–9961. doi: 10.1523/JNEUROSCI.1633-07.2007

Winner, B., Cooper-Kuhn, C. M., Aigner, R., Winkler, J., and Kuhn, H. G. (2002). Long-term survival and cell death of newly generated neurons in the adult rat olfactory bulb. *Eur. J. Neurosci.* 16, 1681–1689. doi: 10.1046/j.1460-9568.2002.02238.x

Yoshihara, S.-I., Takahashi, H., Nishimura, N., Kinoshita, M., Asahina, R., Kitsuki, M., et al. (2014). Npas4 regulates Mdm2 and thus dcx in experience-dependent dendritic spine development of newborn olfactory bulb interneurons. *Cell Rep.* 8, 843–857. doi: 10.1016/j.celrep.2014.06.056

Yoshihara, S., Takahashi, H., Nishimura, N., Naritsuka, H., Shirao, T., Hirai, H., et al. (2012). 5T4 glycoprotein regulates the sensory input-dependent development of a specific subtype of newborn interneurons in the mouse olfactory bulb. *J. Neurosci.* 32, 2217–2226. doi: 10.1523/JNEUROSCI.5907-11.2012

Youssef, M., Atsak, P., Cardenas, J., Kosmidis, S., Leonardo, E. D., and Dranovsky, A. (2019). Early life stress delays hippocampal development and diminishes the adult stem cell pool in mice. *Sci. Rep.* 9:4120. doi: 10.1038/s41598-019-40868-0

Zhou, P., Liu, P., Zhang, Y., Wang, D., and Li, A. (2022). The response dynamics and function of cholinergic and GABAergic neurons in the basal forebrain during olfactory learning. *Front. Cell. Neurosci.* 16:911439. doi: 10.3389/fncel.2022.911439

frontiers | Frontiers in Neural Circuits

TYPE Original Research
PUBLISHED 09 August 2024
DOI 10.3389/fncir.2024.1430598

OPEN ACCESS

EDITED BY
Charles A. Greer,
Yale University, United States

REVIEWED BY
Eike Budinger,
Leibniz Institute for Neurobiology (LG), Germany
Shin Nagayama,
Texas Medical Center, United States

*CORRESPONDENCE
Isabella R. Williams
✉ i.williams@garvan.org.au

RECEIVED 10 May 2024
ACCEPTED 10 July 2024
PUBLISHED 09 August 2024

CITATION
Williams IR and Ryugo DK (2024) Bilateral and symmetric glycinergic and glutamatergic projections from the LSO to the IC in the CBA/CaH mouse. *Front. Neural Circuits* 18:1430598. doi: 10.3389/fncir.2024.1430598

Bilateral and symmetric glycinergic and glutamatergic projections from the LSO to the IC in the CBA/CaH mouse

Isabella R. Williams[1,2]* and David K. Ryugo[1,2,3]

[1]Garvan Institute of Medical Research, Darlinghurst, NSW, Australia, [2]School of Medical Sciences, University of New South Wales, Kensington, NSW, Australia, [3]Department of Otolaryngology, Head, Neck and Skull Base Surgery, St. Vincent's Hospital, Darlinghurst, NSW, Australia

Auditory space has been conceptualized as a matrix of systematically arranged combinations of binaural disparity cues that arise in the superior olivary complex (SOC). The computational code for interaural time and intensity differences utilizes excitatory and inhibitory projections that converge in the inferior colliculus (IC). The challenge is to determine the neural circuits underlying this convergence and to model how the binaural cues encode location. It has been shown that midbrain neurons are largely excited by sound from the contralateral ear and inhibited by sound leading at the ipsilateral ear. In this context, ascending projections from the lateral superior olive (LSO) to the IC have been reported to be ipsilaterally glycinergic and contralaterally glutamatergic. This study used CBA/CaH mice (3–6 months old) and applied unilateral retrograde tracing techniques into the IC in conjunction with immunocytochemical methods with glycine and glutamate transporters (GlyT2 and vGLUT2, respectively) to analyze the projection patterns from the LSO to the IC. Glycinergic and glutamatergic neurons were spatially intermixed within the LSO, and both types projected to the IC. For GlyT2 and vGLUT2 neurons, the average percentage of ipsilaterally and contralaterally projecting cells was similar (ANOVA, $p = 0.48$). A roughly equal number of GlyT2 and vGLUT2 neurons did not project to the IC. The somatic size and shape of these neurons match the descriptions of LSO principal cells. A minor but distinct population of small ($< 40\ \mu m^2$) neurons that labeled for GlyT2 did not project to the IC; these cells emerge as candidates for inhibitory local circuit neurons. Our findings indicate a symmetric and bilateral projection of glycine and glutamate neurons from the LSO to the IC. The differences between our results and those from previous studies suggest that species and habitat differences have a significant role in mechanisms of binaural processing and highlight the importance of research methods and comparative neuroscience. These data will be important for modeling how excitatory and inhibitory systems converge to create auditory space in the CBA/CaH mouse.

KEYWORDS

binaural hearing, sound localization, lateral superior olive, glycine, glutamate, principal cells

1 Introduction

The auditory system is constantly tracking inputs received from the two ears. Principal neurons of the lateral superior olive (LSO) combine excitatory glutamatergic projections from the ipsilateral cochlear nucleus (Cant and Casseday, 1986; Doucet and Ryugo, 2003) with inhibitory glycinergic input from the homolateral medial nucleus of the trapezoid body (MNTB) that is driven by activation of the contralateral cochlear nucleus (Kuwabara and Zook, 1991; Banks and Smith, 1992). The convergence of this binaural information using interaural level and timing differences is sent to the inferior colliculus (IC) (Grothe and Park, 1995; Franken et al., 2018; Williams et al., 2022). Electrophysiological recordings from the inferior colliculus reflect the output of the LSO with maximal excitation leading from the contralateral ear and inhibition when the sound is delivered to the ipsilateral ear (Hind et al., 1963; Kuwada et al., 1984; Grothe and Park, 1995; Park et al., 2004; Ono and Ito, 2015; Ono et al., 2020). The computation of sound location is achieved by the manner in which the auditory system utilizes neural responses created by ongoing interaural differences in time, level, and spectral cues (Mosieff and Konishi, 1981; Tollin and Yin, 2005; Yin et al., 2019). These binaural functions are crucial for the brain to sort the various auditory streams that bombard the system constantly and to make sense of our auditory scene.

The lateral superior olive (LSO) contains a heterogenous population of neurons with either ascending or descending projections, which are suggested to function separately in information processing (Ryugo et al., 2011; Williams et al., 2022). Defining its ascending circuitry is considered crucial to understanding mechanisms of auditory stream segregation. It had been suggested using tract-tracing methods that principal neurons of the LSO have bilateral and symmetric projections to the IC (cat. Adams, 1979; greater horseshoe bat, Schweizer, 1981; gerbil, Nordeen et al., 1983; mustache bat, Ross et al., 1988; Mexican free-tailed bat, Grothe, 1994; Wistar albino rat, Kelly et al., 1998); we quantitatively support this conclusion for the CBA/CaH mouse (Williams et al., 2022). There are, however, disagreements as to the symmetry and chemical nature of these projections: (1) ipsilateral projections are entirely glycinergic and inhibitory (Willard and Martin, 1984; Saint Marie et al., 1989; Moore et al., 1995; Mellott et al., 2021), (2) low frequency neurons project ipsilaterally, whereas high frequency neurons project contralaterally (Glendenning and Mastereton, 1983; Oliver, 2000), and (3) low frequencies project contralaterally and high frequencies project ipsilaterally (Henkel and Brunso-Bechtold, 1993).

The data that include transmitter chemistry with the corresponding laterality of LSO projections to the IC are also conflicting. Published reports to date suggest that ipsilateral projections are primarily glycinergic, and the contralateral projections are glutamatergic. These differences, however, could be due to variations across species (cats, Saint Marie et al., 1989) or chinchillas and guinea pigs, Saint Marie and Baker, 1990; bat, Klug et al., 1995; Long-Evans rats and Swiss Webster mice, Ito and Oliver, 2010; gerbils, Mellott et al., 2021; CBA/CaH mouse, Williams et al., 2022), age (Helfert et al., 1989; Nerlich et al., 2017), cell staining methods for determining amino acid chemistry including in situ hybridization (Mellott et al., 2021); immunohistochemistry (Storm-Mathisen et al., 1983; Wenthold et al., 1986; Koch and Sanes, 1998; Williams et al., 2022); and pathway tracing such as HRP histochemistry (Glendenning et al., 1992), dextran amines (Williams et al., 2022), and selective uptake and transport of radiolabeled glycine (Saint Marie and Baker, 1990; Glendenning et al., 1992). In the context of differences in the species, age of the subjects at the time of examination, and methods employed, variations in the results should not be surprising. The challenge is to advance our knowledge about binaural hearing by understanding the brain differences as they relate to species, species habitat, and methods of research.

This present study sought to confirm the bilateral and symmetrical LSO projections to the IC (Williams et al., 2022) and to extend our understanding of excitatory and inhibitory effects in the mouse. Using retrograde labeling and antibody staining methods in the CBA/CaH mouse, we sought the following: (1) to determine the projection pattern of glycinergic and glutamatergic LSO neurons to the IC, (2) to assess somatic size of the different classes of LSO neurons, and (3) to infer LSO influences on sound localization mechanisms.

2 Materials and methods

2.1 Mouse model of hearing

This study was conducted in line with the Australian Code for the Care and Use of Animals for Scientific Purposes (2013). Usage of all animals were in accord to the Animal Ethics Committee protocols (Animal Research Authority: 20-02 and 21-13) and utilizing the principals of Replacement, Reduction and Refinement with the approval from the Garvan Institute of Medical Research Animal Ethics Committee. A total of 20 CBA/CaH mice of either sex and aged between 4 and 6 months old were used. CBA/CaJ mice (Strain #000654) were imported from The Jackson Laboratory (Bar Harbor, ME) by the Australian BioResources Facility (Mossvale, New South Wales, AUS), renamed CBA/CaH as requested by The Jackson Laboratory, and an inbred colony established. These mice were chosen because they exhibit exhibits stable auditory brainstem response (ABR) thresholds for up to one year (Zheng et al., 1999; Sergeyenko et al., 2013; Muniak et al., 2018) and are commonly used to model normal animal hearing (Berlin, 1963; Ohlemiller et al., 2016).

2.2 Hearing status

All animals underwent ABR testing prior to experimentation. Mice were anesthetized using ketamine/xylazine (100 mg/kg; 20 mg/kg), and placed in a double-walled, sound-attenuating chamber (Sonora Technology, Gotenba, Japan) on a heating pad. Once areflexic to a toe-pinch, the recording, reference, and ground electrodes were placed in the skin on the cranial vertex, left pinna, and biceps femoris, respectively. A MF-1 speaker (Tucker-Davis Technologies, TDT) was positioned 45° off the midline and 10 cm from the pinna where alternating condensation and rarefaction click stimuli (100 μsec square wave pulses) and tone stimuli at 4, 8, 16, 24, 32, 40, and 48 kHz (5 ms duration,

0.5 ms rise/fall) were generated using a software-controlled signal processor, RZ6/BioSigRZ (TDT), and delivered from 90 to 30 dB SPL in 10 dB decremental steps to either ear separately. Stimulus presentations (n = 512) were delivered at a rate of 10/s for each level and the evoked responses were amplified (RA16PA/RA4LI; TDT), bandpass filtered from 0.5 to 3 kHz, recorded, and averaged (RZ6; TDT). Hearing threshold was defined as the sound level at which the peak ABR amplitude was four times the standard deviation of the average baseline noise level (Bogaerts et al., 2009). Only mice with normal auditory brainstem response thresholds and audiograms (Zheng et al., 1999; Taberner and Liberman, 2005; Muniak et al., 2018) were used in this study.

2.3 Tract tracing from the inferior colliculus to the lateral superior olive

Following ABR testing, each individual animal was placed in an atraumatic DKI stereotaxic head holder. The surgical approach to the IC began by making a skin incision on the dorsal surface of the head to expose the cranial sutures, bregma, and lambda. Approximately 5.2 mm posterior to bregma, a unilateral craniotomy (roughly 2 mm^2) was made overlying the IC using a #11 scalpel and a surgical pick. Pressure injections (0.5 µl at a rate of 100 nl per minute) of the retrograde tracer, Fluorogold (FG; 4% in saline, Fluorochrome, Denver, CO, USA) were made using a manual microinjector (Sutter Instruments, Novato, CA) with the needle tip directed into the central nucleus of the IC at a depth of 1.0– 1.5 mm by a micro manipulator (DKI Model 961, Tujunga, CA) using the stereotaxic coordinates of Paxinos and Franklin (2008). Following the IC injection, bone wax was applied to cover the craniotomy, and VetBond tissue adhesive was used to close the incision site for the post-surgical survival period. Retrograde tracer was placed in only one ICs in order to distinguish LSO neurons with ipsilateral or contralateral ascending projections (Supplementary Figure 1).

2.4 Tissue preparation

Fourteen days after an IC injection, animals were administered an intraperitoneal, lethal injection of Lethabarb (200 mg/kg bodyweight). When the animal was unresponsive to a paw pinch, the chest cavity was surgically opened and the heart isolated. The descending aorta was clamped, the right atrium punctured, and an 20g surgical needle, connected to a feeding syringe by flexible tubing, inserted into the left ventricle. The upper body and head were perfused transcardially with 3–5 ml of 1% sodium nitrate in phosphate-buffered saline, followed by 60 ml of 4% paraformaldehyde (in 0.1M phosphate buffer, pH 7.4) delivered at a rate of approximately 20 ml per minute. The head was removed, the calvaria partially opened to expose the brain, and the head post-fixed for another 2–3 h. The brain was then completely dissected out of the skull under an operating microscope and the brain post-fixed overnight at room temperature in 0.1M buffered 4% paraformaldehyde. The following day, the brain was embedded in a gelatin-albumin mixture hardened with 4% paraformaldehyde, sectioned into 60 µm-thick sections using a vibrating microtome (Leica VT1200S, Nussloch, DE), and collected in serial order in buffer using 24-well tissue culture plates.

2.5 Immunostaining with either GlyT2 or vGLUT2

FG-labeling of the LSO principal cells was observed following unilateral FG injections into one IC. Sections containing the SOC were counterstained for the glycine transporter 2 (GlyT2) using rabbit anti-GlyT2 (n = 7, Cat# PA5-69264, Thermofisher, Massachusetts, USA) or for the vesicular glutamate transporter 2 (vGLUT2) using rabbit anti-vGLUT2 (n = 5, Cat# 42-7800, Thermofisher, Massachusetts, USA). Sections were incubated in 0.1% Photoflo (Kodak, Rochester, NY, USA) for one hour, followed by an hour in 20% normal goat serum. Sections were washed three times in buffer and incubated at 4°C overnight in either 1:1000 rabbit anti-GlyT2 primary antibody and 2% normal goat serum or in 1:1000 rabbit anti-vGLUT2 primary antibody and 2% normal goat serum. One section per case was not exposed to the primary antibody and used as a negative control.

The following day, sections were exposed to either rabbit anti-GlyT2 or rabbit anti-vGLUT2 antibodies, rinsed in buffer, and placed in 1:200 goat anti-rabbit IgG cross-absorbed secondary antibody, Alexa FluorTM 488 (Cat# A-11008, RRID:AB_143165, Thermofisher, Massachusetts, USA). After one hour, sections were rinsed in buffer, mounted on standard microscope slides, and coverslipped with VectaShield (H-1400; Vector Labs, California, USA).

The principal neurons labeled from FG injections were viewed under the fluorescent microscope with a wide band ultraviolet excitation filter (Zeiss 19012 AT Filter). GlyT2 or vGLUT2 was viewed under the fluorescent microscope using 499 nm excitation filter [Zeiss (Colibri) Filter Set 59 HE]. The specific fluorescent label from the IC injections and antibody staining prevents cross-over of the label when viewing through the microscope. The MNTB served as a positive control for the GlyT2 neuronal labelling (Supplementary Figure 2).

2.6 Cresyl violet Nissl stain

Cresyl violet (CV) staining was performed on separate cases or sections whose fluorescent signals had faded using a protocol modified from Humason (1979). This basophilic dye stains acidic components of Nissl bodies, ribosomes, and chromatin to reveal the cell bodies and nuclei of neurons (and supporting cells and vasculature). The sections were hydrated in distilled water for 5 min, followed by a 10-min incubation in 0.1% CV dye at room temperature. The slides were rinsed in distilled water, followed by rinses in 70% alcohol, 95% alcohol and then differentiated (95% alcohol with 10 drops of glacial acetic acid) for one minute to remove excess staining. Rehydration in decreasing concentration of alcohol (one-minute periods in 70, 50, 30%, and distilled water) further removes excess CV for air-drying overnight and cover slipping with Permount the next day.

2.7 Quantification of LSO neurons and microscopy

Examination of tissue was conducted using a Zeiss AxioPlan microscope fitted for brightfield and fluorescent microscopy. The following objectives were used with our Zeiss AxioPlan microscope: 100x Oil Plan Neuofluar, NA 1.3; 40x Plan Apochromat NA 1.2; 25x Plan Neofluar NA 0.60; and 10x Planachromat NA 0.25). The high numerical aperture (NA) of each objective optimized final image resolution (300 dpi) and avoided empty magnification. Serial sections of the CV-stained LSO were imaged from the rostral to caudal extremities of the nucleus, guided by the facial and pontine nuclei respectively, to determine the boundaries of the LSO. Criteria for neuron identification and counting were established to reveal three cytologic categories: large periolivary (PO) cells, medium-sized principal cells, and small cells (Supplementary Figure 3).

Further analyses of neuron types were made using projection data and transmitter histochemistry for all sections through each LSO. Cell counts were performed in the contralateral and ipsilateral LSO nucleus for principal projecting (FG) neurons, GlyT2+ only neurons, vGLUT2+ only neurons, and those that double-labeled (FG and GlyT2 neurons or FG and vGLUT2 neurons). Brightfield photomontages (40x objective) at 3 focal planes through each section containing the LSO were compiled and stacked (300 dpi resolution, Adobe Photoshop 2024). Without moving the x-y position of the microscope stage, z-stacks of fluorescent photomicrographs through the same LSO were collected using the UV excitation filter, and the GlyT2 and vGLUT2 neurons from images taken with the 499 nm filter. Manual counts were conducted for the principal cells and for cells labeled with the antibodies; counts for double labeled neurons were made by superimposing the micrographs from the two different filters to determine which cells were double-labeled.

Neuronal criteria were established for the counts and included only cells with a clear, sharp somatic outline and a visible nucleus (Supplementary Figure 4 and Supplementary Table 1). Other blurry globules, holes, and artifacts in the tissue were ruled out using the criteria for labeled cells. A ratio of all the principal IC projecting neurons labeled in the ipsilateral and contralateral LSO was calculated for all cases. Photomicrographs (40x objective) of neurons labeled with either GlyT2 or vGLUT2 were imported into *Photoshop* and the cell body outline was drawn and filled on a separate layer to represent the cell body silhouette area. TIFF files of the drawn silhouette area were loaded into FIJI ImageJ2 (V 2.14.0/1.54f) to quantify the area of the GlyT2 and vGLUT2 somata.

Counts for the projecting neurons, glycinergic neurons, glutamatergic neurons, and CV-stained neurons were compared and related to previous counts reported in the literature. No correction factor was applied in these counts (Hedreen, 1998). Statistical analyses were performed on the data output from the neuronal counts, ratios, and cell size using Descriptive Statistics, Mann Whitney two-tailed test, and Two-way ANOVA using Šídák's Multiple Comparison Test (Prism 9, 2021 GraphPad software, San Diego, CA USA). Means, standard deviations, p-values, and statistical tests are provided.

3 Results

Principal neurons with ascending projections and intrinsic neurons with descending projections exhibited similar somatic anatomy using standard tracing techniques, but could be differentiated by chemical stains: intrinsic efferent neurons stained with cholinergic markers, whereas principal neurons did not. Within this grouping, there are principal cells with ipsilateral or contralateral projections that have been inferred to be glycinergic or glutamatergic, respectively (Glendenning and Mastereton, 1983; Saint Marie et al., 1989; Saint Marie and Baker, 1990; Moore et al., 1995; Mellott et al., 2021). In most studies, glycinergic neurons are reported to project almost entirely to the ipsilateral IC (Saint Marie and Baker, 1990). In the gerbil, 76% of the principal neurons are glutamatergic with contralateral projections to the IC (Mellott et al., 2021), whereas in the C57BL/6 mouse, 98.6% of vGLUT2 neurons projected to the contralateral IC (Haragopal et al., 2023). In the CBA/CaH mouse, half of the retrogradely labeled cells had projections to the ipsilateral IC and the other half to the contralateral IC (Williams et al., 2022). Our goal was to determine the chemistry associated with the laterality of these IC projections. We labeled glycinergic and glutamatergic neurons using antibodies directed against the transporters, GlyT2 and vGLUT2, respectively, in tissue that contained retrogradely labeled LSO principal cells following retrograde tracer injections into the IC.

3.1 Labeling of LSO principal cells co-labeled with GlyT2

Large unilateral retrograde tracer (FG) injections were made into the CNIC to label LSO principal neurons. A bilateral, mostly homogeneous labeling pattern of neurons filled both LSO nuclei (Figure 1, yellow). Within the LSO, a few larger, polygonal neurons were somewhat concentrated around the dorsal hilus within the borders of the LSO. These multipolar cells were distinctly larger than principal cells and could also be found lightly scattered throughout the LSO. They resembled the previously described periolivary neurons (PO) located within and around the LSO (Williams et al., 2022).

In the same tissue, GlyT2 immunohistochemistry was performed to reveal labeled cells and fibers (Figure 1A-row 2 and Figure 1B-row 4). The majority of GlyT2 labeled neurons were medium in size, fusiform in shape, and resembled principal cells (Williams et al., 2022). These cells were distributed throughout the LSO. A subset of GlyT2-labeled neurons was small and oval-shaped, featuring scant cytoplasmic staining by CV; these did not co-label with the retrograde tracer injected in the IC. Another small population of neurons had larger, oblong somata residing within and around the LSO, and resembled previously described PO cells (Supplementary Figure 5A).

Principal cells projecting to the IC were co-labeled by GlyT2 in the ipsilateral and contralateral LSO (Figure 2), were surrounded by neighboring GlyT2 positive axons and dendrites, and featured an opaque nucleus that was readily identifiable. The nuclei in FG-labeled neurons were obscured by the cytoplasmic fluorescence. By illuminating and photographing the fluorescence of the retrograde tracer using one fluorescent filter, and capturing the fluorescence

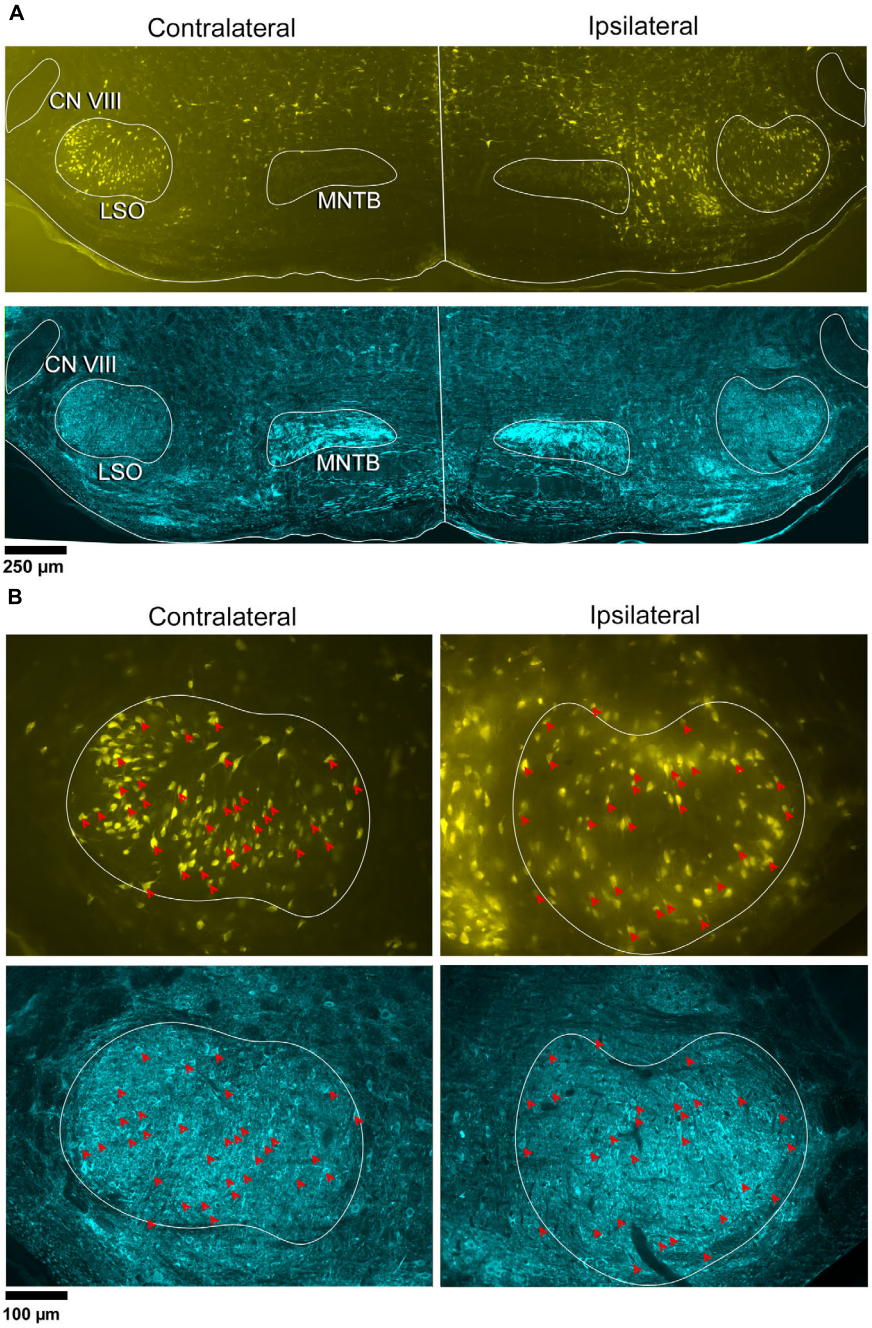

FIGURE 1
Photomicrographs of IC projecting neurons (yellow) and GlyT2 neurons (blue) in the LSO. Principal neurons were labeled via a unilateral injection of FluoroGold (FG) into the right IC. This tissue was then counterstained by GlyT2 immunohistochemistry. **(A)** Low magnification montages of the SOC (10x objective) show the contralateral and ipsilateral LSO with retrogradely labeled principal neurons (top panels, yellow) and GlyT2 staining (bottom panels, blue). Micrographs of the same LSO were captured using a different fluorescent filter to reveal both types of labeled neurons. The MNTB contains well-labeled GlyT2 neurons as a positive control. **(B)** Higher magnification images (25x objective) of the same LSOs shown in A, illustrating double-labeled FG and GlyT2 neurons (red arrowheads) in relatively equal numbers. These results also show that some GlyT2 neurons project to the ipsilateral IC, some to the contralateral IC, and some to neither. FG, FluoroGold; GlyT2, glycine transporter 2; LSO, lateral superior olive; CN VIII, vestibulocochlear nerve; IC, inferior colliculus; MNTB, medial nucleus of the trapezoid body; SOC, superior olivary complex. Scale bar equals 250 µm **(A)** and 100 µm **(B)**.

of the GlyT2 label with another filter, the two images of the same section were overlayed to reveal a population retrogradely labeled cells that co-labeled with GlyT2 (Figure 3). Notably, not all labeled IC-projecting neurons were GlyT2-positive, and not all GlyT2-positive neurons were IC-projecting. Unlike previous reports (Glendenning and Mastereton, 1983; Saint Marie et al., 1989; Saint Marie and Baker, 1990; Mellott et al., 2021; Haragopal et al., 2023), the co-labeled neurons in our study demonstrated that glycinergic neurons projected in equal numbers to the ipsilateral and contralateral IC.

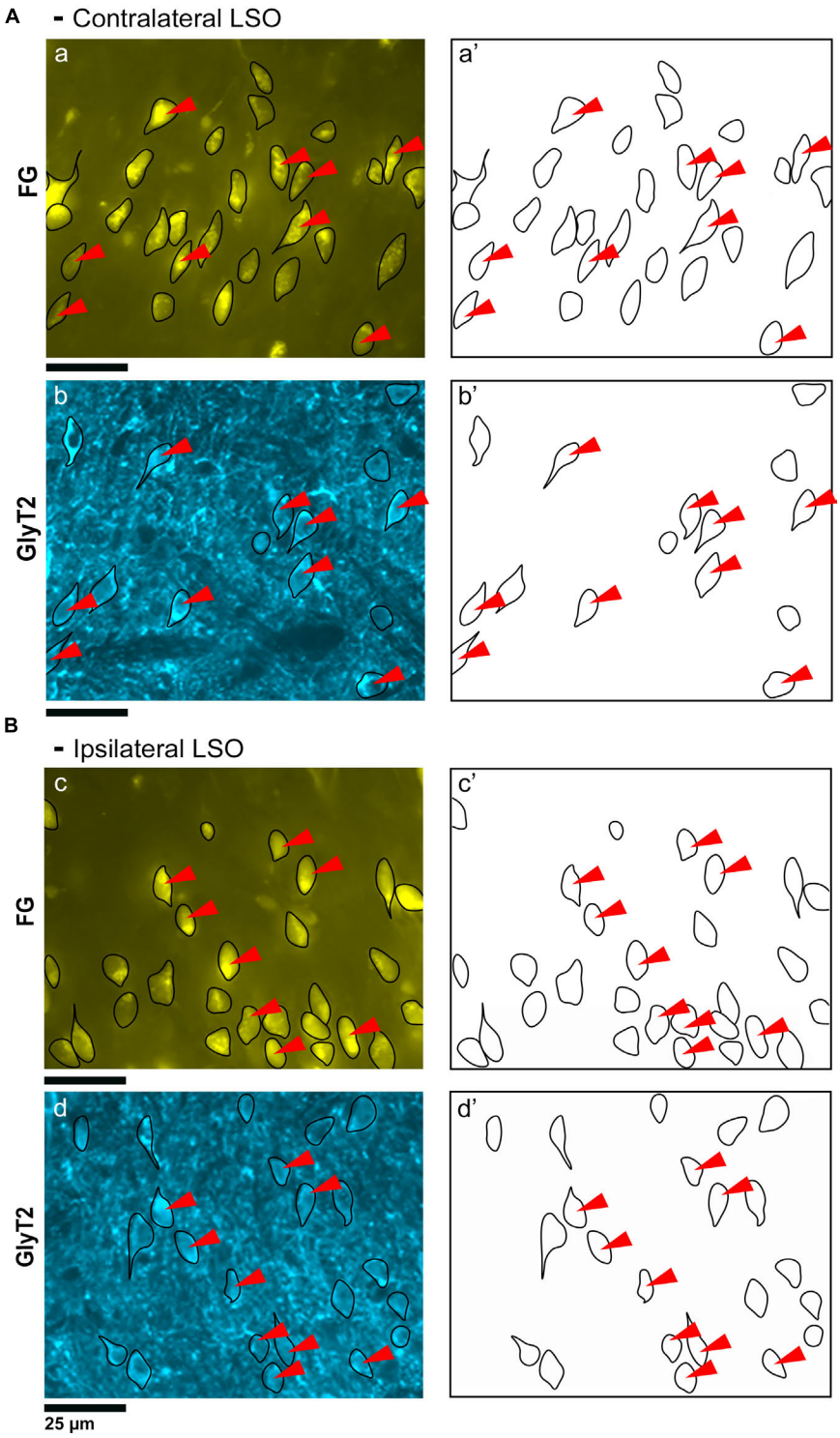

FIGURE 2
Photomicrographs (40x objective) and drawings of LSO principal neurons (yellow) labeled via FG injections into the IC and counterstained with GlyT2 (blue). **(A)** Top row shows FG-labeled neurons (a, yellow with black outlines) and corresponding drawing of the labeled cells (a') from the contralateral LSO. In row 2, GlyT2-labeled cells are shown with black outlines (b) and corresponding drawings (b'). The red arrowheads indicate the double-labeled cells in the photomicrographs and drawings. **(B)** Upper row shows ipsilateral projecting neurons (FG, yellow) with black outlines (c) and corresponding drawings of the labeled cells (c'). The bottom row shows that the ipsilateral projecting GlyT2-labeled neurons (d, d') have a similar size and shape compared to the contralateral-projecting neurons. The IC-projecting cells that co- label with GlyT2 immunostaining are indicated by red arrowheads. FG, FluoroGold; GlyT2, glycine transporter 2; LSO, lateral superior olive; CN VIII, vestibulocochlear nerve; IC, inferior colliculus; MNTB, medial nucleus of the trapezoid body; SOC, superior olivary complex. Scale bar equals 25 µm.

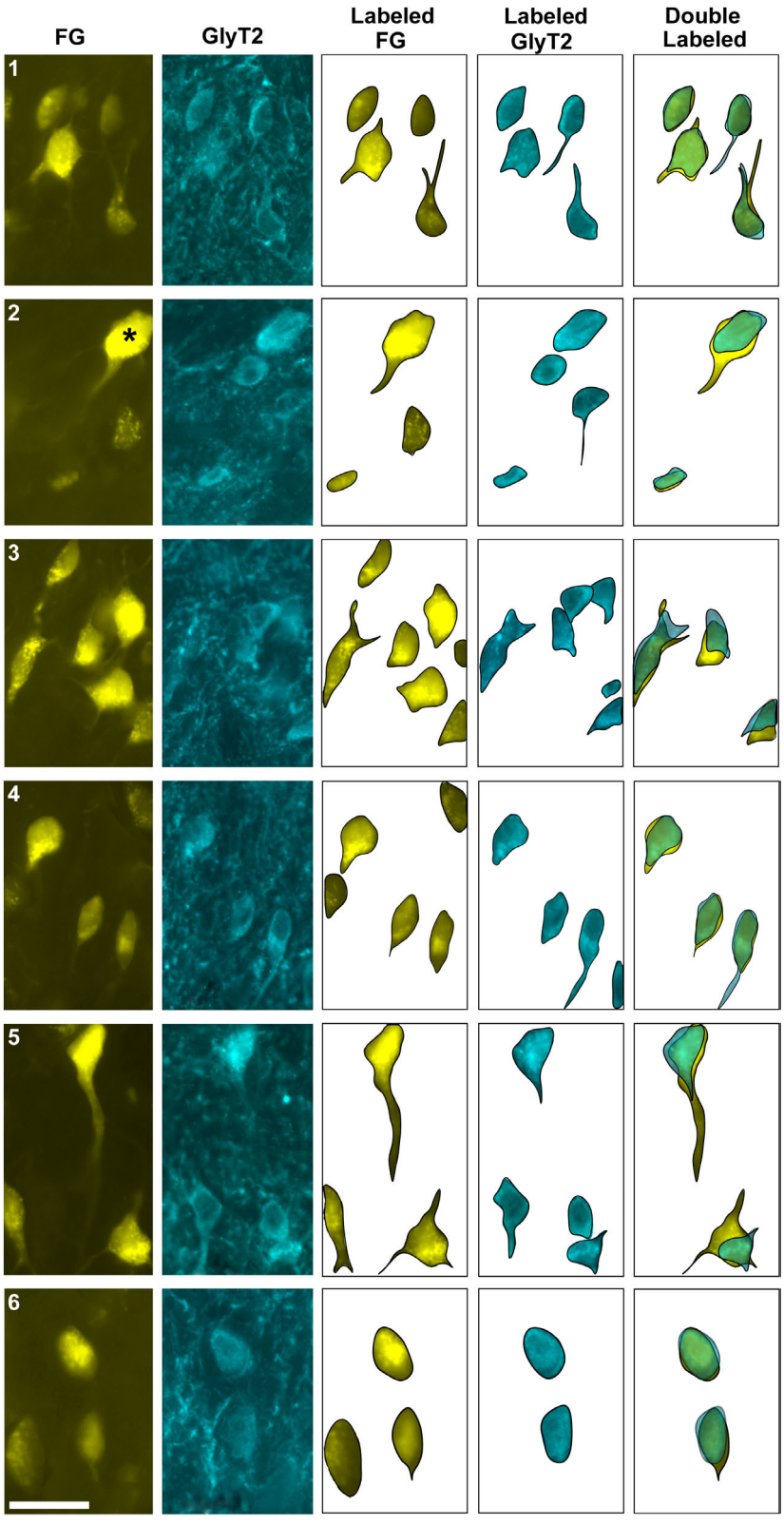

FIGURE 3
Photomicrographs (100x oil objective) and drawings of double-labeled LSO neurons (rows 1–6). Principal neurons were first labeled via a unilateral injection of the retrograde tracer (FG) into the IC (column 1). This tissue was then stained by GlyT2 antibodies (column 2) revealing that some FG neurons were also labeled for GlyT2 in either the ipsilateral or contralateral LSO. Not all principal neurons were double labeled. The neuronal shape of FG and GlyT2 neurons from either the ipsilateral or contralateral LSO are shown (columns 3–4). Double-labeled neurons containing FG and GlyT2 are identified by their overlapping position and near identical somatic features (column 5). An occasional large neuron resembling periolivary neurons (* in row 2) was doubled labeled. Not all GlyT2-stained principal neurons project to the IC, and not all IC-projecting neurons co-label with GlyT2. FG, FluoroGold; GlyT2, glycine transporter 2; LSO, lateral superior olive; CN VIII, vestibulocochlear nerve; IC, inferior colliculus; MNTB, medial nucleus of the trapezoid body; SOC, superior olivary complex. Scale bar equals 25 μm.

3.2 Labeling of LSO principal cells co-labeled with vGLUT2

In a separate set of animals, vGLUT2 immunohistochemistry was used to counterstain the retrogradely labeled IC-projecting neurons in order to compare and contrast co-labeled neurons within the ipsilateral and contralateral LSO. The labeling pattern of vGLUT2 for retrogradely labeled principal neurons was similar to that of GlyT2 labeling: there was a population of ipsilateral and contralateral IC-projecting neurons that co-labeled for vGLUT2. Not all IC-projecting neurons labeled with vGLUT2, and not all vGLUT2-labeled neurons were IC-projecting (Figure 4). The vGLUT2 antibodies labeled cell bodies and surrounding fibers, which created a level of background staining. Regardless, the fusiform appearance of principal neurons was evident (Figures 4, 5). Consistent with other staining techniques in the LSO, a small population of distinctly larger, multipolar neurons tended to reside around the dorsal hilus and resembledPO neurons (Supplementary Figure 5B).

Two different fluorescent filters were used for separately illuminating the IC-projecting neurons and the vGLUT2 neurons so that the images could be superimposed to reveal three types of neurons: (1) retrogradely labeled principal cells that co-labeled with vGLUT2; (2) principal cells that were vGLUT2 negative; and (3) vGLUT2 neurons that did not co-label with principal neurons projecting to the IC (Figures 5, 6). These neurons were observed bilaterally in the LSO.

3.3 Distribution of labeled LSO neurons

The LSO of representative IC injection cases, counterstained by GlyT2 and vGLUT2 antibodies, were drawn, aligned in register, and stacked in the z-plane. The positions retrogradely labeled LSO principal neurons, immunostained GlyT2 neurons, immunostained vGLUT2 neurons, and double-labeled neurons (FG and GlyT2 or FG and vGLUT2) were mapped. The results demonstrate that these various principal neurons are intermixed and distributed relatively uniformly throughout the LSO (Figure 7). The double-labeled neurons represent a smaller population compared to that of the IC projecting neurons or the GlyT2 and vGLUT2 immunolabeled neurons alone. Importantly, double-labeled IC projecting cells were observed in both the ipsilateral and contralateral LSO.

3.4 Counts of double-labeled neurons

The double-labeled neurons (FG and GlyT2 or FG and vGLUT2) were quantified by performing neuronal counts across serial sections from separate GlyT2 (n = 7) and vGLUT2 (n = 5) cases (Table 1). These cases received a single unilateral injection of a retrograde tracer, FG, into the IC. We observed an average of 704 ± 201.6 labeled neurons in the ipsilateral LSO and 701.6 ± 152.2 labeled neurons in the contralateral LSO. The spatial distribution of the projecting neurons in the LSO nuclei appeared symmetrical (Figure 7). This qualitative assessment was confirmed by the near-equal numbers of ipsilateral and contralateral projecting neurons whose ratio averaged near unity (Tables 1, 2A-projecting cells).

The experiments on retrograde labeling coupled to transmitter immunocytochemistry were conducted in two separate series, separated in time by several months. We first made IC injections for the GlyT2 counterstaining (n = 7 mice), and after the resulting histology was finished, initiated IC injections for the vGLUT2 counterstaining (n = 5 mice). In spite of following the same procedures for both sets of experiments, injections from the second set resulted in a larger number of retrogradely-labeled cells compared to those of the first. As a result, we performed an ipsilateral:contralateral ratio analysis within each individual mouse rather than on raw counts; this strategy normalized the data from all the animals (Table 2). The IC-projecting GlyT2 neurons yielded an average ipsilateral:contralateral count ratio of 0.98 ± 0.29 (Table 2B), whereas the ipsilateral:contralateral count ratio for IC-projecting vGLUT2 neurons was 0.98 ± 0.08 (Table 2C). There was no statistical difference between these two sets of ratios (Mann Whitney two-tailed test, $p = 0.876$).

The IC-projecting neurons that doubled-labeled with GlyT2 exhibited bilateral symmetry in the labeling pattern across all seven cases, with a count ratio equal to 1.05 ± 0.23 (Table 2D). The average number of double-labeled neurons in the ipsilateral (GlyT2: 168.6 ± 31.8; vGLUT2: 187.0 ± 27.2) and contralateral (GlyT2: 161.0 ± 47.6; vGLUT2: 197.6 ± 25.7) LSO was also relatively consistent across animals (n = 12; Table 1) and revealed no statistical difference (Table 3, 2-way ANOVA).

The symmetry in the labeling pattern for GlyT2 double-labeled projecting neurons was further evident across all cases by dividing the number of double-labeled neurons in the ipsilateral nucleus by the total number of IC projecting neurons in the ipsilateral nucleus, which revealed 29.7 ± 6.3% of neurons in the ipsilateral LSO were co-labeled and 26.3 ± 8.3% of neurons in the contralateral LSO were co-labeled (Table 1). The double-labeled neurons were intermixed with single-labeled projecting neurons and single-labeled GlyT2 neurons. There was no significant difference in the percentages when comparing the co-labeled neurons in the ipsilateral versus the contralateral LSO (2-way ANOVA, $p = 0.88$; Figure 8A and Table 3).

When double-labeled vGLUT2 neurons were averaged across five cases, the ipsilateral LSO contained 21.4 ± 2.3% IC-projecting neurons compared to the 24.6 ± 2.8% contralateral IC-projecting neurons (Table 1). No significant difference was found in the percentages of double-labeled vGLUT2 neurons with ipsilateral or contralateral projections (2-way ANOVA, p = 0.79; Figure 8A and Table 3). In a similar way, the percentages of doubled-labeled GlyT2 projecting neurons and vGLUT2 projecting neurons in the ipsilateral and contralateral LSO nuclei also revealed no significant differences (Table 3).

3.5 Cresyl violet staining features

In CV-stained material, the cytoplasm of principal cells lacked large stacks of rough endoplasmic reticulum, also known as Nissl bodies. Free ribosomes, however, were plentiful and gave the cytoplasm a fine, granular light-blue texture. A pale spherical

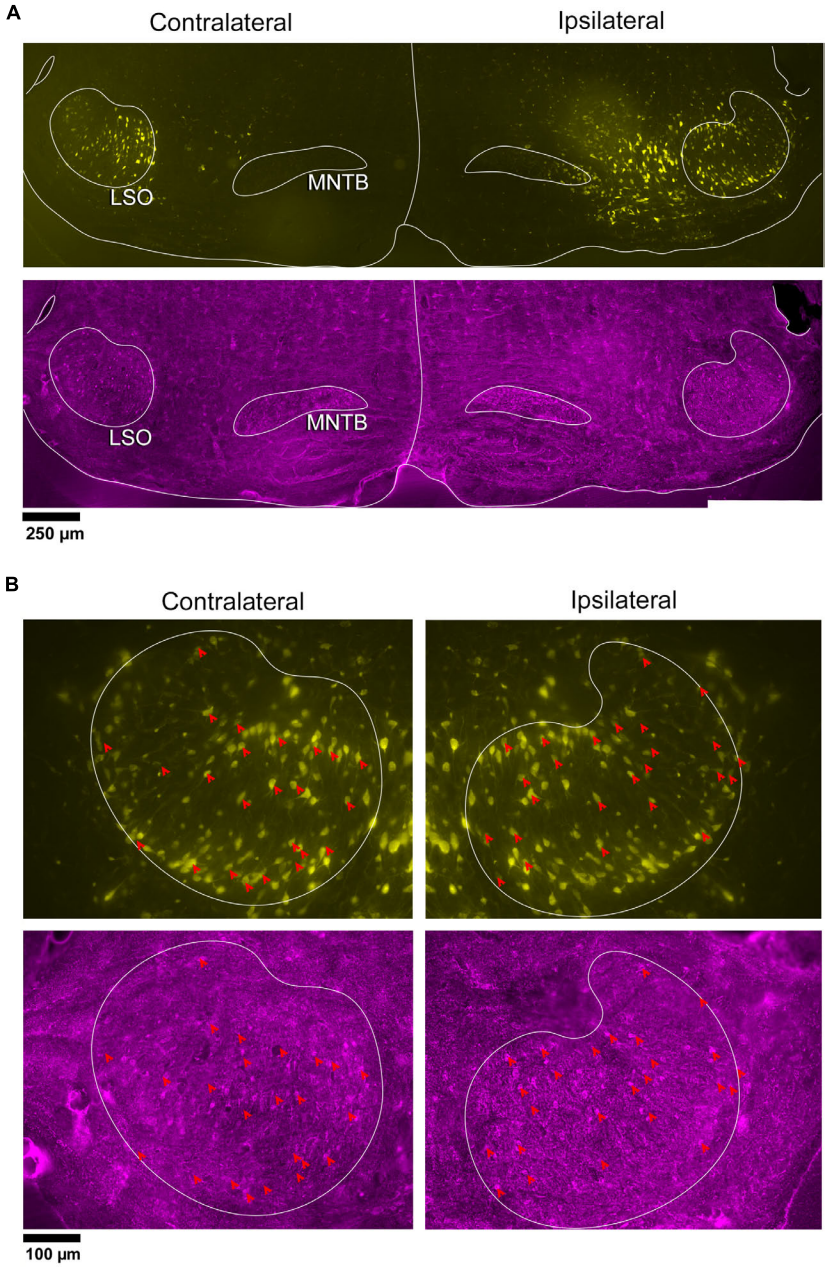

FIGURE 4
Photomicrographs of IC projecting neurons (yellow) and vGLUT2 neurons in the LSO. Principal neurons were labeled via a unilateral injection of the retrograde tracer, FG (yellow), into the right IC and counterstained with vGLUT2 immunohistochemistry (magenta fluorescence). **(A)** Low magnification montages of the SOC (10x objective) show the contralateral and ipsilateral LSO with retrogradely labeled principal neurons (top panels, yellow) and vGLUT2 staining (bottom panels, magenta). **(B)** Higher magnification images (25x objective) of the same tissue in A, revealed double-labeled neurons for FG (upper panels) and vGLUT2 (bottom panels) in the contralateral and ipsilateral LSO (red arrowheads) in approximately equal numbers. Some vGLUT2 neurons project to the ipsilateral IC, some to the contralateral IC, and some to neither. vGLUT2, vesicular glutamate transporter 2; others as in Figure 1.

nucleus with a single nucleolus occupied the middle of the spindle-shaped cell body. Views of the principal cell away from its center-of-gravity often missed the pointed ends of the spindle but revealed an oval cell body dominated by the presence of the central nucleus (Williams et al., 2022).

Counts in CV material were made according to four types of cells identifiable in the tissue (Supplementary Figure 3 and Supplementary Table 1): principal cell with nucleus present, principal cell with no nucleus present, small cell with nucleus present, small cell with no nucleus present. A total of 2277 neurons were counted in the left LSO, and a total of 2785 counted in the right LSO. For the IC projecting neurons, we counted 703 ± 174.7 labeled neurons per LSO. From previous work (Williams et al., 2022), there is an average of 362 ± 25.4 lateral olivocochlear efferents and from this study, an average of 412 ± 54.5 GlyT2 and 528 ± 106.6 vGLUT2 neurons in each LSO nucleus. The sum of

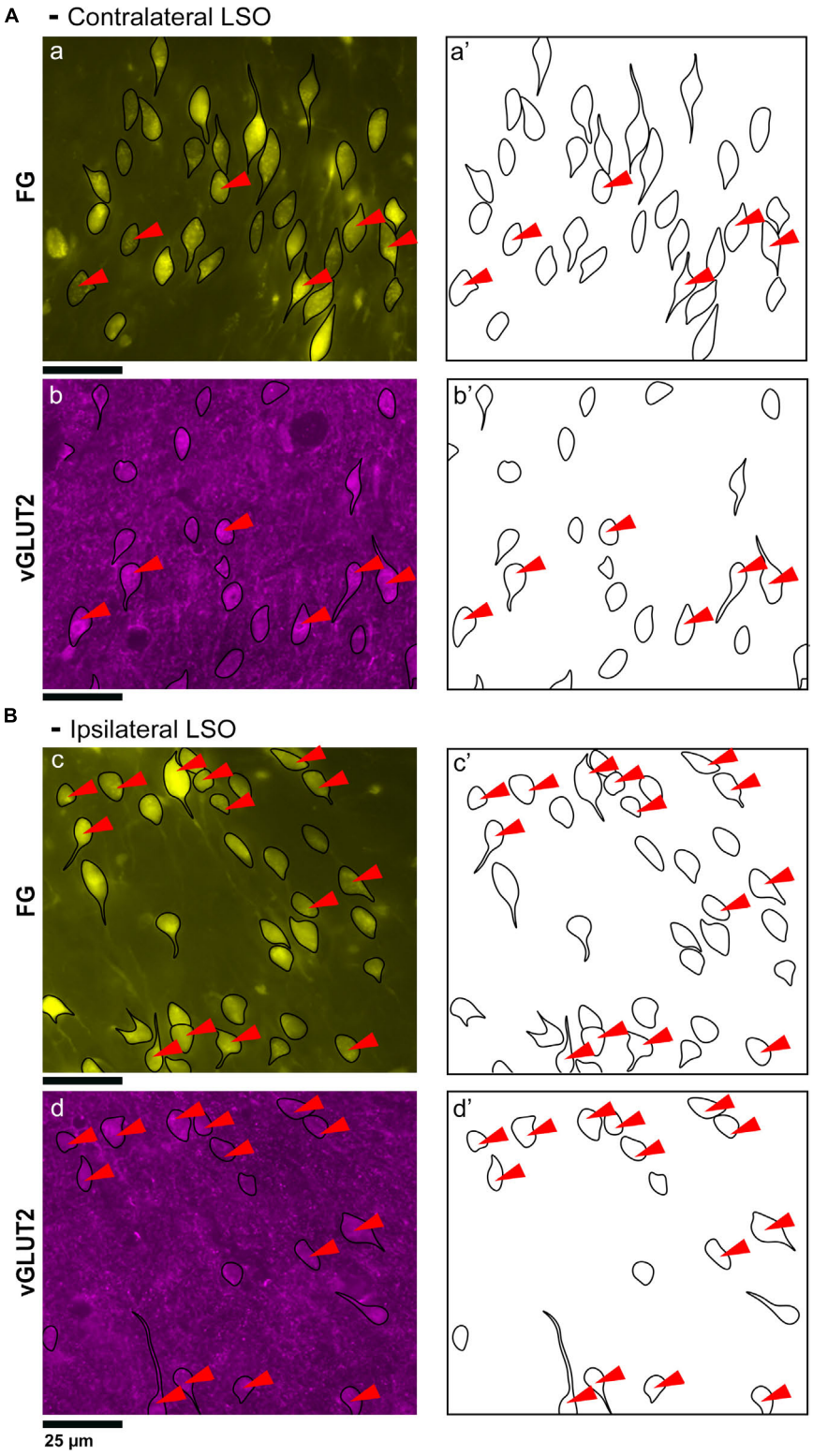

FIGURE 5
Photomicrographs (40x objective) and drawings of LSO principal neurons (yellow) labeled by FG injections into the IC and immunostained for vGLUT2 (magenta). **(A)** Top row shows FG-labeled neurons (a, yellow with black outlines) and corresponding drawing of the labeled cells (a') from the contralateral LSO. In row 2, vGLUT2-labeled cells are shown (b, with black outlines) and drawings only (b'). The red arrowheads indicate the double-labeled cells in the photomicrographs (a, b) and schematic drawings (a', b'). **(B)** Row c shows ipsilateral projecting neurons (FG, yellow with black outlines) and corresponding drawings of the labeled cells (c'). The bottom row shows that the ipsilateral vGLUT2-labeled neurons (d) can be matched to the contralateral-projecting neurons by location and somatic shape (d'). The double-labeled neurons are indicated by red arrowheads. These results confirm that some vGLUT2 neurons project to the ipsilateral IC, some to the contralateral IC, and some not to either. FG, FluoroGold; GlyT2, glycine transporter 2; LSO, lateral superior olive; CN VIII, vestibulocochlear nerve; IC, inferior colliculus; MNTB, medial nucleus of the trapezoid body; SOC, superior olivary complex. Scale bars equal 25 µm.

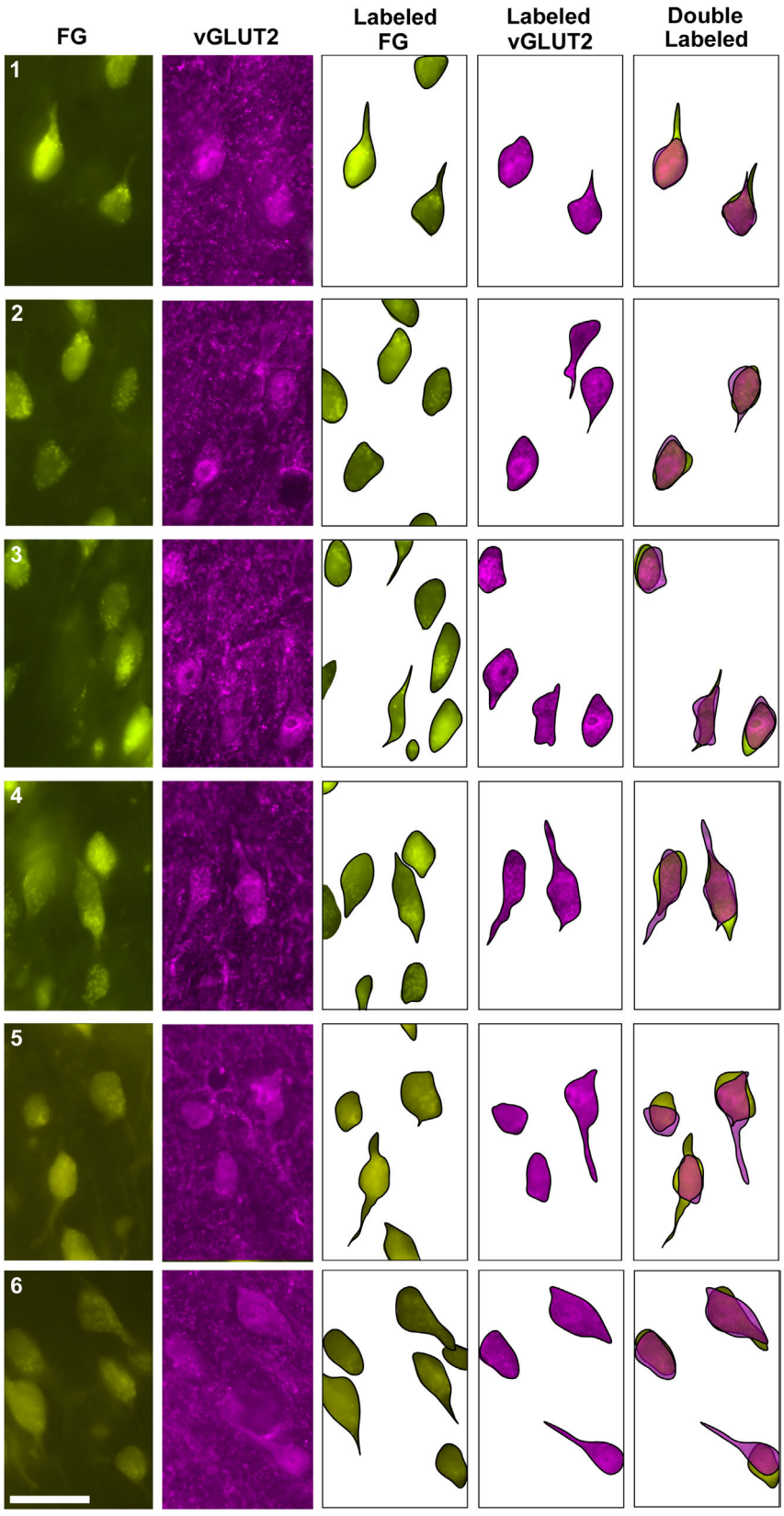

FIGURE 6
Photomicrographs (100x oil objective) and drawings of double-labeled LSO neurons (rows 1–6). Principal neurons were first retrogradely labeled via a unilateral injection of FG into the IC (column 1). This tissue was then stained by vGLUT2 antibodies (column 2) revealing that some FG neurons were co-labeled by a vGLUT2 antibody in either the ipsilateral or contralateral LSO. Not all principal neurons were double labeled. The neuronal shape of FG and vGLUT2 neurons from either the ipsilateral or contralateral LSO are shown (columns 3–4). Double-labeled neurons containing FG and vGLUT2 are identified by their overlapping position and near identical somatic features (column 5). Not all vGLUT2-stained neurons project to the IC, and not all IC-projecting neurons co-label with vGLUT2. Scale bar equals 25 μm.

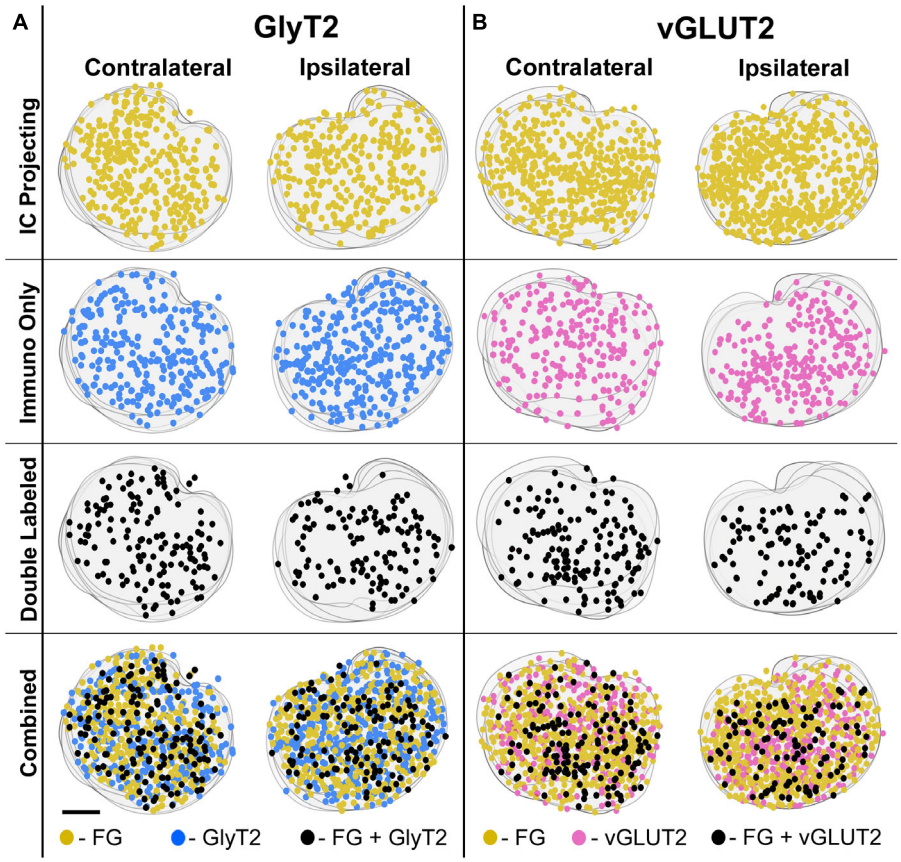

FIGURE 7
Representative IC-injection cases counterstained by GlyT2 antibodies or vGLUT2 antibodies demonstrate their bilateral distribution in the LSO. Neurons that project to the IC and/or are immunostained by GlyT2 **(A)** or vGLUT2 **(B)** antibodies were mapped onto outlines of their corresponding sections and collapsed in a z-stack for the contralateral and ipsilateral LSO. The distribution of labeled cells was relatively uniform and bilaterally symmetrical across the LSO for all cases, consistent with the tonotopic results of Williams et al. (2022). FG, FluoroGold; GlyT2, glycine transporter 2; LSO, lateral superior olive; CN VIII, vestibulocochlear nerve; IC, inferior colliculus; MNTB, medial nucleus of the trapezoid body; SOC, superior olivary complex. Scale bar equals 100 μm.

the average number of IC-projecting neurons, LOCs, GlyT2 and vGLUT2 neurons in one LSO equals 2005. The projection pattern of these neurons is summarized in Figure 8B.

3.6 Soma silhouette area of the labeled neurons

Neuronal size variations were observed from the different sets of stained tissue—LSO projecting neurons revealed qualitative medium and large neurons; GlyT2-labeled neurons were small, medium, and large (Figures 9A–C); and vGLUT2-stained neurons were medium and large. These qualitative observations were confirmed in quantitative analyses using soma silhouette area. The data confirmed a small population of small glycinergic neurons that were revealed by GlyT2 antibodies and related to small LSO neurons stained by CV (Figure 9).

Analysis of soma silhouette area was used to analyze neuron size groups in the LSO (Supplementary Figure 6). In our previous study (Williams et al., 2022), we determined that the principal neurons have an average cell area of 123.9 ± 26.6 μm^2, comparable to medium sized GlyT2- and vGLUT2-labeled neurons in this study.

GlyT2 neurons could be classified into three size categories (Figure 9): large cells, which had polygonal somata and resided around the borders of the LSO; medium-sized neurons, corresponding to descriptions of the principal cells with fusiform somata and unipolar or bipolar dendritic extensions; and small cells featuring somata that were < 40 μm^2, oval, and containing a pale spherical nucleus.

Soma silhouette values for GlyT2 neurons were consistent with a tri-modal distribution (Figure 10 and Table 4): small GlyT2 neurons had an average cell size equal to 37.73 ± 8.30 μm^2, the medium sized neurons had an average size equal to 100.9 ± 25.54 μm^2, and the large neurons had an average cell size equal to 215.0 ± 48.46 μm^2 (Supplementary Figure 6A). In the population of LSO-projecting neurons that co-labeled with GlyT2, these small neurons of the mouse LSO had not been previously described.

Neurons labeled with vGLUT2 antibodies revealed a relatively uniform group of cells that resembled the descriptions of the principal neurons. These neurons were medium sized, averaging 114.0 ± 40.61 μm^2 (Figure 10). A small population of large polygonal neurons were observed around the LSO borders and fit

TABLE 1 Counts for LSO neurons in the ipsilateral and contralateral LSO nuclei.

Animal ID	Immuno label stain	Total IC projecting	IC projecting without immuno	Immuno label	Double labeled	% Double labeled
Ipsilateral						
AM1634	GlyT2	559	439	327	120	21.5
AM1643	GlyT2	603	415	485	188	31.2
AM1644	GlyT2	625	410	447	215	34.4
AM1655	GlyT2	651	494	468	157	24.1
AM1656	GlyT2	465	280	323	185	39.8
AM1657	GlyT2	661	487	381	174	26.3
AM1671	GlyT2	464	323	424	141	30.4
Average ± SD		575.4 ± 82.8	406.9 ± 79.8	407.9 ± 65.6	168.6 ± 31.8	29.7 ± 6.3%
Contralateral						
AM1634	GlyT2	619	542	352	77	12.4
AM1643	GlyT2	676	530	491	146	21.6
AM1644	GlyT2	558	401	427	157	28.1
AM1655	GlyT2	783	601	431	182	23.2
AM1656	GlyT2	582	356	415	226	38.8
AM1657	GlyT2	704	507	432	197	27.9
AM1671	GlyT2	446	304	369	142	31.8
Average ± SD		624 ± 109.7	463 ± 109.8	416.7 ± 45.7	161.0 ± 47.6	26.3 ± 8.3%
Ipsilateral						
AM1664	vGLUT2	1129	921	555	208	18.4
AM1665	vGLUT2	740	556	574	184	24.9
AM1671	vGLUT2	691	548	339	143	20.7
AM1672	vGLUT2	876	687	546	189	21.6
AM1673	vGLUT2	984	773	603	211	21.4
Average ± SD		884 ± 108.9	697 ± 156.6	523.4 ± 105.4	187.0 ± 27.2	21.4 ± 2.3%
Contralateral						
AM1664	vGLUT2	1020	791	593	229	22.5
AM1665	vGLUT2	703	509	576	194	27.6
AM1671	vGLUT2	699	541	319	158	22.6
AM1672	vGLUT2	732	528	591	204	27.9
AM1673	vGLUT2	897	694	588	203	22.6
Average ± SD		810.2 ± 42.8	612.6 ± 124	533.4 ± 120.0	197.6 ± 25.7	24.6 ± 2.8

Manual counts for LSO neurons labeled via IC retrograde injections and immune-histochemistry with GlyT2 ($n = 7$) or vGLUT2 ($n = 5$) were counted to reveal populations of single and double labeled neurons.

the descriptions of PO neurons (mean 230.4 ± 42.15 μm^2; Table 4 and Supplementary Figure 6B). The IC-projecting neurons that co-labeled with vGLUT2 showed similar sizes to vGLUT2 neurons that did not project to the IC. No small neurons were stained by vGLUT2 antibodies.

3.7 Summary

The present findings demonstrate that the population of principal cells of the LSO include bilateral and symmetric projections of glycine and glutamate cells to the IC in the CBA/CaH mouse. We previously documented that these projections are tonotopic (Williams et al., 2022). The organization of these projections to the IC add to our knowledge of how excitation and inhibition contribute to the separate binaural processing demands for localizing high and low frequency sounds. We also observed that not all GlyT2- or vGLUT2-labeled neurons project to the IC: these must project to other brain stem sites, such as the cochlear nucleus, superior olivary complex, nuclei of the lateral lemniscus, or thalamus.

TABLE 2 Ratio between neurons in the ipsilateral and contralateral LSO nuclei labeled with either FG, GlyT2, vGLUT2, or double labeled.

Counts	Label	Ipsilateral	Contralateral	Ratio
A Projecting cells				
Case				
AM1634	FG	559	619	0.91
AM1643	FG	603	676	0.89
AM1644	FG	625	558	1.12
AM1655	FG	651	783	0.83
AM1656	FG	465	582	0.79
AM1657	FG	661	704	0.94
AM1671	FG	464	446	1.04
AM1664	FG	1129	1020	1.10
AM1665	FG	740	703	1.05
AM1671	FG	691	699	0.98
AM1672	FG	876	732	1.19
AM1673	FG	984	897	1.09
Total	–	8448	8419	1.00
B GlyT2 cells				
Case				
AM1634	GlyT2	337	352	0.96
AM1643	GlyT2	485	491	0.99
AM1644	GlyT2	447	427	1.05
AM1655	GlyT2	468	431	1.09
AM1656	GlyT2	323	415	0.78
AM1657	GlyT2	381	432	0.88
AM1671	GlyT2	424	369	1.14
Total	–	2865	2917	0.98
C vGLUT2 cells				
Case				
AM1664	vGLUT2	555	593	0.94
AM1665	vGLUT2	574	576	0.99
AM1671	vGLUT2	339	319	1.06
AM1672	vGLUT2	546	591	0.92
AM1673	vGLUT2	603	588	1.02
Total	–	2617	2667	0.98
D Double labeled cells				
Case				
AM1634	FG + GlyT2	120	77	1.56
AM1643	FG + GlyT2	188	146	1.29
AM1644	FG + GlyT2	215	157	1.37
AM1655	FG + GlyT2	157	182	0.86
AM1656	FG+ GlyT2	185	226	0.82
AM1657	FG + GlyT2	174	197	0.88
AM1671	FG + GlyT2	141	142	0.99
Total FG + GlyT2	–	1180	1127	1.05
AM1664	FG + vGLUT2	208	229	0.91
AM1665	FG + vGLUT2	184	194	0.95
AM1671	FG + vGLUT2	143	158	0.91
AM1672	FG + vGLUT2	189	204	0.93
AM1673	FG + vGLUT2	211	203	1.04
Total FG + vGLUT2	–	935	988	0.95

The ratio of labeled neurons between ipsilateral and contralateral neuronal counts was calculated for each case by dividing the ipsilateral count by the contralateral count. A ratio closest to 1.0 inferred symmetrical labeling between neuronal counts of both nuclei. **(A)** Principal neurons labeled via retrograde tracing in ipsilateral and contralateral LSO nuclei were counted. The total average ratio for the 11 cases is 1.0. Cases with alternate sections labeled with either GlyT2 or vGLUT2 and were counted for the principal neurons independently. **(B)** GlyT2 neurons labeled in the ipsilateral and contralateral LSO nuclei were counted. The average ratio of GlyT2 neurons between both nuclei was 0.98. **(C)** vGLUT2 neurons labeled in the ipsilateral and contralateral LSO nuclei were counted and the resulted in an average ratio equal to 0.98. The ratio of GlyT2 neurons between both nuclei was 0.98. **(D)** Doubled neurons were those retrogradely labeled neurons counterstained with either GlyT2 or vGLUT2. The average ratio of principal neurons double labeled with GlyT2 equalled 1.05; and the average ratio of principal neurons double labeled with vGLUT2 equalled 0.95.

TABLE 3 2-WAY ANOVA results comparing projecting neurons double labeled with GlyT2 or vGLUT2 immuno-histochemistry.

Double label projecting cell comparison				
Average % of double labeled cells		Mean Diff.	*P*-value	Outcome
GlyT2-ipsi	GlyT2-contra	3.4	0.88	ns
29.7	26.3			
GlyT2-ipsi	vGLUT2-ipsi	7.8	0.24	ns
29.7	21.4			
GlyT2-ipsi	vGLUT2-contra	3.2	0.94	ns
29.7	24.6			
GlyT2-contra	vGLUT2-ipsi	4.4	0.79	ns
26.3	21.4			
GlyT2-contra	vGLUT2-contra	−0.17	>0.99	ns
26.3	24.6			
vGLUT2-ipsi	vGLUT2-contra	−4.6	0.79	ns
21.4	24.6			

Comparisons were made between the ipsilateral and contralateral LSO nuclei and between stains. The results revealed no significant difference across all comparisons. Data expanded from Table 1. ipsilateral, ipsi; contralateral; contra.

4 Discussion

The ability to determine the spatial location of a sound is a remarkable accomplishment of the ears and brain. The localization of a sound source is computed by acoustic cues that are created by the physical interactions of the sound with the head and the two ears, including pinna and ear canals. The cues are analyzed by the central auditory system, which uses the neural signals to create

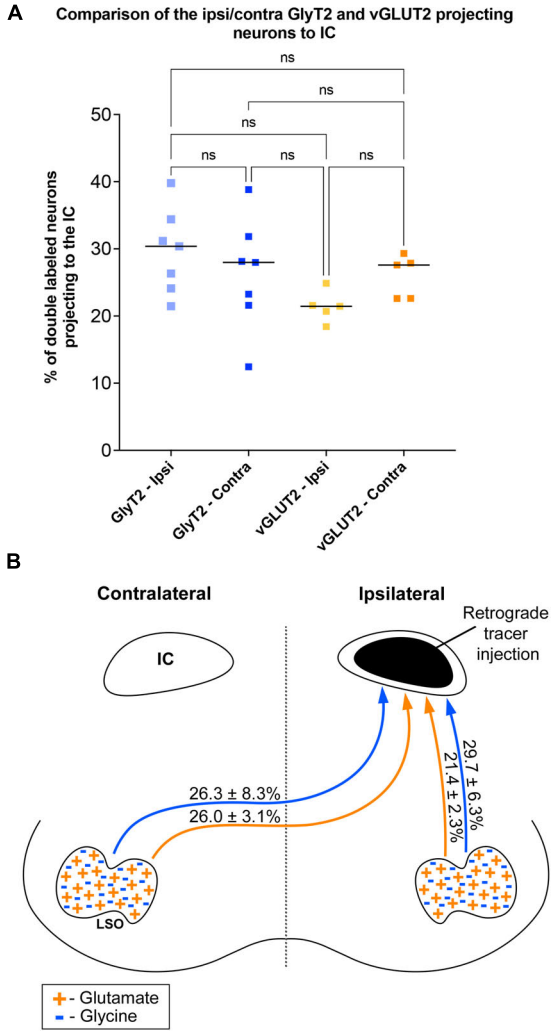

FIGURE 8
Summary of normalized numbers of GlyT2- and vGLUT2-projections to the IC. **(A)** Counts of double-stained neurons were normalized for each animal against the total number of IC projecting cells due to uncontrollable individual differences as well as variations in IC injections placement and size, retrograde transport efficiency, sensitivity of antibody lots, and degree of tissue fixation. The plot confirms what histological analyses suggested: there is no statistical difference between the relative numbers of GlyT2 and vGLUT2 staining of LSO principal cells or between their ipsilateral and contralateral projections to the IC. **(B)** Graphic illustration of the projection ratios of GlyT2 and vGLUT2 to a single IC. The inputs to the opposite IC are not shown but would be a mirror image.

a representation of auditory space. The practical consequence of this ability is to avoid unseen dangers, to orient to the sounds of a potential mate or foe, and to separate simultaneously occurring acoustic streams.

Two ears are clearly important because differences in timing and intensity of arrival of sound at the ears provide binaural cues for sound localization in the azimuthal plane (Jeffress, 1948; Boudreau and Tsuchitani, 1970; Guinan et al., 1972; Grothe, 2000; Konishi, 2000). In the classic model, low frequency sounds produce binaural timing differences, whereas high frequency sounds yield interaural sound level differences (Stevens and Newman, 1936). In addition, the reflections of sounds off the head and pinna and within the ear canals create spectral cues crucial for distinguishing sound distance, elevation, and front-back positioning (Reiss and Young, 2005).

Interaural distance, the distance between the two ears, is a factor that is related to LSO development and to the range of sound localizing abilities across species (Masterton et al., 1969). In a general way, animals with smaller heads have better sound localizing abilities but other factors such as animal niche and considerations of predator vs. prey also play a role. A relationship between interaural distance and high frequency hearing has been noted, but there are exceptions (Irving and Harrison, 1967; Masterton et al., 1969; Moore and Moore, 1971; Heffner and Masterton, 1990). The LSO is a major nucleus in the SOC that is involved in transmitting binaural auditory signals to higher structures and controlling cochlear receptor sensitivity via its descending projections (Dewson, 1967; Liberman, 1980; Darrow et al., 2006; Malmierca and Ryugo, 2011). All extant animals are specialized and adapted to survive in their particular environmental niche, whether it be by reproduction strategies, predation, or complex social systems (Dunbar, 2009). These specializations will be reflected in brain anatomy and physiology.

4.1 Cell types and neurotransmitters

LSO principal neurons that project to the IC are crucial for modeling the role of excitation and inhibition in binaural hearing (Finlayson and Caspary, 1991; Glendenning et al., 1992; Henkel and Brunso-Bechtold, 1993; Brunso-Bechtold et al., 1994; Franken et al., 2018). Not surprisingly, the exploration of cell types and neurotransmitter expression involved in the auditory pathways have been a subject of extensive study over the years and across species including cats, mice, rats, humans, and ferrets (Adams, 1979; Ollo and Schwartz, 1979; Glendenning and Mastereton, 1983; Cant, 1984; Helfert and Schwartz, 1986, 1987; Helfert et al., 1989; Eybalin, 1993; Henkel and Brunso-Bechtold, 1993; Rietzel and Friauf, 1998; Kulesza, 2008).

Generalities regarding cell types have been impeded by variations in cell staining such as *basophilic and silver proteinate dyes* (Taber, 1961; Irving and Harrison, 1967; Fech et al., 2017), *histochemistry* (Warr, 1975), *immunocytochemistry* (Storm-Mathisen et al., 1983; Wenthold et al., 1986; Vetter et al., 1991; Helfert et al., 1992; Berrebi and Spirou, 1998; Kulesza, 2014; Williams et al., 2022), and *Golgi techniques* (Scheibel and Scheibel, 1974; Ollo and Schwartz, 1979; Rietzel and Friauf, 1998). The Golgi-method has had more limited utility because of its preference to work in younger animals (Ryugo and Fekete, 1982). Different staining methods inherently require separate criteria for names because different stains are designed to reveal distinct features of the neurons. Cross validation for different methods has only become available recently with the advent of immunocytochemical double-labeling procedures.

Studies also used different *pathway tracing* techniques that varied in sensitivity and therefore in reliability. *HRP histochemistry* (Adams, 1979; Schweizer, 1981; Nordeen et al., 1983; Glendenning et al., 1992) was the first true neuronal tracer (LaVail et al., 1973) and its sensitivity was dependent on a variety of conditions, particularly on the chromogen used (Mesulam, 1978; Adams,

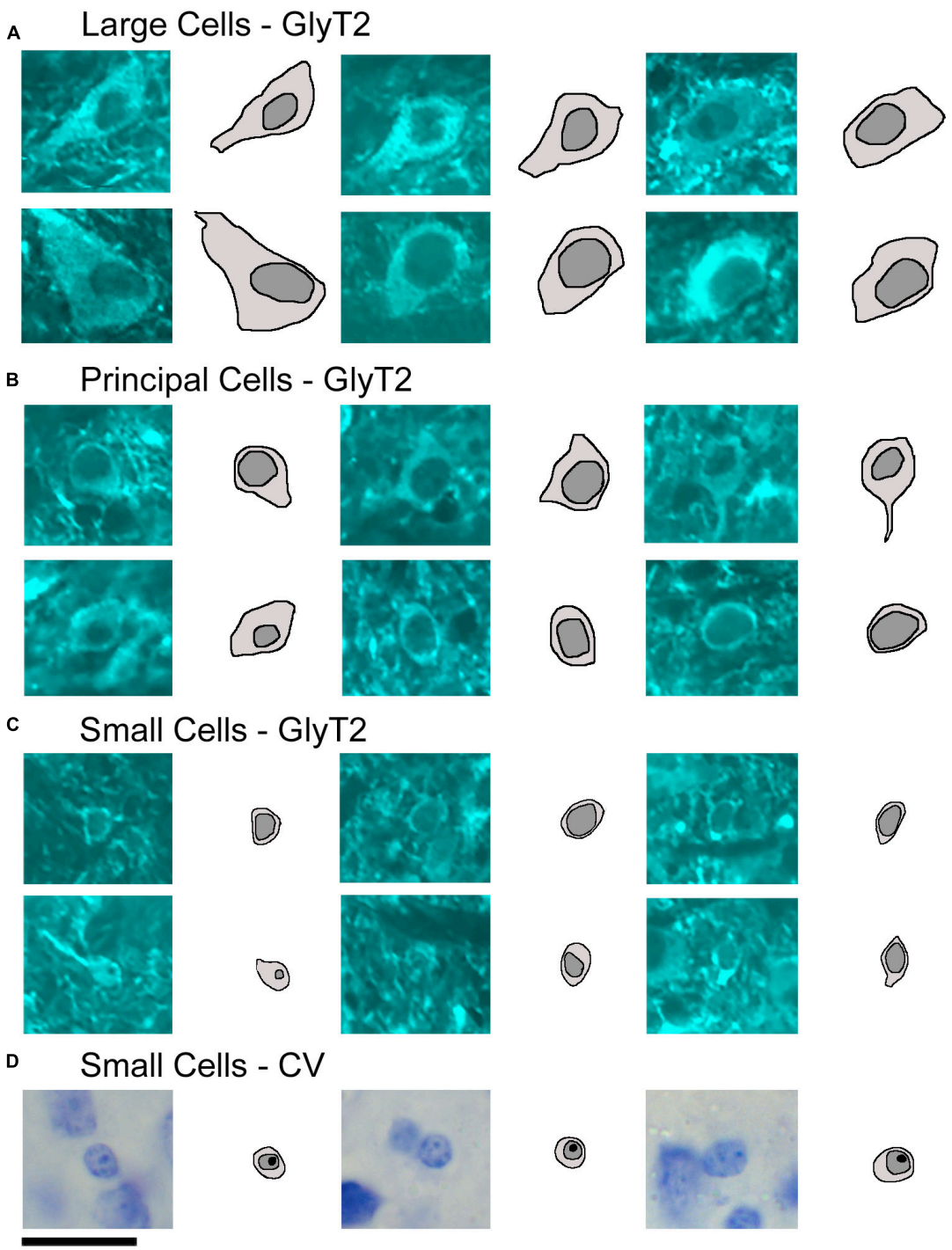

FIGURE 9
Photomicrographs (100x oil) with corresponding drawings of large, medium, and small GlyT2-labeled neurons of the LSO. GlyT2 immunostaining revealed a small population of large and small GlyT2-labeled cells that were intermixed with the dominant, medium-sized principal neurons. GlyT2 neurons were traced to illustrate the cell body silhouette and its resident nucleus. **(A)** Large GlyT2-labeled neurons were sprinkled around the borders of the nucleus and the dorsal hilus. These border neurons were similar in size, shape, and location to previously described periolivary neurons (Williams et al., 2022). **(B)** Medium-sized GlyT2-labeled neurons met the criteria of principal neurons. **(C)** The cell bodies of the small GlyT2-labeled neurons were round-to-oval in shape and never labeled by retrograde tracer injections in the IC. **(D)** CV staining revealed small cells to have granular and slightly lumpy cytoplasm and a round nucleus with pale grainy chromatin and prominent nucleolus. Scale bar equals 25 μm.

1981). The discovery that biotinylated dextran amines could be transported along axons and finely visualized by reactions with diaminobenzidine represented a crucial advance in pathway tracing sensitivity (Reiner et al., 2000). This new method became the standard for identifying pathways in the auditory brain stem (Loftus et al., 2004; Gómez-Álvarez and Saldaña, 2016; Williams et al., 2022), but could be replaced by the constantly evolving technology that has introduced a perhaps even more selective and

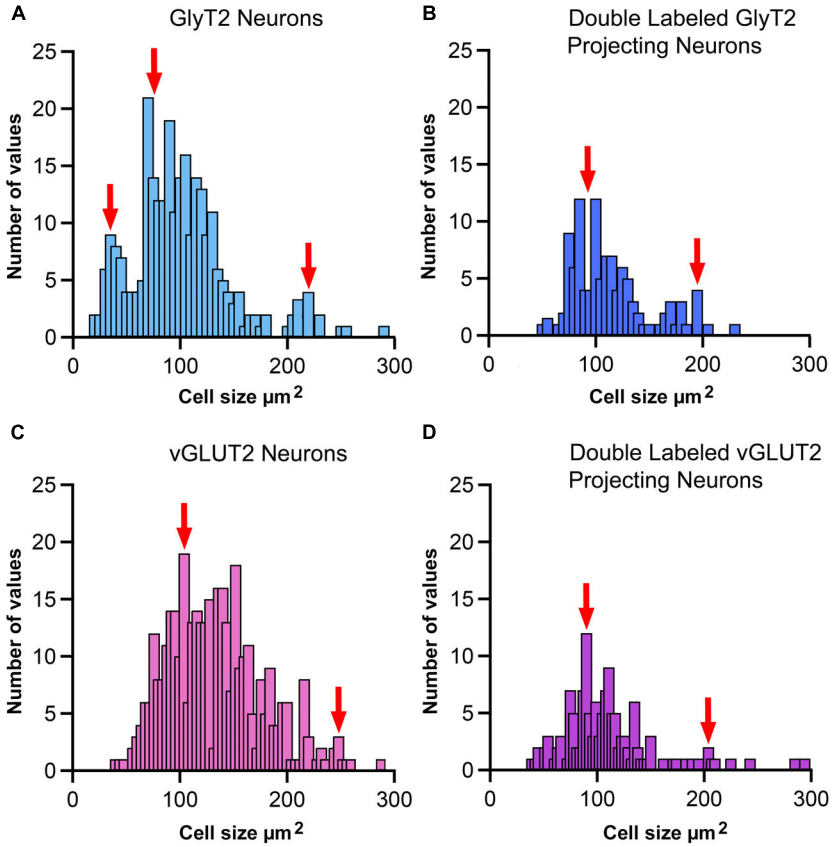

FIGURE 10
Cell size histogram for labeled LSO neurons. The outlines of cell bodies exhibiting a distinct nucleus were drawn from photomicrographs (100x oil) so that somatic silhouette area and shape could be calculated: **(A)** GlyT2 immunostaining, **(B)** double-labeled by FG and GlyT2, **(C)** vGLUT2 immunostaining, and **(D)** double-labeled by FG and vGLUT2. (A) GlyT2 labeling revealed three population based on somatic size: small, medium and large, which aligned with qualitative descriptions provided in Figure 9. A histogram of somatic area showed three peaks (red arrows) that were consistent with three populations based on somatic size. Panel **(B)** Somatic size differences revealed two population peaks (red arrows) for GlyT2 neurons that projected to the IC: medium-sized and large neurons. No small GlyT2 neurons were observed projecting to the IC. Panel **(C)** vGLUT2 antibodies labeled medium-sized and large neurons in the LSO; these two populations resembled the previously described LSO principal and PO neurons, respectively. No small neurons were observed in the LSO stained by vGLUT2 antibodies. Panel **(D)** Neurons double-labeled by FG and vGLUT2 antibodies revealed two population peaks (red arrows) for medium-sized and large neurons attributed to the principal and periolivary neuronal classes. These histograms demonstrate that principal/medium-sized neurons dominate the LSO but that small and large neurons are also present. Histogram bin width equalled 5 µm2.

sensitive method of axon tracing using viral vectors (Lanciego and Wouterlood, 2020; Qiu et al., 2022). A less common method using the *selective uptake and transport of radiolabeled glycine* (Saint Marie and Baker, 1990; Glendenning et al., 1992) and *amino acid receptor immunolabeling* (Koch and Sanes, 1998) have contributed to the literature on cell types, potential transmitter, and cell type location in the LSO. All of these various methods fundamentally require replication using different methods but in the same species. In short, global conclusions regarding cell types, transmitter chemistry, and IC projections have been generally hampered by studies using different species, ages, methods, and naming criteria.

The investigation of neurotransmitter expression, particularly regarding glycine and glutamate, has yielded general agreement where the ipsilateral projection from the LSO to the IC was inhibitory and glycinergic and the contralateral projection from the LSO to the IC was excitatory and glutamatergic (Figure 11). There were, however, differences regarding the extent of contralaterally projecting glycinergic neurons and/or ipsilaterally projecting glutamatergic neurons (Helfert et al., 1989; Saint Marie et al., 1989; Saint Marie and Baker, 1990; Klug et al., 1995; Cant and Benson, 2006; Mellott et al., 2021; Haragopal et al., 2023). In studies that did not analyze cell chemistry, projections were reported as bilateral and symmetrical (Adams, 1979; Schweizer, 1981; Nordeen et al., 1983; Ross et al., 1988; Grothe, 1994; Kelly et al., 1998). We have shown in the CBA/CaH mouse that glycinergic and glutamatergic principal cells of the LSO project bilaterally, symmetrically, and topographically to the IC (Williams et al., 2022; present report).

A comment of cell chemistry seems in order. It has been reported that vGLUT2 is found only in a subset of "nerve terminals" whose distribution appears sorted by "level" along the neuraxis. However, the expression and distribution might also be dependent on the excitatory state or the neuron's packaging/release properties at the time (Fremeau et al., 2004). It has also been reported that vGLUT2 is present in cell bodies (Fremeau et al., 2001; Li et al., 2020). Since vGLUT2 is reported to be distributed extrasynaptically (Gomeza et al., 2003), it is not surprising that it has also been observed in LSO principal cells using

TABLE 4 Representative cell size of GlyT2, vGLUT2, and projecting neurons, and double labeled neurons.

GLYT2					
	GlyT2 (small)	GlyT2 (medium)	GlyT2(large)	GlyT2 IC projecting (medium)	GlyT2 IC projecting (large)
Number of cells	38	212	18	94	18
Area median (μ m^2)	38.2	99.5	208.7	100.5	180.8
Area mean ± standard deviation (μ m^2)	37.73 ± 8.3	100.9 ± 25.5	215.0 ± 48.5	99.14 ± 22.9	180.8 ± 21.2
vGLUT2					
	vGLUT2(medium)	vGLUT2(large)	vGLUT2 IC projecting (medium)	vGLUT2 IC Projecting (large)	
Number of cells	346	38	122	16	
Area median (μ m^2)	123.3	222.8	99.4	200.7	
Area mean ± SD (μ m^2)	114.0 ± 40.6	230.4 ± 42.2	103.1 ± 24.8	202.7 ± 44.0	
FG					
	IC projecting principal cells(medium)		IC projecting principal cells (large)		
Number of cells	551		64		
Area median (μ m^2)	95.9		148.0		
Area mean ± SD (μ m^2)	96.9 ± 22.5		157.2 ± 28.4		

Labeled LSO neurons were divided into categories based on their labeling technique and drawn and measured for cell size silhouette area (μm^2) from multiple cases. GlyT2 featured a population of small neurons that were not seen in vGLUT2 material.

immunostaining (Blaesse et al., 2005; Ito and Oliver, 2010) or *in situ* hybridization (Ito et al., 2010). There remains much to be learned about vGLUT2—its synthesis, regulation, trafficking, and activity-dependence (Martinez-Lozada and Ortega, 2023). In our hands, the vGLUT2 antibody behaves like a specific marker for glutamatergic LSO neurons, which was our goal in the first place.

There is also an issue as to the distribution of GlyT2 staining. GlyT2 has been reported to be primarily in terminal endings (Altieri et al., 2014; Gessele et al., 2016; Mellott et al., 2021), although in our work, GlyT2 antibodies clearly label what may be interpreted as glycinergic cell bodies. Neurons of the MNTB are known to be glycinergic (e.g., Helfert et al., 1989), and MNTB somata stain prominently in our material using GlyT2 antibodies (Supplementary Figure 2; Milinkeviciute et al., 2017 using a CBGlyT2-EGFP mouse). The MNTB staining serves as a positive control for our LSO staining. This staining of MNTB and LSO neurons using GlyT2 antibodies is also consistent with images shown by others (Friauf et al., 1999; Ngodup et al., 2020). These variations may be related to why the contralateral glycinergic projections from the LSO to the IC was not observed in the C57BL/6 mouse (Haragopal et al., 2023) or the gerbil (Mellott et al., 2021). Alternatively, the variations may be strain-specific or due to differences in technique.

4.2 Excitation and inhibition

The physiological features of LSO cells have been featured by no activity in the absence of sound, excitatory responses from ipsilateral sounds, and suppressed activity by contralateral sounds. Single-unit, extracellular recordings revealed the narrow, V-shaped excitatory and inhibitory tuning curves with similar characteristic frequencies (Tsuchitani and Boudreau, 1966, 1967; Guinan et al., 1972). While the LSO is best known for processing interaural level differences, the inhibitory effects of the contralateral ear are most pronounced when the stimuli are closely matched in frequency (Boudreau and Tsuchitani, 1968, 1970; Tollin and Yin, 2002) although there are more recent data suggesting that LSO neurons are also sensitive to the timing of sound onset (Franken et al., 2018), sound envelope emphasizing interaural time differences (Joris and Yin, 1998), or timing information extracted from binaural interactions (Benichoux et al., 2018). These data clearly reveal that the binaural balancing of excitation and inhibition for incoming signals in the LSO is influenced by the various spectral and temporal properties of the sound.

Excitation of a cell by presenting a CF tone in the ipsilateral ear increases as the intensity with which that sound is played increases until reaching a plateau. In parallel, contralateral inhibition measured by a decrease in spikes occurs with increasing intensity of the sound. It is the intensity difference between the ipsilateral and contralateral sound that will elicit or inhibit the spike output. The LSO is equipped to carry out differentiation of incoming sounds based on their level differences while the frequency involvement of this phenomenon remains vital (Goupell and Stakhovskaya, 2018). The convergence of excitatory and inhibitory inputs within the LSO will determine how principal cells acquire their sensitivity for binaural level and time differences.

4.3 Projections

The establishment of excitatory and inhibitory neurons in the LSO represents the next stage in the mechanics of sound localization. It is at this level where excitatory inputs converge onto certain types of neurons in the LSO, leading to the initiation of second-order excitatory and inhibitory

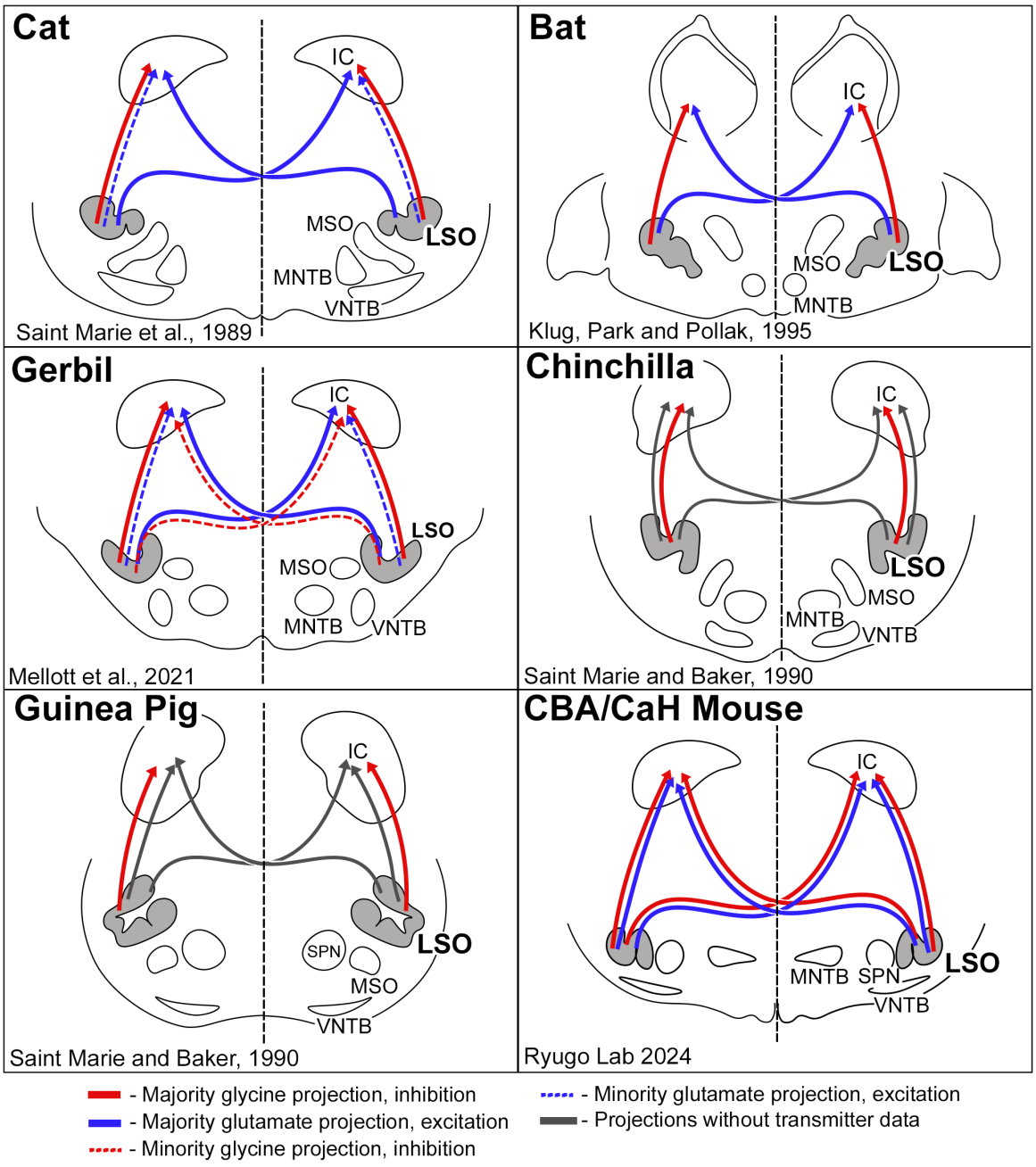

FIGURE 11
Schematic diagram of excitatory and inhibitory projections from LSO cells as reported for a few species of mammals. The pattern of glycinergic and glutamatergic projections in the cat suggested that inhibitory projections were entirely ipsilateral, and that excitatory projections were predominately contralateral (Saint Marie et al., 1989). This pattern was essentially replicated in the bat (Klug et al., 1995). The gerbil resembled the cat, with the additional observation that there was a small group of glycinergic neurons that projected to the contralateral IC (Mellott et al., 2021). The chinchilla and guinea pig featured only ipsilateral glycinergic projections; no glutamate labeling was shown. Contralateral projections were shown by retrograde transport of horseradish peroxidase but without transmitter information (Saint Marie and Baker, 1990). In the CBA/CaH mouse, we observed a bilateral and symmetric projection to the IC for both glycinergic and glutamatergic LSO neurons. These variations in projection patterns are hypothesized to reflect processing differences forged by adaptive mechanisms for different habitats and survival demands.

projections. The distribution of these projections is important for thinking about how auditory space is constructed, at least in terms of following how ipsilateral ear excitation becomes transformed into binaural responses that convey excitation or inhibition.

When considering the nature of IC-projecting principal cells, approximately 25% of them were double labeled bilaterally by GlyT2 or vGlUT2. We did not perform double immunolabeling with the projection experiments, but if we consider both types of staining separately, half of the IC-projecting cells were labeled by GlyT2 or vGLUT2. This situation implies that the other half of the IC-projecting cells are not using glycine or glutamate. Another consideration must deal with the GlyT2 and vGLUT2 immunolabelled cells that do not appear to project to the IC.

We need to know what the chemistry is for these cells and where they project.

In the mouse, it would appear that the mechanisms for binaural processing between the LSO and IC could have a basic repetitive organization. Such a prediction is based on our observation that projections of principal cells are bilateral, topographic, and symmetrical. As such, we propose that a binaural spatial processing unit in the IC could be modeled by bilaterally-matched pairs of isofrequency laminae. This idea is consistent with observed on-going binaural disparity in frequency-intensity spectra as one of the cues for determining the direction of a sound, especially in species with a small head (Harper and McAlpine, 2004; Harper et al., 2014) or a small or absent medial superior olive (Irving and Harrison, 1967; Masterton et al., 1967). The test of such a hypothesis still requires new knowledge about brain stem circuits of the auditory system (Glendenning and Masterton, 1998) and how the various ascending projections are synaptically arranged with the multiple cell types comprising an IC lamina (Oliver, 2000; Loftus et al., 2004, 2010).

An important issue is to understand the differences in results reported for the C57BL/6 mouse (Haragopal et al., 2023) versus what we report for the CBA/CaH mouse. One possibility concerns the mouse strain: the use of the C57BL/6 strain is advantageous for genetic manipulations (Hasan et al., 2004; Hawrylycz et al., 2011) but perhaps not for hearing research. C57BL/6 mice progressively lose hearing starting at 2 months of age (Henry and Chole, 1980; Willott et al., 1985; Ison and Allen, 2003), and high frequency hearing loss starts as early as 6 weeks of age (Ouagazzal et al., 2006). In addition, auditory efferents decline rapidly after 6 weeks of age (Zhu et al., 2007, and there is evidence for central compensatory plasticity Willott and Turner, 1999). In contrast, the stable hearing thresholds of CBA/CaJ mice over time provide a more reliable model and reference for normal hearing mouse strains (Zheng et al., 1999).

There are also technical details in the Haragopal et al. (2023) publication that should be considered. The IC injection volume of only 80 nl of Fluoro-Ruby may not be sufficient to yield a reliable labeling pattern vis-à-vis the contralateral and ipsilateral distribution. The injection site in their (Figure 2) does not include the lateral third of the CNIC. Our pressure injection volumes were significantly greater. In addition, the use of *in vitro* hybridization is reported to weaken the fluorescent signal of their retrograde tracer, Fluoro-Ruby, but the authors do not show the effectiveness of the anti-TRICT retrieval treatment or include *in situ* hybridization controls. The authors do not provide criteria for what they consider labeling nor provide photographic evidence for such labeling. The low magnification of their photomicrographs and undefined arrows and arrowheads likewise raise issues in their cell counts and the ipsilateral/contralateral nature of their projections.

There remains the question for how the "what" component of sound is integrated with the "where" component (Romanski et al., 1999; Cloutman, 2013; Rauschecker, 2018). Binaural networks are important in dynamic sound processing. Proprioceptive, visual, and vestibular systems provide additional information about head and body position, movement, and gravity, and as such, contribute significantly to the "where" component (Rice et al., 1992; Wright and Ryugo, 1996; Kanold and Young, 2001; Kanold et al., 2011). These multisensory systems establish and maintain on-going relationships between sound sources and the position of the listener in space (Ryugo et al., 2003; Wu and Shore, 2018; Ansorge et al., 2021; Ryugo and Milinkeviciute, 2023). Understanding how these sensory circuits and their cellular constituents work together are key to grasping how mammals cope in an acoustic environment where sound is constantly changing in spectral-temporal features, loudness, and position.

4.4 LSO counts

In our study, we performed unilateral IC injections, which labeled neurons in the LSO that double labeled with approximately 20–30% of neurons labeled with either GlyT2 or vGLUT2 in the ipsilateral or contralateral nuclei. We would expect that for bilateral IC injections, the number of double labeled neurons in each LSO for GlyT2 and vGLUT2 cases would increase by twofold. When trying to resolve the overall number of neurons in the LSO, we must consider not just the principal cells, or those that project to the IC, but also the principal neurons who project DNLL or CN and the LSO efferents that project to the ipsilateral cochlea.

The number of AChE-stained cells of the LSO was concluded to represent the total number of LOC neurons because the number of retrogradely labeled, HRP-neurons equaled the number of AChE-stained neurons in adjacent sections and because HRP labeled neurons showed close correspondence to AChE staining when double-labeling methods were used (Warr, 1975). Similar results were found in the CBA/CaH mouse using the retrograde tracer, FluoroGold, with AChE and ChAT (Suthakar, 2017; Williams et al., 2022). These results imply that cholinergic staining of LOC efferents avoids the question of incomplete marking of LOCs due to inadequate access to the tracer.

The relative presence of other neuroactive substances In LOC neurons such as GABA, glycine, dopamine, dynorphin, and nitric oxide seems to vary with age, species, method of staining, laterality of projection, and history of noise exposure (Helfert et al., 1989; Vetter et al., 1991; Vetter and Mugnaini, 1992; Kandler et al., 2002; Maison et al., 2002; Nabekura et al., 2003; Schaeffer et al., 2003; Niu et al., 2004; Jenkins and Simmons, 2006; Wu et al., 2020). In our hands, the retrograde labeling of LOC efferents using FG injections in the cochlea did not co-label with GAD67 positive cells from our transgenic GAD67/EGFP mice (Suthakar, 2017) or with GAD67 positive immunostained cells in CBA/CaH mice. A summary of LSO neuronal counts across studies and involving different labels is provided in Supplementary Table 1.

4.5 Consideration of methods of study

The variety of results that accompany differences in species, age, habitat, and hearing range and sensitivity could provide important links to the study data and some variable that might not have been previously considered, perhaps yielding novel insight into its neural substrate. In our study, we attempted to label LSO neurons using a CBGlyT2-EGFP (Zeilhofer et al., 2005) backcrossed > 10 generations with CBA/CaH mice but could not detect label in LSO neurons. Our attempts to label LSO neurons in the mouse with antibodies against vGLUT1 was also unsuccessful, whereas this method did stain LSO neurons in the rat (Ito and Oliver,

2010). We were unable to determine if the CBA/CaH mouse LSO did not use vGLUT1 transporter or if the antibody or our method was flawed. Superimposed on the inherent differences between species is the fact that different research methods will also yield different kinds of data: (1) intact animal versus *in vitro* slice preparations for physiologically characterizing cell properties; (2) basic dyes, immunocytochemistry, *in situ* hybridization, or transgenic animals for specific cell staining; (3) age of subject for examining growth and development; (4) anterograde, retrograde or viral tracing for describing neuronal circuits; and (5) microscopic visualization technique (brightfield, fluorescent, confocal, light sheet, multiphoton, scanning and electron microscopy). Simple things like staining artifacts—fixation and tissue preservation, tissue distortion while staining, tissue stretching when mounting sections on microscope slides, tissue shrinkage when dehydrating sections for coverslipping—all contribute to microscopic changes. By recognizing the potential sources of variability inherent to any study, we will be better prepared to interpret comparative data.

4.6 Species differences

It has been shown that different species exhibit varying immunochemical and IC-projection characteristics related to the frequency response properties of the neurons under study (Saint Marie et al., 1989; Brunso-Bechtold et al., 1994; Barnes-Davies et al., 2004; Mellott et al., 2021). There are reports of a low frequency bias for ipsilateral projections to the IC and a high frequency bias for contralateral projections (*cat*, Glendenning and Mastereton, 1983; *gerbil*, Mellott et al., 2021). A quite different conclusion was reached in the ferret where the laterally-situated low frequency neurons preferentially projected to the contralateral IC, whereas the medially-situated high frequency neurons projected to the ipsilateral IC (Henkel and Brunso-Bechtold, 1993). Because cats and ferrets are both small carnivoran species and potent predators, such differences might not be expected. Species by itself, however, does not ensure trait uniformity: there are many different strains of mice that are specialized for one feature or another (e.g., Fontaine and Davis, 2016; Smith, 2019).[1] The available data suggest that there is still much to be learned about brain size and circuits as they relate to evolution, species, habitat, and behavior.

Perhaps we need to consider additional details that influence body anatomy, behaviour, reproduction, and ecology. For example, cats and ferrets are both carnivorous mammals with flexible body structure adapted for hunting (Barratt, 1997; Marshall, 2020), but belong to different families: cats are felines, whereas ferrets are weasels. Cats are solitary hunters with distinct predatory behaviors (Marshall, 2020) and are found in various habitats, occupying a wide range of ecological niches (Miller, 1996), not unlike that of ferrets (McKay, 2012). It is of some interest that the cat was domesticated some 10,000 years ago (Driscoll et al., 2009). In contrast, the ferret was domesticated roughly 2,000 years ago (Davison et al., 1999), providing less time for environmental pressures to induce brain and behavior changes.

Mice and rats are small rodents, herbivorous, and thigmotaxic with whiskers that guide them to walls or other points of hiding (Harris, 1979; Traweger et al., 2006). They belong to the same taxonomic family, live in colonies, occupy simple burrows, and display complex social behaviors in fields, forests, or domestic regions (Rossi, 1975; Ehret and Riecke, 2001; Bonthuis et al., 2010; Hikishima et al., 2017; Netser et al., 2020). However, rats are considered natural predators of mice (Liu et al., 2017), and predator-prey relationships are suspected to contribute to differences in brain circuitry (Apfelbach et al., 2005).. Gerbils live in family groups, are gregarious, and known for their more elaborate burrows and burrowing behavior (Fisher and Llewellyn, 1978). Because of these variations in habitat and behavior, we can infer that they have an impact on how each species processes and locates sound.

The natural habitats of the chipmunk, gerbil, and kangaroo rat are moderately elaborate underground burrows, whereas the rat and the mouse are known to create shallow and somewhat simple burrows (Supplementary Figure 7; Storer, 1948; Elliott, 1978, Avenant and Smith, 2003; Scheibler et al., 2006; Weber et al., 2013; Vorhies and Taylor, 2015). In marked contrast, the naked mole rat lives in complex burrows, highly branched with up to 6 km of total tunnel length and extending across as much as 6 football fields (Buffenstein et al., 2012; Park and Buffenstsein, 2012). In burrows, the transmission of high frequency sounds is significantly reduced and the need for sound localization is generally limited to front-back distinctions (Heth et al., 1986; Begall et al., 2007; Okanoya et al., 2018; Barker et al., 2021). It should not be surprising that the auditory system of burrowing animals differs from that of above-ground mammals, and these differences can be reflected their audiograms (Supplementary Figure 8) as well as how sound is processed by the LSO (Moore and Moore, 1971). The differences between common auditory research subjects such as gerbils, guinea pigs, chinchillas, cats, and mice could be associated with anatomical specializations that underlie mechanisms of binaural processing.

Differences in results and/or conclusions presented in published reports are worthy of additional mention. In terms of comparative neurobiology, there is an unstated assumption that there should be a basic blueprint of the mammalian brain, upon which evolution adds, modifies, and improves the plan and adapts novel solutions to help resolve challenging circumstances. The selection of a research subject is often guided by the premise that a specific feature of the subject can be related back to some human quality for translational medical relevance, to a basic generalizable plan of the nervous system, or to some remarkable specialization such as echo location. The immediate aim might be to identify in a simpler system how a particular process works, and the bigger picture might be to reveal brain specializations that evolved to optimize a process that ensures a species survival in a particular habitat. There is, rightly or wrongly, an assumption that the nervous system uses a fixed set of solutions to improve information processing and species survival. In the face of species specializations and even minor genetic variations in the same species, cognitive demands placed on communication, hunting, predator avoidance, and reproductive success could have consequences on brain structure and function yet to be determined. The fine details of how auditory circuits are conceptually and technically constructed are crucial for understanding the biology of hearing.

1 https://www.jax.org

Data availability statement

The original contributions presented in the study are included in the article/Supplementary material, further inquiries can be directed to the corresponding author.

Ethics statement

This study was reviewed and approved by the Garvan Institute of Medical Research and St Vincent's Hospital Animal Ethics Committee. This study was performed in strict accordance with the Australian Code for the Care and Use of Animals for Scientific Purposes (2013) and the ethical guidelines of the National Health and Medical Research Council (NHMRC) of Australia. All animals were handled according to Animal Ethics Committee protocols (Animal Research Authority: 19-33, 20-02, and 21-13).

Author contributions

IW: Writing–review and editing, Writing–original draft, Visualization, Software, Resources, Project administration, Methodology, Investigation, Formal analysis, Data curation, Conceptualization. DR: Writing–review and editing, Writing–original draft, Validation, Supervision, Project administration, Funding acquisition, Conceptualization.

Funding

The author(s) declare financial support was received for the research, authorship, and/or publication of the article. This research was made possible from the following funding sources: NHMRC Grant 1080652 to DR, a bequest from Helen Morgan, and donations to the Hearing Research Lab from Charlene and Graham Bradley, Sue and Haydn Daw, and Alan and Lynn Rydge. The donors had no role in the direction, analysis, or publication of this work.

Acknowledgments

We thank Dr. Thomas Parks for his comments on earlier versions of the manuscript and Anastasia Filimontseva for technical assistance. We also acknowledge the long standing support to the lab by Katanyu Pongstaphone. We also thank the reviewers for their constructive criticisms.

Conflict of interest

The authors declare that the research was conducted in the absence of any commercial or financial relationships that could be construed as a potential conflict of interest.

Publisher's note

Supplementary material

The Supplementary Material for this article can be found online at: https://www.frontiersin.org/articles/10.3389/fncir.2024.1430598/full#supplementary-material

References

Adams, J. (1979). Ascending projections to the inferior colliculus. *J. Comp. Neurol.* 183, 519–538. doi: 10.1002/cne.901830305

Adams, J. C. (1981). Heavy metal intensification of DAB-based HRP reaction product. *J. Histochem. Chytochem.* 29:775. doi: 10.1177/29.6.7252134

Altieri, S. C., Zhao, T., Jalabi, W., and Maricich, S. M. (2014). Development of glycinergic innervation to the murine LSO and SPN in the presence and absence of the MNTB. *Front. Neural Circuits* 8:109. doi: 10.3389/fncir.2014.00109

Ansorge, J., Wu, C., Shore, S. E., and Krieger, P. (2021). Audiotactile interactions in the mouse cochlear nucleus. *Sci. Rep.* 11:6887. doi: 10.1038/s41598-021-86236-9

Apfelbach, R., Blanchard, C. D., Blanchard, R. J., Hayes, R. A. and McGregor, I. S. (2005). The effects of predator odors in mammalian prey species: a review of field and laboratory studies. *Neurosci. Biobehav. Rev.* 29, 1123-1144. doi: 10.1016/j.neubiorev.2005.05.005

Avenant, N. L., and Smith, V. R. (2003). The microenvironment of house mice on Marion Island (sub-Antarctic). *Polar Biol.* 26, 129–141. doi: 10.1007/s00300-002-0464-x

Banks, M. I., and Smith, P. H. (1992). Intracellular recordings from Neurobiotin-labeled cells in brain slices of the rat medial nucleus of the trapezoid body. *J. Neurosci.* 12, 2819–2837. doi: 10.1523/JNEUROSCI.12-07-02819.1992

Barker, A. J., Koch Lewin, G. R., and Pyott, S. J. (2021). Hearing and vocalizations in the naked mole-rat. *Adv. Exp. Med. Biol.* 1319, 157–195. doi: 10.1007/978- 3- 030-65943- 1

Barnes-Davies, M., Barker, M. C., Osmani, F., and Forsythe, I. D. (2004). Kv1 currents mediate a gradient of principal neuron excitability across the tonotopic axis in the rat lateral superior olive. *Eur. J. Neurosci.* 19, 325–333. doi: 10.1111/j.0953-816x.2003.03133.x

Barratt, D. G. (1997). Home range size, habitat utilisation and movement patterns of suburban and farm cats *Felis catus*. *Ecography* 20, 271–280. doi: 10.1111/j.1600-0587.1997.tb00371.x

Begall, S., Burda, H., and Schleich, C. (2007). *Subterranean rodents: News from underground*. Berlin: Springer Science+Business Media.

Benichoux, V., Ferber, A., Hunt, S., Hughes, E., and Tollin, D. (2018). Across species "natural ablation" reveals the brainstem source of a noninvasive biomarker of binaural hearing. *J. Neurosci.* 38, 8563–8573. doi: 10.1523/jneurosci.1211-18.2018

Berlin, C. L. (1963). Hearing in mice via GSR audiometry. *J. Speech Hear. Res.* 6, 359–368. doi: 10.1044/jshr.0604.359

Berrebi, A. S., and Spirou, G. A. (1998). PEP-19 immunoreactivity in the cochlear nucleus and superior olive of the cat. *Neuroscience* 83, 535–554. doi: 10.1016/s0306-4522(97)00407-7

Blaesse, P., Ehrhardt, S., Friauf, E., and Nothwang, H.G. (2005). Developmental pattern of three vesicular glutamate transporters in the rat superior olivary complex. *Cell Tissue Res.* 320, 33–50. doi: 10.1007/s00441-004-1054-8

Bogaerts, S., Clements, J. D., Sullivan, J. M., and Oleskevich, S. (2009). Automated threshold detection for auditory brainstem responses: Comparison with visual estimation in a stem cell transplantation study. *BMC Neurosci.* 10:104. doi: 10.1186/1471-2202-10-104

Bonthuis, P. J., Cox, K. H., Searcy, B. T., Kumar, P., Tobet, S., and Rissman, E. F. (2010). Of mice and rats: Key species variations in the sexual differentiation of brain and behavior. *Front. Neuroendocrinol.* 31:341–358. doi: 10.1016/j.yfrne.2010.05.001

Boudreau, J. C., and Tsuchitani, C. (1968). Binaural interaction in the cat superior olive s segment. *J. Neurophysiol.* 31, 442–454. doi: 10.1152/jn.1968.31.3.442

Boudreau, J. C., and Tsuchitani, C. (1970). Cat superior olive S-segment cell discharge to tonal stimulation. *Contrib. Sens. Physiol.* 4, 143–213. doi: 10.1016/ B978-0- 12- 151804- 2.50011- 5

Brunso-Bechtold, J. K., Linville, M. C., and Henkel, C. K. (1994). Terminal types on ipsilaterally and contralaterally projecting lateral superior olive cells. *Hear. Res.* 77, 99–104. doi: 10.1016/0378-5955(94)90257-7

Buffenstein, R., Park, T., Hanes, M., and Artwohl, J. E. (2012). *Naked mole rat. The laboratory rabbit, guinea pig, hamster, and other rodents*. New York, NY: Elsevier, 1055–1074. doi: 10.1016/b978-0-12-380920-9.00045-6

Cant, N. B. (1984). The fine structure of the lateral superior olivary nucleus of the cat. *J. Comp. Neurol.* 227, 63–77. doi: 10.1002/cne.90227 0108

Cant, N. B., and Benson, C. G. (2006). Wisteria floribunda lectin is associated with specific cell types in the ventral cochlear nucleus of the gerbil, *Meriones unguiculatus*. *Hear. Res.* 216–217, 64–72. doi: 10.1016/j.heares.2006.01.008

Cant, N. B., and Casseday, J. H. (1986). Projections from the anteroventral cochlear nucleyus to the lateral and medial superior olivary nuclei. *J. Comp. Neurol.* 247, 457–476. doi: 10.1002/cne.902470406

Cloutman, L. L. (2013). Interaction between dorsal and ventral processing streams: Where, when and how? *Brain Lang.* 127, 251–263. doi: 10.1016/j.bandl.2012.08.003

Darrow, K. N., Maison, S. F., and Liberman, M. C. (2006). Cochlear efferent feedback balances interaural sensitivity. *Nat. Neurosci.* 9, 1474–1476. doi: 10.1038/nn1807

Davison, A., Birks, J. D. S., Griffiths, H. I., Kitchener, A. C., Biggins, D., and Butlin, R. K. (1999). Hybridization and the phylogenetic relationship between polecats and domestic ferrets in Britain. *Biol. Conserv.* 87, 155–161. doi: 10.1016/S0006-3207(98)00067-6

Dewson, J. H. (1967). Efferent Olivocochlear Bundle: Some relationships to noise masking and to stimulus attenuation. *J. Neurophysiol.* 30, 817–832. doi: 10.1152/jn.1967.30.4.817

Doucet, J. R., and Ryugo, D. K. (2003). Axonal pathways to the lateral superior olive labeled with biotinylated dextran amine injections in the dorsal cochlear nucleus of rats. *J. Comp. Neurol.* 461, 452–465. doi: 10.1002/cne.10722

Driscoll, C. A., Clutton-Brock, J., Kitchener, A. C., and O'Brien, S. J. (2009). The taming of the cat. *Sci. Am.* 30, 68–75.

Dunbar, R. I. M. (2009). Darwin and the ghost of phineas gage: Neuro-evolution and the social brain. *Cortex* 45, 1119–1125. doi: 10.1016/j.cortex.2009.05.005

Ehret, G., and Riecke, S. (2001). Mice and humans perceive multiharmonic communication sounds in the same way. *Proc. Natl. Acad. Sci. U.S.A.* 99, 479–482. doi: 10.1073/pnas.012361999

Elliott, L. (1978). Social behavior and foraging ecology of the Eastern Chipmunk (*Tamias striatus*) in the Adirondack mountains. *Smithsonian Contrib. Zool.* 265, 1–107. doi: 10.5479/si.00810282.265

Eybalin, M. (1993). Neurotransmitters and neuromodulators of the mammalian cochlea. *Physiol. Rev.* 73, 309–373. doi: 10.1152/physrev.1993.73.2.309

Fech, T., Calderón-Garcidueñas, and Kulesza, R. J. Jr. (2017). Characterization of the superior olivary complex of *Canis lupus* domesticus. *Hear. Res.* 351, 130–140. doi: 10.1016/j.heares.2017.06.010

Finlayson, P. G., and Caspary, D. M. (1991). Low-frequency neurons in the lateral superior olive exhibit phase-sensitive binaural inhibition. *J. Neurophysiol.* 65, 598–605. doi: 10.1152/jn.1991.65.3.598

Fisher, M. F., and Llewellyn, G. C. (1978). The Mongolian gerbil: Natural history, care, and maintenance. *Am. Biol. Teach.* 40, 557–560. doi: 10.2307/4446413

Fontaine, D. A., and Davis, D. B. (2016). Attention to background strain is essential for metabolic research: C57BL/6 and the international knockout mouse consortium. *Diabetes* 65, 25–33. doi: 10.2337/db15-0982

Franken, T. P., Joris, P. X., and Smith, P. H. (2018). Principal cells of the brainstem's interaural sound level detector are temporal differentiators rather than integrators. *Elife* 7:e33854. doi: 10.7554/eLife.33854

Fremeau, R. T., Troyer, M. D., Pahner, I., Nygaard, G. O., Tran, C. H., Reimer, R. J., et al. (2001). The expression of vesicular glutamate transporters defines two classes of excitatory synapse. *Neuron* 31, 247–260. doi: 10.1016/s0896-6273(01)00344-0

Fremeau, R. T., Voglmaier, S., Seal, R. P., and Edwards, R. H. (2004). VGLUTs define subsets of excitatory neurons and suggest novel roles for glutamate. *Trends Neurosci.* 27, 98–103. doi: 10.1016/j.tins.2003.11.005

Friauf, E., Aragón, C., Löhrke, S., Westenfelder, B., and Zafra, F. (1999). Developmental expression of the GlycineTransporter GLYT2 in the auditory system of rats suggests involvement in synapse maturation. *J. Comp. Neurol.* 412, 17–37. doi: 10.1002/(SICI)1096-9861(19990913)412:1<17::AID-CNE2<3.0.CO;2-E

Gessele, N., Garcia-Pino, E., Omerbašić, D., Park, T. J., and Koch, U. (2016). Structural changes and lack of HCN1 channels in the binaural auditory brainstem of the naked mole-rat (*Heterocephalus glaber*). *PLoS One* 11:e0146428. doi: 10.1371/journal/pone.0146428

Glendenning, K. K., and Mastereton, R. B. (1983). Acoustic chiasm: Efferent projections of the lateral superior olive. *J. Neurosci.* 3, 1521–1537. doi: 10.1523/JNEUROSCI.03-08-01521.1983

Glendenning, K. K., and Masterton, R. B. (1998). Comparative morphometry of mammalian central auditory systems: Variation in nucleiu and form of the ascending system. *Brain Behav. Evol.* 51, 59–89. doi: 10.1159/000006530

Glendenning, K. K., Baker, B. N., Hutson, K. A., and Masterton, R. B. (1992). Acoustic chiasm V: Inhibition and excitation in the ipsilateral and contralateral projections of LSO. *J. Comp. Neurol.* 319, 100–122. doi: 10.1002/cne.903190110

Gomeza, J., Ohno, K., and Betz, H. (2003). Glycine transporter isoforms in the mammalian central nervous system: Structures, functions and therapeutic promises. *Curr. Opin. Drug Discov. Dev.* 6, 675–682.

Gómez-Álvarez, M., and Saldaña, E. (2016). Different tonotopic regions of the lateral superior olive receive a similar combination of afferent inputs. *J. Comp. Neurol.* 524, 2230–2250. doi: 10.1002/cne.23942

Goupell, M. J., and Stakhovskaya, O. A. (2018). Across-channel interaural-level-difference processing demonstrates frequency dependence. *J. Acoust. Soc. Am.* 143, 645–658. doi: 10.1121/1.5021552

Grothe, B. (1994). Interaction of excitation and inhibition in processing of pure tone and amplitude-modulated stimuli in the medial superior olive of the mustached bat. *J. Neurophysiol.* 71, 706–721. doi: 10.1152/jn.1994.71.2.706

Grothe, B. (2000). The evolution of temporal processing in the medial superior olive, an auditory brainstem structure. *Prog. Neurobiol.* 61, 581–610. doi: 10.1016/s0301-0082(99)00068-4

Grothe, B., and Park, T. J. (1995). Time can be traded for intensity in the lower auditory system. *Naturwissenschaften* 82, 521–523. doi: 10.1007/bf01134488

Guinan, J. J., Norris, B. E., and Guinan, S. S. (1972). Single auditory units in the superior olivary complex: II: Locations of unit categories and tonotopic organization. *Int. J. Neurosci.* 4, 147–166. doi: 10.3109/00207457209164756

Haragopal, H., Mellott, J. G., Dhar, M., Kanel, A., Mafi, A., Tokar, N., et al. (2023). Tonotopic distribution and inferior colliculus projection pattern of inhibitory and excitatory cell types in the lateral superior olive of mice. *J. Comp. Neurol.* 531, 1381–1388. doi: 10.1002/cne.25515

Harper, N. S., and McAlpine, D. (2004). Optimal neural population coding of an auditory spatial cue. *Nature* 430, 682–686. doi: 10.1038/nature02768

Harper, N. S., Scott, B. H., Semple, M. N., and McAlpine, D. (2014). The neural code for auditoryu space depends on sound frequency and head size in an optimal manner. *PLoS One* 9:e108154. doi: 10.137/journal.pone.0108154

Harris, S. (1979). History, distribution, status and habitat requirements of the harvest mouse (*Micromys minutus*) in Britain. *Mammal. Rev.* 9, 159–171. doi: 10.1111/j.1365-2907.1979.tb00253.x

Hasan, M. T., Friedrich, R. W., Euler, T., Larkum, M. E., and Giese, G. (2004). Functional fluorescent Ca2+ indicator proteins in transgenic mice under TET control. *PLoS Biol.* 2:0763. doi: 10.1371/journal.pbio.0020163

Hawrylycz, M., Baldock, R. A., Burger, A., Hashikawa, T., and Johnson, G. A. (2011). Digital atlasing and standardization in the mouse brain. *PLoS Comp. Biol.* 7:e1001065. doi: 10.1371/journal.pcbi.1001065

Hedreen, J. C. (1998). What was wrong with the Abercrombie and empirical cell counting methods? A review. *Anat. Rec.* 250, 373–380.

Heffner, R. S., and Masterton, R. B. (1990). "Sound localization in mammals: Brainstem mechanisms," in *Comparative perception*, Vol. 1, eds M. A. Berkley and W. C. Stebbins (New York, NY: John Wiley & Sons), 285–314.

Helfert, R. H., and Schwartz, I. R. (1986). Morphological evidence for the existence of multiple neuronal classes in the cat lateral superior olivary nucleus. *J. Comp. Neurol.* 244, 533–549. doi: 10.1002/cne.902440409

Helfert, R. H., and Schwartz, I. R. (1987). Morphological features of five neuronal classes in the gerbil lateral superior olive. *Am. J. Anat.* 179, 55–69. doi: 10.1002/aja.1001790108

Helfert, R. H., Bonneau, J. M., Wenthold, R. J., and Altschuler, R. A. (1989). GABA and glycine immunoreactivity in the guinea pig superior olivary complex. *Brain Res.* 501, 269–286. doi: 10.1016/0006-8993(89)90644-6

Helfert, R. H., Juiz, J. J., Bledsoe, S. C., Bonneau, J. M., Wenthold, R. J., and Altschuler, R. A. (1992). Patterns of glutamate, glycine, and GABA immunolabeling

in four synaptic terminal classes in the lateral superior olive of the guinea pig. *J. Comp. Neurol.* 323, 305–325. doi: 10.1002/cne.903230302

Henkel, C. K., and Brunso-Bechtold, J. K. (1993). Laterality of superior olive projections to the inferior colliculus in adult and developing ferret. *J. Comp. Neurol.* 331, 458–468. doi: 10.1002/cne.903310403

Henry, K. R., and Chole, R. A. (1980). Genotypic differences in behavioral, physiological and anatomical expressions of age-related hearing loss in the laboratory mouse. *Audiology* 19, 369–383. doi: 10.3109/00206098009070071

Heth, G., Frankenberg, E., and Nevo, E. (1986). Adaptive optimal sound for vocal communication in tunnels of a subterranean mammal (*Spalax ehrenbergi*). *Experientia* 42, 1287–1289. doi: 10.1007/BF01946426

Hikishima, K., Komaki, Y., Seki, F., Ohnishi, Y., Okano, H. J., and Okano, H. (2017). In vivo microscopic voxel-based morphometry with a brain template to characterize strain-specific structures in the Mouse Brain. *Sci. Rep.* 7:85. doi: 10.1038/s41598-017-00148-1

Hind, J. E., Goldberg, J. M., Greenwood, D. D., and Rose, J. E. (1963). Some discharge characteristics of single neurons in the inferior colliculus of the cat. II. Timing of the discharges and observations on binaural stimulation. *J. Neurophysiol.* 26, 321–341. doi: 10.1152/jn.1963.26.2.321

Humason, G. L. (1979). *Animal tissue techniques*, 4th Edn. San Francisco, CA: W.H.Freeman and Company.

Irving, R., and Harrison, J. (1967). The superior olivary complex and audition: A comparative study. *J. Comp. Neurol.* 130, 77–86. doi: 10.1002/cne.901300105

Ison, J. R., and Allen, P. D. (2003). Low-frequency tone pips elicit exaggerated startle reflex in C57BL/6J mice with hearing loss. *J. Assoc. Res. Otolaryngol.* 4, 495–504. doi: 10.1007/s10162-002-3046-2

Ito, T., and Oliver, D. L. (2010). Origins of glutamatergic terminals in the inferior colliculus identified by retrograde transport and expression of VGLUT1 and VGLUT2 genes. *Front. Neuroanat.* 4:135. doi: 10.3389/fnana.2010.00135

Ito, T., Bishop, D. C., and Oliver, D. L. (2010). Expression of Glutamate and inhibitory amino acid vesicular transporters in the rodent auditory brainstem. *J. Comp. Neurol.* 519, 316–340. doi: 10.1002/cne.22521

Jeffress, L. A. (1948). A place theory of sound localization. *J. Comp. Physiol. Psychol.* 41, 35–39. doi: 10.1037/h0061495

Jenkins, S. A., and Simmons, D. D. (2006). GABAergic neurons in the lateral superior olive of the hamster are distinguished by differential expression of gad isoforms during development. *Brain Res.* 1111, 12–25. doi: 10.1016/j.brainres.2006.06.067

Joris, P. X., and Yin, T. C. T. (1998). Envelope coding in the lateral superior olive. III. Comparison with afferent pathways. *J. Neurophysiol.* 79, 253–269. doi: 10.1152/jn.1998.79.1.253

Kandler, K., Kullmann, P., Ene, F., and Kim, G. (2002). Excitatory action of an immature glycinergic/GABAergic sound localization pathway. *Physiol. Behav.* 77, 583–587. doi: 10.1016/S0031-9384(02)00905-8

Kanold, P. O., and Young, E. D. (2001). Proprioceptive information from the pinna provides somatosensory input to cat dorsal cochlear nucleus. *J. Neurosci.* 21, 7848–7858. doi: 10.1523/jneurosci.21-19-07848.2001

Kanold, P. O., Davis, K. A., and Young, E. D. (2011). Somatosensory context alters auditory responses in the cochlear nucleus. *J. Neurophysiol.* 105, 1063–1070. doi: 10.1152/jn.00807.2010

Kelly, J. B., Liscum, A., van Adel, B., and Ito, M. (1998). Projections from the superior olive and lateral lemniscus to tonotopic regions of the rat's inferior colliculus. *Hear. Res.* 116, 43–54. doi: 10.1016/S0378-5955(97)00195-0

Klug, A., Park, T. J., and Pollak, G. D. (1995). Glycine and GABA influence binaural processing in the inferior colliculus of the mustache bat. *J. Neurophysiol.* 74, 1701–1713. doi: 10.1152/jn.1995.74.4.1701

Koch, U., and Sanes, D. H. (1998). Afferent regulation of glycine receptor distribution in the gerbil LSO. *Microsc. Res. Tech.* 41, 263–269. doi: 10.1002/(sici)1097-0029(19980501)41:3\<263::aid-jemt9\>3.0.co;2-u

Konishi, M. (2000). Study of sound localization by owls and its relevance to humans. *Comp. Biochem. Physiol. A Mol. Integr. Physiol.* 126, 459–469. doi: 10.1016/s1095-6433(00)00232-4

Kulesza, R. J. Jr. (2008). Cytoarchitecture of the human superior olivary complex: Nuclei of the trapezoid body and posterior tier. *Hear. Res.* 241, 52–63. doi: 10.1016/j.heares.2008.04.010

Kulesza, R. J. Jr. (2014). Characterization of human auditory brainstem circuits by calcium-binding protein immunohistochemistry. *Neuroscience* 258, 318–331. doi: 10.1016/j.neuroscience.2013.11.035

Kuwabara, N., and Zook, J. M. (1991). Classification of the principal cells of the medial nucleus of the trapezoid body. *J. Comp. Neurol.* 314, 707–720. doi: 10.1002/cne.903140406

Kuwada, S., Yin, T. C., Buunen, T. J., and Wickesberg, R. E. (1984). Binaural interaction in low-frequency neurons in inferior colliculus of the cat. IV. Comparison of monaural and binaural response properties. *J. Neurophysiol.* 51, 1306–1325. doi: 10.1152/jn.1984.51.6.1306

Lanciego, J. L., and Wouterlood, F. G. (2020). Neuroanatomical tract-tracing techniques that did go viral. *Brain Struct. Funct.* 225, 1193–1224. doi: 10.1007/s00429-020-02041-6

LaVail, J. H., Winston, K. R., and Tish, A. (1973). A method based on retrograde intraaxonal transport of protein for identification of cell bodies of origin of axons terminating within the CNS. *Brain Res.* 58, 470–477. doi: 10.1016/0006-8993(73)90016-4

Li, S.-H., Zhang, C.-K., Qiao, Y., Ge, S.-N., Zhang, T., and Li, J.-L. (2020). Coexpression of VGLUT1 and VGLUT2 in precerebellar neurons in the lateral reticular nucleus of the rat. *Brain Res. Bull.* 162, 94–106. doi: 10.1016/j.brainresbull.2020.06.008

Liberman, M. C. (1980). Efferent synapses in the inner hair cell area of the cat cochlea: An electron microscopic study of serial sections. *Hear. Res.* 3, 189–204. doi: 10.1016/0378-5955(80)90046-5

Liu, Y.-J., Li, L.-F., Zhang, Y.-H., Guo, H.-F., Xia, M., Zhang, M.-W., et al. (2017). Chronic co-species housing mice and rats increased the competitiveness of male mice. *Chem. Sens.* 42, 247–257. doi: 10.1093/chemse/bjw164

Loftus, W. C., Bishop, D. C., and Oliver, D. L. (2010). Differential patterns pof inputs create functional zones in central nucleus of inferior colliculus. *J. Neurosci.* 30, 13396–133408. doi: 10.1523/JNEUROSCI.0338-10.2010

Loftus, W. C., Bishop, D. C., Saint Marie, R. L., and Oliver, D. L. (2004). Organization of binaural excitatory and inhibitory inputs to the inferior colliculus from the superior olive. *J. Comp. Neurol.* 472, 330–344. doi: 10.1002/cne.20070

McKay, J. (2012). *New complete guide to ferrets*. Stroud: Quiller Publishing Ltd.

Maison, S. F., Adams, J. C., and Liberman, M. C. (2002). Olivocochlear innervation in the mouse: Immunocytochemical maps, crossed versus uncrossed contributions, and transmitter colocalization. *J. Comp. Neurol.* 455, 406–416. doi: 10.1002/cne.10490

Malmierca, M. S., and Ryugo, D. K. (2011). "Descending connections of auditory cortex to the midbrain and brain stem," in *The auditory cortex*, eds J. A. Winer and C. E. Schriener (New York, NY: Springer), 189–208. doi: 10.1007/978-1-4419-0074-6_9

Marshall, F. (2020). Cats as predators and early domesticates in ancient human landscapes. *Proc. Nat. Acad. Sci. U.S.A.* 117, 18154–18156. doi: 10.1073/pnas.2011993117

Martinez-Lozada, Z., and Ortega, A. (2023). Milestone review: Excitatory amino acid transporters – beyond their expected function. *J. Neurochem.* 165, 457–466. doi: 10.1111/jnc.15809

Masterton, B., Heffner, H., and Ravizza, R. (1969). The evolution of human hearing. *J. Acoust. Soc. Am.* 45, 966–985. doi: 10.1121/1.1911574

Masterton, R. B., Diamond, I. T., Harrison, J. M., and Beecher, M. D. (1967). Medial superior olive and sound localization. *Science* 155, 1696–1697. doi: 10.1126/science.155.3770.1696-a

Mellott, J. G., Dhar, M., Mafi, A., Tokar, N., and Winters, B. D. (2021). Tonotopic distribution and inferior colliculus projection pattern of inhibitory and excitatory cell types in the lateral superior olive of Mongolian gerbils. *J. Comp. Neurol.* 530, 506–517. doi: 10.1002/cne.25226

Mesulam, M. M. (1978). Tetramethyl benzidine for horseradish peroxidase neurohistochemistry: A non-carcinogenic blue reaction product with superior sensitivity for visualizing neural afferents and efferents. *J. Histochem. Cytochem.* 26, 106–117. doi: 10.1177/26.2.24068

Milinkeviciute, G., Muniak, M. A., and Ryugo, D. K. (2017). Descending projections from the inferior colliculus to the dorsal cochlear nucleus are excitatory. *J. Comp. Neurol.* 525, 773–793. doi: 10.1002/cne.24095

Miller, J. (1996). The domestic cat: Perspective on the nature and diversity of cats. *J. Am. Vet. Med. Assoc.* 208, 498–502. doi: 10.2460/javma.1996.208.04.498a

Moore, D. R., Russell, F. A., and Cathcart, N. C. (1995). Lateral superior olive projections to the inferior colliculus in normal and unilaterally deafened ferrets. *J. Comp. Neurol.* 357, 204–216. doi: 10.1002/cne.903570203

Moore, J. K., and Moore, R. Y. (1971). A comparative study of the superior olivary complex in the primate brain. *Folia Primatol.* 16, 35–51. doi: 10.1159/000155390

Mosieff, A., and Konishi, M. (1981). Neuronal and behavioral sensitivity to binaural time differences in the owl. *J. Neurosci.* 1, 40–48. doi: 10.1523/JNEUROSSCI.01-01-00040.1981

Muniak, M. A., Ayeni, F. E., and Ryugo, D. K. (2018). Hidden hearing loss and endbulbs of Held: Evidence for central pathology before detection of ABR threshold increases. *Hear. Res.* 364, 104–117. doi: 10.1016/j.heares.2018.03.021

Nabekura, J., Katsurabayashi, S., Kakazu, Y., Shibata, S., Matsubara, A., Jinno, S., et al. (2003). Developmental switch from GABA to glycine release in single central synaptic terminals. *Nat. Neurosci.* 7, 17–23. doi: 10.1038/nn1170

Nerlich, J., Rübsamen, R., and Milenkovic, I. (2017). Developmental shift of inhibitory transmitter content at a central auditory synapse. *Front. Cell. Neurosci.* 11:211. doi: 10.3389/fncel.2017.00211

Netser, S., Meyer, A., Magalnik, H., Zylbertal, A., de la Zerda, S. H., Briller, M., et al. (2020). Distinct dynamics of social motivation drive differential social behavior in laboratory rat and mouse strains. *Nat. Commun.* 11:5908. doi: 10.1038/s41467-020-19569-0

Ngodup, T., Romero, G. E., and Trussell, L. O. (2020). Identification of an inhibitory neuron subtype, the L-stellate cell of the cochlear nucleus. *eLife* 9:e54350. doi: 10.7554/eLife.54350

Niu, X., Bogdanovic, N., and Canlon, B. (2004). The distribution and the modulation of tyrosine hydroxylase immunoreactivity in the lateral olivocochlear system of the guinea-pig. *Neuroscience* 125, 725–733. doi: 10.1016/j.neuroscience 2004.02.023

Nordeen, K. W., Killackey, H. P., and Kitzes, L. M. (1983). Ascending auditory projections to the inferior colliculus in the adult gerbil, *Meriones unguiculatus*. *J. Comp. Neurol.* 214, 131–143. doi: 10.1002/cne.902140203

Ohlemiller, K. K., Jones, S. M., and Johnson, K. R. (2016). Application of mouse models to research in hearing and balance. *J. Assoc. Res. Otolaryngol.* 17:493e523. doi: 10.1007/s10162-016-0589-1

Okanoya, K., Yosida, S., Barone, C. M., Applegate, D. T., Brittan-Powell, E. F., Dooling, R. J., et al. (2018). Auditory-vocal coupling in the naked mole-rat, a mammal with poor auditory thresholds. *J. Comp. Physiol. A Neuroethol. Sens. Neural Behav. Physiol.* 204, 905–914. doi: 10.1007/s00359- 018- 1287- 8

Oliver, D. L. (2000). Ascending efferent projections of the superior olivary complex. *Microsc. Res. Tech.* 51, 355–363. doi: 10.1002/1097-0029(20001115)51: 4< 355::AID-JEMT5> 3.0.CO;2- J

Ollo, C., and Schwartz, I. R. (1979). The superior olivary complex in C57BL/6 mice. *Am. J. Anat.* 155, 349–373. doi: 10.1002/aja.1001550306

Ono, M., and Ito, T. (2015). Functional organization of the mammalian auditory midbrain. *J. Physiol. Sci.* 65, 499–506. doi: 10.1007/s12576-015-0394-3

Ono, M., Bishop, D. C., and Oliver, D. L. (2020). Neuronal sensitivity to the interaural time difference of the sound envelope in the mouse inferior colliculus. *Hear. Res.* 385:107844. doi: 10.1016/j.heares.2019.107844

Ouagazzal, A.-M., Reiss, D., and Romand, R. (2006). Effeccts of age-related hearing loss on startle reflex and prepulse inhibition in mice on pure and mixed C57BL and 129 genetic background. *Behav. Brain Res.* 172, 307–315. doi: 10.1016/j.bbr.2006.05.018

Park, T. J., and Buffenstsein, R. (2012). *Digging the underground lif e. The Scientist*.*

Park, T. J., Klug, A., Holinstat, M., and Grothe, B. (2004). Interaural level difference processing in the lateral superior olive and the inferior colliculus. *J. Neurophysiol.* 92, 289–301. doi: 10.1152/jn.00961.2003

Paxinos, G., and Franklin, B. J. (2008). *The mouse brain in stereotaxic coordinates*, 3rd Edn. Sydney, NSW: Elsevier.

Qiu, L., Zhang, B., and Gao, Z. (2022). Lighting up neural circuits by viral tracing. *Neurosci. Bull.* 38, 1383–1396. doi: 10.1007/s12264-022-00860-7

Rauschecker, J. P. (2018). Where, when, and how: Are they all sensorimotor? Towards a unified view of the dorsal pathway in vision and audition. *Cortex* 98, 262–268. doi: 10.1016/j.cortex.2017.10.020

Reiner, A., Veenman, C. L., Medina, L., Jiao, Y., Del Mar, N., and Honig, M. G. (2000). Pathway tracing using biotinylated dextran amines. *J. Neurosci Methods* 15, 23–37. doi: 10.1016/s0165-0270(00)00293-4

Reiss, L. A., and Young, E. D. (2005). Spectral edge sensitivity in neural circuits of the dorsal cochlear nucleus. *J. Neurosci.* 25, 3680–3691. doi: 10.1523/ JNEUROSCI.4963-04.2005

Rice, J. J., May, B. J., Spirou, G. A., and Young, E. D. (1992). Pinna-based spectral cues for sound localization in cat. *Hear. Res.* 58, 132–152. doi: 10.1016/0378-5955(92)90123-5

Rietzel, H. J., and Friauf, E. (1998). Neuron types in the rat lateral superior olive and developmental changes in the complexity of their dendritic arbors. *J. Comp. Neurol.* 390, 20–40. doi: 10.1002/(SICI)1096-9861(19980105)390:1<20::AID-CNE3$>$3.0.CO;2-S

Romanski, L. M., Tian, B., Fritz, J., Mishkin, M., Goldman-Rakic, P. S., and Rauschecker, J. P. (1999). Dual streams of auditory afferents target multiple domains in the primate prefrontal cortex. *Nat. Neurosci.* 2, 1131–1136. doi: 10.1038/16056

Ross, L. S., Pollak, G. D., and Zook, J. M. (1988). Origin of ascending projections to an isofrequency region of the mustache bat's inferior colliculus. *J. Comp. Neurol.* 270, 488–505. doi: 10.1002/cne.902700403

Rossi, A. C. (1975). The "mouse-killing" rat: Ethological discussion on an experimental model of aggression. *Pharmacol. Res. Commun.* 7, 199–216. doi: 10.1016/0031-6989(75)90020-x

Ryugo, D. K., and Fekete, D. M. (1982). Morphology of primary axosomatic endings in the anteroventral cochlear nucleus of the cat: A study of the endbulbs of Held. *J. Comp. Neurol.* 210, 239–257. doi: 10.1002/cne.902100304

Ryugo, D. K., and Milinkeviciute, G. (2023). Differential projections from the cochlear nucleus to the inferior colliculus in the mouse. *Front. Neural Circuits* 17:1229746. doi: 10.3389/fncir.2023.1229746

Ryugo, D. K., Haenggeli, C.-A., and Doucet, J. R. (2003). Multimodal inputs to the granule cell domain of the cochlear nucleus. *Exp. Brain Res.* 153, 477–485. doi: 10.1007/s00221-003-1605-3

Ryugo, D. K., Popper, A. N., and Fay, R. R. (2011). *Auditory and vestibular efferents*. New York, NY: Springer-Verlag.

Saint Marie, R. L. S., Ostapoff, E.-M., Morest, D. K., and Wenthold, R. J. (1989). Glycine-immunoreactive projection of the cat lateral superior olive: Possible role in midbrain ear dominance. *J. Comp. Neurol.* 279, 382–396. doi: 10.1002/cne 902790305

Saint Marie, R. L., and Baker, R. A. (1990). Neurotransmitter-specific uptake and retrograde transport of [3H]glycine from the inferior colliculus by ipsilateral projections of the superior olivary complex and nuclei of the lateral lemniscus. *Brain Res.* 524, 244–253. doi: 10.1016/0006-8993(90)90698-B

Schaeffer, D. F., Reuss, M. H., Riemann, R., and Reuss, S. (2003). A nitrergic projection from the superior olivary complex to the inferior colliculus of the rat. *Hear. Res.* 183, 67–72. doi: 10.1016/s0378-5955(03)00219-3

Scheibel, M. E., and Scheibel, A. B. (1974). Neuropil organization in the superior olive of the cat. *Exp. Neurol.* 43, 339–348. doi: 10.1016/0014-4886(74)90175-7

Scheibler, E., Liu, W., Weinandy, R., and Gattermann, R. (2006). Burrow systems of the Mongolian gerbil (*Meriones unguiculatus* Milne Edwards, 1867). *Mammal. Biol.* 71, 178–182. doi: 10.1016/j.mambio.2005.11.007

Schweizer, H. (1981). The connections of the inferior colliculus and the organization of the brainstem auditory system in the greater horseshoe bat (*Rhinolophus ferrumequinum*). *J. Comp. Neurol.* 201, 25–49. doi: 10.1002/cne 902010104

Sergeyenko, Y., Lall, K., Liberman, M. C., and Kujawa, S. G. (2013). Age-related cochlear synaptopathy: An early-onset contributor to auditory functional decline. *J. Neurosci.* 33, 13686–13694. doi: 10.1523/JNEUROSCI.1783-13.2013

Smith, J. C. (2019). A review of strain and sex differences in response to pain and analgesia in mice. *Comp. Med.* 69, 490–500. doi: 10.30802/AALAS-CM-19-000066

Stevens, S. S., and Newman, E. B. (1936). The localization of actual sources of sound. *Am. J. Psychol.* 48:297. doi: 10.2307/1415748

Storer, T. I. (1948). Control of rats and mice. California agricultural extension service. *Circular* 138:142. doi: 10.5962/bhl.title.53398

Storm-Mathisen, J., Leknes, A. K., Bore, A. T., Vaaland, J. L., Edminson, P., Haug, F.-M., et al. (1983). First visualization of glutamate and GABA in neurones by immunocytochemistry. *Nature* 301, 517–520. doi: 10.1038/301517a0

Suthakar, K. (2017). *Changes in the descending auditory system in hearing loss: Focus on auditory efferents*. Ph.D. thesis. Sydney, NSW: University of New South Wales.

Taber, E. (1961). The cytoarchitecture of the brain stem of the cat. I. Brain stem nuclei of cat. *J. Comp. Neurol.* 116, 27–69. doi: 10.1002/cne.901160104

Taberner, A. M., and Liberman, M. C. (2005). Response properties of single auditory nerve fibers in the mouse. *J. Neurophysiol.* 93:557e569. doi: 10.1152/jn00574.2004

Tollin, D. J., and Yin, T. C. (2002). The coding of spatial location by single units in the lateral superior olive of the cat. I. Spatial receptive fields in azimuth. *J. Neurosci.* 22, 1454–1467. doi: 10.1523/jneurosci.22-04-01454.2002

Tollin, D. J., and Yin, T. C. (2005). Interaural phase and level difference sensitivity in low-frequency neurons in the lateral superior olive. *J. Neurosci.* 25, 10648–10657. doi: 10.1523/jneurosci.1609-05.2005

Traweger, D., Travnitzky, R., Moser, C., Walzer, C., and Bernatzky, G. (2006). Habitat preferences and distribution of the brown rat (rattus Norvegicus Berk.) in the city of Salzburg (Austria): Implications for an urban rat management. *J. Pest Sci.* 79, 113–125. doi: 10.1007/s10340-006-0123-z

Tsuchitani, C., and Boudreau, J. C. (1966). Single unit analysis of cat superior olive s segment with tonal stimuli. *J. Neurophysiol.* 29, 684–697. doi: 10.1152/jn.1966.29.4.684

Tsuchitani, C., and Boudreau, J. C. (1967). Encoding of stimulus frequency and intensity by cat superior olive S-segment cells. *J. Acoust. Soc. Am.* 42, 794–805. doi: 10.1121/1.1910651

Vetter, D. E., Adams, J. C., and Mugnaini, E. (1991). Chemically distinct rat olivocochlear neurons. *Synapse* 7, 21–43. doi: 10.1002/syn.890070104

Vetter, D. E., and Mugnaini, E. (1992). Distribution and dendritic features of three groups of rat olivocochlear neurons. *Anat. Embryol.* 185, 1–16. doi: 10.1007/BF00213596

Vorhies, C. T., and Taylor, W. P. (2015). *Life history of the kangaroo rat: Dipodomys spectabilis spectabilis merriam*. Boulder, CO: Palala Press.

Warr, W. B. (1975). Olivocochlear and vestibular efferent neurons of the feline brain stem: Their location, morphology and number determined by retrograde axonal transport and acetylcholinesterase histochemistry. *J. Comp. Neurol.* 161, 159–181. doi: 10.1002/cne.901610203

Weber, J. N., Peterson, B. K., and Hoekstra, H. E. (2013). Discrete genetic modules are responsible for complex burrow evolution in Peromyscus mice. *Nature* 493, 402–405. doi: 10.1038/nature11816

Wenthold, R. J., Huie, D., Altschuler, R. A., and Reeks, K. A. (1986). Glycine immunoreactivity localized in the cochlear nucleus and superior olivary complex. *Neuroscience* 22, 897–912. doi: 10.1016/0306-4522(87)92968-x

Willard, F. H., and Martin, G. F. (1984). Collateral innervation of the inferior colliculus in the North American opossum: A study using fluorescent markers in a double-labeling paradigm. *Brain Res.* 303, 171–182. doi: 10.1016/0006-8993(84)90225- 7

Williams, I. R., Filimontseva, A., Connelly, C. J., and Ryugo, D. K. (2022). The lateral superior olive in the mouse: Two systems of projecting neurons. *Front. Neural Circuits* 16:1038500. doi: 10.37247/pans2ed.2.23.13

Willott, J. F., and Turner, J. T. (1999). Prolonged exposure to an augmented acoustic environment ameliorates age-related auditory changes in C59BL/6J and DB A/2J mice. *Hear. Res.* 135, 78–88. doi: 10.1016/s0378-5955(99)00094-5

Willott, J. F., Pankow, D., Hunter, K. P., and Kordyban, M. (1985). Projections from the anterior ventral cochlear nucleus to the central nucleus of the inferior colliculus iin young and aging C57BL/6 mice. *J. Comp. Neurol.* 238, 545–551. doi: 10.1002/cne.902370410

Wright, D. D., and Ryugo, D. K. (1996). Mossy fiber projections from the cuneate nucleus to the cochlear nucleus in the rat. *J. Comp. Neurol.* 365, 159–172. doi: 10.1002/(sici)1096-9861(19960129)365:1<159::aid-cne12>3.0.co;2-l

Wu, C., and Shore, S. E. (2018). Multisensory activation of ventral cochlear nucleus d-stellate cells modulates dorsal cochlear nucleus principal cell spatial coding. *J. Physiol.* 596, 4537–4548. doi: 10.1113/jp276280

Wu, J. S., Yi, E., Manca, M., Javaid, H., Lauer, A. M., and Glowatzki, E. (2020). Sound exposure dynamically induces dopamine synthesis in cholinergic LOC efferents for feedback to auditory nerve fibers. *Elife* 9:e52419. doi: 10.7554/eLife.52419

Yin, T. C. T., Smith, P. H., and Joris, P. X. (2019). Neural mechanisms of binaural processing in the auditory brainstem. *Comp. Physiol.* 9, 1503–1575. doi: 10.1002/cphy.c180036

Zeilhofer, H. U., Studler, B., Arabadzisz, D., Schweizer, C., Ahmadi, S., Layh, B., et al. (2005). Glycinergic neurons expressing enhanced green fluorescent protein in bacterial artificial chromosome transgenic mice. *J. Comp. Neurol.* 482, 123–141. doi: 10.1002/cne.20349

Zheng, Q. Y., Johnson, K. R., and Erway, L. C. (1999). Assessment of hearing in 80 inbred strains of mice by ABR threshold analyses. *Hear. Res.* 130, 94–107. doi: 10.1016/s0378-5955(99)00003-9

Zhu, X., Vasilyeve, O. N., Kim, S., Jacobson, M., and Romney, J. (2007). Auditory efferent feedback system deficits precede age-related hearing loss: Contralateral suppression of otoacoustic emissions in mice. *J. Comp. Neurol.* 503, 593–604. doi: 10.1002/cne.21402

frontiers | Frontiers in Neural Circuits

TYPE Original Research
PUBLISHED 29 August 2024
DOI 10.3389/fncir.2024.1448592

OPEN ACCESS

EDITED BY
Kensaku Mori,
RIKEN,'Japan

REVIEWED BY
Shin Nagayama,
Texas Medical Center, United States
Jackson Cioni Bittencourt,
University of São Paulo, Brazil

*CORRESPONDENCE
Hajime Suyama
✉ hajime.suyama@ovgu.de

†PRESENT ADDRESS
Hajime Suyama,
Institute of Biology, Otto-von-Guericke University Magdeburg, Magdeburg, Germany

RECEIVED 13 June 2024
ACCEPTED 13 August 2024
PUBLISHED 29 August 2024

CITATION
Suyama H, Bianchini G and Lukas M (2024) Vasopressin differentially modulates the excitability of rat olfactory bulb neuron subtypes.
Front. Neural Circuits 18:1448592.
doi: 10.3389/fncir.2024.1448592

Vasopressin differentially modulates the excitability of rat olfactory bulb neuron subtypes

Hajime Suyama[1]*†, Gaia Bianchini[2] and Michael Lukas[1]

[1]Institute of Zoology, Neurophysiology, University of Regensburg, Regensburg, Germany, [2]Neural Circuits and Behavior Laboratory, The Francis Crick Institute, London, United Kingdom

Vasopressin (VP) plays a crucial role in social memory even at the level of the olfactory bulb (OB), where OB VP cells are activated during social interactions. However, it remains unclear how VP modulates olfactory processing to enable enhanced discrimination of very similar odors, e.g., rat body odors. Thus far, it has been shown that VP reduces firing rates in mitral cells (MCs) during odor presentation *in vivo* and decreases the amplitudes of olfactory nerve-evoked excitatory postsynaptic potentials (ON-evoked EPSPs) in external tufted cells *in vitro*. We performed whole-cell patch-clamp recordings and population Ca^{2+} imaging on acute rat OB slices. We recorded ON-evoked EPSPs as well as spontaneous inhibitory postsynaptic currents (IPSCs) from two types of projection neurons: middle tufted cells (mTCs) and MCs. VP bath application reduced the amplitudes of ON-evoked EPSPs and the frequencies of spontaneous IPSCs in mTCs but did not change those in MCs. Therefore, we analyzed ON-evoked EPSPs in inhibitory interneurons, i.e., periglomerular cells (PGCs) and granule cells (GCs), to search for the origin of increased inhibition in mTCs. However, VP did not increase the amplitudes of evoked EPSPs in either type of interneurons. We next performed two-photon population Ca^{2+} imaging in the glomerular layer and the superficial GC layer of responses to stronger ON stimulation than during patch-clamp experiments that should evoke action potentials in the measured cells. We observed that VP application increased ON-evoked Ca^{2+} influx in juxtaglomerular cells and GC somata. Thus, our findings indicate inhibition by VP on projection neurons via strong ON input-mediated inhibitory interneuron activity. This neural modulation could improve representation of odors, hence, better discriminability of similar odors, e.g., conspecific body odors.

KEYWORDS

vasopressin, olfactory bulb, social discrimination, neuromodulation, neuropeptide

Introduction

Various mammalian species rely on olfaction to identify environmental stimuli, such as food, predators, or individual conspecifics. Thus, rodents sniff conspecifics at the initiation of social behaviors, allowing them to assess characteristics such as sex or familiarity. For example, male mice can discriminate urine from males and females even when they are not able to establish physical contact with them (Pankevich et al., 2004). Another example is social memory, also known as social discrimination (Engelmann et al., 2011), which is based on recognition of individual conspecifics encountered previously. This ability can be quantified experimentally as rats investigate an unknown stimulus rat longer than another with whom they recently interacted. Social memory is suggested to be highly dependent on olfaction since the olfactory bulb (OB) is essential for social discrimination (Dantzer et al., 1990).

The central actions of the neuropeptide vasopressin (VP) include the modulation of social behavior. Moreover, VP is an important enhancer of social memory (Dantzer et al., 1988). More specifically, local OB injection of a VP receptor antagonist blocks the ability to form memories of conspecifics, whereas additional local application of VP prolongs the memory for conspecifics (Dluzen et al., 1998; Tobin et al., 2010).

The OB is the very first brain region for processing and filtering olfactory signals in mammals. Neural microcircuits in the OB are known to integrate and modify signals from the olfactory epithelium before transmitting those to the olfactory cortex and other higher brain areas, which then trigger behavioral responses. Approximately 80% of all neurons in the OB are inhibitory interneurons (Shepherd et al., 2004), such as periglomerular cells (PGCs) in the glomerular layer (GL) and granule cells (GC) in the GC layer (GCL) (Nagayama et al., 2014). Interneurons form synaptic connections onto other interneurons or projection neurons, such as middle tufted cells (mTCs) and mitral cells (MCs), to inhibit them. The major portion of inhibition in the GL is suggested to function as gain control of incoming olfactory signals (e.g., Linster and Hasselmo, 1997; Cleland and Sethupathy, 2006; Cleland et al., 2007), whereas GCs organize spike timing and synchronization of projection neurons (e.g., McTavish et al., 2012; Fukunaga et al., 2014; Osinski and Kay, 2016; Egger and Kuner, 2021). Although most bulbar neurons express the classical neurotransmitter glutamate or GABA, it is known that various other substances that are released from either bulbar neurons or centrifugal projections affect neural communication in the OB as well, including neuromodulators, e.g., dopamine or acetylcholine, and neuromodulatory neuropeptides, like VP or cholecystokinin (Nagayama et al., 2014; Imamura et al., 2020; Brunert and Rothermel, 2021; Suyama et al., 2022). A source of endogenous VP that acts on social discrimination in the OB is an innate population of VP-expressing cells (VPCs) that were characterized as a subpopulation of superficial tufted cells (Tobin et al., 2010; Lukas et al., 2019). As mentioned above, VP signaling at the level of the OB is essential for the social memory of conspecifics (Tobin et al., 2010).

Several of our previous findings support the importance of VP neuromodulation in the OB during social memory establishment and thereby indicate intrabulbar VP release from VPCs. Thus, bulbar VPCs react with increased numbers of activated cells, i.e., positive for phosphorylated extracellular signal-regulated kinase, following social interaction *in vivo* and with action potential firing following olfactory nerve stimulation during acetylcholine application in *in-vitro* OB slice experiments (Suyama et al., 2021). However, it is still not clear how VP modulates olfactory processing on the cellular level to enable enhanced discrimination of very similar odor mixtures, such as conspecific body odors (Singer et al., 1997).

Tobin et al. (2010) showed that spontaneous firing rates and firing rates after odor stimulation in MCs decrease upon VP administration *in vivo*, and we showed that VP bath application decreases the amplitudes of electrical olfactory nerve (ON) stimulation-evoked excitatory postsynaptic potentials (EPSPs) in eTCs *in vitro* (Lukas et al., 2019). These initial findings suggest that VP has inhibitory effects on excitatory neurons in the OB. Since the prevalent OB VP receptors are Gq-coupled excitatory V1a receptors (V1aRs), it is unlikely that VP acts directly on excitatory neurons. Therefore, the origin of VP inhibitory effects is not yet determined. However, we have suggestions from the morphology of VPCs. We previously showed the neurite reconstruction of VPCs, including apical dendritic tufts in the GL and axons in the GCL (Lukas et al., 2019). VP-neurophysin was found in somata, dendrites, and axons, which indicates that VP could be released from dendrites, e.g., apical dendritic tufts, and axons. Biocytin-DAB reconstruction revealed that aside from apical dendritic tufts in the glomeruli, VPCs innervate densely in the GL and EPL, and in the superficial GCL, they have either numerous short but localized branches (type 1) or long-range projection along the internal plexiform layer (type 2) (Lukas et al., 2019). The observation leads to the hypothesis that VP is released in the GL and the superficial GCL binds to cells located there. In line with the hypothesis, strong signals of V1aR staining were observed in the GL (Ostrowski et al., 1994) and in the superficial part of the GCL (Tobin et al., 2010). Moreover, the discriminability of similar odors, including social discrimination, is regulated by bulbar interneurons, which in turn modulate excitatory/projection neurons (Abraham et al., 2010; Oettl et al., 2016). Thus, we hypothesized that an excitatory action of VP on inhibitory neurons in the GL or the GCL enhances the inhibition of excitatory neurons during social interactions.

As a first step to examine how VP might enhance the inhibition of excitatory neurons during odor processing, we investigated VP effects on the responses of different cell types, including both excitatory and inhibitory neurons, to ON stimulation in acute OB slices, which mimics sensory activation. Therefore, we recorded ON-evoked EPSPs and spontaneous inhibitory postsynaptic currents (IPSCs) in mTCs and MCs that project to the cortices, and ON-evoked EPSPs in PGCs and GCs. Furthermore, we performed Ca^{2+} population imaging of ON-evoked responses in the GL and the superficial GCL using two-photon microscopy.

Materials and methods

Animals

All procedures were conducted according to the guidelines for the care and use of laboratory animals by the local government of Oberpfalz and Unterfranken, and we are monitored and certified regarding animal handling and slice preparation by institutional veterinarians.

Wistar rats of either sex were purchased from Charles River Laboratories (Sulzfeld, Germany) or bred onsite in the animal facilities at the University of Regensburg. The light in the rooms was set to an automatic 12-h cycle (lights on 07:00–19:00).

Slice preparation

Eleven- to 18-day-old juvenile rats of either sex were used for *in-vitro* electrophysiology and Ca^{2+} imaging experiments. The rats were deeply anesthetized with isoflurane and quickly decapitated. Horizontal slices (300 µm) of the OB were cut in ice-cold, carbogenated ACSF (artificial cerebrospinal fluid; in mM: 125 NaCl, 26 $NaHCO_3$, 1.25 NaH_2PO_4, 20 glucose, 2.5 KCl, 1 MgCl, and 2 $CaCl_2$) using a vibratome (VT 1200, LEICA, Wetzlar, Germany) and afterward incubated in ACSF at 36°C for 45 min. Until experiments, the slices were kept at room temperature (~21°C) in ACSF.

Electrophysiology

Brain slices were placed in a recording chamber on the microscope's stage and continuously perfused with carbogenated ACSF circulated using a perfusion pump (ISM 850, Cole-Parmer, Wertheim, Germany). To perform whole-cell patch-clamp recordings, cells were visualized by infrared gradient-contrast illumination via an IR filter (Hoya, Tokyo, Japan). Glass pipettes for recordings were pulled by a pipette puller (Narishige, Tokyo, Japan) sized 4–6 MΩ and filled with intracellular solution. The intracellular solution for current-clamp recordings contained 130 K-methylsulfate, 10 HEPES, 4 $MgCl_2$, 4 Na_2ATP, 0.4 NaGTP, 10 Na phosphocreatine, and 2 ascorbate (in mM) at pH 7.2, and the intracellular solution for voltage-clamp recordings contained 110 CsCl, 10 HEPES, 4 $MgCl_2$, 10 TEA, 10 QX-314, 2.5 Na_2ATP, 0.4 NaGTP, 10 Na Phosphocreatine, and 2 ascorbate (in mM) at pH 7.2. Recordings were performed with an EPC-10 (HEKA, Lambrecht, Germany) digital oscilloscope. The series resistance ranged between 10 and 30 MΩ. The average resting membrane potentials were −60 to −70 mV in MCs and mTCs, −50 to −60 mV in PGCs, and −70 to −80 mV in GCs. Experiments were only started in cases where the patched cells had a holding current below approximately −50 pA and a stable resting membrane potential. When the resting membrane potential is shifted during the ON stimulation experiments, the holding current is adjusted to bring the membrane potential back to the initial value in order to avoid the effects of leakage and the possible direct effects of VP on the resting membrane potentials (Table 1). Experiments were performed at room temperature (~21°C).

ON stimulation was performed with a glass pipette stimulation electrode sized around 2 MΩ. Glass pipettes were filled with ACSF. The unipolar electrode was connected to an external stimulator (STG 1004, Multi-Channel Systems, Reutlingen, Germany). The stimulation strength was adjusted via the stimulator's software (MC_Stimulus, v 2.1.5), and stimulation was triggered by the amplifier software (Patchmaster, v2x73.5, HEKA). Stimulation pipettes were gently placed in the ON layer anterior to the area selected for patching using a manual manipulator (LBM-7, Scientifica, East Sussex, UK) under optical control with the microscope. The stimulation lasted for 100 µs, with a current of 20–200 µA for mTCs, 25–350 µA for MCs, 9–100 µA for PGCs, or 5–150 µA for GCs. We confirmed the identity of PGCs with *post-hoc* morphological examination. We added biocytin (5 mg/mL, Sigma-Aldrich, Darmstadt, Germany) in the intracellular solution to fill cells during recording and subsequently visualized apical dendrite arbors using enzymatic 3,3′-diaminobenzidine-based staining (Vector Laboratories, CA, USA) (Lukas et al., 2019). All patched putative PGCs had a soma sized <10 µm and no long-range laterally projecting neurite, confirming their identity as PGCs (Nagayama et al., 2014).

TABLE 1 Holding currents during experiments with olfactory nerve stimulation.

	ACSF (pA)	VP (pA)	Changes (pA)
mTCs	−40.1 ± 25.3	−42.2 ± 23.9	−1.3 ± 3.7
MCs	−34.9 ± 16.6	−37.6 ± 16.3	−2.7 ± 8.9
PGCs	−11.9 ± 15.2	−14.7 ± 15.7	−2.9 ± 4.0
GCs	−13.4 ± 17.3	−17.4 ± 18.0	−4.0 ± 5.6

mTCs, middle tufted cells; MCs, mitral cells; PGCs, periglomerular cells; GCs, granule cells.

Experimental design

In current-clamp experiments recording ON-evoked EPSPs, ON stimulation was triggered only every 30 s to prevent run-down (Lukas et al., 2019). VP was diluted in ACSF ([Arg^8]-vasopressin acetate salt, Sigma-Aldrich, Darmstadt, Germany, 1 µM) and bath-applied via the perfusing system after a baseline recording of 5 min. Traces in the VP condition were recorded no earlier than 5 min after the onset of administration. Traces were averaged over five stimulations, and two such averaged traces, each in the ACSF condition and in the VP condition, were analyzed. Averaged amplitudes within conditions were normalized to the ACSF condition (100%). The data were analyzed with Origin 2020 (Origin Lab Corporation, Northampton, MA, USA).

In voltage-clamp experiments, spontaneous IPSCs were recorded at 0 mV for 10 min during each condition. VP (1 µM) was bath-applied via the perfusion system, and the VP condition was recorded 5 min after the onset of administration for 5 min. The frequencies and amplitudes of IPSCs were normalized to the ACSF condition (100%). The data were analyzed with the Peak Analyzer in Origin 2020.

Population Ca^{2+} imaging

For population Ca^{2+} imaging, the AM-dye Cal-520 (1 µM, AAT Bioquest, CA, USA) and Alexa 594 (50 µM, Invitrogen) were loaded into the superficial GCL or the GL via a glass pipette sized around 2 MΩ. Loading pipettes were guided by light microscopy and the Alexa 594 fluorescence. The Ca^{2+} dye was loaded for 15 s using the Picospritzer III device (Parker Hannifin, NH, USA), followed by 20 min incubation to allow the Ca^{2+} dye to be taken up by cells. The fluorescence was imaged at a wavelength of 850 nm in raster-scan mode using a two-photon resonant scanner (frame rate of 31.5 Hz). Femto-2D microscope (Femtonics) was equipped with a Mai Tai wideband, mode-locked Ti:Sapphire laser (Spectra-Physics, CA, USA) and a 20× Zeiss water immersion objective (Carl Zeiss, Oberkochen, Germany). The microscope was controlled by MESc v3.3.4290 software (Femtonics). ON stimulation (400 µA, 100 µs) was applied three times for each condition: control (ACSF) and VP (1 µM). VP was bath-applied via the perfusion system, and the VP condition was recorded 10 min after the onset of administration.

The raw data of the experiments were imported to Fiji[1] and ΔF/F in the somata of GCs, juxtaglomerular cells (JGCs, decided by the small cell bodies), and the glomeruli were extracted using the ROI selection tool. The resulting traces from the three stimulations per condition were averaged. ΔF/F amplitudes and integral (from the onset of the signal until the signal is back to the baseline or the end of the session) were analyzed with Origin 2020. ΔF/F in the VP condition was corrected according to the ratio of the basal fluorescence (F0) in the VP condition to that in the ACSF condition. Corrected ΔF/F

1 ImageJ, downloaded from: https://imagej.net/Fiji/Downloads.

(VP) = ΔF/F (VP) × F0 (VP) / F0 (ACSF). Averaged amplitudes and integral within conditions were normalized to the ACSF condition (100%).

Ca^{2+} imaging experiments were performed at room temperature (~21°C).

Statistics

Statistics were performed with SPSS (version 26, IBM, Armonk, NY, USA). All statistical analysis performed was two-sided, and significance was accepted at $p < 0.05$. All data in the text are shown with average ± standard deviation.

Results

VP reduced ON-mediated excitation and increased spontaneous inhibition in mTCs but not in MCs

We performed patch-clamp recordings in either current-clamp or voltage-clamp configuration in mTCs and MCs in acute OB slices (Figure 1A). Electrical ON stimulation reliably evoked EPSPs in mTCs and MCs. We then compared EPSP amplitudes in the presence of VP (1 µM in ACSF) to the control condition (ACSF). In mTCs, VP reduced the amplitudes of ON-evoked EPSPs to 60.4 ± 20.5% of control ($p = 0.012$, $z = -2.521$, related samples Wilcoxon test, $n = 8$ from six rats; Figures 1B,C). The amplitudes of ON-evoked EPSPs without VP application were stable over time compared to the VP condition (95.0 ± 4.6% of control, 10 min after the start of the measurement, $n = 5$ from four rats, $p = 0.004$, $t(11) = 3.657$, t-test vs. VP). Therefore, we concluded that the reduction is due to VP application but not desensitization of bulbar circuits to ON stimulation. In another set of experiments using voltage-clamp recordings, VP increased the frequencies of spontaneous IPSCs to 123.3 ± 23.6% of control ($p = 0.012$, $z = 2.521$, related samples Wilcoxon test, $n = 8$ from four rats; Figures 1D,E). However, the amplitudes of spontaneous IPSCs were not changed (106.9 ± 24.3%, $p = 0.263$, $z = 1.120$, related samples Wilcoxon test, $n = 8$ from four rats; Figure 1F), indicating a predominantly presynaptic effect. Furthermore, in all experiments ($n = 8$ from four rats), spontaneous IPSCs were abolished following bath application of bicuculline (a GABA receptor antagonist, 50 µM), confirming the GABAergic origin of these signals (data not shown). Therefore, the data imply that VP enhances both ON-evoked and tonic inhibitory modulation of mTCs. Surprisingly, we did not observe any of those VP inhibitory effects in MCs, even though broad distributions in evoked EPSP amplitudes and IPSC frequencies in the VP condition were observed [ON-evoked EPSPs: 99.4 ± 20.2% of control, $p = 0.929$, $z = -0.089$,

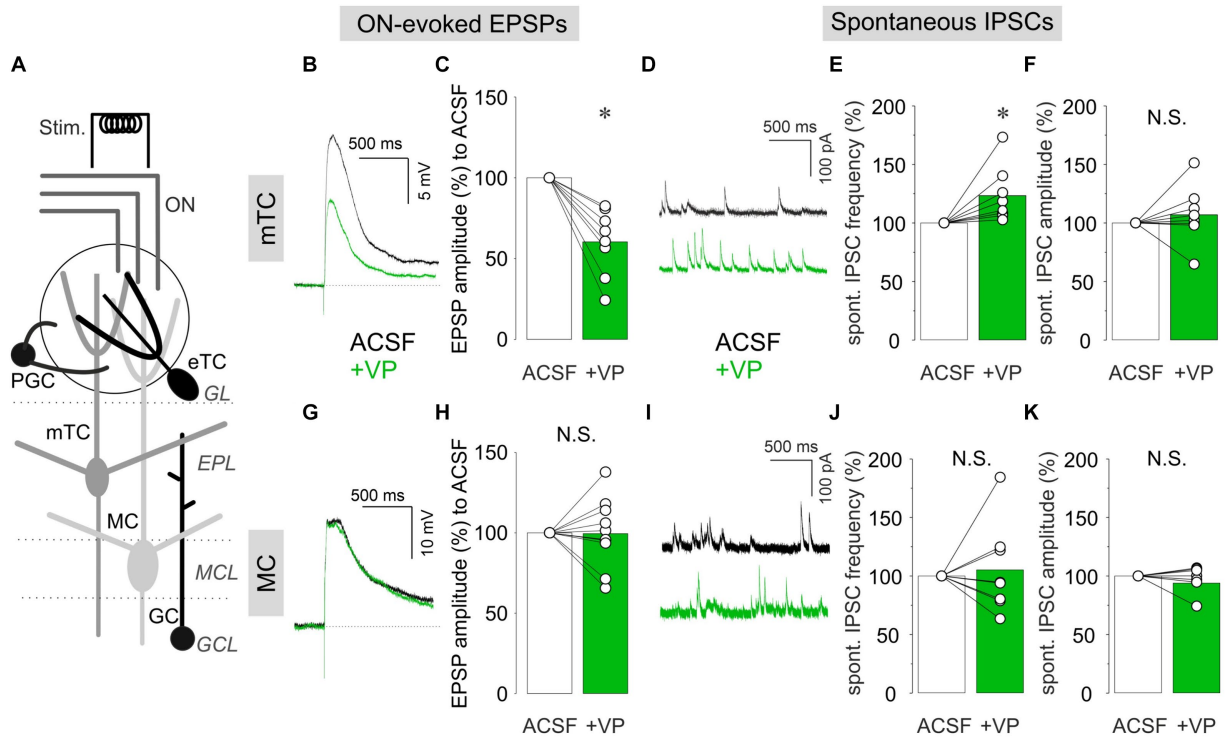

FIGURE 1
Patch-clamp recordings from mTCs and MCs. **(A)** The schematic image of the OB slice. ON, olfactory nerve; GL, glomerular layer; EPL, external plexiform layer; MCL, mitral cell layer; GCL, granule cell layer; Stim., electrical ON stimulation; PGC, periglomerular cell; eTC, external tufted cell; mTC, middle tufted cell; MC, mitral cell; GC, granule cell. Representative current-clamp traces of ON-evoked EPSPs and cumulative data of ON-evoked EPSP amplitudes in % to control in mTCs **(B,C)** and MCs **(G,H)**. Representative voltage-clamp traces of spontaneous IPSCs and cumulative data of spontaneous IPSC frequencies and amplitudes in % to control in mTCs **(D–F)** and MCs **(I–K)**. The bar graphs show average values. Individual data points are shown as open circles, and points from the same cell are connected by a line. *$p < 0.05$; N.S., non-significant. Black traces: ACSF (control); Green traces: VP.

related samples Wilcoxon test, $n = 11$ from nine rats (Figures 1G,H); frequencies of spontaneous IPSCs: 105.3 ± 38.2% of control, $p = 0.889$, $z = 0.140$, related samples Wilcoxon test, $n = 8$ from six rats (Figures 1I,J); amplitudes of spontaneous IPSCs: 97.2 ± 10.6% of control, $p = 0.779$, $z = -0.280$, related samples Wilcoxon test, $n = 8$ from six rats (Figures 1I,K)]. This lack of consistent inhibitory effects in MCs was somewhat unexpected, as Tobin et al. (2010) showed *in vivo* that VP reduces spontaneous and odor-evoked spiking rates in MCs.

VP did not increase evoked EPSPs in inhibitory neurons

Where does the inhibition of excitatory projection neurons, e.g., eTCs or mTCs, originate from? There are two main populations of inhibitory interneurons in the OB. One is in the glomerular layer (GL), where synapses between the ON and bulbar neurons reside within the glomerular neuropil. Thus, the first modulation of olfactory inputs takes place in this layer. There are many cell types of inhibitory neurons in the GL, and the most numerous are PGCs (Nagayama et al., 2014). We performed patch-clamp recordings in PGCs regardless of subtypes, as we were not able to differentiate them in our experimental setup. ON stimulation-evoked EPSPs in PGCs. We observed mixed effects of VP (1 μM) on the amplitudes of evoked EPSPs, including increase, decrease, or no changes (Figure 2A). Consequently, there was no overall significant difference between VP application compared to the control condition (85.4 ± 26.1% of control, $p = 0.131$, $z = -1.511$, paired Wilcoxon test, $n = 11$ from nine rats; Figure 2B). We further categorized PGCs into either Type A or Type C according to their firing patterns, as described by Tavakoli et al. (2018). In addition, we examined if hyperpolarizing currents evoked sags due to hyperpolarization-induced depolarization. Moreover, we visualized patched putative PGCs by filling cells with biocytin (see methods) to investigate their morphology. However, we could not find any correlation between these electrophysiological or morphological characteristics and the different directions of VP effects (data not shown).

We next examined the second main population of inhibitory interneurons in the OB, the GCs (Nagayama et al., 2014). Unlike PGCs, VP consistently decreased the amplitudes of ON-evoked EPSPs in GCs to 85.0 ± 11.7% of control ($p = 0.012$, $z = -2.521$, related samples Wilcoxon test, $n = 8$ from eight rats; Figures 2C,D). Thus, ON-evoked EPSPs were not increased upon VP administration in both inhibitory interneuron populations, arguing against an increased excitation of interneurons via the sensory afferents as a mechanism for the inhibitory action of VP on eTCs and mTCs.

VP increased evoked Ca^{2+} influx in inhibitory neurons

While VP did not increase the subthreshold excitability of inhibitory neurons, we next wondered whether suprathreshold activation might be enhanced. Therefore, we performed two-photon population Ca^{2+} imaging to examine VP effects on Ca^{2+} influx in inhibitory interneurons with strong ON stimulation, which is likely to evoke action potentials in stimulated cells from our experience (400 μA, up to 100 μA, or 150 μA for EPSP experiments in PGCs or GCs, respectively). We injected the AM-dye Cal-520 into the GL, followed by two-photon imaging with a resonant scanner. After JGCs took up the dye into their somata, we stimulated the ON and measured ΔF/F in the JGC somata as well as in the neuropil in the glomeruli (Figures 3A,B; Egger et al., 2003). F0 in JGCs increased in the VP condition to 125 ± 29.3% of control ($p < 0.001$, $z = 8.882$, related samples Wilcoxon test; Figure 3C). While there were mixed effects, on average VP significantly increased the amplitudes and the integral of ON-evoked ΔF/F changes to 156 ± 101% and 143 ± 106% of control, respectively [Amplitudes: $p < 0.001$, $z = 6.376$, related samples Wilcoxon test; Integral: $p < 0.001$, $z = 3.775$, related samples Wilcoxon test, $n = 166$ from five rats (Figures 3B,C)]. F0 in the glomeruli increased in the VP condition to 110 ± 14.8% of control ($p = 0.041$, $z = 2.040$, related samples Wilcoxon test; Figure 3D). The amplitudes and the

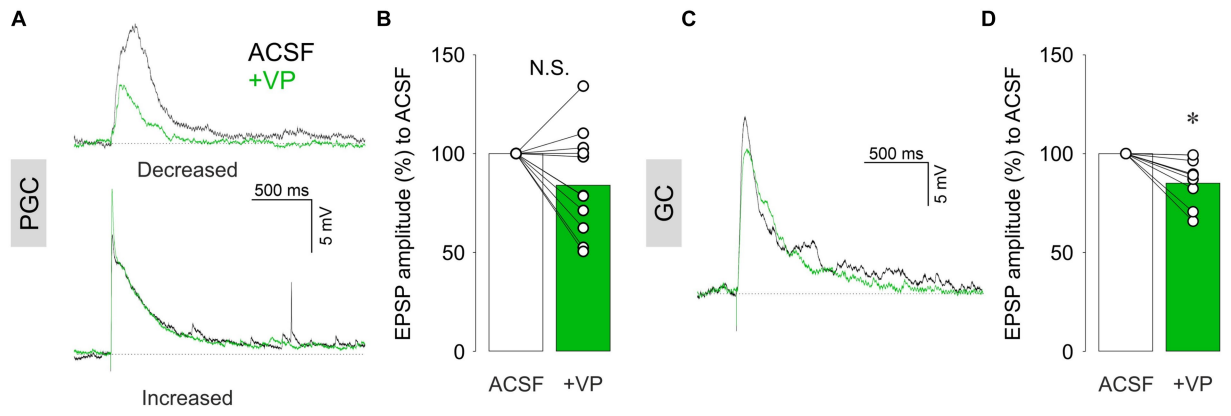

FIGURE 2
Representative current-clamp traces of ON-evoked EPSPs and cumulative data of ON-evoked EPSP amplitudes in % to control in PGCs **(A,B)** and GCs **(C,D)**. The bar graphs show average values. Individual data points are shown as open circles, and points from the same cell are connected by a line. *$p < 0.05$; N.S., non-significant. Black traces: ACSF (control); Green traces: VP.

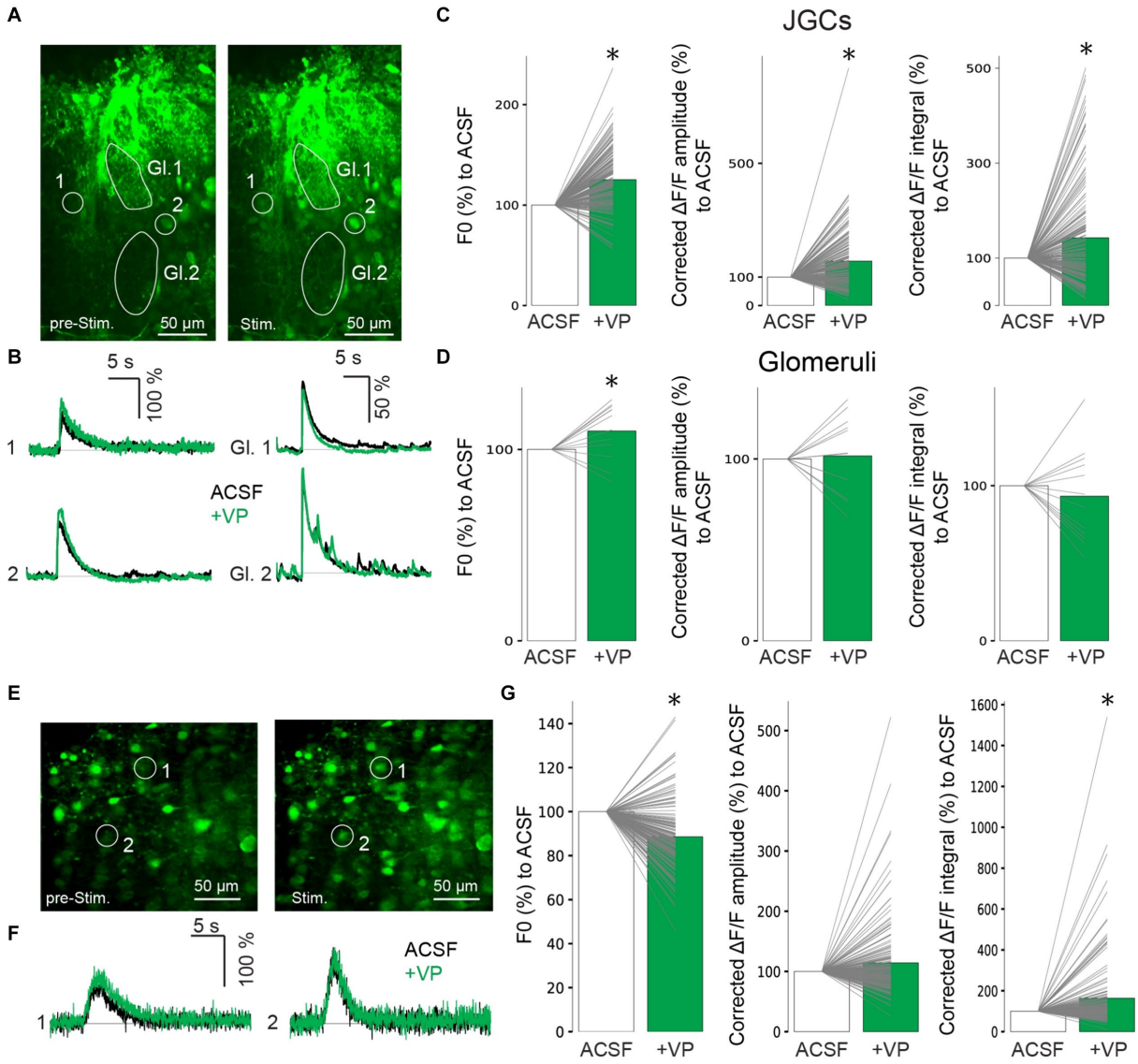

FIGURE 3
Representative images of Ca^{2+} imaging before ON stimulation (left) and after ON stimulation (right) in the GL **(A)**. Gl., glomerulus. Representative traces of Ca^{2+} imaging from corresponding JGCs (left) and from corresponding glomeruli (right) in A **(B)**. Cumulative data of F0 (left) and amplitudes (middle) and integral (right) of ΔF/F in JGCs **(C)** and glomeruli **(D)**. Bar graphs show average values. Individual data points from the same cell are connected by a line. *$p < 0.05$. Black traces: ACSF (control); Green traces: VP. Representative images of Ca^{2+} imaging before ON stimulation (left) and after ON stimulation (right) in the GCL **(E)**. Representative traces of Ca^{2+} imaging from the corresponding GCs are shown in E **(F)**. Cumulative data of F0 (left) and amplitudes (middle) and integral (right) of ΔF/F in GCs **(G)**. The bar graphs show average values. Individual data points from the same cell are connected by a line. *$p < 0.05$. Black traces: ACSF (control); Green traces: VP.

integral of ON-evoked ΔF/F in the glomeruli were similar to control, 102 ± 21.6% and 93.3 ± 30.3% of control, respectively [Amplitudes: $p = 0.754$, $z = 0.314$, related samples Wilcoxon test; Integral: $p = 0.388$, $z = -0.863$, related samples Wilcoxon test, $n = 12$ from five rats (Figures 3B,D)].

We also performed dye injections in the superficial GCL and measured changes in intracellular Ca^{2+} levels in the GC somata (Figures 3E,F). F0 decreased in the VP condition to 88.6 ± 15.3% of the control ($p < 0.001$, $z = -7.973$, related samples Wilcoxon test; Figure 3G). In these experiments, again, there were mixed effects, but on average, VP significantly increased the integral but not the amplitudes of ON-evoked ΔF/F changes to 164 ± 181% and 114 ± 63% of control, respectively [Integral: $p < 0.001$, $z = 3.832$, related samples Wilcoxon test; Amplitudes: $p = 0.558$, $z = 0.587$, related samples Wilcoxon test, $n = 165$ from six rats (Figures 3F,G)].

Therefore, we suggest that VP enhances evoked Ca^{2+} influx in those inhibitory interneurons (Table 2).

Discussion

Origin of VP inhibitory effects in the OB

V1aRs that are predominantly expressed in the olfactory bulb are $G\alpha_{q/11}$-coupled receptors and thus act in an excitatory manner (Birnbaumer, 2002). As mentioned in the introduction, V1aRs are

TABLE 2 Summary of results regarding ON-evoked responses in different neuron types.

		Subthreshold activation (E/IPSPs) Weak ON stimulation	Suprathreshold activation (Ca^{2+} influx) Strong ON stimulation
Excitatory neurons	eTCs (Lukas et al., 2019)	↓ (ON-evoked EPSPs)	–
	mTCs	↓ (ON-evoked EPSPs)↑ (spontaneous IPSPs)	–
	MCs	N.S. (ON-evoked EPSPs, spontaneous IPSPs)	–
Inhibitory neurons	JGCs/PGCs	N.S. (ON-evoked EPSPs)	↑ (amplitude, integral)
	GCs	↓ (ON-evoked EPSPs)	N.S. (amplitude)/ ↑ (integral)

eTCs, external tufted cells; mTCs, middle tufted cells; MCs, mitral cells; JGCs, juxtaglomerular cells; PGCs, periglomerular cells; GCs, granule cells; N.S., non-significant.

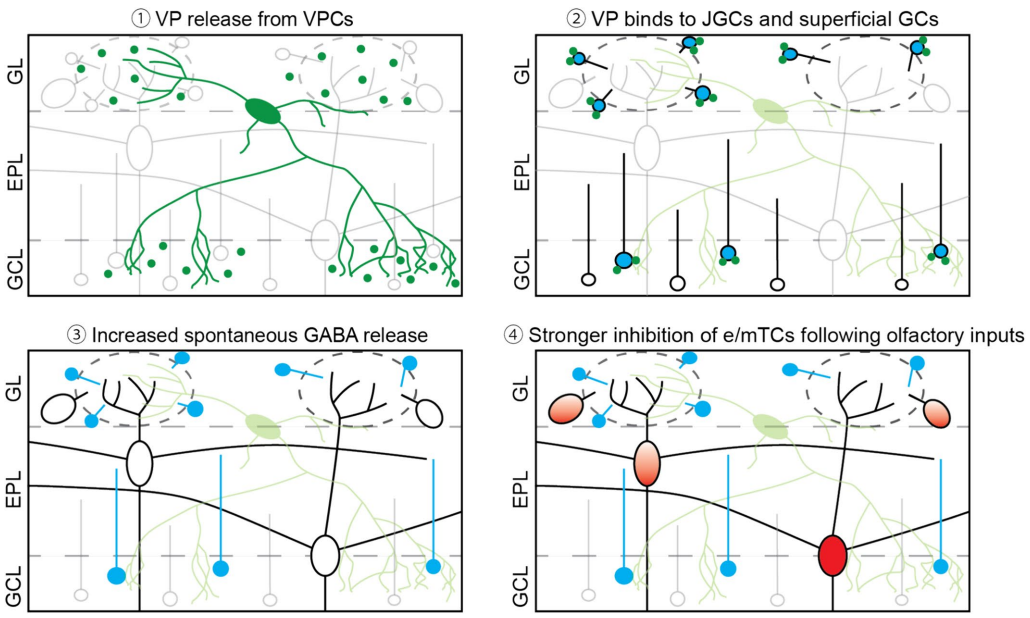

FIGURE 4
Scheme of the overview. (1) Once VPCs are activated, VP is released from their dendrites and axons in both the GL and the superficial GCL. (2) Released VP binds to VP receptors, which are expressed in the GL and the superficial GCL, likely on JGCs and GCs. (3) Through VP receptor activation, spontaneous GABA release occurs more frequently, leading to more spontaneous inhibitory inputs onto mTCs. (4) Following suprathreshold olfactory inputs, VP-bound interneurons are activated stronger and then inhibit e/mTCs and MCs (Tobin et al., 2010).

expressed in the GL and the superficial part of the GCL (Ostrowski et al., 1994; Tobin et al., 2010). In addition, VPCs innervate densely those two layers in the OB (Figure 4; Lukas et al., 2019). This distribution of V1aRs and VPC's innervation fits our data, showing that VP increased the ON-evoked Ca^{2+} signal in JGCs and GCs in those layers. Moreover, VP increases the inhibition of eTCs (Lukas et al., 2019) and mTCs (Figure 1). A similar VP-mediated increase of inhibition has been shown in other brain regions. For example, VP increases the frequency of spontaneous IPSP/Cs in magnocellular paraventricular nucleus neurons (Hermes et al., 2000), as well as spontaneous spikes in hippocampal GABAergic neurons, which results in an increase in the number of spontaneous IPSCs in pyramidal neurons (Ramanathan et al., 2012). Ramanathan et al. (2012) suggested that increased hippocampal GABAergic inhibition of pyramidal cells may result in organized inhibition to establish fine-tuning of excitation and rhythmic synchronized activity of pyramidal neurons that are important for memory consolidation. Since the function of bulbar inhibitory networks is suggested to tune excitation and modulate oscillatory activity as well, VP effects on bulbar inhibitory neurons may help organize excitatory neuron activity.

In current-clamp experiments, we did not observe significant changes in the holding current to keep the basal membrane potentials the same as the initial values between control and the VP condition, and the changes are not different between cell types (Table 1; mTCs: $p = 0.348$, $t(7) = 1.006$, paired t-test; MCs: $p = 0.341$, $t(10) = 1.000$, paired t-test; PGCs: $p = 0.061$, $t(10) = 2.108$, paired t-test; GCs: $p = 0.082$, $t(7) = 2.028$, paired t-test; Between cell types: $p = 0.285$, $H = 3.788$, $df = 3$, Kruskal–Wallis test). Even though holding currents tend to be more negative in the VP condition, implying depolarization, changes are not statistically significant, and we cannot differentiate potential VP effects and the increase of leakage currents over time. F0 in the Ca^{2+} population imaging showed different results in the GL and the GCL. F0 in JGCs and glomeruli significantly increased (Figures 3C,D), and F0 in GCs significantly decreased (Figure 3G) in the VP condition. One can assume that VP increases the basal Ca^{2+} concentration in JGCs and

decreases it in GCs. However, the dye has been shown to suffer from F0 increases over time (Tada et al., 2014). In addition, photobleaching should be considered. As a result, we cannot definitely conclude what causes the F0 changes from our experiments. Therefore, further experiments focusing on the VP effects on the resting membrane potentials or basal Ca^{2+} concentrations in OB neurons would be beneficial to better understand the direct effects of VP. Previous studies on the VP effects on the hippocampus (Urban and Killian, 1990) and the lateral septum (Van Den Hooff and Urban, 1990) showed that only a subset of neurons depolarized and/or fired upon VP application. However, even neurons that did not get directly excited by VP showed synaptic modulation by VP. Thus, even if VP does not change their resting membrane potentials, other mechanisms, e.g., intracellular cascades involving ER Ca^{2+} or DAG (Birnbaumer, 2002), would contribute to changing the response to the inputs, such as greater Ca^{2+} influx.

Functional implication of the VP effects: different results with weak or strong ON inputs

Functional differences between PGCs (inhibition in the GL) and GCs have been discussed extensively elsewhere (see review, Devore and Linster, 2012, D'Souza and Vijayaraghavan, 2014). Briefly, inhibition in the GL tunes activation patterns of projection neurons, such as contrast enhancement or concentration invariance (e.g., Linster and Hasselmo, 1997; Cleland and Sethupathy, 2006; Cleland et al., 2007). For instance, acetylcholine (ACh), which is known to activate GL interneurons (Devore and Linster, 2012), enhances the contrast of projection neural representation responding to very similar odors. Thus, neostigmine (an acetylcholinesterase inhibitor) administration in the OB increases differences in the number of MC spikes between responses to ethers differing by single carbon chain in *in-vivo* electrophysiology. For example, an MC responds strongest to E2 (ethyl acetate) and second strongest to E3 (ethyl propionate), differing by only one carbon chain, but the responses are not significantly different from each other. In the presence of neostigmine, the MC responds less strongly to or gets more inhibited by E3 than control. Therefore, responses of the MC to E2 and E3 are discriminable (Chaudhury et al., 2009). Moreover, electrical stimulation of the horizontal limb of the diagonal band of Broca (HDB), the center of cholinergic top-down projections, decreases glomerular M/TC-tuft activity following odor presentation with high concentration, whereas increases glomerular activity following low-concentration odor presentation in *in-vivo* Ca^{2+} imaging, indicating responses are less varied to different concentrations of the same odor (Bendahmane et al., 2016). These authors suggested that the less variation of responses to different odor concentrations makes neural representation reflect more purely the identity of odors. In our hands, VP increased the amplitudes of ON-evoked Ca^{2+} influx into JGCs in population imaging. If VP effects and ACh effects on the GL interneurons are similar, VP might prevent excitatory neurons from firing when they are weakly activated. Therefore, we observed inhibitory VP effects on the amplitudes of subthreshold-evoked EPSPs in eTCs (Lukas et al., 2019) and mTCs (Figure 1). The lack of inhibitory effects on MCs is discussed below.

GCs are responsible for the organization of spike timing and synchronization of projection neurons that further refine contrast and representations of odors (e.g., McTavish et al., 2012; Osinski and Kay, 2016). Computational analysis showed that the level of GC excitability might tune oscillatory frequency in MCs; thus, with low excitability of GCs, MCs fire in the gamma range, however high excitability allows MCs to fire in beta oscillation (Osinski and Kay, 2016). Oettl et al. (2016) showed the modulation of GCs via the oxytocin system in the anterior olfactory nucleus (AON). An oxytocin receptor agonist increases the frequency of spontaneous EPSCs in GCs from AON excitatory neurons, resulting in increased spontaneous IPSCs in MCs. In *in-vivo* electrophysiological recordings in M/TCs, an oxytocin receptor agonist applied in the AON lowers basal spiking rates and increases odor-evoked spiking rates, thus improving the signal-to-noise ratio. Conditional oxytocin receptor knockout in the AON impairs social memory, showing that the enhanced signal-to-noise ratio in M/TCs by activation of GCs is important for discrimination of conspecific body odors (Oettl et al., 2016).

Interestingly, the results of ON-evoked EPSPs and ON-evoked Ca^{2+} influx in PGCs (or JGCs) and GCs contradict each other (Figures 2, 3). This discrepancy may be explained by the fact that what we were observing during recording EPSPs and imaging Ca^{2+} influx is different. During slice experiments, we performed subthreshold activation, whereas, during Ca^{2+} imaging, we performed suprathreshold activation by ON stimulation. Possibly, VP can enhance Ca^{2+} entry selectively for suprathreshold activation, which is probably not related to the initial depolarization but to later phases of the signal which involve contributions from NMDARs. V1aRs and NMDARs are present at GC somata (Personal communication with M. Sassoe-Pognetto; Stroh et al., 2012). In the rat ventral hippocampus, VP excites neurons, and the VP effects are blocked by both V1aR and NMDAR antagonists, indicating VP effects via modulation of NMDARs. Moreover, VP enhances glutamate-evoked spiking (Urban and Killian, 1990). In contrast, EPSPs are subthreshold activation that are highly dependent on the inputs of the cells. We observed the inhibitory VP effects on excitatory neurons (Figure 1; Tobin et al., 2010, Lukas et al., 2019). The results indicate that the inputs of inhibitory interneurons, e.g., glutamate released from excitatory neurons, are less in the presence of VP. Hence, smaller amplitudes of evoked EPSPs in GCs in the VP condition that we observed. Mixed results in PGCs might be due to the differences in connectivity, either directly connected with the ON or with eTCs (Shao et al., 2009), e.g., the ON-driven population is resistant and the eTC-driven population is susceptible to the VP administration because eTCs are susceptible. Although we did not observe subpopulations that can be divided by the VP effects on EPSP amplitudes, morphology, or firing pattern, it is worth examining further characteristics, such as molecular markers. We have not performed experiments on interneurons in the EPL (Nagayama et al., 2014). Since VPC's neurites are found in the EPL, it would be informative to investigate VP effects on them as well.

Our data showed that VP reduced the amplitudes of ON-evoked EPSPs in eTCs (Lukas et al., 2019) and mTCs. These data indicate that eTCs and mTCs need stronger ON inputs to fire under the VP condition. The suppression of those neurons could result in contrast enhancement of the neural representation in the OB (Chaudhury et al., 2009). The glomerular GABAergic inhibition includes $GABA_A$ receptor- and $GABA_B$ receptor-mediated pathways. For instance, cholecystokinin, which is also expressed in a subpopulation of superficial tufted cells, acts on SACs to inhibit presynaptically the ON via $GABA_B$ receptors, resulting in smaller ON-evoked EPSCs in eTCs (Liu and Liu, 2018). Therefore, a similar mechanism is conceivable for

VP modulation, and further examination of the involvement of SACs or $GABA_B$ receptors would give us more insights into the VP-mediated inhibition of eTCs and mTCs. Interestingly, unlike for mTCs or eTCs, VP did not reduce the amplitudes of evoked EPSPs or increase frequencies of spontaneous IPSCs in MCs. This variance in our data between mTCs and MCs could be due to the difference in input sources of the two cell types. MCs receive indirect excitatory inputs from eTCs (De Saint Jan et al., 2009; Najac et al., 2011), and MCs are less sensitive to odor inputs than e/mTCs (Igarashi et al., 2012). If the ON-evoked EPSPs in MCs are consequences of the firing of eTCs, the ON stimulation intensity in MC experiments may be strong for eTCs, so that also during VP application, APs are still evoked in eTCs. Thus, during VP application, the same net amount of excitation is transmitted to MCs as without VP. Tobin et al. (2010) showed that odor-evoked MC firing decreased upon VP administration, although we did not observe reduced amplitudes of ON-evoked EPSPs in MCs in our experiments (Figure 1). In their *in-vivo* experiments, Tobin et al. (2010) presented odors that were able to fire MCs. We purposefully stimulated the ON electrically in *in-vitro* slices to evoke EPSPs in MCs. Thus, we suggest that the discrepancy between the results from Tobin et al. (2010) and ours might be due to differences in subthreshold and suprathreshold activation of MCs in the different experimental setups. The main inputs of GCs are dendrodendritic glutamatergic signals from TCs or MCs. If the somata of MCs do not show active conduction like in our slice experiments, it is unlikely that their lateral dendrites release glutamate to excite GCs. As a result, inhibition of MC firing via dendrodendritically induced GABA release from GCs cannot be triggered or modulated by VP. However, during strong ON stimulation, like odor stimulation, MCs fire and excite GCs. If the excitation is strong enough, VP could enhance the GC activity as also shown in our Ca^{2+} imaging experiments using suprathreshold ON stimulation (Figure 3). Under these conditions, VP-modulated enhanced activation of GCs might be responsible for an increased dendrodenritic GABAergic suppression of MC firing as shown in the *in-vivo* experiments of Tobin et al. (2010). However, to finally confirm this hypothesis, further Ca^{2+} imaging or spike analysis experiments using strong ON stimulation would be needed. Since Tobin et al. (2010) reported that V1aRs are expressed in MCs as well, we cannot exclude that VP directly excites MCs, even though we could not see excitatory effects in our experiments. In CA1, VP increases not only the number of spontaneous IPSCs but also the number of spontaneous spikes under the conditions of glutamatergic and GABAergic receptor antagonists in pyramidal neurons (Ramanathan et al., 2012). Therefore, the non-synaptic excitability of projection neurons would be intriguing to examine, as mentioned above. Sun et al. (2021) showed interesting effects of oxytocin, which also modulates social discrimination at the level of the OB (Dluzen et al., 1998; Sun et al., 2021). The authors demonstrated that oxytocin directly reduces the excitability of MCs via the Gq protein pathway, which, in turn, results in less activation of GCs responding to odor presentation. As a direct mechanism like that one is also conceivable for VP via V1aR on MCs, these results further encourage the examination of direct VP effects on MCs.

In addition to VP and oxytocin, various other neuropeptides are involved in the modulation of OB neuron activity (Stark, 2024). For instance, Decoster et al. (2024) recently showed that GnRH (gonadotropin-releasing hormone)-expressing neurons in male mice are activated upon the presentation of estrus female urine, and silencing of GnRH neurons impairs preference toward estrus female urine over male urine in male mice. Although it is not clear yet how other neuropeptides modulate neural activity in the OB in social contexts, it is worth paying attention to other neuropeptidergic systems. In addition, there might be synergic effects of different neuropeptides, especially ones that are known to have similar behavioral effects, such as VP and oxytocin (Dluzen et al., 1998; Tobin et al., 2010; Sun et al., 2021; Suyama et al., 2021).

Possible consequences of VP-mediated OB modulation

We previously suggested that social discrimination is a variation of perceptual learning because of the association with ACh and the close similarity of stimuli, i.e., conspecific body odors, that rats discriminate (Suyama et al., 2021). Perceptual learning is possible because a subject pays attention to a stimulus during exposures, and sensory acuity against the stimulus is enhanced due to a finer neural representation. As mentioned above, ACh, an important substance for perceptual learning, increases differences in the number of MC spikes reacted to odors differing by a single carbon (Chaudhury et al., 2009). This change in neural representation results in behavioral outputs like habituation. Rats lose their motivation to investigate odor if rats perceive it as the same one as they previously investigated, i.e., habituation. In controls, rats show habituation to an odor differing by a single carbon from a previously exposed odor, suggesting that rats cannot distinguish odors differing by one carbon. However, injection of neostigmine into the OB enables rats to discriminate those odors (Chaudhury et al., 2009). Therefore, neuromodulation of projection neuron activity seems to be important for sensory perception, hence discrimination as the behavioral output of this enhanced sensory perception. We demonstrated that VP modulation may result in less mTCs firing via GL contrast enhancement. Furthermore, VP inhibits the firing rates of MCs (Tobin et al., 2010), which can result in improved neural representation (Linster and Hasselmo, 1997). Although Tobin et al. (2010) did not record the firing rates of mTCs, it is plausible that this is the same for all projection neurons. Thus, in the VP condition, M/TCs may transmit more precise information to higher brain regions, like during the modulatory action of ACh (Chaudhury et al., 2009). Taken together, we hypothesize that VP inhibits projection neurons differently to reduce sensitivity and improve representation in the olfactory cortex.

Data availability statement

The raw data supporting the conclusions of this article will be made available by the authors, without undue reservation.

Ethics statement

Ethical approval was not required for the study involving animals in accordance with the local legislation and institutional requirements because according to the German Animal Ethics Legislature, killing animals exclusively for the purposes of using their organs or tissues is not considered as an animal experiment (Tierschutzgesetz, Section 4,

Paragraph 3). We are monitored and certified regarding animal handling and slice preparation by institutional veterinarians.

Author contributions

HS: Funding acquisition, Writing – review & editing, Writing – original draft, Visualization, Supervision, Methodology, Investigation, Formal analysis, Data curation, Conceptualization. GB: Writing – review & editing, Data curation. ML: Writing – review & editing, Writing – original draft, Visualization, Supervision, Project administration, Methodology, Investigation, Funding acquisition, Formal analysis, Data curation, Conceptualization.

Funding

The author(s) declare that financial support was received for the research, authorship, and/or publication of this article. This research was supported by the German Research Foundation (DFG LU2164/1-1), the Boehringer Ingelheim Fonds (travel grant), and the University of Regensburg (RU5424).

Acknowledgments

We would like to thank Anne Pietryga-Krieger for experimental support, Christoph Schmid and Atefeh Akbari for help with experimentation, and Veronica Egger for experimental equipment such as electrophysiology rigs and Ca^{2+} imaging setups and advice.

Conflict of interest

The authors declare that the research was conducted in the absence of any commercial or financial relationships that could be construed as a potential conflict of interest.

Publisher's note

References

Abraham, N. M., Egger, V., Shimshek, D. R., Renden, R., Fukunaga, I., Sprengel, R., et al. (2010). Synaptic inhibition in the olfactory bulb accelerates odor discrimination in mice. *Neuron* 65, 399–411. doi: 10.1016/j.neuron.2010.01.009

Bendahmane, M., Ogg, M. C., Ennis, M., and Fletcher, M. L. (2016). Increased olfactory bulb acetylcholine bi-directionally modulates glomerular odor sensitivity. *Sci. Rep.* 6:25808. doi: 10.1038/srep25808

Birnbaumer, M. (2002). "58 - vasopressin receptors" in Hormones, brain and behavior. eds. D. W. Pfaff, A. P. Arnold, S. E. Fahrbach, A. M. Etgen and R. T. Rubin (San Diego: Academic Press).

Brunert, D., and Rothermel, M. (2021). Extrinsic neuromodulation in the rodent olfactory bulb. *Cell Tissue Res.* 383, 507–524. doi: 10.1007/s00441-020-03365-9

Chaudhury, D., Escanilla, O., and Linster, C. (2009). Bulbar acetylcholine enhances neural and perceptual odor discrimination. *J. Neurosci.* 29, 52–60. doi: 10.1523/JNEUROSCI.4036-08.2009

Cleland, T. A., Johnson, B. A., Leon, M., and Linster, C. (2007). Relational representation in the olfactory system. *Proc. Natl. Acad. Sci.* 104, 1953–1958. doi: 10.1073/pnas.0608564104

Cleland, T. A., and Sethupathy, P. (2006). Non-topographical contrast enhancement in the olfactory bulb. *BMC Neurosci.* 7:7. doi: 10.1186/1471-2202-7-7

D'souza, R. D., and Vijayaraghavan, S. (2014). Paying attention to smell: cholinergic signaling in the olfactory bulb. *Front. Synaptic Neurosci.* 6:21. doi: 10.3389/fnsyn.2014.00021

Dantzer, R., Koob, G. F., Bluthe, R. M., and Lemoal, M. (1988). Septal vasopressin modulates social memory in male-rats. *Brain Res.* 457, 143–147. doi: 10.1016/0006-8993(88)90066-2

Dantzer, R., Tazi, A., and Bluthe, R. M. (1990). Cerebral lateralization of olfactory-mediated affective processes in rats. *Behav. Brain Res.* 40, 53–60. doi: 10.1016/0166-4328(90)90042-D

De Saint Jan, D., Hirnet, D., Westbrook, G. L., and Charpak, S. (2009). External tufted cells drive the output of olfactory bulb glomeruli. *J. Neurosci.* 29, 2043–2052. doi: 10.1523/JNEUROSCI.5317-08.2009

Decoster, L., Trova, S., Zucca, S., Bulk, J., Gouveia, A., Ternier, G., et al. (2024). A Gnrh neuronal population in the olfactory bulb translates socially relevant odors into reproductive behavior in male mice. *Nature Neurosci.* doi: 10.1038/s41593-024-01724-1

Devore, S., and Linster, C. (2012). Noradrenergic and cholinergic modulation of olfactory bulb sensory processing. *Front. Behav. Neurosci.* 6:52. doi: 10.3389/fnbeh.2012.00052

Dluzen, D. E., Muraoka, S., Engelmann, M., and Landgraf, R. (1998). The effects of infusion of arginine vasopressin, oxytocin, or their antagonists into the olfactory bulb upon social recognition responses in male rats. *Peptides* 19, 999–1005. doi: 10.1016/S0196-9781(98)00047-3

Egger, V., and Kuner, T. (2021). Olfactory bulb granule cells: specialized to link coactive glomerular columns for percept generation and discrimination of odors. *Cell Tissue Res.* 383, 495–506. doi: 10.1007/s00441-020-03402-7

Egger, V., Svoboda, K., and Mainen, Z. F. (2003). Mechanisms of lateral inhibition in the olfactory bulb: efficiency and modulation of spike-evoked calcium influx into granule cells. *J. Neurosci.* 23, 7551–7558. doi: 10.1523/JNEUROSCI.23-20-07551.2003

Engelmann, M., Hadicke, J., and Noack, J. (2011). Testing declarative memory in laboratory rats and mice using the nonconditioned social discrimination procedure. *Nat. Protoc.* 6, 1152–1162. doi: 10.1038/nprot.2011.353

Fukunaga, I., Herb, J. T., Kollo, M., Boyden, E. S., and Schaefer, A. T. (2014). Independent control of gamma and theta activity by distinct interneuron networks in the olfactory bulb. *Nat. Neurosci.* 17, 1208–1216. doi: 10.1038/nn.3760

Hermes, M. L. H. J., Ruijter, J. M., Klop, A., Buijs, R. M., and Renaud, L. P. (2000). Vasopressin increases Gabaergic inhibition of rat hypothalamic paraventricular nucleus neurons *in vitro*. *J. Neurophysiol.* 83, 705–711. doi: 10.1152/jn.2000.83.2.705

Igarashi, K. M., Ieki, N., An, M., Yamaguchi, Y., Nagayama, S., Kobayakawa, K., et al. (2012). Parallel mitral and tufted cell pathways route distinct odor information to different targets in the olfactory cortex. *J. Neurosci.* 32, 7970–7985. doi: 10.1523/JNEUROSCI.0154-12.2012

Imamura, F., Ito, A., and Lafever, B. J. (2020). Subpopulations of projection neurons in the olfactory bulb. *Front. Neural Circuits* 14. doi: 10.3389/fncir.2020.561822

Linster, C., and Hasselmo, M. (1997). Modulation of inhibition in a model of olfactory bulb reduces overlap in the neural representation of olfactory stimuli. *Behav. Brain Res.* 84, 117–127. doi: 10.1016/S0166-4328(97)83331-1

Liu, X., and Liu, S. (2018). Cholecystokinin selectively activates short axon cells to enhance inhibition of olfactory bulb output neurons. *J. Physiol.* 596, 2185–2207. doi: 10.1113/JP275511

Lukas, M., Suyama, H., and Egger, V. (2019). Vasopressin cells in the rodent olfactory bulb resemble non-bursting superficial tufted cells and are primarily inhibited upon olfactory nerve stimulation. *eNeuro* 6:2019. doi: 10.1523/ENEURO.0431-18.2019

Mctavish, T. S., Migliore, M., Shepherd, G. M., and Hines, M. L. (2012). Mitral cell spike synchrony modulated by dendrodendritic synapse location. *Front. Comput. Neurosci.* 6:3. doi: 10.3389/fncom.2012.00003

Nagayama, S., Homma, R., and Imamura, F. (2014). Neuronal organization of olfactory bulb circuits. *Front. Neural Circuits* 8:98. doi: 10.3389/fncir.2014.00098

Najac, M., De Saint Jan, D., Reguero, L., Grandes, P., and Charpak, S. (2011). Monosynaptic and polysynaptic feed-forward inputs to mitral cells from olfactory sensory neurons. *J. Neurosci.* 31, 8722–8729. doi: 10.1523/JNEUROSCI.0527-11.2011

Oettl, L. L., Ravi, N., Schneider, M., Scheller, M. F., Schneider, P., Mitre, M., et al. (2016). Oxytocin enhances social recognition by modulating cortical control of early olfactory processing. *Neuron* 90, 609–621. doi: 10.1016/j.neuron.2016.03.033

Osinski, B. L., and Kay, L. M. (2016). Granule cell excitability regulates gamma and beta oscillations in a model of the olfactory bulb dendrodendritic microcircuit. *J. Neurophysiol.* 116, 522–539. doi: 10.1152/jn.00988.2015

Ostrowski, N., Lolait, S., and Young, W. (1994). Cellular localization of vasopressin V1a receptor messenger ribonucleic acid in adult male rat brain, pineal, and brain vasculature. *Endocrinology* 135, 1511–1528. doi: 10.1210/endo.135.4.7925112

Pankevich, D. E., Baum, M. J., and Cherry, J. A. (2004). Olfactory sex discrimination persists, whereas the preference for urinary odorants from estrous females disappears in male mice after vomeronasal organ removal. *J. Neurosci.* 24, 9451–9457. doi: 10.1523/JNEUROSCI.2376-04.2004

Ramanathan, G., Cilz, N. I., Kurada, L., Hu, B., Wang, X., and Lei, S. (2012). Vasopressin facilitates Gabaergic transmission in rat hippocampus via activation of V1A receptors. *Neuropharmacology* 63, 1218–1226. doi: 10.1016/j.neuropharm.2012.07.043

Shao, Z., Puche, A. C., Kiyokage, E., Szabo, G., and Shipley, M. T. (2009). Two Gabaergic Intraglomerular circuits differentially regulate tonic and phasic presynaptic inhibition of olfactory nerve terminals. *J. Neurophysiol.* 101, 1988–2001. doi: 10.1152/jn.91116.2008

Shepherd, G. M., Chen, W. R., and Greer, C. A. (2004). "Olfactory bulb" in The synaptic organization of the brain. ed. G. M. Shepherd (Oxford: Oxford University Press).

Singer, A. G., Beauchamp, G. K., and Yamazaki, K. (1997). Volatile signals of the major histocompatibility complex in male mouse urine. *Proc. Natl. Acad. Sci. USA* 94, 2210–2214. doi: 10.1073/pnas.94.6.2210

Stark, R. (2024). The olfactory bulb: a neuroendocrine spotlight on feeding and metabolism. *J. Neuroendocrinol.* 36:e13382. doi: 10.1111/jne.13382

Stroh, O., Freichel, M., Kretz, O., Birnbaumer, L., Hartmann, J., and Egger, V. (2012). Nmda receptor-dependent synaptic activation of Trpc channels in olfactory bulb granule cells. *J. Neurosci.* 32, 5737–5746. doi: 10.1523/JNEUROSCI.3753-11.2012

Sun, C., Yin, Z., Li, B.-Z., Du, H., Tang, K., Liu, P., et al. (2021). Oxytocin modulates neural processing of mitral/tufted cells in the olfactory bulb. *Acta Physiol.*:e13626. doi: 10.1111/apha.13626

Suyama, H., Egger, V., and Lukas, M. (2021). Top-down acetylcholine signaling via olfactory bulb vasopressin cells contributes to social discrimination in rats. *Commun. Biol.* 4:603. doi: 10.1038/s42003-021-02129-7

Suyama, H., Egger, V., and Lukas, M. (2022). Mammalian social memory relies on neuromodulation in the olfactory bulb. *e-Neuroforum* 28, 143–150. doi: 10.1515/nf-2022-0004

Tada, M., Takeuchi, A., Hashizume, M., Kitamura, K., and Kano, M. (2014). A highly sensitive fluorescent indicator dye for calcium imaging of neural activity in vitro and in vivo. *Eur. J. Neurosci.* 39, 1720–1728. doi: 10.1111/ejn.12476

Tavakoli, A., Schmaltz, A., Schwarz, D., Margrie, T. W., Schaefer, A. T., and Kollo, M. (2018). Quantitative Association of Anatomical and Functional Classes of olfactory bulb neurons. *J. Neurosci.* 38, 7204–7220. doi: 10.1523/JNEUROSCI.0303-18.2018

Tobin, V. A., Hashimoto, H., Wacker, D. W., Takayanagi, Y., Langnaese, K., Caquineau, C., et al. (2010). An intrinsic vasopressin system in the olfactory bulb is involved in social recognition. *Nature* 464, 413–417. doi: 10.1038/nature08826

Urban, I. J. A., and Killian, M. J. P. (1990). Two actions of vasopressin on neurons in the rat ventral hippocampus: a microiontophoretic study. *Neuropeptides* 16, 83–90. doi: 10.1016/0143-4179(90)90116-G

Van Den Hooff, P., and Urban, I. J. A. (1990). Vasopressin facilitates excitatory transmission in slices of the rat dorso-lateral septum. *Synapse* 5, 201–206. doi: 10.1002/syn.890050305

Frontiers in
Neural Circuits

Explores the emergent properties of neural circuits - the brain's elementary modules

Part of the most cited neuroscience journal series, focuses on the anatomy, physiology, development and function of neural circuitry, exploring how plasticity shapes the architecture of the brain's elementary modules.

Discover the latest Research Topics

See more →

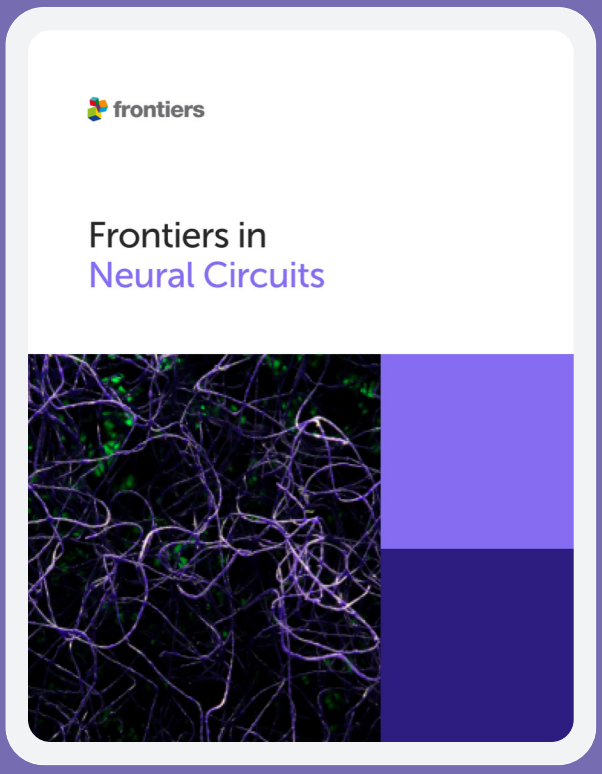

Frontiers

Avenue du Tribunal-Fédéral 34
1005 Lausanne, Switzerland
frontiersin.org

Contact us

+41 (0)21 510 17 00
frontiersin.org/about/contact